Synthesis, Characterisation and Transition Metal Ion Complexation Studies of "Pocket-Like" Imine and Amide Derivatives

A thesis submitted to the National University of Ireland in fulfilment of the requirements for the degree of

Doctor of Philosophy

By

Haixin Gao

NUI MAYNOOTH

Ollscoil na hÉireann Má Nuad

Department of Chemistry,

Faculty of Science and Engineering,

National University of Ireland, Maynooth,

Maynooth,

Co. Kildare,

Ireland

December 2013

Research Supervisor: Dr. John McGinley

Head of Department: Dr. John Stephens

Table of Contents

Contents

Declaration

This is to certify that the material presented within this thesis has not been submitted previously for a Degree to this or any other University. All material presented, except where acknowledged and cited, is the original work of the author.

Haixin Gao

_____

December 2013

Dedication

To my parents, ZhaoFu Gao (高兆福) and Xia Zhang （张侠）, with love.

Thank you for everything.

List of abbreviations

Ac	Acetyl
AcOH	Acetic acid
Anal. Calc.	Analytical calculation
Ar	Aryl
B.M.	Böhr Magneton
br	Broad
t-Bu	*tert*-Butyl
Boc	*tert*-Butyloxycarbonyl
$CDCl_3$	Deuterated chloroform
cm	Centimetre
cm^{-1}	Wavenumbers
d	Doublet
℃	Degrees Celsius
dd	Doublet of doublets
d.e.	Diastereomeric excess
Δ	Reflux temperature
δ	Chemical shift
DMF	*N*,*N*-dimethylformamide
d_6-DMSO	Deuterated dimethyl sulphoxide
dt	Doublet of triplets
e.e.	Enantiomeric excess
en	Ethylenediamine
EtOH	Ethanol
FTIR	Fourier Transform Infrared
h	Hour
HCl	Hydrochloric acid
HOMO	Highest occupied molecular orbital
Hz	Hertz
IR	Infrared
J	Coupling constant
KBr	Potassium bromide
KOH	Potassium hydroxide
λ	Wavelength (nm)
lit	Literature value
LUMO	Lowest unoccupied molecular orbital
M	Molar
m	Multiplet
Me	Methyl
MeOH	Methanol
Me_4Si	Tetramethylsilane

MHz	Megahertz
min	Minute
mL	Millilitre
mmol	Millimole
m.p.	Melting point
μ_{eff}	Effective magnetic moment
N_2	Dinitrogen
NaCl	Sodium chloride
NaOH	Sodium hydroxide
NMR	Nuclear magnetic resonance
nm	Nanometre
OEt	Ethoxide anion
O_2	Molecular oxygen
pH	Logarithmic scale of concentration of hydronium ions ($-\log[H_3O^+]$)
PhMe	Toluene
pK_a	Minus log of association constant K_a of a given solution ($-\log K_a$)
ppm	Parts per million
py	Pyridine
q	Quartet
s	Singlet
t	Triplet
TFA	Trifluoroacetic acid

Acknowledgements

My deepest gratitude goes first and foremost to Dr. John McGinley, my supervisor, for his constant encouragement and guidance. He has walked me through all the stages of the writing of this thesis. Without his consistent and illuminating instruction, this thesis could not have reached its present form. His keen and rigorous academic observation enlightens me not only in this thesis but also in my future study.

I would like to extend my sincere gratitude to both the current and former heads of the Chemistry Department at NUI Maynooth, Dr John Stephens and Prof. John Lowry, as well as for the technical staff Ollie, Mary Anne, Barbara, Ria, Orla, Ken, Niamh, Anne, Carol, Donna and Noel for their help during this time.

How time flies. I am missing this three and half years working on this project already. All the people in this department are very kind and warm to me. I need to thank McGinley's group particularly, who welcomed me so wholeheartedly when I started. Thanks to my seniors Dr.s: John W, Denis D, Niall M. and Laura O.T who help in my first years and teach me a lot. My English could not be worse when I stated the PhD, without your help, I could not adapt to the life of a chemistry PhD candidate so quickly. Special thanks to Ursula S. and Sam B. who were absolutely baby teachers, correcting my pronunciation every day. (You all say NMR sounds a whole word, but till now, I still say N-M-R-, you need put more effort on me). But, Niall and John, your genuine Irish pronunciation was really confusing during my whole PhD time. The words I said to you most frequently were: 'sorry', 'what', 'say again'. Laura, if we would have been in a team again, I will definitely ask you to slow down a little bit when talking to me. Anyway, I really appreciate all your help, and regard you as my brothers and sisters.

To the rest in the lab, Dr. John M (how could you answer every questions in every Wednesday's group meetings), Dr. Declan (I remembered you taught me the Irish men words), Dr. Trish (you should play tennis with me), Dr. Niall (your pet phrase, could be worse); to the other Dr.s, Carol, Louise, Wayne, Dean, the Johns (too many Johns), Lorna, Róis ín, Alanna, Colin, Vickie, Niall Mc (Joey); and to the people who are working in the lab or waiting for their vivas, Niamh, Rob D, Gama, Andrea (Andy), Justine, Ross, Andrew: I wish you all the best in the future.

Any craic?

Abstract

New families of [1+2] and [1+3] acyclic Schiff-base (imine) ligands using both di- or tri-aldehyde compounds and a variety of primary amines as precursors were prepared and fully characterised. These acyclic ligands have several extra functional groups attached, such as an OH or pyridine or imidazole rings. The imine ligands were prepared by using anhydrous magnesium sulphate and DCM/$CHCl_3$ solution in order to prevent potential hydrolysis from occurring. Four imine ligands, due to the presence of four different primary amines (2-, 3- or 4-aminomethylpyridine and 3-aminopropylimidazole (APIM)), were formed from the various aldehydes in each of the sections in this thesis. The aldehydes chosen for this study included 4-*tert*-2,6-benzenedicarboxyaldehyde, 2,5-diformyl-1,4-dihydroxybenzene, 5,5'-methylene-bis-salicylaldehyde and 2,4,6-triformylphloroglucinol as well as pyridine-2,6-dicarboxaldhyde. These ligands were reacted with various MX_2 salts (M = Cu, Ni, Zn, Co and Hg, and X = chloride, acetate and perchlorate). The metal complexation reactions were carried out in MeOH solution with stirring for about 2 hours. In the case of most complexation reactions, highly coloured precipitates were formed immediately.

All ligands were characterised by a combination of NMR spectroscopy, IR spectroscopy and either mass spectrometry or elemental analyses. The metal complexes were analysed by NMR spectroscopy (where appropriate), IR spectroscopy, magnetic moments and elemental analyses. Despite all our efforts, no crystals, suitable for an X-ray crystallographic study, were obtained. In several cases, the formation of polymeric materials was obtained which made the determination of structures of those complexes difficult.

1 Introduction

1.1 Schiff-base ligands and metal complexes

1.1.1 Overview

Schiff-base ligands and corresponding metal complexes have received much attention in recent years due to their wide use as dyes and pigments, catalysts, intermediates in organic synthesis, polymer stabilizers and due to their broad range of biological activities, including anti-fungal, anti-bacterial, anti-malarial, anti-proliferative, anti-inflammatory, anti-viral, and anti-pyretic properties.[1-4] Schiff bases are aldehyde or ketone like compounds in which the carbonyl group is replaced by an imine or azomethine group. It contains a carbon-nitrogen double bond with the nitrogen atom connected to an aryl or alkyl group but not hydrogen.

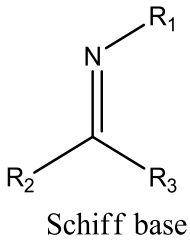

Schiff base

Figure 1.1: The structure of a Schiff base.

Schiff bases are of general formula $R_1N=CR_2R_3$, where R_1 is a phenyl or alkyl group which gives the Schiff base its stability.[5] Although the formation of Schiff bases is reversible, due to the hydrolysis of the imine under certain conditions, it is still straight forward for the reaction to succeed. It is still unknown what type of Schiff base is stable in the presence of water even with acidic solution, while others are very sensitive to water and easily hydrolyse back to aldehyde. To overcome this potential hydrolysis, the reaction of Schiff bases should be undertaken under dry solvent conditions or using some additional procedure to remove the side product, water, in the imine formation. (Further discussion of this will occur in Section 1.1.3 dealing with the synthesis of Schiff base ligands). The lone pair on the nitrogen atom of the imine part can supply electrons which enable the formation of a proper donor bond to a metal ion for complexation to occur. Many Schiff bases have a second functional group, normally OH and SH groups or another N atom, which are near to imine group. These functional groups can allow the formation of five or six member chelate rings when coordinated with different metal ions. The work described in this thesis concentrates on synthesising some novel Schiff-base ligands with several functional groups, such as phenol OH and

N from pyridine ring ligands and to generate their corresponding Zn(II), Hg(II), Cu(II), Ni(II) and Co(II) metal complexes.

1.1.2 History of Schiff-bases

Schiff bases are named after Hugo (Ugo) Schiff (1834-1915), a German chemist. He discovered Schiff bases in 1864[6] and other imines, and was responsible for research into aldehydes and had the Schiff test named after him. Fuchsine (shown in Figure 1.2) was studied by Schiff as a Schiff reagent in 1866, which was apparently widely used during the last decades of the 19th century for industrial dyes.

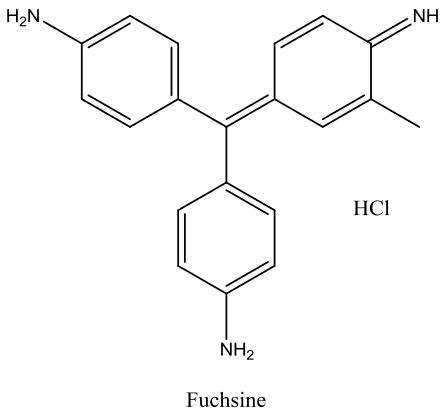

Figure 1.2: Structure of Fuchsine.

A well-known Schiff base ligand is a salen-type[7] (shown in Figure 1.3) with a bi-functional and tetradentate(ONNO) ligand. Several asymmetric salen type Schiff bases were reported by R. Atkins[8] in 1985, who suggested a more general term salen-type of tetradentate (ONNO) ligands. The 2-hydroxybenzaldehyde is a suitable building block due to the substitution pattern hydroxyl group of the ring. Once the imine bond is formed from primary amine and aldehyde, this orientation of salen-type Schiff bases will form a more stable six member ring when binding to metal ion.

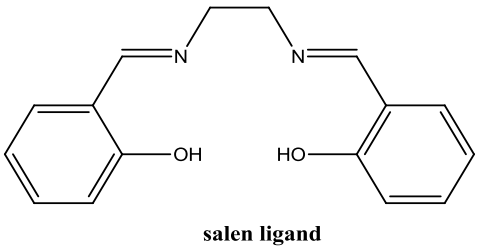

Figure 1.3: Typical structure of salen-type ligand.

1.1.3 Synthesis of Schiff-base ligands

A Schiff base reaction is a reversible, acid-catalysed condensation between a primary amine (not ammonia) and either an aldehyde or ketone. A Schiff base is the nitrogen analogue of an aldehyde or ketone, where the carbonyl group is replaced by an imine group (C=N-R), which is shown in Figure 1.4 where R may be an alkyl or an aryl group.

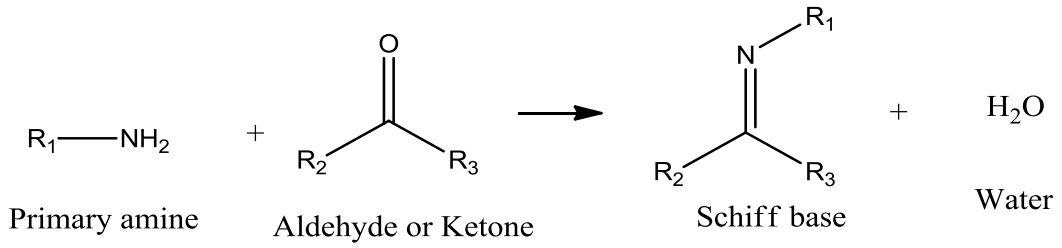

Figure 1.4: Preparation of Schiff Base.

Schiff bases which contain aryl substituents are more stable and more easily synthesized than those that contain alkyl substituents. This means that Schiff bases of aliphatic aldehydes are relatively unstable and they readily undergo polymerisation in comparison to products from conjugation of aromatic aldehydes.[9,10,11,12,13]

Typically, the formation of Schiff bases from aldehydes or ketones requires a protic solvent which is sufficiently dry in order to prevent potential hydrolysis of the newly formed imine bond. The formation is generally undertaken under acid or base catalysis, or upon heating. The completion of imine formation is controlled by the separation of the product or removal of water, or both.

1.1.3.1 Mechanism of Schiff bases formation

The general consensus of the mechanism of Schiff base formation, as shown in Figure 1.5, is nucleophilic addition to the carbonyl group. In the Schiff base formation, the nucleophile is the primary amine. In the first part of the mechanism, the lone pair of electrons in the amine nitrogen attacks the aldehyde or ketone to give an unstable addition compound called a carbinolamine.[14] Then a 1,3-hydrogen shift follows which facilitates losing water by either acid or base catalysis. Since the carbinolamine is an alcohol, it undergoes acid catalysed dehydration.

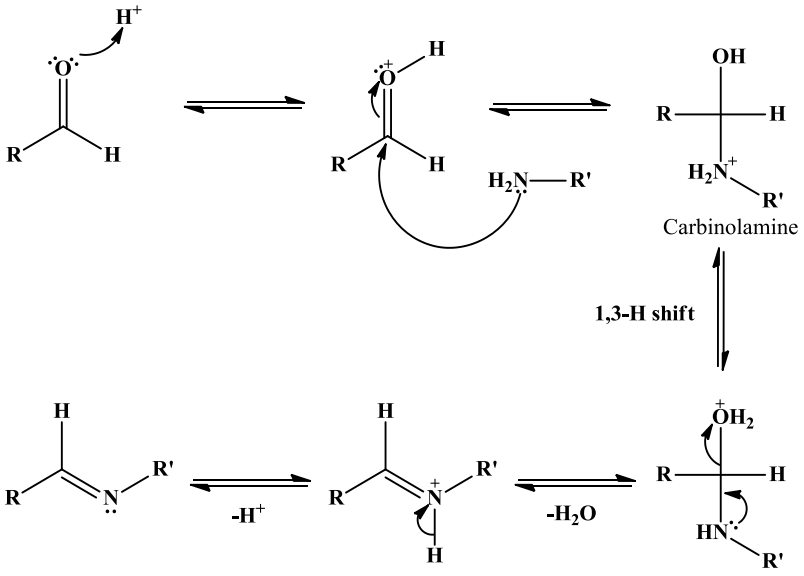

Figure 1.5: Mechanism of Schiff base formation.

The rate-determining step of Schiff base formation is the dehydration of carbinolamine, and that is the reason why the reaction is catalyzed by acids or Lewis acid. But the concentration of acid present for the catalysis cannot be too high as amines are basic compounds. If the amine is deprotonated and becomes non-nucleophilic, equilibrium is pulled to the left and the carbinolamine will go back to aldehyde or ketone and primary amine.

Base catalysis is also used for the dehydration of carbinolamines. The reaction of elimination is analogous to the E_2 elimination of alkyl halides. Schiff base formation can be divided into two steps through an anionic intermediate, i.e. addition followed by elimination.

The geometry of the imine double bond generally adopts a *trans* orientation, which limits the steric interactions of the bulkier R group, with R being either aryl or alkyl substituents.[15]

1.1.3.2 Potential problem in Schiff base formation - Hydrolysis

As mentioned previously during the mechanism of Schiff base formation, it is known that the formation of the imine can lead to a potential problem in which the imine double bond could be hydrolysed back to the starting materials. The successful completion is to separate the Schiff base compound or remove side product, H_2O, or both. Although most Schiff base formation reactions are generally undertaken smoothly in normal co-ordinated dry solvent such as MeOH or EtOH, it still has the potential

problem in which the Schiff bases might be hydrolysed. The following three ways are focused on removing side product, water. (I), Schiff base formation involves drying agents such as anhydrous sodium sulphate or anhydrous magnesium sulphate in DCM or chloroform solvent; (II), in the 1990s an in situ method for water elimination was developed, using dehydrating solvents such as tetramethyl orthosilicate or trimethyl orthoformate;[16] (III), For some reactants require forcing conditions such as heating to reflux in a high boiling solvent and may include the use of a Dean-Stark apparatus or molecular sieves.[17,18,19]

1.1.3.3 Catalytic activities of Schiff base transition metal complexes[4]

Many salen Schiff bases complexes of metal ions show high catalytic activity.

Polymerization reactions

Britovsek and co-workers[20] claimed a new active family of olefin polymerization catalysts. These homogeneous catalysts are based on 2,6-bis(imino)pyridyl Schiff base ligands complexed to iron(II) or cobalt(II) ions (shown in Figure 1.6). With the data they observed that both Fe(II) and Co(II) had high activities, however the activities of the iron are exceptionally higher. When the substituents R_1, R_2, R_3 and R_4 are equal to methyl, the Fe(II) complex achieved the highest result in ethylene polymerisation.[20] It was notable that the activities had a dramatic decrease when the *ortho*-substituent R_3 was changed to hydrogen. The reason for this could be explained by steric protection of the active site in controlling activities and molecular weight.

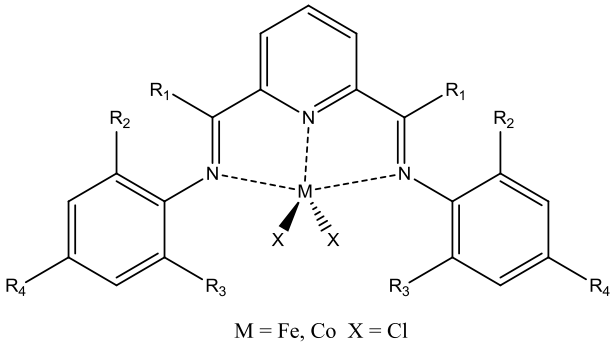

Figure 1.6: The structure of homogeneous catalysts based on Schiff base complexes.

In order to optimise this homogeneous catalyst, heterogenization is required by avoiding fouling the reactor, overheating of the particle and melting of the polymer. Most often, inorganic support materials such as silica[21] has been used to heterogenize soluble polymerization catalysts.[22] Kim and co-workers[23] reported silica-supported Fe(II) and

Co(II) catalysts based on bis(imino)-pyridyl group (shown in Figure 1.7) with silicon ethoxide functionality on the top of the pyridine ring. Both silica-supported (shown in Figure 1.7) and non-supported (shown in Figure 1.6) bis-(imino)pyridyl Co(II) and Fe(II) complexes were carried out as catalysts in polymerizations. A comparison of the catalytic activities between homo- and hetero-geneous catalysts established that the silica-supported heterogeneous iron and cobalt catalysts showed high activities in ethylene polymerization (supported iron catalysts observed activity of 4.87×10^7 (g of PE/(mol of Fe-cat. h bar)) at 50 ℃, while the cobalt supported catalysts showed 1.60×10^7 (g of PE/(mol of Co-cat. h bar)) at same temperature). Though due to the reduced activated site or limited diffusion of monomer into the interior pores of the supported catalysts, both homogeneous catalysts observed 100-folder higher activity than the heterogeneous, the resulted molecular weight of the polyethylene produced by silica-supported catalysts were higher than that of polyethylene by analogue homogeneous catalysts (up to 2.02×10^5).

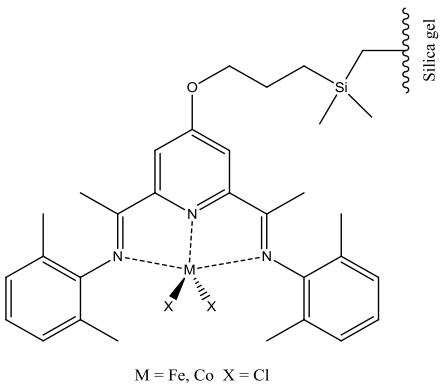

Figure 1.7: Silica-supported 2,6-bis(imino)pyridyl Fe(III) and Co(II) complexes.[24,20,25]

Oxidation reactions

Schiff base complexes with various *d*-block metals such as cobalt,[26] copper[27] and manganese[28] are widely used as catalysts in oxidation reactions. These complexes are effective and selective catalysts in a variety of organic reactions, as well as they are easily prepared, cheap, stable.[3] The Schiff bases are based usually on salicylaldehyde or salen-type ligands. The high electron-donating ability of the Schiff base ligands are able to promote the electron transfer rate. So, these ligands are supposed to increase the overall catalytic activity of an imine-functionalized composite.[29,30]

The oxidation of alcohols to aldehydes and ketones has been widely used in organic synthesis. Adam and co-workers[31] reported a convenient catalytic (shown in Figure 1.8)

oxidation (PhIO/cat, CH_2Cl_2, ca. 20 ℃) of primary and secondary alcohols with allylically and benzylically activated CH bonds. With the analytic data they obtained, they were able to establish that the corresponding carbonyl compounds had been achieved in good yield (up to > 95 %), and the chemo-selectivity of oxidizing alcohols to enones was higher than epoxidation of the double bond (up to 95:5).

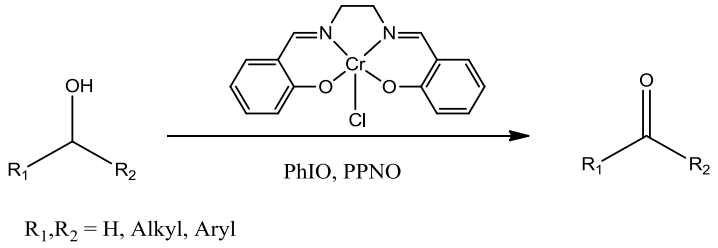

Figure 1.8: Catalytic activity of Cr(III) salen-Schiff base complex in oxidation reaction.

Although these transition metal complexes catalysts afford interesting results in organic synthesis, these catalysts are still related to some problems of corrosion, contamination of reaction products and difficulties in separation.[32,33] In order to overcome these drawbacks, the development of the heterogenization of homogeneous catalysts have been attracted much attention. These catalysts have advantages, such as, ease of separation from reaction mixture, reduction in problems of waste disposal, and they are recyclable.[34,35,36] Polymer-supported catalysts are one of the most useful heterogeneous catalysts in organic oxidation synthesis.[3] The polymer-supported catalytic system relates to an energetic polymer support and an active species immobilized either by forming chemical bonds or through physical interactions, e.g. hydrogen bonding or donor-acceptor interactions. Silica SBA-15 is one of the most common types of mesoporous silica. It provides hexagonal channels ranging from 5 to 30 nm and a very narrow pore-size distribution. Due to its large internal surface area (>800 m^2 g^{-1}), it allows for the dispersion of a large number of catalytically active centers.[37,38]

Recently, Massah and co-workers[39] developed a novel Schiff base Mn(II) complex with salicylaldehyde-poly(vinylamine) supported by SBA-15 as a heterogeneous catalyst. The catalyst was synthesized via a simple method (shown in Figure 1.9) without using any organo silica precursors which are expensive and involved some complicated synthesis and purification. Benzyl alcohol was tested as a model in their work. According to the observed analytical data, they were able to establish that the SBA-15 supported catalyst increased the activity in comparison to the non-supported catalyst (yield %, 90:50) due to site-isolation and cooperative effects between the SBA-15 and

the metal complex. The SBA-15 supported Schiff base complex also plays an important role in observing high reactivity (90 % yield) and selectivity (>99 %) in benzyl alcohol oxidation reaction. In addition, this catalyst was also found to be reusable (at least 5 times) and was also environmental friendly.[39]

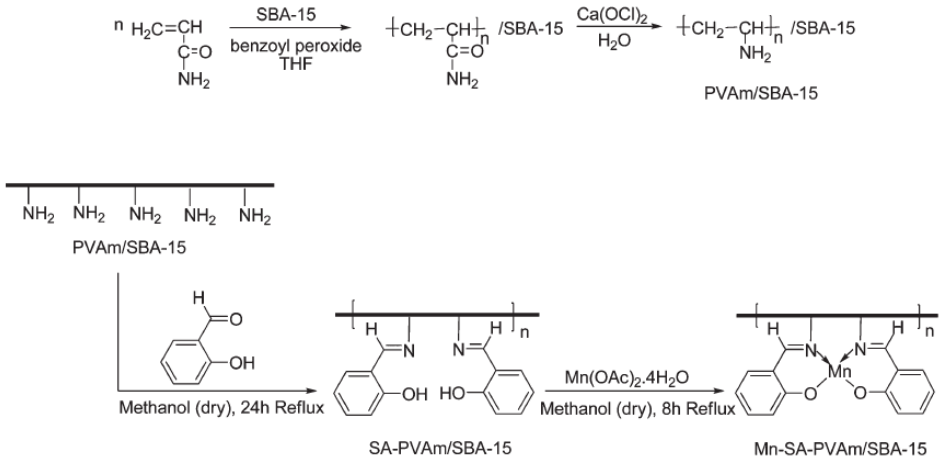

Figure 1.9: Preparation of SBA-15 supported Mn(II) Schiff base catalyst.

Epoxidation reactions

Chromium and manganese Schiff base complexes are widely used as catalysts in epoxidation reactions. The reason for this could be that chromium and manganese have a variety of stable oxidation states, more than the other *d*-block metals. Schiff base complexes with hydroxyl groups have shown high activity in epoxidation of alkenes than un-substituted or aryl substituted ligands. The best known epoxidation reaction with a Schiff base catalyst involves Jacobsen's catalyst[40,41] which is shown in Figure 1.10. This manganese(III) coordination complex stereoselectively converts un-functionalised *cis*-alkenes to epoxides, with the largest enantiomeric excess (e.e) reported at 97 %.[41]

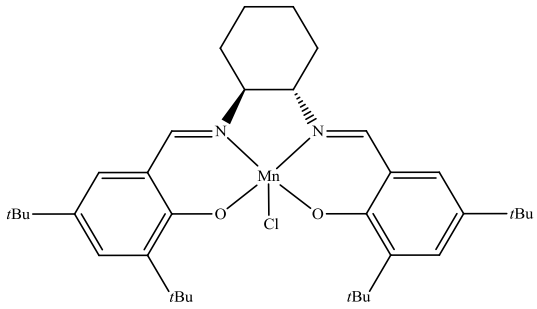

Figure 1.10: Jacobsen's catalyst[40,41] for epoxidation.

The mechanism of the catalytic cycle (shown in Figure 1.11) for the epoxidation of alkenes by Mn(salen) complexes was proposed by Kochi and co-workers.[42] The oxygen transfer in this mechanism involves a two-step catalytic cycle. The reactive intermediate $O=Mn^{V}(salen)^{+}$ oxo complex was suggested when Mn(III)Cl(salen) was reacted with an oxidizing agent in the first step. This Mn(V) complex was regarded as a responsible species for epoxidation. In addition, the μ-oxo-Mn(IV) dimer species were detected as transient species. This manganese complex, in the second step, carries the activated oxygen to the olefinic double bond.

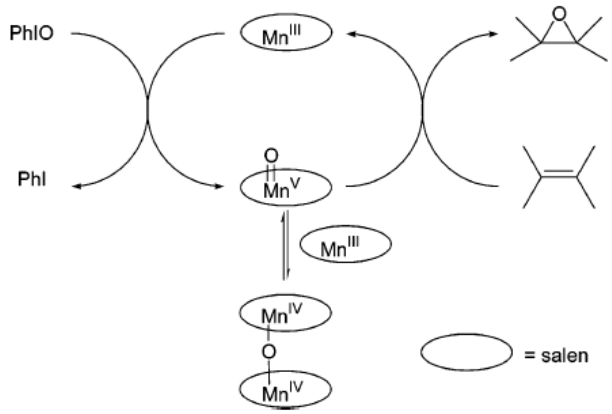

Figure 1.11: Proposed catalytic cycle of the alkenes epoxidation.[42]

At the same time, the Japanese chemists Katsuki and co-workers reported a very closely related asymmetric epoxidation. The chiral catalyst[43] shown in Figure 1.12 is also a salen derivative and the metal ion is again manganese(III). The oxidant is iodosobenzene (PhI=O) but this method works best for *E*-alkenes.

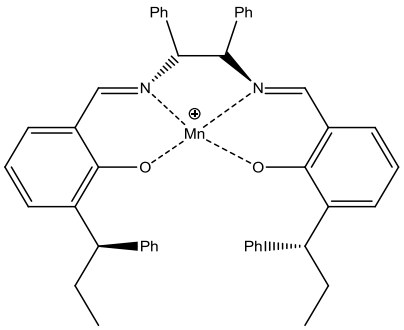

Figure 1.12: Katsuki catalyst for epoxidation.[43]

Numerous substituents at 3,3' and 5,5' positions and diimine backbone based on Jacobsen's catalyst were investigated. In the first investigations of the (salen)Mn(III)-catalyzed epoxidation, Zhang observed that steric bulk (phenyl and *t*-butyl) at the 3,3' position of the salen ligand is essential in order to achieve high enantioselectivity.[40] In

addition, the electronic properties of the substituents at the 5,5' position also have a significant effect on the enantioselectivity of the epoxidation reaction.[41] Electron-withdrawing substituents at 5,5' position were found to have more reactivity in (salen)Mn(V) oxo intermediate, which leads olefin to a comparatively early transition state and affords lower levels of enantioselectivity.[44] Different substituents[45,46,47] were also investigated on a two carbon chain, such as phenyl, alkyl and so on. With the analytical data they observed, they were able to establish that the donor ligands were again shown to be capable of altering enantioselectivities and yields.[46,47]

Diels-Alder reactions

The Diels-Alder reaction is a standard method for six-membered ring formation (shown in Figure 1.13). Many natural products can be prepared by taking advantage of an asymmetric Diels-Alder reaction[48] at an early stage of the synthetic scheme.

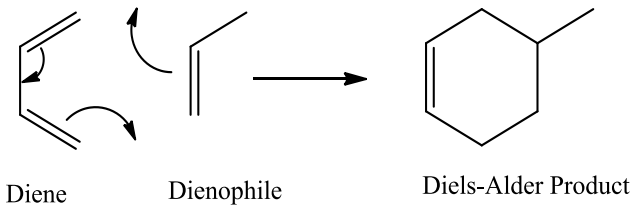

Figure 1.13: Typical Diels-Alder reaction.

The reason why the Diels-Alder reaction goes so well under simply heating is that the transition state has six delocalized π electrons (shown in Figure 1.14) and thus is aromatic in character, having similar stabilization to benzene.

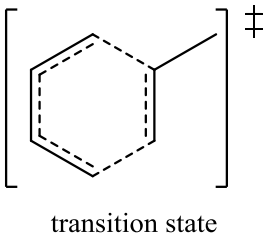

Figure 1.14: Transition state in Diels-Alder reaction.

Salen-type Schiff bases complexes also play an important role in Diels-Alder reactions[4] as catalysts. Magesh and co-workers reported a *exo*-diastereomer (shown in Figure 1.15) of pyranoquinolines which were regarded as potential antibacterial agents.

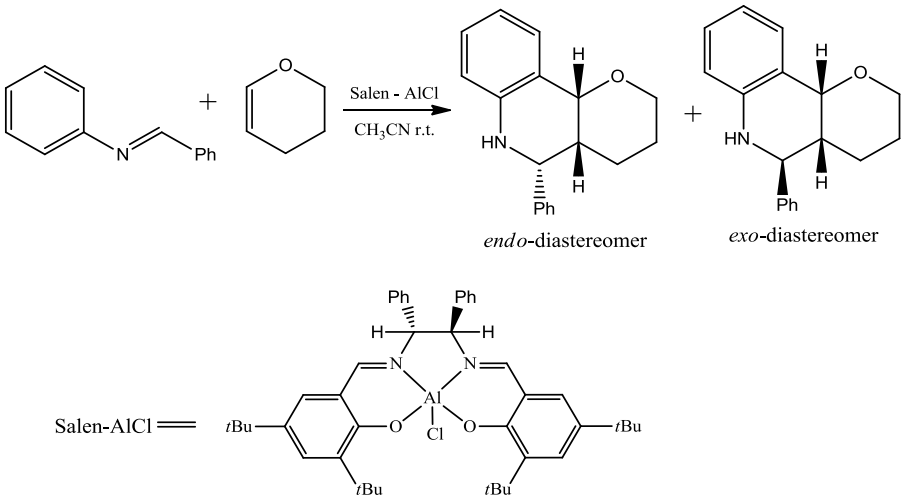

Figure 1.15: Catalytic activity of salen-Al(III) complex in Diels-Alder reaction.

With the analytical data they obtained, they identified that only the *exo*-diastereomer exhibited potential bacteriolytic activity against bacteria such as *Vibrio parahaemolyticus* and *Vibro vulnificus* while the inactive *endo*-diasereomer was claimed to bond either to the receptor sites on the bacteria or to some component of the effector mechanism, in order to prevent the target-oriented synthesis. Magesh and co-workers also established that Al(III) salen Schiff bases complexes functioned as catalysts in forming *exo*-diastereomer with 90 % selectivity. Several substituents (in both aromatic ring and salen backbone) of salen-AlCl complexes were also examined as catalysts, all of which achieved more than 90 % diastereoselectivity of exo-diastereomer. In addition, the salen-Al(III) complex (shown in Figure 1.15) was used as a catalyst in the Diels-Alder reaction (Figure 1.15). The *exo*-diastereomer was generated in excellent diastereoselectivity (100 %) though overall yield obtained was only 43 %.[49]

1.1.4 Schiff-base metal complexation

1.1.4.1 Overview

Schiff bases are very efficient as ligands. The presence of the lone pair of electrons on the nitrogen atom of the imine bond means that they can be donated to the appropriated metal ion. Many Schiff base ligands have a second or even third functional group, such as an OH (salicylaldehyde or its derivatives) and the nitrogen atoms from heterocyclic rings, e.g. pyridine or imidazole rings. This electron donation, in conjunction with a functional group, implies that a vast number of transition metal complexes could be prepared. From recent reviews, a large number of Schiff base complexes have been used in catalytic activities,[4] polymer supported in oxidations,[3] biological activities[2] and so on.

The aim of this chapter, is to provide an overview on only Zn(II), Hg(II), Ni(II), Cu(II) and Co(II) coordination chemistry with Schiff base ligands.

1.1.4.2 Zn(II) Schiff-base complexes

Zinc occurs in low amounts in nature. But, large amounts of zinc ores have been found in the Earth's crust.[50] Zinc is a late first row transition metal which has an electronic configuration of [Ar]3d^{10}4s^2 and is a member of group 12 of the periodic table. The chemistry of zinc is controlled by the +2 oxidation state. When Zn is formed in this state, the outer shell *s*-electrons are lost, which yields a bare zinc ion with electronic configuration [Ar]3d^{10}. The full *d*-orbitals implies that Zn(II) complexes are diamagnetic and are mostly colourless. It also suggests that the coordination complexes of Zn(II) ions do not have a ligand field stabilisation effect. The stereo-chemistries of these species are determined by considerations of electrostatic forces, covalent bonding forces and the size of the metal ion.[51]

With respect to organometallic compounds, organozinc compounds were first found by Edward Frankland in 1849. The first organozinc compound, diethylzinc, was the first compound discovered with a sigma bond between a metal atom and carbon atom. Organozinc compounds are consisted of three main types, which are organozinc halides, diorganozincs and lithium/magnesium zincates with alkyl or aryl groups. Examples of applications of organozinc compounds include the Reformatskii[52] reaction, and the Simmons-Smith[53,54] reaction. The Reformatskii reaction involves transferring α-halo-esters and aldehydes to β-hydroxy-esters through an intermediate organozinc halide.[52] The Simmons-Smith reaction involves the carbenoid (i.e. iodomethyl) zinc iodide reacting with alkenes to give cyclopropanes.[53]

Zn(II) Schiff base complexes are well known in coordination chemistry, although not in same large number as reported for copper and nickel derivatives. The Zn(II) ion is dominated by either four-, five- or six-coordinate geometry with the four- and five-coordinate geometries being the most common.[51] Examples of high/low coordination numbers for Zn^{2+} ions are rare, but still can be found. Sun and co-workers[55] reported a pentadentate Schiff base ligand in 2006 (Figure 1.16, a), and established the Zn(II) complex was seven-coordinate with a pentadentate N_3O_2 Schiff base ligand and two remaining coordination sites occupied by donor solvent molecules.

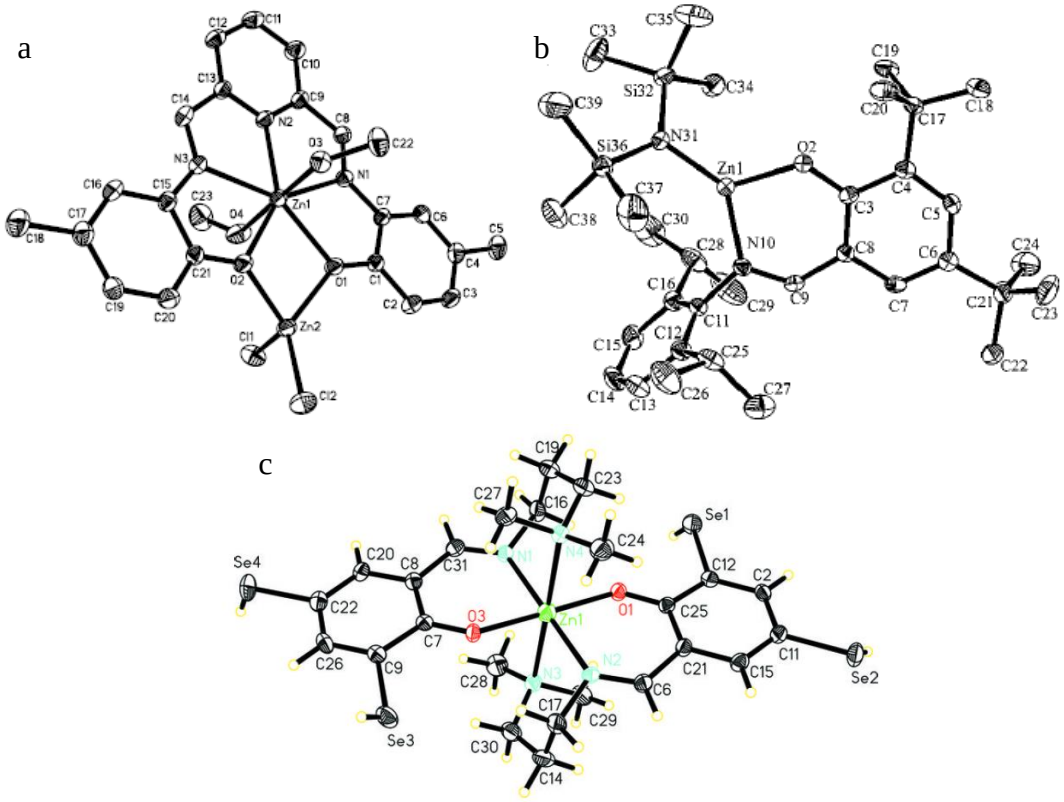

Figure 1.16: Examples of Zn(II) Schiff bases complexes for seven-coordinated (dinuclear) (a),[55] three-coordinated (b)[56] and six-coordinated (c).[57]

Chisholm and co-workers synthesized a three-coordinate monomeric Zn(II) Schiff base complex (Figure 1.16, b) in 2001.[56] Six-coordinated Zn(II) Schiff bases complexes are much more common than either the seven- or three-coordinate, Yang and co-workers reported a six-coordinated Zn(II) complex (Figure 1.16, c) by two N,N'O-tridentate Schiff base ligands, resulting in a slight distorted *trans*-ZnO_2N_4 octahedral coordination for the metal ion.[57]

There are a large number of donor atoms in Zn(II) Schiff base complexes such as hard N-, O- and soft S-donors. Zn(II) compounds include zinc chloride, zinc carbonate, zinc sulphate and zinc nitrate, as well as zinc oxide which is perhaps the most significant according to its commercial significance as a semiconductor.[51]

Although Zn(II) Schiff bases complexes show less catalytic activity (e.g. Zn(II) Schiff base complexes achieved low activity for the decomposition of hydrogen peroxide (H_2O_2)[58]) in transition metal complexes than the other metal ions (Ni, Co, Mn or Cu) complexes, it showed widely ranged bio-applications as reviewed by Anand.[2] The interaction of Zn(II) Schiff base complex with DNA was reported by Kumaran and co-workers.[59] It was investigated with *in silico* methods and suggested that it could

complex with DNA though the minor groove and have high activity on anti-bacterial and antifungal testing.

1.1.4.3 Hg(II) Schiff-base complexes

Mercury has many unusual properties, one of these is that it is the only metal that is a liquid at standard temperature and pressure.[60] Mercury is less reactive in comparison to zinc. It can dissolve many metals to form mercury amalgams.[61] Mercury is a late third row transition metal which has an electronic configuration of $[Ar]4f^{14}5d^{10}6s^2$ and is a member of group 12 of the periodic table. The common oxidation states of mercury ion are the +1 and +2 states. The chemistry of Hg(I) compounds usually result in the formation of simple stable compounds with Hg-Hg metal bonds, which is different from its neighbours, cadmium and zinc. Most Hg(I) compounds are diamagnetic and feature the dimeric cation, Hg_2^{2+}, (except mercury(I) hydride). The most common oxidation state of mercury is +2, which is the main oxidation state found in nature as well. However higher oxidation states are detected with evidence for the biological oxidation of mercury(II) to mercury(III),[60] while the mercury(IV) compound, HgF_4 was published in 2007.[62] In this thesis, only the Hg(II) oxidation state will be discussed with counter ions of chloride and perchlorate.

A wide range of coordination geometries is obtained for Hg(II) complexes with coordination numbers from 2 to 6 with geometry variations including linear, trigonal planar, tetrahedral, trigonal bipyramidal, square-based pyramidal and octahedral geometries.[50] The full *d*-orbitals of Hg(II) ion which is similar to Zn(II), indicates that Hg(II) ion are diamagnetic. It also suggests that the coordination complexes of Hg(II) ions do not have ligand field stabilisation effect.

The coordination number of Hg(II) Schiff base complexes are generally from 2 to 4. Khalaji and co-workers[63,64,65] recently reported a tetrahedral geometry Hg(II) Schiff base complexes based on the substituents benzaldehyde with ethylenediamine (shown in Figure 1.17) with corresponding analysis.

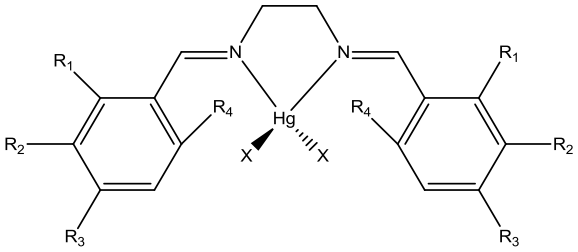

Figure 1.17: R_1=R_2=R_3=OMe; R_4=H; X=I;[63] R_1=R_4=H; R_2=R_3=OMe; X=I;[64] R_1=R_4=Cl; R_2=R_3=H; X=Br.[65]

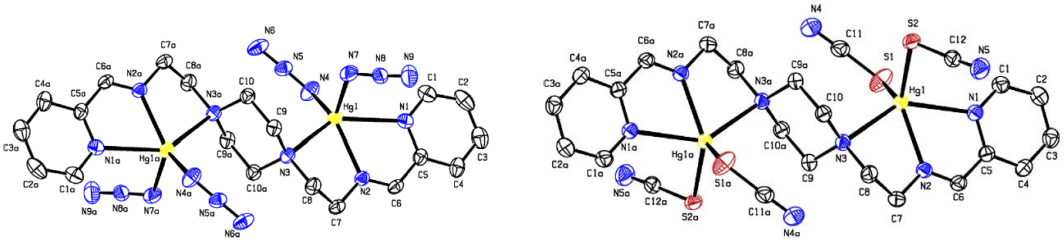

Figure 1.18: Bis(tridentate) Schiff base Hg(II) complexes with azide HgN_5(left) and thiocyanate HgN_3S_2(right)

Chattopadhyay and co-workers[66] reported two bis(tridentate) Schiff base bridged dinuclear Hg(II) pseudohalides complexes which used azide and thiocyanate to replace the acetate ions. The geometry of both complexes adopted a distorted square pyramidal geometry (shown in Figure 1.18, HgN_5 left and HgN_3S_2 right).

Different counter ions influenced the structures of Hg(II) Schiff base complexes based on (*E*)-*N*-(pyridine-2-ylmethylidene) as reported by Basu Baul and co-workers.[67] With the data observed based on that ligand, they suggested iodide preferred the monomeric complexes, chloride and bromide yield binuclear complexes, while the nitrate and azide lead to polymers. From their obtained crystal structures, octahedral geometry of Hg(II) Schiff base complex as polymer was found with nitrate counter ions (shown in Figure 1.19 right) compared to square pyramidal geometry of the same complex with azide ions (shown in Figure 1.19, left).

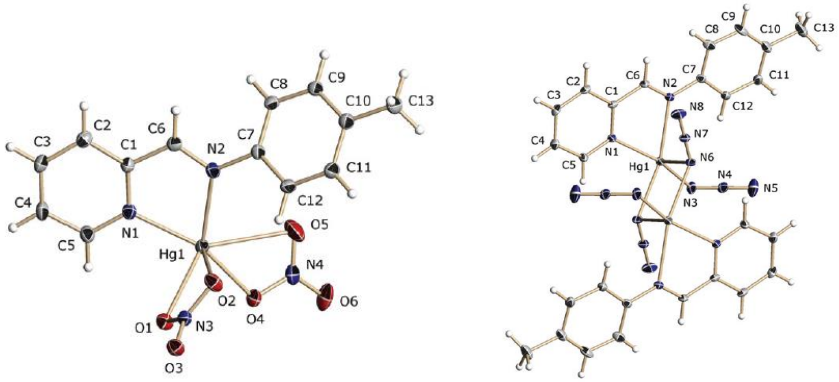

Figure 1.19: The crystal structures of octahedral geometry of Hg(II) complex (left) and square pyramidal geometry of Hg(II) complex (right).

The application of Hg(II) Schiff base complexes have not been reported much yet, probably due to its high toxicity. However, the heavy atoms such as palladium(II) or mercury(II) tridentate Schiff base complexes also have a good catalytic activity in Heck and Suzuki coupling reactions.[68] In addition, mercury has a special affinity for N and S atoms rather than O atom, which appears a potential ligator atoms in biochemistry.[69]

1.1.4.4 Ni(II) Schiff-base complexes

Nickel is a late first row transition metal which is a member of group 10 of the periodic table. It has two electronic configurations of [Ar]3$d^8$4s^2 or [Ar]3$d^9$4s^1 which are very close in energy. The most common oxidation state of nickel is +2 oxidation state, but the oxidation state of 0, +1, and +3 states are also known, even +4 state has been indicated.[70] Both Ni(III) and Ni(IV) are known as powerful oxidants. Ni(IV) is present in only a few species, and its formation requires extremely strong oxidants,[61] e.g. $K_2[NiF_6]$ which is used as an oxidizing agent in some solid propellants, is synthesised from $NiCl_2$, F_2 and KCl. Ni(III) is a very good oxidizing agent as well, but it is stabilized by σ-donor ligands such as thiols and phosphines.[71] The black hydrous oxide Ni(O)OH is achieved by alkaline hypochlorite oxidation of aqueous Ni(II) salts and is widely used in NiCd rechargeable batteries.[72] However, in this thesis, only the Ni(II) oxidation state will be discussed.

The common anions of Ni(II) compounds include sulfide, sulfate, carbonate, hydroxide, carboxylates and halides. A wide range of coordination geometries is obtained for Ni(II) complexes with coordination numbers of 4 to 6 being common. The octahedral and square planar geometries are most usual, but tetrahedral, trigonal bipyramidal and square-based pyramidal geometries are not unusual.[61]

Magnetic moments of Ni(II) complexes are used as proof of their corresponding geometries. Both octahedral and tetrahedral are paramagnetic complexes, in contrast to the square planar geometry which is diamagnetic.[61] The octahedral Ni(II) complexes with d^8 configuration result in paramagnetic complexes which are usually close to the spin-only value of 2.83 B.M. This can be explained by the splitting of the *d*-orbitals in crystal field theory[73] (shown in Figure 1.20). In contrast, tetrahedral complexes possess magnetic moments of about 4 B.M. due to orbital contributions in comparison to octahedral complexes. One of the *d*-orbitals ($d_x^2 - d_y^2$) is in high energy, with the eight *d*-electrons occupying the four remaining d-orbitals. The tetrahedral geometry is enforced by the use of bulky substituents on the ligands which sterically hinder the formation of the square planar derivative. These differences in magnetic moments are invaluable in providing information about the coordination geometry in a Ni(II) complex.[61]

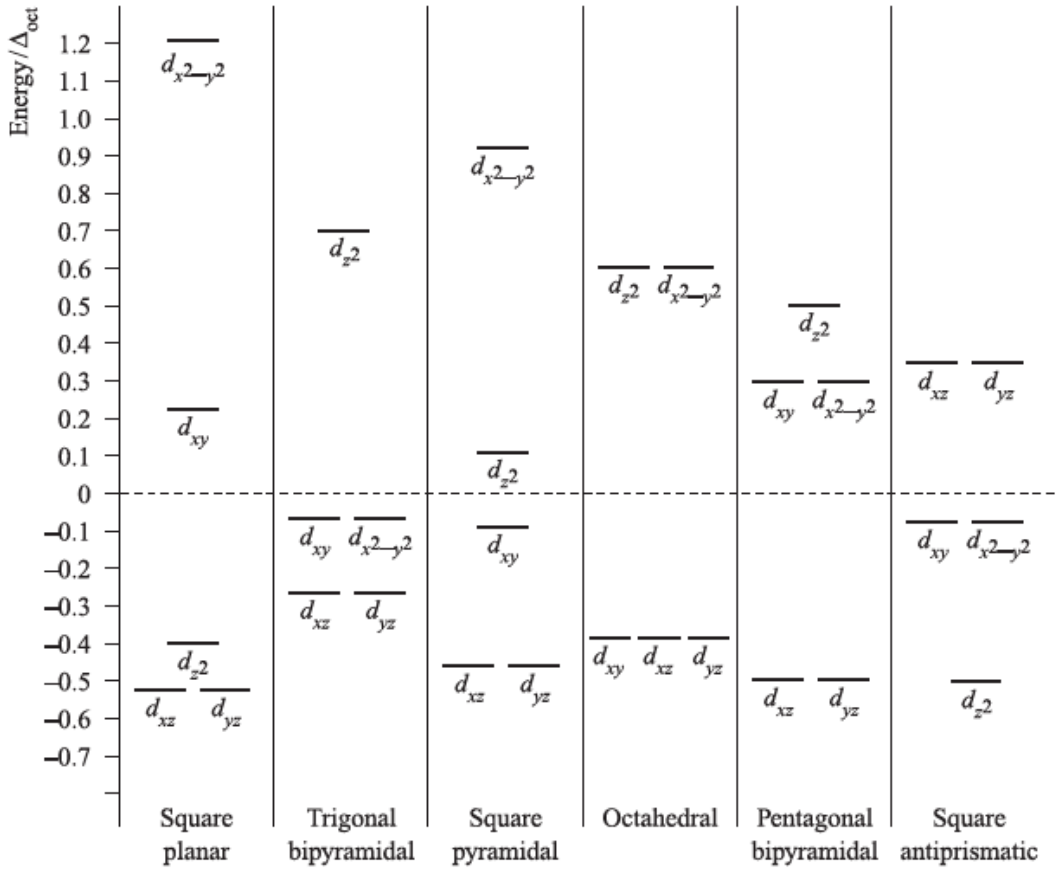

Figure 1.20: Energy levels of the *d*-orbitals in common stereo-chemistries.[73]

The use of Schiff base ligands based on salicylaldehyde in the preparation of nickel(II) complexes generally results in the formation of square planar geometries of Ni(II)

complexes.[74] However, there are some exceptions in which Ni(II) complexes have five coordinated or octahedral geometries. Recently, Franks *et. al.*[75] introduced five-coordinate Ni(II)-diphenolate Schiff base complex, which exhibited two reversible oxidation processes. In addition, the five-coordinate complexes possessed an unsaturated coordination sphere which might afford further promises toward the development of novel catalytic systems. However, Ni(II) complexes employing octahedral geometries are more common than the five-coordinate complexes. The six-coordination sphere which is normally completed by coordinating solvents such as water[76] or methanol[77] solvents are obtained. Different coordinated anions such as thiocyanates are also prepared in the complexes reported by Mukherjee.[78]

The salen-type Ni(II) complexes are also found as having potential catalytic activities.[4] High-density and linear polyethylenes were produced by ethylene polymerization with Ni(II) complexes, as was suggested by Gibson.[79] Ni(II) salen complexes also claimed catalytic activity in asymmetric benzylation reaction of an alanine enolate (Figure 1.21). The reason for salen ligands derived from acyclic chiral 1,2-diamines achieved low catalytic activities, is that the presence of diamine substituents could adopt anti-conformations to each other.[78]

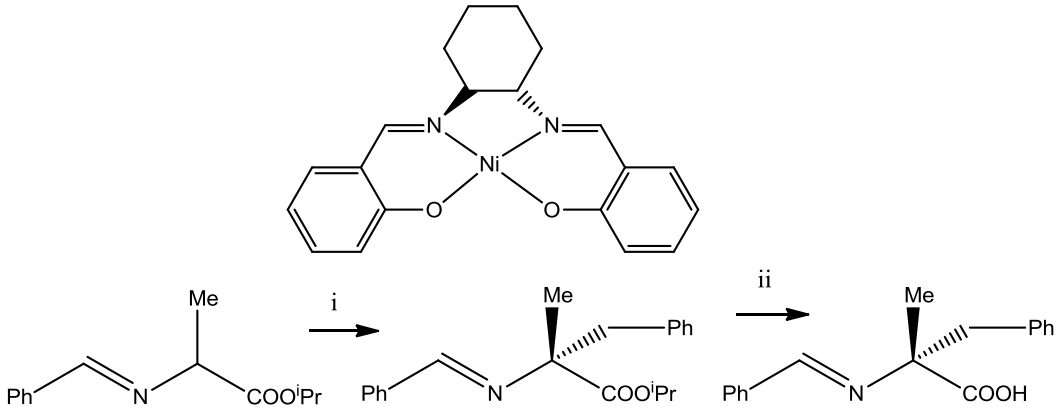

condition: (i) cat. (2-10 %) NaOH, (solid)/BnBr; (ii) H_3O^+/heat

Figure 1.21: The formation of α-methyl phenylalanine by Ni(II) salen Schiff base complex catalyzed.[78]

1.1.4.5 Cu(II) Schiff-base complexes

Copper is a late first row transition metal which is a member of group 11 of the periodic table. It has an electronic configurations of [Ar]$3d^{10}4s^1$. Copper forms a wide variety of compounds with different oxidation states usually +1 and +2, which are often called

cuprous and cupric, respectively. Cu(I) is the only first row *d*-block metal to adopt a stable +1 oxidation state. The Cu(I) ion has a d^{10} electronic configuration which means the complexes of Cu(I) ions are diamagnetic and colourless (except if the counter-ion is coloured or charge transfer absorptions occur in the visible region, e.g. Cu_2O). Cu(III) and Cu(IV) are also observed but are relatively rare.[51] In this chapter, only the coordination chemistry of Cu(II) ion will be focussed on.

Cupric is the old name for the copper(II) ion. The Cu(II) ion has a d^9 configuration which means it is paramagnetic due to its single unpaired electron. This d^9 configuration indicates that the Cu(II) ion in coordination chemistry is subject to Jahn-Teller distortions when present in an octahedral or tetrahedral environment. This effect implies that it 'requires molecules to adopt geometries that do not lead to a degeneracy in valence level orbitals'.[51] For example, Cu(II) ion when six coordinated is generally observed in a distorted octahedral geometry, which consists four short copper-ligand bonds and two long trans bonds.

The coordination number of Cu(II) Schiff base complexes is dominated by 4, 5 and 6. Octahedral Schiff base complexes of Cu(II) ion are the most common in which most axial groups are coordinating solvents or counter ions. This axial phenomenon is almost similar to five-coordinate complexes with the exception of Cu(II)-diphenolate complex. Franks *et al.*[75] recently reported Cu(II) complexes containing pentadentate N_3O_2 Schiff base ligand with Cu(II) ion having a trigonal bipyriamidal geometry. Anuradha and co-workers[80] confirmed a new macrocyclic binuclear Cu(II) complex which adopted four-coordinate square planar geometry.

The Cu(II) Schiff base complexes based on salicylaldehyde are well known and have a vast number applications in the literature. This type of Cu(II) complexes are widely used as catalysts[4] and for their biological relevance[81] such as antimicrobial activities.[82]

Ourari and co-workers[83] had reported a novel Cu(II) Schiff base complex with pyrrole rings in 2013. The new Cu(II) complex they reported has square planar geometry (shown is the Figure 1.22) and the structure was elucidated by X-ray diffraction, and the catalytic properties for alcohol oxidation and CO_2 reduction were also tested by them. This Cu(II) complex seems to be more efficient in the electro-oxidation of isopropylic alcohol than other kinds of alcohol, e.g. methanol, ethanol and benzyl alcohol.

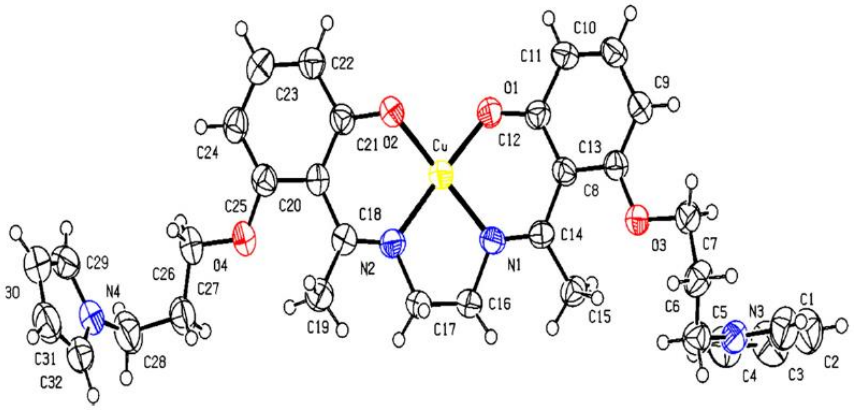

Figure 1.22: Novel Cu(II) complex used as catalyst in alcohols oxidation and CO_2 reduction.

Mishra and co-workers[84] recently reported two microwave synthesized Schiff base ligands (shown in Figure 1.23, named **MKN** and **HAN**). Both ligands and Cu(II) complexes were tested on selected bacteria *E. coli* and *S. aureus* and fungi *A. niger* and *C. albicans*. The data they obtained showed good biological activity as anti-microbials, and complexes are more active than their corresponding ligands. The reason for this is explained: the polarity of the metal ion will be decreased by chelation, and increase the delocalization of π-electrons and enhance the penetration of the complexes into lipid membranes, so that the metal binding sites would block the enzymes of the microorganisms from working efficiently.[84]

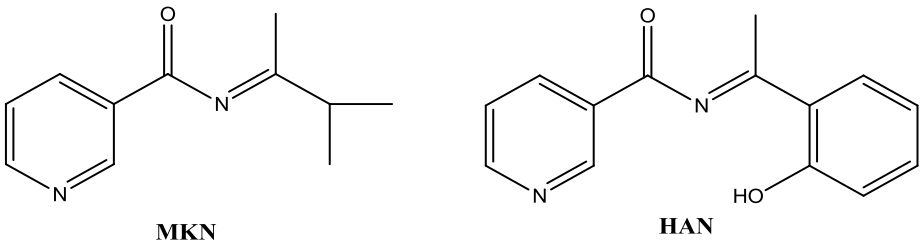

Figure 1.23: The structure of MKN and HAN Schiff base ligands.[84]

1.1.4.6 Co(II) Schiff-base complexes

Cobalt is a late first row transition metal which is a member of group 9 of the periodic table. It has an electronic configurations of $[Ar]4s^2 3d^7$. Like nickel, cobalt in the Earth's crust is found only in combined form. While the range of oxidation states of cobalt from -1 to + 5 are known, the states of +2 (cobaltous) and +3 (cobaltic) are more common than the others. The Co(IV) and Co(V) are rare but have also been stabilized by the presence of fluorine or oxygen atoms, e.g. Cs_2CoF_6 and K_3CoO_4[61,85] This thesis will

mainly focus on the coordination chemistry of Co(II) ion with counter ions of chloride and perchlorate. However, a mixed valued Co(II)-Co(III) complex has also been reported in this thesis.

The Co(II) ion has an electronic configuration d^7, and is paramagnetic due to its single unpaired electrons. The coordination numbers of Co(II) ion is various from 2 to 8, with the vast number of coordination geometries ranging from linear to dodecahedral geometries.[61] But generally, the coordination numbers of Co(II) complexes are six- or four-coordinate. Most Co(II) complexes are high-spin with magnetic moments being higher than spin-only value. Typically, the magnetic moments of high-spin Co(II) octahedral geometry complexes are in the range of 4.3-5.2 B.M., while 4.2-4.8 B.M. for tetrahedral species.[86] It was found that more tetrahedral Co(II) complexes than any other transition metal ion exist. The reason for this could be the difference in energy of the crystal field stabilization between the octahedral and tetrahedral geometries is small for a high-spin d^7 electron configuration.[87]

The use of Schiff base ligands based on salicylaldehyde derivatives or salen-type in the preparation of cobalt(II) complexes generally results in four-, five- or six-coordinated. Chen and co-workers[88] had reported a large number of salen-type Schiff base (shown in Figure 1.24, left) Co(II) complexes which were tested as oxygen carriers. Most of these type of Co(II) complexes have square planar geometries due to the rigid multidentate salen Schiff base ligands.[87] Interestingly, Boca and co-workers[89] suggested a trigonal bipyramid geometry of Co(II) complex based on H_2(t-Bu)(Me) salmdptn (shown in Figure 1.24, right) Schiff base complex which established potential reversible binding to dioxygen. Rajnak and co-workers[90] reported a self-assembled octahedral geometry of Co(II) Schiff base complex.

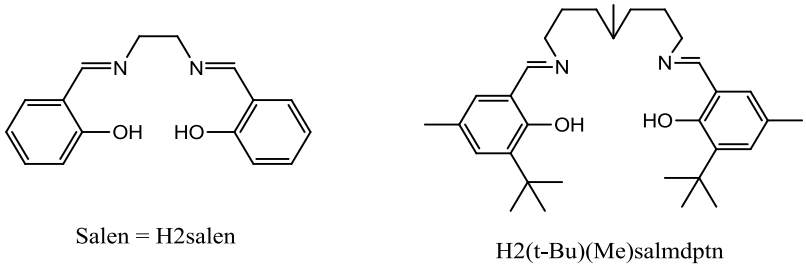

Figure 1.24: Schiff base ligands, salen(left), salmdptn(right).

Table 1.1: Permeances and selectivity factors of O_2 and N_2 through the SiO_2–PVP–salcomine and SiO_2–PVP hybrid membranes at 298, 373 and 423 K.[91]

Membrane	T/K	10^{-10} Permeance/ mol m^{-2} s^{-1} Pa^{-1}		Selectivity factor P_{O_2}/P_{N_2}[a]
		O_2	N_2	
SiO_2–PVP–salcomine	298	1.2	0.84	1.4
	373	4.0	0.87	4.6
	423	5.0	0.84	6.1
SiO_2–PVP	298	1.5	1.5	1.0
	373	1.2	1.1	1.0
	423	0.77	0.77	0.99

[a] Theoretical selectivity factor based on Knudsen flow is 0.94.

Cobalt(II) salen-Schiff base complexes have found use in 'Oxygen Carrier Complexes', which were first described by Pfeiffer *et al.*[91] in 1933. Since then, a large number of Co(II) complexes have been found to reversibly bind dioxygen, and salen or other Schiff base ligands have been extensively studied in there.

A novel Co(II)–salcomine Schiff base complex was reported by Kuraoka et. al. and with the data observed (shown in Table 1.1), they reported that in membranes of SiO_2-PVP-salcomine of Co(II) complexes at 298 and 423K, the selectivity factor is raised from 1.4 to 6.1.

The Schiff bases complexes of Co(II) ion also found good catalytic activities,[4] such as epoxidation,[92] catalyzed on oxidative carbonylation of amines.[93] The Co(II) complexes play an important role in biochemistry as well.[2]

1.2 Macro-cyclic and acyclic Schiff base ligands

1.2.1 Overview

Macro-cyclic and acyclic compounds have received much attention in the last twenty years. These compounds play an important role in the understanding of molecular processes in biochemistry, material science, catalysis, activation, transport and separation phenomena and so on.[94,1] Many of these cyclic and acyclic ligands have been created to mimic the function of natural compounds in order to recognize and transport the specific metal ions, anions or neutral molecules, and also to realize and reproduce the catalytic activity in metallo-enzymes and proteins.[95,96,97] In these studies, Schiff bases compounds have been extensively employed as they are easily prepared (see

section of Synthesis of Schiff-base ligands), obtained in high yield and formed usually without any side products. A vast amount of macro-cyclic and acyclic Schiff base ligands have been synthesized in order to find out the important role of different donor atoms, such as their relative position, the number and size of the chelating rings formed, and the flexibility of the coordinating moiety on the selective species.[98] The hole size of different macro-cyclic ligands represents an additional parameter for the selectivity of different charged or neutral species which can be recognized. However, the interesting properties of acyclic Schiff base ligands may increase as they have more flexibility than macro-cyclic compounds.[94]

1.2.2 Macro-cyclic Schiff base ligands

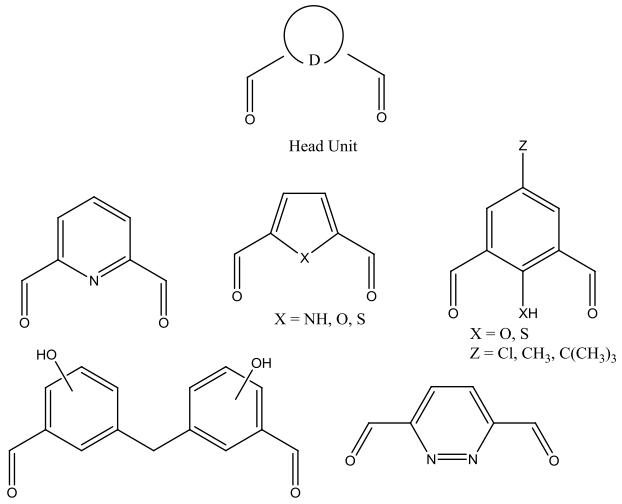

Figure 1.25: Different di-formyl precursors of head units.

Macro-cyclic Schiff base ligands have been prepared by condensation of different di-carbonyl precursors based on head units and analogous (shown in Figure 1.25) with different lateral di-amines. The macro-cyclic compounds are usually formed at [1+1] and [2+2] depending on the number of head and lateral units present. In the conditions of certain precursors, such as 2,6-diacetylpyridine and 1,3-diamino-2-hydroxypropane, the [3+3] and [4+4] macro-cyclic ligands have also been investigated.[99,100] The [3+2] bicyclic[101] condensation ligands have also been prepared by reaction of tri-amines with di-carbonyl precursors to achieve hexa-imine macro-bicyclic compounds (shown in Figure 1.26).

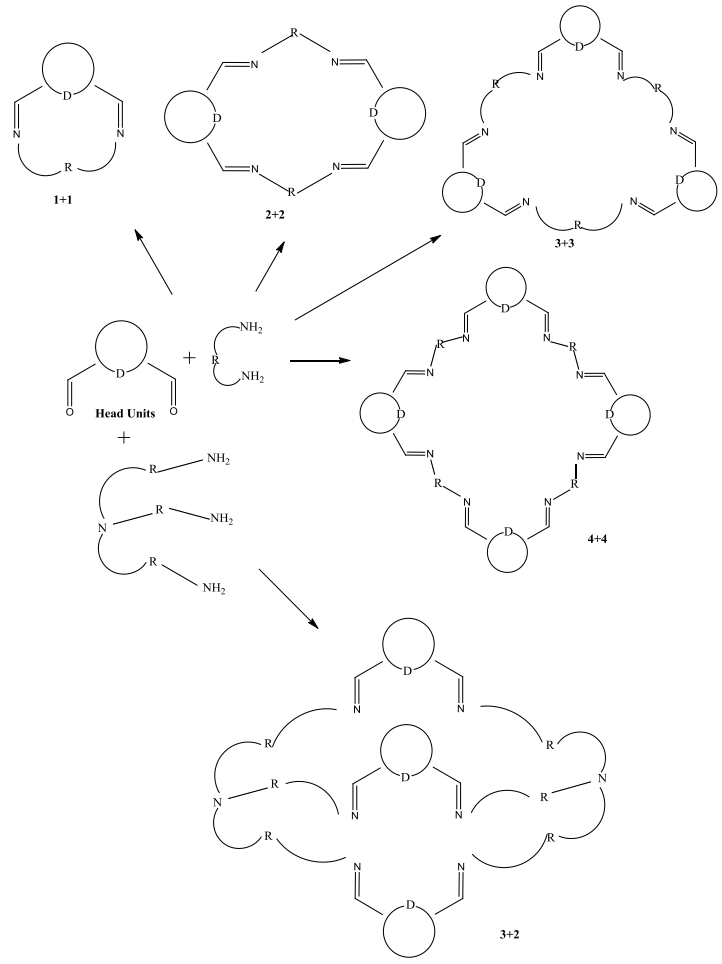

Figure 1.26: Different types of formation of macro-cyclic Schiff base ligands.

1.2.2.1 Macro-cyclic Schiff bases complexes

The word 'template' is reported by Curtis *et al.*[102] in early 1960s who explored the use of metal template procedures for obtaining a wide range of macro-cyclic systems, and it has been widely used since that time to now. The use of template also has been utilised in the synthesis of macro-cyclic Schiff bases complexations by the cyclocondensation of dicarbonyl compounds and lateral diamines, because they are simple 'one-pot reaction', cheap and performed in high yield. New template synthesis of [1+1] macro-cyclic Schiff base copper(II) and nickel(II) complexes based on cyclocondensation of 2,6-diformyl-4-metyl-phenol and two different lateral di-amines chain (e.g. diethylenetriamine and 1,2-bis(3-aminopropylamino)ethane, respectively), have been reported by Gurumoorthy and co-workers.[103] According to the analytical data they observed, they were able to establish that the attempt to synthesize the [1+1] macro-cyclic ligands using diformyl compounds and diamines under different conditions without metal template did not achieve the expected results, where [2+2] macro-cycles were formed in all case. However, the use of metal(II) perchlorate as metal templates

for the macro-cyclic reactions resulted in the [1+1] macro-cycles formation (shown in Figure 1.27).

Moreover, the antimicrobial activity of macro-cyclic complexes of **L1** and **L2** with Cu(II) and Ni(II) salts, respectively, were examined *in vitro* with a comparison against two standard drugs, Ciprofloxacin and Clotrimazole (shown in Table 1.2).

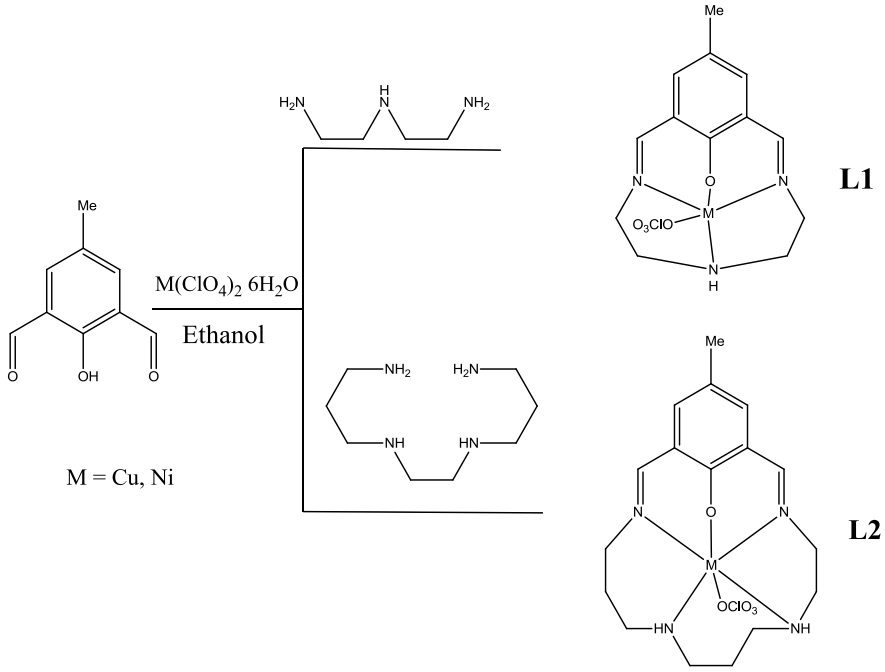

Figure 1.27: Metal template cyclocondensation in the presence of M(II) perchlorate salts.

Table 1.2: The activities of antibacterial and antifungal of four synthesized macro-cyclic complexes (*E.c – Escherichia coli*; *S.a – Staphylococcus aureus*; *K.p – Klebsiella pneumoniae*; *A.o – Aspergillus ochraceus*; *P.v – Paecilomyces variotii*; *B.c – Botrytis cinerea*.[103]

Compounds	Representation zone of inhibition (mm)					
	Antibacterial			Antifungal		
	E.c	*S.a*	*K.p*	*A.o*	*P.v*	*B.c*
Ciprofloxacin	24.0	25.0	25.0	-	-	-
Clotrimazole	-	-	-	26	29	25
CuL^1	13.0	11.1	12.3	11.7	14.5	12.8
CuL^2	15.5	15.2	12.9	14.6	18.2	16.6
NiL^1	15.9	19.3	15.6	14.8	18.0	17.8
NiL^2	18.2	19.6	18.3	16.8	18.5	18.2

They were also able to shown that all the synthesized macrocyclic metal complexes showed good antimicrobial activities against the tested microorganisms. And Ni(II) complexes have better activities in antibacterial and antifungal testing in comparison to Cu(II) complexes. The reason for the higher anti-microbial activity of the complexes could be explained by the coordination and chelation. These make the metal complexes become more powerful and potent bacteriostatic agents, which will inhibit the growth of the microorganisms.[104,105]

1.2.3 Acyclic Schiff base ligands

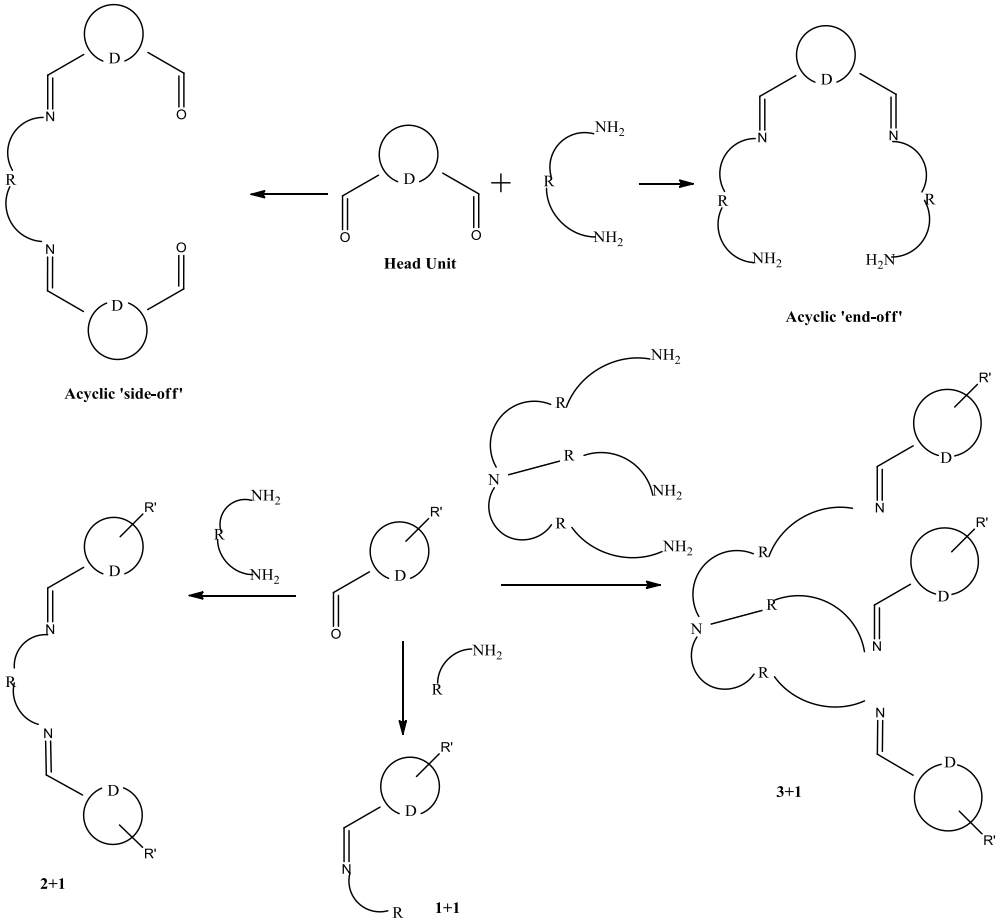

Figure 1.30: Different formations of acyclic Schiff base ligands.

The acyclic Schiff bases compounds have received much more attention with a comparison to macro-cyclic compounds due to their similar properties to macro-cycles but exhibiting a smaller molecular weight and higher flexibility. The preparation of acyclic Schiff base compounds are synthesized by the self-condensation of formyl- or keto-compounds and primary amines-precursors. While the synthetic procedure is quite successful, the acyclic ligands are generally obtained in pure and suitable forms. The acyclic Schiff base ligands are usually formed in several types (shown in Figure 1.28),

[1+1], [2+1] and [1+3] are the acyclic in the condensation of a substituted formyl derivatives with the appropriate amines while the acyclic Schiff bases compounds in [2+1] and [1+2] formation which were called acyclic 'side-off' and acyclic 'end-off', respectively, are the di-formyl derivatives (see Head Units in Figure 1.25) with related amines precursors.

However, in this thesis, it will mainly focus on symmetric [1+2] acyclic 'end-off' Schiff base ligands and their corresponding complexes.

1.2.3.1 [1+2] symmetric end-off systems

The [1+2] symmetric end-off Schiff base ligands are derived from the condensation of the diformyl precrusors (see Head Units in Figure 1.25) with the primary mono-amine derivatives. The reaction of these Schiff bases, consisting of two identical adjacent coordination chambers. The corresponding homodinuclear complexes are prepared with such ligands and in the presence of base as deprotonating agent and *d*-metal ions in a molar ratio of 1:2 (ligand to metal ratio). However, the mononuclear complexation could be also achieved by occupying a 1:1 (ligand to metal) molar ratio. The both di- and mono-nuclear complexation could be also prepared in the presence of a template. Similarly, the different polyamine derivatives also could be used for the synthesis of [1+2] acyclic Schiff base ligands in the presence of a template in order to prevent the polymerize action. These polyamine derivatives ligands in the preparation of the appropriate metal salts and base, generally result in homonuclear complexes as well. The resulting dinuclear or mononuclear complexes normally contain endogenous donor atoms, such as pyridazine N, N; pyridine, N; phenolate -O- or a thiophenolate sulfur -S-.

1.2.3.2 Symmetric acyclic end-off systems containing one phenolate endogenous bridging group

A dinucleating compartmental ligand of 'end-off' type, 2,6-bis[N-(2-pyridylethyl)iminomethyl]-4-methylphenol (shown in Figure 1.29), was reported by Matsufuji and co-workers.[106]

The ligand HL was used for the preparation of two dinucleating complexes in the presence of Zn(II) and Ni(II) perchlorate salts, respectively. Moreover, the two crystal structures of both $[Zn_2(L)(OH)(py)_3](ClO_4)_2]$ and $[Ni_2(L)(OH)(py)_4](ClO_4)_2]$ were also observed (shown in Figure 1.30).

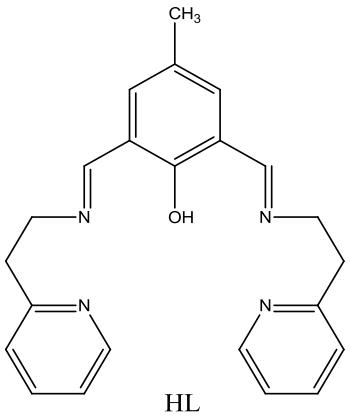

HL

Figure 1.29: Structure of 2,6-bis[*N*-(2-pyridylethyl)iminomethyl]-4-methylphenol.

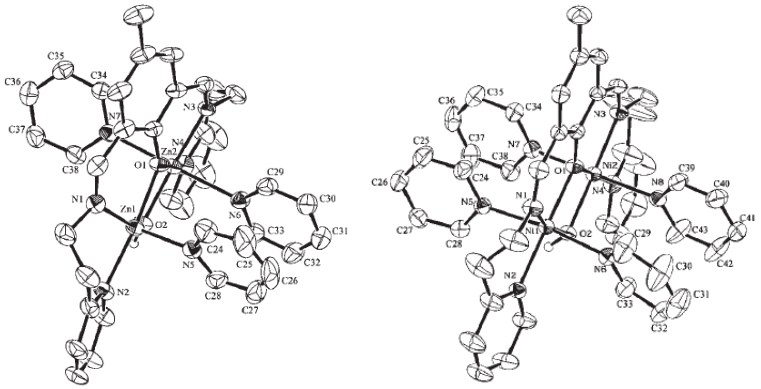

Figure 1.30: Crystal structures of $[Zn_2(L)(OH)(py)_3]^{2+}$ (left) and $[Ni_2(L)(OH)(py)_4]^{3+}$ (right).[106]

With the crystal structures, they were able to establish that both complexes are dinucleating and compartmental. The two Zn(II) ions in the complex were in different geometries, one Zn(II) ion is five-coordinated geometry which is intermediate between square-pyramid and trigonal-bipyramid, with further coordination of one pyridine molecule, whereas the other Zn(II) ion has a six-coordinate octahedral geometry with two coordinated pyridine molecules. However, both Ni(II) ions in the complex were observed to have the same geometries, six-coordinated octahedral geometry, with two pyridine molecules at *axial* sites in each Ni(II) ion.

The Zn(II) complex is diamagnetic while in the Ni(II) complex an antiferromagnetic interaction operates between the two Ni(II) ions. The magnetic moment of $[Ni_2(L)(OH)(py)_4](ClO_4)_2]$ at room temperature is 2.92 B.M., and moments decrease to

0.28 B.M. with temperature falling down to 2K. This suggested antiferromagnetic interaction operated between each pair of nickel ions.[106]

Ye and co-workers[107] also reported a di- and a tetranuclear Zn(II)-carboxylate compartmental complex in different coordination modes based on ligand HL (HL is shown in Figure 1.29) with phenolate and carboxylate bridges. A vast number of examples from both experiment and calculation have proven that 'carboxylate shift' is a low-energy path in the altering of binding mode in catalytic cycles of metalloenzymes.[108] The two di-Zn(II) carboxylate complexes, $[Zn_2L(\mu_{1,3}\text{-}OAc)_2](ClO_4)$ and $[Zn_2L(\mu_{1,3}\text{-}Pro)_2](ClO_4)$ were prepared by condensation of 2,6-diformyl-4-methylphenol with 2-(2-aminoethane)-pyridine in the presence of the Zn(II) carboxylate and $NaClO_4$. The condensation in the presence of HCOONa and Zn(II) perchlorate salts with ligand HL resulted to a tetranuclear Zn(II) complex, $[Zn_4(L)_2(\mu_{1,1}\text{-}HCOO)_2(\mu_{1,3}\text{-}HCOO)_2](ClO_4)_2$. The three crystal structures (two di-nuclear and one tetra-nuclear complexes) were also obtained. But both di-nucleating complexes showed almost same observation. So, the crystal structures of di-nucleating and tetra-nucleating Zn(II) complexes are shown in left and right, respectively, in Figure 1.31.

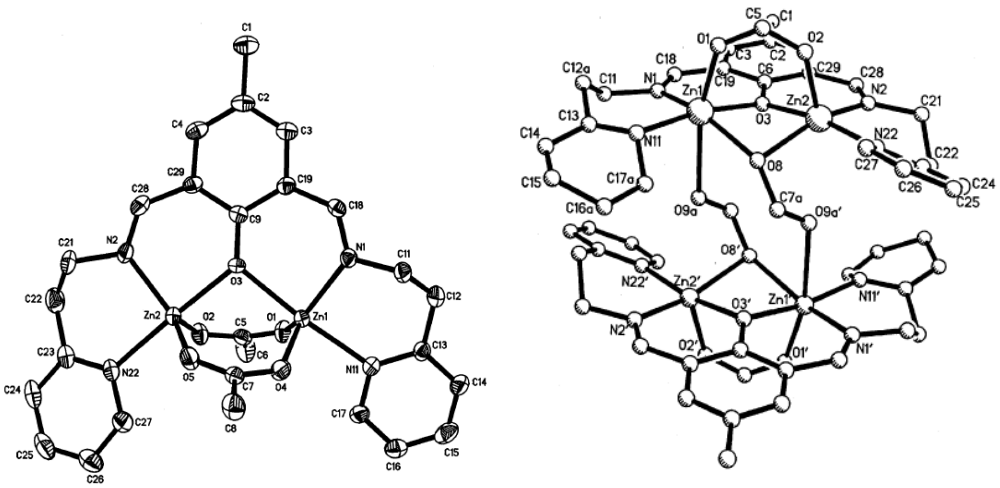

Figure 1.31: Crystal structures of di-nuclear $[Zn_2L(\mu_{1,3}\text{-}OAc)_2]^+$ (left) and tetra-nuclear $[Zn_4(L)_2(\mu_{1,1}\text{-}HCOO)_2(\mu_{1,3}\text{-}HCOO)_2]^{2+}$ (right).[107]

In both di-nucleating complexes, the coordination of each Zn(II) ion is penta-coordinate and the polyhedron around each Zn(II) ions could be described as slightly distorted trigonal bipyraminal geometry. While the geometry of the tetranuclear core is emphasized an arrangement occurred between the Zn(II) ions and the carboxylates group. This could be described that the tetranulcear complex is comprised of two

identical dinuclear $[Zn_2L(\mu_{1,1}\text{-}HCO_2)(\mu_{1,3}\text{-}HCO_2)]^+$ species which were connected to each other *via* the carboxylate groups. It is interesting that the two Zn(II) ions within each subunit species display two different coordination geometries (shown in Figure 1.31, right). One Zn(II) ion in each subunit has a five-coordinate N_2O_3 (*via* three oxygen atoms from a phenolate and two formate groups, and further two nitrogens from ligand L) as distorted square pyramidal geometry, while the other Zn(II) ion is six-coordinate with an additional coordinating oxygen atom from carboxylate groups, resulting in a N_2O_4 distorted octahedral geometry.

An interesting strategy in the formation of polynuclear Zn(II) complexes starting from dinuclear end-off compartmental complexes which were synthesized by end-off ligand HL in the presence of Zn(II) ions salts and appropriate base was successfully prepared.[109,110] A similar tetra-nuclear Zn(II) complex based on end-off ligand HL was also achieved by Giannis and co-workers.[110] The subunit $[Zn_2(L)(OH)](ClO_4)_2$ was prepared by reaction of HL with Zn(II) perchlorate salts in the presence of LiOH. The diffusion of *trans*-1,2-bis(4-pyridyl)ethylene (4,4'-bpe) into a methanol solution with subunit $[Zn_2(L)(OH)](ClO_4)_2$ resulted to the formation of tetra-nucleating complex $[Zn_4(L)_2(\mu\text{-}OH)_2(\mu\text{-}4,4'\text{-}bpe)_2](ClO_4)_4{\cdot}4H_2O$ (shown in Figure 1.32, a) within a period of two weeks.[110] However, the ability to assemble a tetra-nucleating complex with 4,4'-bpe in the formation of an infinite polynuclear ladder-like complex $[[Zn_2(L)(\mu\text{-}OH)(\mu\text{-}4,4'\text{-}bpe)](ClO_4)_2\ 2H_2O]_\infty$ (shown in Figure 1.32, b) was also found by Giannis and co-workers.[109]

The structure of tetra-nucleating Zn(II) complex (shown in Figure 1.32, a) was performed by two identical subunits $[Zn_2(L)(OH)]^{2+}$, and they were assembled with two 4,4'-bpe molecules to form the tetra-nuclear complex $[Zn_4(L)_2(\mu\text{-}OH)_2(\mu\text{-}4,4'\text{-}bpe)_2]^{4+}$. The structure is similar to the tetra-nuclear complex which was discussed earlier in Figure 1.31, with the exception that each Zn(II) ion in the complex $[Zn_4(L)_2(\mu\text{-}OH)_2(\mu\text{-}4,4'\text{-}bpe)_2]^{4+}$ adopts the same geometry, a square pyramidal geometry, where the pyridyl nitrogen in 4,4'-bpe presents at the apical positions while the remaining sites are occupied by a phenolate and two nitrogens from ligand L and an additional OH ion.[110]

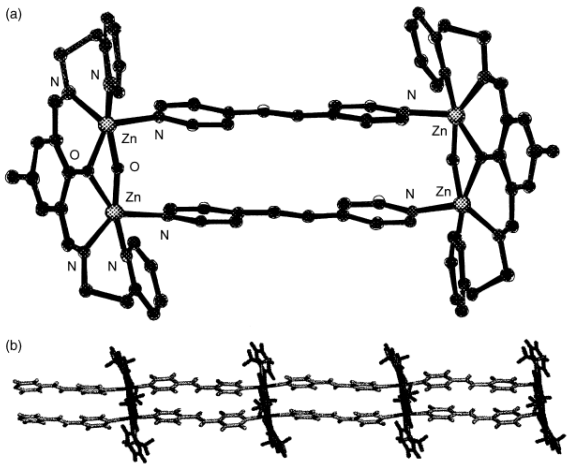

Figure 1.32: Structures of complexes tetra-nucleating $[Zn_4(L)_2(\mu\text{-}OH)_2(\mu\text{-}4,4'\text{-bpe})_2](ClO_4)_4{\cdot}4H_2O$ (a) and poly-nucleating $[[Zn_2(L)(\mu\text{-}OH)(\mu\text{-}4,4'\text{-bpe})](ClO_4)_2\ 2H_2O]_\infty$ (b).

Additionally, the polymeric complex $[[Zn_2(L)(\mu\text{-}OH)(\mu\text{-}4,4'\text{-bpe})](ClO_4)_2\ 2H_2O]_\infty$ was found by the same synthetic route with a tetra-nuclear complex.[109] In contrast to tetra-nuclear complex, the geometry of the polymeric complex (shown in Figure 1.32, b) has each Zn(II) ions is octahedral geometry rather than a square pyramidal geometry, with an additional nitrogen atom from 4,4'-bpe group. The coordination environment in such a situation means that the two nitrogen atoms of two 4,4'-bpe adopt a *transoid* arrangement,[110] and the other coordination sites are similar to the tetra-nuclear complex. In addition, the pentadentate ligand L units are oriented anti-parallel along the polymer backbone.[109]

Moreover, it was observed that both the tetra-nuclear and the poly-nuclear complexes had a suitable configuration in the preparation of [2+2] photo-dimerization in the solid state, resulted in dimerization 4,4'-tpcb (where 4,4'-tpcb = *rctt*-tetrakis(4-pyridyl)-cyclobutane) from 4,4'-bpe complexes (shown in Figure 1.33). Thus, a 100% yield of 4,4'-tpcb tetra-nuclear complex was achieved by exposing either the 4,4'-bpe single crystals or a powdered crystalline complex under UV radiation over a period of approximately 5 h. Optical microscopy as well as single crystal X-ray diffraction, established that this reaction occurred *via* a single crystal to single crystal (SCSC) transformation. Similarly, the powdered crystalline complex of poly-nuclear $[[Zn_2(L)(\mu\text{-}OH)(\mu\text{-}4,4'\text{-bpe})](ClO_4)_2\ 2H_2O]_\infty$ under UV-irradiation produced the similar complex of 4,4'-tpcb over a period of 32 h. This transformation was determined by ^1H NMR

spectroscopy, which was suggested by the disappearance of an olefinic singlet at 7.54 ppm and the appearance of a cyclo butane singlet at 4.66 ppm.

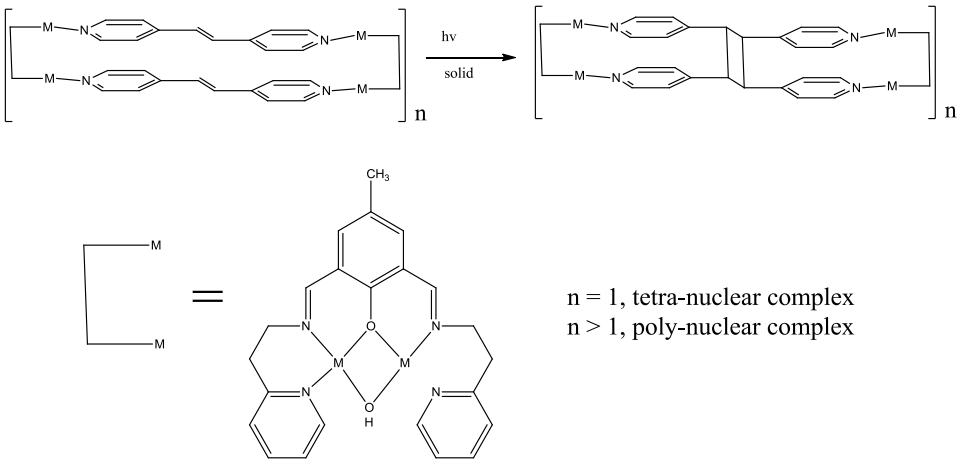

Figure 1.33: [2+2] photodimerization reaction of tetra and poly-nuclear complexes.[109,110]

1.3 Pyridine amides and metal complexes

1.3.1 Overview

Amide is another widely used group in nature. It is named peptide in biochemical context forming the main chain of a protein. The formation of amide bond is a fundamentally important reaction in lots of areas and occurs in good yields with the assistance of different coupling reagents, hence the synthesis of the amide bond is not as straightforward to prepare as imine. It has also exhibited the ability of conferring structural rigidity and preventing hydrolysis which suggest interesting properties in coordination chemistry.[111] Neutral amides can give rise to the formation of regioisomers when amides are bonding to metal salts, due to the possibility of coordination *via* either the lone pair of the nitrogen atom (amide conjugate base) or the lone pair of the carbonyl oxygen atom.[112,113] However, the deprotonated amide by a strong base (e.g. sodium hydride) preferably coordinates to metal ions through the amido nitrogen atom.[114] Recently, several reviews based on amide functional groups such as multi-pyridyl amide complexes,[111,115] macrocyclic and acyclic amide complexes[116] have also received much attention in coordination chemistry and applications in catalytic reactions.

1.3.2 The formation of amide ligands

Generally, the formation of amide bonds (-C(O)-NH-) occurs typically in a condensation reaction between a carboxylic acid and either primary or secondary amines.[117] However, several problems are observed in this condensation. The carboxylic acid and amine base can react with each other in an acid-base reaction resulting in the formation of an ammonium carboxylate salt (shown in Figure 1.34). In addition, this reaction does not occur spontaneously at ambient temperature, except in the case where water is removed and occurred at a high temperature (e.g. >200 ℃)[118] which will force the reaction equilibrium turn to right.

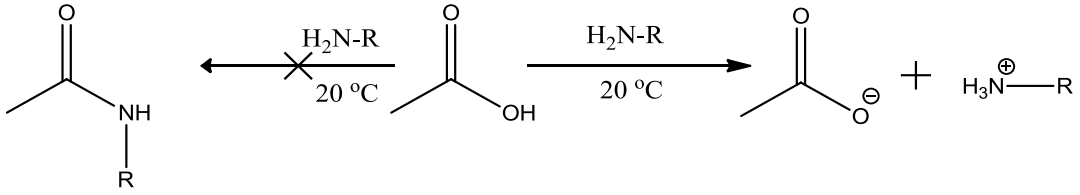

Figure 1.34: The formation of ammonium carboxylate salt.

In order to overcome these problems, it is necessary to find a species to activate the carboxylic acid since the hydroxyl moiety in the carboxylic acid functional group is a poor leaving group. This process is occurred by converting the hydroxyl group of the acid into a superior good leaving group first, then with the treatment of the amine compounds. Using the generally known coupling reagents[119] can achieve the aim of activating the carboxylic acid. These coupling reagents can act as stand-alone reagents to generate compounds, such as acid chloride, (mixed) anhydrides, carbonic anhydrides or active ester. One of first widely used coupling reagents is carbodiimides, e.g. dicyclohexylcarbodiimide (DCC) (shown in Figure 1.35) which has been used for coupling since 1955.[120] The mechanism of using these coupling reagents will not be discussed here as it is irrelevant to the work done in this thesis.

In addition to the carbodiimide derivatives, another coupling reagent based on triazine[121] derivatives are also attractive and are much more interesting due to the fact that they have the advantage of promoting the formation of amides in alcohols or aqueous solvent, without ester formation or generating acid halides. One example of these triazine derivatives is 4-(4,6-dimethoxy-1,3,5-triazin-2-yl)-4-methyl-morpholinium (or DMT-MM)[121] chloride (shown in Figure 1.35), which does not need inert atmosphere or dry solvents for the reaction process in contrast to carbodiimides coupling reagents. Moreover, the easy elimination of the co-product which arises from

using DMT-MM *via* straightforward filtration is another advantage for using triazine derivatives for the amide formation.[122]

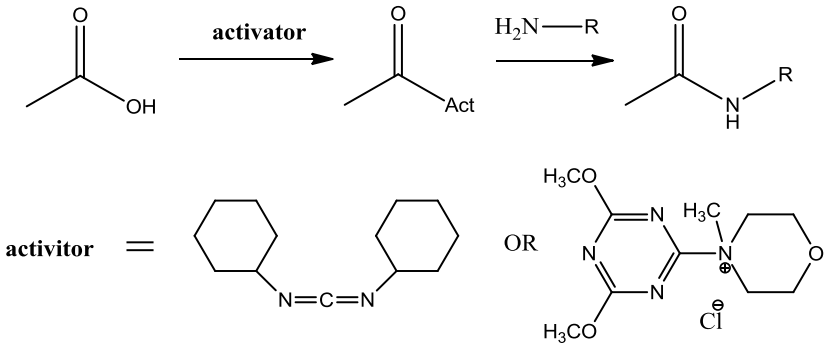

Figure 1.35: Coupling reagents DCC (bottom left) and DMT-MM (bottom right) used as activator in the formation of amide bonds.

Another preparation of amide bond is through the method of converting the carboxylic acid into ester precursor which can be regarded as a superior leaving group in order to facilitate the nucleophilic substitution. One example of formation of calix[4]arene di-amide by transforming the ester to amide has been reported by McGinley *et. al.*[123] The diethyl ester of calix[4]arene in the mixture solvents of toluene-methanol was heated to reflux in the presence of di-amine precursors. The calix[4]arene di-amide compounds were achieved in good yield and in easily purified. However, the reaction time in this process lasts for several days which might be due to the large calix[4]arene molecule.

The use of acid halides which exhibit highly reactive carbonyl derivatives were also employed for the synthesis of amide bonds. The first synthesis of a dipeptide (Gly-Gly) by using acid chlorides was reported by Fischer *et. al.*[124] in 1901. The most common reagents are using thionyl chloride, phosphorus pentachloride or oxalyl chloride.[125] These reagents generate acid chloride which react with amine precursors leading to the formation of amide compounds. The reagent phosphorus pentachloride was most commonly used until it was replaced by thionyl chloride, due to the generated co-products, sulfur dioxide and hydrogen chloride. However, the products of thionyl chloride reactions are more easily removed in the elimination step in comparison to those of phosphorus pentachloride. In addition, the boiling point of thionyl chloride is 74.6 ℃, i.e. the excess of thionyl chloride can be easily removed under reduced pressure to isolate product.

1.3.3 Zn(II), Hg(II), Ni(II), Cu(II) and Co(II) amide complexes

Metal complexes with a vast amounts of metal ions, including both hard-valent and soft-valent ions and even zerovalent metals have been employed in forming metal-amide complexes. As has been talked about previously, amide groups are rigid and versatile ambidentate donor ligands. The resistance to hydrolysis of the amide group (which is thought of as the main advantage with a comparison to imine group), indicates that by-products resulting from amide ligand cleavage are unlikely to occur. However, this does not suggest that the amide group cannot be broken up. In this thesis, the metal coordination amide chemistry will focus on *d*-block divalent metals salts such as Zn(II), Hg(II), Ni(II), Cu(II) and Co(II) with corresponding chloride, perchlorate and acetate ions.

The synthesis of Co^{3+}-centered-Zn^{2+}-peripheral heterobimetallic complexes (shown in Figure 1.36) based on ligand 2,6-diamidopyridine derivatives have been reported by Mishra and co-workers.[126] The coordination geometry of the central Co(III) ion is octahedral with four deprotonated amide nitrogen atoms in the equatorial planar and two pyridyl nitrogen atoms in the axial positions. Both Zn(II) ions have tetrahedral geometries and they are situated in two clefts which were created by the hanging pyridine rings, and are also coordinated to the pyridine nitrogen atoms. The remaining two coordination groups of each Zn(II) ion were observed to be slightly different. One Zn(II) ion is externally coordinated by two Cl^- ions whereas the other Zn(II) ion is occupied by one Cl- and one DMA (N,N'-dimethylacetamide) molecule. In addition, this compound, shown in Figure 1.36, exhibited reasonable catalytic activity in the Beckmann rearrangement of the aldoximes and ketoximes to their respective amides.[126]

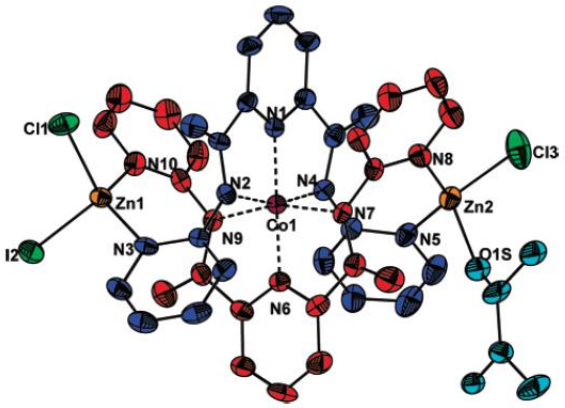

Figure 1.36: The structure of Co(III)-Zn(II) heterometallic complex.

The reaction of ligand 2,6-bis[*N*-(2'-pyridylmethyl)carbamyl]pyridine (H_2L) with Ni(II) ions in solution resulted in two complexes which are a minor red 1:1 (Ni:L) species [NiL] and a major dark brown 3:2 (Ni:L) species $[Ni_3(L)_2(OAc)_2(MeOH)_2]$, respectively, reported by Alcock *et. al.*[127] The complex of NiL, which is shown in Figure 1.37, proved to be diamagnetic suggesting that the Ni(II) ion is four-coordinate square planar geometry even though the ligand L is a pendantate ligand. Both amide groups are deprotonated and coordinated to the Ni(II) ion centre contributed by the fact that the amide hydrogen atoms have disappeared in the ^{1}H NMR spectrum. They were able to establish that both amido nitrogen atoms, and central pyridine nitrogen atoms were coordinated to Ni(II) ion centre and with only one pyridine groups to bind while the other being an unbound pendant arm.

The trinuclear Ni(II) complex $[Ni_3(L)_2(OAc)_2(MeOH)_2]$ which was formed by the reaction of H_2L with Ni(II) acetate as major product was also reported by the same group. The geometry of each Ni(II) ion is a distorted octahedral. The crystal structure of trinuclear Ni(II) complex was also solved and shown in Figure 1.37. All the amide hydrogen were deprotonated to form the amido group which participated in the Ni(II) complexation. The three Ni(II) ions were bonded by two ligands (L), and the central pyridine group in each ligands were observed at trans axial locations, while the amido nitrogen atoms occupied the planar and were bonding to the metal ions.

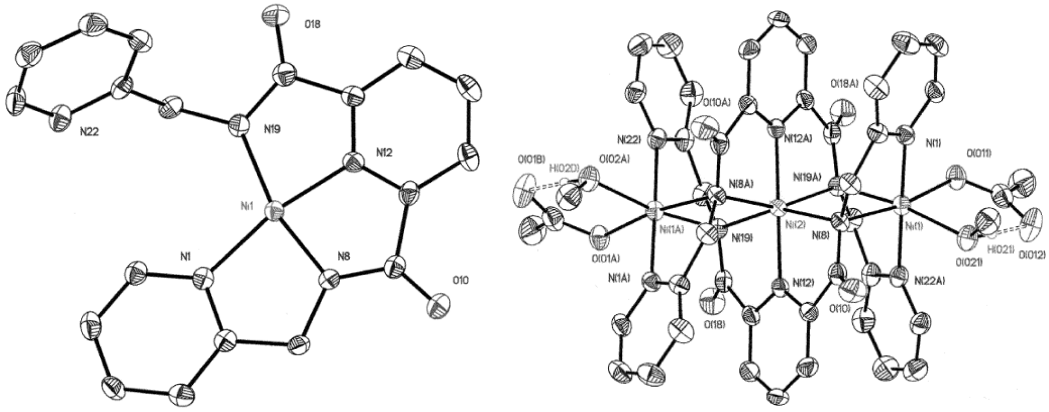

Figure 1.37: Crystal structures of mononuclear complex [NiL] and trinuclear complex $[Ni_3(L)_2(OAc)_2(MeOH)_2]$.

The pentadentate di-amide ligand N,N'-bis[2-(1-pyrazolyl)ethyl]pyridine-2,6-dicarhoxamide [H_2L'] with the Cu(II) ions has been reported by Chavez and co-workers.[128] The complex [CuL'] was synthesized in the presence of strong base ($Me_4N(OH)$) and Cu(II) perchlorate which the ligand H_2L' could be fully deprotonated

in order to generate the Cu(II) complex. The resulting $Me_4N(ClO_4)$ is insoluble and could be easily removed by filtration. The crystal structure of [CuL'] was also obtained and shown in Figure 1.38. The Cu(II) ion is coordinated to five nitrogen atoms, and the Cu(II) ion centre adopts a square-pyramidal geometry. Two deprotonated amido nitrogen atoms, one central pyridyl nitrogen atoms and one 2-pyrazole nitrogen atom occupy the equatorial plane while the other 2-pyrazole nitrogen atom adopts at the axial position to complete the square-pyriamidal geometry. In addition, the electronic absorption spectrum (maximum at 600 nm and shoulder at about 735 nm) of [CuL'] also suggested the Cu(II) complex is typical of tetragonally distorted Cu(II) in a square-pyramidal coordination geometry.

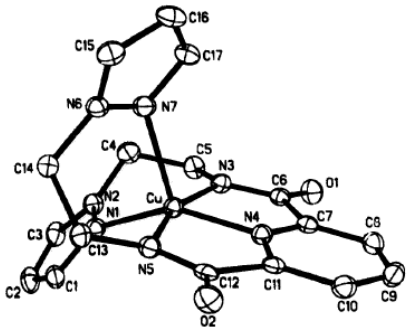

Figure 1.38: Crystal structure of mononuclear complex CuL'

1.4 The aim of thesis

The aim of this thesis was to expand the chemistry of both acyclic Schiff-base and amide ligands and to study their coordination complexes. These acyclic ligands have several extra functional groups attached, such as an OH or pyridine or imidazole rings. Different divalent d-block metal salts were involved in the metal complexation reactions of the various ligands formed with MX_2 (M = Cu, Ni, Zn, Co and Hg, and X = chloride, acetate and perchlorate). This thesis has been divided into six parts where five of them are concerned with different imine ligands and their corresponding metal complexes while the remaining section deals with an amide derivative and its metal complexes. All metal complexes will be examined through a comparison with the novel acyclic ligands by the analytical methods of ^{1}H and ^{13}C NMR spectroscopy, IR spectroscopy, mass spectrometry and microanalyses.

2 Experimental

2.1 Instrumentation

Reagents and reactants were supplied by either Alfa Aesar, Fluorochem or Sigma-Aldrich and were used as received without further purification. Solvents were distilled before use and purified according to standard procedures. Products were characterised by NMR and IR spectroscopy unless otherwise indicated. ^{1}H and ^{13}C NMR (δ ppm; J Hz) spectra were recorded on a Bruker Avance 300 MHz spectrometer at a probe temperature of 25 ℃ using saturated $CDCl_3$ solutions with Me_4Si reference, and resolutions of 0.18 Hz and 0.01 ppm, respectively, unless otherwise indicated. ^{1}H NMR and ^{13}C NMR spectra were run at 300 MHz and 75 MHz, respectively. Infrared spectra (cm^{-1}) were recorded as KBr discs or liquid films between NaCl plates using a Perkin Elmer system 2000 FT-IR spectrophotometer. Melting point analyses were carried out using a Stewart Scientific SMP 1 melting point apparatus and are uncorrected. Mass spectrometry was carried out on a LC/TOF-MS model 6210 Time-Of-Flight LC/MS with an electrospray source positive and negative (ESI+/−), capillary 3500 V, nebuliser spray 30 psig, drying gas 5 L/min and source temperature 325 ℃. The fragmentor was used at 175 V. The LC was run on a 1200 series model and injection volumes were typically 10 μL. Column used was an Agilent Eclipse XBD-C18. A diameter of 5-micron was employed. The mobile phase constituted A (acetonitrile with 0.1 % formic acid) and B (0.1 % aqueous formic acid) with a gradient of 5 % A to 100 % at a flow rate of 0.5 mL/min over 15 minutes. Microanalyses were carried out at the National University of Ireland, Maynooth, using a Thermo Finnigan Elementary Analyzer Flash EA 1112. The results of which were analysed using the Eager 300 software.

2.2 Section 1

2.2.1 4-*tert*-Butyl-2,6-Dihydroxymethylphenol (**1**)[129]

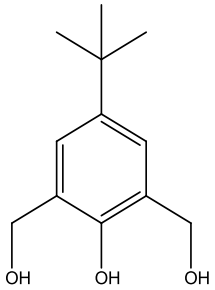

p-*tert*-Butylphenol (24 g, 0.16 mol), 40% aqueous formaldehyde (24 g, 0.32 mol) and 2% aqueous NaOH (320 mL, 0.16 mol) were stirred at 30-40 ℃ for 2 days. Then 2 L of acetone was added to the solution until no more white solid crashed out. The white solid was filtered, washed with acetone and dried in air to give a white sodium salt. This white solid was redissolved in water (100 mL), and acidified by 25% H_2SO_4 solution (15.66 g, 0.16 mmol). The resulting white solid was collected by filtration and dried in air overnight to give the product **1**. This was recrystallized from ether and hexane.

White solid. Yield: 23.7 g, 70%, $\delta_H(CDCl_3)$: 8.00 (1H, s, br, Ar-OH), 7.06 (2H, s, ArH), 4.77 (4H, s, CH_2OH), 2.81 (2H, s, br, CH_2OH), 1.27 (9H, s, t-Butyl). These match reported data.

2.2.2 4-*tert*-Butyl-2,6-diformylphenol (**2**)[130]

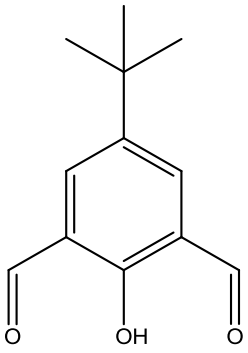

Compound **2** was synthesised according to the literature reference.[130] To a 100 mL round-bottomed flask, was added compound **1** (1 g, 4.85 mmol) and activated MnO_2 (7 g, 80 mmol) in $CHCl_3$ (50 mL). The mixture was heated to reflux with stirring for 15 hrs. After the reaction cooled down, the mixture was filtered by gravity, then washed

with $CHCl_3$. Activated carbon was added to the mixture and heated gently for 5-10 min. This was filtered to give a yellow filtrate. The excess solvent was removed under reduced pressure to give compound **2** as a yellow solid.

Yield: 0.54g, 55%. $\delta_H(CDCl_3)$: 11.47 (1H, s, ArOH), 10.25 (2H, s, -CHO), 7.98 (2H, s, ArH), 1.33 (9H, s, t-butyl). ν_{max} (KBr): 2964 (OH), 2866 (-CH_2-), 1686 (C=O), 1660 (C=O associated with OH), 1222 (C-O) cm^{-1}. These match reported data.

2.2.3 4-(*tert*-Butyl)-2,6-bis((*E*)-((pyridine-2-ylmethyl)imino)methyl)phenol (**3**)

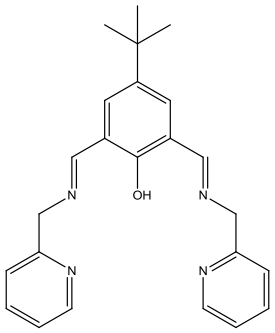

To a suspension of anhydrous $MgSO_4$ (1.46 g, 10.5 mmol) in CH_2Cl_2 was added compound **2** (0.5 g, 2.42 mmol) followed by 2-aminomethyl pyridine (0.52 g, 4.84 mmol). The mixture was stirred at room temperature overnight. The resulting suspension was filtered, washed with CH_2Cl_2, and the solution was removed under vacuum to give compound **3** as yellow oil.

Yield: 0.93 g, 99%. $\delta_H(CDCl_3)$: 13.87 (1H, s, ArOH), 8.78 (2H, s, br, CH=N-), 8.58 (2H, d, py-H, J = 3.8 Hz), 7.69 (2H, t, pyridine-H, J = 8.3 Hz), 7.78 (2H, s, br, ArH), 7.40 (2H, d, py-H, J = 8.3 Hz), 7.20 (2H, m, py-H), 4.98 (4H, s, CH_2), 1.33 (9H, s, t-butyl) ppm. $\delta_C(CDCl_3)$: 159.0, 149.6, 141.4, 137.1, 122.1, 53.4, 34.2, 31.4 ppm. ν_{max} (KBr): 3375, 1959, 1630, 1600, 1480, 1415, 1220, 819, 800 cm^{-1}. HR-MS: calcd $C_{24}H_{27}N_4O$, m/z: $[M+H]^+$, 387.2179. Found: 387.2163. [Diff(ppm)]: -4.17.

2.2.4 Metal complexes of **3**

General procedure:

Ligand **3** (100 mg, 0.259 mmol) was dissolved in MeOH (10 mL). To this was added, dropwise, the appropriate metal salt (0.518 mmol) in MeOH (5 mL). A coloured solid precipitated immediately. The mixture was kept stirring for additional 2 hours. The

coloured solid was removed by filtration, washed with MeOH, and dried in oven (75 ℃) overnight.

2.2.4.1 Reaction of **3** with $ZnCl_2$

Yellow solid. Yield: 70 mg, 43%. δ_H(DMSO): 8.85 (2H, s, -CH=N-), 8.72 (2H, s, br, py-H), 8.14 (2H, s, br, py-H), 7.77 (2H, s, ArH), 7.67 (4H, br, py-H) 5.17 (4H, s, $-CH_2-$), 1.33 (9H, s, t-butyl) ppm. ν_{max} (KBr): 3487, 2964, 1655, 1607, 1572, 1542, 1484, 1446, 1422, 1286, 1232, 1067, 1020, 766 cm^{-1}. Calcd for: [Zn_2(**3**)Cl_3], $C_{24}H_{25}Cl_3N_4OZn_2$, C, 46.30; H, 4.05; N, 9.00 %. Found: C, 46.57; H, 3.68; N, 8.89 %.

2.2.4.2 Reaction of **3** with $Hg(ClO_4)_2 \cdot 6H_2O$

Yellow solid. Yield: 47 mg, 48%. δ_H(DMSO): 8.94 (2H, s, -CH=N-), 7.89 (2H, s, ArH), 7.84-7.89 (4H, m, pyridine-H, ArH), 7.55 (2H, d, pyridine-H, J = 4.3 Hz), 7.46 (2H, d, pyridine-H, J = 7.9 Hz), 7.25 (2H, t, pyridine), 5.01 (4H, s, $-CH_2-$), 1.43 (9H, s, t-butyl) ppm. ν_{max} (KBr): 3443, 2960, 1638, 1600, 1531, 1477, 1442, 1396, 1362, 1246, 1094, 1008, 766, 623 cm^{-1}. Calcd for: [Hg(**3**)ClO_4], $C_{24}H_{26}ClHgN_4O_5$, C, 42.05; H, 3.68; N, 8.17 %. Found: C, 41.65; H, 3.62; N, 8.23 %.

2.2.5 4-(tert-Butyl)-2,6-bis((*E*)-((pyridin-3-ylmethyl)imino)methyl)phenol (**4**)

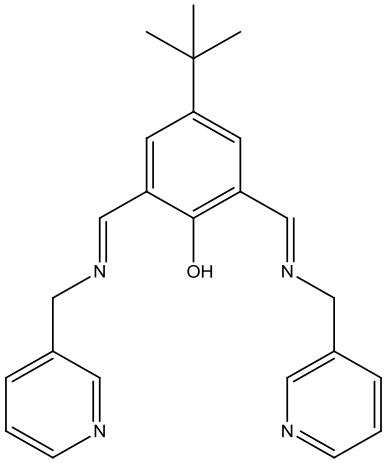

To a suspension of anhydrous $MgSO_4$ (1.46 g, 10.5 mmol) in CH_2Cl_2 was added compound **2** (0.5 g, 2.42 mmol). This was followed by 3-aminomethyl pyridine (0.52 g, 4.84 mmol). The mixture was stirred at room temperature overnight. The resulting suspension was filtered, washed with CH_2Cl_2, and the excess filtrate was removed under vacuum to give compound **4** as a yellow solid.

Experimental

Yield: 0.93 g, 99%. $\delta_H(CDCl_3)$: 13.60 (1H, s, ArOH), 8.73 (2H, s, br, CH=N), 8.63 (2H, s, py-H), 8.55 (2H, d, py-H, J = 5.3 Hz), 7.67 (2H, d, ArH, J = 9 Hz), 7.31 (2H, m, py-H), 4.84 (4H, s, CH_2), 1.33 (9H, s, t-butyl) ppm. $\delta_C(CDCl_3)$: 158.7, 149.3, 148.1, 141.6, 135.5, 134.8, 123.5, 34.2, 31.3 ppm. ν_{max} (KBr): 3054, 2987, 1635, 1591, 1474, 1422, 1150, 896 cm^{-1}. Calcd for: $C_{24}H_{26}N_4O$, C, 74.58; H, 6.35; N, 14.87 %. Found: C, 74.84; H, 6.35; N, 14.87 %. M.P : 126-127 ℃.

2.2.6 Metal complexes of **4**

General procedure:

Compound **4** (100 mg, 0.259 mmol) was dissolved in MeOH (10 mL). To this was added, dropwise, the appropriate metal salt (0.259 mmol) in MeOH (5 mL). A coloured solid precipitated immediately. The mixture was kept stirring for an additional 2 hours. The coloured solid was removed by filtration, washed with MeOH and dried in oven (75 C) overnight.

2.2.6.1 Reaction of **4** with $ZnCl_2$

Yellow solid. Yield: 82 mg, 54%. δ_H(DMSO): (T=50 ℃) 8.78 (2H, s, br, CH=N-), 8.47-8.65 (4H, m, br, py-H), 7.65 (4H, s, br, py-H), 7.36 (2H, s, br, ArH), 4.79 (4H, s, br, CH_2), 1.29 (9H, s, t-butyl) ppm. ν_{max} (KBr): 3502, 2959, 1661, 1657, 1558, 1540, 1435, 1231, 1074, 840, 702 cm^{-1}. Calcd for: [Zn_2(**4**)Cl_3·MeOH], $C_{25}H_{29}Cl_3N_4O_2Zn_2$, C, 45.87; N, 8.56; H, 4.47 %, Found: C, 46.57; N, 9.06; H, 4.41 %.

2.2.6.2 Reaction of **4** with $Zn(ClO_4)_2·6H_2O$

Yellow solid. Yield: 116 mg, 69%. δ_H(DMSO): 8.65 (2H, s, -CH=N-), 8.52 (2H, s, pyridine), 8.30 (2H, s, br, pyridine), 7.81 (4H, br, pyridine, ArH), 7.44 (2H, s, br, pyridine), 4.85 (4H, s, CH_2), 1.27 (9H, m, t-butyl) ppm. ν_{max} (KBr): 3427, 2961, 1650, 1542, 1434, 1233, 1099 (br), 841, 709, 623 cm^{-1}. Calcd for: [Zn(**4**)(ClO_4)·$4H_2O$], $C_{24}H_{33}ClN_4O_9Zn$, C, 46.32; H, 5.34; N, 9.00 %. Found: C: 46.06; H, 4.50; N: 8.66 %.

2.2.6.3 Reaction of **4** with $HgCl_2$

Yellow solid. Yield: 149 mg, 48%. δ_H(DMSO): 8.84 (2H, s, -CH=N-), 8.59 (2H, s, pyridine), 8.51 (2H, br, pyridine), 7.88 (2H, br, pyridine), 7.80 (2H, s, ArH), 7.45 (2H, br, pyridine), 4.86 (4H, s, CH_2), 1.27 (9H, s, t-butyl) ppm. ν_{max} (KBr): 3439, 2960, 1630, 1600, 1531, 1433, 1363, 1228, 1127, 1067, 840, 798 cm^{-1}. Calcd for: [Hg(**4**)Cl], $C_{24}H_{25}ClHgN_4O$, C, 46.38; H, 4.05; N, 9.01 %. Found: C, 46.75; N, 3.85; H, 8.86 %.

2.2.6.4 Reaction of **4** with $Hg(ClO_4)_2 \cdot H_2O$

Yellow solid. Yield: 0.18 g, 58%. δ_H(DMSO): 9.02 (1H, s, br, ArOH), 8.49 (2H, d, py-H, J = 6 Hz), 8.40 (2H, s, py-H), 7.79 (2H, s, ArH), 7.59 (2H, s, py-H), 7.37-7.42 (2H, m, py-H), 5.02 (4H, s, br, CH_2), 1.32 (9H, s, t-butyl) ppm. ν_{max} (KBr): 3523, 2961, 1651, 1619, 1530, 1447, 1233, 1095(br), 623 cm^{-1}. Calcd for: [Hg_2(**4**)$(ClO_4)_3 \cdot 2H_2O$], $C_{24}H_{29}Cl_3Hg_2N_4O_{15}$, C, 25.71; N, 5.00; H, 2.61 %. Found: C, 25.35; N, 5.18; H, 2.66 %.

2.2.6.5 Reaction of **4** with $NiCl_2 \cdot 6H_2O$

Dark green solid. Yield: 80 mg, 44%. ν_{max} (KBr): 3366, 2959, 1645, 1540, 1484, 1434, 1231, 1073, 842, 802, 705 cm^{-1}. Calcd for: [Ni_2(**4**)$Cl_3 \cdot 5H_2O$], $C_{24}H_{35}Cl_3N_4Ni_2O_6$, C, 41.22; H, 5.04; N, 8.01 %. Found: C, 40.62; H, 4.77; N, 7.97 %. μ_{eff} = 4.06 B.M.

2.2.6.6 Reaction of **4** with $Ni(ClO_4)_2 \cdot 6H_2O$

Green solid. Yield: 80 mg, 46%. ν_{max} (KBr): 3424, 2961, 1651, 1628, 1540, 1486, 1432, 1364, 1232, 1099(br), 800, 709, 624 cm^{-1}. Calcd for: [Ni(**4**)$(ClO_4) \cdot 4H_2O$], $C_{24}H_{33}ClN_4NiO_9$, C, 46.82; H, 5.40; N, 9.10 %. Found: C, 46.44; H, 4.47; N, 8.39 %. μ_{eff} = 3.06 B.M.

2.2.6.7 Reaction of **4** with $CuCl_2 \cdot 2H_2O$

Green solid. Yield: 88 mg, 55%. ν_{max} (KBr): 3429, 2957, 1662, 1656, 1557, 1541, 1436, 1234, 1075, 841, 701 cm^{-1}. Calcd for: [Cu_2(**4**)$Cl_3 \cdot$MeOH], $C_{25}H_{29}Cl_3Cu_2N_4O_2$, C, 46.13; H, 4.49; N, 8.61 %. Found: C, 46.49; H, 4.48; N, 8.91 %. μ_{eff} = 2.19 B.M.

2.2.6.8 Reaction of **4** with $Cu(ClO_4)_2 \cdot 6H_2O$

Green solid. Yield: 92 mg, 55%. ν_{max} (KBr): 3432, 2962, 1655, 1633, 1547, 1484, 1438, 1365, 1236, 1090(br), 864, 799, 703, 623 cm^{-1}. Calcd for: [Cu(**4**)$(ClO_4) \cdot 3H_2O$], $C_{24}H_{31}ClCuN_4O_8$, C, 47.84; H, 5.19; N, 9.30 %. Found: C, 48.02; H, 5.22; N, 9.11 %. μ_{eff} = 2.23 B.M.

2.2.7 4-(tert-butyl)-2,6-bis((*E*)-((pyridin-4-ylmethyl)imino)methyl)phenol (**5**)

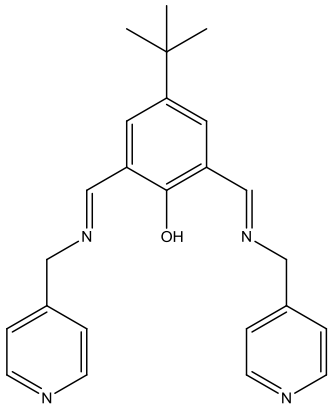

To a suspension of anhydrous $MgSO_4$ (1.46 g, 10.5 mmol) in CH_2Cl_2 was added compound **2** (0.5 g, 2.42 mmol). This was followed by 4-aminomethyl pyridine (0.52 g, 4.84 mmol). The mixture was stirred at room temperature overnight. The resulting suspension was filtered, washed with CH_2Cl_2, and the filtrate was removed under vacuum to give compound **3** as yellow oil.

Yield: 0.93 g, 99%. $\delta_H(CDCl_3)$: 13.62 (1H, s, ArOH), 8.74 (2H, s, br, CH=N), 8.57-8.59 (4H, m, py-H), 7.25-7.29 (6H, m, pyridine-H, ArH), 4.84 (4H, s, CH_2), 1.35 (9H, s, t-butyl) ppm. $\delta_C(CDCl_3)$: 158.7, 150.0, 141.7, 122.6, 121.9, 53.4, 45.2, 34.2, 31.4 ppm. ν_{max} (DCM): 3054, 2987, 1633, 1599, 1561, 1476, 1413, 1308, 1219, 1118, 1063, 991 cm^{-1}. HR-MS: calcd $C_{24}H_{27}N_4O$, m/z: $[M+H]^+$, 387.2179. Found: 387.2164. [Diff(ppm)]: -4.01.

2.2.8 Metal complexes of **5**

General procedure:

Compound **5** (100 mg, 0.259 mmol) was dissolved in MeOH (10 mL). To this was added, dropwise, the appropriate metal salt (0.259 mmol) in MeOH (5 mL). A coloured solid precipitated immediately. The mixture was kept stirring for additional 2 hours. The coloured solid was collected by filtration, washed with MeOH and dried in oven overnight (75-80 ℃).

The ^1H NMR spectra of the complexes obtained from the reactions of ligand **5** with Zn(II) and Hg(II) salts are very broad and weak, indicating a polymeric type material is present. Furthermore, no hydrolysis of the ligand appears to have taken place.

2.2.9 2,6-bis((*E*)-((3-(1H-imidazol-1-yl)propyl)imino)methyl)-4-(tert-butyl)phenol (**6**)

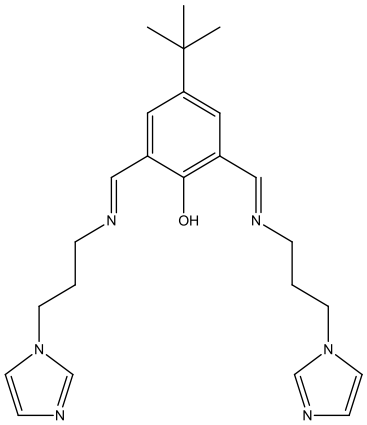

To a suspension of anhydrous $MgSO_4$ (1.46 g, 10.5 mmol) in CH_2Cl_2 was added compound **2** (0.5 g, 2.42 mmol). This was followed by 1-(3-aminopropyl)-imidazole (0.61 g, 4.84 mmol). The mixture was stirred at room temperature overnight. The resulting suspension was filtered, washed with CH_2Cl_2, and the filtrate was removed under vacuum to give compound **6** as yellow oil.

Yield: > 99 %. δ_H(CDCl3): 13.7 (1H, s, ArOH), 8.58 (2H, s, br, CH=N), 7.67 (2H, s, br, ArH), 7.50 (2H, s, imidazole-H), 7.09 (2H, s, imidazole-H), 6.96 (2H, s, imidazole-H), 4.09 (4H, t, N-CH_2, J = 6.9 Hz), 3.60 (4H, t, imidazole-CH_2, J = 6.4 Hz), 2.17-2.25 (4H, m, CH_2) ppm. δ_C($CDCl_3$): 158.6, 141.6, 137.2, 129.7, 118.7, 56.8, 53.4, 44.4, 34.1, 31.9, 31.4 ppm. ν_{max} (DCM): 3053, 2966, 2685, 1639, 1508, 1460, 1422, 1364, 1265, 1229, 1109, 1078, 895, 737, 663 cm^{-1}. HR-MS: calcd $C_{24}H_{33}N_6O$ m/z: $[M+H]^+$, 421.2716. Found: 421.2701. [Diff(ppm)]: -4.16.

2.2.10 Metal complexes of compound **6**

General procedure:

Compound **6** (55 mg, 0.129 mmol) was dissolved in MeOH (10 mL). To this was added, dropwise, the appropriate metal salt (0.129 mmol) in MeOH (5 mL). A coloured solid precipitated immediately. The mixture was kept stirring for an additional 2 hours. The coloured solid was collected by filtration, washed with MeOH and dried in oven overnight (75-80 ℃).

2.2.10.1 Reaction of **6** with $ZnCl_2$

Yellow solid. Yield: 50mg, 62%. δ_H(DMSO): 8.55 (2H, s, br, -CH=N-), 8.09 (2H, s, imidazole-H), 7.71 (2H, s, imidazole-H), 7.46 (2H, s, imidazole-H), 7.04 (2H, s, ArH), 4.15 (4H, s, br, -HC=N-CH_2), 3.58 (4H, s, br, imidazole-CH_2-), 2.16 (4H, s, br, CH_2-$\underline{CH_2}$-CH_2), 1.27 (9H, s, t-butyl) ppm. ν_{max} (KBr): 3437, 3122, 2959, 2869, 1656, 1632, 1538, 1456, 1236, 952, 754, 656 cm^{-1}. Calcd for: [Zn_2(**6**)Cl_3·MeOH], $C_{25}H_{39}Cl_3N_6O_2Zn_2$, C, 43.35; H, 12.13; N, 5.67 %. Found: C, 43.39; H, 4.77; N, 12.60 %.

2.2.10.2 Reaction of **6** with $Zn(ClO_4)_2 \cdot 6H_2O$

Yellow solid. Yield: 73 mg, 90%. δ_H(DMSO): 8.58 (2H, s, br, -CH=N-), 7.97 (2H, s, br, imidazole-H), 7.76 (2H, s, imidazole-H), 7.37 (2H, s, imidazole-H), 7.05 (2H, s, ArH), 4.10 (4H, s, br, -HC=N-CH_2), 3.56 (4H, s, br, N-CH_2-), 2.08 (4H, s, br, CH_2-$\underline{CH_2}$-CH_2), 1.27 (9H, s, t-butyl) ppm. ν_{max} (KBr): 3439, 3132, 2960, 2870, 1658, 1633, 1539, 1460, 1364, 1238, 1121, 841, 758, 623 cm^{-1}. Calcd for: [Zn(**6**)(ClO_4)·$4H_2O$], $C_{24}H_{39}ClN_6O_9Zn$, C, 43.91; H, 5.99; N, 12.80 %. Found: C, 43.79; H, 5.85; N, 12.42 %.

2.2.10.3 Reaction of **6** with $HgCl_2$

Yellow solid. Yield: 68mg, 54%. δ_H(DMSO): 8.59 (2H, s, br, -CH=N-), 7.98 (2H, s, br, imidazole-H), 7.77 (2H, s, imidazole-H), 7.48 (2H, s, imidazole-H), 7.05 (2H, s, ArH), 4.16 (4H, t, -HC=N-CH_2, J = 6.7 Hz), 3.56 (4H, t, imidazole-CH_2, J = 6 Hz), 2.15 (4H, m, CH_2-$\underline{CH_2}$-CH_2), 1.27 (9H, s, t-butyl) ppm. ν_{max} (KBr): 3415, 3119, 2955, 2865, 1638, 1526, 1456, 1362, 1234, 1109, 1025, 837, 751, 649 cm^{-1}. Calcd for: [Hg_2(**6**)Cl_3·(OMe)], $C_{25}H_{35}Cl_3Hg_2N_6O_2$, C, 31.31; H, 3.68; N, 8.76 %. Found: C, 32.08; H, 3.37; N, 9.37 %.

2.2.10.4 Reaction of **6** with $Hg(ClO_4)_2 \cdot H_2O$

Yellow solid. Yield: 87 mg, 67%. δ_H(DMSO): 13.77 (1H, s, br, ArOH), 8.56 (2H, s, br, -CH=N-), 8.29 (2H, s, br, imidazole-H), 7.75 (2H, s, imidazole-H), 7.72 (2H, s, ArH), 7.24 (2H, s, imidazole-H), 4.31 (4H, t, -HC=N-CH_2), 3.60 (4H, s, br, N-CH_2-), 2.21 (4H, s, br, CH_2-$\underline{CH_2}$-CH_2), 1.29 (9H, s, t-butyl) ppm. ν_{max} (KBr): 3445, 3134, 2960, 2870, 1640, 1528, 1459, 1364, 1236, 1108, 838, 754, 623 cm^{-1}. Calcd for: [Hg(**6**)$(ClO_4)_2$], $C_{24}H_{32}Cl_2HgN_6O_9$, C, 35.15; H, 3.93; N, 10.25 %. Found: C, 34.72; H, 3.82; N, 10.13 %.

2.2.10.5 Reaction of **6** with $Cu(ClO_4)_2 \cdot 6H_2O$

Green solid. Yield: 70 mg, 80%. ν_{max} (KBr): 3421, 3134, 2959, 2872, 1655, 1634, 1547, 1459, 1365, 1237, 1120, 844, 660, 624 cm^{-1}. Calcd for: [Cu(**6**)$(ClO_4)_2$·$2H_2O$],

$C_{24}H_{36}Cl_2CuN_6O_{11}$, C, 40.09; H, 5.05; N, 11.69 %. Found: C, 40.63; H, 5.04; N, 11.79 %. μ_{eff} = 1.91 B.M.

2.2.10.6 Reaction of **6** with $Ni(ClO_4)_2 \cdot 6H_2O$

Brown solid. Yield: 55 mg, 86%. ν_{max} (KBr): 3420, 3134, 2958, 2870, 1652, 1633, 1459, 1364, 1284, 1234, 1108, 941, 840, 624 cm^{-1}. Calcd for: [Ni(**6**)$(ClO_4)_2 \cdot H_2O$], $C_{24}H_{34}Cl_2N_6NiO_{10}$, C, 41.41; H, 4.92; N, 12.07 %. Found: C, 41.99; H, 4.85; N, 12.21 %. μ_{eff} = 3.13 B.M.

2.3 Section 2

2.3.1 5,5'-Methylene-bis-salicylaldehyde (**7**)[131]

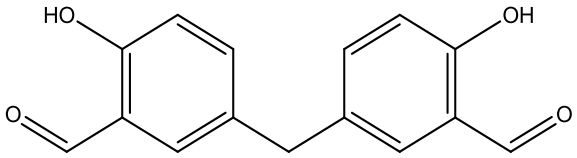

To a solution of 13.8 mL (16 g, 0.131 mol) of distilled salicylaldehyde in 10 mL of glacial acetic acid, in which 1.4 g (41.2 mmol) of trioxane was dissolved, a mixture of 0.1 mL of concentrated sulphuric acid and 0.5 mL of glacial acetic acid was added slowly with stirring under nitrogen atmosphere at 95 ℃. The stirring was continued for 24 hours at that temperature. The reaction mixture was then poured into 1 litre ice-cold water and allowed to stand overnight. The deposited solid was filtered and extracted twice with 100 mL of petroleum ether in order to remove unreacted salicylaldehyde. The isolated solid was then triturated three times with 40 mL of ether and recrystallized from 30 mL of acetone to obtain white crystals.[131]

Yield: 7.6 g, 37.5 %. $\delta_H(CDCl_3)$: 10.91 (2H, s, ArOH), 9.86 (2H, s, -CHO), 7.33 (4H, d, ArH), 6.96 (2H, s, ArH), 3.96 (2H, s, $ArCH_2Ar$) ppm. ν_{max} (KBr): 3438, 1655, 1482, 1275, 746 cm^{-1}. These match reported data.

2.3.2 (*E*)-4,4'-methylenebis(2-((*E*)-((pyridin-2-ylmethyl)imino)methyl)phenol) (**8**)

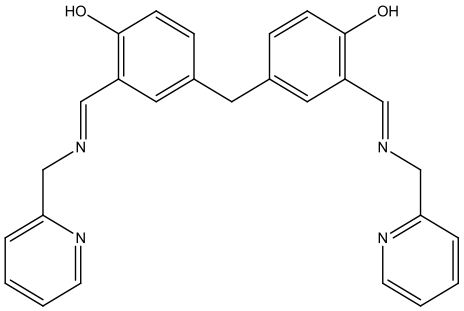

Compound **7** (1.28 g, 5 mmol) was dissolved in 50 mL of MeOH. To this was added, dropwise, 2-aminomethyl pyridine (1.08 g, 10 mmol) in MeOH (30 mL). The solvent was heated to reflux for 2 hours. Then the solvent was cooled down to room temperature. The excess solvent was reduced under vacuum. The yellow compound **8** will be formed as a yellow oil.

Yield: > 99 %. $\delta_H(CDCl_3)$: 13.15 (2H, s, br, ArOH), 8.56 (2H, d, py-H, J = 3.7 Hz), 8.48 (2H, s, -CH=N-), 7.68 (2H, dt, py-H, J = 7.9, 2.0 Hz), 7.34 (2H, d, ArH, J = 7.8 Hz), 7.13-7.27 (4H, m, py-H), 7.07 (2H, s, ArH), 6.91 (2H, d, ArH, J = 9.6 Hz), 4.92 (4H, s, $-CH_2-$), 3.88 (2H, s, $ArCH_2Ar$) ppm. $\delta_C(CDCl_3)$: 166.8, 159.4, 157.9, 149.4, 136.9, 133.1, 131.5, 122.4, 122.0, 118.6, 117.1, 65.11, 51.5, 39.7 ppm. ν_{max} (KBr): 3432, 1634, 1589, 1491, 1434, 1274, 1224, 821, 783, 754 cm^{-1}. HR-MS: calcd: $C_{27}H_{25}N_4O_2$ m/z: $[M+H]^+$, 438.2003. Found: 438.1992. [Diff(ppm)]: -2.47.

2.3.3 Metal complexes of **8**

General procedure:

Compound **7** (128 mg, 0.5 mmol) was dissolved in MeOH (20 mL). To this was added, dropwise, 2-aminometyl pyridine (108 mg, 1.0 mmol) in MeOH (10 mL). The solution was heated to reflux for 2 hours. Then the solution was cooled down to room temperature. The appropriate metal salt (1.0 mmol) in MeOH (10 mL) was added to solution. A coloured solid precipitated immediately. The mixture was kept stirring for additional 1 hour at room temperature. The coloured solid was collected by filtration, washed with MeOH, and dried in air overnight.

[a] If the complex was found as a very small, coloured suspension, which cannot be filtrated. Then the solution was removed under vacuum. MeOH (10 mL) was added, the

resulting solid was collected by filtration, washed with MeOH, and dried in air overnight.

[b] For the metal complexes of $Zn(SCN)_2$ and $Ni(SCN)_2$

Procedure:

Compound **7** (128 mg, 0.5 mmol) was dissolved in MeOH (20 mL). To this was added, dropwise, 2-aminometyl pyridine (108 mg, 1.0 mmol) in MeOH (10 mL). The solution was heated to reflux for 2 hours. Then the solution was cooled down to room temperature. $Zn(OAc)_2{\cdot}2H_2O$ or $Ni(OAc)_2{\cdot}4H_2O$ (1.0 mmol) in MeOH (10 mL) was added to solution. This was kept stirring for 30 min, with colour changed. Sodium thiocyanate (81 mg, 1.0 mmol) in 10 mL of MeOH was added to solution. A coloured solid precipitated immediately. The mixture was kept stirring for additional 1 hour at room temperature. The yellow solid was collected by filtration, washed with MeOH, and dried in air overnight.

2.3.3.1 Reaction of **8** with $Zn(OAc)_2{\cdot}2H_2O$, then with NaSCN

Yellow solid. Yield: 0.22 g, 62 %. δ_H(DMSO): 8.56 (2H, s, br, py-H), 8.50 (2H, s, CH=N-), 8.03 (2H, t, py-H, J = 7.3 Hz), 7.53-7.56 (4H, m, ArH, py-H), 7.01-7.05 (4H, m, py-H, ArH), 6.54 (2H, d, ArH, J = 8.1 Hz), 4.95 (4H, s, $-CH_2-$), 3.66 (2H, s, $ArCH_2Ar$) ppm. ν_{max} (KBr): 3432, 2902, 2079, 1634, 1474, 1395, 1283, 1158, 1049, 763 cm^{-1}. Calcd for: $[Zn_2(\mathbf{8})(SCN)_2{\cdot}MeOH]$, $C_{30}H_{26}N_6O_3S_2Zn_2$, C, 50.50; H, 3.67; N, 11.78 %. Found: C, 51.02; H, 3.47; N, 11.28 %.

2.3.3.2 Reaction of **8** with $Zn(OAc)_2{\cdot}2H_2O$

White crystals. Yield: 0.15 g, 49%. δ_H(DMSO): 8.56 (2H, d, py-H, J = 5.0 Hz), 8.51 (2H, s, CH=N-), 8.02 (2H, dt, py-H, J = 1.5, 7.7 Hz), 7.49-7.55 (4H, m, ArH, py-H), 7.07 (4H, s, br, ArH, py-H), 6.72 (2H, d, ArH, J = 9.1 Hz), 4.98 (4H, s, $N\text{-}CH_2\text{-}py$), 3.70 (2H, s, $ArCH_2Ar$), ppm. ν_{max} (KBr): 3433, 1639, 1593, 1573, 1484, 1418, 1397, 1283, 1049, 1021, 673 cm^{-1}. Calcd for: $C_{31}H_{28}N_4O_6Zn_2$, $[Zn_2(\mathbf{8})(OAc)_2]$, C, 54.49; H, 4.13; N, 8.20 %. Found: C, 54.34; H, 4.43; N, 7.85 %.

2.3.3.3 Reaction of **8** with $ZnCl_2$

Yellow solid. Yield: 0.23 g, 69 %. δ_H(DMSO): 8.58 (4H, br, -CH=N-, ArH), 7.94 (2H, br, py-H), 7.47 (4H, br, ArH, py-H), 7.10 (4H, br, py-H), 6.66 (2H, br, ArH), 4.93 (4H, s, $-CH_2-$), 3.74 (2H, s, $ArCH_2Ar$) ppm. ν_{max} (KBr): 3438, 2913, 1638, 1608, 1484, 1283,

1157, 1049, 766 cm^{-1}. Calcd for: [Zn_2(**8**)Cl_2·MeOH], $C_{28}H_{26}Cl_2N_4O_3Zn_2$, C, 50.33; H, 3.92; N, 8.38 %. Found: C, 49.67; H, 3.73; N, 8.06 %.

2.3.3.4 Reaction of **8** with $Ni(OAc)_2·4H_2O$, then with NaSCN

Green solid. Yield: 0.18 g, 54 %. ν_{max} (KBr): 3438, 2102, 1639, 1471, 1393, 1283, 1157, 764 cm^{-1}. Calcd for: [Ni_2(**8**)$(SCN)_2$], $C_{29}H_{22}N_6Ni_2O_2S_2$, C, 52.13; H, 3.31; N, 12.58 %. Found: C, 51.69; H, 3.57; N, 12.36 %. μ_{eff} = 3.54 B.M.

2.3.3.5 Reaction of **8** with $Ni(NO_3)_2·6H_2O$

Dark green solid. Yield: 0.12 g, 36 %. ν_{max} (KBr): 3408, 1642, 1608, 1484, 1384, 1283, 1050, 765 cm^{-1}. Calcd for: [Ni_2(**8**)(NO_3)·(OH)·MeOH], $C_{28}H_{27}N_5Ni_2O_7$, C, 50.56; H, 4.10; N, 10.56 %. Found: C, 50.29; H, 4.07; N, 11.02 %. μ_{eff} = 3.32 B.M.

2.3.3.6 Reaction of **8** with $NiCl_2·6H_2O$

Reddish solid. Yield: 0.21 g, 64 %. ν_{max} (KBr): 3406, 1641, 1608, 1484, 1050, 831, 765 cm^{-1}. Calcd for: [Ni_2(**8**)Cl_2·MeOH], $C_{28}H_{26}Cl_2N_4Ni_2O_3$, C, 51.36; H, 4.00; N, 8.56 %. Found: C, 52.20; H, 4.57; N, 8.07 %. μ_{eff} = 3.44 B.M.

2.3.3.7 Reaction of **8** with $Ni(ClO_4)_2·6H_2O$

Grey solid. Yield: 0.24 g, 43.2 %. ν_{max} (KBr): 3415, 1644, 1609, 1484, 1144, 1120, 1190, 1090, 966, 627 cm^{-1}. Calcd for: [Ni_2(**8**)(ClO_4)(OH)·2MeOH], $C_{29}H_{31}ClN_4Ni_2O_9$, C, 47.56; H, 4.27; N, 7.65 %. Found: C, 47.68; H, 4.21; N, 7.90 %. μ_{eff} = 3.38 B.M.

2.3.3.8 Reaction of **8** with $CuCl_2·2H_2O$

Green solid. Yield: 0.28 g, 81 %. ν_{max} (KBr): 3440, 1627, 1533, 1470, 1393, 1284, 1168, 832, 770 cm^{-1}. Calcd for: [Cu_2(**8**)Cl_2·$2H_2O$], $C_{27}H_{26}Cl_2Cu_2N_4O_4$, C, 48.51; H, 3.92; N, 8.38 %. Found: C, 48.54; H, 3.31; N, 8.42 %. μ_{eff} = 2.15 B.M.

2.3.3.9 Reaction of **8** with $Cu(OAc)_2·H_2O$

Green solid. Yield: 0.11 g, 30 %. ν_{max} (KBr): 3413, 1627, 1571, 1530, 1397, 1321, 1283, 1165, 768, 677 cm^{-1}. Calcd for: [Cu_2(**8**)$(OAc)_2$·$3H_2O$], $C_{31}H_{34}Cu_2N_4O_9$, C, 50.75; H, 4.67; N, 7.64 %. Found: C, 50.50; H, 4.30; N, 7.30 %. μ_{eff} = 2.18 B.M.

2.3.3.10 Reaction of **8** with $Cu(ClO_4)_2·6H_2O$

Dark green solid. Yield: 0.35 g, 88 %. ν_{max} (KBr): 3409, 1627, 1533, 1469, 1392, 1285, 1109(br), 768, 627 cm^{-1}. Calcd for: $C_{28}H_{26}Cl_2Cu_2N_4O_{11}$, [$Cu_2$(**8**)$(ClO_4)_2$·MeOH], C, 42.43; H, 3.31; N, 7.07 %. Found: C, 42.92; H, 2.98; N, 6.80 %. μ_{eff} = 2.16 B.M.

2.3.3.11 Reaction of **8** with $Co(SCN)_2$

Green solid. Yield: 0.24 g, 72%. ν_{max} (KBr): 3453, 2066, 1631, 1532, 1464, 1281, 1161, 1074, 765 cm^{-1}. Calcd for: $[Co^{(III)}Co^{(II)}(\mathbf{8})(SCN)_2(OH)\cdot H_2O]$, $C_{29}H_{25}Co_2N_6O_4S_2$, C, 49.51; H, 3.58; N, 11.95 %. Found: C, 50.23; H, 3.58; N, 11.86 %. μ_{eff} = 0.98 B.M.

2.3.3.12 Reaction of **8** with $CoCl_2\cdot 6H_2O$

Black solid. Yield: 0.125 g, 39 %. ν_{max} (KBr): 3413, 1633, 1533, 1465, 1281, 1073, 829, 768 cm^{-1}. Calcd for: $[Co_2(\mathbf{8})Cl_2\cdot H_2O]$, $C_{27}H_{24}Cl_2Co_2N_4O_3$, C, 50.57; H, 3.77; N, 8.74 %. Found: C, 50.96; H, 4.24; N, 8.16 %. μ_{eff} = 4.65 B.M.

2.3.4 (*E*)-4,4'-methylenebis(2-((*E*)-((pyridin-3-ylmethyl)imino)methyl)phenol) (**9**)

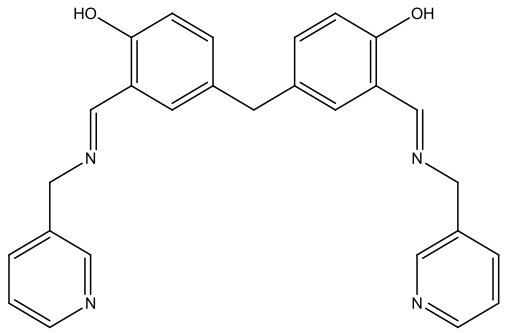

Compound **7** (1.28 g, 5 mmol) was dissolved in 50 mL of MeOH. To this was added, dropwise, 3-aminomethyl pyridine (1.08 g, 10 mmol) in MeOH (30 mL). The solution was heated to reflux for 2 hours. Then the solution was cooled down to room temperature. The excess solution was reduced to 15 mL under vacuum. The yellow compound **8** crystallized overnight.

Yield: 0.85 g, 40 %. $\delta_H(CDCl_3)$: 12.90 (2H, s, br, ArOH), 8.57 (2H, s, py-H), 8.54 (2H, dd, py-H, J = 4.8, 1.5 Hz), 8.41 (2H, s, CHN), 7.63 (2H, d, py-H, J = 7.8 Hz), 7.26-7.30 (2H, m, py-H), 7.16 (2H, dd, ArH, J = 8.4, 2.2 Hz), 7.04 (2H, s, ArH), 6.91 (2H, d, ArH, J = 8.4 Hz), 4.78 (4H, s, CH_2), 3.88 (2H, s, $ArCH_2Ar$) ppm. $\delta_C(CDCl_3)$: 166.3 159.3, 149.2, 148.9, 135.4, 133.7, 133.3, 131.4, 123.6, 118.4, 117.2, 60.7, 39.7 ppm. ν_{max} (KBr): 3450, 1640, 1592, 1575, 1492, 1422, 1280, 1227, 1065, 816 cm^{-1}. Calcd for: $C_{27}H_{24}N_4O_2$, C, 74.29; H, 5.54; N, 12.83. Found: C, 73.60; H, 6.00; N, 12.81. m.p: 103-104 ℃.

2.3.5 Metal complexes of compound **9**

General procedure:

Experimental

Compound **7** (128 mg, 0.5 mmol) was dissolved in MeOH (20 mL). To this was added, dropwise, 3-aminometyl pyridine (108 mg, 1.0 mmol) in MeOH (10 mL). The solution was heated to reflux for 2 hours. Then the solution was cooled down to room temperature. Metal salt (0.213 g, 1.0 mmol) in MeOH (10 mL) was added to solution. A coloured solid precipitated immediately. The mixture was kept stirring for additional 1 hour at room temperature. The coloured solid was collected by filtration, washed with MeOH, and dried in air overnight.

2.3.5.1 Reaction of **9** with $ZnCl_2$

Yellow solid. Yield: 0.25 g, 83 %. δ_H(DMSO): 12.98 (2H, s, br, ArOH), 8.69 (2H, s, CH=N-), 8.57 (2H, s, py-H), 8.51 (2H, d, py-H, J = 5.0 Hz), 7.78 (2H, d, ArH, J = 7.8 Hz), 7.40-7.44 (2H, m, py-H), 7.31 (2H, s, ArH), 7.21 (2H, d, py-H, J = 9.3 Hz), 6.83 (2H, d, ArH, J = 8.3 Hz), 4.83 (4H, s, N=CH_2-py), 3.85 (2H, s, ArCH_2Ar) ppm. ν_{max} (KBr): 3445, 1628, 1536, 1470, 1435, 1397, 1318, 1198, 1161, 1060, 823, 702 cm^{-1}. Calcd for: $C_{54}H_{48}Cl_6N_4O_2Zn_3$, [$Zn_3$(**9**)$_2Cl_6$], C, 50.60; H, 3.77; N, 8.74 %. Found: C, 51.38; H, 3.69; N, 8.59 %.

2.3.5.2 Reaction of **9** with $Zn(ClO_4)_2 \cdot 6H_2O$

Yellow solid. Yield: 0.28 g, 88 %. δ_H(DMSO): Can't dissolve in any solvent even in very hot DMSO. ν_{max} (KBr): 3427, 1621, 1536, 1472, 1436, 1400, 1121, 1108, 831, 624 cm^{-1}. Calcd for: [Zn(**9**)$(ClO_4)\cdot 2H_2O$], $C_{27}H_{27}ClN_4O_8Zn$, C, 50.96; H, 4.28; N, 8.80 %. Found: C, 51.22; H, 3.98; N, 8.78 %.

2.3.5.3 Reaction of **9** with $Zn(OAc)_2 \cdot 2H_2O$

Yellow solid. Yield: 0.30 g, 83 %. δ_H(DMSO): (only dissolved in hot DMSO) 8.49 (4H, br, CH=N-, py-H), 8.24 (2H, br, py-H), 7.78 (2H, br, py-H), 7.31 (2H, br, ArH), 7.11 (2H, br, py-H), 7.03 (2H, s, ArH), 6.57 (2H, br, ArH) 4.81 (4H, br, N-CH_2-py) 3.68 (2H, br, ArCH_2Ar) ppm. ν_{max} (KBr): 3419, 1626, 1533, 1470, 1433, 1397, 1196, 1156, 1056, 830, 702 cm^{-1}. Calcd for: [Zn_2(**9**)$(OAc)_2\cdot 2H_2O$], $C_{31}H_{32}N_4O_8Zn_2$, C, 51.75; H, 4.48; N, 7.79 %. Found: C, 51.91; H, 4.35; N, 8.14 %.

2.3.5.4 Reaction of **9** with $HgCl_2$

Yellow solid. Yield: 0.33 g, 76 %. δ_H(DMSO): 13.06 (2H, s, br, ArOH), 8.69 (2H, s, -CH=N-), 8.58 (2H, s, py-H), 7.51 (2H, d, py-H, J = 9.3 Hz), 7.75 (2H, d, ArH, J = 7.8), 7.37-7.41 (2H, m, py-H), 7.31 (2H, s, ArH), 7.19-7.23 (2H, m, py-H), 6.83 (2H, d, ArH, J = 8.3 Hz), 4.82 (4H, s, -CH_2-), 3.85 (2H, s, ArCH_2Ar) ppm. ν_{max} (KBr): 3445, 1633,

1490, 1433, 1274, 1048, 797, 704, 645 cm^{-1}. Calcd for: $[Hg_3(\mathbf{9})_2Cl_6]$, $C_{54}H_{48}Cl_6Hg_3N_8O_4$, C, 38.43; H, 2.87; N, 6.64 %. Found: C, 38.54; H, 2.78; N, 6.86 %.

2.3.5.5 Reaction of **9** with $NiCl_2 \cdot 6H_2O$

Green solid. Yield: 0.263 g, 85 %. ν_{max} (KBr): 3404, 1625, 1536, 1475, 1431, 1396, 1324, 1276, 1160, 1037, 830, 408 cm^{-1}. Calcd for: $[Ni_3(\mathbf{9})_2Cl_6]$, $C_{54}H_{48}Cl_6N_8Ni_3O_4$, C, 51.40; H, 3.83; N, 8.88 %. Found: C, 52.28; H, 4.28; N, 8.95 %. μ_{eff} = 3.40 B.M.

2.3.5.6 Reaction of **9** with $Ni(OAc)_2 \cdot 4H_2O$

Green solid. Yield: 0.335 g, 93 %. ν_{max} (KBr): 3430, 2902, 1624, 1539, 1475, 1430, 1397, 1324, 1160, 1036, 837, 708 cm^{-1}. Calcd for: $[Ni_2(\mathbf{9})(OAc)_2 \cdot MeOH \cdot H_2O]$, $C_{32}H_{34}N_4Ni_2O_8$, C, 53.38; H, 4.76; N, 7.78 %. Found: C, 53.19; H, 4.71; N, 8.66 %. μ_{eff} = 4.05 B.M.

2.3.5.7 Reaction of **9** with $Ni(ClO_4)_2 \cdot 6H_2O$

Green solid. Yield: 0.212 g, 65 %. ν_{max} (KBr): 3473, 1626, 1536, 1475, 1432, 1398, 1324, 1121, 834, 709, 636 cm^{-1}. Calcd for: $[Ni(\mathbf{9})(ClO_4) \cdot 2MeOH]$, $C_{29}H_{31}ClN_4NiO_8$, C, 52.96; H, 4.75; N, 8.52 %. Found: C, 52.94; H, 4.14; N, 7.98 %. μ_{eff} = 3.28 B.M.

2.3.5.8 Reaction of **9** with $Ni(NO_3)_2 \cdot 6H_2O$

Green solid. Yield: 0.266 g, 87 %. ν_{max} (KBr): 3410, 2904, 1626, 1535, 1475, 1432, 1384, 1323, 1160, 1037, 834, 708 cm^{-1}. Calcd for: $[Ni(\mathbf{9})(NO_3) \cdot 3H_2O]$, $C_{27}H_{29}N_5NiO_8$, C, 53.14; H, 4.79; N, 11.48 %. Found: C, 52.72; H, 4.21; N, 11.23 %. μ_{eff} = 3.37 B.M.

2.3.5.9 Reaction of **9** with $CuCl_2 \cdot 2H_2O$

Grey solid. Yield: 0.266 g, 77 %. ν_{max} (KBr): 3423, 1622, 1536, 1471, 1434, 1394, 1323, 1220, 1164, 1058, 830, 702 cm^{-1}. Calcd for: $[Cu_3(\mathbf{9})_2Cl_6 \cdot 4H_2O]$, $C_{54}H_{56}Cl_6Cu_3N_8O_8$, C, 48.10; H, 4.19; N, 8.31 %. Found: C, 47.17; H, 3.86; N, 7.88 %. μ_{eff} = 2.03 B.M.

2.3.5.10 Reaction of **9** with $Cu(OAc) \cdot 2H_2O$

Green solid. Yield: 0.21 g, 62 %. ν_{max} (KBr): 3412, 1622, 1536, 1472, 1428, 1393, 1324, 1163, 830, 708 cm^{-1}. Calcd for: $[Cu_2(\mathbf{9})(OAc)_2]$, $C_{31}H_{28}Cu_2N_4O_6$, C, 54.78; H, 4.15; N, 8.24 %. Found: C, 54.20; H, 4.26; N, 8.45 %. μ_{eff} = 2.17 B.M.

2.3.5.11 Reaction of **9** with $Cu(ClO_4)_2 \cdot 6H_2O$

Green solid. Yield: 0.295 g, 84 %. ν_{max} (KBr): 3442, 1622, 1536, 1472, 1433, 1395, 1323, 1109, 1091, 831, 706, 626 cm^{-1}. Calcd for: [Cu(**9**)$(ClO_4)_2$], $C_{27}H_{24}Cl_2CuN_4O_{10}$, C, 46.40; H, 3.46; N, 8.02 %. Found: C, 46.30; H, 3.71; N, 7.95 %. μ_{eff} = 2.21 B.M.

2.3.5.12 Reaction of **9** with $CoCl_2 \cdot 6H_2O$

Green solid. Yield: 0.222 g, 76 %. ν_{max} (KBr): 3430, 1619, 1535, 1470, 1432, 1395, 1315, 1192, 1161, 1054, 828, 707 cm^{-1}. Calcd for: [Co_3(**9**)$_2Cl_2 \cdot 4H_2O$], $C_{54}H_{56}Cl_6Co_3N_8O_8$, C, 48.60; H, 4.23; H, 8.40 %. Found: C, 48.84; H, 4.16; N, 8.56 %. μ_{eff} = 4.71 B.M.

2.3.5.13 Reaction of **9** with $Co(ClO_4)_2 \cdot 6H_2O$

Green solid. Yield: 0.24 g, 77 %. ν_{max} (KBr): 3437, 1619, 1537, 1471, 1430, 1395, 1316, 1121, 1108, 832, 711 cm^{-1}. Calcd for: $C_{29}H_{31}ClCoN_4O_8$, [Co(**9**)$(ClO_4)\cdot 2MeOH$], C, 52.93; H, 4.74; N, 8.51 %. Found: C, 53.29; H, 3.78; N, 8.27 %. μ_{eff} = 4.82 B.M.

2.3.5.14 Reaction of **9** with $Co(SCN)_2$

Green solid. Yield: 0.253 g, 80 %. ν_{max} (KBr): 3438, 2068, 1620, 1535, 1471, 1431, 1394, 1316, 1277, 1160, 1036, 826, 708 cm^{-1}. Calcd for: [Co(**9**)$(CSN)\cdot H_2O$], $C_{28}H_{25}CoN_5O_3S$, C, 58.95; H, 4.42; N, 12.28 %. Found: C, 59.40; H, 3.93; N, 12.77 %. μ_{eff} = 5.12 B.M.

2.3.6 (*E*)-4,4'-methylenebis(2-((*E*)-((pyridin-4-ylmethyl)imino)methyl)phenol) (**10**)

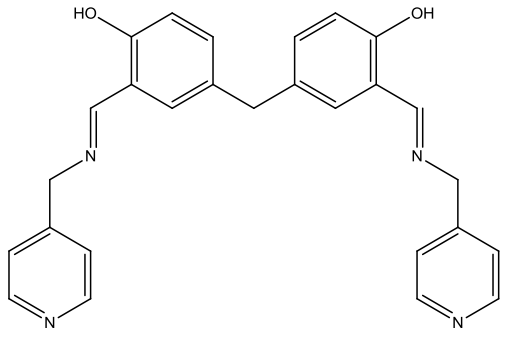

Compound **7** (1.28 g, 5 mmol) was dissolved in 50 mL of MeOH. To this was added, dropwise, 4-aminomethyl pyridine (1.08 g, 10 mmol) in MeOH (30 mL). The solvent was heated to reflux for 2 hours. Then the solvent was cooled down to room temperature. The excess solvent was reduced to 15 mL under vacuum to give compound **10** as a yellow oil.

Yield: 2 g, 94 %. $\delta_H(CDCl_3)$: 12.92 (2H, s, ArOH), 8.56-8.58 (4H, dd, py-H, J = 4.5, 1.6 Hz), 8.41 (2H, s, CH=N-), 7.23 (4H, d, py-H, J = 5.8 Hz), 7.18 (2H, dd, ArH, J = 8.4, 2.2 Hz), 7.05 (2H, s, ArH), 6..94 (2H, d, ArH, J = 8.5 Hz), 4.87 (4H, s, =N-CH_2-py), 3.89 (2H, s, ArCH_2Ar) ppm. $\delta_C(CDCl_3)$: 167.0, 159.3, 150.0, 147.1, 133.4, 131.5, 122.4, 118.4, 117.2, 62.0, 53.4, 39.7 ppm. ν_{max} (DCM): 3410, 3054, 2945, 2833, 1636, 1605, 1492, 1421, 1281, 1027, 896 739 cm^{-1}. HR-MS: calcd: $C_{27}H_{25}N_4O_2$ m/z: $[M+H]^+$, 438.2003. Found: 438.1995. [Diff(ppm)]: -1.98.

2.3.7 Metal complexes of compound **10**

General procedure:

Compound **7** (128 mg, 0.5 mmol) was dissolved in MeOH (20 mL). To this was added, dropwise, 4-aminometyl pyridine (108 mg, 1.0 mmol) in MeOH (10 mL). The solution was heated to reflux for 2 hours. Then the solution was cooled down to room temperature. The appropriate metal salt (0.213 g, 1.0 mmol) in MeOH (10 mL) was added to solution. A coloured solid precipitated immediately. The mixture was kept stirring for additional 1 hour at room temperature. The coloured solid was collected by filtration, washed with MeOH, and dried in air overnight.

[a] If the complex was found as a very small, coloured suspension, which cannot be filtrated. Then the solution was removed under vacuum. MeOH (10 mL) was added, the resulting solid was collected by filtration, washed with MeOH, and dried in air overnight.

2.3.7.1 Reaction of **10** with $ZnCl_2$

Yellow solid. Yield: 0.293 g, 96 %. δ_H(DMSO): 12.95 (2H, s, ArOH), 8.69 (2H, s, -CH=N-), 8.54 (4H, d, py-H, J = 5.9 Hz), 7.36 (4H, d, py-H, J = 5.7 Hz), 7.32 (2H, s, ArH), 7.23 (2H, s, br, ArH), 6.84 (2H, d, ArH, J = 8.4 Hz), 4.84 (4H, s, =N-CH_2-), 3.86 (2H, br, ArCH_2Ar) ppm. ν_{max} (KBr): 3425, 1621, 1536, 1492, 1473, 1431, 1277, 1224, 1161, 1067, 1031, 817 cm^{-1}. Calcd for: [Zn(**10**)Cl_2·$2H_2O$], $C_{27}H_{28}Cl_2N_4O_4Zn$, C, 53.27; H, 4.64; N, 9.20 %. Found: C, 53.94; H, 4.10; N, 9.05 %.

2.3.7.2 Reaction of **10** with $Zn(OAc)_2$·$2H_2O$

Yellow solid. Yield: 0.334 g, 92 %. δ_H(DMSO): can't dissolve in hot DMSO. ν_{max} (KBr): 3424, 2896, 1619, 1537, 1475, 1430, 1398, 1316, 1162, 1030, 815, 684 cm^{-1}. Calcd for: [Zn_2(**10**)$(OAc)_2$·$2H_2O$·2MeOH], $C_{31}H_{32}N_4O_8Zn_2$, C, 51.75; H, 4.48; N, 7.79 %. Found: C, 52.09; H, 4.45; N, 7.62 %.

2.3.7.3 Reaction of **10** with $Zn(ClO_4)_2 \cdot 6H_2O$

Yellow solid. Yield: 0.264 g, 81 %. δ_H(DMSO): (can't dissolve in any solvents even hot DMSO) ν_{max} (KBr): 3445, 1621, 1537, 1473, 1431, 1399, 1313, 1277, 1121, 1109, 816, 625 cm^{-1}. Calcd for: [Zn(**10**)$(ClO_4)\cdot 3H_2O$], $C_{27}H_{29}ClN_4O_9Zn$, C, 49.56; H, 4.47; N, 8.56 %. Found: C, 50.02; H, 4.13; N, 8.05 %.

2.3.7.4 Reaction of **10** with $HgCl_2$

Yellow solid. Yield: 0.35 g, 65 %. δ_H(DMSO): 8.71 (2H, s, CHN), 8.57 (4H, d, py-H, J = 6 Hz), 7.40 (4H, d, py-H, J = 6.4 Hz), 7.33 (2H, s, ArH), 7.24 (2H, dd, ArH, J = 7.3, 2.0 Hz), 6.86 (2H, d, ArH, J = 8.6 Hz), 4.86 (4H, s, N-CH_2-py), 3.87 (2H, s, $ArCH_2Ar$) ppm. ν_{max} (KBr): 3473, 1632, 1607, 1492, 1423, 1381, 1273, 1222, 1156, 1064, 1013, 818 cm^{-1}. Calcd for: $C_{27}H_{26}Cl_2Hg_2N_4O_4$, [$Hg_2$(**10**)$Cl_2\cdot 2H_2O$], C, 34.40; H, 2.78; N, 5.94 %. Found: C, 34.01; H, 3.21; N, 5.85 %.

2.3.7.5 Reaction of **10** with $NiCl_2 \cdot 6H_2O$

Green solid. Yield: 0.288 g, 96 %. ν_{max} (KBr): 3442, 1622, 1536, 1474, 1424, 1396, 1321, 1276, 1222, 1160, 815, 620 cm^{-1}. Calcd for: [Ni(**10**)$Cl_2\cdot 2H_2O$], $C_{27}H_{28}Cl_2N_4NiO_4$, C, 53.86; H, 4.69; N, 9.30 %. Found: C, 53.94; H, 4.66; N, 8.46 %. μ_{eff} = 3.46 B.M.

2.3.7.6 Reaction of **10** with $Ni(OAc)_2 \cdot 4H_2O$[a]

Green solid. Yield: 0.3 g, 85 %. ν_{max} (KBr): 3436, 1622, 1540, 1475, 1423, 1398, 1323, 1221, 1161, 815 cm^{-1}. Calcd for: [Ni_2(**10**)$(OAc)_2\cdot 2MeOH\cdot 2H_2O$], $C_{31}H_{32}N_4Ni_2O_8$, C, 52.73; H, 4.56; N, 7.93 %. Found: C, 53.40; H, 4.83; N, 8.23 %. μ_{eff} = 4.03 B.M.

2.3.7.7 Reaction of **10** with $Ni(ClO_4)_2 \cdot 6H_2O$

Green solid. Yield: 0.28 g, 85 %. ν_{max} (KBr): 3453, 2906, 1622, 1536, 1474, 1424, 1397, 1322, 1276, 1222, 1120, 1108, 824, 626 cm^{-1}. Calcd for: [Ni(**10**)$(ClO_4)\cdot 2MeOH$], $C_{29}H_{31}ClN_4NiO_8$, C, 52.96; H, 4.75; N, 8.52 %. Found: C, 53.65; H, 4.52; N, 8.18 %. μ_{eff} = 2.97 B.M.

2.3.7.8 Reaction of **10** with $Ni(NO_3)_2 \cdot 6H_2O$

Green solid. Yield: 0.295 g, 94 %. ν_{max} (KBr): 3416, 1622, 1535, 1475, 1384, 1322, 814 cm^{-1}. Calcd for: [Ni(**10**)$(NO_3)\cdot MeOH\cdot 2H_2O$], $C_{28}H_{32}N_5NiO_8$, C, 53.78; H, 5.16; N, 11.20 %. Found: C, 53.79; H, 4.42; N, 11.16 %. μ_{eff} = 3.31 B.M.

2.3.7.9 Reaction of **10** with $CuCl_2 \cdot 2H_2O$

Brown green solid. Yield: 0.313 g, 94 %. ν_{max} (KBr): 3436, 1619, 1535, 1470, 1427, 1393, 1320, 1222, 1065, 824 cm^{-1}. Calcd for: $[Cu_2(\mathbf{10})Cl_2 \cdot MeOH]$, $C_{28}H_{26}Cl_2Cu_2N_4O_3$, C, 50.61; H, 3.94; N, 8.43 %. Found: C, 50.19; H, 4.05; N, 8.99 %. μ_{eff} = 2.11 B.M.

2.3.7.10 Reaction of **10** with $Cu(OAc)_2 \cdot H_2O$

Brown green solid. Yield: 0.319 g, 97 %. ν_{max} (KBr): 3430, 1621, 1536, 1471, 1425, 1394, 1325, 1221, 1164, 830 cm^{-1}. Calcd for: $[Cu_2(\mathbf{10})(OAc)_2]$, $C_{31}H_{28}Cu_2N_4O_6$, C, 54.78; H, 4.15; N, 8.24 %. Found: C, 55.07; H, 4.60; N, 8.77 %. μ_{eff} = 2.16 B.M.

2.3.7.11 Reaction of **10** with $Cu(ClO_4)_2 \cdot 6H_2O$

Green solid. Yield: 0.35 g, 95 %. ν_{max} (KBr): 3473, 1622, 1536, 1472, 1427, 1395, 1323, 1222, 1144, 1120, 1090, 825, 627 cm^{-1}. Calcd for: $[Cu_2(\mathbf{10})(ClO_4)_2 \cdot 2H_2O]$, $C_{27}H_{26}Cl_2Cu_2N_4O_{12}$, C, 40.71; H, 3.29; N, 7.03 %. Found: C, 40.83; H, 3.50; N, 7.52 %. μ_{eff} = 2.21 B.M.

2.3.7.12 Reaction of **10** with $CoCl_2 \cdot 6H_2O$

Black solid. Yield: 0.35 g, 99 %. ν_{max} (KBr): 3401, 2898, 1616, 1537, 1471, 1426, 1391, 1310, 1276, 1220, 1162, 1066, 1052, 815 cm^{-1}. Calcd for: $[Co(\mathbf{10})Cl_2 \cdot MeOH \cdot H_2O]$, $C_{28}H_{30}Cl_2CoN_4O_4$, C, 54.56; H, 4.91; N, 9.09 %. Found: C, 54.35; N, H, 4.43; 9.24 %. μ_{eff} = 5.03 B.M.

2.3.7.13 Reaction of **10** with $Co(ClO_4)_2 \cdot 6H_2O$

Green solid. Yield: 0.31 g, 97 %. ν_{max} (KBr): 3428, 1619, 1536, 1471, 1423, 1395, 1315, 1277, 1221, 1121, 1108, 1090, 819, 626 cm^{-1}. Calcd for: $[Co(\mathbf{10})(ClO_4) \cdot 2H_2O]$, $C_{27}H_{27}ClCoN_4O_8$, C, 51.48; H, 4.32; N, 8.89 %. Found: C, 51.94; H, 4.16; N, 8.45 %. μ_{eff} = 3.41 B.M.

2.3.7.14 Reaction of **10** with $Co(SCN)_2$

Green solid. Yield: 0.3 g, 93 %. ν_{max} (KBr): 3432, 2904, 2070, 1633, 1608, 1491, 1422, 1394, 1314, 1222, 816 cm^{-1}. Calcd for: $[Co_2(\mathbf{10})(SCN)_2 \cdot 2MeOH \cdot 2H_2O]$, $C_{29}H_{26}Co_2N_6O_6S_2$, C, 49.44; H, 3.72; N, 11.93 %. Found: C, 50.27; H, 4.23; N, 12.28 %. U_{eff} = 4.23 B.M.

2.3.8 (*E*)-4,4'-methylenebis(2-((*E*)-((3-(1H-imidazol-1-yl)propyl)imino)methyl)phenol) (**11**)

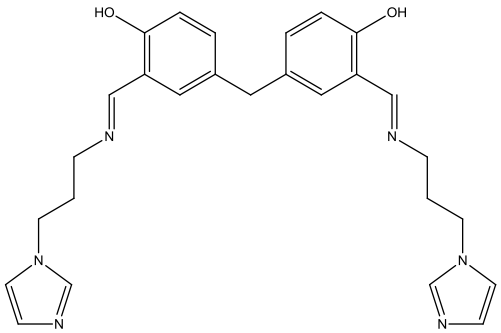

Yield: 2.2 g, 93 %. δ_H($CDCl_3$): 13.04 (2H, s, ArOH), 8.28 (2H, s, CH=N-), 7.45 (2H, s, imidazole-H), 7.16 (2H, dd, ArH, J = 8.4, 2.5 Hz), 7.07 (2H, s, imidazole-H), 7.02 (2H, s, ArH), 6.90-6.92 (4H, m, imidazole-H, ArH), 4.06 (4H, t, =N-CH_2, J = 6.8 Hz), 3.87 (2H, s, ArCH_2Ar), 3.52 (4H, t, CH_2-imidazole, J = 6.6 Hz), 2.13-2.22 (4H, m, =NCH_2-$\underline{CH_2}$-) ppm. δ_C($CDCl_3$): 166.2, 159.3, 137.1, 133.1, 132.5, 131.5, 129.8, 118.8, 117.1, 55.8, 44.2, 39.7, 31.7 ppm. ν_{max} (DCM): 3584, 3054, 2987, 1636, 1506, 1493, 1437, 1421, 1078, 896, 738 cm^{-1}. HR-MS: calcd: $C_{27}H_{31}N_6O_2$ m/z: $[M+H]^+$, 471.2508. Found: 471.2497. [Diff(ppm)]: -3.06.

2.3.9 The metal complexes of compound **11**

General procedure:

Compound **7** (128 mg, 0.5 mmol) was dissolved in MeOH (20 mL). To this was added, dropwise, 1-(3-Aminopropyl)-imidazole (125 mg, 1.0 mmol) in MeOH (10 mL). The solution was heated to reflux for 2 hours. Then the solution was cooled down to room temperature. The appropriate metal salt (0.136 g, 1.0 mmol) in MeOH (10 mL) was added to solution. A coloured solid precipitated immediately. The mixture was kept stirring for additional 1 hour at room temperature. The coloured solid was collected by filtration, washed with MeOH, and dried in air overnight.

[a] If the complex was found as a very small, coloured suspension, which cannot be filtrated. Then the solution was removed under vacuum. MeOH (10 mL) was added, the resulting solid was collected by filtration, washed with MeOH, and dried in air overnight.

2.3.9.1 Reaction of **11** with $ZnCl_2$

Yellow solid. Yield: 0.338 g, 96 %. ν_{max} (KBr): 3484, 3122, 2930, 1626, 1533, 1473, 1399, 1276, 1096, 953, 832, 656 cm^{-1}. Calcd for: $[Zn_3(\mathbf{11})_2Cl_4{\cdot}4H_2O]$, $C_{54}H_{66}Cl_4N_{12}O_8Zn_3$, C, 48.07; H, 4.93; N, 12.46 %. Found: C, 47.77; H, 4.57; N, 12.56 %.

2.3.9.2 Reaction of **11** with $Zn(ClO_4)_2{\cdot}6H_2O$

Yellow solid. Yield: 0.308 g, 84 %. δ_H(DMSO):13.00-13.50 (2H, br, ArOH), 8.46 (2H, s, CH=N-), 8.08 (2H, s, imidazole-H), 7.47 (2H, s, imidazole-H), 7.20-7.23 (4H, m, ArH), 7.09 (2H, s, imidazole-H), 6.81-6.83 (2H, d, ArH, J = 7.6 Hz), 4.11 (4H, t, CH=N-CH_2, J = 7.6), 3.82 (2H, s, $ArCH_2Ar$), 3.52-3.55 (4H, t, CH_2-imidazole, J = 5.5 Hz), 2.08-2.17 (4H, m, CH=N-$CH_2\underline{CH_2}$) ppm. ν_{max} (KBr): 3450, 3131, 2941, 1630, 1537, 1493, 1475, 1276, 1244, 1120, 1108, 624 cm^{-1}. Calcd for: $[Zn(\mathbf{11})(ClO_4)_2]$, $C_{27}H_{30}Cl_2N_6O_{10}Zn$, C, 44.13; H, 4.11; N, 11.44 %. Found: C, 44.63; H, 4.46; N, 11.35 %.

2.3.9.3 Reaction of **11** with $Zn(OAc)_2{\cdot}2H_2O$[a]

Yellow solid. Yield: 0.336 g, 87%. δ_H(DMSO): (Can't dissolve in DMSO). ν_{max} (KBr): 3417, 3126, 2928, 1625, 1533, 1474, 1398, 1320, 1095, 952, 825, 958 cm^{-1}. Calcd for: $[Zn_2(\mathbf{11})(OAc)_2{\cdot}3H_2O]$, $C_{31}H_{30}N_6O_9Zn_2$, C, 48.26; H, 5.23; N, 10.89 %. Found: C, 48.08; H, 5.04; N, 10.57 %.

2.3.9.4 Reaction of **11** with $HgCl_2$

Yellow solid. Yield: 0.492 g, 99 %. δ_H(DMSO): 13.09 (2H, s, br, ArOH), 8.47 (2H, s, CH=N-), 7.92 (2H, s, imidazole-H), 7.38 (2H, s, ArH), 7.30 (2H, d, imidazole-H, J = 8.3 Hz), 7.20 (2H, dd, ArH, J = 8.6, 2.2 Hz), 7.01 (2H, d, imidazole-H, J = 7.7 Hz), 6.82 (2H, d, ArH, J = 8.0 Hz), 4.09-4.11 (4H, m, =N-CH_2-), 3.82 (2H, s, $ArCH_2Ar$), 3.49-3.53 (4H, m, =N-$CH_2CH_2\underline{CH_2}$), 2.10-2.15 (4H, m, =N-$CH_2\underline{CH_2}CH_2$) ppm. ν_{max} (KBr): 3452, 3120, 2930, 2850, 1633, 1518, 1492, 1452, 1273, 1235, 1109, 826, 750, 648 cm^{-1}. Calcd for: $[Hg_2(\mathbf{11})Cl_4]$, $C_{27}H_{30}Cl_4Hg_2N_6O_5$, C 32.00; H, 2.98; N, 8.29 %. Found: 32.35; H, 3.45; N, 8.92 %.

2.3.9.5 Reaction of 11 with $Ni(OAc)_2{\cdot}4H_2O$[a]

Green solid. Yield: 0.306 g, 71 %. ν_{max} (KBr): 3415, 3130, 2929, 1631, 1547, 1479, 1399, 1311, 1277, 1109, 942, 833, 663 cm^{-1}. Calcd for: $[Ni_2(\mathbf{11})(OAc)_2{\cdot}2H_2O{\cdot}2MeOH]$,

$C_{33}H_{46}N_6Ni_2O_{10}$, C, 49.29; H, 5.77; N, 10.45 %. Found: C, 48.61; H, 5.44; N, 10.37 %. μ_{eff} = 4.42 B.M.

2.3.9.6 Reaction of **11** with $Ni(ClO_4)_2 \cdot 6H_2O$

Green solid. Yield: 0.285 g, 72 %. ν_{max} (KBr): 3424, 3133, 2939, 1628, 1527, 1492, 1398, 1279, 1232, 1108, 1092, 833, 663, 625 cm^{-1}. Calcd for: [Ni(**11**)$(ClO_4)_2 \cdot 2MeOH$], $C_{29}H_{38}Cl_2N_6NiO_{12}$, C, 43.97; H, 4.83; N, 10.61 %. Found: C, 43.97; H, 4.61; N, 10.16 %. μ_{eff} = 4.23 B.M.

2.3.9.7 Reaction of **11** with $CuCl_2 \cdot 2H_2O$

Grey solid. Yield: 0.32 g, 85 %. ν_{max} (KBr): 3441, 3130, 2930, 1623, 1535, 1473, 1395, 1322, 1292, 1228, 1095, 831, 654 cm^{-1}. Calcd for: [Cu_2(**11**)$Cl_3 \cdot 2H_2O$], $C_{27}H_{33}Cl_3Cu_2N_6O_4$, C, 43.88; H, 4.50; N, 11.37 %. Found: C, 43.27; H, 4.18; N, 10.92 %. μ_{eff} = 1.82 B.M.

2.3.9.8 Reaction of **11** with $Cu(ClO_4)_2 \cdot 6H_2O$

Brown green solid. Yield: 0.34 g, 80 %. ν_{max} (KBr): 3426, 3133, 2936, 1623, 1536, 1475, 1396, 1318, 1283, 1143, 1120, 1109, 831, 626 cm^{-1}. Calcd for: [Cu_2(**11**)$(ClO_4)_2 \cdot 3H_2O$], $C_{27}H_{34}Cl_2Cu_2N_6O_{13}$, C, 38.22; H, 4.04; N, 9.90 %. Found: C, 38.80; H, 3.91; N, 9.53 %. μ_{eff} = 2.14 B.M.

2.3.9.9 Reaction of **11** with $CoCl_2 \cdot 6H_2O$

Green solid. Yield: 0.355 g, 97 %. ν_{max} (KBr): 3435, 3123, 2933, 1619, 1533, 1470, 1397, 1314, 1277, 1232, 1161, 1095, 829, 657 cm^{-1}. Calcd for: [Co_3(**11**)$_2Cl_4 \cdot 4H_2O$], $C_{54}H_{66}Cl_3Co_3N_{12}O_8$, C, 48.77; H, 5.00; N, 12.64 %. Found: C, 48.27; H, 4.37; N, 12.38 %. μ_{eff} = 5.78 B.M.

2.3.9.10 Reaction of **11** with $Co(SCN)_2$

Dark green solid. Yield: 0.356 g, 99 %. ν_{max} (KBr): 3428, 3122, 2924, 2066, 1633, 1522, 1491, 1274, 1229, 1107, 1092, 827, 658 cm^{-1}. Calcd for: [Co(**11**)$(SCN)_2 \cdot 4H_2O$], $C_{29}H_{38}CoN_8O_6S_2$, C, 48.53; H, 5.34; N, 15.61 %. Found: C, 48.99; H, 5.35; N, 15.59 %. μ_{eff} = 4.63 B.M.

2.3.9.11 Reaction of **11** with $Co(ClO_4)_2 \cdot 6H_2O$

Brown green solid. Yield: 0.362 g, %. ν_{max} (KBr): 3424, 3132, 2943, 1620, 1534, 1472, 1397, 1278, 1108, 831, 625 cm^{-1}. Calcd for: [Co(**11**)$(ClO_4)_2$], $C_{27}H_{30}Cl_2N_6O_{10}$, C, 44.52; H, 4.15; N, 11.54 %. Found: C, 45.07; H, 4.29; N, 11.54 %. μ_{eff} = 4.62 B.M.

2.4 Section 3

2.4.1 Dipicolinic acid (**12**)[132]

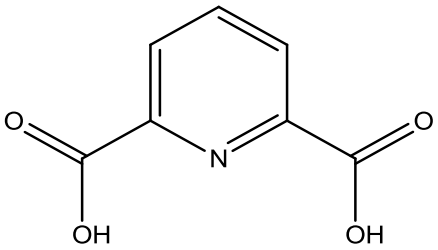

A mixture of $KMnO_4$ (8.848 g, 56 mmol) and 2,6-dimethylpyridine (1.2 mL, 10 mmol) in water (85 mL) was heated to reflux for 5 h, and on cooling, the inorganic salts were removed by filtration. Then the filtrate was concentrated to the 1/5 of original volume. Finally, when the pH value of the mixture was adjusted to 2 by using 70% H_2SO_4, compound **12** was obtained as a white solid. Yield: 90 %, m.p. 226-227 ℃.[132] These match reported data.

2.4.2 Dimethyl dipicolinate (**13**)[133]

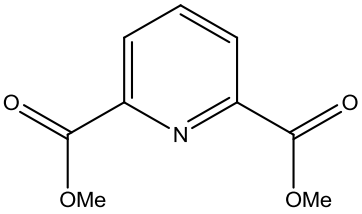

A solution of dipicolinic acid (**12**) (4 g, 24 mmol) in MeOH (50 mL) and conc. H_2SO_4 (10 mL) was heated for 18 h. Water (30 mL) was added and the aqueous solution was neutralised with saturated sodium carbonate solution. The resulting solution was extracted with $CHCl_3$ (3 × 40 ml). The combined extracts were dried with $MgSO_4$, filtered and the solvent was removed under vacuum to give a white solid.[133]

Yield: 1.82 g, 61 %. $\delta_H(CDCl_3)$: 8.32 (2H, d, py-H), 8.03 (1H, t, py-H), 4.03 (6H, s, OMe) ppm. These match reported data.

2.4.3 N^2,N^6-bis(pyridin-3-ylmethyl)pyridine-2,6-dicarboxamide (**14**)

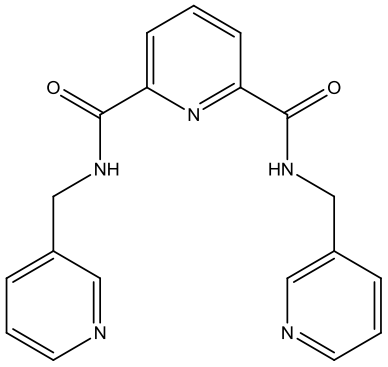

To a solution of compound **13** (1.95 g, 10 mmol) in toluene (50 mL) was added 3-aminomethyl pyridine (4.32 g, 40 mmol). The suspension was then refluxed for 48 h. The solution was then cooled down to room temperature, and reduced under vacuum to give a crude yellow oil. The oil was redissolved in $CHCl_3$ (50 mL), washed with H_2O (4 × 40 mL). The organic layer was dried with $MgSO_4$, filtered, and concentrated under vacuum to give compound **14** as yellow oil. This was recrystallized from benzene to give off-white crystals.

Yield: 1.5 g, 43 %. $\delta_H(CDCl_3)$: 8.86 (2H, t, CONH, J = 6.0 Hz), 8.41-8.43 (4H, m, py-H), 8.23 (2H, s, py-H), 8.09 (1H, t, py-H, J = 8.0 Hz), 7.61 (2H, d, py-H, J = 8 Hz), 7.20 (2H, dd, py-H, J = 5.0, 7.9 Hz), 4.48-4.50 (4H, d, CH_2, J = 6.3 Hz) ppm. $\delta_C(CDCl_3)$: 163.9, 148.7, 148.6, 139.1, 135.9, 134.3, 125.4, 123.8, 40.5 ppm. ν_{max} (KBr): 3551, 3319, 3262, 3091, 1674, 1660, 1534, 1435, 1170, 1077, 999, 812 cm^{-1}. Calcd for: $C_{19}H_{17}N_5O_2$, C, 65.69; H, 4.93; N, 20.16 %. Found: C, 65.29; H, 4.21; N, 19.74 %. m.p: 168-169 ℃.

2.4.4 Metal complexes of **14**

General procedure:

Compound **14** (100 mg, 0.289 mmol) was dissolved in MeOH (20 mL). To this was added, dropwise, the appropriate metal salt (0.289 mmol) in MeOH (10 mL). A coloured solid precipitated immediately. The mixture was kept stirring for an additional 1 hour at room temperature. The coloured solid was collected by filtration, washed with MeOH, and dried in air overnight.

[a] If the complex was found as a very small, coloured suspension, which cannot be filtrated. Then the solution was removed under vacuum. MeOH (10 mL) was added, the resulting solid was collected by filtration, washed with MeOH, and dried in air overnight.

2.4.4.1 Reaction of **14** with $ZnCl_2$

White solid. Yield: 0.138 g, 92 %. δ_H(DMSO): 9.92 (2H, t, CONH, J = 6.2 Hz), 8.59 (2H, s, py-H), 8.48 (2H, s, br, py-H), 8.20-8.27 (3H, m, py-H), 7.79 (2H, d, py-H, J = 7.7 Hz), 7.39-7.44 (2H, m, py-H), 4.64 (4H, d, CH_2, J = 6.1 Hz) ppm. ν_{max} (KBr): 3350, 1675, 1610, 1529, 1440, 1311, 1171, 1059, 1003, 700 cm^{-1}. Calcd for: [Zn(**14**)Cl_2·$2H_2O$], $C_{19}H_{21}Cl_2N_5O_4Zn$, C, 43.91; H, 4.07; N, 13.48 %. Found: C, 44.01; H, 3.35; N, 13.34 %.

2.4.4.2 Reaction of **14** with $Zn(ClO_4)_2·6H_2O$

White solid. Yield: 0.185 g, 95 %. δ_H(DMSO): 9.90 (2H, t, CONH, J = 6.2 Hz), 8.57 (2H, s, br, py-H), 8.47 (2H, s, br, py-H), 8.18-8.28 (3H, m, py-H), 7.75 (2H, d, py-H, J = 8.0 Hz), 7.36-7.40 (2H, m, py-H), 4.64 (4H, d, CH_2, J = 6.3 Hz) ppm. ν_{max} (KBr): 3533, 3342, 3097, 1643, 1615, 1566, 1443, 1290, 1198, 1108(br), 752, 703, 624 cm^{-1}. Calcd for: [Zn(**14**)$(ClO_4)_2$], $C_{19}H_{17}Cl_2Zn_2N_5O_{10}$, C, 33.70; H, 2.53; N, 10.34 %. Found: C, 33.60; H, 2.57; N, 9.94 %.

2.4.4.3 Reaction of **14** with $HgCl_2$

White solid. Yield: 0.165 g, 93 %. δ_H(DMSO): 9.90 (2H, t, CONH, J = 6.5 Hz), 8.59 (2H, s, py-H), 8.47 (2H, d, py-H, J = 1.3 Hz), 8.21-8.26 (3H, m, py-H), 7.77 (2H, d, py-H, J = 7.9 Hz), 7.42 (2H, d, py-H, J = 4.8, 7.8 Hz), 4.65 (4H, d, CH_2, J = 6.3 Hz) ppm. ν_{max} (KBr): 3356, 1690, 1677, 1527, 1436, 1303, 1169, 1049, 1000, 788, 700, 635 cm^{-1}. Calcd for: [Hg(**14**)Cl_2], $C_{19}H_{17}Cl_2HgN_5O_2$, C, 36.87; H, 2.76; N, 11.31 %. Found: C, 36.50; H, 2.58; N, 10.66 %.

2.4.4.4 Reaction of **14** with $Hg(ClO_4)_2·6H_2O$

White solid. Yield: 0.167 g, 74 %. δ_H(DMSO): 9.96-10.00 (2H, m, CONH), 8.54-8.60 (4H, m, py-H), 8.28 (5H, s, br, py-H), 7.85-7.90 (2H, m, py-H), 4.78 (4H, s, br, CH_2) ppm. ν_{max} (KBr): 3530, 3356, 1660, 1591, 1539, 1447, 1109(br), 692, 625 cm^{-1}. Calcd for: [Hg(**14**)$(ClO_4)_2$·$2H_2O$], $C_{19}H_{21}Cl_2HgN_5O_{12}$, C, 29.15; H, 2.70; N, 8.95 %. Found: C, 28.86; H, 2.76; N, 8.47 %.

2.4.4.5 Reaction of **14** with $NiCl_2 \cdot 6H_2O$

Pale green solid. Yield: 0.11 g, 78 %. ν_{max} (KBr): 3338, 1670, 1607, 1532, 1444, 1430, 1238, 709, 648 cm^{-1}. Calcd for: [Ni(**14**)(Cl)·(OH)·2MeOH], $C_{20}H_{22}ClN_5NiO_4$, C, 48.97; H, 4.52; N, 14.28 %. Found: C, 49.35; H, 4.70; N, 14.89 %. μ_{eff} = 1.58 B.M.

2.4.4.6 Reaction of **14** with $Ni(ClO_4)_2 \cdot 6H_2O$

Pale green solid. Yield: 0.13 g, 81 %. ν_{max} (KBr): 3357, 1645, 1629, 1537, 1485, 1436, 1108(br), 708, 626 cm^{-1}. Calcd for: [Ni(**14**)(ClO_4)(OH)·$2H_2O$], $C_{19}H_{22}ClN_5NiO_9$, C, 40.86; H, 3.97; N, 12.54 %. Found: C, 41.69; H, 3.89; N, 12.47 %. μ_{eff} = 2.54 B.M.

2.4.4.7 Reaction of **14** with $CuCl_2 \cdot 2H_2O$

Blue solid. Yield: 0.13 g, 85 %. ν_{max} (KBr): 3436, 3343, 1670, 1535, 1438, 1196, 1069, 698, 649 cm^{-1}. Calcd for: [Cu(**14**)Cl_2·H_2O·MeOH], $C_{20}H_{23}Cl_2CuN_5O_4$, C, 45.16; H, 4.36; N, 13.17 %. Found: C, 44.67; H, 4.11; N, 13.29 %. μ_{eff} = 1.74 B.M.

2.4.4.8 Reaction of **14** with $Cu(ClO_4)_2 \cdot 6H_2O$

Blue solid. Yield: 0.14 g, 83 %. ν_{max} (KBr): 3550, 3358, 1659, 1596, 1540, 1439, 1276, 1096(br), 756, 704, 626 cm-1. Calcd for: [Cu(**14**)(ClO_4)(OH)·$3H_2O$], $C_{19}H_{24}ClCuN_5O_{10}$, C, 39.25; H, 4.16; N, 12.05 %. Found: C, 39.20; H, 3.58; N, 11.72 %. μ_{eff} = 1.65 B.M.

2.4.4.9 Reaction of **14** with $Cu(NO_3)_2 \cdot 3H_2O$[a]

Pale blue solid. Yield: 0.06 g, 41 %. ν_{max} (KBr): 3306, 1647, 1629, 1538, 1435, 1384, 1334 (br), 682, 649 cm^{-1}. Calcd for: [Cu(**14**)(NO_3)(OH)], $C_{19}H_{20}CuN_6O_7$, C, 44.93; H, 3.97; N, 16.55 %. Found: C, 45.32; H, 3.99; N, 16.65 %. μ_{eff} = 1.82 B.M.

2.4.4.10 Reaction of **14** with $Cu(OAc)_2 \cdot H_2O$

Blue solid. Yield: 0.126 g, 75 %. ν_{max} (KBr): 3408, 1578, 1481, 1427, 1387, 1303, 1190, 803, 766, 705 cm^{-1}. Calcd for: [Cu(**14**)$(OAc)_2$·$4H_2O$], $C_{23}H_{29}CuN_5O_9$, C, 45.96; H, 4.23; N, 12.37 %. Found: C, 46.04; H, 4.24; N, 12.37 %. μ_{eff} = 1.79 B.M.

2.4.4.11 Reaction of **14** with $CoCl_2 \cdot 6H_2O$

Blue solid. Yield: 0.113 g, 82 %. ν_{max} (KBr): 3342, 1670, 1605, 1529, 1479, 1444, 1428, 1188, 842, 811, 709, 647 cm^{-1}. Calcd for: [Co(**14**)Cl_2·MeOH], $C_{20}H_{21}Cl_2CoN_5O_3$, C, 47.17; H, 4.16; N, 13.75 %. Found: C, 48.10; H, 4.35; N, 14.46 %. μ_{eff} = 3.48 B.M.

2.4.5 N^2,N^6-bis(pyridin-4-ylmethyl)pyridine-2,6-dicarboxamide (15)

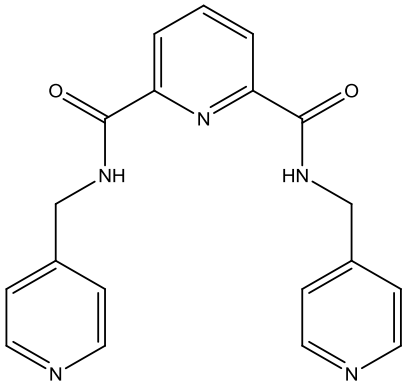

To a solution of compound **13** (1.95 g, 10 mmol) in toluene (50 mL) was added 4-aminomethyl pyridine (4.32 g, 40 mmol). The suspension was then refluxed for 48 h. The solvent was then cooled down to room temperature, and reduced under vacuum. The filtrate was redissolved in $CHCl_3$ (50 mL), washed with H_2O (4 × 40 mL). The organic layer was dried with $MgSO_4$, filtered, and concentrated under vacuum to give a compound **15** as yellow oil.

Yield: 3.1 g, 90 %. $\delta_H(CDCl_3)$: 8.86 (2H, t, CONH, J = 6.1 Hz), 8.45 (2H, d, py-H, J = 7.7 Hz), 8.39 (4H, dd, py-H, J = 4.3, 1.5 Hz), 8.12 (1H, t, py-H, J = 7.8 Hz), 7.06 (4H, dd, py-H, J = 1.2, 4.2 Hz), 4.57 (4H, d, CH_2, J = 6.2 Hz) ppm. $\delta_C(CDCl_3)$: 164.0, 149.5, 148.5, 147.6, 139.3, 128.3, 125.6, 122.3, 42.1 ppm. ν_{max} (DCM): 3054, 2987, 1681, 1602, 1527, 1421, 1156, 896 cm^{-1}. HR-MS: calcd: $C_{19}H_8N_5O_2$ m/z: $[M+H]^+$, 348.1455. Found: 348.1468. [Diff(ppm)]: 3.734.

2.4.6 Metal complexes of **15**

General procedure:

Compound **15** (100 mg, 0.289 mmol) was dissolved in MeOH (20 mL). To this was added, dropwise, the appropriate metal salt (0.289 mmol) in MeOH (10 mL). A coloured solid precipitated immediately. The mixture was kept stirring for an additional 1 hour at room temperature. The coloured solid was collected by filtration, washed with MeOH, and dried in air overnight.

2.4.6.1 Reaction of **15** with $ZnCl_2$

White solid. Yield: 0.122 g, 80 %. δ_H(DMSO): 9.95 (2H, t, CONH, J = 6.7 Hz), 8.52 (4H, d, py-H, J = 6.0 Hz), 8.23-8.28 (3H, m, py-H), 7.36 (4H, d, py-H, J = 6.0 Hz), 4.65

(4H, d, CH_2, J = 6.3 Hz) ppm. ν_{max} (KBr): 3468, 3362, 1675, 1620, 1563, 1535, 1432, 1226, 1068, 1031, 1002, 809, 648 cm^{-1}. Calcd for: [Zn(**15**)Cl_2·MeOH·H_2O], $C_{20}H_{23}Cl_2N_5OZn$, C, 45.01; H, 4.34; N, 13.12 %. Found: C, 44.71; H, 3.62; N, 13.49 %.

2.4.6.2 Reaction of **15** with $Zn(ClO_4)_2·6H_2O$

White solid. Yield: 0.124 g, 69 %. δ_H(DMSO): 9.95 (2H, t, CONH, J = 6.5 Hz), 8.51 (4H, d, py-H, J = 6.2 Hz), 8.25-8.28 (3H, m, py-H), 7.33 (4H, d, py-H, J = 5.8 Hz), 4.64 (4H, d, CH_2, J = 6.3 Hz) ppm. ν_{max} (KBr): 3340, 3104, 1659, 1643, 1624, 1563, 1536, 1434, 1109(br), 750, 626 cm^{-1}. Calcd for: [Zn(**15**)$(ClO_4)_2$·H_2O], C, 36.24; H, 3.04; N, 11.12 %. Found: C, 36.91; H, 3.04; N, 11.60 %.

2.4.6.3 Reaction of **15** with $Zn(OAc)_2·2H_2O$

Yellow solid. Yield: 0.03 g, 13 %. δ_H(DMSO): 10.42 (2H, s, br, CONH), 8.50-8.58 (2H, m, py-H), 8.41 (5H, s, br, py-H, py-H), 7.36 (4H, s, br, py-H), 4.63 (4H, s, br, CH_2), 1.79 (6H, s, OAc) ppm. ν_{max} (KBr): 3432, 3235, 3096, 1674, 1649, 1621, 1595, 1565, 1431, 1415, 1387, 1364, 1330, 679 cm^{-1}. Calcd for: [Zn_2(**15**)$(OAc)_2(OH)_2$·$2H_2O$], $C_{23}H_{29}N_5O_{10}Zn_3$, C, 41.46; H, 4.39; N, 10.51 %. Found: C, 41.35; H, 3.93; N, 9.83 %.

2.4.6.4 Reaction of **15** with $HgCl_2$

Colourless crystals. Yield: 0.05 g, 27 %. δ_H(DMSO): 9.95 (2H, t, CONH, J = 6.3 Hz), 8.52 (4H, d, py-H, J = 4.4 Hz), 8.23-8.29 (3H, m, py-H), 7.36 (4H, d, py-H, J = 5.6 Hz), 4.65 (4H, d, CH_2, J = 6.2 Hz) ppm. ν_{max} (KBr): 3491, 3365, 1682, 1612, 1563, 1533, 1429, 1224, 1067, 1001, 648 cm^{-1}. Calcd for: [Hg(**15**)Cl_2·H_2O], $C_{19}H_{19}Cl_2HgN_5O_3$, C, 35.83; H, 3.01; N, 11.00 %. Found: C, 35.75; H, 2.76; N, 10.96 %.

2.4.6.5 Reaction of **15** with $Hg(ClO_4)_2·6H_2O$

White solid. Yield: 0.174 g, 91 %. δ_H(DMSO): Calcd for: 10.03-10.07 (2H, t, CONH), 8.65 (4H, d, py-H), 8.24-8.30 (3H, m, py-H), 7.72-7.74 (4H, d, py-H), 4.75-7.80 (4H, d, CH_2) ppm. ν_{max} (KBr): 3361, 1678, 1646, 1624, 1562, 1538, 1438, 1108(br), 1003, 623 cm^{-1}. Calcd for: [Hg(**15**)(ClO_4)(OH)], $C_{19}H_{18}ClHgN_5O_7$, C, 34.35; H, 2.73; N, 10.54 %. Found: C, 34.93; H, 2.85; N, 10.45 %.

2.4.6.6 Reaction of **15** with $NiCl_2·6H_2O$

Brown green solid. Yield: 0.04 g, 33 %. ν_{max} (KBr): 3271, 1662, 1618, 1534, 1525, 1313, 1225, 1067, 1001, 747, 684 cm^{-1}. Calcd for: [Ni(**15**)Cl_2·$4H_2O$], $C_{19}H_{25}Cl_2N_5NiO_6$, C, 41.56; H, 4.59; N, 12.76 %. Found: C, 41.89; H, 4.32; N, 13.19 %. μ_{eff} = 2.86 B.M.

2.4.6.7 Reaction of **15** with $Ni(ClO_4)_2 \cdot 6H_2O$

Pale green solid. Yield: 0.129 g, 74 %. ν_{max} (KBr): 3366, 1646, 1619, 1538, 1427, 1108(br), 683, 626 cm^{-1}. Calcd for: [Ni(**15**)$(ClO_4)_2$], $C_{19}H_{17}Cl_2N_5NiO_{10}$, C, 37.72; H, 2.83; N, 11.58 %. Found: C, 37.64; H, 3.59; N, 11.85 %. μ_{eff} = 2.73 B.M.

2.4.6.8 Reaction of **15** with $Ni(NO_3)_2 \cdot 6H_2O$

Brown green solid. Yield: 0.09 g, 56 %. ν_{max} (KBr): 3295, 1648, 1618, 1563, 1538, 1426, 1384, 1352, 1225, 1023, 618 cm^{-1}. Calcd for: [Ni(**15**)$(NO_3)_2 \cdot MeOH \cdot 2H_2O$], $C_{20}H_{25}NiN_7O_{11}$, C, 40.16; H, 4.21; N, 15.39 %. Found: C, 40.30; H, 4.41; N, 15.71 %. μ_{eff} = 2.81 B.M.

2.4.6.9 Reaction of **15** with $Cu(ClO_4)_2 \cdot 6H_2O$

Green solid. Yield: 0.179 g, 99 %. ν_{max} (KBr): 3427, 1659, 1618, 1538, 1429, 1108(br), 636, 626 cm^{-1}. Calcd for: [Cu(**15**)$(ClO_4)_2 \cdot H_2O$], $C_{19}H_{19}Cl_2CuN_5O_{11}$, C, 36.35; H, 3.05; N, 11.15 %. Found: C, 35.98; H, 3.07; N, 11.04 %. μ_{eff} = 1.87 B.M.

2.4.6.10 Reaction of **15** with $Cu(NO_3)_2 \cdot 6H_2O$

Green solid. Yield: 0.09 g, 50 %. ν_{max} (KBr): 3412, 1659, 1619, 1538, 1428, 1384, 1351, 1224, 1065, 1029, 833, 620 cm^{-1}. Calcd for: [Cu(**15**)$(NO_3)_2 \cdot 2MeOH \cdot H_2O$], $C_{21}H_{27}CuN_7O_{11}$, C, 40.88; H, 4.41; N, 15.89 %. Found: C, 40.52; H, 4.23; N, 16.08 %. μ_{eff} = 1.78 B.M.

2.4.6.11 Reaction of **15** with $CoCl_2 \cdot 6H_2O$

Green solid. Yield: 0.07 g, 46 %. ν_{max} (KBr):3325, 1666, 1613, 1561, 1533, 1426, 1223, 1065, 819, 682, 648 cm^{-1}. Calcd for: [Co(**15**)$Cl_2 \cdot MeOH \cdot H_2O$], $C_{20}H_{23}Cl_2CoN_5O_4$, C, 45.56; H, 4.40; N, 13.28 %. Found: C, 45.95; H, 4.19; N, 13.26 %. μ_{eff} = 4.77 B.M.

2.4.6.12 Reaction of **15** with $Co(ClO_4)_2 \cdot 6H_2O$

Yellow solid. Yield: 0.03 g, 20 %. ν_{max} (KBr): 3372, 1659, 1617, 1562, 1538, 1424, 1109(br), 636, 626 cm^{-1}. Calcd for: [Co(**15**)$(ClO_4)_2 \cdot 3H_2O$], $C_{19}H_{23}Cl_2CoN_5O_{13}$, C, 34.62; H, 3.52; N, 10.62 %. Found: C, 34.77; H, 3.09; N, 10.34 %. μ_{eff} = 3.87 B.M.

2.4.7 N^2,N^6-bis(3-(4,5-dihydro-1H-imidazol-1-yl)propyl)pyridine-2,6-dicarboxamide (**16**)

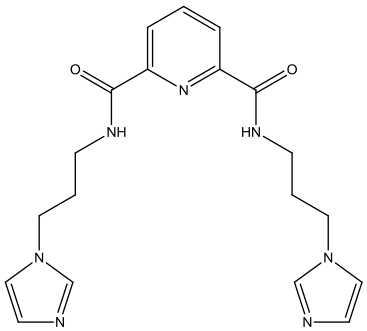

To a solution of compound **13** (1.95 g, 10 mmol) in toluene (50 mL) was added 1-(3-aminopropyl)-imidazole (5 g, 40 mmol). The solution was then refluxed for 48 h. This solution was then cooled down to room temperature, and reduced under vacuum. The remaining yellow oil was redissolved in $CHCl_3$ (50 mL), washed with H_2O (4 × 40 mL). The organic layer was dried with $MgSO_4$, filtered, and concentrated under vacuum to give a compound **16** as colourless oil.

Yield: 3.5 g, 92 %. $\delta_H(CDCl_3)$: 8.55 (2H, t, CONH, J = 6.3 Hz), 8.32 (2H, d, py-H, J = 7.8 Hz), 8.01 (1H, t, py-H, J = 7.5 Hz), 9.61 (2H, s, imidazole-H), 7.00 (2H, s, imidazole-H), 6.91 (2H, s, imidazole-H), 4.05 (4H, t, NH-CH_2-, J = 6.7 Hz), 3.40-3.47 (4H, m, $NHCH_2CH_2\underline{CH_2}$-), 2.00-2.17 (4H, m, $NHCH_2$-$\underline{CH_2}$-) ppm. $\delta_C(CDCl_3)$: 164.2, 148.8, 138.8, 137.1, 129.4, 129.0, 128.2, 124.9, 119.3, 45.1, 38.7, 34.4 ppm. ν_{max} (DCM): 3305, 3054, 2986, 1672, 1537, 1508, 1446, 1422, 1230, 1078, 896 cm^{-1}. HR-MS: calcd: $C_{19}H_{24}N_7O_2$ m/z: $[M+H]^+$, 382.1991. Found: 382.2005. [Diff(ppm)]: 4.78.

2.4.8 Metal complexes of **16**

General procedure:

Compound **16** (110 mg, 0.289 mmol) was dissolved in MeOH (20 mL). To this was added, dropwise, the appropriate metal salt (0.289 mmol) in MeOH (10 mL). A coloured solid precipitated immediately. The mixture was kept stirring for additional 1 hour at room temperature. The coloured solid was collected by filtration, washed with MeOH, and dried in air overnight.

[a] If the complex was found as a very small, coloured suspension, which cannot be filtrated. Then the solution was removed under vacuum. MeOH (10 mL) was added, the

resulting solid was collected by filtration, washed with MeOH, and dried in air overnight.

[b] If did not form the precipitate, then the solvent was reduced to half under vacuum. And the solvent was left under air for couple of days. The coloured solids will be precipitated. The coloured solids were collected by filtration, washed with MeOH, dried in air overnight.

2.4.8.1 Reaction of **16** with $ZnCl_2$

White solid. Yield: 0.15 g, 94 %. δ_H(DMSO): 9.28 (2H, t, CONH, J = 5.9 Hz), 8.19-8.25 (5H, s, br, py-H, imidazole-H), 7.51 (2H, s, br, imidazole-H), 7.18 (2H, s, br, imidazole-H), 4.16 (4H, t, NH-$\underline{CH_2}$, J = 6.3 Hz), 3.30 (4H, s, br, $\underline{CH_2}$-imidazole), 2.09-2.13 (4H, m, NHCH$_2\underline{CH_2}$) ppm. ν_{max} (KBr): 3486, 3344, 3120, 1663, 1536, 1446, 1241, 1099, 954, 845, 753, 657 cm^{-1}. Calcd for: [Zn(**16**)Cl_2·2H_2O], $C_{19}H_{27}Cl_2N_7O_4Zn$, C, 41.21; H, 4.91; N, 17.71 %. Found: C, 40.80; H, 4.65; N, 17.18 %.

2.4.8.2 Reaction of **16** with $Zn(ClO_4)_2$·6H_2O

White solid. Yield: 0.17 g, 98 %. δ_H(DMSO): 9.16-9.20 (2H, t, CONH), 8.28 (2H, s, imidazole-H), 8.16 (3H, s, py-H), 7.61 (2H, s, imidazole-H), 7.17 (2H, s, imidazole-H), 4.19 (4H, s, br, NH$\underline{CH_2}$), 3.30 (4H, d, CH_2-imidazole), 2.13 (4H, s, br, NHCH$_2\underline{CH_2}$) ppm. ν_{max} (KBr): 3361, 3128, 1663, 1540, 1446, 1242, 1106(br), 957, 845, 752, 623 cm^{-1}. Calcd for: [Zn(**16**)(ClO_4)(OH)·2H_2O], $C_{19}H_{28}ClN_7O_9Zn$, C, 38.08; H, 4.71; N, 16.36 %. Found: C, 38.21; H, 4.41; N, 16.20 %.

2.4.8.3 Reaction of **16** with $Zn(OAc)_2$·2H_2O

Colourless crystals. Yield: 0.158 g, 83 %. δ_H(DMSO): 9.27-9.28 (2H, m, br, CONH), 8.16-8.22 (5H, py-H, imidazole-H), 7.42 (2H, s, imidazole-H), 7.13 (2H, s, imidazole-H), 4.12-4.14 (4H, m, br NH-$\underline{CH_2}$), 3.29-3.31 (4H, m, NHCH$_2$-$\underline{CH_2}$), 2.07-2.11 (4H, m, br, $\underline{CH_2}$-imidazole), 1.81 (6H, s, OAc) ppm. ν_{max} (KBr): 3426, 3299, 3126, 2935, 1668, 1611, 1590, 1537, 1438, 1394, 1333, 1243, 1110, 1097, 747, 682, 657 cm^{-1}. Calcd for: [Zn(**16**)$(OAc)_2$·2H_2O], $C_{23}H_{33}N_7O_8Zn$, C, 45.97; H, 5.54; N, 16.32 %. Found: C, 45.81; H, 4.91; N, 15.78 %.

2.4.8.4 Reaction of **16** with $HgCl_2$

White solid. Yield: 0.18 g, 99 %. δ_H(DMSO): 9.32 (2H, t, CONH, J = 6.3 Hz), 8.17-8.21 (3H, m, py-H), 8.03 (2H, s, imidazole-H), 7.47 (2H, s, imidazole-H), 7.05 (2H, s, imidazole-H), 4.13 (4H, t, NH-$\underline{CH_2}$, J = 6.5 Hz), 3.32 (4H, m, $\underline{CH_2}$-imidazole), 2.04-

2.09 (4H, m, $NHCH_2$-$\underline{CH_2}$) ppm. ν_{max} (KBr): 3381, 3123, 2942, 1664, 1539, 1446, 1239, 1107, 754, 649 cm^{-1}. Calcd for: [Hg(**16**)Cl_2·$2H_2O$], $C_{19}H_{27}Cl_2HgN_7O_4$, C, 33.12; H, 3.95; N, 14.23 %. Found: C, 32.88; H, 3.30; N, 13.87 %.

2.4.8.5 Reaction of **16** with $Hg(ClO_4)_2$·$6H_2O$

White solid. Yield: 0.165 g, 81 %. δ_H(DMSO): 9.40 (2H, t, CONH, J = 6.6 Hz), 8.43 (2H, s, imidazole-H), 8.20-8.22 (3H, m, py-H), 7.77 (2H, s, imidazole-H), 7.35 (2H, s, imidazole-H), 4.28-4.30 (4H, s, br, $NH\underline{CH_2}$), 3.36 (4H, s, br, $\underline{CH_2}$-imidazole), 2.08-2.13 (4H, m, $NHCH_2\underline{CH_2}$) ppm. ν_{max} (KBr): 3362, 3133, 2945, 1673, 1654, 1546, 1448, 1246, 1115(br), 623 cm-1. Calcd for: [Hg(**16**)(ClO_4)(OH)·H_2O], $C_{19}H_{26}ClHgN_7O_8$, C, 31.85; H, 3.66; N, 13.68 %. Found: C, 31.91; H, 3.35; N, 13.67 %.

2.4.8.6 Reaction of **16** with $Ni(ClO_4)_2$·$6H_2O$

Green solid. Yield: 0.1 g, 63 %. ν_{max} (KBr): 3362, 3132, 2946, 1674, 1650, 1632, 1539, 1448, 1287, 1239, 1090(br), 753, 662 cm^{-1}. Calcd for: [Ni(**16**)(ClO_4)(OH)·$2H_2O$], $C_{19}H_{28}ClN_7NiO_9$, C, 38.43; H, 4.24; N, 16.51 %. Found: C, 38.97; H, 4.28; N, 16.79 %. μ_{eff} = 2.60 B.M.

2.4.8.7 Reaction of **16** with $Ni(NO_3)_2$·$6H_2O$[b]

Green solid. Yield: 0.125 g, 71 %. ν_{max} (KBr): 3430, 3319, 1669, 1656, 1632, 1544, 1530, 1384, 1343, 1331, 1235, 1100, 841, 746, 665 cm^{-1}. Calcd for: [Ni(**16**)$(NO_3)_2$·MeOH·H_2O], $C_{20}H_{29}N_9NiO_{10}$, C, 39.11; H, 4.76; N, 20.52 %. Found: C, 39.17; H, 4.45; N, 20.82 %. μ_{eff} = 3.67 B.M.

2.4.8.8 Reaction of **16** with $CuCl_2$·$2H_2O$[a]

Blue solid. Yield: 0.148 g, 98 %. ν_{max} (KBr): 3286, 3127, 2938, 1663, 1533, 1445, 1237, 1096, 747, 655 cm^{-1}. Calcd for: [Cu(**16**)Cl_2·H_2O·MeOH], $C_{20}H_{29}Cl_2CuN_7O_4$, C, 42.45; H, 5.16; N, 17.32 %. Found: C, 42.37; H, 4.92; N, 17.93 %. μ_{eff} = 1.77 B.M.

2.4.8.9 Reaction of **16** with $Cu(ClO_4)_2$·$6H_2O$

Blue solid. Yield: 0.148 g, 80 %. ν_{max} (KBr): 3365, 3135, 2949, 1659, 1536, 1447, 1241, 1098(br), 754, 658, 624 cm^{-1}. Calcd for: [Cu(**16**)$(ClO_4)_2$·H_2O], $C_{19}H_{25}Cl_2CuN_7O_{11}$, C, 34.48; H, 3.81; N, 14.81 %. Found: C, 33.72; H, 3.72; N, 14.52 %. μ_{eff} = 1.82 B.M.

2.4.8.10 Reaction of **16** with $Cu(NO_3)_2$·$3H_2O$[a]

Blue solid. Yield: 0.11 g, 64 %. ν_{max} (KBr): 3421, 3273, 3127, 2942, 1647, 1534, 1444, 1384, 1351, 1237, 1096, 753, 655 cm^{-1}. Calcd for: [Cu(**16**)$(NO_3)_2$·$2H_2O$],

$C_{19}H_{27}CuN_9O_{10}$, C, 37.72; H, 4.50; N, 21.04 %. Found: C, 37.92; H, 4.43; N, 21.04 %. μ_{eff} = 1.79 B.M.

2.4.8.11 Reaction of **16** with $CoCl_2 \cdot 6H_2O$

Blue solid. Yield: 0.135 g, 93 %. ν_{max} (KBr): 3343, 3118, 2944, 1660, 1539, 1446, 1240, 1097, 748, 659 cm^{-1}. Calcd for: [Co(**16**)Cl_2], $C_{19}H_{23}Cl_2CoN_7O_2$, C, 44.63; H, 4.53; N, 19.18 %. Found: C, 44.47; H, 4.83; N, 19.15 %. μ_{eff} = 4.41 B.M.

2.4.8.12 Reaction of **16** with $Co(ClO_4)_2 \cdot 6H_2O$

Light pink solid. Yield: 0.121 g, 66 %. ν_{max} (KBr): 3391, 3355, 3129, 2933, 1675, 1660, 1446, 1234, 1101(br), 1000, 941, 842, 748, 666 cm^{-1}. Calcd for: [Co(**16**)$(ClO_4)_2$], $C_{19}H_{23}Cl_2CoN_7O_{10}$, C, 35.70; H, 3.63; N, 15.34 %. Found: C, 36.54; H, 4.07; N, 15.64 %. μ_{eff} = 4.19 B.M.

2.5 Section 4

2.5.1 Triformylphloroglucinol (**17**)[134]

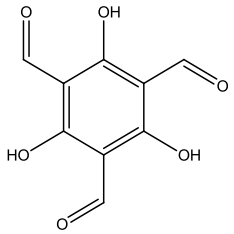

To the solution of hexamethylenetetramine (10 g, 72 mmol) in 30 ml of trifluoroacetic acid was added phloroglucinol (4 g, 31.7 mmol). The solution was heated to reflux at 100 ℃ for 3 h under N_2. Approximiately 50 mL of 3M HCl was added and the solution was heated at 100 ℃ for additional 1 hour. Then the solution was cooled down to room temperature, passed through Celite. The remaining solvent was extracted with DCM (3 × 50 mL). The solvent was dried with $MgSO_4$, filtered. The solvent was removed under vacuum to give the product as a yellow solid. The product was left overnight in fumehood to get rid of all acid.[134]

Yield: 0.99 g, 15 %. $\delta_H(CDCl_3)$: 14.11 (3H, s, ArOH), 10.18 (3H, s, CHO) ppm. These match reported data.

2.5.2 (*Z*)-2,4,6-tris(((pyridin-2-ylmethyl)amino)methylene)cyclohexane-1,3,5-trione (**18**)

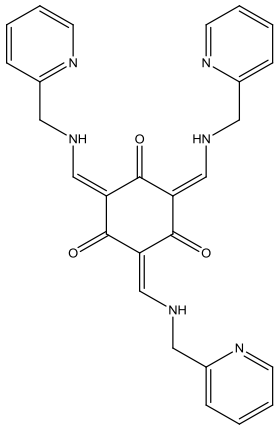

To a suspension of anhydrous $MgSO_4$ (4.14 g, 30 mmol) in CH_2Cl_2 (50 mL) was added compound **17** (0.63 g, 3 mmol). This was followed by 2-aminomethyl pyridine (0.97 g, 9 mmol). The mixture was stirred at room temperature overnight. The resulting suspension was filtered, washed with CH_2Cl_2, and the excess filtrate was removed under vacuum to give compound **18** as a yellow oil.

Yield: 1.4 g, 97 %. $\delta_H(CDCl_3)$: 11.86, 11.43 (3H, m, NH), 8.59-8.60 (3H, m, py-H), 8.25-8.40 (3H, m, CH-NH), 7.65-7.71 (3H, m, py-H), 7.20-7.28 (6H, m, py-H), 4.68-4.73 (6H, m, CH_2) ppm. $\delta_C(CDCl_3)$: 185.5, 157.7, 157.0, 156.1, 149.8, 137.0, 122.8, 121.4, 105.4, 55.1 ppm. ν_{max} (DCM): 3054, 2987, 1609, 1572, 1552, 1436, 1422, 1324, 1201 cm^{-1}. HR-MS: calcd: $C_{27}H_{25}N_6O_3$ m/z: $[M+H]^+$, 481.1991. Found: 481.1983. [Diff(ppm)]: 1.78.

2.5.3 Metal complexes of **18**

General procedure:

Compound **18** (100 mg, 0.208 mmol) was dissolved in MeOH (20 mL). To this was added, dropwise, the appropriate metal salt (0.625 mmol) in MeOH (10 mL). A coloured solid precipitated immediately. The mixture was kept stirring for additional 1 hour at room temperature. The coloured solid was collected by filtration, washed with MeOH, and dried in air overnight.

2.5.3.1 Reaction of **18** with $ZnCl_2$

Yellow solid. Yield: 77 mg, 48 %. δ_H(DMSO): 11.14-11.26, 11.57-11.67 (3H, m, NH), 8.56-8.57 (3H, m, py-H), 8.17-8.28 (3H, m, CH-NH), 7.79-7.84 (3H, m, py-H), 7.31-

7.37 (6H, m, py-H), 4.76-4.78 (6H, m, CH_2) ppm. ν_{max} (KBr): 3450, 3223, 1607, 1571, 1546, 1509, 1440, 1371, 1326, 1209, 1021, 838, 767 cm^{-1}. Calcd for: $[Zn_2(\mathbf{18})Cl_4 \cdot H_2O]$, $C_{27}H_{26}Cl_4N_6O_4Zn_2$, C, 42.06; H, 3.40; N, 10.90 %. Found: C, 42.36; H, 3.25; N, 10.98 %.

2.5.3.2 Reaction of **18** with $Zn(ClO_4)_2 \cdot 6H_2O$

Yellow solid. Yield: 60 mg, 32 %. δ_H(DMSO): 11.18, 11.58 (3H, m, NH), 8.65 (3H, s, py-H), 8.19-8.31 (3H, m, CH-NH), 8.01-8.03 (3H, m, py-H), 7.51-7.54 (6H, m, py-H), 4.85 (6H, s, CH_2) ppm. ν_{max} (KBr): 3434, 311, 1607, 1571, 1545, 1468, 1433, 1371, 1328, 1215, 1108(br), 1022, 836, 766, 626 cm^{-1}. Calcd for: $[Zn_3(\mathbf{18})_2(ClO_4)_6 \cdot 2H_2O]$, $C_{54}H_{52}Cl_6N_{12}O_{32}Zn_3$, C, 36.24; H, 2.93; N, 9.39 %. Found: C, 35.87; H, 3.22; N, 9.41 %.

2.5.3.3 Reaction of **18** with $Zn(OAc)_2 \cdot 2H_2O$

Yellow solid. Yield: 100 mg, 46 %. δ_H(DMSO): 8.84, 8.99, 9.04 (3H, s, CH=N), 8.50 (3H, s, br, py-H), 8.01-8.06 (2H, m, py-H), 7.91-7.96 (1H, m, py-H), 7.51-7.56 (4H, m, py-H), 7.41-7.47 (2H, m, py-H), 4.91 (4H, s, CH_2), 4.80 (2H, s, CH_2) ppm. ν_{max} (KBr): 3432, 2928, 1607, 1571, 1512, 1443, 1429, 1369, 1320, 1283, 1217, 1044, 1019, 763 cm^{-1}. Calcd for: $[Zn_4(\mathbf{18\text{-}C_3})(OAc)_5]$, $C_{37}H_{36}N_6O_{13}Zn_4$, C, 42.97; H, 3.51; N, 8.13 %. Found: C, 43.50; H, 3.11; N, 8.70 %.

2.5.3.4 Reaction of **18** with $HgCl_2$

Yellow solid. Yield: 86 mg, 47 %. δ_H(DMSO): 11.61, 11.19 (3H, m, NH), 8.58-8.59 (3H, d, py-H), 8.17-8.28 (3H, m, CH-NH), 7.84-7.90 (3H, m, py-H), 7.36-7.43 (6H, m, py-H), 4.80 (6H, m, CH_2) ppm. ν_{max} (KBr): 3431, 3240, 2937, 1610, 1543, 1463, 1438, 1353, 1326, 1205, 1093, 838, 765, 625 cm^{-1}. Calcd for: $[Hg_3(\mathbf{18})_2Cl_6]$, $C_{54}H_{48}Cl_6Hg_3N_{12}O_6$, C, 36.53; H, 2.72; N, 9.47 %. Found: C, 36.65, H, 2.89; N, 9.15 %.

2.5.3.5 Reaction of **18** with $Hg(ClO_4)_2 \cdot 6H_2O$

Yellow solid. Yield: 180 mg, 86 %. δ_H(DMSO): 11.19, 11.60 (3H, s, br, NH), 8.59 (3H, s, py-H), 8.23 (3H, s, br, CH-NH), 7.92 (3H, s, br, py-H), 7.45 (6H, s, br, py-H), 4.83 (6H, s, br, CH_2) ppm. ν_{max} (KBr): 3438, 3121, 1606, 1549, 1463, 1438, 1374, 1327, 1209, 1108(br), 766, 625 cm^{-1}. Calcd for: $[Hg_3(\mathbf{18})_2(ClO_4)_6]$, $C_{54}H_{48}Cl_6Hg_3N_{12}O_{30}$, C, 30.03; H, 2.24; N, 7.78 %. Found: C, 29.91; H, 1.82; N, 8.32 %.

2.5.3.6 Reaction of **18** with $CuCl_2 \cdot 2H_2O$

Green solid. Yield: 110 mg, 61 %. ν_{max} (KBr): 3428, 3068, 1599, 1567, 1501, 1444, 1423, 1368, 1339, 1247, 1217, 1089, 1026, 765 cm^{-1}. Calcd for: $[Cu_2(\mathbf{18})Cl_4 \cdot MeOH \cdot 3H_2O]$, $C_{27}H_{26}Cl_4Cu_2N_6O_4$, C, 42.26; H, 3.41; N, 10.95 %. Found: C, 42.00; H, 3.16; N, 10.10 %. μ_{eff} = 1.95 B.M.

2.5.3.7 Reaction of **18** with $CoCl_2 \cdot 6H_2O$

Dark yellow solid. Yield: 110 mg, 65 %. ν_{max} (KBr): 3431, 1615, 1569, 1499, 1445, 1417, 1373, 1240, 1093, 769 cm^{-1}. Calcd for: $[Co_2(\mathbf{18})Cl_4 \cdot 2MeOH]$, $C_{29}H_{32}Cl_4Co_2N_6O_5$, C, 43.31; H, 4.01; N, 10.45 %. Found: C, 42.95; H, 3.46; N, 9.94 %. μ_{eff} = 2.83 B.M.

2.5.3.8 Reaction of **18** with $Co(ClO_4)_2 \cdot 6H_2O$

Dark yellow solid. Yield: 144 mg, ν_{max} (KBr): 3427, 1607, 1569, 1496, 1426, 1372, 1242, 1108(br), 768, 626 cm^{-1}. Calcd for: $[Co(II)Co(III)(\mathbf{18})(OH)_4(ClO_4)]$ $C_{27}H_{28}ClCo_2N_6O_{11}$, C, 42.43; H, 3.69; N, 10.97 %. Found: C, 42.25; H, 3.32; N, 10.42 %. μ_{eff} = 0.67 B.M.

2.5.4 (*Z*)-2,4,6-tris(((pyridin-3-ylmethyl)amino)methylene)cyclohexane-1,3,5-trione (**19**)

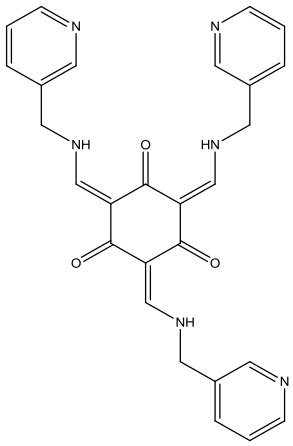

To a suspension of anhydrous $MgSO_4$ (4.14 g, 30 mmol) in CH_2Cl_2 (50 mL) was added compound **17** (0.63 g, 3 mmol). This was followed by 3-aminomethyl pyridine (0.97 g, 9 mmol). The mixture was stirred at room temperature overnight. The resulting suspension was filtered, washed with CH_2Cl_2, and the excess filtrate was removed under vacuum to give compound **19** as a yellow oil.

Yield: 1.4 g, 97 %. $\delta_H(CDCl_3)$: 11.19-11.25, 11.67-11.71 (3H, m, NH), 8.49-8.58 (6H, m, py-H), 8.32-8.39 (1H, q, CH-NH), 8.16-8.25 (2H, t, CH-NH), 7.61-7.69 (6H, m, py-

H), 7.25-7.32 (3H, m, py-H), 4.57-4.63 (6H, m, CH_2) ppm. δ_C($CDCl_3$): 185.4, 158.2, 157.3, 156.5, 151.8, 149.7, 148.9, 148.3, 135.0, 134.8, 123.8, 123.5, 105.3, 51.3, 43.9 ppm. ν_{max} (DCM): 3054, 2987, 1607, 1578, 1553, 1443, 1423, 1316, 896 cm^{-1}. HR-MS: calcd: $C_{27}H_{24}N_6NaO_3$ m/z: $[M+Na]^+$, 503.1802. Found: 503.1823. [Diff(ppm)]: 4.09.

2.5.5 Metal complexes of **19**

General procedure:

Compound **19** (100 mg, 0.208 mmol) was dissolved in MeOH (20 mL). To this was added, dropwise, the appropriate metal salt (0.625 mmol) in MeOH (10 mL). A coloured solid precipitated immediately. The mixture was kept stirring for additional 1 hour at room temperature. The coloured solid was collected by filtration, washed with MeOH, and dried in air overnight.

2.5.5.1 Reaction of **19** with $ZnCl_2$

Off-white solid. Yield: 100 mg, 64 %. δ_H(DMSO):11.03-11.14, 11.46-11.55 (3H, m, NH), 8.51- 8.57 (6H, m, py-H), 8.13-8.28 (3H, m, CH-NH), 7.78-7.80 (3H, m, py-H), 7.41-7.46 (3H, m, py-H), 4.67-4.73 (6H, m, CH_2) ppm. ν_{max} (KBr): 3435, 1606, 1551, 1506, 1485, 1438, 1370, 1193, 1060, 838, 702, 656 cm^{-1}. Calcd for: [Zn_2(**19**)Cl_4], $C_{27}H_{24}Cl_4N_6O_3Zn_2$, C43.06; H, 3.21; N, 11.16 %. Found: C, 43.77; H, 3.42; N, 11.04 %.

2.5.5.2 Reaction of **19** with $Zn(ClO_4)_2{\cdot}6H_2O$

Off-white solid. Yield: 83 mg, 53 %. δ_H(DMSO): 11.05-11.16, 11.46-11.55 (3H, m, NH), 8.50-8.56 (6H, m, py-H), 8.14-8.28 (3H, m, CH-NH), 7.75-7.78 (3H, m, py-H), 7.40-7.44 (3H, m, py-H), 4.68-4.70 (6H, d, CH_2) ppm. ν_{max} (KBr): 3427, 3235, 1607, 1548, 1485, 1459, 1436, 1372, 1354, 1323, 1209, 1107(br), 706, 624 cm^{-1}. Calcd for: [Zn(**19**)$(ClO_4)_2$], $C_{27}H_{24}Cl_2N_6O_{11}Zn$, C43.54; H, 3.25; N, 11.28 %. Found: C, 43.92; H, 2.59; N, 10.83 %.

2.5.5.3 Reaction of **19** with $HgCl_2$

Off-white solid. Yield: 160 mg, 73 %. δ_H(DMSO): 11.02-11.15, 11.45-11.54 (3H, m, NH), 8.52-8.62 (6H, m, py-H), 8.13-8.27 (3H, m, CH-NH), 7.75-7.77 (3H, m, py-H), 7.40-7.44 (3H, m, py-H), 4.66-4.72 (6H, m, CH_2) ppm. ν_{max} (KBr): 3435, 3233, 1607, 1582, 1546, 1459, 1434, 1352, 1325, 1208, 1188, 102, 837, 704 cm^{-1}. Calcd for: [Hg(**19**)$Cl_2{\cdot}2H_2O$], $C_{27}H_{28}Cl_4Hg_2N_6O_5$, C, 30.61; H, 2.66; N, 7.93 %. Found: C, 30.12; H, 2.38; N, 7.59 %.

2.5.5.4 Reaction of **19** with $Hg(ClO_4)_2 \cdot 6H_2O$

Yellow solid. Yield: 200 mg, 76 %. δ_H(DMSO): 11.09-11.17, 11.44-11.51 (3H, m, NH), 8.58-8.65 (6H, m, py-H), 8.17-8.35 (6H, m, CH-NH, py-H), 7.86-7.96 (3H, m, py-H), 4.89-4.90 (6H, m, CH_2) ppm. ν_{max} (KBr): 3460, 3233, 1607, 1489, 1446, 1356, 1325, 1201, 1107(br), 837, 693, 624 cm^{-1}. Calcd for: [Hg_2(**19**)$(ClO_4)_4$], $C_{27}H_{24}Cl_4Hg_2N_6O_{19}$, C, 25.34; H, 1.89; N, 6.57 %. Found: C, 25.74; H, 1.48; N, 6.57 %.

2.5.5.5 Reaction of **19** with $NiCl_2 \cdot 6H_2O$

Pale red solid. Yield: 89 mg, 53 %. ν_{max} (KBr): 3376, 1603, 1521, 1457, 1432, 1351, 1322, 1206, 1190, 1055, 1035, 707 cm^{-1}. Calcd for: [Ni_2(**19**)$Cl_4 \cdot$MeOH$\cdot 2H_2O$], $C_{28}H_{32}Cl_4N_6Ni_2O_6$, C, 41.63; H, 3.99; N, 10.40 %. Found: C, 41.46; H, 4.39; N, 10.23 %. μ_{eff} = 3.92 B.M.

2.5.5.6 Reaction of **19** with $Ni(ClO_4)_2 \cdot 6H_2O$

Dark red solid. Yield: 76 mg, 45 %. ν_{max} (KBr): 3405, 1604, 1521, 1459, 1434, 1353, 1324, 1108(br), 709, 627 cm_{-1}. Calcd for: [Ni(**19**)$(ClO_4)_2 \cdot 4H_2O$], $C_{27}H_{32}Cl_2N_6NiO_{15}$, C, 40.03; H, 3.98; N, 10.37 %. Found: C, 39.52; H, 3.66; N, 9.73 %. μ_{eff} = 4.29 B.M.

2.5.5.7 Reaction of **19** with $Ni(OAc)_2 \cdot 4H_2O$

Light red solid. Yield: 112 mg, 61 %. ν_{max} (KBr): 3387, 1599, 1520, 1430, 1379, 1322, 1254, 1191, 1109, 1020, 800, 706 cm^{-1}. Calcd for: [Ni_3(**19**)$(OH)_3(OAc)_3 \cdot 3H_2O$], $C_{33}H_{42}N_6Ni_3O_{15}$, C, 42.22; H, 4.51; N, 8.95 %. Found: C, 42.00; H, 4.28; N, 9.00 %. μ_{eff} = 3.27 B.M.

2.5.5.8 Reaction of **19** with $CuCl_2 \cdot 2H_2O$

Brown solid. Yield: 85 mg, 52 %. ν_{max} (KBr): 3417, 1603, 1539, 1435, 1375, 1324, 1256, 1193, 1060, 801, 701 cm^{-1}. Calcd for: [Cu_2(**19**)$Cl_4 \cdot 2H_2O$], $C_{27}H_{28}Cl_4Cu_2N_6O_5$, C, 41.29; H, 3.59; N, 10.70 %. Found: C, 41.20; H, 3.32; N, 10.14 %. μ_{eff} = 2.38 B.M.

2.5.5.9 Reaction of **19** with $Cu(OAc)_2 \cdot H_2O$

Dark green solid. Yield: 45 mg, 20 %. ν_{max} (KBr): 3430, 1580, 502, 1428, 1376, 1333, 1261, 1194, 1026, 802, 705 cm^{-1}. Calcd for: [Cu_3(**19**)$(OH)_3(OAc)_3 \cdot 3H_2O$], $C_{33}H_{42}Cu_3N_6O_{15}$, C, 41.57; H, 4.44; N, 8.82 %. Found: C, 41.35; H, 3.65; N, 8.08 %. μ_{eff} = 2.82 B.M.

2.5.5.10 Reaction of **19** with $Cu(NO_3)_2 \cdot 6H_2O$

Brown solid. Yield: 86 mg, 45 %. ν_{max} (KBr): 3420, 3078, 1591, 1505, 1434, 1384, 1318, 1195, 1020, 801, 703 cm^{-1}. Calcd for: $[Cu_3(\mathbf{19})(OH)_3(NO_3)_3]$, $C_{27}H_{27}Cu_3N_9O_{15}$, C, 35.71; H, 3.00; N, 13.88 %. Found: C, 36.21; H, 3.25; N, 13.58 %. μ_{eff} = 2.87 B.M.

2.5.5.11 Reaction of **19** with $CoCl_2 \cdot 6H_2O$

Black solid. Yield: 58 mg, 38 %. ν_{max} (KBr): 3406, 1603, 1542, 1483, 1459, 1432, 1355, 1324, 1033, 837, 706 cm^{-1}. Calcd for: $[Co_3(\mathbf{19})_2Cl_6 \cdot 2MeOH]$, $C_{56}H_{60}Cl_6Co_3N_{12}O_{10}$, C, 46.36; H, 4.17; N, 11.59 %. Found: C, 45.58; H, 3.99; N, 11.15 %. μ_{eff} = 5.45 B.M.

2.5.5.12 Reaction of **19** with $Co(ClO_4)_2 \cdot 6H_2O$

Pale solid. Yield: 68 mg, 43 %. ν_{max} (KBr): 3431, 1606, 1543, 1484, 1462, 1434, 1353, 1323, 1209, 1108(br), 709, 624 cm^{-1}. Calcd for: $[Co(\mathbf{19})(ClO_4)_2]$, $C_{27}H_{24}Cl_2CoN_6O_{11}$, C, 43.92; H, 3.28; N, 11.38 %. Found: C, 44.21; H, 3.02; N, 10.91 %. μ_{eff} = 4.25 B.M.

2.5.6 (*Z*)-2,4,6-tris(((pyridin-4-ylmethyl)amino)methylene)cyclohexane-1,3,5-trione (**20**)

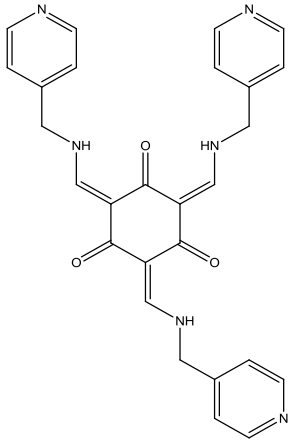

To a suspension of anhydrous $MgSO_4$ (4.14 g, 30 mmol) in CH_2Cl_2 (50 mL) was added compound **17** (0.63 g, 3 mmol). This was followed by 4-aminomethyl pyridine (0.97 g, 9 mmol). The mixture was stirred at room temperature overnight. The resulting suspension was filtered, washed with CH_2Cl_2, and the excess filtrate was removed under vacuum to give compound **20** as a yellow oil.

Yield: 1.4 g, 97 %. $\delta_H(CDCl_3)$: 11.28, 11.76 (3H, m, NH), 8.54-8.61 (6H, m, py-H), 8.17-8.36 (3H, m, CH-NH), 7.20-7.25 (6H, m, py-H), 4.58-4.62 (6H, m, py-H) ppm. $\delta_C(CDCl_3)$: 188.3, 185.4, 182.5, 161.2, 158.7, 158.2, 157.8, 157.1, 150.5, 149.9, 145.4, 122.7, 122.0, 121.8, 105.5, 52.6, 45.2 ppm. ν_{max} (DCM): 3055, 1987, 1610, 1553, 1437,

1421, 1322, 896 cm^{-1}. HR-MS: calcd: $C_{27}H_{24}N_6NaO_3$ m/z: $[M+Na]^+$, 503.1802. Found: 503.1824. [Diff(ppm)]: 4.41.

2.5.7 Metal complexes of **20**

General procedure:

Compound **20** (100 mg, 0.208 mmol) was dissolved in MeOH (20 mL). To this was added, dropwise, the appropriate metal salt (0.625 mmol) in MeOH (10 mL). A coloured solid precipitated immediately. The mixture was kept stirring for additional 1 hour at room temperature. The coloured solid was collected by filtration, washed with MeOH, and dried in air overnight.

2.5.7.1 Reaction of **20** with $ZnCl_2$

Off-white solid. Yield: 121 mg, 77 %. δ_H(DMSO): 11.13, 11.51 (3H, m, NH), 8.53-8.59 (6H, m, py-H), 8.15-8.28 (3H, m, CH-NH), 7.34-7.37 (6H, m, py-H), 4.73-4.75 (6H, m, CH_2) ppm. ν_{max} (KBr): 3447, 1607, 1548, 1460, 1431, 1354, 1328, 107, 1031, 837, 809 cm^{-1}. Calcd for: [Zn_2(**20**)Cl_4], $C_{27}H_{24}Cl_4N_6O_3Zn$, C, 42.06; H, 3.40; N, 10.90 %. Found: C, 41.70; H, 3.52; N, 10.66 %.

2.5.7.2 Reaction of **20** with $Zn(ClO_4)_2{\cdot}6H_2O$

Off-white solid. Yield: 87 mg, 56 %. δ_H(DMSO): 11.13, 11.51 (3H, m, NH), 8.54-8.56 (6H, d, py-H), 8.15-8.27 (3H, m, CH-NH), 7.31 (6H, s, br, py-H), 4.72 (6H, s, br, CH_2) ppm. ν_{max} (KBr): 3423, 1606, 1546, 1459, 1431, 1354, 1328, 1221, 1109(br), 807, 626 cm^{-1}. Calcd for: [Zn(**20**)$(ClO_4)_2$], $C_{27}H_{24}Cl_2N_6O_{11}Zn$, C, 43.54; H, 3.25; N, 11.28 %. Found: C, 44.01; H, 2.82; N, 10.78 %.

2.5.7.3 Reaction of **20** with $HgCl_2$

Off-white solid. Yield: 195 mg, 78 %. δ_H(DMSO): 11.13, 11.51 (3H, m, NH), 8.55-8.60 (6H, d, py-H), 8.16-8.28 (3H, m, CH-NH), 7.35-7.38 (6H, m, py-H), 4.73-4.75 (6H, d, CH_2) ppm. ν_{max} (KBr): 3444, 1603, 1532, 1459, 1426, 1353, 1327, 1220, 1067, 1015, 837 cm^{-1}. Calcd for: [Hg_5(**20**)$_2Cl_{10}{\cdot}2H_2O$], $C_{54}H_{52}Cl_{10}Hg_5N_{12}O_8$, C, 27.55; H, 2.23; N, 7.14 %. Found: C, 27.20; H, 2.12; N, 6.85 %.

2.5.7.4 Reaction of **20** with $Hg(ClO_4)_2{\cdot}6H_2O$

Off-white solid. Yield: 194 mg, 73 %. δ_H(DMSO): 11.20, 11.50 (3H, m, NH), 8.70 (6H, s, br, py-H), 8.22-8.35 (3H, m, CH-NH), 7.80 (6H, s, br, py-H), 4.97 (6H, s, br, CH_2) ppm. ν_{max} (KBr): 3455, 1605, 1546, 1427, 1356, 1328, 1220, 1109(br), 626 cm^{-1}. Calcd

for: $[Hg_2(\mathbf{20})(ClO_4)_4]$, $C_{27}H_{24}Cl_4Hg_2N_6O_{19}$, C, 25.34; H, 1.89; N, 6.57 %. Found: C, 25.32; H, 1.54; N, 6.54 %.

2.5.7.5 Reaction of **20** with $NiCl_2 \cdot 6H_2O$

Pale pink solid. Yield: 105 mg, 68 %. ν_{max} (KBr): 3388, 1603, 1520, 1459, 1426, 1353, 1328, 1067, 809 cm^{-1}. Calcd for: $[Ni_2(\mathbf{20})Cl_4]$, $C_{27}H_{24}Cl_4N_6Ni_2O_3$, C, 43.84; H, 3.27; N, 11.36 %. Found: C, 43.37; H, 3.26; N, 10.62 %. μ_{eff} = 3.50 B.M.

2.5.7.6 Reaction of **20** with $Ni(ClO_4)_2 \cdot 6H_2O$

Pale pink solid. Yield: 111 mg, 72 %. ν_{max} (KBr): 3407, 1604, 1521, 1459, 1426, 1354, 1328, 1222, 1109(br), 807, 627 cm^{-1}. Calcd for: $[Ni(\mathbf{20})(ClO_4)_2 \cdot MeOH \cdot H_2O]$, $C_{28}H_{30}Cl_2N_6NiO_{13}$, C, 42.67; H, 3.84; N, 10.66 %. Found: C, 43.19; H, 2.96; N, 10.66 %. μ_{eff} = 2.87 B.M.

2.5.7.7 Reaction of **20** with $Ni(OAc)_2 \cdot 4H_2O$

Pale pink solid. Yield: 120 mg, 66 %. ν_{max} (KBr): 3414, 1599, 1520, 1424, 1351, 1350, 1325, 1222, 1067, 809 cm^{-1}. Calcd for: $[Ni_3(\mathbf{20})(OH)_4(OAc)_2 \cdot H_2O]$, $C_{31}H_{36}N_6Ni_3O_{12}$, C, 43.26; H, 4.22; N, 9.76 %. Found: C, 43.27; H, 4.14; N, 9.47 %. μ_{eff} = 4.32 B.M.

2.5.7.8 Reaction of **20** with $CuCl_2 \cdot 2H_2O$

Brown solid. Yield: 137 mg, 77 %. ν_{max} (KBr): 3433, 1603, 1506, 1428, 1377, 1353, 1330, 1223, 1066, 811 cm^{-1}. Calcd for: $[Cu_5(\mathbf{20})_2Cl_{10} \cdot 4H_2O]$, $C_{54}H_{56}Cl_{10}Cu_5N_{12}O_{10}$, C, 38.03; H, 3.31; N, 9.86 %. Found: C, 38.39; H, 3.34; N, 9.56 %. μ_{eff} = 2.06 B.M.

2.5.7.9 Reaction of **20** with $Cu(ClO_4)_2 \cdot 6H_2O$

Brown solid. Yield: 125 mg, 62 %. ν_{max} (KBr): 3436, 1602, 1504, 1429, 1379, 1353, 1328, 1225, 1108(br), 810, 626 cm^{-1}. Calcd for: $[Cu_2(\mathbf{20})(ClO_4)_3 \cdot (OH)]$, $C_{27}H_{35}Cl_3Cu_2N_6O_{16}$, C, 35.14; H, 2.73; N, 9.11 %. Found: C, 35.10; H, 3.29; N, 8.78 %. μ_{eff} = 2.11 B.M.

2.5.7.10 Reaction of **20** with $Cu(NO_3)_2 \cdot 6H_2O$

Dark green solid. Yield: 112 mg, 57 %. ν_{max} (KBr): 3431, 3077, 1588, 1504, 1427, 1384, 1224, 1066, 1028, 833, 809 cm^{-1}. Calcd for: $[Cu_3(\mathbf{20})(NO_3)_3(OH)_3 \cdot 2H_2O]$, $C_{27}H_{31}Cu_3N_9O_{17}$, C, 34.34; H, 3.31; N, 13.35 %. Found: C, 34.18; H, 3.16; N, 13.40 %. μ_{eff} = 2.99 B.M.

2.5.7.11 Reaction of **20** with $CoCl_2 \cdot 6H_2O$

Green solid. Yield: 94 mg, 57 %. ν_{max} (KBr): 3383, 1606, 1540, 1460, 1426, 1354, 1328, 1222, 1066, 1019, 808 cm^{-1}. Calcd for: $[Co_2(\mathbf{20})Cl_4 \cdot 2MeOH \cdot 2H_2O]$, $C_{29}H_{36}Cl_4Co_2N_6O_7$, C, 41.45; H, 4.32; N, 10.00 %. Found: C, 42.03; H, 4.32; N, 10.46 %. μ_{eff} = 5.70 B.M.

2.5.7.12 Reaction of **20** with $Co(ClO_4)_2 \cdot 6H_2O$

Yellow solid. Yield: 94 mg, 57 %. ν_{max} (KBr): 3428, 1606, 1544, 1462, 1426, 1353, 1328, 1108(br), 806, 626 cm^{-1}. Calcd for: $[Co(\mathbf{20})(ClO_4)_2 \cdot MeOH \cdot H_2O]$, $C_{28}H_{30}Cl_2CoN_6O_{13}$, C, 42.66; H, 3.84; N, 10.66 %. μ_{eff} = 4.05 B.M.

2.5.8 (*Z*)-2,4,6-tris(((3-(1H-imidazol-1-yl)propyl)amino)methylene)cyclohexane-1,3,5-trione (**21**)

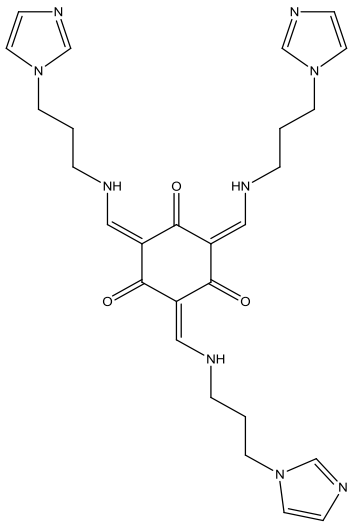

To a suspension of anhydrous $MgSO_4$ (4.14 g, 30 mmol) in CH_2Cl_2 (50 mL) was added compound **17** (0.63 g, 3 mmol). This was followed by 2-aminomethyl pyridine (1.125 g, 9 mmol). The mixture was stirred at room temperature overnight. The resulting suspension was filtered, washed with CH_2Cl_2, and the excess filtrate was removed under vacuum to give compound **21** as a yellow oil.

Yiled: 1.6 g, 96 %. $\delta_H(CDCl_3)$: 11.05, 11.51 (3H, m, NH), 8.05-8.23 (3H, m, CH-NH), 7.50-7.53 (3H, d, imidazole-H), 7.11 (3H, s, imidazole-H), 6.93 (3H, s, imidazole-H), 4.07 (6H, m, NH-$\underline{CH_2}$), 3.38 (6H, m, $\underline{CH_2}$-imidazole), 2.02-2.20 (6H, m, $NHCH_2$-$\underline{CH_2}$) ppm. $\delta_C(CDCl_3)$: 185.2, 157.6, 154.9, 137.1, 130.1, 118.6, 104.9, 46.6, 43.6, 31.7 ppm. ν_{max} (DCM): 3055, 2987, 1610, 1551, 1508, 1450, 1422, 1180, 896 cm^{-1}. $[M+Na]^+$: 568.27. HR-MS: calcd: $C_{27}H_{33}N_9NaO_3$ m/z: $[M+Na]^+$, 554.2604. Found: 554.2592. [Diff(ppm)]: -4.11.

2.5.9 Metal complexes of **21**

General procedure:

Compound **21** (100 mg, 0.188 mmol) was dissolved in MeOH (20 mL). To this was added, dropwise, the appropriate metal salt (0.565 mmol) in MeOH (10 mL). A coloured solid precipitated immediately. The mixture was kept stirring for additional 1 hour at room temperature. The coloured solid was collected by filtration, washed with MeOH, and dried in air overnight.

2.5.9.1 Reaction of **21** with $ZnCl_2$

Off-white solid. Yield: 133 mg, 80 %. δ_H(DMSO): 11.12, 10.80 (3H, m, NH), 7.89-8.13 (6H, m, CH-NH, imidazole-H), 7.41-7.47 (3H, m, imidazole-H), 7.06-7.08 (3H, m, imidazole-H), 4.14 (6H, s, br, $NHCH_2$), 3.23 (6H, s, br, CH_2-imidazole), 2.09 (6H, s, br, $NHCH_2CH_2$) ppm. ν_{max} (KBr): 3468, 3122, 2947, 1614, 1535, 1453, 1354, 1320, 1240, 1186, 1098, 953, 840, 626 cm^{-1}. Calcd for: $[Zn_5(\mathbf{21})_2Cl_{10}\cdot 2H_2O]$, $C_{52}H_{70}Cl_{10}N_{18}O_8Zn_5$, C, 36.42; H, 3.96; N, 14.16 %. Found: C, 36.62; H, 3.80; N, 13.77 %.

2.5.9.2 Reaction of **21** with $Zn(ClO_4)_2\cdot 6H_2O$

Off-white solid. Yield: 128 mg, 78 %. δ_H(DMSO): 10.46-10.92 (3H, m, NH), 7.90-8.09 (6H, m, CH-NH, imidazole-H), 7.55-7.62 (3H, m, imidazole-H), 6.92-7.26 (3H, m, imidazole-H), 4.03-4.31 (6H, m, NH-CH_2), 3.50-3.58 (6H, m, CH_2-imidazole), 1.95-2.13 (6H, m, $NHCH_2$-CH_2) ppm. ν_{max} (KBr): 3428, 3122, 2948, 1614, 1539, 1452, 1355, 1329, 1243, 1184, 1109(br), 839, 636 cm^{-1}. Calcd for: $[Zn(\mathbf{21})(ClO_4)_2\cdot 4H_2O]$, $C_{27}H_{41}Cl_2N_9O_{15}Zn$, C, 37.36; H, 4.76; N, 14.52 %. Found: C, 37.66; H, 4.12; N, 14.53 %.

2.5.9.3 Reaction of **21** with $HgCl_2$

Off-white solid. Yield: 180 mg, 71 %. δ_H(DMSO): 11.18, 10.83 (3H, m, NH), 7.96 (6H, m, NH-CH, imidazole-H), 7.44 (3H, s, br, imidazole-H), 7.05 (3H, s, br, imidazole-H), 4.11 (6H, s, br, NH-CH_2), 3.35 (6H, s, br, CH_2-imidazole), 2.08 (6H, s, br, $NHCH_2$-CH_2) ppm. ν_{max} (KBr): 3442, 3121, 2943, 1610, 1540, 1451, 1352, 1318, 1239, 1109, 837, 647 cm^{-1}. Calcd for: $[Hg_3(\mathbf{21})Cl_6]$, $C_{27}H_{33}Cl_6Hg_3N_9O_3$, C, 24.09; H, 2.47; N, 9.36 %. Found: C, 23.81; H, 2.32; N, 9.02 %.

2.5.9.4 Reaction of **21** with $Hg(ClO_4)_2 \cdot 6H_2O$

Off-white solid. Yield: 177 mg, 68 %. δ_H(DMSO): 10.89, 11.22 (3H, br, NH), 8.46 (3H, s, br, imidazole-H), 7.84 (6H, s, br, CH-NH, imidazole-H), 7.43 (3H, s, br, imidazole-H), 4.32 (6H, s, br, NH-$\underline{CH_2}$), 3.50 (6H, s, br, CH_2-imidazole), 2.17 (6H, s, br, $NHCH_2$-$\underline{CH_2}$) ppm. ν_{max} (KBr): 3527, 3141, 1614, 1529, 1453, 1356, 1109(br), 840, 757, 623 cm^{-1}. Calcd for: [Hg_2(**21**)$(ClO_4)_4 \cdot 2H_2O$], $C_{28}H_{39}Cl_4N_9O_{21}$, C, 24.36; H, 2.85; N, 9.13 %. Found: C, 23.96; H, 2.86; N, 9.44 %.

2.5.9.5 Reaction of **21** with $Ni(ClO_4)_2 \cdot 6H_2O$

Yield: 109 mg, 66 %. ν_{max} (KBr): 3426, 3132, 2947, 1611, 1524, 1453, 1353, 1321, 1108(br), 836, 665, 626 cm-1. Calcd for: [Ni(**21**)$(ClO_4)_2 \cdot MeOH \cdot 2H_2O$], $C_{29}H_{43}Cl_2N_9NiO_{14}$, C, 39.98; H, 4.97; N, 14.47 %. Found: C, 39.75; H, 4.84; N, 14.78 %. μ_{eff} = 3.07 B.M.

2.5.9.6 Reaction of **21** with $CuCl_2 \cdot 2H_2O$

Yield: 116 mg, 65 %. ν_{max} (KBr): 3433, 3126, 1610, 1520, 1452, 1383, 1317, 1234, 1186, 1098, 837, 751, 655 cm^{-1}. Calcd for: [Cu_3(**21**)Cl_6], $C_{28}H_{35}Cl_6Cu_3N_9O_3$, C, 35.44; H, 3.72; N, 13.28 %. Found: C, 35.60; H, 3.94 N, 13.34 %. μ_{eff} = 2.86 B.M.

2.5.9.7 Reaction of **21** with $CoCl_2 \cdot 6H_2O$

Yield: 133 mg, 74 %. ν_{max} (KBr): 3392, 3119, 2942, 1610, 1521, 1451, 1380, 1312, 1236, 1184, 1094, 659 cm^{-1}. Calcd for: [Co_3(**21**)$Cl_6 \cdot H_2O$], $C_{28}H_{37}Cl_6Co_3N_9O_4$, C, 35.28; H, 3.91; N, 13.23 %. Found: C, 35.39; H, 3.75; N, 13.03 %. μ_{eff} = 5.35 B.M.

2.6 Section 5

2.6.1 2,5-Dibromo-1,4-dimethoxybenzene (**22**)[135]

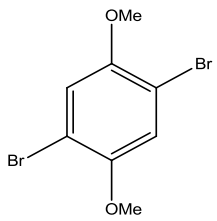

To the solution of 1,4-dimethoxybenzene (10 g, 74.5 mmol) in acetic acid (20 mL) was slowly added bromine (23.15 g, 145 mmol, 7.46 mL) in acetic acid (10 mL) at room temperature. The solution turned to red, and a white solid precipitated after 15 minutes. The mixture was stirred for an additional 2 h then was cooled down in ice. The white

solid was collected by filtration, and washed with cooled MeOH and dried in an oven (75 ℃) overnight.

Yield: 13.2 g, 62 %. $\delta_H(CDCl_3)$: 7.10 (2H, s, ArH), 3.85 (6H, s, OMe) ppm. These match reported data.

2.6.2 1,4-Dimethoxy-2,5-diformylbenzene (**23**)[136]

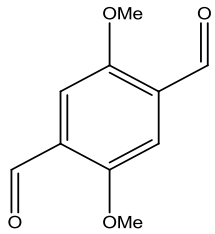

To a solution of 1,4-dibromo-2,5-dimethoxybenzene (**22**) (2 g, 60 mmol) in dry THF (30 mL) was added n-butyllithium 2.5 M in hexane (10 mL 24 mmol) at -78 ℃ under argon and stirred for 2 h. To this was added additional THF (30 mL) and DMF (6 mL, 78 mmol). The solution was stirred at that temperature for extra 1 h and hydrolysed with 3 M HCl (20 mL). The reaction mixture was allowed to warm to room temperature. The yellow solid was collected by filtration, dried in oven (75 ℃) overnight.

Yield: 0.65 g, 49 %. $\delta_H(CDCl_3)$: 10.50 (2H, s, CHO), 7.46 (2H, s, ArH) 3.95 (6H, s, OMe) ppm. These match reported data.

2.6.3 1,4-Dihydroxy-2,5-diformylbenzene (**24**)[137]

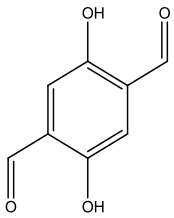

To a mixture of 1,4-dimethoxy-2,5-diformylbenzene (**23**) (0.6 g, 3.15 mmol) in acetic acid (30 mL) was added HBr (48 % w/w, 25 mL). The mixture was heated to reflux for 20 h under argon. Then the solution was cooled on ice. The dark yellow precipitate which formed was collected by filtration, washed with water, and dried in oven (75 ℃) overnight.

Yield: 0.3 g, 61 %. δ_H(DMSO): 10.62 (2H, s, br, ArOH), 10.25 (2H, s, CHO), 7.20 (2H, s, ArH) ppm. These match reported data.

2.6.4 2,5-bis((*E*)-((pyridin-2-ylmethyl)imino)methyl)benzene-1,4-diol (**25**)

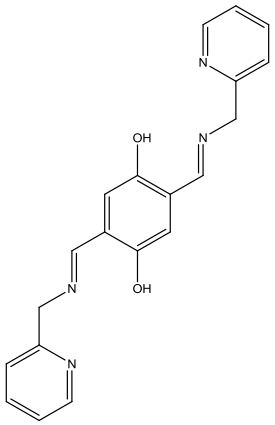

To a mixture of compound **24** (0.465 g, 2.8 mmol) in MeOH (30 mL) was slowly add 2-aminomethyl pyridine (0.6 g, 5.6 mmol) in MeOH (10 mL). The mixture was turned to transparent then small yellow crystals were crashed. The mixture was stirred at room temperature for additional 2 h. The crystals were collected by filtration, washed with cold MeOH, dried in air. The mother solvent was reduced to 10 mL under vacuum. The more solid would be precipitated overnight.

Yield: 0.647 g, 68 %. δ_H(DMSO): 12.45 (2H, s, ArOH), 8.73 (2H, s, CHN), 8.54-8.56 (2H, d, py-H, J = 4.8 Hz), 7.82 (2H, dt, py-H, J = 1.8, 7.6 Hz), 7.42 (2H, d, py-H, J = 7.8 Hz), 7.30-7.34 (2H, m, py-H), 7.09 (2H, s, ArH), 4.91 (4H, s, CH_2) ppm. δ_C(DMSO): 166.5, 157.6, 151.9, 149.2, 137.0, 122., 122.2, 1221.6, 117.9, 64.3 ppm. ν_{max} (KBr): 3437, 3006, 2885, 1642, 1590, , 1430, 1360, 1311, 1155, 1066, 791, 743 cm^{-1}. m.p : 170-171 ℃. Calcd for: $C_{20}H_{18}N_4O_2$, C, 69.35; H, 5.24; N, 16.17 %. Found: C, 69.54; H, 5.33; N, 15.89 %.

2.6.5 Metal complexes of **25**

General procedure:

To a mixture of compound **25** (0.05 g, 0.144 mmol) in MeOH (25 mL) was added appropriate metal salt (0.289 mmol) in MeOH (10 mL). The mixture was heated to reflux overnight. The coloured solid would be precipitated after the reaction cooled down. The precipitate was collected by filtration, washed with MeOH, and dried in air overnight.

2.6.5.1 Reaction of **25** with $Zn(ClO_4)_2 \cdot 6H_2O$

Dark yellow solid. Yield: 61 mg, 60 %. δ_H(DMSO): 8.63 (2H, s, CHN), 8.58 (2H, d, py-H, J = 5.7 Hz), 8.10 (2H, t, py-H, J = 6.2 Hz), 7.56-7.65 (4H, m, py-H), 6.74 (2H, s, ArH), 5.05 (4H, s, CH_2) ppm. ν_{max} (KBr): 3391, 1636, 1572, 1471, 1369, 1232, 1144, 1109(br), 844, 765, 627 cm^{-1}. Calcd for: [Zn_2(**25**)$(ClO_4)_2 \cdot$MeOH], $C_{21}H_{20}Cl_2N_4O_{11}Zn_2$, C, 35.72; H, 2.86; N, 7.94 %. Found: C, 35.75; H, 2.75; N, 7.23 %.

2.6.5.2 Reaction of **25** with $Zn(OAc)_2 \cdot 2H_2O$

Dark purple solid. Yield: 48 mg, 56 %. ν_{max} (KBr): 3397, 1625, 1575, 1443, 1428, 1377, 1321, 1140, 1050, 1020, 853, 762 cm^{-1}. Calcd for: [Zn_2(**25**)$(OAc)_2 \cdot 2H_2O$], $C_{24}H_{22}N_4O_6Zn_2$, C, 45.81; H, 4.16; N, 8.90 %. Found: C, 46.30; H, 3.68; N, 9.14 %.

2.6.6 2,5-bis((*E*)-((pyridin-3-ylmethyl)imino)methyl)benzene-1,4-diol (**26**)

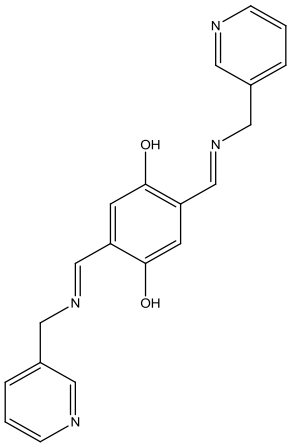

To a mixture of compound **24** (0.465 g, 2.8 mmol) in MeOH (30 mL) was slowly add 2-aminomethyl pyridine (0.6 g, 5.6 mmol) in MeOH (10 mL). The mixture was turned to transparent then small yellow crystals were crashed. The mixture was stirred at room temperature for additional 2 h. The crystals were collected by filtration, washed with cold MeOH, dried in air. The mother solvent was reduced to 10 mL under vacuum. The more solids would be precipitated overnight.

Yield: 0.82 g, 85 %. δ_H(DMSO): 12.30 (2H, s, ArOH), 8.73 (2H, s, CHN), 8.59 (2H, s, py-H), 8.52 (2H, d, py-H, J = 4.7 Hz), 7.75-7.79 (2H, m, py-H), 7.39-7.43 (2H, m, py-H), 7.08 (2H, s, ArH), 4.86 (4H, s, CH_2) ppm. δ_C(DMSO): 166.1, 151.8, 149.1, 148.5, 135.6, 134.1, 123.7, 121.6, 117.8, 59.8 ppm. ν_{max} (KBr): 3327, 1636, 1576, 1512, 1437,

1426, 1363, 1312, 1218, 1156, 1067, 854, 705 cm^{-1}. m.p: 170-171 ℃. Calcd for: $C_{20}H_{18}N_4O_2$, C, 69.35; H, 5.24; N, 16.17 %. Found: C, 68.92; H, 4.88; N, 15.88 %.

2.6.7 Metal complexes of **26**

General procedure

To a mixture of compound **26** (0.05 g, 0.144 mmol) in MeOH (25 mL) was added appropriate metal salt (0.289 mmol) in MeOH (10 mL). The mixture was heated to reflux overnight. The coloured solid would be precipitated after the reaction cooled down. The solids collected by filtration, washed with MeOH, and dried in air overnight.

2.6.7.1 Reaction of **26** with $ZnCl_2$

Brown orange solid. Yield: 33 mg, 47.8 %. δ_H(DMSO): 12.30 (2H, s, ArOH), 8.73 (2H, s, CHN), 8.59 (2H, s, py-H), 8.52 (2H, d, py-H, J = 4.7 Hz), 7.75-7.79 (2H, m, py-H), 7.39-7.43 (2H, m, py-H), 7.08 (2H, s, ArH), 4.86 (4H, s, CH_2) ppm. ν_{max} (KBr): 3414, 1629, 1611, 1484, 1436, 1362, 1346, 1311, 1159, 1061, 787, 703 cm^{-1}. Calcd for: [Zn(**26**)Cl_2], $C_{20}H_{18}Cl_2N_4O_2Zn$, C, 49.77; H, 3.76; N, 11.61 %. Found: C, 49.85; H, 3.62; N, 11.15 %.

2.6.7.2 Reaction of **26** with $Zn(ClO_4)_2 \cdot 6H_2O$

Dark red solid. Yield: 40 mg, 47.1 %. ν_{max} (KBr): 3452, 1613, 1471, 1436, 1374, 1316, 1231, 1108, 873 cm^{-1}. Calcd for: [Zn(**26**)$(ClO_4)\cdot(OH)\cdot 2MeOH$], $C_{22}H_{26}ClN_4O_9Zn$, C, 44.69; H, 4.43; N, 9.48 %. Found: C, 44.86; H, 4.69; N, 9.47 %

2.6.7.3 Reaction of **26** with $Zn(OAc)_2 \cdot 2H_2O$

Red solid. Yield: 67 mg, 69.8 %. δ_H(DMSO): 8.32-8.56 (6H, m, py-H, CHN), 7.78 (2H, s, br, py-H), 7.31-7.43 (2H, m, py-H), 6.63-6.79 (2H, m, ArH), 4.77-4.84 (4H, m, CH_2) ppm. ν_{max} (KBr): 3385, 1621, 1608, 1561, 1476, 1431, 1366, 1315, 1240, 1171, 1048, 872, 704 cm^{-1}. Calcd for: [Zn_2(**26**)$(OAc)_2 \cdot 4H_2O$], $C_{24}H_{32}N_4O_{10}Zn_2$, C, 43.20; H, 4.83; N, 8.40 %. Found: C, 43.45; H, 4.97; N, 7.98 %.

2.6.7.4 Reaction of **26** with $HgCl_2$

Yellow solid. Yield: 72 mg, 76.9 %. δ_H(DMSO): 12.30 (2H, s, ArOH), 8.73 (2H, s, CHN), 8.59 (2H, s, py-H), 8.52 (2H, d, py-H, J = 4.7 Hz), 7.78-7.80 (2H, m, py-H), 7.41-7.45 (2H, m, py-H), 7.08 (2H, s, ArH), 4.86 (4H, s, CH_2) ppm. ν_{max} (KBr): 3439, 1629, 1586, 1431, 360, 1312, 1214, 1195, 1157, 1055, 784, 701 cm^{-1}. Calcd for:

[Hg(**26**)Cl_2·MeOH], $C_{21}H_{22}Cl_2HgN_4O_3$, C, 38.81; H, 3.41; N, 8.62 %. Found: C, 38.95; H, 3.66; N, 8.66 %.

2.7 Section 6

2.7.1 2,6-bis-(Hydroxymethyl)-pyridine (**27**)[138]

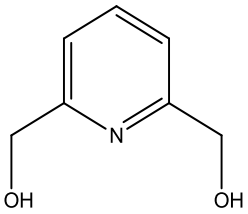

To pyridine-2,6-dicarboxylic acid dimethyl ester **13** 5.00 g (25.6 mmol) in THF (50 mL) was slowly added $NaBH_4$ 4.21 g (110.5 mmol), and the solution was then stirred at room temperature for 12 h. After evaporation of the solvent, the residue was dissolved in 30 mL water, adjusted to pH 3 with 2M HCl, and then adjusted to pH 9 with saturated aqueous Na_2CO_3 solution. The solvent was removed under vacuum, the residue was extracted with $CHCl_3$ (300 mL) by continuous liquid – liquid extraction for 10 h. The organic solvent was dried with $MgSO_4$ and removed under vacuum to give a white product which was washed with Et_2O and dried in vacuum to give compound **27**.

Yield: 2.5 g, 68 %. $\delta_H(CDCl_3)$: 8.19 (2H, d, py-H, J = 7.59), 8.10 (1H, t, py-H, J = 7.41), 4.78 (4H, s, CH_2). These match reported data.

2.7.2 Pyridine-2,6-dicarboxaldehyde (**28**)[139]

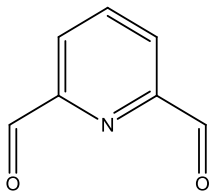

To the mixture of 2,6-bis-(hydroxymethyl)-pyridine (11.51 g, 82.8 mmol) and SeO_2 (9.99 g, 90 mmol), was added 1,4-dioxane (200 mL). The mixture was then reflux for 4 h and filtered. The solvent was removed under vacuum to give a crude product as off-white solid. The solid was dissolved in DCM, and passed through a silica gel plug. The solvent was concentrated, and the solid was recrystallized from a mixture of 100 mL of acetone and 100 mL of hexane to afford 9.2 g of white crystals, which was kept under argon.

Yield: 9.2 g, 82 %. $\delta_H(CDCl_3)$: 10.18 (2H, s, CHO), 8.19 (2H, d, py-H, J = 7.59 Hz), 8.10 (1H, t, py-H, J = 7.41 Hz) ppm. These match reported data.

2.7.3 (N,N'E,N,N'E)-N,N'-(pyridine-2,6-diylbis(methanylylidene))bis(1-(pyridin-2-yl)methanamine) (29)

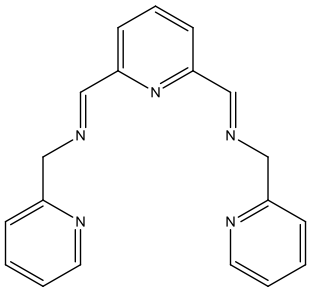

To a suspension of anhydrous $MgSO_4$ (13.8 g, 100 mmol) in $CHCl_3$ (100 mL) was added compound **28** (1.35 g, 10 mmol). This was followed by 2-aminomethyl pyridine (2.16 g, 20 mmol). The mixture was heated to reflux for 24 h. The resulting suspension was filtered, washed with $CHCl_3$, and the solution was removed under vacuum to give compound **29** as a yellow oil.

Yield: 2.95 g, 94 %. $\delta_H(CDCl_3)$: 8.62 (2H, s, CHN), 8.58-8.60 (2H, m, py-H), 8.22 (2H, d, py-H, J = 7.5 Hz), 7.83 (2H, t, py-H, J = 7.5 Hz), 7.69 (2H, td, py-H, J = 7.5, J = 1.8 Hz), 7.42 (2H, d, py-H, J = 7.8 Hz), 7.18-7.22 (2H, m, py-H), 5.04 (4H, s, CH_2) ppm. $\delta_C(CDCl_3)$: 163.9, 158.7, 149.5, 149.3, 136.7, 124.9, 122.5, 122.4, 121.5, 66.5 ppm. ν_{max} (DCM): 3020, 1652, 1594, 1573, 1521. 1475, 1436, 1048, 929 cm^{-1}. HR-MS: calcd: $C_{19}H_{18}N_5$ m/z: $[M+H]^+$, 316.1562. Found: 316.1556. [Diff(ppm)]: -2.47.

2.7.4 (N,N'E,N,N'E)-N,N'-(pyridine-2,6-diylbis(methanylylidene))bis(1-(pyridin-3-yl)methanamine) (30)

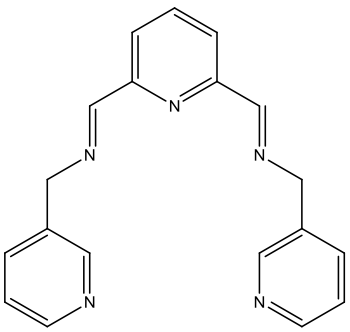

Experimental

To a suspension of anhydrous $MgSO_4$ (13.8 g, 100 mmol) in $CHCl_3$ (100 mL) was added compound **28** (1.35 g, 10 mmol). This was followed by 3-aminomethyl pyridine (2.16 g, 20 mmol). The mixture was heated to reflux for 24 h. The resulting suspension was filtered, washed with $CHCl_3$, and the excess filtrate was removed under vacuum to give compound **30** as a yellow oil.

Yield: > 99 %. $\delta_H(CDCl_3)$: 8.64 (2H, d, py-H, J = 1.8 Hz), 8.56 (2H, s, CHN), 8.54 (2H, dd, py-H, J = 1.5, 4.8 Hz), 8.10 (2H, d, py-H, J = 9 Hz), 7.84 (1H, t, py-H, J = 7.8 Hz), 7.69 (2H, dt, py-H, J = 7.8, 2.1 Hz), 7.30 (2H, m, py-H), 4.90 (4H, s, CH_2) ppm. $\delta_C(CDCl_3)$: 163.1, 154.0, 149.5, 148.7, 137.1, 135.7, 134.1, 123.5, 122.8, 62.2 ppm. ν_{max} (DCM): 3054, 2986, 1648, 1591, 1576, 1479, 1454, 1424, 1027 cm^{-1}. HR-MS: calcd: $C_{19}H_{18}N_5$ m/z: $[M+H]^+$, 316.1562. Found: 316.1558. [Diff(ppm)]: -1.66.

3 Results and Discussion

3.1 Introduction

This thesis presents the results of an investigation into the development of novel divalent metal ion binders using a small molecular weight compound which contains at least two imine groups and one phenol group. The two imine groups are formed from 2-, 3-, or 4-aminomethylpyridine, or 1-(3-aminopropyl)-imidazole (APIM), which affords one or two more N donor atom in each bridging side. This feature provides a 'pocket' for the metal ion to bind into.

Different divalent metal ion salts (MX_2), with M = Zn(II), Hg(II), Ni(II), Cu(II) and Co(II) and X = chloride, perchlorate and acetate, are used in forming novel metal complexes.

The results from these corresponding complexes could be distinguished from ^{1}H NMR spectroscopy, IR spectroscopy and elemental analysis.

3.2 Schiff base ligand formation and hydrolysis

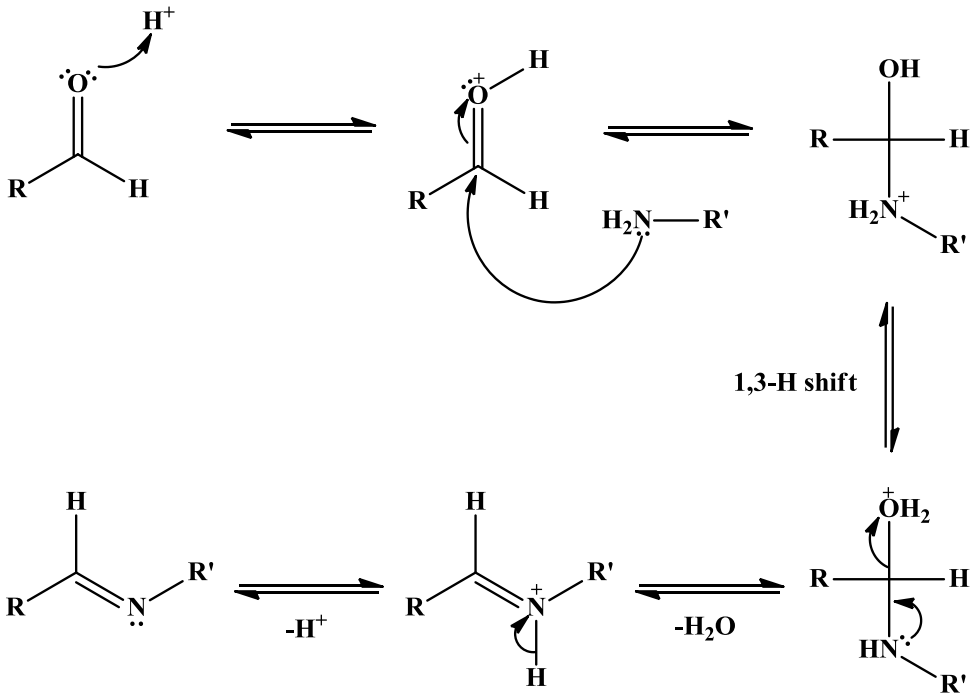

Figure 1.5: Mechanism of imine formation.

Hydrolysis of the Schiff-base ligands proves highly problematic with cleavage of the imine bond occurring under mild conditions. Although anhydrous solvents were used throughout, the commercially obtained salts, as their hydrated forms, supplied enough water into the system for hydrolysis of imine bond to occur. The problem was

exacerbated by the presence of the metal cations which have Lewis acid properties and can accelerate this bond cleavage. The mechanism for imine formation and its reversible reaction are shown in the Figure 3.2.1.

This hydrolysis even could be reversible in the imine-ligand formation. But sometimes imine-ligands are very stable even in acidic conditions. It is still unknown why some imine compounds undergo hydrolysis, while others are stable in similar conditions. In order to stop the hydrolysis of the imine group, anhydrous $MgSO_4$ was used to stop potential hydrolysis in chloroform/DCM in mild conditions.

3.3 Section 1

3.3.1 Pseudo Calixarenes

The synthesis of compound (5-*tert*-butyl-2-hydroxy-1,3-phenylene)dimethanol **1** is shown in Figure 3.3.1 which is reported by Kwanghyun and co-workers[129] by using 4-*tert*-butylphenol, aqueous formaldehyde, and 2 % sodium hydroxide solution at 40 ℃ for 2 days. However, the generated crude product is formed as a yellow oil and it was hard to solidify the crude compound **1** from a mixture (ether/hexane) solution.

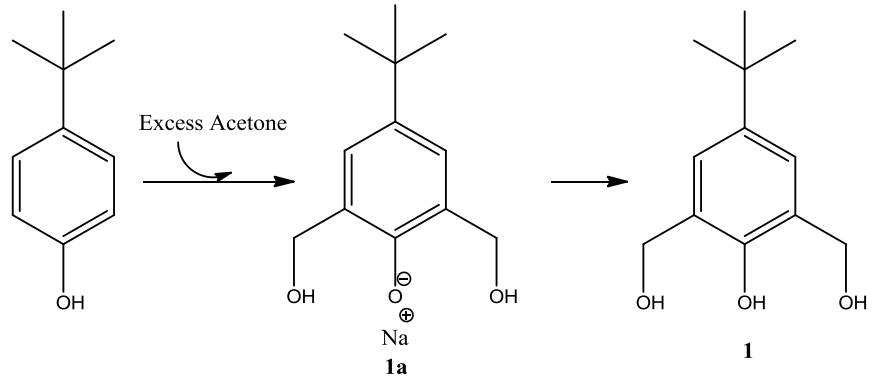

Figure 3.3.1: The formation of compound **1**.

Hence, the purification of the intermediate (sodium 2,6-bis(hydroxymethyl)-4-tert-butylphenolate) **1a** (shown in Figure 3.3.1) was necessary due to the straightforward synthetic route from **1a** to **1**. The excess acetone was used in order to solidify the intermediate. The ^{1}H NMR spectrum of **1a** is shown in Figure 3.3.2 suggesting the intermediate was clean. The signal of the aromatic protons are resonating at 6.54 ppm, and the bridging methylene protons can be seen at 4.42 ppm. There was no peak at around 7-9 ppm indicating that the phenol group was deprotonated. The signal of the alcohol protons occurred at 2.09 ppm.

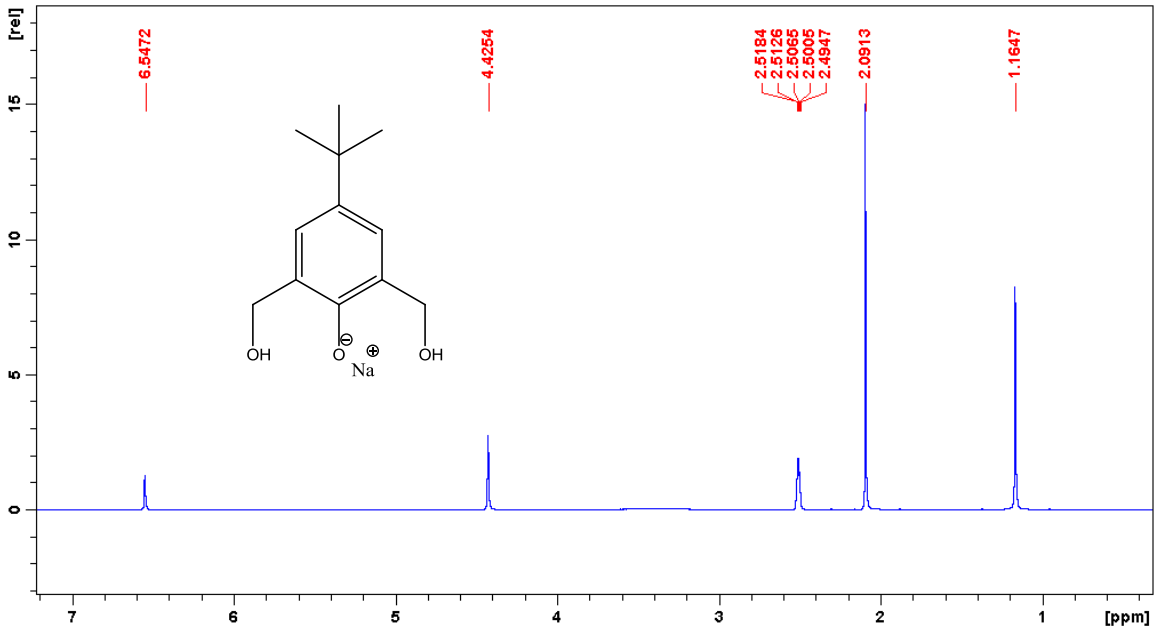

Figure 3.3.2: The ^{1}H NMR spectrum of compound **1a** in d_6-DMSO.

The IR spectrum of intermediate **1a** contains the aromatic C=C stretches which occurrs at 1480 cm^{-1} which has shifted from 1490 cm^{-1} in compound **1**. The C-O bend from the phenol group appears as a weak broad peak at 1218 cm^{-1} in compound **1**, while with alkalized **1a** appears as a sharp peak at 1221 cm^{-1}.

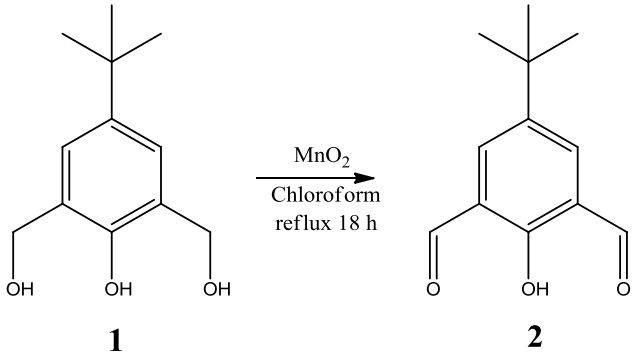

Figure 3.3.3: Synthesis of compound **2**.

Adjusting of **1a** with 25 % H_2SO_4 in H_2O to pH 2 yielded compound **1** as a white solid. It was recrystallized from a mixture of ether/hexane and obtained as a white crystalline solid. The presence of a singlet at 8.00 ppm in the ^{1}H NMR spectrum is indicative of the formation of the phenol group.

Compound 5-(1,1-dimethylethyl)-2-hydroxy-1,3-benzenedicarboxaldehyde **2** was synthesised *via* the method reported by Yong and co-workers[140] (shown in Figure 3.3.3). Compound **1** reacted with activated MnO_2 in chloroform for 18 h under reflux yielding

compound **2** with no further oxidation to the carboxylic acid groups. The mechanism could be explained either by the formation of a π-complex between the aromatic ring containing the alcohol, and some Lewis acid site on the surface of MnO_2 particles or by the favourable thermodynamics involved in the formation of a carbonyl conjugated with an unsaturated system. During the course of the reaction, the MnO_2 particles changed from being large and coarse to being very fine particles which then caused a problem when it came to remove them from the reaction. To overcome this, activated carbon was added to the remaining brown mixture. Activated carbon is a form of carbon processed to be riddled with small, low-volume pores that increase the surface area available for adsorption. The mixture was gently heated to reflux for an additional 15 min to let all the MnO_2 particles be absorbed by activated carbon. It was then filtered while hot to remove more than 90 % of MnO_2. The remaining mixture was passed through a silica gel plug to leave a clean light yellow solution. The excess chloroform was removed under vacuum.

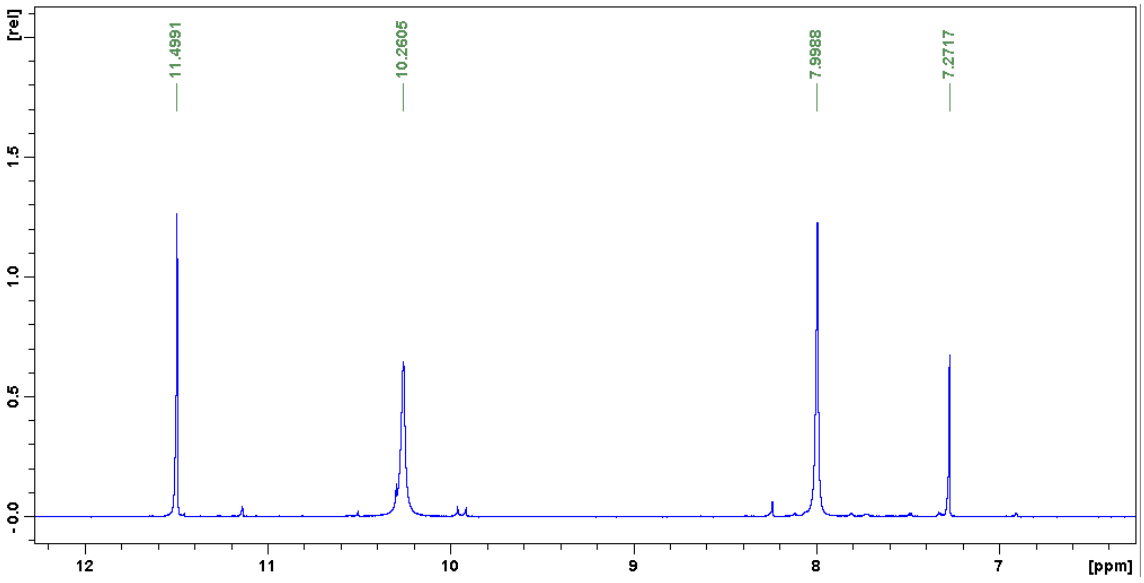

Figure 3.3.3.1: The ^{1}H NMR spectrum of compound **2** in $CDCl_3$.

It was found that compound **2** could be also synthesised directly from 4-*tert*-butyl phenol with hexamethylenetetramine in trifluoroacetic acid (TFA) under inert conditions. This is only one-step reaction in comparison to the early experiment with a good yield (65 %) which was reported by Yim-Pan and co-workers.[141]

In the both synthetic routes, the disappearance of a singlet at 4.77 ppm and the presence of a aldehyde peak at 10.25 ppm in the ^{1}H NMR spectrum indicate that all alcohol groups were oxidised to carbonyl groups. The phenol proton signal shifts from 8.00

ppm to 11.47 ppm due to a strong hydrogen bonding. The IR spectrum of compound **2** shows the presence of a carbonyl group at 1686, 1660 cm^{-1} and OH at 2964 cm^{-1}, respectively.

Due to the difficulty in removing MnO_2 particles, the second way proved to be a better way to synthesise the target compound.

3.3.2 Pseudo Calixarene Schiff Base Ligands

Compound **2** can be used to form four new ligands (**3** – **6**) as shown in Figure 3.3.4. All the ligands were synthesised using the same reaction strategy, which was one equivalent of compound **2**, two equivalents of the appropriate amine precursors and ten equivalents of anhydrous $MgSO_4$ in DCM with stirring for 12 hours at room temperature.

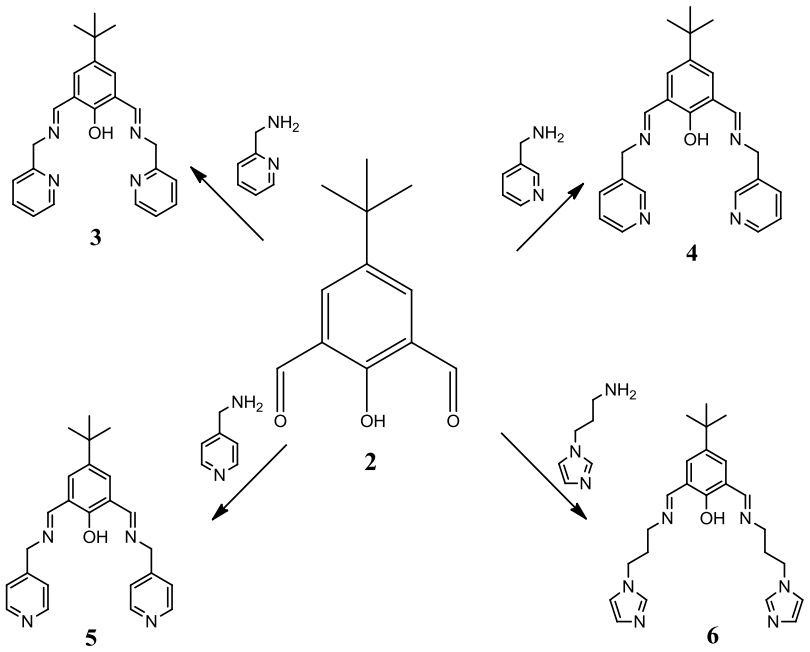

Figure 3.3.4: Synthesis of ligands **3** – **6**.

3.3.3 Ligand 3

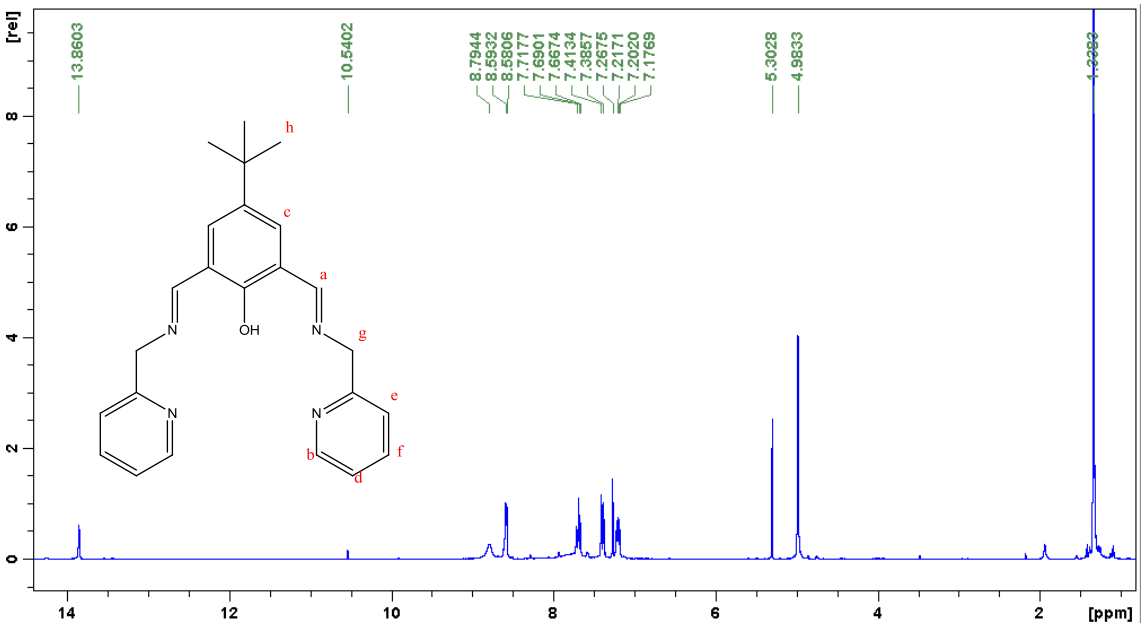

Figure 3.3.5: The ^{1}H NMR of ligand **3** in $CDCl_3$.

The ligand **3** was isolated as a yellow oil. The ^{1}H NMR spectrum of ligand **3** is shown in Figure 3.3.5. The signal of phenol proton occurring at 13.86 ppm in comparison to the di-carbonyl compound **2** at 11.47 ppm suggested that a stronger hydrogen bond is formed between the imine and the phenol rather than the one formed between the aldehyde and the phenol. The appearance of the imine proton Ha which was present at 8.79 ppm as a broad peak and the disappearances of the aldehyde proton at around 10 ppm of compound **2** were indicative of the imine formation. Interestingly, the aromatic proton Hc was present as a small broad peak at 7.78 ppm. The protons Hb, Hd, He and Hf in the pyridine rings of the side chains are represented at 8.58, 7.69, 7.40 and 7.20 ppm, respectively. The bridging methylene protons Hg which appear at 4.98 ppm indicated that the reaction had occurred.

The IR spectrum of ligand **3** was run under DCM. As imine electrons are more delocalised than aldehyde, the C=N stretch signal of imine group is present at 1635 cm^{-1}. In addition, the C=N stretch for the lower pyridine rings appears at 1592 cm^{-1} but it was difficult to assign the other peaks from the pyridine rings. The signal of C-O stretch which should be at around 1270 cm^{-1} was blocked by DCM solvent stretches.

The mass spectrum has suggested that ligand **3** is pure.

3.3.4 Metal complexes of ligand 3

Metal complex reactions of ligand **3** with various metal(II) salts were carried out in MeOH. The reactions were carried out by stirring in MeOH for 2 hours. The resulting coloured solids were obtained by filtration.

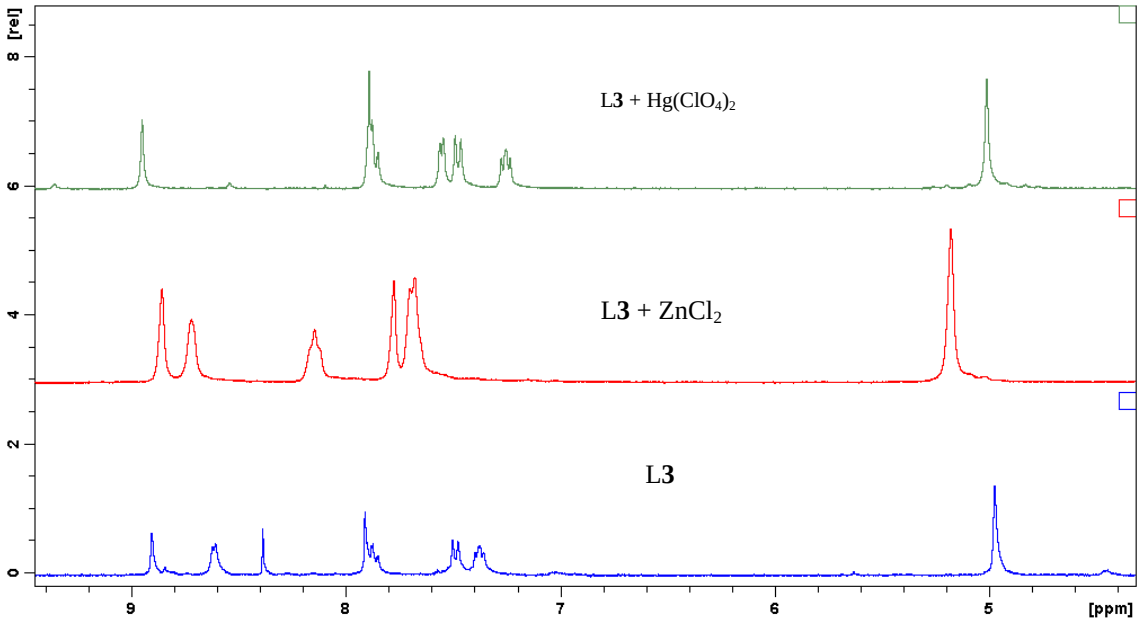

Figure 3.3.6: A comparison of the ^{1}H NMR spectra of ligand **3** and its corresponding Zn(II) chloride and Hg(II) perchlorate complexes in DMSO-d_6.

3.3.4.1 [Zn_2(**3**)Cl_3]

The complex [Zn_2(**3**)Cl_3] is formed as a yellow solid. The ^{1}H NMR spectrum of compound [Zn_2(**3**)Cl_3] is shown in Figure 3.3.6 (in red). The disappearance of the phenol proton at around 13 ppm has suggested the phenol group was deprotonated by metal ion and coordinated to the Zn(II) ion centre. Imine proton Ha resonates at 8.90 ppm in ligand **3** in comparison to the original peak at 8.58 ppm indicating that the nitrogen atoms from the imine group are binding to the metal centre. While the protons in the pyridine rings, Hb and Hd are observed at 8.72 and 8.14 ppm which were seen the previous positions at 8.61 and 7.87 ppm in ligand **3**, respectively. The protons He and Hf are obtained at 7.77 ppm as a broad singlet where the two protons have moved from 7.50 and 7.36 ppm in ligand **3**. These protons shifts are pointing out that nitrogen atoms from the pyridine rings are binding to the Zn(II) ion centre as well. Slight chemical shifts are also occurring at either the aromatic proton Hc or the bridging methylene proton Hg. The signals of protons Hc and Hg are represented at 7.70 and 5.17 ppm which have moved from 7.91 and 4.97 ppm in ligand **3**.

In the IR spectrum of compound [Zn_2(**3**)Cl_3], the signal of the imine group which is obtained at 1655 and 1637 cm^{-1}, respectively, has suggested the two imine groups are in the slight different environment. In addition, the C=N stretch from the lower pyridine rings is present at 1608 cm^{-1} in comparison to the original one at 1592 cm^{-1}, indicating the occurrence of the pyridyl nitrogens coordination to the Zn(II) ion centre.

Elemental analysis indicated that the complex had the formula [Zn_2(**3**)Cl_3]. This would also imply that two zinc ions were bonded to the ligand and that three chloride ions were also involved. The ligand itself is deprotonated to account for the neutral charge. The coordination number of each Zn(II) ion is four. The bonding similarity of each Zn(II) ion is through one nitrogen atom of imine group and one nitrogen atom from a pyridine ring, as well as one chloride ion. The only difference is that one Zn(II) ion is bonded to the oxygen atom from the phenol group, while the other one Zn(II) ion is coordinated to the third chloride ion. Hence, the possible structure of [Zn_2(**3**)Cl_3] is depicted in Figure 3.3.7.

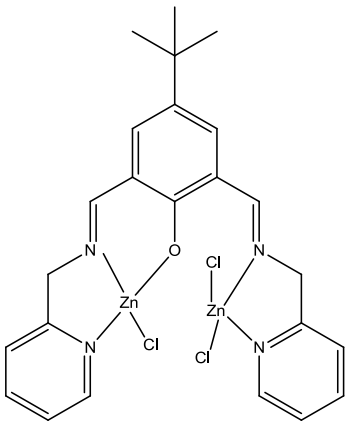

Figure 3.3.7: Possible structure for Zn_2(**3**)Cl_3.

3.3.4.2 [Hg(**3**)(ClO_4)]

The complex [Hg(**3**)(ClO_4)] was isolated as a yellow solid. The ^{1}H NMR spectrum of compound [Hg(**3**)(ClO_4)] is shown in Figure 3.3.6 (in green). The phenol proton was deprotonated by the Hg(II) ion as no signal appearing around 13-15 ppm in the ^{1}H NMR spectrum. The signal of the imine proton Ha has slightly shifted to 8.95 ppm in the Hg(II) complex which was seen at 8.90 ppm in free ligand spectrum, therefore a weak bonding could be occurred between the imine nitrogen atoms and the Hg(II) ion. A big difference of the proton signals of the lower pyridine rings was found between the ligand and the Hg(II) complex. Proton Hb has significantly shifted to 7.55 ppm when compared with the original peak at 8.61 ppm in ligand **3** while proton Hf which

presented at 7.37 ppm in ligand **3** has moved to 7.25 ppm. These shifts would indicate that the nitrogen atoms from the pyridine rings could be coordinated to the Hg(II) ion centre. The bridging methylene proton Hg resonates at 5.01 ppm which was seen to have a slight change from ligand **3** at 4.95 ppm.

The IR spectrum of complex [Hg(**3**)(ClO_4)] contains a broad signal $\nu_{C=N}$ at 1638 cm^{-1} which is similar to that of ligand **3** at 1635 cm^{-1} suggesting that the nitrogen atoms from the imine groups could be binding to the metal ion centre which is in agreement with the results discussed earlier in the ^1H NMR section. The C=N signal for the pyridine rings is obtained at 1600 cm^{-1} which was seen to have a slight change from the original spectrum at 1592 cm^{-1} indicating that the nitrogen atoms from pyridine rings are coordinated to the Hg(II) ion centre. The appearance of perchlorate group stretches at 1094 cm^{-1} as a strong broad signal indicated that metal complexation had occurred.

Elemental analysis indicated the complex had formula [Hg(**3**)(ClO_4)]. This would also imply that Hg(II) ion is bonded to the ligand and that one perchlorate group is also involved. The ligand itself is deprotonated to account for neutral charge. The bonding of the Hg(II) ion is through the deprotonated phenol oxygen atom, and two nitrogen atoms from the pyridine rings and two imine nitrogen atoms. The coordination number of the Hg(II) ion is five. So, the possible structure of compound [Hg(**3**)(ClO_4)] is depicted in Figure 3.3.8.

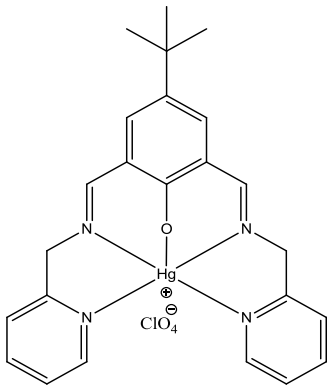

Figure 3.3.8: Possible structure for [Hg(**3**)(ClO_4)].

3.3.5 Ligand 4

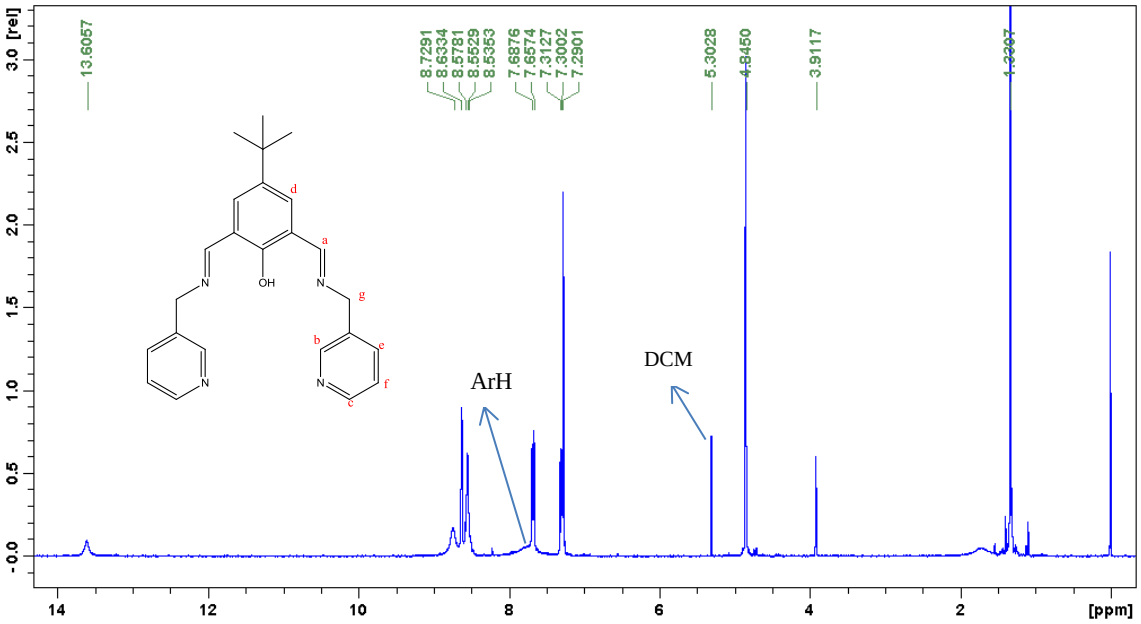

Figure 3.3.9: The ^{1}H NMR spectrum of ligand **4** in $CDCl_3$.

The ligand **4** is formed as a yellow solid which recrystallized from MeOH. The ^{1}H NMR spectrum of ligand **4** is shown in Figure 3.3.9, and the signal of the phenol proton appears as a singlet at 13.60 ppm in comparison to the original spectrum at 11.47 ppm from di-carbonyl compound **2**. The reason for this has been explained earlier for ligand **3** in section 3.3.3. The signal of the imine proton Ha is occurring at 8.73 ppm as a broad peak and there is no peak appearing at around 10 ppm suggesting that imine formation had occurred. The aromatic proton Hd is present as a small broad peak at 7.78 ppm. In addition, the signals of protons from the lower pyridine rings, protons Hb, Hc, He and Hf are represented at 8.63, 8.55, 7.66 and 7.30 ppm, respectively. The bridging methylene protons Hg is seen at 4.84 ppm.

The IR spectrum of ligand **4** contains the OH stretch at 3375 cm^{-1} as a broad peak. The signal of the imine group $\nu_{C=N}$ at 1630 and 1600 cm^{-1}, respectively, suggests that the two imine groups are in different environments, perhaps due to hydrogen bonding between one imine nitrogen atom and phenol proton. In addition, the signal of the C=N stretch from the lower pyridine ring is present at 1562 cm^{-1}. It is difficult to assign specific bands for pyridine rings in the IR spectrum of ligand **4** and its corresponding metal complexes due to the large number of bands already present. The elemental analysis has indicated ligand **4** is pure.

3.3.6 Metal complexes of ligand 4

Metal complexation reactions of ligand **4** with various metal(II) salts were carried out in MeOH. The reactions were carried out by stirring the ligand the metal salt for 2 hours in MeOH. The resulting coloured solids were collected by filtration.

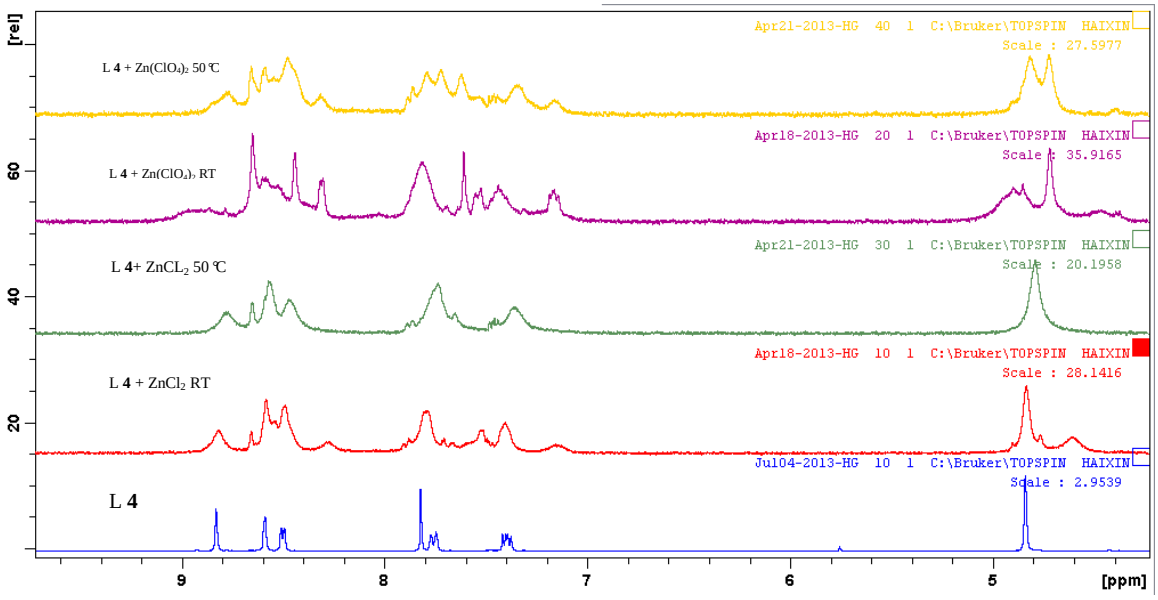

Figure 3.3.10: A comparison of the ^{1}H NMR spectra of ligand **4** and its corresponding Zn(II) chloride and Zn(II) perchlorate complexes at room temperature and 50 ℃, respectively, in DMSO-d_6.

The comparison of ^{1}H NMR spectra of ligand **4** and its corresponding Zn(II) complexes at either room temperature or 50 ℃ is shown in Figure 3.3.10. Although the spectra of the Zn(II) metal complexes are not clear, it still indicates some basic information, 1) The broad peaks and the disappearance of phenol proton indicate the Zn(II) complexation occurred successfully and the complexes are probably polymeric complexes. 2) The imine group in the complexes are not hydrolysed which is due to no peak at around 10 ppm.

3.3.6.1 [Zn_2(**4**)Cl_3·MeOH]

The complex of [Zn_2(**4**)Cl_3·MeOH] is isolated as a yellow solid. The ^{1}H NMR spectra of compound [Zn_2(**4**)Cl_3·MeOH] at room temperature and 50 ℃ are shown in Figure 3.3.10 in red and green, respectively. All protons of the Zn(II) complexes at different temperatures are obtained as broad signals which would imply that polymeric Zn(II) complexes were formed.

In the IR spectrum of compound [Zn_2(**4**)Cl_3·MeOH], the signal of imine group $\nu_{C=N}$ is observed at 1648 and 1630 cm^{-1} in comparison to original ligand **4** at 1630 and 1600 cm^{-1}, respectively, indicating the two imine groups are in different environments. The appearance of a signal of C=N stretch for the lower pyridine rings is occurring at 1540 cm^{-1} which has moved from 1561 cm^{-1} in ligand **4**, has pointed out that the two nitrogen atoms from pyridine rings are binding to the Zn(II) ion centre. The signal ν_{C-O} stretch appearing at 1220 cm^{-1} in ligand **4** shifts to 1231 cm^{-1} in the metal complex which is thought of as another donor O atom.

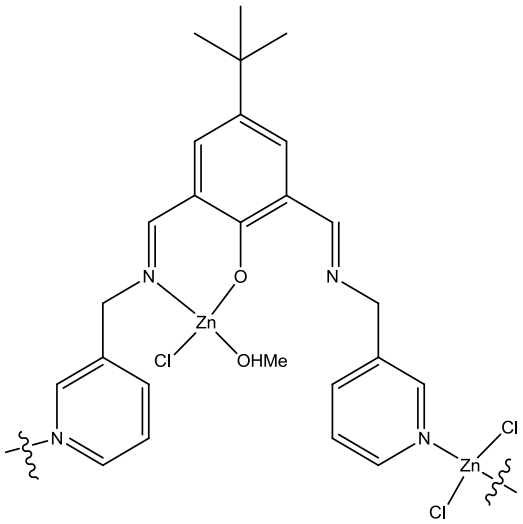

Figure 3.3.11: Possible structure for [Zn_2(**4**)Cl_3·MeOH].

Elemental analysis indicated that the complex had the formula [Zn_2(**4**)Cl_3·MeOH]. This would also imply that two Zn(II) ions were bonded to the ligand and that three chloride ions as well as one coordination MeOH molecule were also involved. The ligand itself is deprotonated to account for the neutral charge. The coordination number of each Zn(II) ion is four. The possible structure of one monomer unit of compound [Zn_2(**4**)Cl_3·MeOH] is depicted in Figure 3.3.11.

3.3.6.2 [Zn(**4**)(ClO_4)·$4H_2O$]

The complex [Zn(**4**)(ClO_4)·$4H_2O$] is formed as a yellow solid. The ^{1}H NMR spectra of compound [Zn(**4**)(ClO_4)·$4H_2O$] at different temperatures are shown in Figure 3.3.10 in purple and yellow, respectively. The polymer complex could be occurring for the Zn(II) perchlorate due to the obtained spectra being very broad and similar to those of the Zn(II) chloride complex. A very broad signal of two imine protons was obtained at around 8.91 ppm suggesting the two imine protons could be in different environments.

In addition, several broad signals for the pyridine rings protons are also occurring at 7 to 8 ppm suggesting two pyridine rings might be in different environments as well.

In the IR spectrum of compound [Zn(**4**)(ClO_4)·$4H_2O$], the observed OH stretch at 3436 cm^{-1} as a strong broad signal is suggesting that coordinated water molecules could be in the complex. Two imine groups are in different environments due to the presence of the C=N stretches signal at 1651 and 1628 cm^{-1} which were seen to have slightly changed from the original ligand **4** at 1630 and 1600 cm^{-1}, respectively. The C=N stretch for the lower pyridine rings is occurring at 1540 cm^{-1} which has moved from 1561 cm^{-1} suggesting that the nitrogen atoms from pyridine rings are binding to the Zn(II) ion centre. The C-O stretch presents at 1234 cm^{-1} in comparison to the original one at 1218 cm^{-1} from ligand **4** pointing out that the oxygen atom from phenol group is deprotonated and coordinated to the Zn(II) ion. The appearance of a perchlorate group at 1099 cm^{-1} as a strong broad signal indicates that the Zn(II) complexation had occurred.

Elemental analysis indicated that the complex had the formula [Zn(**4**)(ClO_4)·$4H_2O$]. This would also imply that one Zn(II) ion was bonded to the ligand and that one perchlorate ion was also involved. The ligand itself is deprotonated to account for neutral charge. The coordination number of the Zn(II) ion is from 3 to 6 (including different number of water molecules). The possible structure of one monomer unit of compound [Zn(**4**)(ClO_4)·$4H_2O$] in four coordination number is depicted in Figure 3.3.12.

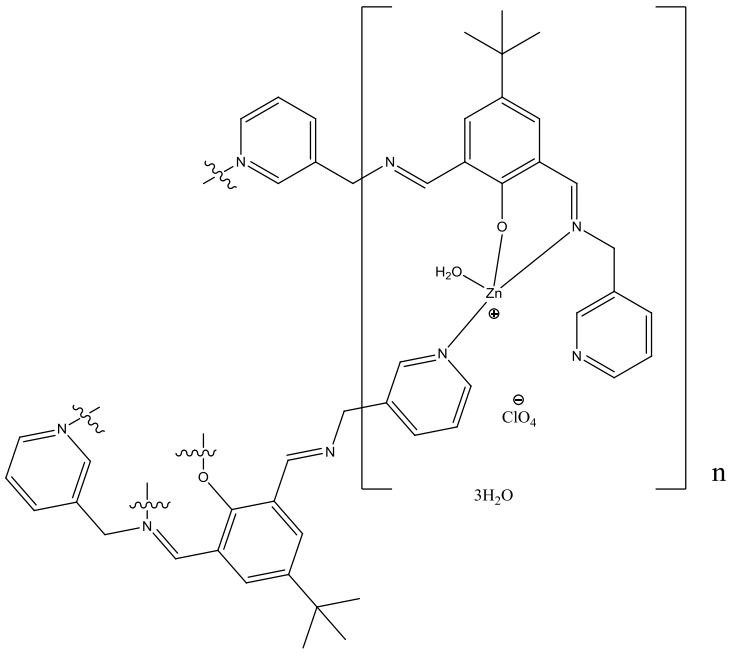

Figure 3.3.12: Possible structure for [Zn(**4**)(ClO_4)·$4H_2O$].

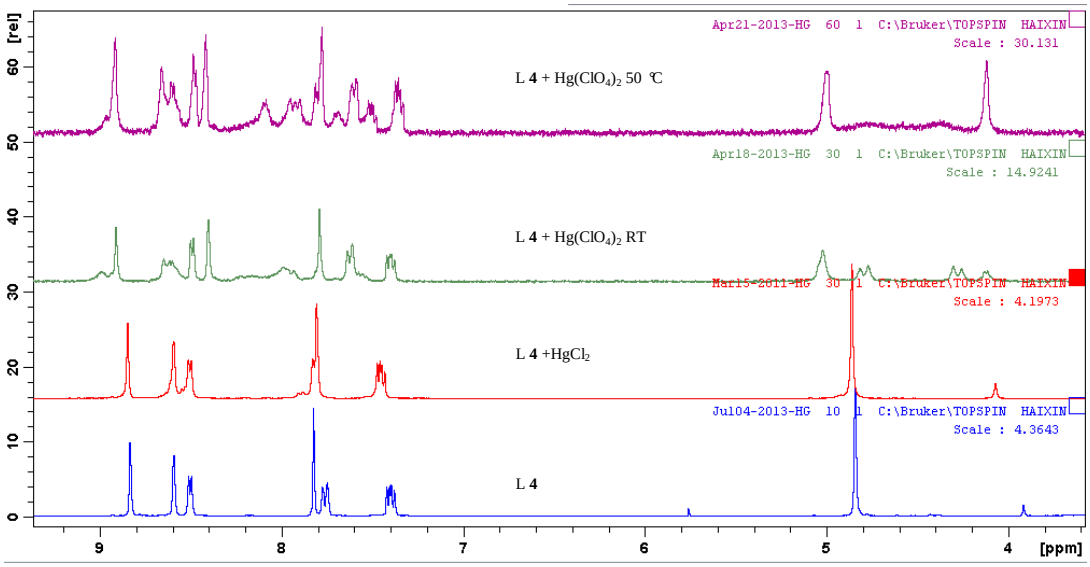

Figure 3.3.13: A comparison of ligand **4** and its corresponding Hg(II) chloride/perchlorate complexes at room temperature and 50 ℃ in DMSO-d_6.

3.3.6.3 [Hg(**4**)Cl]

The complex [Hg(**4**)Cl] was isolated as a yellow solid. The ^{1}H NMR spectrum of compound [Hg(**4**)Cl] is shown in Figure 3.3.13 (in red). The phenolic proton is deprotonated by Hg(II) ion due to the fact that there is no peak at around 13-15 ppm. The spectrum of the Hg(II) chloride complex is very similar to that of ligand **4** with the exception of the pyridine protons, which has suggested a weak bonding could be occurring between the Hg(II) ion and the ligand, and the bonding of the Hg(II) ion is possible through the two nitrogen atoms at the lower pyridine rings. The two signals of protons He and Hf from the pyridine rings are observed at 7.82 and 7.45 ppm which have moved from 7.76 and 7.40 ppm in ligand **4**.

The IR spectrum of compound [Hg(**4**)Cl] contains the C=N stretch of the C=N stretch for the imine group at 1651 cm^{-1} which has moved from 1630 cm^{-1} of ligand **4**. This implies the nitrogen atoms of the imine group could be coordinated to the Hg(II) ion. The C=N stretch of the pyridine rings was occurred at 1531 cm^{-1} which was seen from the original ligand at 1561 cm^{-1} suggesting that the two nitrogen atoms from the lower pyridine rings are coordinated to the metal ion. This would also agree with the result which was discussed earlier in the ^{1}H NMR spectrum in the Hg(II) chloride complex.

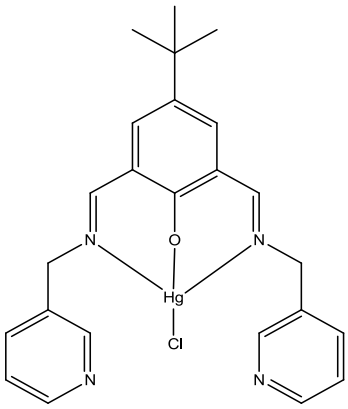

Figure 3.3.14: Possible structure for compound [Hg(**4**)Cl].

The elemental analysis indicated that the complex had the formula [Hg(**4**)Cl]. This would also imply that one Hg(II) ion was bonded to the ligand and that one chloride ion was also involved. The ligand itself was deprotonated to account for neural charge. The bonding of the Hg(II) ion is through the oxygen atom from the deprotonated phenol group as well as one chloride ion. The two nitrogen atoms at the lower pyridine rings could be involved in binding to the metal ion of an adjacent molecule. The possible structure of compound is depicted in Figure 3.3.14.

3.3.6.4 [Hg_2(**4**)$(ClO_4)_3 \cdot 2H_2O$]

The complex [Hg_2(**4**)$(ClO_4)_3 \cdot 2H_2O$] was isolated as a yellow solid. The spectra of compound [Hg_2(**4**)$(ClO_4)_3 \cdot 2H_2O$] at different temperatures are shown in Figure 3.3.13 in green and purple, respectively. Several more signals are obtained which suggests that the complex is an unsymmetrical complex and the two pyridine rings in side chains could be in different environments. Two signals of the are observed for the imine proton signals at 9.01 and 8.91 ppm, respectively, suggesting that one imine is coordinated to the Hg(II) ion while the other is not. This can be seen in particular in the ^{1}H NMR spectra recorded at 50 ℃, the presenting two broad singlets at 5.0 and 4.1 ppm, respectively, with a ratio of integral is approximately 1:1 has agreed with the formation of unsymmetrical complex. In addition, the disappearance of phenol proton signal is indicating the phenol proton was deprotonated and coordinated to the Hg(II) ion centre.

The IR spectrum of compound [Hg_2(**4**)$(ClO_4)_3 \cdot 2H_2O$] contains a C=N stretch of imine group at 1651 cm^{-1} and 1619 cm^{-1} which were seen in the original ligand **4** at 1630 cm^{-1} and 1600 cm^{-1} suggesting that the two imine nitrogen atoms are in different environments and coordinated to the metal centre. In addition, the signal of the C=N stretch from the lower pyridine ring is obtained at 1530 cm^{-1} in comparison to the

previous one at 1561 cm^{-1} indicating the nitrogen atoms from the pyridine rings are binding to the Hg(II) ion centre as well. Hg(II) complexation has occurred due to the presence of a strong broad signal at 1095 cm^{-1}.

The elemental analysis suggested that the complex had the formula $[Hg_2(\mathbf{4})(ClO_4)_3{\cdot}2H_2O]$. This would also imply that two Hg(II) ions were bonded to the ligand and that three perchlorate ions were also involved. The ligand itself was deprotonated to account for neutral charge. The possible structure of one monomer unit of compound $[Hg_2(\mathbf{4})(ClO_4)_3{\cdot}2H_2O]$ is depicted in Figure 3.3.15.

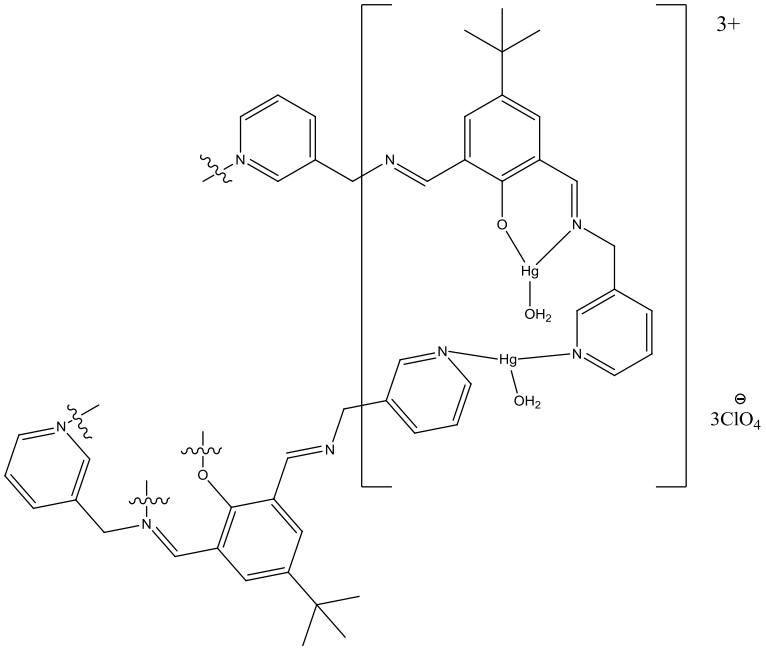

Figure 3.3.15: Possible structure for $[Hg_2(\mathbf{4})(ClO_4)_3{\cdot}2H_2O]$.

3.3.6.5 $[Ni_2(\mathbf{4})Cl_3{\cdot}5H_2O]$

The complex $[Ni_2(\mathbf{4})Cl_3{\cdot}5H_2O]$ is formed as a dark green solid. The obtained data of complex $[Ni_2(\mathbf{4})Cl_3{\cdot}5H_2O]$ in either the IR spectrum or the elemental analysis is very similar to that of Zn(II) chloride complex which indicates the bonding of the Ni(II) ion should be analogous to that of Zn(II) ion as well. The magnetic moment of complex $[Ni_2(\mathbf{4})Cl_3{\cdot}5H_2O]$ is 4.06 B.M. which implied the geometries of the Ni(II) ions are tetrahedral. So, the possible structure of one monomer unit of complex $[Ni_2(\mathbf{4})Cl_3{\cdot}5H_2O]$ is shown in Figure 3.3.16.

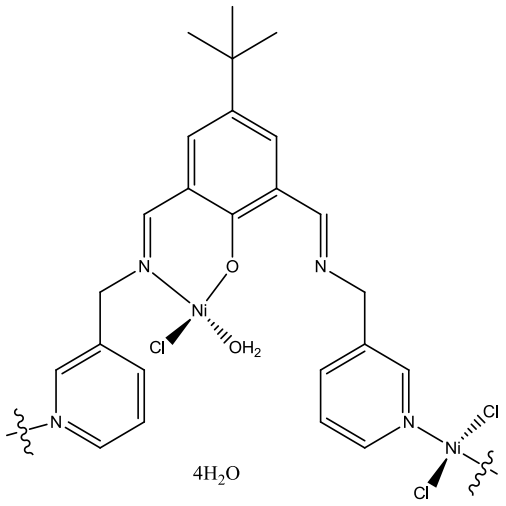

Figure 3.3.16: Possible structure for $[Ni_2(\mathbf{4})Cl_3{\cdot}5H_2O]$.

3.3.6.6 $[Ni(\mathbf{4})(ClO_4){\cdot}4H_2O]$

The complex $[Zn(\mathbf{4})(ClO_4){\cdot}4H_2O]$ was isolated as a green solid. The bonding of the Ni(II) perchlorate complex is similar to that of the Zn(II) perchlorate complex due to the observations that both IR spectrum and elemental analysis are similar to those of Zn(II) perchlorate complex. For example, two separate imine C=N stretch signals are observed at 1651 and 1628 cm^{-1} in the IR spectrum suggesting that one imine nitrogen atom is coordinated to the Ni(II) ion centre while the other is not. In addition, the magnetic moment of the Ni(II) complex which is 3.06 B.M. suggests the geometry of the Ni(II) ion is octahedral. Hence, the possible structure of one monomer unit of complex $[Zn(\mathbf{4})(ClO_4){\cdot}4H_2O]$ is shown in Figure 3.3.17.

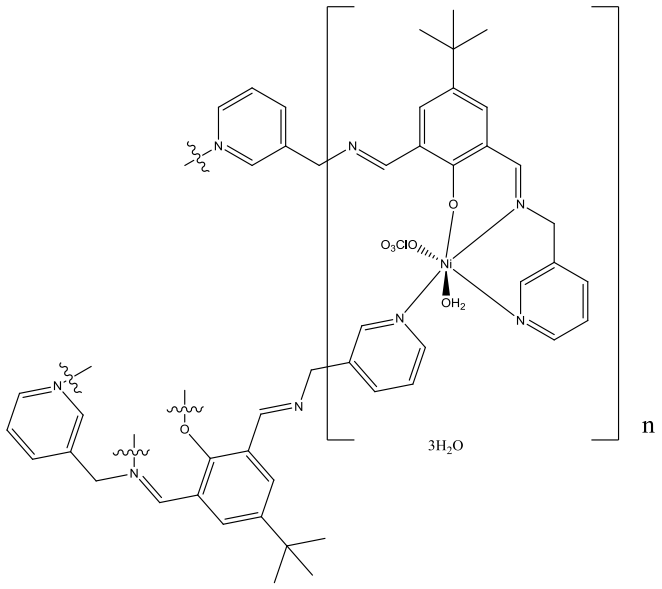

Figure 3.3.17: Possible structure of compound $[Zn(\mathbf{4})(ClO_4){\cdot}4H_2O]$.

3.3.6.7 [Cu_2(**4**)Cl_3·MeOH]

The complex of [Cu_2(**4**)Cl_3·MeOH] was isolated as a green solid. The IR spectrum of the complex is similar to that of Zn(II) chloride complex with only the exception of the signal of the C=N stretch for the imine group. The signal is obtained at 1658 and 1631 cm^{-1} in comparison to the Zn(II) chloride complex at 1648 and 1630 cm^{-1}, respectively, without significant change. In total, this similarity would imply the bonding of the Cu(II) ion should be analogous to that of the Zn(II) ion.

The elemental analysis indicated the complex had the formula [Cu_2(**4**)Cl_3·MeOH]. This would also imply that two Cu(II) ions were bonded to the ligand and that three chloride ions were also involved. The ligand itself was deprotonated to account for the neutral charge. One coordination methanol solvent was also involved. The bonding of the Cu(II) ions are similar to that of the Zn(II) ion in the chloride complex. The magnetic moment of the complex [Cu_2(**4**)Cl_3·MeOH] is 2.19 B.M. So, the possible structure of one monomer unit of complex [Cu_2(**4**)Cl_3·MeOH] is depicted in Figure 3.3.18.

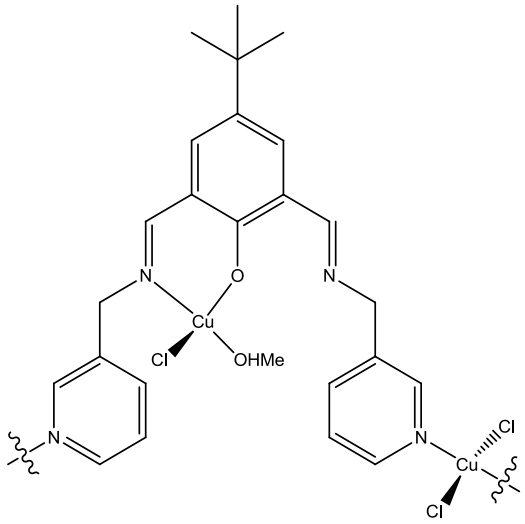

Figure 3.3.18: Possible structure for [Cu_2(**4**)Cl_3·MeOH].

3.3.6.8 [Cu(**4**)(ClO_4)·3H_2O]

The Cu(II) perchlorate complex with ligand **4** was formed as a green solid. The proposed complex [Cu(**4**)(ClO_4)·3H_2O] in both the IR spectrum and the elemental analysis is very similar to that of the Zn(II) perchlorate complex which suggests that the bonding of the Cu(II) ion should be similar to that of the Zn(II) ion. The only slight change that could be observed was that of the C=N stretch for the imine group where obtained at 1655 and 1634 cm^{-1} in the Cu(II) complex in comparison to the 1651 and 1628 cm^{-1} from the Zn(II) complex. These two imine stretches are suggesting that one

imine nitrogen atom might be coordinated to the Cu(II) ion while the other one is not. The magnetic moment of the complex [Cu(**4**)(ClO_4)·$3H_2O$] is 2.23 B.M. The possible structure of one monomer unit of compound [Cu(**4**)(ClO_4)·$3H_2O$] is depicted in Figure 3.3.19.

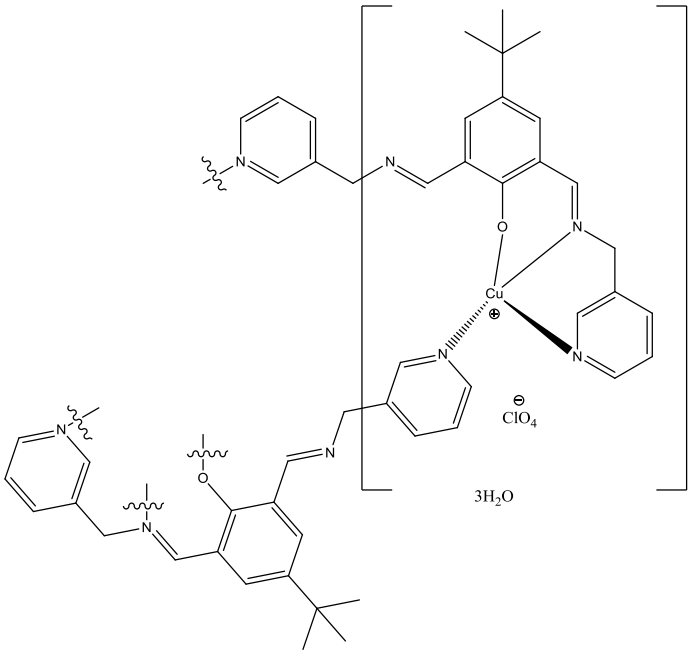

Figure 3.3.19: Possible structure for [Cu(**4**)(ClO_4)·$3H_2O$].

3.3.7 Ligand 5

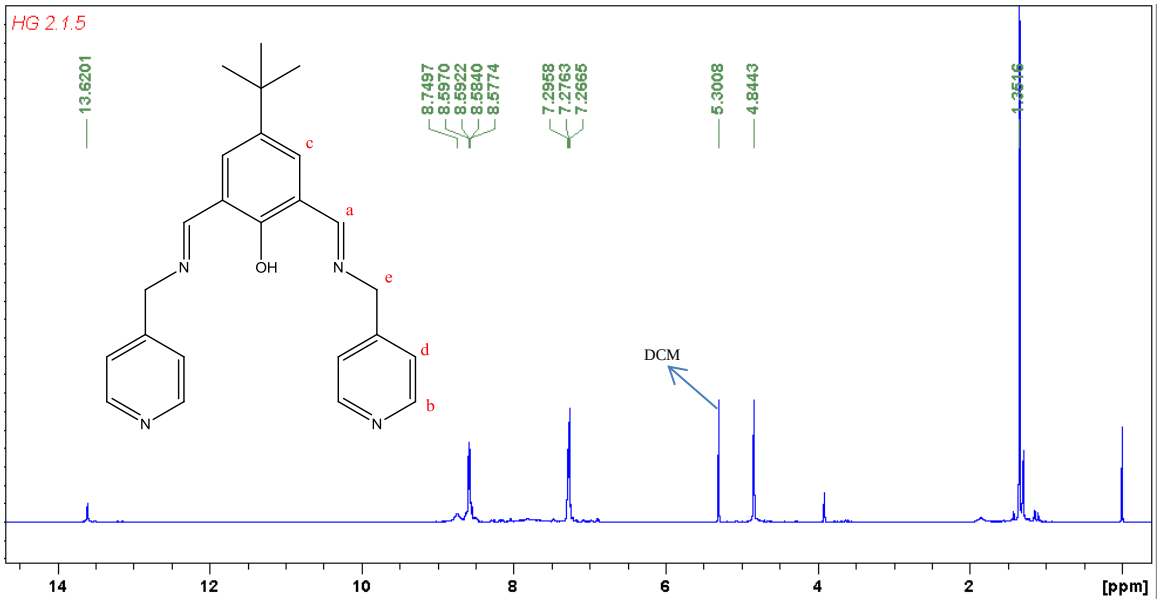

Figure 3.3.20: The ^{1}H NMR spectrum of ligand **5** in $CDCl_3$.

The ligand **5** is formed as a yellow oil. The ^{1}H NMR spectrum of ligand **5** is shown in Figure 3.3.20. The phenolic proton gives rise to a signal at 13.62 ppm when this is

compared to the signals in compound **2** at 11.47 ppm, it would suggest that a stronger H-bond exists between the imine and the phenol rather than formed between the aldehyde and the phenol. The reason for imine formation is due to the appearance of an imine proton, Ha, at 8.75 ppm as a broad peak and the disappearance of the aldehyde signal from compound **2** at 10 ppm. Aromatic proton Hc is present as a small broad peak at about 7.78 ppm, while the proton signals from the lower pyridine rings, Hb and Hd are occurring at 8.59 and 7.27 ppm, respectively. The bridging methylene protons He is obtained at 4.84 ppm.

The IR spectrum of ligand **5** was run under the DCM. The signal of $\nu_{C\text{-}H}$ resonating at 2866 cm^{-1} in carbonyl group increases to 2987 cm^{-1}, showing that the imine is more delocalised than aldehyde. In addition, the C=N stretch for the imine group is obtained at 1630 cm^{-1}. The reason for this could be that one imine N is associated with OH from a phenol group while the other remains as a normal imine. The C=N stretch for the pyridine appears at 1561 cm^{-1}. The signal of C-O stretch from the phenol group could be present around 1220 cm^{-1} which is blocked by DCM solvent in the IR spectrum. It is difficult to assign other specific bands for pyridine rings in the IR spectrum of ligand **5** and its corresponding metal complexes due to large number of bands already present. The mass spectrum shows ligand **5** is pure.

3.3.8 Metal complexes of ligand 5

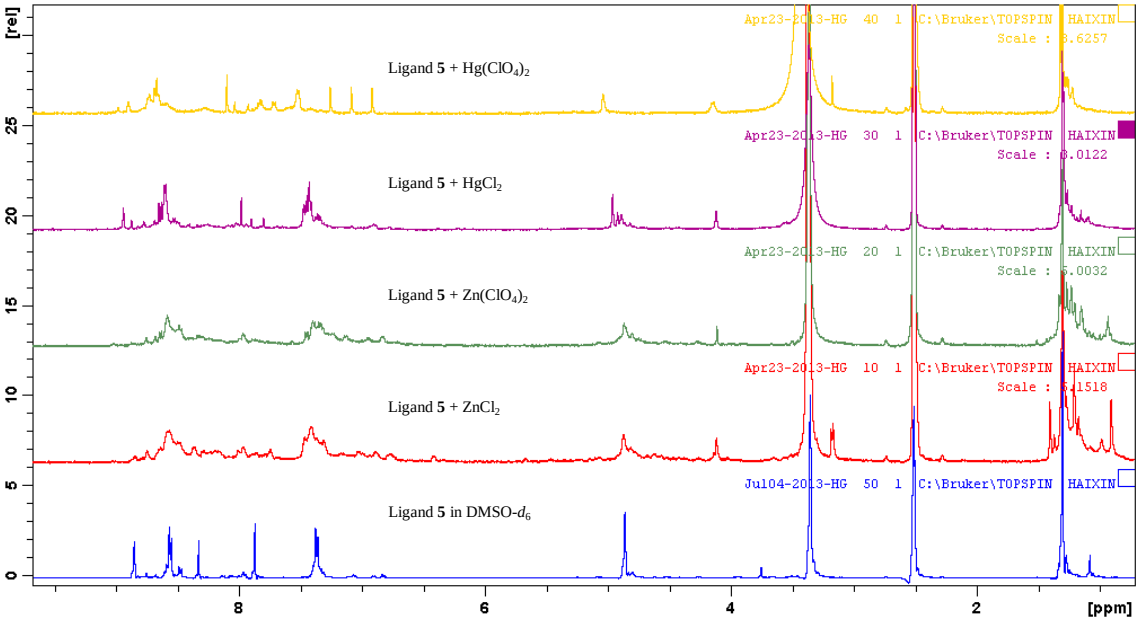

Figure 3.3.21: A comparison of ^{1}H NMR spectra of ligand **5** and its corresponding ZnX_2 and HgX_2 (X = chloride and perchlorate) complexes in DMSO-d_6.

Metal complexation reactions of ligand **5** with various metal(II) salts were carried out in MeOH, but the resulting solids were difficult to characterise and analyse due to the formation of insoluble polymeric species. No discussion of these reactions will be under taken.

The ^{1}H NMR spectra signals of the complexes obtained from the reactions of ligand **5** with Zn(II) and Hg(II) salts are very broad and weak, indicating a polymeric type material is present. Furthermore, no hydrolysis of the ligand appears to have taken place.

3.3.9 Ligand 6

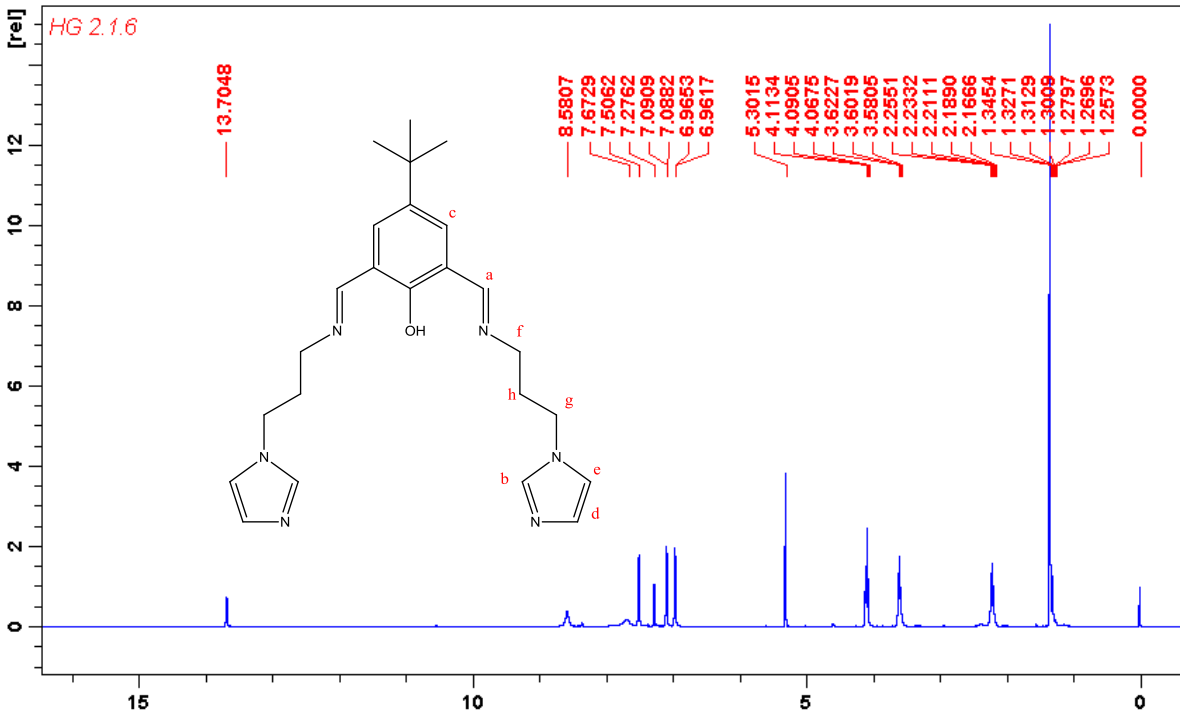

Figure 3.3.22: The ^{1}H NMR spectrum of ligand **6** in $CDCl_3$

Ligand **6** is formed as a yellow oil. The ^{1}H NMR spectrum of ligand **6** is shown in Figure 3.3.22. The signal for the phenolic proton appears at 13.70 ppm which has moved from 11.47 ppm in di-carbonyl compound **2** indicating that a stronger hydrogen bond is formed between the imine and the phenol rather than between the aldehyde and the phenol. Both the imine proton Ha which is occurring as a broad singlet at 8.58 ppm and the disappearance of the aldehyde proton of compound **2** at around 10 ppm are implying that imine formation has occurred. The aromatic proton, Hc, which presents at 7.67 ppm has shifted from 7.98 ppm in compound **2**. In addition, the signals of protons Hb, Hc and Hd from the imidazole rings are also obtained at 7.50, 7.09 and 6.96 ppm,

respectively, while the three methylene protons Hf, Hg and Hh are present at 4.05, 3.53 and 2.10 ppm as a triplet, triplet and multiplet, respectively.

The IR spectrum of ligand **6** was run in DCM. The C=N stretch signal at 1639 cm^{-1} is due to the imine group. In addition, the signal C=C stretch for the imidazole rings is occurring at 1508 cm^{-1}. The signals of aromatic and C-O stretches are observed at 1460 cm^{-1} and it 1230 cm^{-1}, respectively.

Mass spectrum indicates that ligand **6** is pure.

3.3.10 Metal complexes of ligand 6

Metal complexes reactions of ligand **6** with various metal(II) salts were carried out in MeOH. The reactions were carried out by stirring the ligand and the appropriate metal salts for 2 hours in MeOH. The resulting coloured solids were collected by filtration.

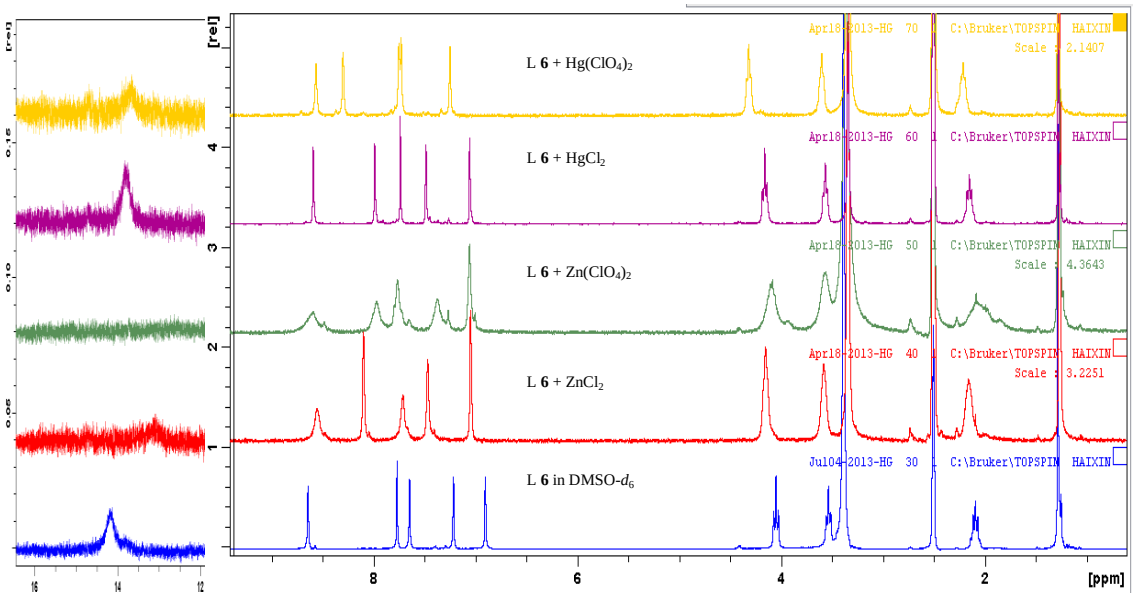

Figure 3.3.23: A comparison of the ^{1}H NMR spectra of ligand **6** and its corresponding ZnX_2 and HgX_2 (X = chloride or perchlorate) complexes in DMSO-d_6.

Table 3.3.24: A comparison of the IR spectra of the ligand **6** and its corresponding metal complexes.

	OH	Phenol-OH	C-H	Imine C=N	Imidazole C=C	C-O
ligand **6**		3054	2967	1639	1508	1230
$ZnCl_2$	3438	3123	2959	1656, 1632	1538	1237
$Zn(ClO_4)_2$	3439	3132	2960	1659, 1633	1539	1238
$HgCl_2$	3423	3119	2956	1638	1527	1234
$Hg(ClO_4)_2$	3428	3134	2960	1640	1529	1236
$Cu(ClO_4)_2$	3434	3134	2960	1655, 1635	1547	1238
$Ni(ClO_4)_2$	3435	3135	2959	1652, 1633	1539	1234

The metal complexes of ligand **6** in the presence of various metal salts were formed successfully. This is contribute to the difference of the analytical data obtained for the ligand and its complexes in either the ^{1}H NMR spectra (in Figure 3.3.23 right) or the IR spectra (in Table 3.3.24). According to these observations, it would imply some empirical results: 1) The metal ions from the 1st row of the d-block group, such as Zn(II), Cu(II) and Ni(II) ions, will deprotonate the phenol group of ligand **6**, while the 3rd row *d*-block ion like Hg(II) is not able to deprotonate the ligand (shown in Figure 3.3.23 left); 2) The two imine groups are in different environments in complexes of the 1st row *d*-block metals, while the imine nitrogen atoms are not coordinated to the 3rd row of the *d*-block metal ions.

3.3.10.1 [Zn_2(**6**)Cl_3·MeOH]

The complex [Zn_2(**6**)Cl_3·MeOH] was isolated as a yellow solid. The ^{1}H NMR spectrum of compound [Zn_2(**6**)Cl_3·MeOH] is shown Figure 3.3.23 (in red). The phenol group was deprotonated and coordinated to the Zn(II) ion confirmed by the fact that there is no signal at around 13-15 ppm. The broad signal of the imine proton Ha at 8.55 ppm which has shifted from the original signal at 8.64 ppm in free ligand **6** indicates that the imine nitrogen atoms might be coordinated to the Zn(II) ion. Several differences in chemical shifts between the ligand and complex are found in the proton signals of the imidazole rings. The protons Hb, Hd and He which were present at 7.76, 7.21 and 6.90 ppm in ligand **6** have shifted to 8.10, 7.46 and 7.04 ppm, respectively, in the Zn(II) complex. This would imply that two nitrogen atoms from imidazole rings are binding to the Zn(II) ion centre. In addition, three bridging methylene protons Hf, Hg and Hh resonate at 4.15,

3.58 and 2.16 ppm as three broad singlets in comparison to the previous three at 4.05, 3.53 and 2.10 ppm with a slight change suggesting metal complexation had occurred.

The IR spectrum of compound [Zn_2(**6**)Cl_3·MeOH] contains a signal due to the OH stretch at 3438 cm^{-1} pointing out that a coordinating methanol molecule might be in the complex. The C=N stretch signal for the imine group is present at 1656 and 1632 cm^{-1} in comparison to the original stretches at 1639 cm^{-1} suggesting that the two imine groups are in different environments. In addition, the nitrogen atoms of the imidazole rings are coordinating to the Zn(II) ion centre as differences in stretches of the C=C stretch for the imidazole rings of the ligand (1508 cm^{-1}) and the Zn(II) chloride complex (1538 cm^{-1}) can be seen.

Elemental analysis indicated that the complex had the formula [Zn_2(**6**)Cl_3·MeOH]. This would also imply that two Zn(II) ions were bonded to the ligand and that three chloride ions were also involved. The ligand itself is deprotonated to account for the neutral charge. The coordination number of each Zn(II) ions is four. So, the possible structure of compound [Zn_2(**6**)Cl_3·MeOH] is depicted in Figure 3.3.25.

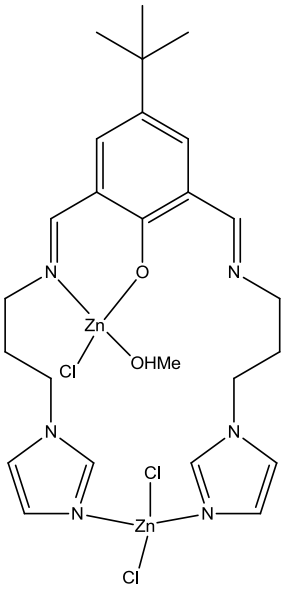

Figure 3.3.25: Possible structure for [Zn_2(**6**)Cl_3·MeOH].

3.3.10.2 [Zn(**6**)(ClO_4)·4H_2O]

The complex [Zn(**6**)(ClO_4)·4H_2O] is formed as a yellow solid. The ^{1}H NMR spectrum of compound [Zn(**6**)(ClO_4)·4H_2O] is shown in Figure 3.3.23 (in green). The phenolic proton was deprotonated as no peak appeared at around 14 ppm suggesting that the oxygen atom from phenol group is coordinated to the Zn(II) ion centre. The signal of

proton Ha of the imine group is obtained at 8.58 ppm as a broad peak which has moved from 8.61 ppm in ligand **6**. Large changes in chemical shifts were found between the protons of the imidazole rings, which indicated that the nitrogen atoms from the imidazole rings are coordinated to the Zn(II) ion centre. The protons Hb, Hd and He are appearing at 7.97, 7.37 and 7.05 ppm which have shifted from 7.76, 7.21 and 6.90 ppm, respectively, from ligand **6**. In addition, the obtained signals of the three methylene protons Hf, Hg and Hh are similar to those of the Zn(II) chloride complex.

The IR spectrum of compound [Zn(**6**)(ClO_4)·$4H_2O$] contains an OH stretch at 3439 cm^{-1} as a broad signal suggesting some coordinated solvent could be in the complex. The two imine groups are in different environments due to the imine signal observed at 1658 and 1633 cm^{-1}, respectively. The C=C stretch for the imidazole rings is obtained at 1539 cm^{-1} which has moved from 1508 cm^{-1} in ligand **6** implying that the two nitrogen atoms from imidazole rings are coordinated to the metal centre. The obtained strong broad signal of the perchlorate group at 1108 cm^{-1} is implying the metal complexation had occurred.

Elemental analysis indicated that the complex had the formula [Zn(**6**)(ClO_4)·$4H_2O$]. This would also imply that one Zn(II) ion was bonded to ligand and that one perchlorate ion was also involved. The ligand itself was deprotonated to account for neutral charge. The bonding of the Zn(II) ion is through one imine nitrogen atom, one oxygen atom from phenol group, and two nitrogen atoms at the lower imidazole rings. The coordination number of the Zn(II) ion could be either five- or six-coordinate (including one water molecule). The possible structure of compound [Zn(**6**)(ClO_4)·$4H_2O$] is depicted in Figure 3.3.26.

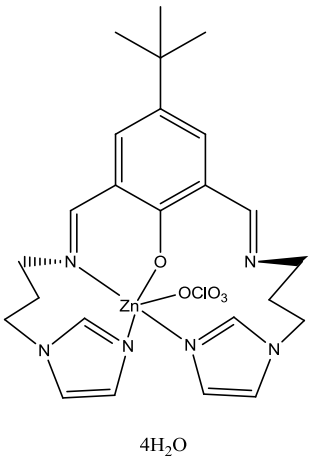

Figure 3.3.26: Possible structure for [Zn(**6**)(ClO_4)$_2$].

3.3.10.3 [Hg_2(**6**)Cl_3·(OMe)]

The complex [Hg_2(**6**)Cl_3·(OMe)] was isolated as a yellow solid. The ^{1}H NMR spectrum of compound [Hg_2(**6**)Cl_3·OMe] is shown in Figure 3.3.23 (in purple). The phenolic proton is observed at 13.81 ppm which has moved from 14.17 ppm in ligand **6** indicating that the oxygen atoms could be associated with the Hg(II) ion centre. The obtained signals of the imine proton Ha in both complex (8.59 ppm) and ligand (8.64 ppm) are very similar suggesting the nitrogen atoms from the imine groups might be not coordinated to the metal centre. The protons at the lower imidazole rings were found to have big difference between the ligand and the complex. The protons Hb, Hd and He which obtained at 7.76, 7.21 and 6.90 ppm have shifted to 7.99, 7.26 and 7.05 ppm, respectively, pointing out the nitrogen atoms at the lower imidazole rings are coordinated to the metal centre. In addition, the observation of three methylene protons, Hf, Hg and Hh is very similar to those of Zn(II) chloride complex.

The IR spectrum of compound [Hg_2(**6**)Cl_3·(OMe)], the signal of the C=N stretch for the imine group occurs very similar but broader wavenumber (1640 cm^{-1}) to that of ligand **6** which suggests that the imine nitrogen atom could be coordinated the Hg(II) ion. In addition, the C=C stretch for the imidazole rings of the complex is obtained at 1527 cm^{-1} in comparison to the previous ligand at 1508 cm^{-1} implying that the nitrogen atoms of imidazole rings are binding to the Hg(II) ion centre.

Elemental analysis indicated that the complex had the formula [Hg_2(**6**)Cl_3·(OMe)]. This was also implied that two Hg(II) ions were bonded to ligand and that three chloride ions and one deprotonated MeOH ion were also involved to account for neutral charge. The possible structure of compound [Hg_2(**6**)Cl_3·OMe] is depicted in Figure 3.3.27

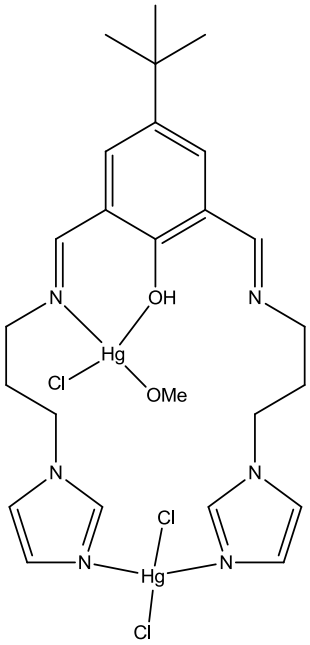

Figure 3.3.27: Possible structure for [Hg_2(**6**)Cl_3·OMe].

3.3.10.4 [Hg(**6**)$(ClO_4)_2$]

The complex [Hg(**6**)$(ClO_4)_2$] was formed as a yellow solid. The ^{1}H NMR spectrum of compound [Hg(**6**)$(ClO_4)_2$] is shown in Figure 3.3.23 (in yellow). The phenolic proton resonates at 13.68 ppm as a broad peak. Comparing this to the original signal at 14.17 ppm in ligand **6** suggests the phenol group is not deprotonated by Hg(II) ion but the oxygen atom could be coordinated to the Hg(II) ion centre. The signal of the imine proton Ha is present at 8.56 ppm which was seen to have a slight shift from ligand **6** at 8.64 ppm. The aromatic proton Hc appears very similar ppm between ligand **6** and Hg(II) complex. However, the protons signals Hb, Hd and He at the lower pyridine rings which were occurred at 7.76, 7.21 and 6.90 ppm has shifted to 8.29, 7.73 and 7.25 ppm suggesting the nitrogen atoms from the imidazole rings are binding to the Hg(II) ion centre. In addition, the obtainment of the three methylene bridging protons Hg, Hf and Hh is similar to that of the Zn(II) chloride complex.

The IR spectrum of compound [Hg(**6**)$(ClO_4)_2$] contains a signal ν_{OH} at 3448 cm^{-1} suggesting that the phenol OH could be in the Hg(II) complex. The C=N stretch of the imine group occurs at 1640 cm^{-1} which is very similar to that of the ligand but appeared broader. This implies that the imine nitrogen atoms are bonding to the Hg(II) ion centre. The C=C stretch for the imidazole rings presents at 1529 cm^{-1} has moved from 1508 cm^{-1}, indicating that the two nitrogen atoms from imidazole rings are coordinated to the Hg(II) ion centre which agrees with the results discussed earlier in the ^{1}H NMR

spectrum in the Hg(II) perchlorate complex. The presence of the perchlorate group as a strong broad signal at 1109 cm^{-1} is further confirmed that the metal complexation had occurred.

Elemental analysis indicated that the complex had the formula [Hg(**6**)$(ClO_4)_2$]. This also implied that one Hg(II) ion was bonded to the ligand and that two perchlorate ions were also involved to account for the neutral charge. The bonding of the Hg(II) ion is through the two nitrogen atoms from the imidazole rings, two imine nitrogen atoms and one oxygen atom from the phenol group. So, the possible structure of compound [Hg(**6**)$(ClO_4)_2$] is depicted in Figure 3.3.28.

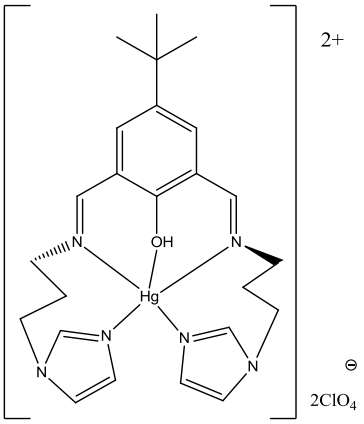

Figure 3.3.28: Possible structure for [Hg(**6**)$(ClO_4)_2$].

3.3.10.5 [Cu(**6**)$(ClO_4)_2 \cdot 2H_2O$]

The complex [Cu(**6**)$(ClO_4)_2 \cdot 2H_2O$] was obtained as a green solid. The analytical data of the complex [Cu(**6**)$(ClO_4)_2 \cdot 2H_2O$] in either the IR spectrum or the elemental analysis is very similar to that of Zn(II) chloride complex with only one exception which is that the signal of the imidazole rings occur at 1647 cm^{-1} in the Cu(II) perchlorate complex, whereas in the Zn(II) complex it occur at 1538 cm^{-1}. The magnetic moment of the Cu(II) perchlorate complex is 1.91 B.M. Hence, the possible structure of complex [Cu(**6**)$(ClO_4)_2 \cdot 2H_2O$] should be very similar to that of the Zn(II) perchlorate complex. So, the proposed structure of complex [Cu(**6**)$(ClO_4)_2 \cdot 2H_2O$] is depicted in Figure 3.3.29.

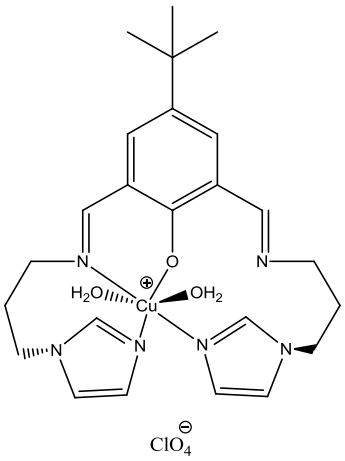

Figure 3.3.29: Possible structure for [Cu(**6**)$(ClO_4)_2$·$2H_2O$]

3.3.10.6 [Ni(**6**)$(ClO_4)_2$·H_2O]

The complex of [Ni(**6**)$(ClO_4)_2$·H_2O] was formed as a brown solid. The analytical data of the complex [Ni(**6**)$(ClO_4)_2$·H_2O] in either the IR spectrum or the elemental analysis is very similar to that of Zn(II) perchlorate complex which indicates that the bonding of the Ni(II) ion should be analogous to that of the Zn(II) ion as well. In addition, the magnetic moment of the Ni(II) perchlorate complex is obtained as 3.13 B.M. which suggests that the geometry of the Ni(II) ion is octahedral sphere. Hence, the possible structure of complex [Ni(**6**)$(ClO_4)_2$·H_2O] is depicted in Figure 3.3.30.

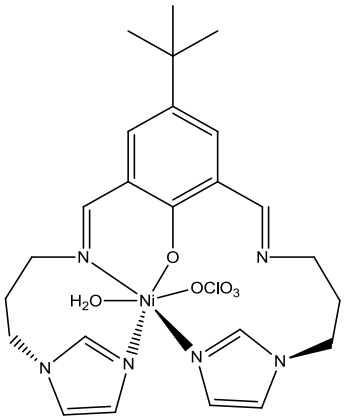

Figure 3.3.30: Possible structure for [Ni(**6**)$(ClO_4)_2$·H_2O].

3.4 Section 2

3.4.1 Preparation

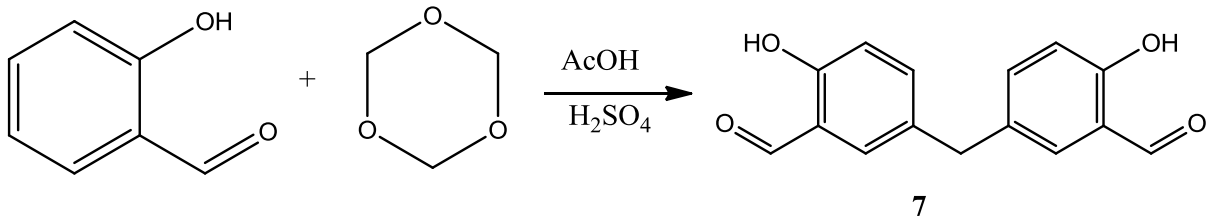

7

Figure 3.4.1: Synthetic route of compound **7**.[131]

The synthesis of compound **7** (5,5'-methylene-bis-salicylaldehyde) which is shown in Figure 3.4.1 was reported by Marvel and co-workers,[131] who generated the compound **7** as a white solid in up to 80 % yield.

The mechanism of formation of compound **7** by using 1,3,5-trioxane is shown in Figure 3.4.2.

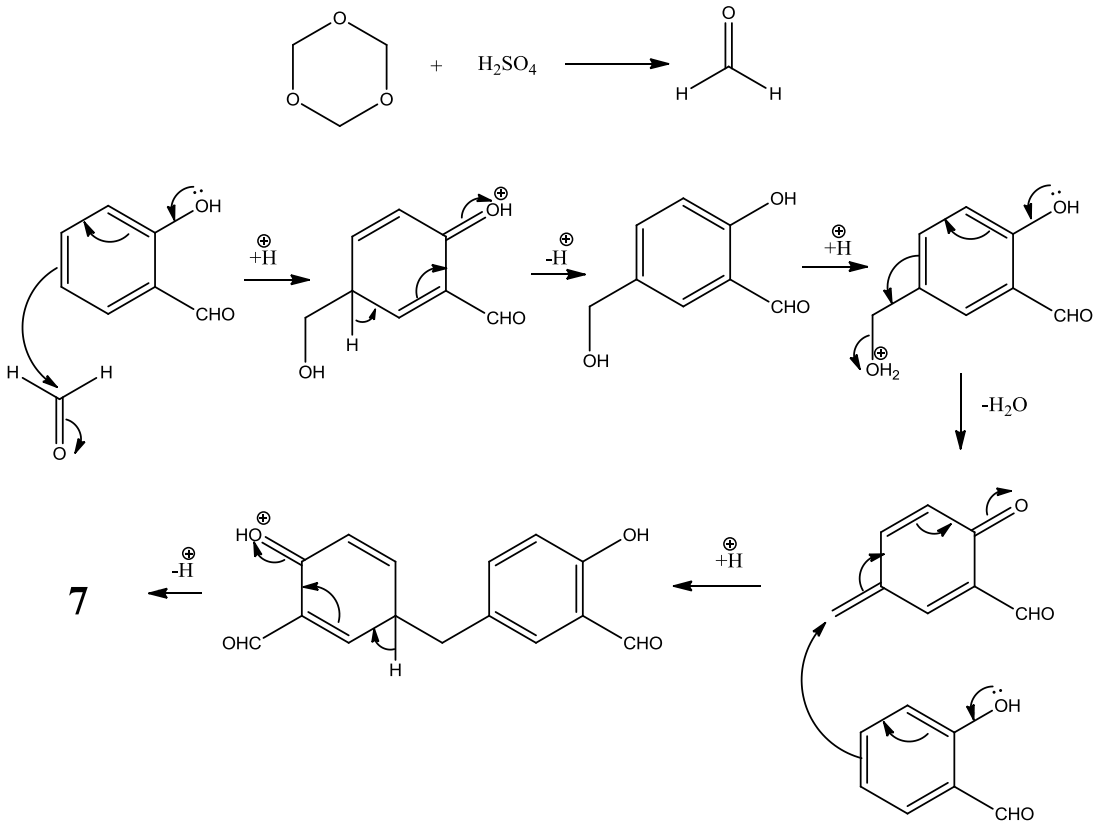

Figure 3.4.2: Mechanism of formation compound **7**.

In the first step, the depolymerisation of 1,3,5-trioxane with concentrated sulfuric acid produced formaldehyde in up to 99 % yield, as reported by Bell and co-workers.[142] The 'phenol formaldehyde resins' of which the most famous, Bakelite,[143] was discovered by Bäkeland at the turn of the century is involved. He combined phenol and formaldehyde in acid solution and observed a reaction similar to the bisphenol compound **7** syntheses[144] which is shown in Figure 3.4.2. In the third step, an acid-catalyzed electrophilic aromatic substitution now occurs to link a second phenol to the first. The rather stable benzylic cation makes a good intermediate.

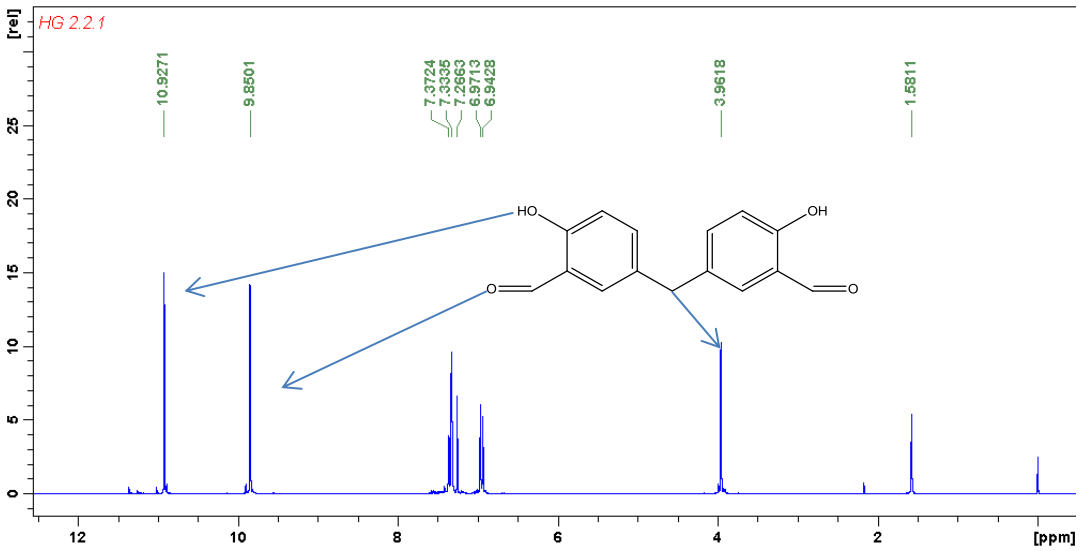

Figure 3.4.3: The ^{1}H NMR spectrum of compound **7** in $CDCl_3$.

The ^{1}H NMR spectrum of compound **7** is shown in the Figure 3.3.3. The observed signals of the protons in either phenol group (10.92 ppm) or the aldehyde group (9.85 ppm) in compound 7 are very similar to those of the starting material salicylaldehyde. In addition, the disappearance of a signal from the aromatic ring which was present at 6.95 ppm suggests that the 'bisphenol' reaction had occurred. The new bridging methylene protons resonate at 3.96 ppm in compound **7** also agree with this result.

The IR spectrum of compound **7** contains a signal ν_{OH} which is observed at 3438 cm^{-1}. In addition, a band at 1656 cm^{-1} is indicative of the carbonyl group. The signals of aromatic C=C stretch and C-O stretch occur at 1482 cm^{-1} and 1275 cm^{-1}, respectively.

The elemental analysis indicated that compound 7 is pure.

Compound **7** was used to synthesize four new ligands (**8** – **11**) as shown in Figure 3.4.4. All the ligands were synthesized using the same reaction strategy, by stirring one

equivalent of compound **7**, two equivalents of the appropriate amines, and ten equivalents of anhydrous $MgSO_4$ in DCM for 12 hours. The reason for this has been discussed previously in the section Schiff base ligand formation and hydrolysis.

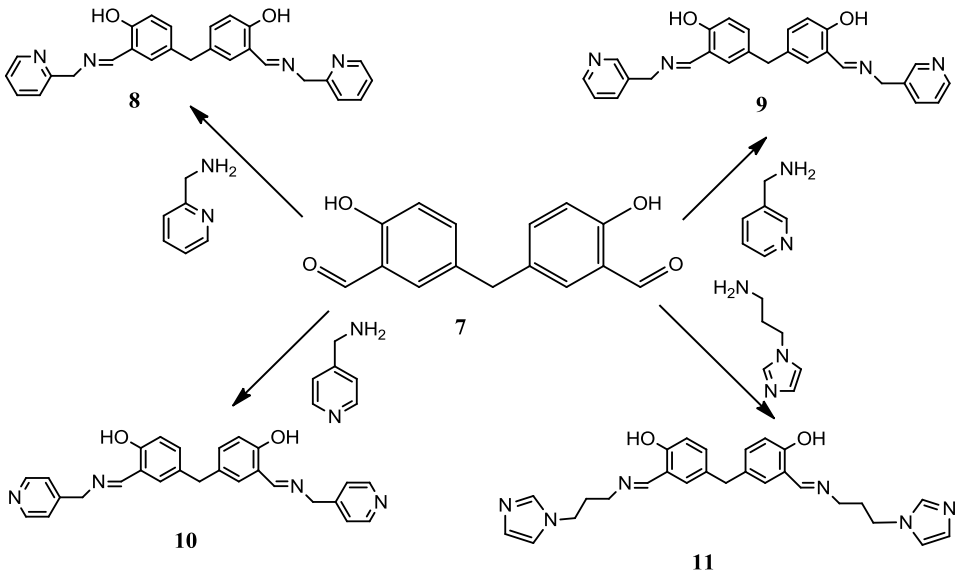

Figure 3.4.4: Synthesis of ligands **8** – **11**.

3.4.2 Ligand 8

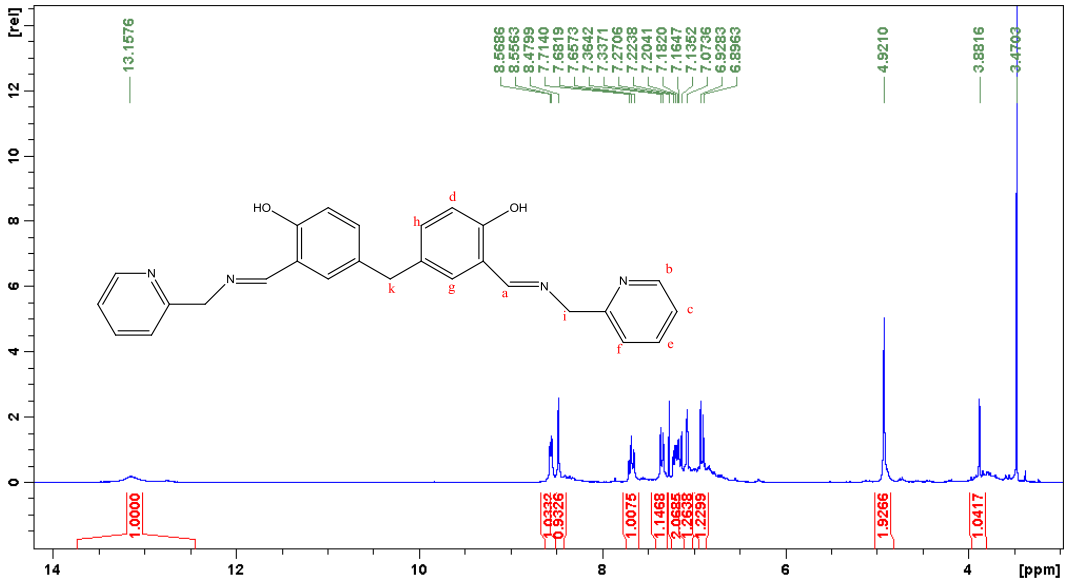

Figure 3.4.5: The ^{1}H NMR spectrum of ligand **8** in $CDCl_3$.

Ligand **8** was isolated as a yellow oil. The ^{1}H NMR spectrum of ligand **8** is shown in the Figure 3.4.5. The signal of the phenol proton resonates at 13.15 ppm which has moved from the diphenol compound **7** at 10.92 ppm suggesting that a stronger hydrogen bond has formed between the imine and the phenol rather than between the aldehyde

and the phenol. The appearance of the signal of imine proton Ha presenting at 8.48 ppm and the disappearance of the aldehyde proton from compound **7** at around 10 ppm has pointed towards imine formation had occurred. In addition, the aromatic protons Hd, Hg and Hh are represented at 7.34, 7.33 and 6.95 ppm, respectively. Aromatic methylene protons Hk are seen at 3.96 ppm in compound **7** which is shifted from their positions of 3.88 ppm in ligand **8**. While the signals of protons at the lower pyridine rings, Hb is observed at 8.56 ppm as a doublet, Hf presents a multiplet from 7.13 to 7.22 ppm. In the ^{13}C NMR spectrum, the imine carbon resonates at 166.8 ppm which confirms that imine formation had occurred. Ligand **8** contains fourteen carbon peaks which are a match with ligand **8**.

The IR spectrum of ligand **8** contains a signal at 3433 cm^{-1} which represents the phenol OH stretch. The band of the C=N stretch for the imine group is obtained at 1634 cm^{-1} in comparison to the di-carbonyl compound **7** at 1656 cm^{-1} indicating the imine formation had occurred. The signal of the C=N stretch for the pyridine rings is occurring at 1589 cm^{-1}. In addition, the signals of the aromatic stretch and the C-O stretch are addressing at 1491 and 1272 cm^{-1} which are very similar to those of compound **7**. It was difficult to assign other peaks from pyridine rings.

The elemental analysis shows the ligand **8** is pure.

3.4.3 Metal complexes of 8

Metal complexation reactions of ligand **8** with various metal(II) salts were carried out in MeOH. The reactions were carried out by stirring the ligand and the appropriate metal salts at room temperature for 2 hours in MeOH. The resulting coloured solids were collected by filtration. In the case of the $Zn(SCN)_2$ and $Ni(SCN)_2$ reactions, the complexation is carried out initially with Zn(II) or Ni(II) acetate salts resulting in a clear solution. The appropriate thiocyanate complexes are formed as coloured solids, which precipitate on the addition of sodium thiocyanate to the solution.

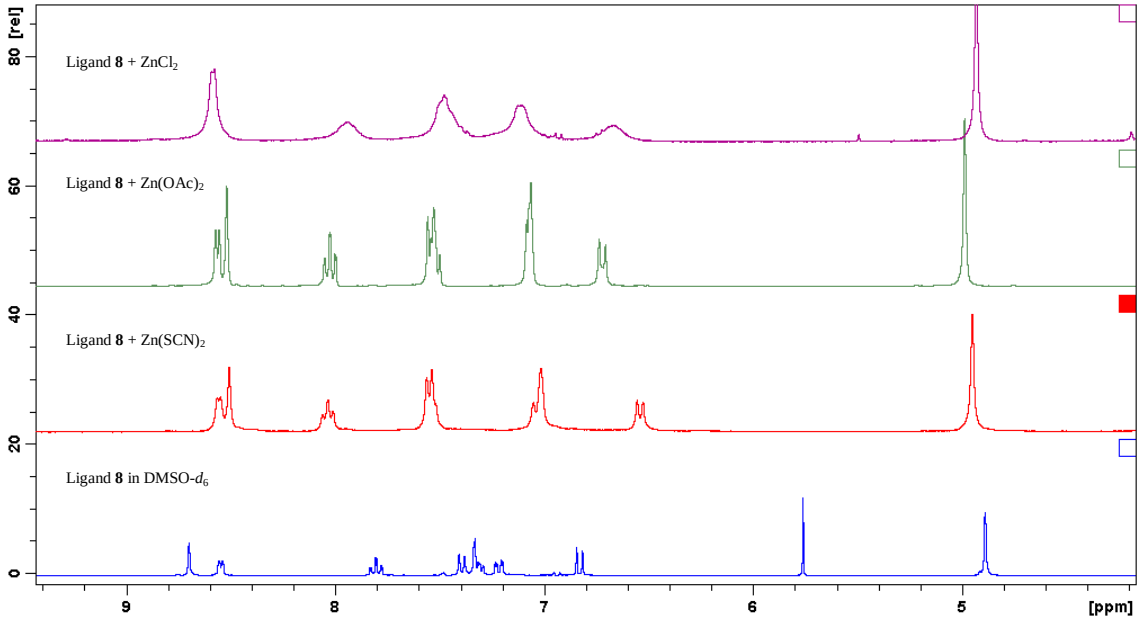

Figure 3.4.6: A comparison of ^{1}H NMR spectra of ligand **8** with its corresponding ZnX_2 (X = Cl/ClO_4/OAc/SCN) complexes in DMSO-d_6.

3.4.3.1 [Zn_2(**8**)$(SCN)_2$·MeOH]

The complex [Zn_2(**8**)$(SCN)_2$·MeOH] was obtained as a yellow solid. The ^{1}H NMR spectrum of compound [Zn_2(**8**)$(SCN)_2$·MeOH] is shown in Figure 3.4.6 (in red). The disappearance of the phenol proton as there is no signal at around 13 ppm has pointed towards the phenol group being deprotonated by the Zn(II) ion and the oxygen atom coordinated to the metal centre. The signal of imine proton Ha is occurring at 8.50 ppm which has moved from 8.70 ppm in the previous ligand implying that the nitrogen atoms from the imine group are coordinated to the Zn(II) ion centre. In addition, the aromatic protons Hd, Hg and Hb, resonate at 7.55, 7.01 and 6.54 ppm in the Zn(II) complex in comparison to the original three at 7.40, 7.33 and 6.83 ppm in ligand **8**, respectively. The reason for these shifts of the aromatic protons is that the deprotonated phenol group is resulting in proton Hd becoming more shielded while the protons Hg and Hh are more deshielded than those of ligand **8**. Several protons shifts from the lower pyridine rings are also observed. The protons Hb, Hc, He and Hf, resonate at 8.55, 8.03, 7.55 and 7.03 ppm which were seen from the original four positions at 8.55, 7.80, 7.31 and 7.21 ppm in ligand **8**, respectively, indicating that the two nitrogen atoms from the pyridine rings are coordinated to the Zn(II) ion centre as well. In addition, the signals of the two methylene protons, Hk and Hi, Hk appear at 3.66 ppm in the Zn(II) complex which was seen to have a slight change from 3.86 ppm in ligand **8** indicates that the length between the two aromatic rings could be decreased in Zn(II) complex.

Another bridging methylene proton Hi is resonating at 4.95 ppm which is similar to that of ligand **8**.

The IR spectrum of compound [Zn_2(**8**)$(SCN)_2$·MeOH] contains a signal ν_{OH} at 3432 cm^{-1} suggesting extra MeOH solvent might be coordinated in the Zn(II) complex. The appearance of the signal of thiocyanate group at 2079 cm^{-1} is indicative of the Zn(II) thiocyanate complexation had occurred. The imine C=N stretch occurred at 1635 cm^{-1} in comparison to 1634 cm^{-1} for ligand **8** with the shape changed from sharp to broad indicating that the two nitrogen atoms from the imine groups could be coordinated to the metal ion centre. The band C=N stretch at 1537 cm^{-1} is from the pyridine rings which has moved from its original signal at 1589 cm^{-1} which suggested that two nitrogen atoms from the pyridine rings are coordinated to the Zn(II) ion centre. In addition, two signals of aromatic stretch and the C-O stretch appear at 1474 and 1284 cm^{-1} in comparison to the two from the original ligand at 1491 and 1274 cm^{-1}.

Elemental analysis indicated that the complex had the formula [Zn_2(**8**)$(SCN)_2$·MeOH]. This also implies that two Zn(II) ions were bonded to the ligand and that two thiocyanate ions were also involved. The ligand itself was deprotonated to account for neutral charge. Each Zn(II) ion centre possesses four-coordination (tetrahedral) geometry, each Zn(II) ion with one nitrogen atom from the pyridine ring and one from the imine moiety, an oxygen and a thiocyanate sulfur complexing the coordination sphere. One equivalent of MeOH is also indicated in the Zn(II) thiocyanate complex. The possible structure of compound [Zn_2(**8**)$(SCN)_2$·MeOH] is depicted in Figure 3.4.7.

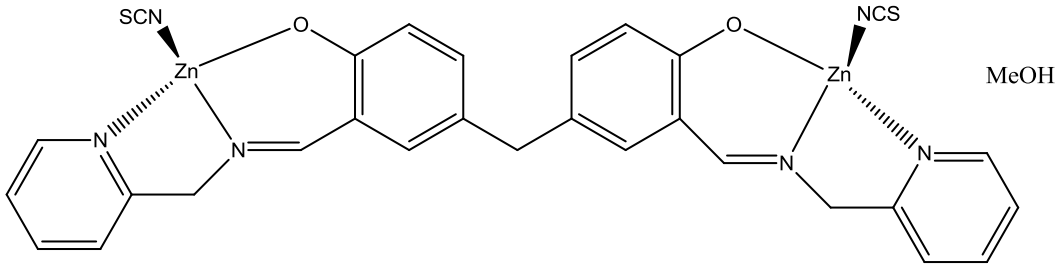

Figure 3.4.7: Possible structure for [Zn_2(**8**)$(SCN)_2$·MeOH].

3.4.3.2 [Zn_2(**8**)$(OAc)_2$]

The complex [Zn_2(**8**)$(OAc)_2$] is formed as a white crystalline solid. The ^{1}H NMR spectrum of complex [Zn_2(**8**)$(OAc)_2$] is shown in Figure 3.4.6 (in green). The ^{1}H NMR spectrum (with the only one exception that the aromatic proton Hb resonates at 6.72 ppm in the Zn(II) acetate complex compared to its corresponding signal from the Zn(II)

thiocyanate complex at 6.54 ppm) and the elemental analysis of compound [Zn_2(**8**)$(OAc)_2$] are very similar to that in Zn(II) thiocyanate complex which implies that the geometry of the Zn(II) ion in complex [Zn_2(**8**)$(OAc)_2$] is analogous to that of the Zn(II) thiocyanate complex.

In the IR spectrum of compound [Zn_2(**8**)$(OAc)_2$], the band of the imine group (C=N stretch) is similar to the one of the Zn(II) thiocyanate complex which suggests that the two nitrogen atoms could be binding to the metal centre. The appearance of the acetate signal at 1594 cm^{-1} has pointed towards fact that the Zn(II) acetate complexation had occurred. In addition, the band C=N stretch for the pyridine rings is occurring at 1573 cm^{-1} which has moved from the previous one at 1589 cm^{-1} in ligand **8** indicating the two nitrogen atoms from the pyridine rings are coordinated to the metal centre as well. The rest of the bands such as aromatic stretch, C-O stretch are observed in very similar positions to those of the Zn(II) thiocyanate complex.

Elemental analysis indicated that the complex had the formula [Zn_2(**8**)$(OAc)_2$], which suggests that the coordination of the Zn(II) ion is analogous to that of Zn(II) thiocyanate complex. Hence, the proposed structure of complex [Zn_2(**8**)$(OAc)_2$] is depicted in Figure 3.4.8.

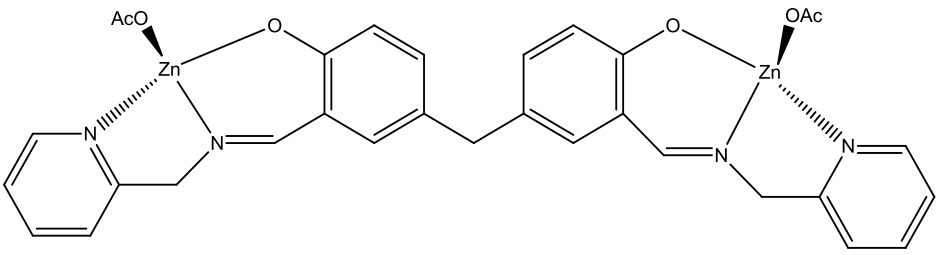

Figure 3.4.8: Possible structure for [Zn_2(**8**)$(OAc)_2$].

3.4.3.3 [Zn_2(**8**)Cl_2·MeOH]

The complex [Zn_2(**8**)Cl_2·MeOH] was isolated as a yellow solid. The ^{1}H NMR spectrum of compound [Zn_2(**8**)Cl_2·MeOH] is shown in Figure 3.4.6 (in purple). Although the spectrum appears as several broad peaks from 6-9 ppm, it is still very similar to that of Zn(II) thiocyanate complex according to the analytical data. This would imply that the bonding of Zn(II) ion in the Zn(II) chloride complex is analogous to the one of Zn(II) thiocyanate complex.

The structure of complex [Zn_2(**8**)Cl_2·MeOH] should be similar to the one of Zn(II) thiocyanate complex due to the similarity of both the IR spectrum and the elemental

analysis to those of Zn(II) thiocyanate complex. This similarity would suggest that the bonding of Zn(II) ion is occurring through the same donating atoms in both complexes. Hence, the proposed structure of complex [Zn_2(**8**)Cl_2·MeOH] is depicted in Figure 3.4.9.

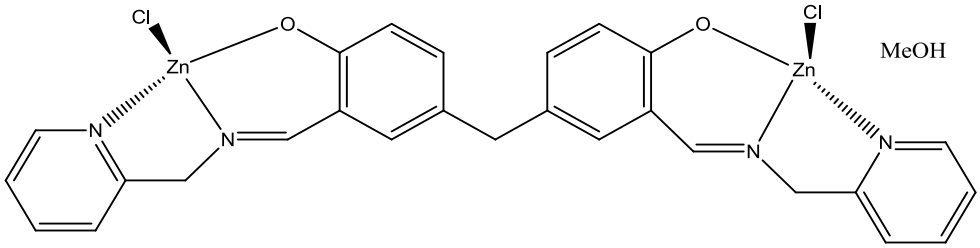

Figure 3.4.9: Possible structure for [Zn_2(**8**)Cl_2·MeOH].

3.4.3.4 [Ni_2(**8**)$(SCN)_2$]

The complex [Ni_2(**8**)$(SCN)_2$] was formed as a green solid. The observations of the complex [Ni_2(**8**)$(SCN)_2$] in either the IR spectrum or the elemental analysis are very similar to those of the Zn(II) thiocyanate complex which suggests that the structure of complex [Ni_2(**8**)$(SCN)_2$] is analogous to that of Zn(II) thiocyanate complex. In addition, the magnetic moment of complex [Ni_2(**8**)$(SCN)_2$] was obtained at 3.54 B.M. It is indicative of a tetrahedral geometry of the Ni(II) ion as the coordination number of Ni(II) thiocyanate complex is only four. The bonding is through one oxygen atom from the deprotonated phenol group, one nitrogen atom from the imine group and the other one from pyridine rings as well as one coordinated thiocyanate ion. Hence, the proposed structure of complex [Ni_2(**8**)$(SCN)_2$] is depicted in Figure 3.4.10.

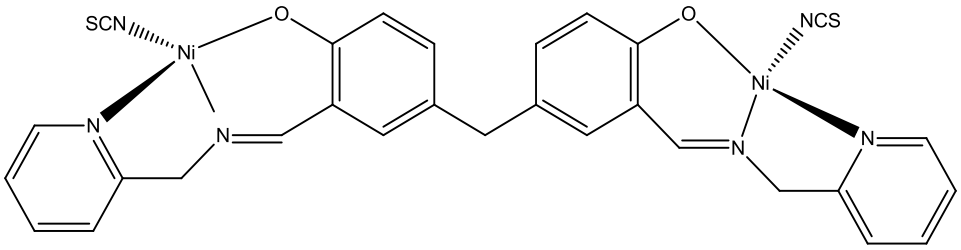

Figure 3.4.10: Possible structure for [Ni_2(**8**)$(SCN)_2$].

3.4.3.5 [Ni_2(**8**)(NO_3)(OH)·MeOH]

The complex [Ni_2(**8**)(NO_3)(OH)·MeOH] was formed as a dark green solid. The IR spectrum of compound [Ni_2(**8**)(NO_3)(OH)·MeOH] contains C=N stretch for the imine group at 1642 cm^{-1} which has shifted from its position in the free ligand at 1634 cm^{-1} indicating that imine nitrogen atoms are coordinated to the Ni(II) ion centre. The presence of a medium band of C=N stretch at 1608 cm^{-1} which is from the pyridine

rings can be compared to the original band at 1589 cm^{-1} implying that two nitrogen atoms from the pyridine rings are binding to the Ni(II) ion centre. The appearance of the nitrate group at 1384 cm^{-1} is pointing out that Ni(II) nitrate complexation had occurred. In addition, the other signals such as aromatic stretch and C-O stretch are obtained similarly to those of Zn(II) thiocyanate complex. The magnetic moment of complex [Ni_2(**8**)(NO_3)(OH)·MeOH] was obtained as 3.32 B.M. This value would imply that the Ni(II) complex adopts a tetrahedral geometry. Elemental analysis indicated that the complex had the formula [Ni_2(**8**)(NO_3)(OH)·MeOH]. This also suggests that two Ni(II) ions were bonded to the ligand and that one nitrate ion and one hydroxyl group from the deprotonated water are also involved. The ligand itself is deprotonated to account for the neutral charge. The bonding of the Ni(II) nitrate complex is very similar to that of Zn(II) thiocyanate complex. So, the possible structure of compound [Ni_2(**8**)(NO_3)(OH)·MeOH] is depicted in Figure 3.4.11.

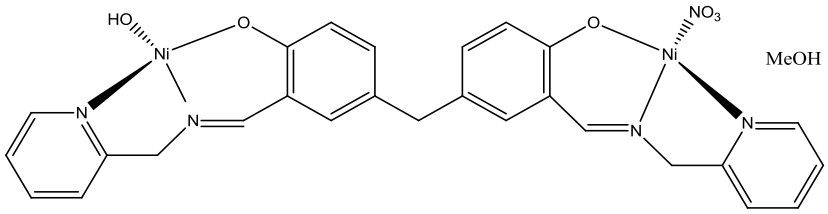

Figure 3.4.11: Possible structure for [Ni_2(**8**)(NO_3)(OH)·MeOH].

3.4.3.6 [Ni_2(**8**)Cl_2·MeOH]

The complex [Ni_2(**8**)Cl_2·MeOH] was formed as a reddish solid. The analytical data of the complex [Ni_2(**8**)Cl_2·MeOH] in both the IR spectrum and the elemental analysis are very similar to those of Zn(II) chloride complex which suggests that the bonding of the Ni(II) ion should be analogous to that of the Zn(II) ion. In addition, the magnetic moment of Ni(II) chloride complex was determined to be 3.44 B.M. This value would suggest that the complex adopts a tetrahedral geometry. Hence, the proposed structure of complex [Ni_2(**8**)Cl_2·MeOH] is depicted in Figure 3.4.12.

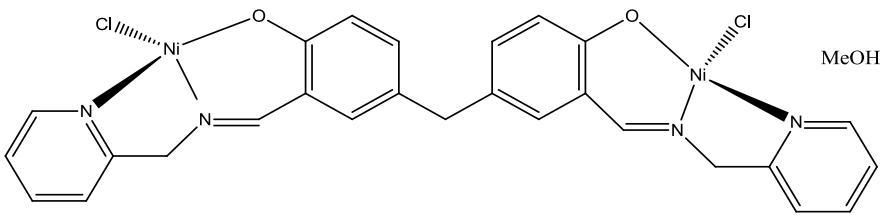

Figure 3.4.12: Possible structure for [Ni_2(**8**)Cl_2·MeOH].

3.4.3.7 [Ni_2(**8**)(ClO_4)(OH)·2MeOH]

The complex [Ni_2(**8**)(ClO_4)(OH)·2MeOH] was formed as a grey solid. The IR spectrum of compound [Ni_2(**8**)(ClO_4)(OH)·2MeOH] contains a signal ν_{OH} at 3415 cm^{-1} implying that MeOH molecules could be coordinated to the Ni(II) ion. The signal of C=N stretch for the imine stretch at 1645 cm^{-1} compares to that of the free ligand at 1634 cm^{-1} suggesting that the two nitrogen atoms from the imine group are binding to the Ni(II) ion centre. In addition, the C=N stretch for the pyridine rings is occurring at 1609 cm^{-1} which has moved from 1589 cm^{-1} in ligand **8**, pointing towards that the two nitrogen atoms from the pyridine rings are also coordinated to the Ni(II) ion centre. The appearance of the perchlorate band at 1090 cm^{-1} as a strong broad signal, has indicated that Ni(II) perchlorate complexation had occurred.

Elemental analysis indicated that the complex had the formula [Ni_2(**8**)(ClO_4)(OH)·2MeOH]. This would also imply that two Ni(II) ions were bonded to the ligand and that one perchlorate ion and one hydroxyl group from a deprotonated water molecule were also involved. The ligand itself is deprotonated to account for the neutral charge. The magnetic moment of complex [Ni_2(**8**)(ClO_4)(OH)·2MeOH] is 3.38 B.M. which suggests that the Ni(II) ion adopts a tetrahedral geometry. Hence, the possible structure of compound [Ni_2(**8**)(ClO_4)(OH)·2MeOH] is depicted in Figure 3.4.13.

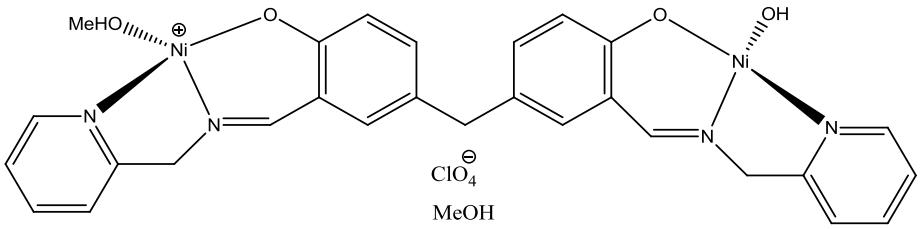

Figure 3.4.13: Possible structure for [Ni_2(**8**)(ClO_4)(OH)·2MeOH].

3.4.3.8 [Cu_2(**8**)Cl_2·2H_2O]

The compound of [Cu_2(**8**)Cl_2·2H_2O] was isolated as a green solid. The IR spectrum of the complex [Cu_2(**8**)Cl_2·2H_2O] is similar to that of the Zn(II) chloride complex with the only one exception of the signal representing the C=N stretch for the imine group occurs at 1628 cm^{-1} in the Cu(II) complex. The other data from the IR spectrum and the elemental analysis of the Cu(II) complex are similar to these of the Zn(II) chloride complex indicating that the bonding of the Cu(II) ion should be analogous to that of the

Zn(II) ion. The magnetic moment of the Cu(II) chloride complex is 2.15 B.M. Hence, the proposed structure of compound [Cu_2(**8**)Cl_2·$2H_2O$] is depicted in Figure 3.4.14.

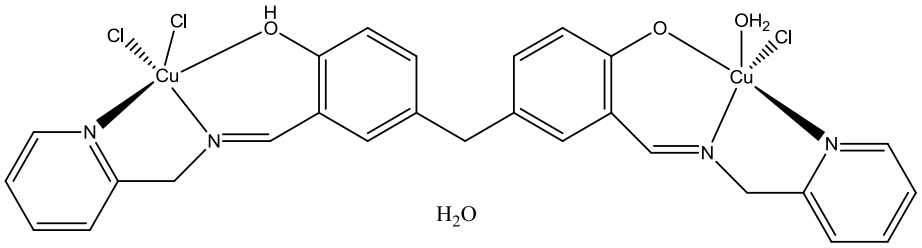

Figure 3.4.14: Possible structure for [Cu_2(**8**)Cl_3·$2H_2O$].

3.4.3.9 [Cu_2(**8**)$(OAc)_2$·$3H_2O$]

The complex [Cu_2(**8**)$(OAc)_2$·$3H_2O$] was formed as a green solid. The IR spectrum of compound [Cu_2(**8**)$(OAc)_2$·$3H_2O$] contains a signal ν_{OH} at 3412 cm^{-1} which suggests that coordinated water molecules are in the Cu(II) complex. The band of the C=N stretch for the imine group is present at 1627 cm^{-1} as a broad signal in comparison to the previous one at 1634 cm^{-1} in ligand **8** with the slight shift indicating that the imine nitrogen atoms are coordinated to the Cu(II) ion centre, and also implies the acetate group is in the complex. The C=N stretch for the pyridine ring is occurring at 1581 cm^{-1} which was shifted slightly from the original position at 1589 cm^{-1} in ligand **8** pointing towards that two nitrogen atoms from the pyridine rings are also binding to Ni(II) ion centre.

Elemental analysis indicated that the complex had the formula [Cu_2(**8**)$(OAc)_2$·$3H_2O$]. This would also imply that two Cu(II) ions were bonded to the ligand and that two acetate ions were also involved. The ligand itself is deprotonated to account for neutral charge. The magnetic moment of the Cu(II) acetate complex is 2.15 B.M. The geometry of the complex could be tetrahedral. Hence, the possible structure of compound [Cu_2(**8**)$(OAc)_2$·$3H_2O$] is depicted in Figure 3.4.15.

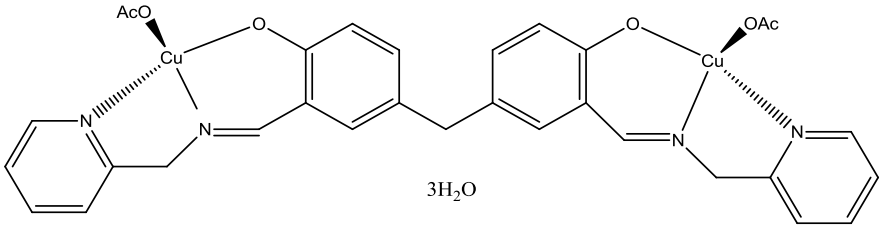

Figure 3.4.15: Possible structure for [Cu_2(**8**)$(OAc)_2$·$3H_2O$].

3.4.3.10 $[Cu_2(\mathbf{8})(ClO_4)_2 \cdot MeOH]$

The compound $[Cu_2(\mathbf{8})(ClO_4)_2 \cdot MeOH]$ was formed as a dark green solid. In the IR spectrum of compound $[Cu_2(\mathbf{8})(ClO_4)_2 \cdot MeOH]$, the appearance of OH stretch at 3409 cm^{-1} has suggested that coordinated MeOH molecule in the complex. The C=N stretch for the imine group presents at 1627 cm^{-1} which shifted from 1634 cm^{-1} in ligand **8** implying that the two nitrogen atoms from the imine group are coordinated to the Cu(II) ion centre. The presence of a band representing the C=N stretch from the pyridine rings occurs at 1571 cm^{-1} has moved from the original position at 1589 cm^{-1} in ligand **8**. This implies that the two nitrogen atoms from the pyridine rings are binding to the metal centre as well. Metal complexation may have occurred due to the appearance of the perchlorate group at 1108 cm^{-1} as a strong broad band.

Elemental analysis indicated that the complex had the formula $[Cu_2(\mathbf{8})(ClO_4)_2 \cdot MeOH]$. This would also imply that two Cu(II) ions were bonded to the ligand and that two perchlorate ions were also involved. The ligand itself is deprotonated to account for neutral charge. The magnetic moment of the Cu(II) perchlorate complex is 2.16 B.M. The geometry of the Cu(II) ion is tetrahedral. The possible structure of compound $[Cu_2(\mathbf{8})(ClO_4)_2 \cdot MeOH]$ is depicted in Figure 3.4.16.

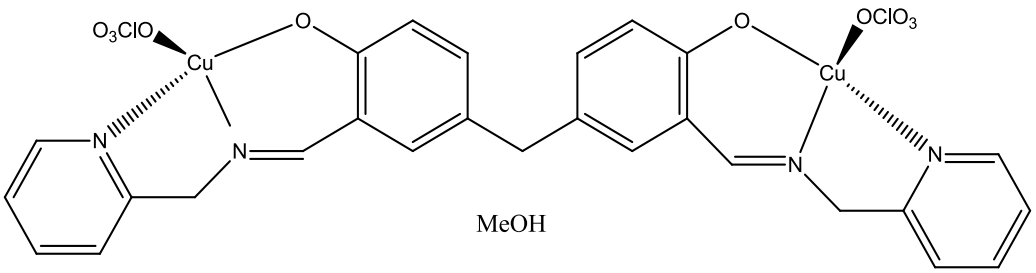

Figure 3.4.16: Possible structure for $[Cu_2(\mathbf{8})(ClO_4)_2 \cdot MeOH]$.

3.4.3.11 $[Co^{(III)}Co^{(II)}(\mathbf{8})(SCN)_2(OH) \cdot H_2O]$

The complex of $[Co^{(III)}Co^{(II)}(\mathbf{8})(SCN)_2(OH) \cdot H_2O]$ is isolated as a green solid. The obtained IR spectrum of compound $[Co^{(III)}Co^{(II)}(\mathbf{8})(SCN)_2(OH) \cdot H_2O]$ is very similar to that of the Zn(II) thiocyanate complex which suggests the bonding of the Co(II) ion should be analogous to that of Zn(II) ion. However, the magnetic moment of the Co(II) thiocyanate complex is 0.98 B.M. This value suggests that in the complex two different cobalt ions are present which are diamagnetic Co(III) ion and low spin Co(II) ion. The elemental analysis suggested the complex had the formula

$[Co^{(III)}Co^{(II)}(\mathbf{8})(SCN)_2(OH)\cdot H_2O]$. The bonding of the metal ions will be either tetrahedral Co(II) or octahedral Co(III), as depicted in Figure 3.4.17.

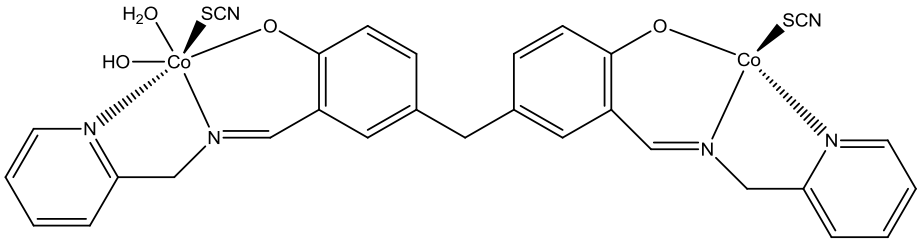

Figure 3.4.17: Possible structure for $[Co^{(III)}Co^{(II)}(\mathbf{8})(SCN)_2(OH)\cdot H_2O]$.

3.4.3.12 $[Co_2(\mathbf{8})Cl_2\cdot H_2O]$

The complex $[Co_2(\mathbf{8})Cl_2\cdot H_2O]$ is formed as a dark green solid. The obtained analytical data of the complex $[Co_2(\mathbf{8})Cl_2\cdot H_2O]$ in either the IR spectrum or the elemental analysis is very similar to that of the Zn(II) chloride complex which indicates that bonding of the Co(II) ion should be analogous to that of Zn(II) ion as well. The magnetic moment of the Co(II) complex is 4.65 B.M. which suggests the Co(II) ion adopts a tetrahedral geometry. Hence, the proposed structure of complex $[Co_2(\mathbf{8})Cl_2\cdot H_2O]$ is depicted in Figure 3.4.18.

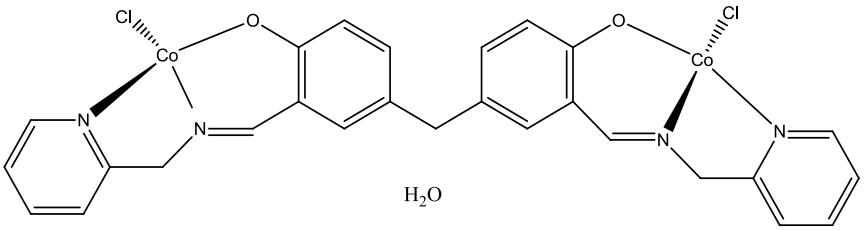

Figure 3.4.18: Possible structure for $[Co_2(\mathbf{8})Cl_2\cdot H_2O]$.

3.4.4 Ligand 9

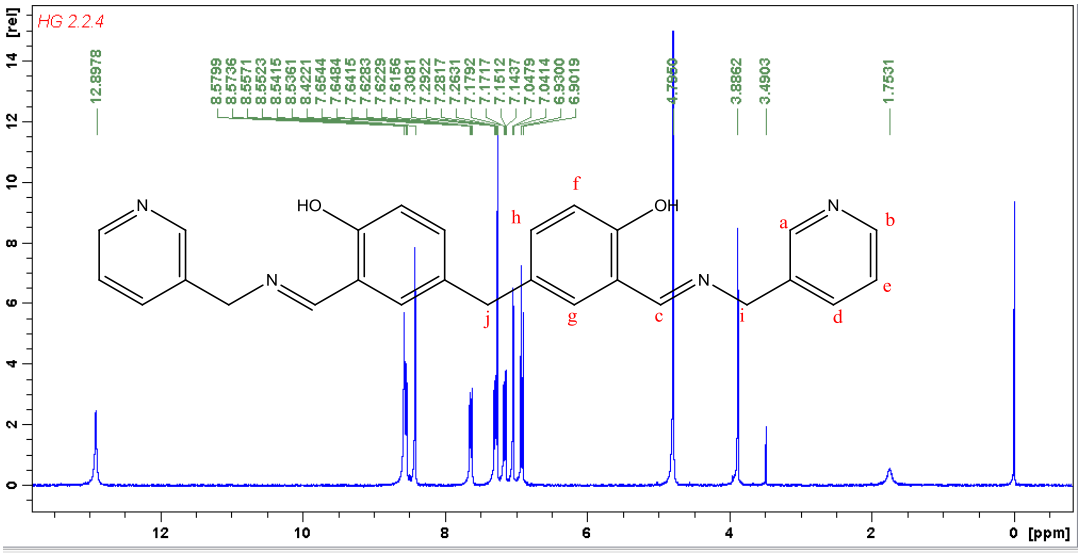

Figure 3.4.19: The ^{1}H NMR spectrum of ligand **9** in $CDCl_3$.

The ligand **9** is formed as a yellow solid which recrystallized from MeOH. The ^{1}H NMR spectrum of ligand **9** is shown in Figure 3.4.19. The phenol proton is resonating at 12.90 ppm in comparison to the one at 10.92 ppm in compound **7** indicating that a stronger hydrogen bond is formed between the imine and the phenol than that formed between the aldehyde and the phenol. The disappearance of the signal representing carbonyl proton at around 10 ppm of compound **7** and the appearance of imine proton Hc at 8.42 ppm imply that imine formation had occurred. Peaks representing the aromatic protons Hf, Hg and Hh are present at 7.16, 7.33 and 6.95 ppm, respectively. The aromatic bridging methylene proton Hj which resonated at 3.96 ppm in compound **7** has shifted to 3.88 ppm in ligand **9**. In addition, the signals of the protons for the pyridine rings, Ha presents at 8.58 ppm as a singlet, Hb resonates as doublet of doublets at 8.54 ppm; Hd and He are observed at 7.63 and 7.29 ppm, respectively, in ligand **9**. In the ^{13}C NMR spectrum, the imine carbon appears at 166.3 ppm which supports that all aldehyde was consumed. The spectrum contains fourteen carbon peaks which matches with ligand **9**. The elemental analysis indicates that the ligand **9** is pure.

The IR spectrum of ligand **9** contains a band ν_{OH} at 3450 cm^{-1} which presents that phenol OH stretch. The peak for the C=N stretch of the imine group appears at 1640 cm^{-1} in comparison to the aldehyde C=O stretch in compound **7** at 1656 cm^{-1} indicating that imine formation had occurred. The appearance of the C=N stretch at 1589 cm^{-1} is due to the pyridine rings. And a C-O stretch was seen at 1281 cm^{-1} which was seen the

previous band at 1272 cm^{-1} in compound **7**. It was difficult to assign other peaks from pyridine rings.

3.4.5 Metal complexes of 9

Metal complexes reactions of ligand **9** with various metal(II) salts were carried out in MeOH. The reactions were carried out by stirring 2 hours in MeOH. The resulting coloured solids were collected by filtration.

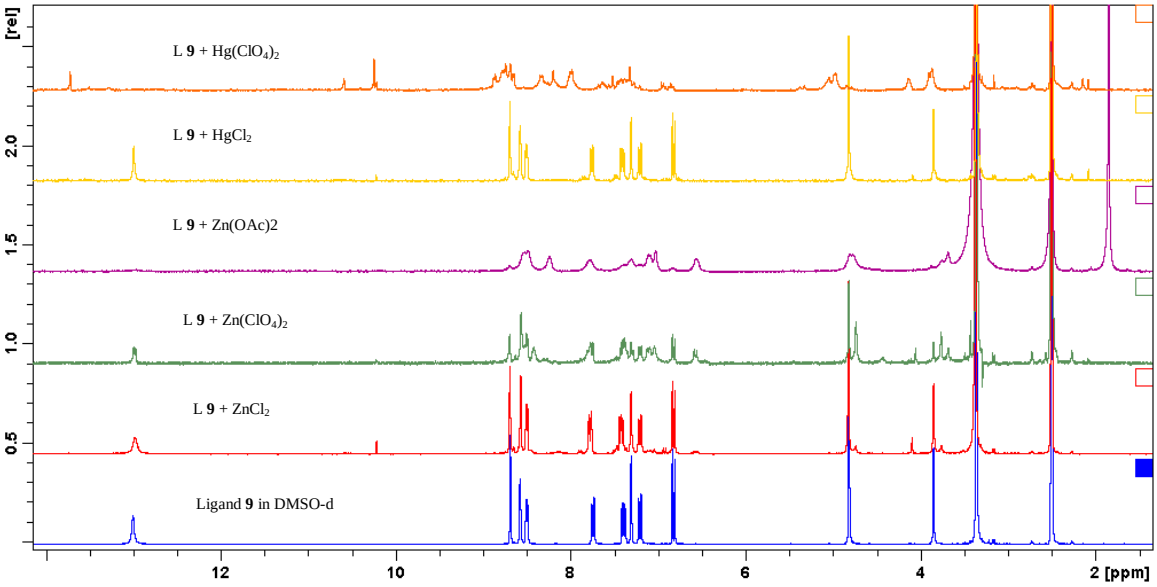

Figure 3.4.20: A comparison of ^{1}H NMR spectra of ligand **9** and its corresponding Zn(II) chloride/acetate/perchlorate complexes and Hg(II) chloride/perchlorate complexes in DMSO-d_6.

As shown in Figure 3.4.20, the blue spectrum is ligand **9** in DMSO-d_6. The Zn(II) chloride complex is shown in red, which is quite similar with ligand **9**. The green spectrum is the Zn(II) perchlorate complex which has several more peaks compared to ligand **9** indicating that the two side chains could be in different environments. The NMR spectrum of the Zn(II) acetate complex is shown as purple, interestingly, the phenol group was deprotonated as there were no signals presenting at more than 10 ppm. The spectrum of the Hg(II) chloride complex is shown in yellow which is similar to the proton spectrum of the Zn(II) chloride complex. The last one is the Hg(II) perchlorate complex which is shown as the orange spectrum implying that the Hg(II) perchlorate complex could be hydrolysed due to a peak at around 10.3 ppm.

3.4.5.1 $[Zn_3(\mathbf{9})_2Cl_6]$

The complex of $[Zn_3(\mathbf{9})_2Cl_6]$ was formed as a yellow solid. The ^{1}H NMR spectrum of the Zn(II) chloride complex is shown in Figure 3.4.20 (in red) which is quite similar to the free ligand, suggesting a weak metal bonding was occurring. The only slight difference on closer inspection is the two signals from the pyridine rings, protons Hd and He which present at 7.75 and 7.40 ppm in ligand **9** but have shifted to 7.78 and 7.43 ppm, respectively, in the Zn(II) chloride complex. This could indicate that two pyridine nitrogen atoms are coordinated to the Zn(II) ion centre.

The IR spectrum compound $[Zn_3(\mathbf{9})_2Cl_6]$ contains a band for the OH stretch at 3446 cm^{-1} which was seen at 3450 cm^{-1} from the original ligand **9** with no significant change. However, the OH bend and C-O stretch occur at 1435 and 1318 cm^{-1} which have moved from 1422 and 1281 cm^{-1}, respectively. These suggest that the oxygen atom from the phenol group might have a weak bonding to the Zn(II) ion centre. The C=N stretch for the imine group presents at 1628 cm^{-1} in comparison to the original band at 1640 cm^{-1}. A large shift was found in the C=N stretch for the pyridine rings which is present at 1536 cm^{-1} in comparison to the previously position at 1591 cm^{-1} in ligand **9**. This implies that the two pyridine nitrogen atoms are binding to the Zn(II) ion. The aromatic stretch is present at 1471 cm^{-1} in the Zn(II) complex which were seen at 1492 cm^{-1} in ligand **9**.

Elemental analysis indicated that the complex had the formula $[Zn_3(\mathbf{9})_2Cl_6]$. This would imply that three Zn(II) ions were bonded to two ligands and that six chloride ions were also involved to account for neutral charge. The bonding of each Zn(II) ion is through one oxygen atoms from the phenol group and one nitrogen from the pyridine rings as well as two chloride ions. The possible structure of compound $[Zn_3(\mathbf{9})_2Cl_6]$ is depicted in Figure 3.4.21.

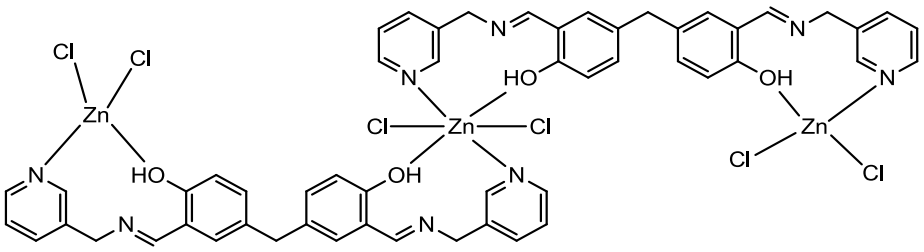

Figure 3.4.21: Possible structure for $[Zn_3(\mathbf{9})_2Cl_6]$.

3.4.5.2 [Zn(**9**)(ClO_4)·$2H_2O$]

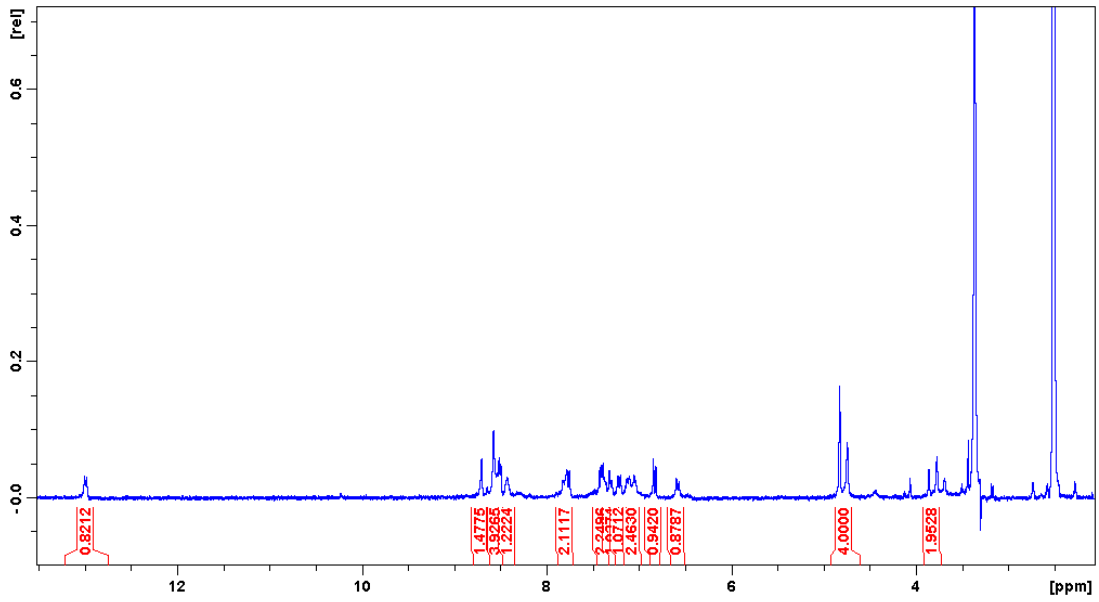

Figure 3.4.22: The ^{1}H NMR spectrum of complex [Zn(**9**)(ClO_4)·$2H_2O$].

The complex of [Zn(**9**)(ClO_4)·$2H_2O$] was formed as a yellow solid. The ^{1}H NMR spectrum of compound [Zn(**9**)(ClO_4)·$2H_2O$] is shown in Figure 3.4.22. The phenol proton is appeared at 13.00 ppm, however, due to the ratio of the integrals, only one phenol proton obtained in spectrum, so the other phenol proton was deprotonated to form the Zn(II) complex. This would also imply that the two side chains could be in different environments. That is why there are so many signals in Figure 3.4.22. In addition, the bridging methylene protons Hi which is occurring as different two singlets at 4.82 and 4.74 ppm, respectively, confirms this result. But it was difficult to assign specific peaks in the spectrum.

The IR spectrum of complex [Zn(**9**)(ClO_4)·$2H_2O$] contains a signal of C=N stretch for the imine group at 1622 cm^{-1} as a strong broad peak which has moved from 1640 cm^{-1} in ligand **9**. The C=N stretch of the pyridine rings occurs at 1536 cm^{-1} which was seen to have a large shift from the original band at 1591 cm^{-1} in ligand **9**. This indicates that the two nitrogen atoms from the pyridine rings are coordinated to the Zn(II) ion centre. In addition, the C-O stretch appears at 1318 and 1277 cm^{-1} in comparison to the original one at 1281 cm^{-1} in ligand **9** pointing towards the C-O stretch could be in different environments in Zn(II) complex. The appearance of a broad strong band at 1108 cm^{-1} is due the perchlorate group, and has indicated the Zn(II) perchlorate complexation had occurred.

Elemental analysis indicated that the complex had the formula [Zn(**9**)(ClO_4)·$2H_2O$]. This would imply that one Zn(II) ion was bonded to the ligand and that one perchlorate ion was also involved. Only one phenol group of the ligand is deprotonated to account for neutral charge. The bonding of the Zn(II) ion is through two oxygen atoms and two nitrogen atoms from the pyridine rings. The coordination number of the Zn(II) ion is either four- or six-coordinate (including two water molecules). The possible structures of compound [Zn(**9**)(ClO_4)·$2H_2O$] are depicted in Figure 3.4.23.

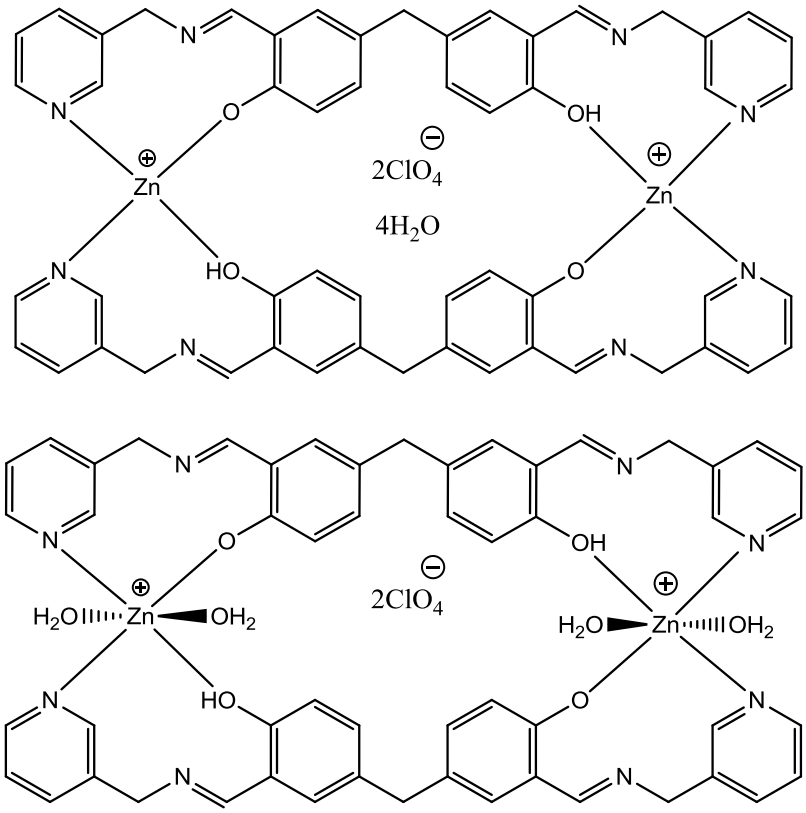

Figure 3.4.23: Possible structures for [Zn(**9**)(ClO_4)·$2H_2O$].

3.4.5.3 [Zn_2(**9**)($OAc)_2$·$2H_2O$]

The complex [Zn_2(**9**)($OAc)_2$·$2H_2O$] is formed as a yellow solid. The ^{1}H NMR spectrum of compound [Zn_2(**9**)($OAc)_2$·$2H_2O$] is shown in Figure 3.4.20 (in purple). Comparing this to other Zn(II) complexes, the phenol group was deprotonated as no peak is present at around 13-15 ppm. The imine proton Hc and the pyridyl proton Ha resonate at 8.50 ppm as a broad singlet in comparison to the original bands, where the protons Hc and Ha at 8.69 and 8.58 ppm, respectively, in ligand **9**. This imine proton shift would imply that the two nitrogen atoms from the imine group are coordinated to the Zn(II) ion centre. The proton Hb resonates at 8.24 ppm which was seen at 8.51 ppm in ligand **9**. Proton Hg appears at 7.32 ppm which is quite similar to the original one at 7.31 ppm.

Protons Hf and Hd are present at 7.11 ppm which were seen Hf at 7.21 ppm and Hd at 7.75 ppm, respectively, in ligand **9**. The chemical shifts of the protons in the pyridine rings suggest that the two nitrogen atoms from the pyridine rings could be coordinated to the Zn(II) ion centre. The shift of the aromatic protons Hf and Hg are very similar to the free ligand with the exception of proton Hh which is present at 6.57 ppm as a broad peak has moved from its original position at 6.83 ppm in ligand **9**. The two bridging methylene protons, Hj and Hi, proton Hj present at 4.81 ppm which was seen from the original one at 4.82 ppm in ligand **9** without significant change. Proton Hi appears at 3.68 ppm comparing the previous one at 3.85 ppm in ligand **9**.

The IR spectrum of compound $[Zn_2(\mathbf{9})(OAc)_2{\cdot}2H_2O]$ contains a signal ν_{OH} at 3417 cm^{-1} which was seen at 3450 cm^{-1} in the original ligand **9** which suggests that some coordinated water molecules are in the Zn(II) complex. The C=N stretch for the imine group is present at 1626 cm^{-1} which has moved from 1640 cm^{-1} in ligand **9** implying that two imine nitrogens could be coordinated to the Zn(II) ion centre. The appearance of the acetate group at 1592 cm^{-1} is implying that the metal complexation had occurred. The C=N stretch of the pyridine rings presents at 1533 cm^{-1} in comparison to the original band at 1591 cm^{-1} in ligand **9** demonstrating that the two pyridine nitrogen atoms are binding to the Zn(II) ion. The aromatic stretch presents at 1470 cm^{-1} in the Zn(II) complex which were seen at 1492 cm^{-1} in ligand **9**. And C-O stretch appears at 1323 cm^{-1} in contrast to the band at 1281 cm^{-1} in ligand **9** which suggests that the oxygen the from phenol is coordinated to the Zn(II) ion.

Elemental analysis indicated that the complex had the formula $[Zn_2(\mathbf{9})(OAc)_2{\cdot}2H_2O]$. This would also imply that two Zn(II) ions were bonded to ligand and that two acetate ions were also involved. The ligand itself is deprotonated to account for neutral charge. The bonding of each Zn(II) ions is the same which is through one oxygen atoms from deprotonated phenol group, and two nitrogen atoms from imine group and the pyridine rings as well as one acetate ion. The geometry of the Zn(II) ion is either four- or five-coordinate (including water molecules) geometry. Hence, the possible structures of compound $[Zn_2(\mathbf{9})(OAc)_2{\cdot}2H_2O]$ are depicted in Figure 3.4.24.

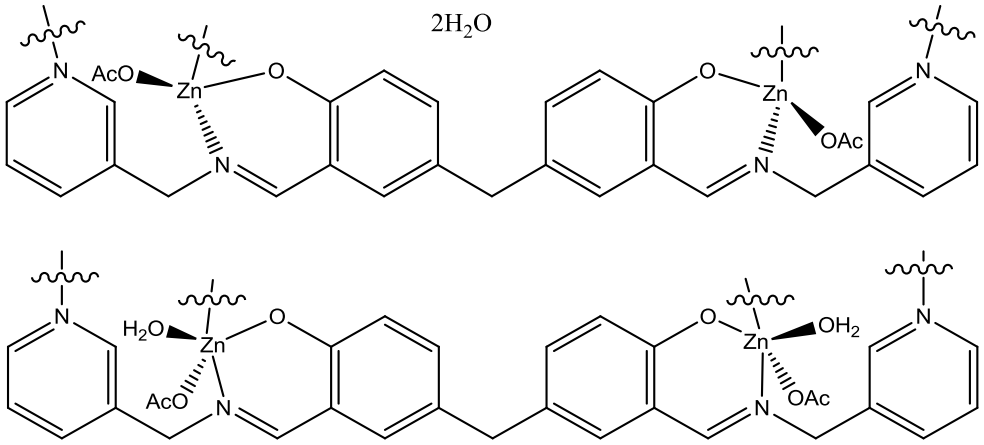

Figure 3.4.24: Possible structures for $[Zn_2(\mathbf{9})(OAc)_2{\cdot}2H_2O]$.

3.4.5.4 $[Hg_3(\mathbf{9})_2Cl_6]$

The complex $[Hg_3(\mathbf{9})_2Cl_6]$ is isolated as a yellow solid. The ^{1}H NMR spectrum of compound $[Hg_3(\mathbf{9})_2Cl_6]$ is shown in Figure 3.4.20 in yellow. The obtained ^{1}H NMR spectrum which is quite similar to that of the Zn(II) chloride complex is indicative of the bonding of the Hg(II) ion should be analogous to that of the Zn(II) ion.

The observations are that the Hg(II) chloride complex in either IR spectrum or the elemental analysis are similar to those of the Zn(II) chloride complex. Hence, the proposed structure of complex $[Hg_3(\mathbf{9})_2Cl_6]$ is depicted in Figure 3.4.25.

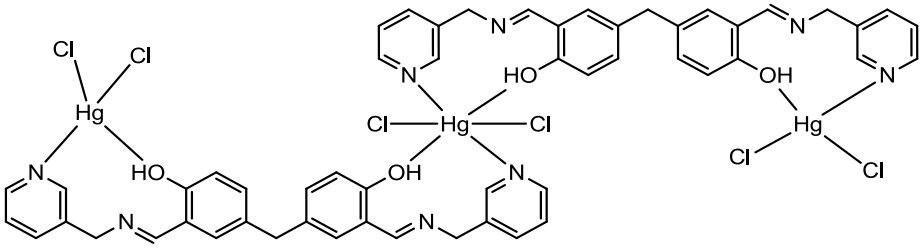

Figure 3.4.25: Possible structure for $[Hg_3(\mathbf{9})_2Cl_6]$.

3.4.5.5 $[Ni_3(\mathbf{9})_2Cl_6]$

The complex of $[Ni_3(\mathbf{9})_2Cl_6]$ is formed as a green solid. The obtained analytical data of the complex $[Ni_3(\mathbf{9})_2Cl_6]$ in both the IR spectrum and the elemental analysis are quite similar to that of the Zn(II) chloride complex which is implying that the bonding of complex $[Ni_3(\mathbf{9})_2Cl_6]$ is analogous to that of the Zn(II) chloride complex. In addition, the magnetic moment of the complex $[Ni_3(\mathbf{9})_2Cl_6]$ is obtained as 3.40 B.M. It is not easy to distinguish the geometry of the Ni(II) complexes, both tetrahedral and octahedral

geometries are possible with this value in the Ni(II) chloride complex. Hence, a proposed structure of complex $[Ni_3(\mathbf{9})_2Cl_6]$ is shown in Figure 3.4.26.

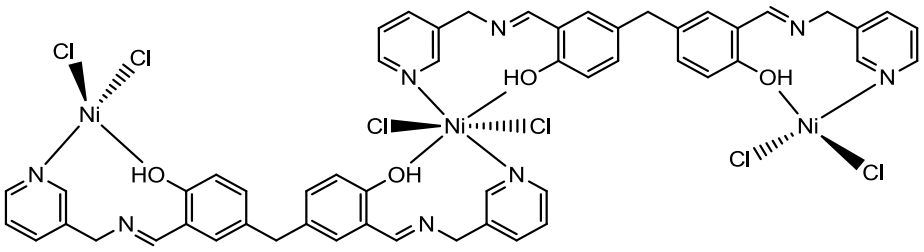

Figure 3.4.26: Possible structure for $[Ni(\mathbf{9})Cl_2{\cdot}3H_2O]$.

3.4.5.6 $[Ni_2(\mathbf{9})(OAc)_2{\cdot}MeOH{\cdot}H_2O]$

The complex $[Ni_2(\mathbf{9})(OAc)_2{\cdot}MeOH{\cdot}H_2O]$ was formed as a green solid. It is presumed that the two phenol groups are deprotonated in the Ni(II) acetate complex which is similar to that of Zn(II) acetate complex as their IR spectra are very similar.

Elemental analysis indicated that the complex had the formula $[Ni_2(\mathbf{9})(OAc)_2{\cdot}MeOH{\cdot}H_2O]$. This formula is also similar to that of the Zn(II) complex as well. In addition, the magnetic moment of the Ni(II) acetate complex is obtained at 4.05 B.M. which is strongly suggesting the geometry of each Ni(II) ions is tetrahedral. Hence, the possible structure of complex $[Ni_2(\mathbf{9})(OAc)_2{\cdot}MeOH{\cdot}H_2O]$ is depicted in Figure 3.4.27.

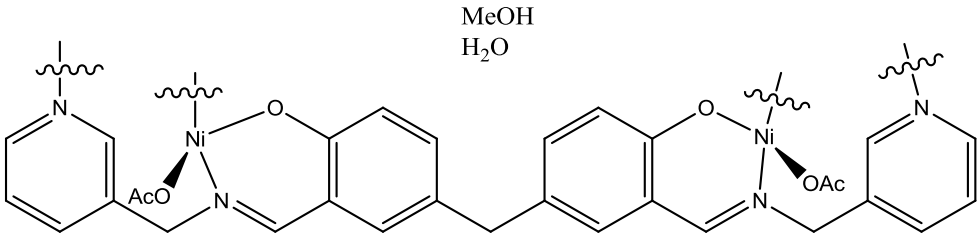

Figure 3.4.27: Possible structure for $[Ni_2(\mathbf{9})(OAc)_2{\cdot}MeOH{\cdot}H_2O]$.

3.4.5.7 $[Ni(\mathbf{9})(ClO_4){\cdot}2MeOH]$

The complex $[Ni(\mathbf{9})(ClO_4){\cdot}2MeOH]$ is formed as a green solid. Due to the observation of the only one phenol group was deprotonated in the Zn(II) perchlorate complex, it is presumed that similar deprotonation would be occurred in the Ni(II) perchlorate complex. In addition, the obtained IR spectrum and the elemental analysis of compound $[Ni(\mathbf{9})(ClO_4){\cdot}2MeOH]$ are similar to those of Zn(II) perchlorate complex as well which suggests the bonding of Ni(II) ion is analogous to the Zn(II) ion. The magnetic moment

of the complex [Ni(**9**)(ClO_4)·2MeOH] is obtained at 3.28 B.M. This implies that the geometry of the Ni(II) ion could adopt either a tetrahedral or an octahedral geometry. Hence, the proposed structures of complex [Ni(**9**)(ClO_4)·2MeOH] are depicted in Figure 3.4.28.

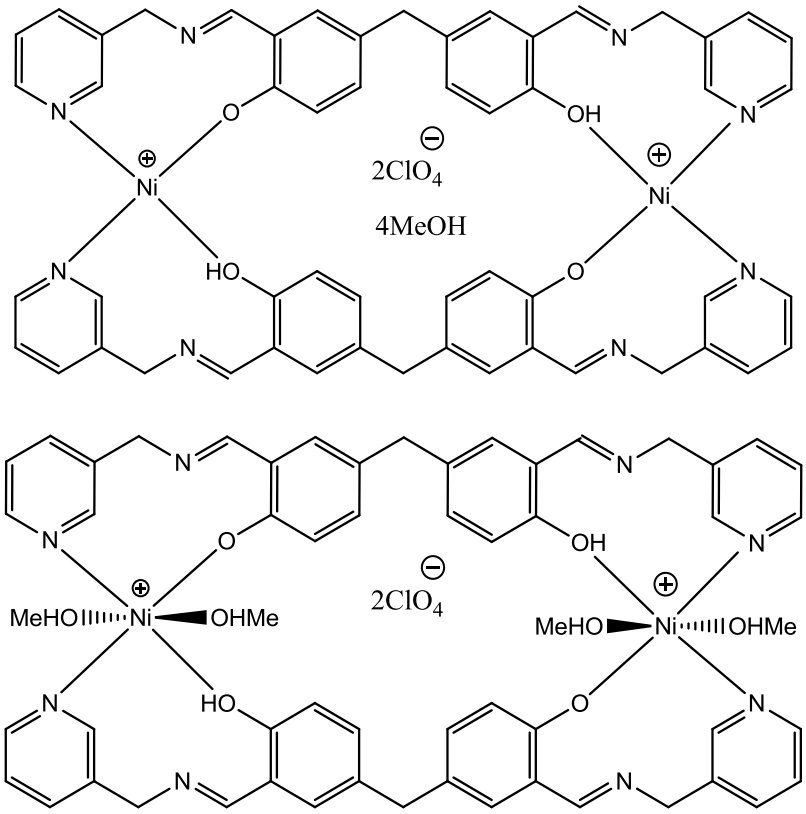

Figure 3.4.28: Possible structures for [Ni(**9**)(ClO_4)·2MeOH].

3.4.5.8 [Ni(**9**)(NO_3)·3H_2O]

The complex [Ni(**9**)(NO_3)·3H_2O] is formed as a green solid. The IR spectrum compound [Ni(**9**)(NO_3)·3H_2O] contains a band ν_{OH} at 3410 cm^{-1} which was seen at 3450 cm^{-1} in the original ligand **9** indicating that phenol OH stretch or coordinated water molecules could be in the Ni(II) complex. The C=N stretch of imine group is present at 1626 cm^{-1} which is similar to that of Zn(II) perchlorate complex. In addition, the C=N stretch of the pyridine rings at 1535 cm^{-1} in comparison to the original one at 1591 cm^{-1} has suggested the two nitrogen atoms from the pyridine rings are coordinated to the Ni(II) ion centre. Interestingly, it is observed that two bands of C-O stretch at 1274 and 1323 cm^{-1}, respectively, implying that the two C-O bonds are in different environments which is similar to that of the Zn(II) perchlorate complex as well. This suggests that the bonding of the Ni(II) nitrate complex is analogous to that of the Zn(II) perchlorate

complex. The appearance of the nitrate signal at 1385 cm^{-1} is indicating that Ni(II) nitrate complexation had occurred.

Elemental analysis indicated that the complex had the formula [Ni(**9**)(NO_3)·$3H_2O$]. This also implied that one Ni(II) ion was bonded to the ligand and that one nitrate ion was also involved. Only one phenol group could be deprotonated in order to account for neutral charge. The magnetic moment of the Ni(II) nitrate complex is obtained at 3.37 B.M. which is quite similar to that of the Ni(II) perchlorate complex suggesting the geometry could be similar to that of the Ni(II) nitrate complex as well. Hence, the possible structures of compound [Ni(**9**)(NO_3)·$3H_2O$] are depicted in Figure 3.4.29.

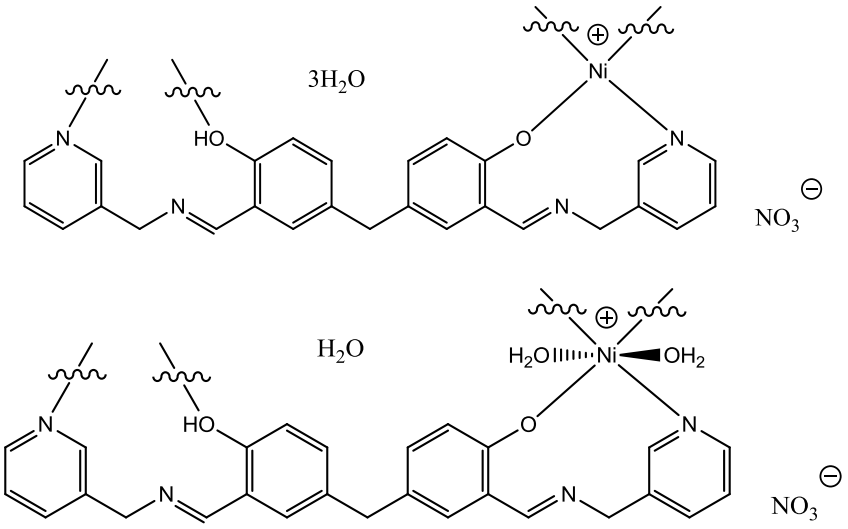

Figure 3.4.29: Possible structures for [Ni(**9**)(NO_3)·$3H_2O$].

3.4.5.9 [Cu_3(**9**)$_2Cl_6$·$4H_2O$]

The complex [Cu_3(**9**)$_2Cl_6$·$4H_2O$] is isolated as a grey solid. The IR spectrum compound [Cu_3(**9**)$_2Cl_6$·$4H_2O$] contains a signal ν_{OH} at 3429 cm^{-1} suggesting that phenol OH stretch or coordinated water might be in the Cu(II) complex. Other bands such as imine group, pyridine rings or the aromatic stretch and C-O stretch are very similar to that of the Zn(II) chloride complex.

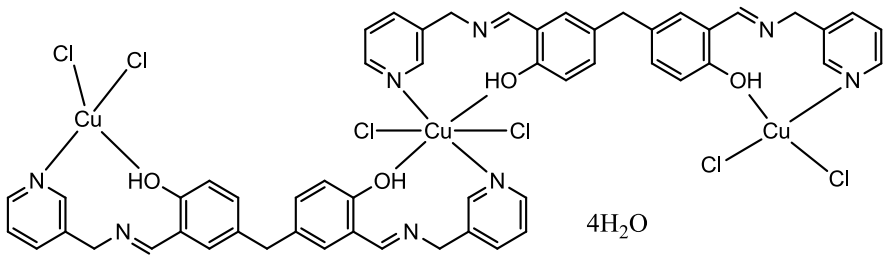

Figure 3.4.30: Possible structure for [Cu_3(**9**)$_2Cl_6$·$4H_2O$].

In addition, the elemental analysis suggested the complex had the formula [Cu_3(**9**)$_2Cl_6$·$4H_2O$] which is similar to that of the Zn(II) complex as well with the exception of four extra water molecules are in the Cu(II) chloride complex. The bonding of the Cu(II) ion is through two oxygen atoms from the phenol group and two nitrogen atoms from the pyridine rings. The magnetic moment of the Cu(II) chloride complex is 2.03 B.M. Hence, the proposed structure of complex [Cu_3(**9**)$_2Cl_6$·$4H_2O$] is depicted in Figure 3.4.30.

3.4.5.10 [Cu_2(**9**)$(OAc)_2$]

The complex of [Cu_2(**9**)$(OAc)_2$] is formed as a green solid. It is presumed that the two phenol groups are deprotonated in the Cu(II) acetate complex as the IR spectrum of the Cu(II) complex is very similar to that of the Zn(II) acetate complex.

Elemental analysis indicated the complex had the formula [Cu_2(**9**)$(OAc)_2$]. This would also imply that two Cu(II) ions were bonded to the ligand and that two acetate ions were also involved. The ligand itself is deprotonated to account for neutral charge. The bonding of each Cu(II) ion is similar which is though one oxygen atom of deprotonated phenol group and one imine nitrogen atom and one pyridine nitrogen atom as well as one acetate ion. In addition, the bonding of the Cu(II) ion is analogous to that of Zn(II) ion. The magnetic moment of the Cu(II) acetate complex is 2.17 B.M. Hence, the geometry of Cu(II) ion is tetrahedral. The possible structure of compound [Cu_2(**9**)$(OAc)_2$] is depicted in Figure 3.4.31.

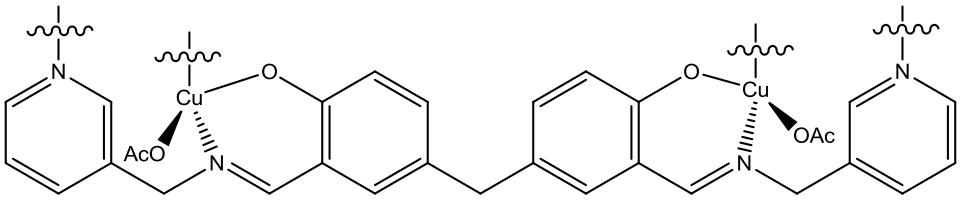

Figure 3.4.31: Possible structure for [Cu_2(**9**)$(OAc)_2$].

3.4.5.11 [Cu(**9**)$(ClO_4)_2$]

The complex [Cu(**9**)$(ClO_4)_2$] is formed as a green solid. The IR spectrum of compound [Cu(**9**)$(ClO_4)_2$] is found to be very similar to that of Zn(II) perchlorate complex with the only one exception of the C-O stretch which presenting only one signal at 1323 cm^{-1} in comparison to the two bands of C-O stretches in the Zn(II) complex. This would suggest that the two C-O stretches are in the same environment in the Cu(II) perchlorate complex. In addition, the appearance of the perchlorate group at 1109 cm^{-1} as a strong

broad signal indicates that Cu(II) perchlorate complexation had occurred. In addition, due to the similar IR spectrum between the Cu(II) and the Zn(II) perchlorate complexes, the bonding of Cu(II) ion should be analogous to that of Zn(II) ion. The magnetic moment of the Cu(II) perchlorate complex is 2.21 B.M. Hence, the proposed structure of the complex [Cu(**9**)$(ClO_4)_2$] is depicted in Figure 3.4.32.

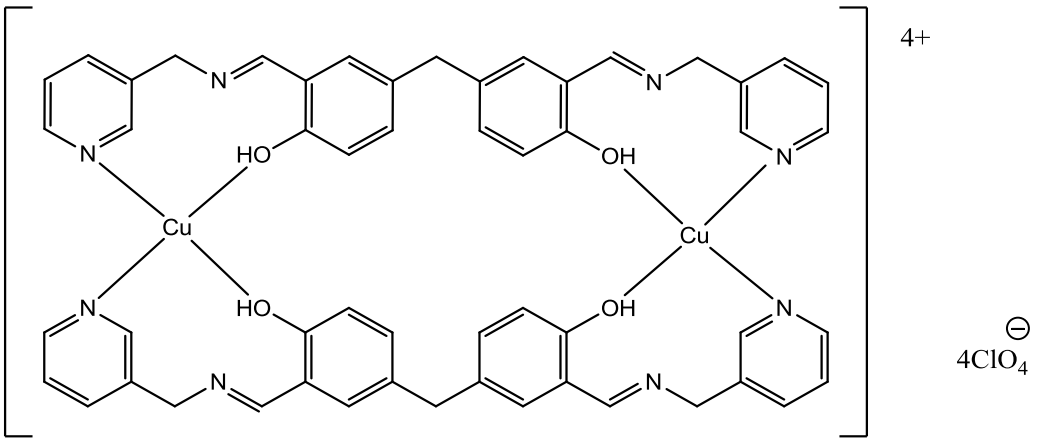

Figure 3.4.32: Possible structure for [Cu(**9**)$(ClO_4)_2$].

3.4.5.12 [Co_3(**9**)$_2Cl_6$·$4H_2O$]

The complex [Co_3(**9**)$_2Cl_6$·$4H_2O$] is isolated as a green solid. The IR spectrum of compound [Co_3(**9**)$_2Cl_6$·$4H_2O$] contains ν_{OH} at 3430 cm^{-1} as a strong broad band indicating either the presence of the phenol OH or some coordinated water molecules are in the Co(II) complex. The observations of the complex in either the IR spectrum or the elemental analysis are very similar to that of Zn(II) chloride complex which would also imply that the bonding of Co(II) ion should be analogous to that of Zn(II) ion as well. In addition, the magnetic moment of the complex [Co_3(**9**)$_2Cl_6$·$4H_2O$] is obtained at 4.71 B.M. which is indicative of an octahedral geometry in the Co(II) complex. Hence, the proposed structure of complex [Co_3(**9**)$_2Cl_6$·$4H_2O$] is depicted in Figure 3.4.33.

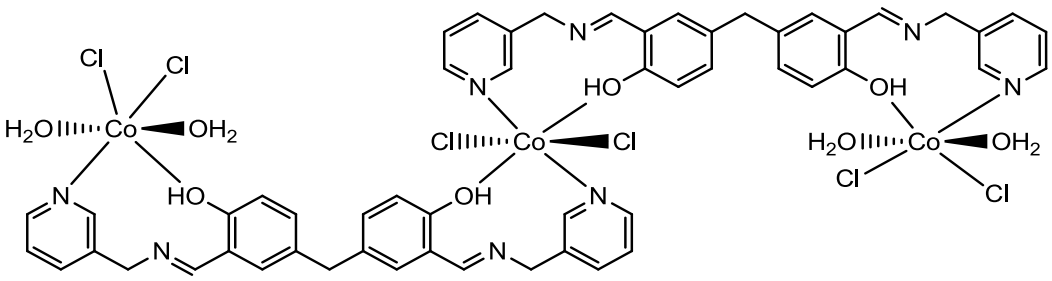

Figure 3.4.33: Possible structure for [Co(**9**)Cl_2·H_2O].

3.4.5.13 [Co(**9**)(ClO_4)·2MeOH]

The complex [Co(**9**)(ClO_4)·2MeOH] is formed as a green solid. As only one phenol group was deprotonated in the Zn(II) perchlorate complex, it is presume that similar deprotonating would occur in the Co(II) perchlorate complex. In addition, the IR spectrum and the elemental analysis of compound [Co(**9**)(ClO_4)·2MeOH] are similar to those of Zn(II) perchlorate complex as well which indicated that the bonding of Co(II) ion is analogous to that of the Zn(II) ion. The magnetic moment of the complex [Co(**9**)(ClO_4)·2MeOH] is obtained as 4.82 B.M. This implies that the of Co(II) ion is adopting an octahedral geometry sphere. Hence, the proposed structure of complex [Co(**9**)(ClO_4)·2MeOH] is depicted in Figure 3.4.34.

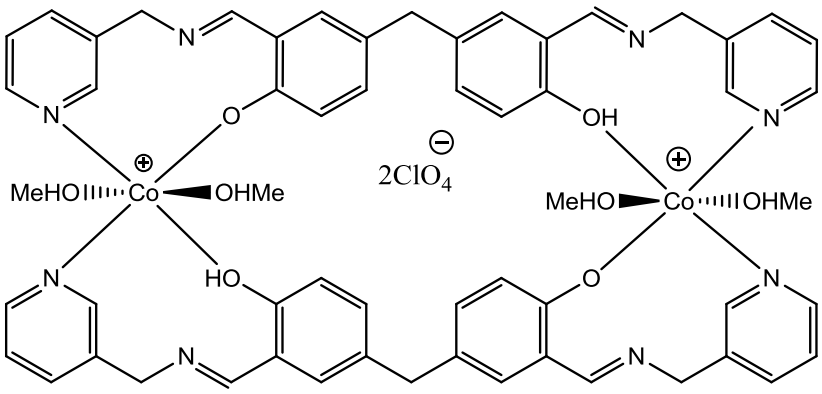

Figure 3.4.34: Possible structure for [Co(**9**)(ClO_4)·2MeOH].

3.4.5.14 [Co(**9**)(SCN)·H_2O]

The complex [Co(**9**)(SCN)·H_2O] is formed as a green solid. In the IR spectrum of compound [Co(**9**)(SCN)·H_2O], the appearance of the thiocyanate stretch at 2067 cm^{-1} is indicative of the Co(II) thiocyanate complexation had occurred. The other signals such as OH stretch, C=N stretch for the imine group and pyridine ring are observed very similar to those of Co(II) perchlorate complex. In addition, two signals of C-O stretches obtained at 1277 and 1316 cm^{-1} imply that the two C-O groups are in different environments, which are similar to that of Co(II) perchlorate complex as well. The magnetic moment of [Co(**9**)(SCN)·H_2O] is occurring at 5.12 B.M. indicating the geometry of the high-spin Co(II) ion is adopting an octahedral geometry sphere. The elemental analysis pointed out the complex had the formula [Co(**9**)(SCN)·H_2O]. According to observations of the IR spectrum and the elemental analysis, the bonding of Co(II) ion in the thiocyanate complex should be analogous to that of Co(II) perchlorate complex as well. Hence, the proposed structure of the complex [Co(**9**)(SCN)·H_2O] is depicted in Figure 3.4.35.

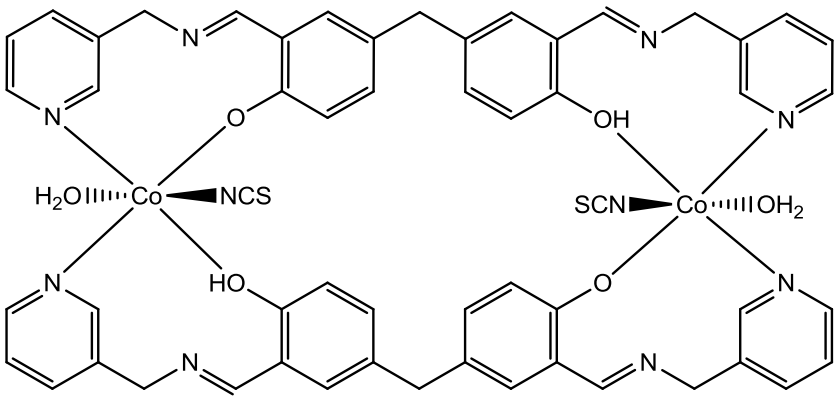

Figure 3.4.35: Possible structure for [Co(**9**)(SCN)·H_2O].

3.4.6 Ligand 10

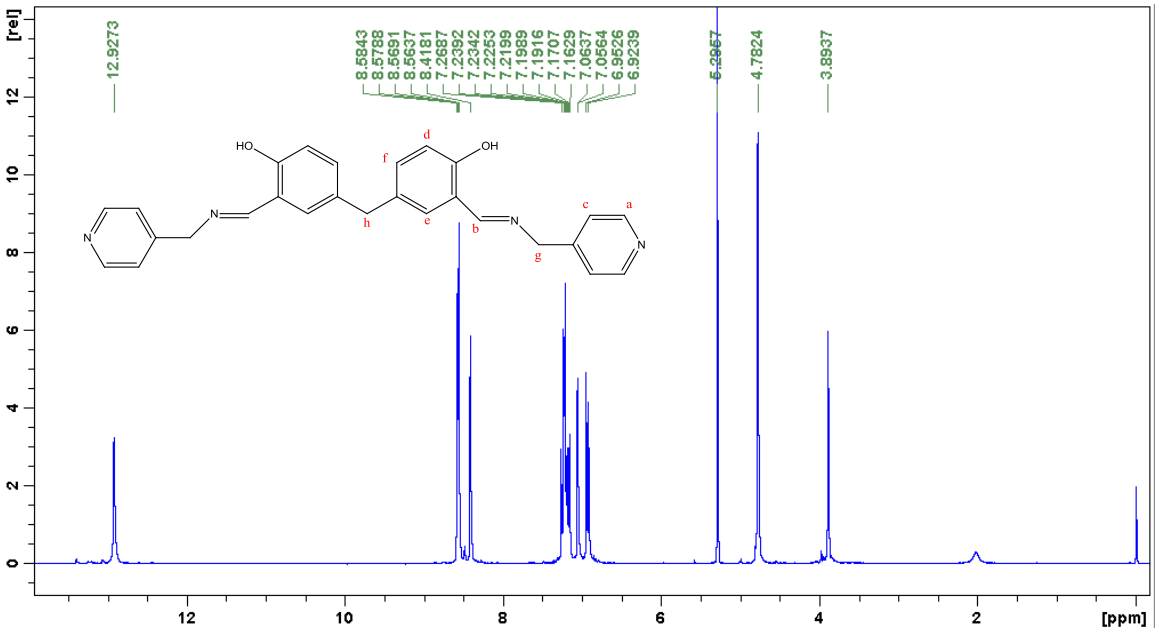

Figure 3.4.36: The ^{1}H NMR spectrum of ligand **10** in $CDCl_3$.

The ligand **10** is formed as a yellow oil. The ^{1}H NMR spectrum of ligand **10** is shown in Figure 3.4.36. The signal of the phenol proton is occurring at 12.92 ppm in comparison to the aldehyde proton at 10.92 ppm in di-carbonyl compound **7** suggesting that a stronger hydrogen bond is formed between the imine and the phenol than that formed between the aldehyde and the phenol. The appearance of the signal of the imine proton Hb at 8.42 ppm and the disappearance of the aldehyde proton signal at around 10 ppm in compound **7** have suggested that imine formation had occurred. Aromatic protons Hd, He and Hf appear at 7.18, 7.06 and 6.94 ppm in ligand **10** comparing the original three peaks for their protons in free ligand at 7.37, 7.33 and 6.95 ppm, respectively. The peak for the aromatic methylene protons Hh are seen at 3.96 ppm in compound **7** which has

shifted to 3.89 ppm in ligand **10**. While the signals of the pyridine rings protons, Ha and Hc, are present at 8.75 and 7.23 ppm, respectively, in ligand **10**. In the ^{13}C NMR spectrum, the imine carbon appears at 167.0 ppm which confirms that imine formation had occurred. The spectrum for the ligand **10** contains twelve carbon signals which matches with ligand **10**.

The IR spectrum of ligand **10** contains a band ν_{OH} at 3474 cm^{-1} for the phenol OH stretch. The C=N stretch for the imine group appears at 1636 cm^{-1} in comparison to the aldehyde stretch at 1656 cm^{-1} indicating that the imine formation had occurred. The presence of a medium band at 1605 cm^{-1} is due to the C=N stretch of the pyridine rings. The absorption of aromatic stretch is present at 1492 cm^{-1} which was seen at 1493 cm^{-1} in compound **7** with no significant change. And the signal of C-O stretch is occurring at 1281 cm^{-1} which has moved from 1272 cm^{-1} in compound **7**. It was difficult to assign other peaks from pyridine rings. The mass spectrum indicates that ligand **10** is pure.

3.4.7 Metal complexes of 10

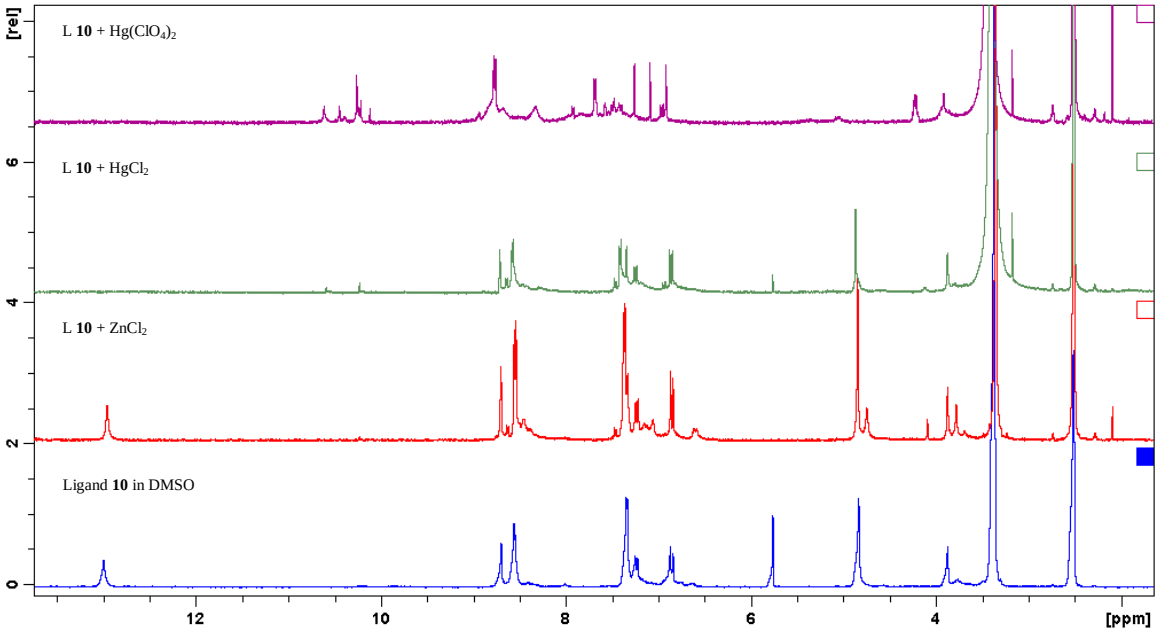

Figure 3.4.37: A comparison of ^{1}H NMR spectra of ligand **10** and its corresponding Zn(II) chloride complex and Hg(II) chloride and perchlorate complexes in DMSO-d_6.

Metal complexes reactions of ligand **10** with various metal(II) salts were carried out by stirring at room temperature for 2 hours in MeOH. The resulting coloured solids were collected by filtration.

As is shown in Figure 3.4.37, the blue spectrum is ligand **10** in DMSO-d_6. The Zn(II) and Hg(II) chloride complexes are shown as red and green spectra, respectively, which are quite similar to that of ligand **10**. But the phenol protons were deprotonated in Hg(II) complex. The Zn(II) acetate and perchlorate complexes cannot dissolve in any solvent even in hot DMSO-d_6 suggesting that polymeric materials are formed in these two complexes. The Hg(II) perchlorate complex, shown as a purple spectrum, indicates that the imine group might be hydrolysed which is due to a couple of peaks around 10.3 ppm. So, no further discussion of Hg(II) perchlorate complex in this chapter.

Table 3.4.1: A comparison of the analytical data of the IR spectra between the ligand **10** and its corresponding metal complexes.

	OH	Imine C=N	Pyridine C=N	Aromatic	C-O stretch
ligand **10**	3474	1636	1605	1492	1281
$ZnCl_2$	3425	1621	1536	1473	1277
$Zn(OAc)_2$	3425	1621	1537	1475	1316
$Zn(ClO4)_2$	3445	1621	1537	1473	1313, 1277
$HgCl_2$	3473	1632	1607	1492	1273
$NiCl_2$	3453	1622	1536	1474	1276
$Ni(OAc)_2$	3436	1622	1540	1475	1323
$Ni(ClO_4)_2$	3453	1622	1536	1474	1322, 1276
$Ni(NO_3)_2$	3416	1622	1535	1475	1323, 1277
$CuCl_2$	3436	1619	1535	1470	1321
$Cu(OAc)_2$	3430	1621	1536	1471	1325
$Cu(ClO_4)_2$	3473	1622	1536	1472	1323
$CoCl_2$	3401	1616	1537	1471	1276
$Co(ClO_4)_2$	3473	1622	1536	1472	1315, 1277
$Co(SCN)_2$	3432	1633	1608	1491	1314

The comparison of the IR spectra between the ligand **10** and its corresponding metal complexes is shown in Table 3.4.1. The OH stretch is obtained at around 3450 cm^{-1} as a broad band in all complexes which imply coordinated solvent (such as water or methanol molecules) could be in metal complexes; The imine stretches are normally occurring at 1620 to 1625 cm^{-1} which have not changed significantly in comparison to

the original stretches of the ligand. So, it is difficult to distinguish whether the imine nitrogen atoms are binding to the metal ion centre or not. However, in the case of complexes which are in the presence of $HgCl_2$ and $Co(SCN)_2$, the signals of imine groups are almost the same as that of the ligand. Moreover, the observed signals of the pyridine rings of these two complexes are similar to that of ligand as well. Only one change is occurring at the C-O group. This would imply that the bonding of these two complexes are only through the oxygen atom from the phenol group. With the other metal complexes, all the bands of the pyridine rings have a large change between the ligand and the complexes implying that bonding of these complexes are *via* the two nitrogen atoms from the pyridine rings; The relationship of the aromatic stretch and the C-O stretch can be described as if the bonding of the complexes is occurring through the oxygen atoms from the phenol group (no matter it is deprotonated or not), it will result the signal of the aromatic stretch changed from 1492 cm^{-1} in the free ligand to about 1470 cm^{-1}.

3.4.7.1 [Zn(**10**)Cl_2·$2H_2O$]

The complex of [Zn(**10**)Cl_2·$2H_2O$] is formed as a yellow solid. The ^1H NMR spectrum of compound [Zn(**10**)Cl_2·$2H_2O$] is shown in Figure 3.4.37 (in red). The observed spectrum of the Zn(II) complex is quite similar to that of the ligand indicating a weak bonding could have occurred between the Zn(II) ion and the ligand. The shift of the imine proton Hb is very small between the complex and the ligand indicating that the imine nitrogen atoms are not coordinated to the Zn(II) ion centre.

The IR spectrum of compound [Zn(**10**)Cl_2·$2H_2O$] contains a band ν_{OH} at 3425 cm^{-1} which suggests that phenol OH stretch and coordinated waters could be in Zn(II) complex. The imine C=N stretch is occurring at 1621 cm^{-1} as a strong peak which has moved from 1636 cm^{-1} in ligand **10**. This indicates that two imine nitrogens could be coordinated to Zn(II) ion centre. A large shift was found in the band of the pyridine ring C=N stretch, it appears at 1536 cm^{-1} in comparison to the band from the free ligand at 1605 cm^{-1} suggesting that two nitrogen atoms from the pyridine rings are coordinated to the Zn(II) ion centre. In addition, the signal of C-O stretch is present at 1277 cm^{-1} in comparison to the original position at 1281 cm^{-1} without significant change pointing towards that the two oxygen atoms are not coordinated to the Zn(II) ion centre.

Elemental analysis indicated that the complex had the formula [Zn(**10**)Cl_2·$2H_2O$]. This would also imply that one Zn(II) ion was bonded to the ligand and that two chloride

ions were also involved to account for neutral charge. The bonding of the Zn(II) ion is through two nitrogen atoms of the pyridine rings as well as two chloride ions. The geometry of the Zn(II) ion is either four- or six-coordinate (including two water molecules). Hence, the possible structures of one monomer unit of compound [Zn(**10**)Cl_2·$2H_2O$] are depicted in Figure 3.4.38.

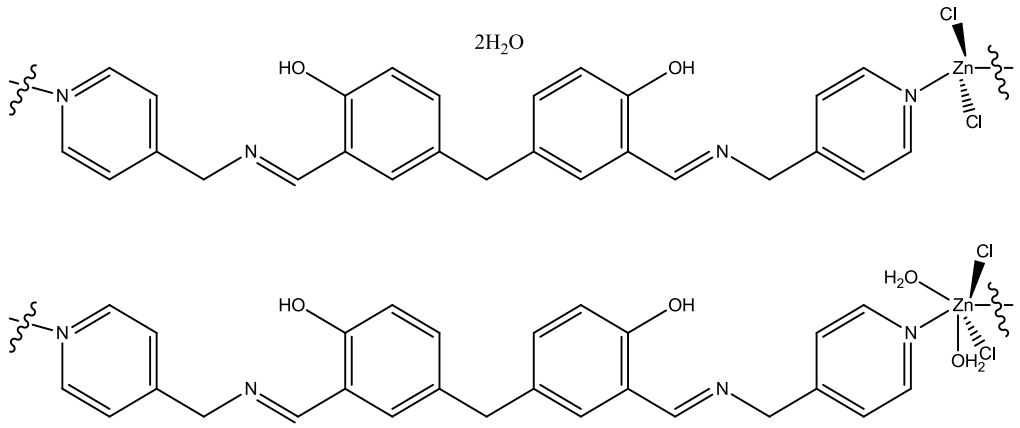

Figure 3.4.38: Possible structures for [Zn(**10**)Cl_2·$2H_2O$].

3.4.7.2 [Zn_2(**10**)$(OAc)_2$·$2H_2O$·2MeOH]

The complex of [Zn_2(**10**)$(OAc)_2$·$2H_2O$·2MeOH] is isolated as a yellow solid. The Zn(II) acetate complex cannot dissolve in any solvent suggesting a polymeric structure had formed between the Zn(II) ion and the ligand.

The IR spectrum of compound [Zn_2(**10**)$(OAc)_2$·$2H_2O$·2MeOH] contains a signal ν_{OH} at 3425 cm^{-1} as a strong broad band which is indicative of some coordinated solvents such as water or methanol molecules are in the complex. The signal of imine C=N stretch is present at 1621 cm^{-1} as a strong broad peak (might be some acetate group involved as well) which is similar to that of Zn(II) chloride complex. A large shift between the complex and the ligand is observed at the C=N stretch of the pyridine rings at 1537 cm^{-1} and 1605 cm^{-1}, respectively, pointing towards that the two nitrogen atoms from the pyridine rings are coordinated to the metal ion centre. The signal of C-O stretch appears at 1316 cm^{-1} in Zn(II) complex which has moved from 1281 cm^{-1} indicating the oxygen atoms from the phenol group are binding to the metal ion centre as well.

Elemental analysis indicated that two Zn(II) ions were bonded to the ligand and that two acetate ions were also involved. The ligand itself is deprotonated to account for the neutral charge. Two water molecules and two methanol molecules could be coordinated to the metal ion. The bonding of each Zn(II) ion is through one oxygen atom from the

deprotonated phenol group, and two nitrogen atoms from pyridine ring and imine group. Hence, the geometry of the Zn(II) ion is either four- or six-coordinate (including one water molecule and one methanol molecule). The possible structures of one monomer unit of compound [Zn_2(**10**)$(OAc)_2 \cdot 2H_2O \cdot 2MeOH$] are depicted in Figure 3.4.39.

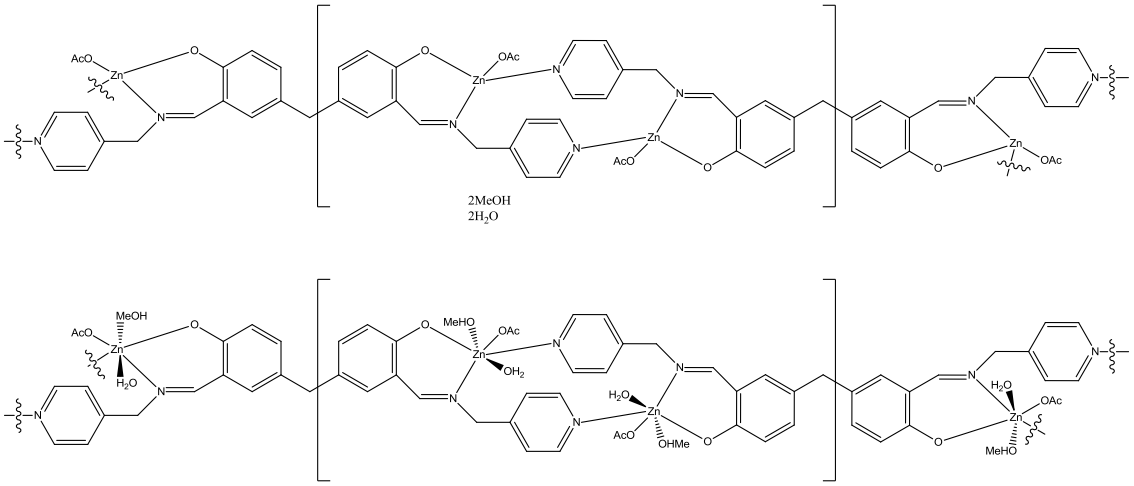

Figure 3.4.39: Possible structures for [Zn(**10**)$(OAc)_2 \cdot 2H_2O \cdot 2MeOH$].

3.4.7.3 [Zn(**10**)$(ClO_4) \cdot 3H_2O$]

The complex [Zn(**10**)$(ClO_4) \cdot 3H_2O$] is formed as a yellow solid. The Zn(II) perchlorate complex from ligand **10** cannot dissolve in any common NMR solvents which suggests a highly polymeric material has been formed.

The IR spectrum of compound [Zn(**10**)$(ClO_4) \cdot 3H_2O$] contains a signal ν_{OH} at 3445 cm^{-1} suggesting coordinated water molecules are in the Zn(II) complex. The imine C=N stretch is present at 1621 cm^{-1} as a strong peak which has moved from 1636 cm^{-1} in ligand **10**. The appearance of the C=N stretch for the pyridine rings at 1537 cm^{-1} compared to the band in free ligand at 1605 cm^{-1} is suggesting that the two nitrogen atoms from the pyridine rings are coordinated to the metal ion centre. In addition, the two signals of the C-O stretch occurring at 1313 and 1277 cm^{-1} which was seen the free ligand at 1281 cm^{-1} implying the two C-O groups in the Zn(II) perchlorate complex are in different environments. The appearance of the perchlorate group at 1109 cm^{-1} as a strong broad signal has pointed out that the Zn(II) perchlorate complexation had occurred.

Elemental analysis indicated that the complex had the formula [Zn(**10**)$(ClO_4) \cdot 3H_2O$]. This would also imply that one Zn(II) ion was bonded to the ligand and that one perchlorate ion was also involved. Only one phenol group of the ligand is deprotonated

to account for neutral charge. The possible structure of one monomer unit of compound [Zn(**10**)(ClO_4)·3H_2O] is depicted in Figure 3.4.40.

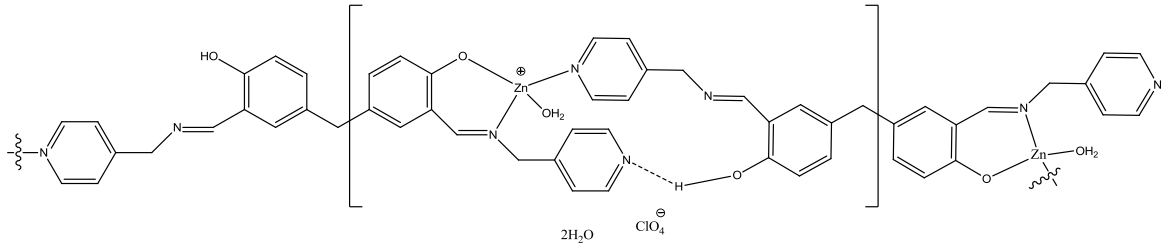

Figure 3.4.40: Possible structure for [Zn(**10**)(ClO_4)·3H_2O].

3.4.7.4 [Hg_2(**10**)Cl_2·2H_2O]

The complex [Hg_2(**10**)Cl_2·2H_2O] is formed as a yellow solid. The ^{1}H NMR spectrum of compound [Hg_2(**10**)Cl_2·2H_2O] is shown in Figure 3.4.37 (in green). The observed spectrum is very similar to that of ligand with the only one exception of the two phenol protons which were not present in the Hg(II) complex. This would imply that the oxygen atoms from the two phenol groups are coordinated.

The IR spectrum of compound [Hg_2(**10**)Cl_2·2H_2O] contains a signal ν_{OH} at 3462 cm^{-1} indicating some coordinated water molecules are in Hg(II) complex. The bands of C=N stretches of the imine group and pyridine rings are obtained at 1632 cm^{-1} and 1607 cm^{-1}, respectively, which are very similar to those of the free ligand pointing that the nitrogen atoms from both the imine group and the pyridine rings are not coordinated to the Hg(II) ion centre. This observation also agrees with the results discussed earlier in the ^{1}H NMR spectrum in Figure 3.4.7. In addition, the signal of the C-O stretch is occurring at 1273 cm^{-1} which has moved from 1281 cm^{-1} in ligand **10**.

Elemental analysis indicated that the complex had the formula [Hg_2(**10**)Cl_2·2H_2O]. This would also imply that two Hg(II) ions were bonded to the ligand and that two chloride ions were also involved. The ligand itself is deprotonated in order to account for the neutral charge. The bonding of each Hg(II) ions is through one oxygen atom from the deprotonated phenol group and one nitrogen atoms of the imine group and as well as one chloride ion. The geometry of each Hg(II) ion is either three- or four-coordinate (including one water molecule). Hence, the proposed structures of the complex [Hg_2(**10**)Cl_2·2H_2O] are depicted in Figure 3.4.41.

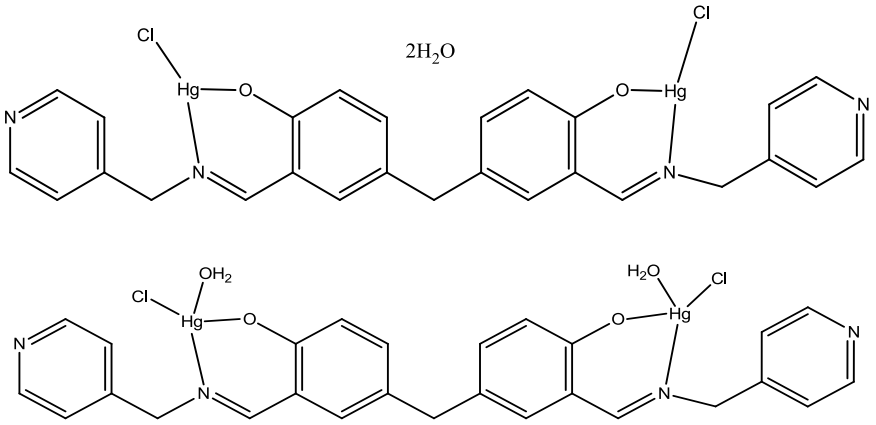

Figure 3.4.41: Possible structures of complex [Hg_2(**10**)Cl_2·$2H_2O$].

3.4.7.5 [Ni(**10**)Cl_2·$2H_2O$]

The complex [Ni(**10**)Cl_2·$2H_2O$] is isolated as a green solid. The observed analytical data of the complex [Ni(**10**)Cl_2·$2H_2O$] in either the IR spectrum or the elemental analysis is very similar to that of Zn(II) chloride complex. This would also imply the bonding the Ni(II) ion should be analogous to that of Zn(II) ion as well. In addition, the magnetic moment of the complex [Ni(**10**)Cl_2·$2H_2O$] is obtained at 3.46 B.M. suggesting that the geometry of the Ni(II) ion could be either tetrahedral or octahedral. Hence, the proposed structures of the complex [Ni(**10**)Cl_2·$2H_2O$] are depicted in Figure 3.4.42.

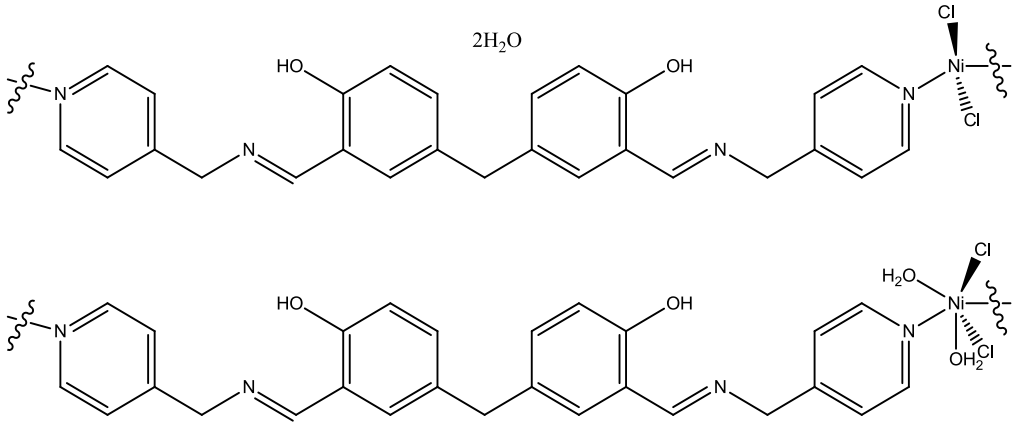

Figure 3.4.42: Possible structure for [Ni(**10**)Cl_2·$2H_2O$].

3.4.7.6 [Ni_2(**10**)$(OAc)_2$·$2H_2O$·2MeOH]

The complex [Ni_2(**10**)$(OAc)_2$·$2H_2O$·2MeOH] is formed as a green solid. It is presumed that the two phenol groups were deprotonated by the Ni(II) ions as the IR spectrum of compound [Ni_2(**10**)$(OAc)_2$·$2H_2O$·2MeOH] is similar to that of the Zn(II) acetate complex. elemental analysis of the Ni(II) acetate complex can also agree with this result. So, the bonding of the Ni(II) ion should be similar to that of Zn(II) ion. In addition, the

magnetic moment of the complex [Ni_2(**10**)$(OAc)_2$·$2H_2O$·2MeOH] is obtained at 4.03 B.M. which is strongly suggesting that the geometry of the each Ni(II) ions carries a tetrahedral geometry. Hence, the proposed structure of the complex [Ni_2(**10**)$(OAc)_2$·$2H_2O$·2MeOH] is depicted in Figure 3.4.33.

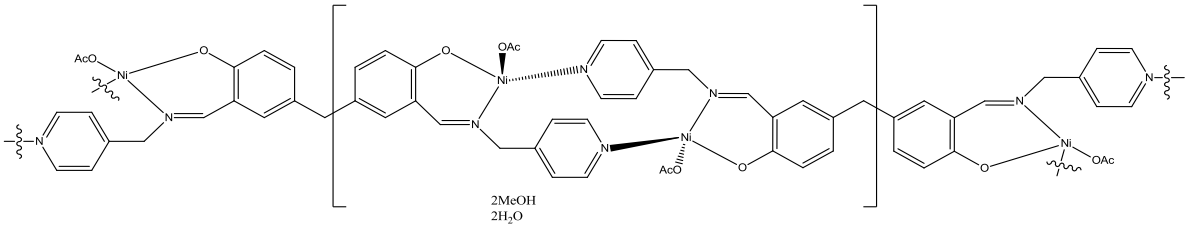

Figure 3.4.43: Possible structure for [Ni(**10**)$(OAc)_2$·$2H_2O$·2MeOH].

3.4.7.7 [Ni(**10**)(ClO_4)·2MeOH]

The complex [Ni(**10**)(ClO_4)·2MeOH] is isolated as a green solid. The bonding of the Ni(II) perchlorate complex is very similar to that of Zn(II) perchlorate complex as that both the IR spectrum and the elemental analysis are similar between the Ni(II) complex and the Zn(II) complex. The one slight difference is the band of the C-O stretch which occurs at 1322 and 1276 cm^{-1} in comparison to that of Zn(II) complex at 1313 and 1277 cm^{-1}, respectively. In addition, the magnetic moment of the complex [Ni(**10**)(ClO_4)·2MeOH] is 2.97 B.M. and suggests that the Ni(II) ion is adopting an octahedral geometry. Hence, the proposed structure of the complex [Ni(**10**)(ClO_4)·2MeOH] is depicted in Figure 3.4.44.

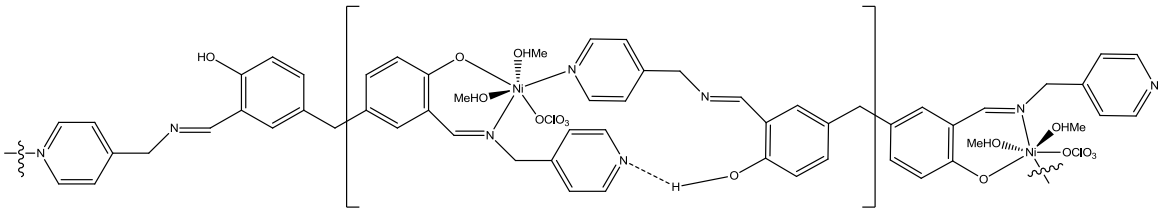

Figure 3.4.44: Possible structure for [Ni(**10**)(ClO_4)·2MeOH].

3.4.7.8 [Ni(**10**)(NO_3)·MeOH·$2H_2O$]

The complex [Ni(**10**)(NO_3)·MeOH·$2H_2O$] is formed as a green solid. The IR spectrum of compound [Ni(**10**)(NO_3)·MeOH·$2H_2O$] is observed to be similar to that of Ni(II) perchlorate complex in the signals of the imine group, pyridine rings, aromatic stretch and C-O stretch which are shown in table 3.4.1. In addition, the appearance of the nitrate group at 1384 cm^{-1} indicates the Ni(II) nitrate complexation had occurred. The

magnetic moment of the complex [Ni(**10**)(NO_3)·MeOH·$2H_2O$] is 3.31 B.M. implying the both tetrahedral geometry and octahedral geometry could be occurring in the Ni(II) complex. According to the observation of the IR spectrum, the bonding of the Ni(II) nitrate complex should be analogous to that of Ni(II) perchlorate complex as well. Hence, the proposed structures of the complex [Ni(**10**)(NO_3)·MeOH·$2H_2O$] are depicted in Figure 3.4.45.

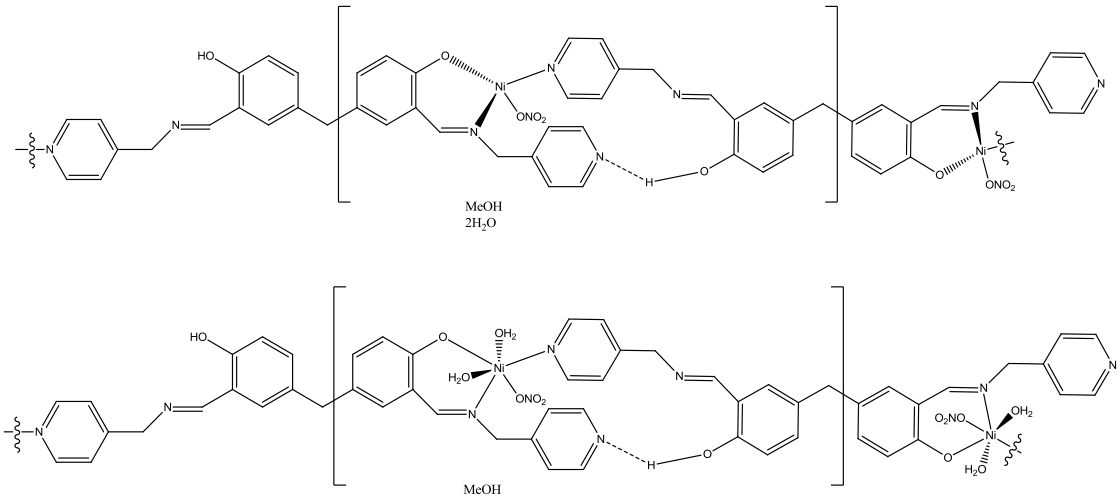

Figure 3.4.45: Possible structures for [Ni(**10**)NO_3·MeOH·$2H_2O$].

3.4.7.9 [Cu_2(**10**)Cl_2·MeOH]

The complex [Cu_2(**10**)Cl_2·MeOH] is formed as a brown green solid. Interestingly, the observed IR spectrum of compound [Cu_2(**10**)Cl_2·MeOH] is similar to that of Zn(II) acetate complex in the signals of the imine group, pyridine rings, and the C-O stretch. The imine C=N stretch at 1619 cm^{-1} in comparison to the original ligand at 1636 cm^{-1} is indicative of the two nitrogen atoms from the imine groups are coordinated to the Cu(II) ion centre. And the signals of the C-O stretch at 1321 cm^{-1} which has moved from 1281 cm^{-1} in ligand **10** is presume the phenol group was deprotonated by the Cu(II) ion.

Elemental analysis indicated that the complex had the formula [Cu_2(**10**)Cl_2·MeOH]. This would also imply that two Cu(II) ions were bonded to ligand and that two chloride ions were also involved. The ligand itself is deprotonated to account for neutral charge. The bonding of each Cu(II) ion is through one oxygen atom from the deprotonated phenol group and two nitrogen atoms from one pyridine ring and one imine group. The magnetic moment of the Cu(II) chloride complex is 2.11 B.M. The geometry of the Cu(II) ion is four-coordinated tetrahedral sphere. Hence, the possible structure of compound [Cu_2(**10**)Cl_2·MeOH] is depicted in Figure 3.4.46.

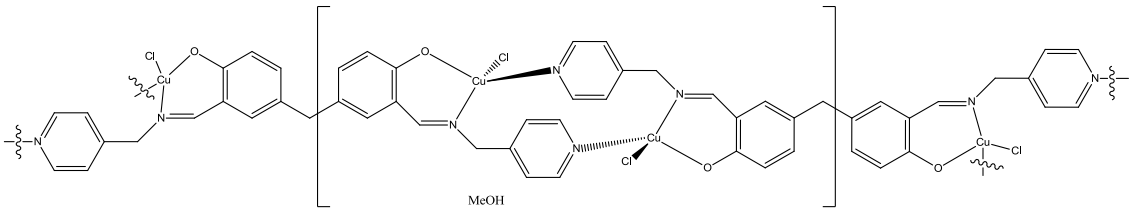

Figure 3.4.46: Possible structure for [Cu_2(**10**)Cl_2·MeOH].

3.4.7.10 [Cu_2(**10**)$(OAc)_2$]

The complex of [Cu_2(**10**)$(OAc)_2$] is obtained as a brown green solid. The signals such as imine group, pyridine rings and C-O stretch of the IR spectrum of compound [Cu_2(**10**)$(OAc)_2$] are occurring similarly to those of Ni(II) acetate complex (shown in Table 3.4.1) implying the bonding of the Cu(II) ion should be similar to that of Ni(II) ion as well. The magnetic moment of the Cu(II) acetate complex is 2.16 B.M. Hence, the proposed structure of the complex [Cu_2(**10**)$(OAc)_2$] is depicted in Figure 3.4.47.

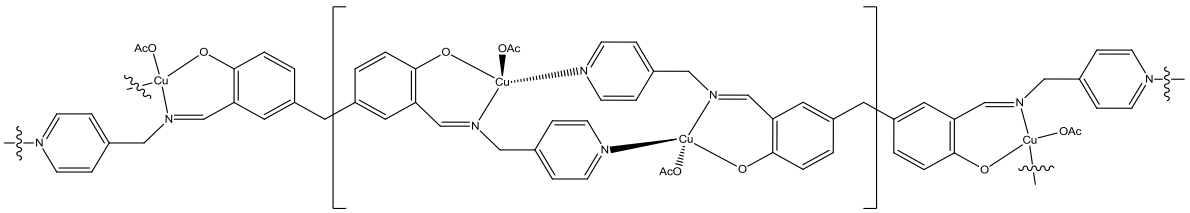

Figure 3.4.47: Possible structure for [Cu(**10**)$(OAc)_2$].

3.4.7.11 [Cu_2(**10**)$(ClO_4)_2$·$2H_2O$]

The complex [Cu_2(**10**)$(ClO_4)_2$·$2H_2O$] is isolated as a green solid. The IR spectrum of the Cu(II) perchlorate complex is similar to that of the Zn(II) acetate complex. However, only one signal of the C-O stretch at 1323 cm^{-1} observed in the Cu(II) perchlorate complex in comparison to the one at 1313 and 1277 cm^{-1} of the Zn(II) perchlorate complex implying the two C-O groups are in the same environment and the two phenol groups are deprotonated.

Elemental analysis indicated that the complex had the formula [Cu_2(**10**)$(ClO_4)_2$·$2H_2O$]. This would also imply that two Cu(II) ions were bonded to the ligand and that two perchlorate ions were also involved. The ligand itself was deprotonated to account for the neutral charge. The bonding of each Cu(II) ions is through one oxygen atom from the deprotonated phenol group and two nitrogen atoms from one imine group and one pyridine ring. The magnetic moment of the Cu(II) perchlorate complex is 2.21 B.M.

The geometry of the Cu(II) ion is four-coordinate tetrahedral. Hence, the proposed structure of the complex $[Cu_2(\mathbf{10})(ClO_4)_2{\cdot}2H_2O]$ is depicted in Figure 3.4.48.

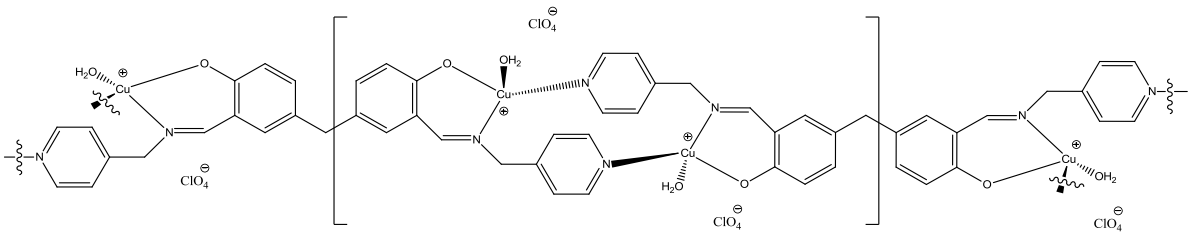

Figure 3.4.48: Possible structure for $[Cu_2(\mathbf{10})(ClO_4)_2{\cdot}2H_2O]$.

3.4.7.12 $[Co(\mathbf{10})Cl_2{\cdot}MeOH{\cdot}H_2O]$

The complex $[Co(\mathbf{10})Cl_2{\cdot}MeOH{\cdot}H_2O]$ is formed as dark brown solid. The obtained analytical data of the complex $[Co(\mathbf{10})Cl_2{\cdot}MeOH{\cdot}H_2O]$ in either the IR spectrum or the elemental analysis is very similar to that of Zn(II) chloride complex which would suggest the bonding of the Co(II) ion should be analogous to that of Zn(II) ion as well. In addition, the magnetic moment of the complex $[Co(\mathbf{10})Cl_2{\cdot}MeOH{\cdot}H_2O]$ is obtained at 5.03 B.M. implying that the Co(II) complex is occupying an octahedral geometry sphere. Hence, the proposed structure of the complex $[Co(\mathbf{10})Cl_2{\cdot}MeOH{\cdot}H_2O]$ is depicted in Figure 3.4.49.

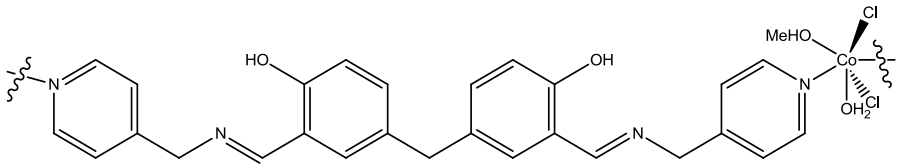

Figure 3.4.49: Possible structure for $[Co(\mathbf{10})Cl_2{\cdot}MeOH{\cdot}H_2O]$.

3.4.7.13 $[Co(\mathbf{10})(ClO_4){\cdot}2H_2O]$

The complex $[Co(\mathbf{10})(ClO_4){\cdot}2H_2O]$ is formed as a green solid. The obtained analytical data of the complex $[Co(\mathbf{10})(ClO_4){\cdot}2H_2O]$ in either the IR spectrum or the elemental analysis is very similar to that of Zn(II) perchlorate complex (shown in Table 3.4.1) which would suggest that the bonding of the Co(II) ion should be analogous to that of the Zn(II) ion as well. In addition, the magnetic moment of the complex $[Co(\mathbf{10})(ClO_4){\cdot}2H_2O]$ is obtained at 3.41 B.M. implying that the Co(II) ion is adopting an tetrahedral geometry sphere. Hence, the proposed structure of the complex $[Co(\mathbf{10})(ClO_4){\cdot}2H_2O]$ is depicted in Figure 3.4.50.

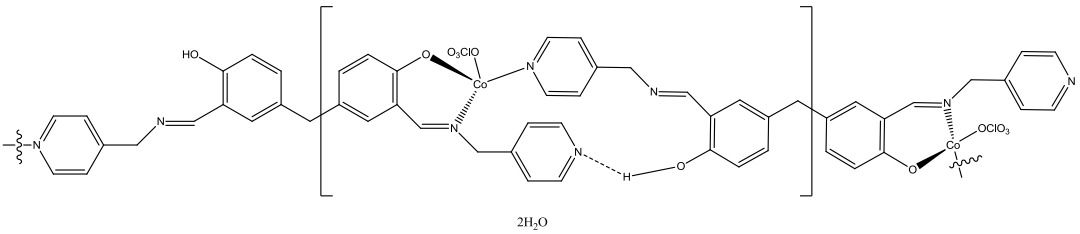

Figure 3.4.50: Possible structure for [Co(**10**)(ClO_4)·$2H_2O$].

3.4.7.14 [Co_2(**10**)$(SCN)_2$·2MeOH·$2H_2O$]

The complex [Co_2(**10**)$(SCN)_2$·2MeOH·$2H_2O$] is formed as a green solid. The IR spectrum of compound [Co_2(**10**)$(SCN)_2$·2MeOH·$2H_2O$] contains a signal ν_{OH} at 3432 cm^{-1} indicating that coordinated methanol molecules or water molecules may be in the Co(II) complex. The appearance of a strong signal at 2070 cm^{-1} is indicative of the Co(II) thiocyanate complexation had occurred. The bands of the C=N stretches of the imine and the pyridine rings occur at 1633 and 1608 cm^{-1} in comparison to those in the free ligand at 1636 and 1605 cm^{-1} without significant change suggesting that the nitrogen atoms from neither the imine group nor the pyridine rings are binding to the Co(II) ion. However, the band of the C-O stretch is present at 1314 cm^{-1} which has moved from 1281 cm^{-1} in ligand **10** presuming that the phenol group was deprotonated. In addition, the analytical data of the Co(II) thiocyanate complex are similar to that of Hg(II) chloride complex which is shown in Table 3.4.1. The magnetic moment of the Co(II) complex is obtained as 4.32 B.M. pointing that a tetrahedral geometry could be present in the Co(II) complex.

Elemental analysis indicated that the complex had the formula [Co_2(**10**)$(SCN)_2$·2MeOH·$2H_2O$]. This would also imply that two Co(II) ions were bonded to the ligand and that two thiocyanate ions were also involved. The ligand itself was deprotonated to account for neutral charge. The bonding of each Co(II) ion is through one oxygen atom from the deprotonated phenol group, and one thiocyanate ion, as well as one water and one methanol molecules. Hence, the possible structure of compound [Co_2(**10**)$(SCN)_2$·2MeOH·$2H_2O$] is depicted in Figure 3.4.51.

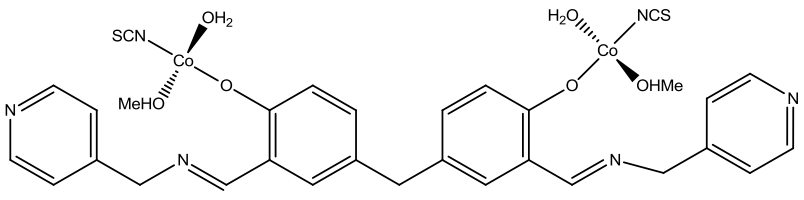

Figure 3.4.51: Possible structure for [Co_2(**10**)$(SCN)_2$·2MeOH·$2H_2O$].

3.4.8 Ligand 11

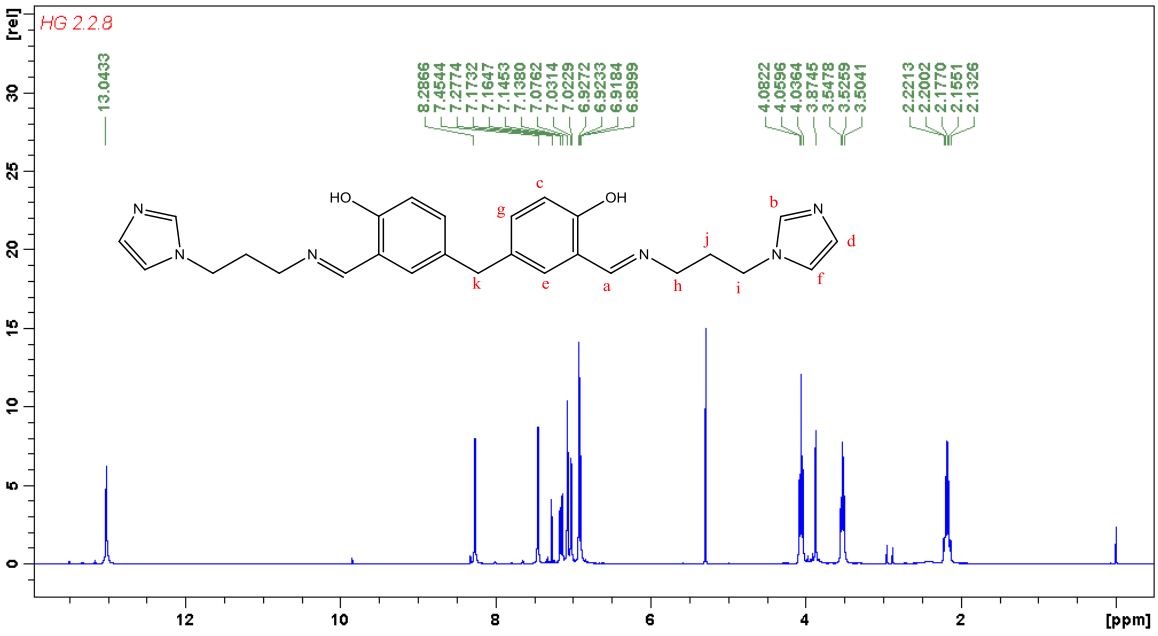

Figure 3.4.52: The ^{1}H NMR spectrum of ligand **11** in $CDCl_3$.

The ligand **11** is formed as a yellow oil. The ^{1}H NMR spectrum of ligand **11** is shown in Figure 3.4.52. The signal of phenol proton resonates at 13.04 ppm in comparison to the aldehyde proton at 10.92 ppm in di-carbonyl compound **7** again indicating that stronger hydrogen bond is formed between the imine and the phenol rather formed between the aldehyde and the phenol. The appearance of the imine proton Ha at 8.28 ppm and the disappearance of the aldehyde proton at around 10 ppm suggests that the imine formation had occurred. Aromatic protons Hc, He and Hg appear at 7.16, 7.02 and 6.91 ppm in ligand **11** which were seen to shift slightly from the original three signals at 7.37, 7.33 and 6.95 ppm, respectively, in di-carbonyl compound **7**. And the aromatic bridging methylene proton Hk which was seen at 3.96 ppm in compound **7** has been shifted to 3.87 ppm in ligand **11**. In addition, the three signals protons of the imidazole rings, protons Hb, Hd and Hf are present at 7.45, 7.07 and 6.92 ppm as three singlets, respectively, in ligand **11**. In the ^{13}C NMR spectrum, the imine carbon appears at 166.2 ppm which is sure that imine formation had occurred. The spectrum of ligand **11** contains fourteen carbons which match with ligand **11**. It is suggested ligand **11** is pure from mass spectrum.

The IR spectrum of ligand **11** is tested under DCM solvent. The imine C=N stretch appears at 1636 cm^{-1} in comparison to the C=O stretch of aldehyde group at 1656 cm^{-1} in compound **7** indicating that the imine formation had occurred. A band C=C stretch at

1590 cm^{-1} is due to the imidazole rings. Aromatic C=C stretch is observed at 1493 cm^{-1} which is similar to a band present in the IR spectrum compound **7** with. In addition, the C-O stretch absorption is occurring at 1283 cm^{-1} which has moved from 1272 cm^{-1} in compound **7**. It was difficult to assign other peaks from pyridine rings.

3.4.9 Metal complexes of 11

Metal complexes reactions of ligand **11** with various metal(II) salts were carried out in MeOH. The reactions were carried out by stirring the ligand and the appropriate metal salts at room temperature for 2 hours in MeOH. The resulting coloured solids were collected by filtration.

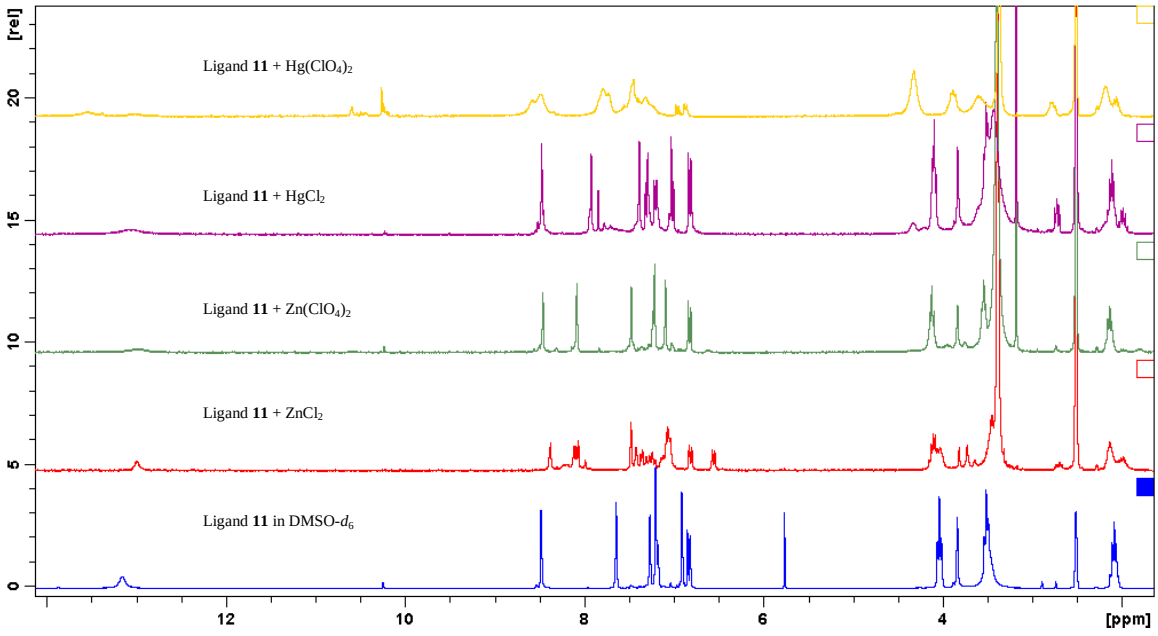

Figure 3.4.53: A comparison of ^{1}H NMR spectra of ligand **11** and its corresponding ZnX_2 and HgX_2 (X = chloride or perchlorate) complexes in DMSO-d_6.

As shown in Figure 3.4.53, the blue spectrum is the ligand **11** in DMSO-d_6. The Zn(II) chloride and perchlorate complexes are shown as red and green spectra, respectively. Zn(II) acetate couldn't dissolve in any solvent even in hot DMSO suggesting a highly polymeric material or stronger bonding between the Zn(II) ion and the ligand could be occurred in the Zn(II) acetate complex. Hg(II) chloride complex, is shown as a purple spectrum. The imine group could be hydrolysed in the Hg(II) perchlorate complex which is due to a couple of peaks around 10.3 ppm. No further discussion of the Hg(II) complex is this chapter.

Table 3.4.2: A comparison of the analytical data of the IR spectra between the ligand **11** and its corresponding complexes (cm^{-1}).

	OH	Imine C=N	Imidazole C=N	Aromatic C=C	C-O
ligand **11**	3054	1636	1590	1493	1283
$ZnCl_2$	3484	1626	1534	1473	1315, 1276
$Zn(ClO_4)_2$	3484	1630	1537	1493	1276
$Zn(OAc)_2$	3417	1625	1533	1475	1320
$HgCl_2$	3452	1633	1518	1492	1274
$Ni(OAc)_2$	3415	1636	1547	1479	1312
$Ni(ClO4)_2$	3424	1628	1527	1492	1279
$CuCl_2$	3441	1623	1535	1474	1322, 1292
$Cu(ClO4)_2$	3425	1623	1536	1475	1319
$CoCl_2$	3435	1619	1533	1470	1314, 1278
$Co(SCN)_2$	3428	1633	1522	1491	1274
$Co(ClO4)_2$	3424	1620	1534	1472	1278

A comparison of the IR spectra of the ligand **11** and its corresponding metal complexes is shown in Table 3.4.2. The nitrogen atoms of the pyridine rings are coordinated to the metal ion centre in these all complexes due to the large difference between the ligand and the complexes in the signal of the imidazole rings. If the band of the aromatic stretch has altered about 20 cm^{-1} between the ligand and the metal complexes, one or two phenol groups would be deprotonated due to the number of the C-O signals. If the band of the aromatic stretch did not change which normally results the signal of C-O stretch did not change, neither, such as in the case of the Zn(II) perchlorate, Hg(II) chloride, Ni(II) perchlorate and Co(II) thiocyanate complexes. This resulted in bonding of these complexes is only through the nitrogen atom of the imidazole rings.

3.4.9.1 $[Zn_3(\mathbf{11})_2Cl_4{\cdot}4H_2O]$

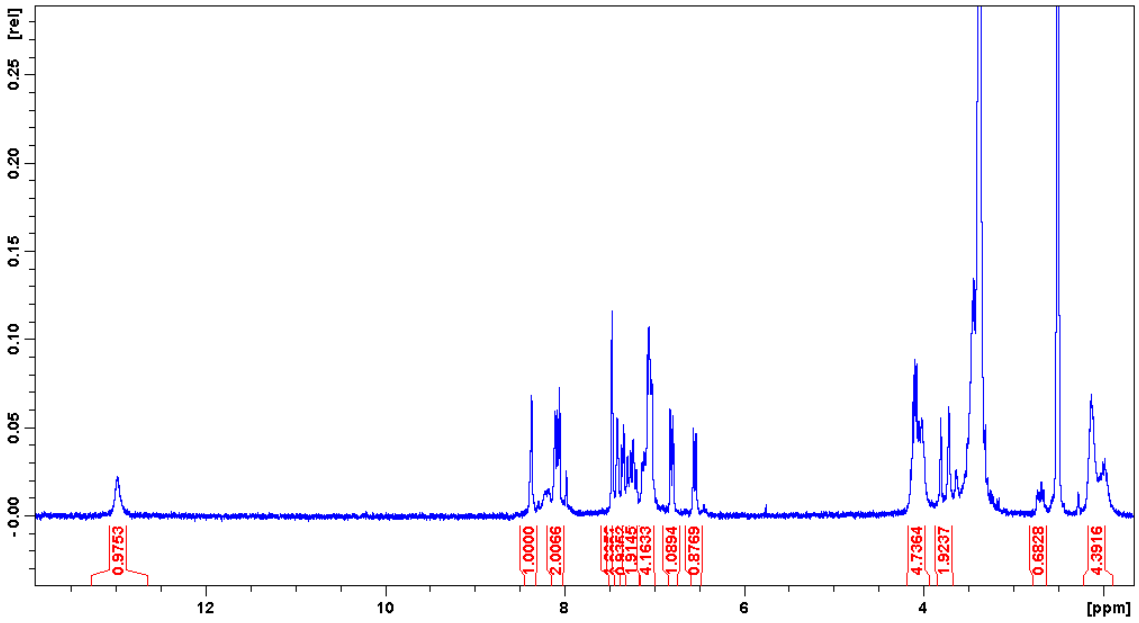

Figure 3.4.54: The ^{1}H NMR spectrum of $[Zn_3(\mathbf{11})_2Cl_4{\cdot}4H_2O]$ in DMSO-d_6.

The complex $[Zn_3(\mathbf{11})_2Cl_4{\cdot}4H_2O]$ is formed as a yellow solid. The ^{1}H NMR spectrum of compound $[Zn_3(\mathbf{11})_2Cl_4{\cdot}4H_2O]$ is shown in Figure 3.4.54. Due to the ratio of the integrals in Figure 3.4.54, only one phenol proton was deprotonated by Zn(II) ion and the other one stays at 12.99 ppm in comparison to the previous ligand at 13.15 ppm. This implies that one of the two phenol groups is deprotonated to form a bond between the oxygen atom and the Zn(II) ion, while the other phenol group could be coordinated to the Zn(II) ion centre as well, but not deprotonated. In addition, so many peaks occurring from 6 to 8 ppm indicates that the two side chains are in different environments. And the chemical shifts of the two signals of the imine proton Ha at 8.37 and 8.06 ppm in comparison to the original ligand at 8.47 ppm and two peaks of the aromatic bridging methylene proton Hk at 3.81 and 3.72 ppm, respectively, also agree with this result. However, it would be difficult to distinguish the specific signals of the aromatic protons and the imidazole protons in Figure 3.4.54.

The IR spectrum of compound $[Zn_3(\mathbf{11})_2Cl_4{\cdot}4H_2O]$ contains a band ν_{OH} at 3484 cm^{-1} as a broad signal suggesting coordinated water molecules are in the Zn(II) complex. The imine C=N stretch is present at 1626 cm^{-1} as a strong peak which has moved from 1636 cm^{-1} in ligand **11**. The appearance of the C=N stretch for the imidazole rings at 1534 cm^{-1} which was seen to have a large shift from the position at 1590 cm^{-1} in ligand **11** suggests that the two nitrogen atoms from the imidazole rings are coordinated to the metal ion centre. The aromatic C=C stretch is observed at 1473 cm^{-1} in the Zn(II)

complex where it was present at 1493 cm^{-1} in ligand **11**. The band of C-O stretch is occurring at 1315 and 1276 cm^{-1} and has moved from 1283 cm^{-1} in ligand **11**. This would also imply that the two C-O groups are in different environments in Zn(II) complex and agree with the results discussed earlier in the ^{1}H NMR spectrum of the Zn(II) chloride complex.

Elemental analysis indicated that the complex had the formula $[Zn_3(\mathbf{11})_2Cl_4{\cdot}4H_2O]$. This also suggested that three Zn(II) ions were bonded to two ligands and that four chloride ions were also involved. Only one phenol group was deprotonated in each ligand to account for neutral charge. The bonding of Zn(II) ions is through the oxygen atoms from the phenol groups and nitrogen atoms from the imidazole rings. The possible structure of compound $[Zn_3(\mathbf{11})_2Cl_4{\cdot}4H_2O]$ is depicted in Figure 3.4.55.

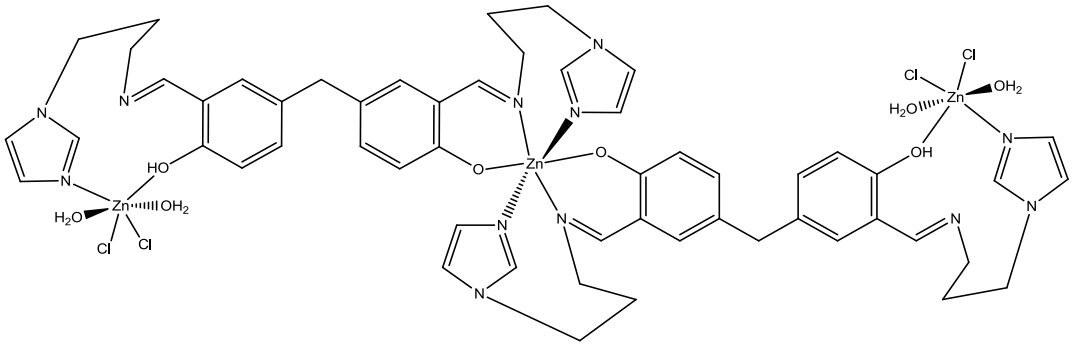

Figure 3.4.55: Possible structure for $[Zn_3(\mathbf{11})_2Cl_4{\cdot}4H_2O]$.

3.4.9.2 $[Zn(\mathbf{11})(ClO_4)_2]$

The complex of $[Zn(\mathbf{11})(ClO_4)_2]$ is formed as a yellow solid. In the ^{1}H NMR spectrum of compound $[Zn(\mathbf{11})(ClO_4)_2]$ in Figure 3.4.53, the signals of phenol proton and the imine proton Ha are occurring at 13.01 and 8.46 ppm which were similar to the free ligand **11** at 13.15 and 8.47 ppm, respectively. This suggests that neither the oxygen atoms from the phenol group nor the nitrogen atoms from the imine group are binding to the metal ion centre. While the signals of aromatic rings protons, Hc, He and Hg, are observed at 7.23, 7.21 and 6.82 ppm in Zn(II) complex which were seen to shift slightly from the original three signals at 7.26, 7.18 and 6.83 ppm in ligand **11**. In addition, a large chemical shift is found in the signals for the protons of the imidazole rings. Protons Hb, Hd and Hf appear at 8.08, 7.47 and 7.09 ppm as three singlets in Zn(II) complex in comparison to those at 7.64, 7.20 and 6.90 ppm from ligand **11** implying that two nitrogen atoms from imidazole rings are coordinated to the Zn(II) ion centre. The aromatic bridging methylene proton Hk at 3.83 ppm in Zn(II) complex is very

similar to that of ligand **11**. For the other bridging methylene protons Hh, Hi and Hj have a slight change from 4.03, 3.51 and 2.08 ppm in ligand **11** to 4.11, 3.4 and 2.13 ppm in Zn(II) complex, respectively.

The IR spectrum of compound [Zn(**11**)$(ClO_4)_2$] contains imine C=N stretch at 1630 cm^{-1} as a strong peak in comparison to the band at 1636 cm^{-1} in ligand **11** without significant change. However, the band of the C=N stretch of the imidazole rings which is present at 1537 cm^{-1} has moved from 1590 cm^{-1} implying that the imidazole nitrogen atoms are binding to the Zn(II) ion. The C=C aromatic stretch and the C-O stretch are very similar to those in free ligand (shown in Table 3.4.2). This would also suggest that the bonding of Zn(II) ion is only occurring at the two nitrogen atoms of the imidazole rings which agree with the results discussed earlier in the ^1H NMR spectrum. The appearance of the perchlorate group at 1108 cm^{-1} as a strong broad signal has suggested the Zn(II) perchlorate complexation had occurred.

Elemental analysis indicated that the complex had the formula [Zn(**11**)$(ClO_4)_2$]. This also suggested that one Zn(II) ion was bonded to the ligand and that two perchlorate ions were also involved to account for the neutral charge. The bonding of the Zn(II) ion is only through two nitrogen atoms of the imidazole rings. The geometry of the Zn(II) ion is four-coordinate tetrahedral. The possible structure of compound [Zn(**11**)$(ClO_4)_2$] is depicted in Figure 3.4.56.

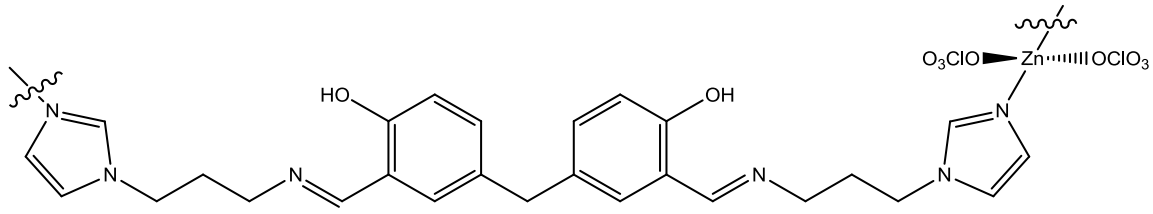

Figure 3.4.56: Possible structure for [Zn(**11**)$(ClO_4)_2$].

3.4.9.3 [Zn_2(**11**)$(OAc)_2 \cdot 3H_2O$]

The complex [Zn_2(**11**)$(OAc)_2 \cdot 3H_2O$] is formed as a yellow solid. The formed Zn(II) acetate complex cannot dissolve in any common NMR solvents, even in hot DMSO-d_6. This implies a polymeric complex could have occurred in the Zn(II) acetate complex.

The IR spectrum of compound [Zn_2(**11**)$(OAc)_2 \cdot 3H_2O$] contains a stretch ν_{OH} at 3417 cm^{-1} indicating some coordinated water molecules are in Zn(II) complex. The Imine stretch is at 1625 cm^{-1} as a strong peak comparing the band at 1636 cm^{-1} in ligand **11**

indicates that two imine nitrogens could be coordinated to the Zn(II) ion centre. The appearance of the C=O stretch from the acetate group at 1588 cm^{-1} is suggesting the Zn(II) acetate complexation had occurred. The band of the imidazole C=N stretch is obtained at 1533 cm^{-1} and has moved from 1590 cm^{-1} in ligand **11** suggesting that two imidazole nitrogen atoms are binding to Zn(II) ion. In addition, the C-O stretch which was seen at 1283 cm^{-1} in ligand **11** has shifted to 1320 cm^{-1} in the Zn(II) complex is presuming that the phenol group was deprotonated.

Elemental analysis indicated that the complex had the formula $[Zn_2(\mathbf{11})(OAc)_2{\cdot}3H_2O]$. This would also imply that two Zn(II) ions were bonded to the ligand and that two acetate ions were also involved. The ligand itself is deprotonated to account for the neutral charge. The bonding of each Zn(II) ion is through one oxygen atom from the deprotonated phenol group and one nitrogen atom of the imidazole ring as well as one acetate ion and one water molecule. Hence, the possible structure of compound $[Zn_2(\mathbf{11})(OAc)_2{\cdot}3H_2O]$ is depicted in Figure 3.4.57.

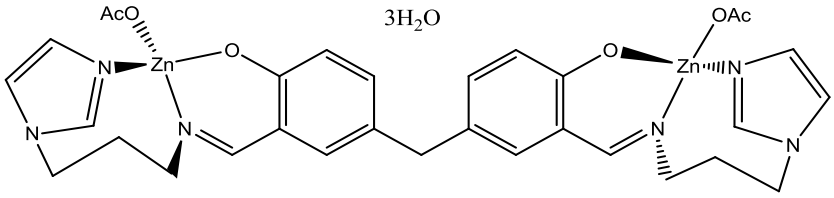

Figure 3.4.57: Possible structure for $[Zn_2(\mathbf{11})(OAc)_2{\cdot}3H_2O]$.

3.4.9.4 $[Hg_2(\mathbf{11})Cl_4]$

The complex $[Hg_2(\mathbf{11})Cl_4]$ is formed as a yellow solid. The ^1H NMR spectrum of compound $[Hg_2(\mathbf{11})Cl_4]$ is shown in Figure 3.4.53 (in purple). The appearance of a signal for the phenol proton at 13.09 which is similar to that obtained in the ^1H NMR spectrum of ligand **11** at 13.15 ppm suggests the oxygen atoms are not binding to the metal ion centre. The small change in chemical shift of imine protons Ha appearing at 8.47 ppm between the Hg(II) chloride complex and the ligand is also implying the two imine nitrogen atoms are not binding to the metal ion centre. The signals protons of aromatic rings, protons Hc, He and Hg resonate at 7.20, 7.38 and 6.82 ppm in Hg(II) complex which were seen to move slightly from 7.26, 7.18 and 6.83 ppm, respectively, in ligand **11**. A large chemical shift is found in the protons of the imidazole rings, Hb, Hd and Hf, appear at 7.90, 7.30 and 7.01 ppm which have moved from 7.64, 7.20 and 6.90 ppm from ligand **11**, indicating that two nitrogen atoms from imidazole rings are

binding to Hg(II) ion centre. The obtained bridging methylene protons Hk, Hh, Hi and Hj are similar to those of Zn(II) perchlorate complex.

The IR spectrum of compound [Hg_2(**11**)Cl_4] contains a imine C=N stretch at 1633 cm^{-1} as a strong peak in comparison to the band at 1636 cm^{-1} in ligand **11** indicating that two imine nitrogen atoms are not coordinated to Hg(II) ion centre. The appearance of the signal of the imidazole C=N stretch at 1518 cm^{-1} which has moved from 1590 cm^{-1} in ligand **11** suggests that the imidazole nitrogen atoms are binding to the Hg(II) ion. The C=C aromatic stretch and C-O stretch appear at 1492 and 1274 cm^{-1}, respectively, which are similar to those two bands of the ligand **11** implying the phenol groups are not deprotonated by the metal ion and not coordinated to the metal ion centre.

Elemental analysis indicated that the complex had the formula [Hg_2(**11**)Cl_4]. This would also imply that two Hg(II) ions were bonded to the ligand and that four chloride ions were also involved to account for the neutral charge. The bonding of each Hg(II) ions is through one nitrogen atom from the imidazole ring and two chloride ions. The coordination geometry of Hg(II) ion is three-coordinate sphere. Hence, the possible structure of compound [Hg_2(**11**)Cl_4] is depicted in Figure 3.4.58.

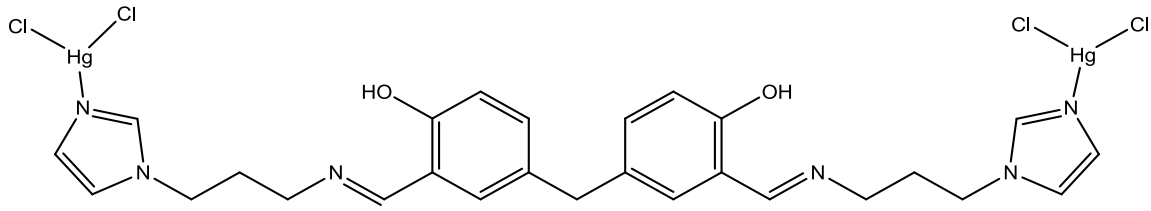

Figure 3.4.58: Possible structure for [Hg_2(**11**)Cl_4].

3.4.9.5 [Ni_2(**11**)$(OAc)_2$·$2H_2O$·2MeOH]

The complex of [Ni_2(**11**)$(OAc)_2$·$2H_2O$·2MeOH] is formed as a green solid. The obtained analytical data of the complex [Ni_2(**11**)$(OAc)_2$·$2H_2O$·2MeOH] in both the IR spectrum and the elemental analysis are very similar to those of Zn(II) acetate complex which imply that the bonding of the Ni(II) ion should be analogous to that of Zn(II) ion. The magnetic moment of the complex is obtained as 4.42 B.M. which indicates the geometry of the Ni(II) ion is a tetrahedral sphere. Hence, the proposed structure of the complex [Ni_2(**11**)$(OAc)_2$·$2H_2O$·2MeOH] is depicted in Figure 3.4.59.

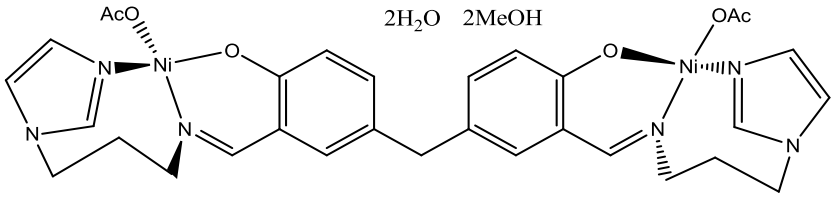

Figure 3.4.59: Possible structure for [Ni_2(**11**)$(OAc)_2$·$2H_2O$·2MeOH].

3.4.9.6 [Ni(**11**)$(ClO_4)_2$·2MeOH]

The complex [Ni(**11**)$(ClO_4)_2$·2MeOH] is obtained as a green solid. The IR spectrum and the elemental analysis of the complex [Ni(**11**)$(ClO_4)_2$·2MeOH] are similar to that of Zn(II) perchlorate complex (shown in Table 3.4.2) which implies that the bonding of the Ni(II) ion should be analogous to that of Zn(II) ion. The magnetic moment of the complex [Ni(**11**)$(ClO_4)_2$·2MeOH] is obtained as 4.23 B.M. indicating that the Ni(II) ion is a tetrahedral geometry sphere. Hence, the proposed structure of the complex [Ni(**11**)$(ClO_4)_2$·2MeOH] is depicted in Figure 3.4.60.

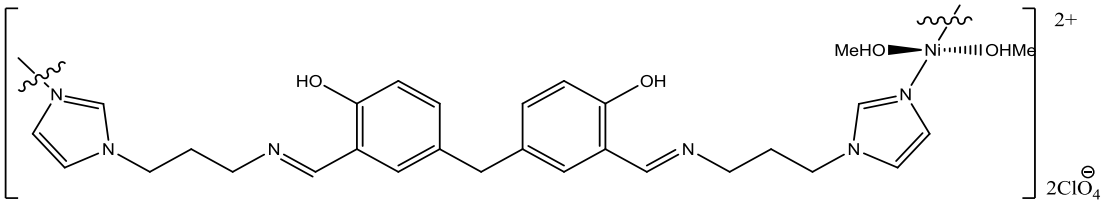

Figure 3.4.60: Possible structure for [Ni(**11**)$(ClO_4)_2$·2MeOH].

3.4.9.7 [Cu_2(**11**)Cl_3·$2H_2O$]

The complex of [Cu_2(**11**)Cl_3·$2H_2O$] is obtained as a grey solid. The observed bands such as the C=N stretches from the imine and the imidazole rings, and the C=C aromatic stretch in the IR spectrum of compound [Cu_2(**11**)Cl_3·$2H_2O$] are very similar to that of Zn(II) chloride complex with one exception of the C-O stretch which presents at 1322 and 1292 cm^{-1} in Cu(II) complex in comparison to the two bands in the Zn(II) chloride complex at 1315 and 1276 cm^{-1}, respectively. This implies the two C-O groups in the Cu(II) complex are in different environments, and one of the phenol groups could be deprotonated by the Cu(II) ion. In addition, the similarity of the signal of imidazole rings is pointing out the two nitrogen atoms from imidazole rings are coordinated to the Cu(II) ion centre.

Elemental analysis indicated that the complex had the formula [Cu_2(**11**)Cl_3·$2H_2O$]. This would also imply that two Cu(II) ions were bonded to ligand and that three chloride ions were also involved. Only one phenol group was deprotonated to account for the neutral

charge. The magnetic moment of the Cu(II) chloride complex is 1.82 B.M. The possible structure of compound [Cu_2(**11**)Cl_3·$2H_2O$] is depicted in Figure 3.4.61.

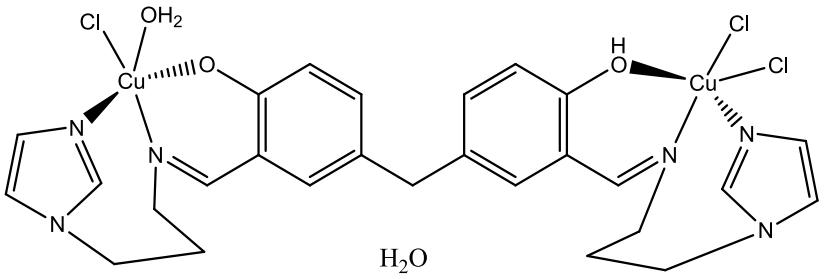

Figure 3.4.61: Possible structure for [Cu_2(**11**)Cl_3·$2H_2O$].

3.4.9.8 [Cu_2(**11**)$(ClO_4)_2$·$3H_2O$]

The complex [Cu_2(**11**)$(ClO_4)_2$·$3H_2O$] is formed as a brown green solid. The IR spectrum of compound [Cu_2(**11**)$(ClO_4)_2$·$3H_2O$] contains a peak ν_{OH} at 3425 cm^{-1} indicating that coordinated water molecules are present in the Cu(II) complex. The imine C=N stretch is present at 1623 cm^{-1} which has moved from 1636 cm^{-1} in ligand **11**. Two nitrogen atoms from imidazole rings are coordinated to the Cu(II) ion centre is due to the large difference of imidazole C=N stretches between the complex (1536 cm^{-1}) and the free ligand (1590 cm^{-1}). The aromatic C=C stretch is present at 1475 cm^{-1} in Cu(II) complex which has moved from 1493 cm^{-1} in ligand **11**. The band of the C-O stretch appears at 1319 cm^{-1} in Cu(II) complex which was seen to have a shift 1283 cm^{-1} in ligand **11** suggesting that oxygen atoms could be coordinated with Cu(II) ion centre. The appearance of the perchlorate group at 1090 cm^{-1} as a strong broad signal has pointed out that the Cu(II) perchlorate complexation had occurred.

Elemental analysis indicated that the complex had the formula [Cu_2(**11**)$(ClO_4)_2$·$3H_2O$]. This would also imply that two Cu(II) ions were bonded to the ligand and that two perchlorate ions were also involved. The ligand itself is deprotonated to account for the neutral charge. The bonding of each Cu(II) ion is through one oxygen atom from the deprotonated phenol group, and one nitrogen atom from imidazole ring as well as one perchlorate ion and one coordinated water molecule. The magnetic moment of the Cu(II) perchlorate complex is 2.14 B.M. The geometry of the Cu(II) ion is four-coordinate tetrahedral sphere. Hence, the possible structure of compound [Cu_2(**11**)$(ClO_4)_2$·$3H_2O$] is depicted in Figure 3.4.62.

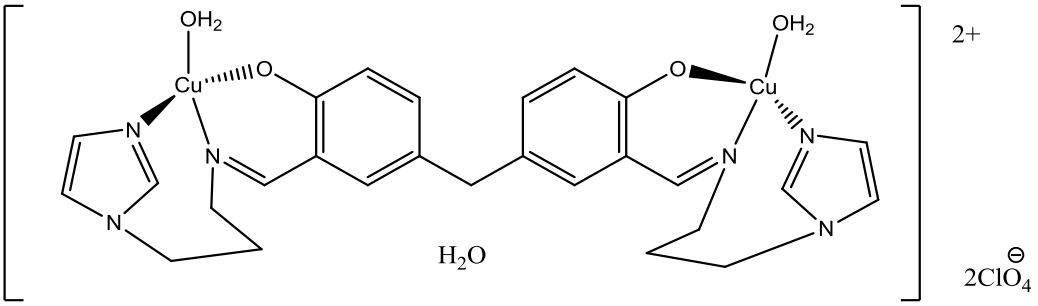

Figure 3.4.62: Possible structure for $[Cu_2(\mathbf{11})(ClO_4)_2{\cdot}3H_2O]$.

3.4.9.9 $[Co_3(\mathbf{11})_2Cl_4{\cdot}4H_2O]$

The complex $[Co_3(\mathbf{11})_2Cl_4{\cdot}4H_2O]$ is obtained as a green solid. The obtained analytical data of the complex $[Co_3(\mathbf{11})_2Cl_4{\cdot}4H_2O]$ in either the IR spectrum or the elemental analysis is very similar to that of Zn(II) chloride complex (shown in Table 3.4.2) which imply that the bonding of the Co(II) ion is analogous to that of Zn(II) ion as well. In addition, the magnetic moment of the complex $[Co_3(\mathbf{11})_2Cl_4{\cdot}4H_2O]$ is obtained at 5.78 B.M. indicating that the geometry of the Co(II) ion is octahedral. Hence, the proposed structure of the complex $[Co_3(\mathbf{11})_2Cl_4{\cdot}4H_2O]$ is depicted in Figure 3.4.63.

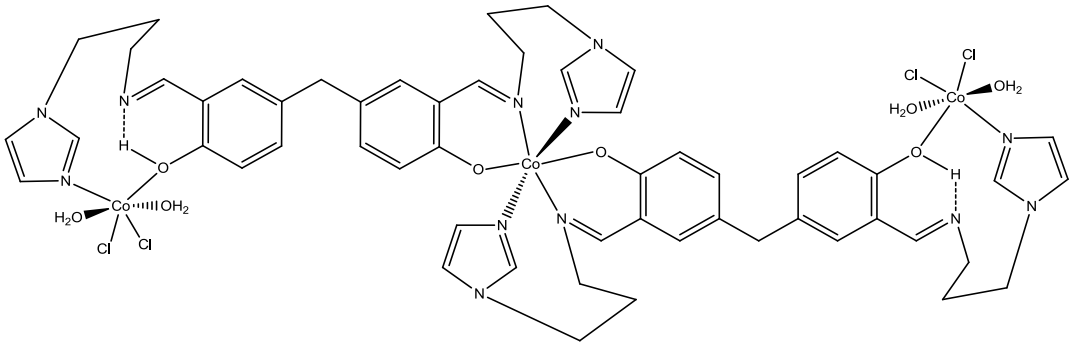

Figure 3.4.63: Possible structure of $[Co_3(\mathbf{11})_2Cl_4{\cdot}4H_2O]$.

3.4.9.10 $[Co(\mathbf{11})(SCN)_2{\cdot}4H_2O]$

The complex $[Co(\mathbf{11})(SCN)_2{\cdot}4H_2O]$ is formed as a dark green solid. The observed bands such as the C=N stretches from the imine and the imidazole rings, and the C=C aromatic stretch in the IR spectrum of the complex $[Co(\mathbf{11})(SCN)_2{\cdot}4H_2O]$ are similar to those of Zn(II) perchlorate complex which suggest that the bonding of the Co(II) ion should be analogous to that of Zn(II) ion. In addition, the magnetic moment of the complex $[Co(\mathbf{11})(SCN)_2{\cdot}4H_2O]$ is 4.63 B.M. This value indicates the Co(II) ion adopts a tetrahedral geometry sphere. Hence, the proposed structure of the complex $[Co(\mathbf{11})(SCN)_2{\cdot}4H_2O]$ is depicted in Figure 3.4.64.

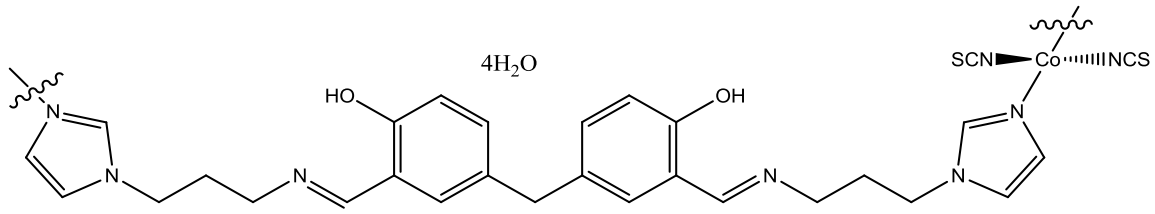

Figure 3.4.64: Possible structure for [Co(**11**)$(SCN)_2 \cdot 4H_2O$].

3.4.9.11 [Co(**11**)$(ClO_4)_2$]

The complex [Co(**11**)$(ClO_4)_2$] is formed as a brown green solid. The obtained analytical data of the complex [Co(**11**)$(ClO_4)_2$] in its IR spectrum and the elemental analysis is very similar to that of Ni(II) perchlorate complex (shown in Table 3.4.2) which imply that the bonding of the Co(II) ion should be analogous to that of Ni(II) ion as well. In addition, the magnetic moment of the complex [Co(**11**)$(ClO_4)_2$] is obtained as 4.62 B.M. This value would suggest that the complex [Co(**11**)$(ClO_4)_2$] adopts a tetrahedral geometry. Hence, the proposed structure of the complex [Co(**11**)$(ClO_4)_2$] is depicted in Figure 3.4.65.

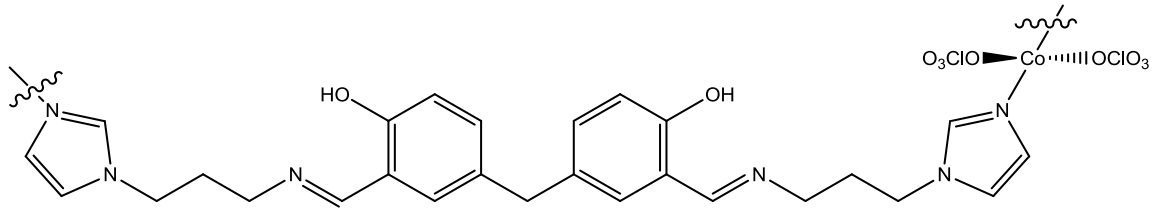

Figure 3.4.65: Possible structure for [Co(**11**)$(ClO_4)_2$].

3.5 Section 3

3.5.1 Preparation of 13

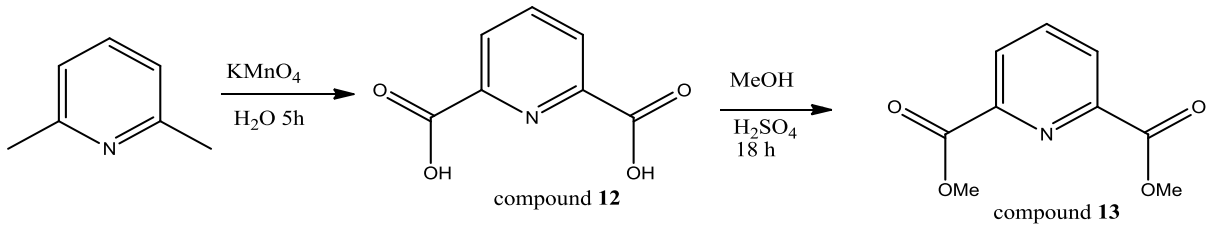

Figure 3.5.1: Synthesis of compound **13**.

The compound 2,6-dilutidine is commercially available. The synthetic route of compound **13** is shown in Figure 3.5.1. The compound pyridine-2,6-dicarboxylic acid (dipicolinic) **12** was synthesized by oxidising 2,6-dilutidine in the presence of potassium permanganate, as has been reported by Dai and co-workers.[145] Dipicolinic **12** is obtained as a white solid which cannot be dissolved in any NMR solvents. However the melting point of dipicolinic **12** was found to be 225-226 ℃ which is similar to the literature value of 226-227 ℃.[145] A white solid of dimethyl dipicolinate (**13**) was formed according to literature.[133]

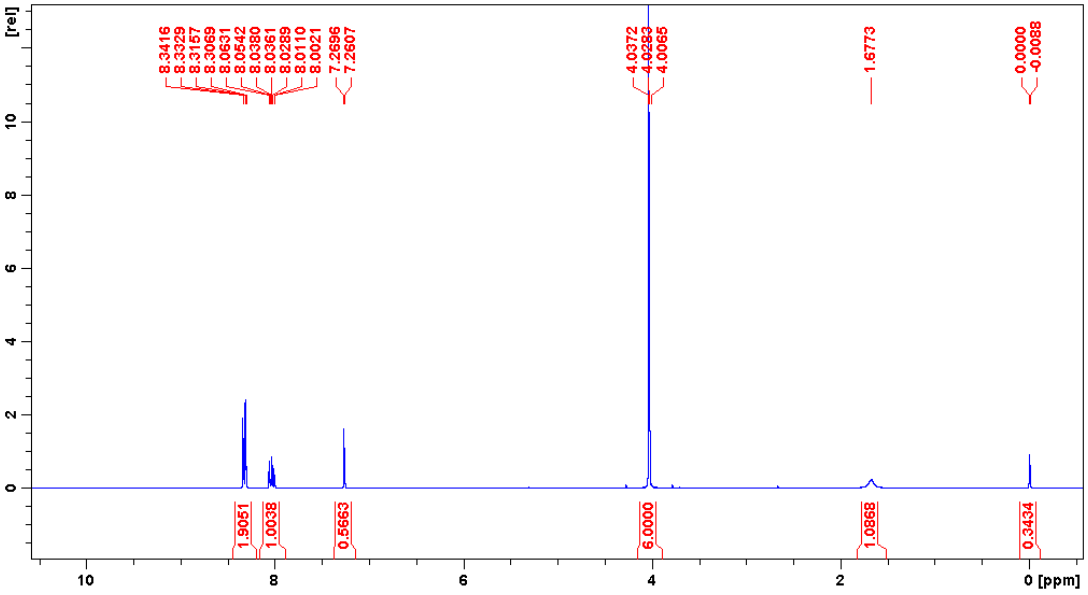

Figure 3.5.2: The ^{1}H NMR spectrum of dipicolinate **13** in $CDCl_3$.

The ^{1}H NMR spectrum of **13** is shown in Figure 3.5.2. The methoxy protons which resonate at 4.03 ppm as a singlet, indicates that the ester formation had occurred. The

two signals of the central pyridine ring were observed at 8.32 ppm and 8.03 ppm as a doublet and a triplet, respectively. These values are quite similar to those previously reported.

3.5.2 Amide ligands synthesis

The conversion of the carboxylic ester into an amide was carried out in a toluene solution and involves the nucleophilic attack by a base (amine) on the electron-deficient carbon of the carbonyl group. This results in the displacement of the alkoxy group (OR) with a NHR group.

The three new di-amide ligands (**14** – **16**) can be synthesized by using dimethyl dipicolinate **13** as shown in Figure 3.5.3. All the ligands were synthesized in the same reaction strategy, with one equivalent of **13** and four equivalents of appropriate amine precursors being heated to reflux for 24-48 hours. The solvent from the resulting solution was removed under reduced pressure to yield the crude di-amide ligands. These ligands were dissolved in DCM (50 mL), washed with water (3×40 mL), dried over anhydrous $MgSO_4$, and the solvent was removed under reduced pressure to generate the purified ligands **14** – **16**. In addition, the ligand **14** was recrystallized from benzene to generate white crystals.

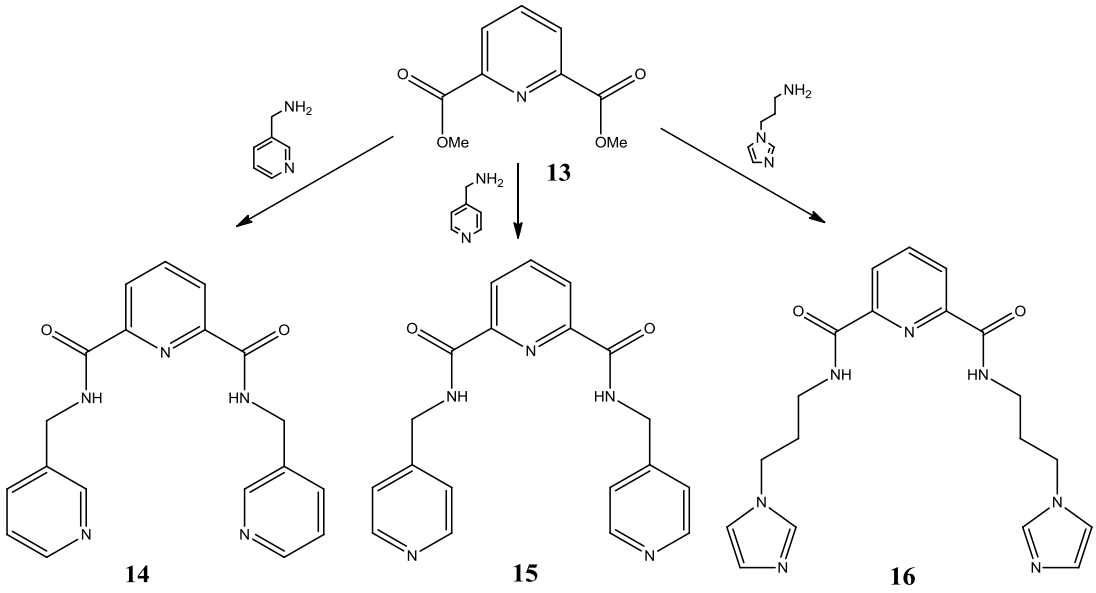

Figure 3.5.3: Synthesis of ligands **14** – **16**.

3.5.3 Ligand 14

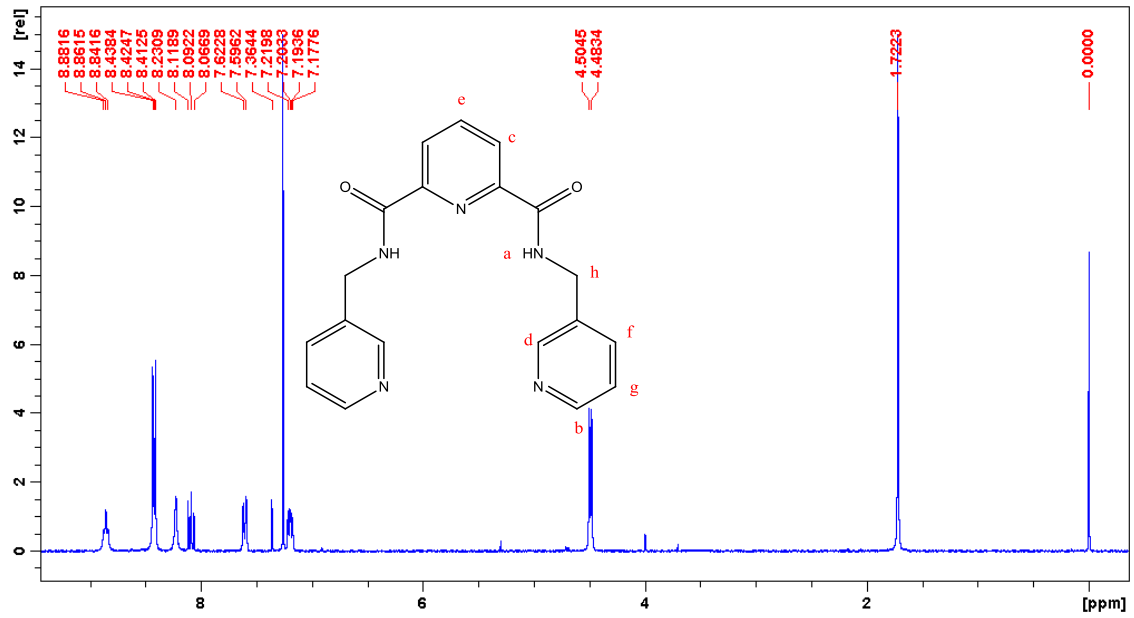

Figure 3.5.4: ^{1}H NMR spectrum of ligand **14** in $CDCl_3$.

Ligand **14** was formed as a white crystalline solid after recrystallized from benzene. The ^{1}H NMR spectrum of ligand **14** is shown in Figure 3.5.4. The signal appearing at 8.86 ppm as a triplet represents the amide proton Ha, implying that amide formation had occurred. The two signals of the central pyridine ring, protons Hc and He, are observed at 8.42 ppm as a doublet and at 8.09 ppm as a triplet, respectively, which have shifted from 8.32 ppm and 8.03 ppm in the previous spectrum of dimethyl dipicolinate **13** (Figure 3.5.2). The signal protons of the lower pyridine rings in ligand **14**, proton Hb appears as a doublet which resonates at the similar ppm with proton Hc at 8.42 ppm; and proton Hd is observed as a singlet at 8.23 ppm in ligand **14**. Protons Hf and Hg are observed at 7.61 ppm as a doublet and 7.20 ppm as a doublet of doublets. The disappearance of methoxy protons at about 4 ppm in dimethyl dipicolinate **13** and the appearance of bridging methylene protons Hh at 4.49 ppm as a doublet suggested that the amide formation had occurred. The ^{13}C NMR spectrum of ligand **14** contains ten carbon peaks to indicate the ten non-equivalent carbons now present in the ligand **14**.

The IR spectrum of ligand **14** contains two signals $\nu_{N\text{-}H}$ stretch at 3319 and 3262 cm^{-1}, indicating that both N-H stretch could be in different stretch. It could be that one hydrogen atom from amide group is forming a hydrogen bond to the nitrogen atom from the central pyridine ring. It would lead to a small different type of amide group. The carbonyl signal occurs at 1674 and 1660 cm^{-1}, which could prove this theory. Aromatic

stretches are present at 1435 cm^{-1}. It was difficult to assign other specific pyridine bends. The elemental analysis shows the ligand **14** is pure.

3.5.4 Metal complexes of 14

Metal complexation reactions of ligand **14** with various metal(II) salts were carried out in MeOH. The reactions were carried out at room temperature with stirring for 2 hours in MeOH. The resulting coloured solids were collected by filtration. The only exception was the Cu(II) nitrate complex in which the solid was formed with slow evaporation of solvent after a couple of days.

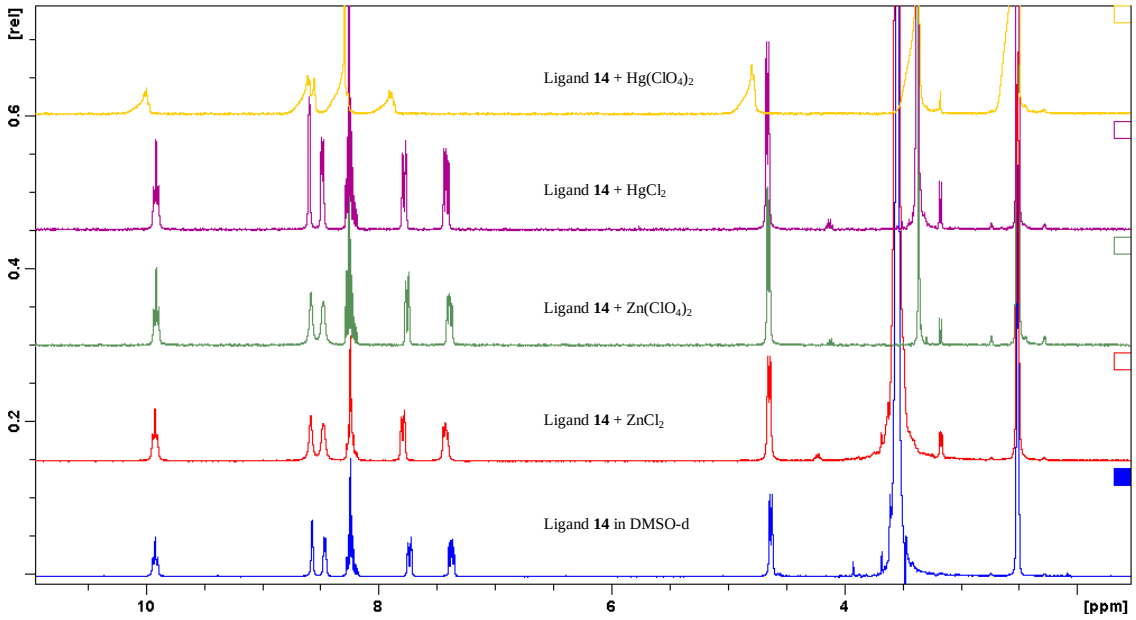

Figure 3.5.5: A comparison of ^{1}H NMR spectra of ligand **14** and its corresponding ZnX_2 and HgX_2 (X= chloride and perchlorate) complexes in DMSO-d_6.

3.5.4.1 [Zn(**14**)Cl_2·2H_2O]

The Zn(II) chloride complex is obtained as a white solid. The ^{1}H NMR spectrum of the complex [Zn(**14**)Cl_2·2H_2O] is shown in Figure 3.5.5 (in red). The amide protons resonate at 9.92 ppm, this does not represents a significant shift in comparison to the previous signal of ligand **14**. The protons Hc and He from the central pyridine rings of in both the ligand and the Zn(II) complex are occurring at 8.19-8.27 ppm as a multiplet. The signals protons of the pyridine rings in the each side chains, protons Hd and Hb are observed at 8.59 ppm and at 8.48 ppm, respectively, which are similar to the previous two signals from ligand **14**. However, a slight change had occurred in the signal position of protons Hf and Hg. Proton Hf is present at 7.79 ppm in Zn(II) complex with a comparison to the previous one at 7.73 ppm in ligand **14**. Proton Hg appears at 7.42

ppm in Zn(II) complex which was seen at 7.36 ppm in ligand **14**. This implies that the pyridine rings for the side chains could be in different environments in Zn(II) complex and the ligand, respectively. The bridging methylene proton Hh is observed at 4.64 ppm in Zn(II) complex which is similar to the one from ligand **14**.

The IR spectrum of complex [Zn(**14**)Cl_2·$2H_2O$], contains a very broad signal at 3351 cm^{-1} which cannot distinguish whether it is the OH stretch or the NH stretch or both. The carbonyl group is present at 1675 cm^{-1} as a broad signal which was seen the previous one at 1674 and 1660 cm^{-1} from ligand **14**. This broad signal suggests that the oxygen atom from amide group is coordinated to the Zn(II) ion centre. In addition, the C=N stretch from the pyridine ring is present at 1610 cm^{-1} compared to the original one at 1577 cm^{-1} in ligand **14**, indicating that the pyridine nitrogen atom of are binding to the Zn(II) ion centre.

Elemental analysis indicated that the complex had the formula [Zn(**14**)Cl_2·$2H_2O$]. This would suggest that one Zn(II) ion was bonded to the ligand and that two chloride ions were also involved to account for neutral charge. The geometries of Zn(II) ion could be octahedral, with two oxygen atoms from the amide group, one nitrogen from the central pyridine ring and two chloride ions, as well as one water molecule. The possible structure of compound [Zn(**14**)Cl_2·$2H_2O$] is depicted in Figure 3.5.6.

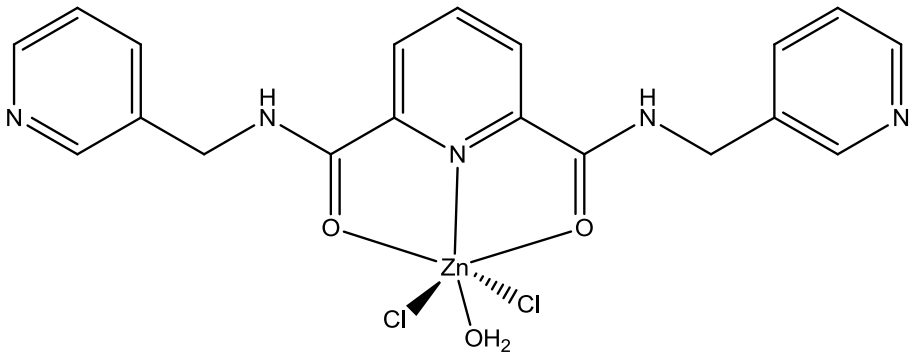

Figure 3.5.6: Possible structure for [Zn(**14**)Cl_2·$2H_2O$].

3.5.4.2 [Zn(**14**)$(ClO_4)_2$]

The complex [Zn(**14**)$(ClO_4)_2$] was obtained as a white solid. The ^{1}H NMR spectrum of compound [Zn(**14**)$(ClO_4)_2$] is shown in Figure 3.5.5 (in green). The spectrum is slight different to the one of Zn(II) chloride complex upon closer inspection, but both of them are very similar. This would indicate that the bonding of the zinc ion is occurring at the

similar positions. As a result, the structure of Zn(II) perchlorate should be similar to that of the Zn(II) chloride complex.

In the IR spectrum of compound [Zn(**14**)$(ClO_4)_2$], the carbonyl group is represented by a band at 1643 cm^{-1} as a broad signal with a comparison to the previous one at 1674 and 1660 cm^{-1} from ligand **14** implying that the amide group (oxygen atom) is coordinated to the metal ion centre. The N-H bend is observed at 1566 cm^{-1} which was seen the free ligand at 1534 cm^{-1}. A signal of the C=N stretch from the pyridine ring is observed at 1615 cm^{-1} which corresponds to the band seen at 1577 cm^{-1} in the spectrum of ligand **14**, indicating that pyridine nitrogen atom is binding to Zn(II) ion centre. The perchlorate group appears a strong broad signal at 1108 cm^{-1} indicative of the Zn(II) complexation had occurred.

Elemental analysis indicated that the complex had the formula [Zn(**14**)$(ClO_4)_2$]. This would suggest that one Zn(II) ion was bonded to the ligand through the two oxygen atoms from the carbonyl group and one nitrogen atom from the central pyridine ring. that two perchlorate ions were also involved to account for neutral charge. One or two perchlorate ions could be also involved. The geometry of Zn(II) ion could be a tetrahedral. The possible structure of compound [Zn(**14**)$(ClO_4)_2$] is depicted in Figure 3.5.7.

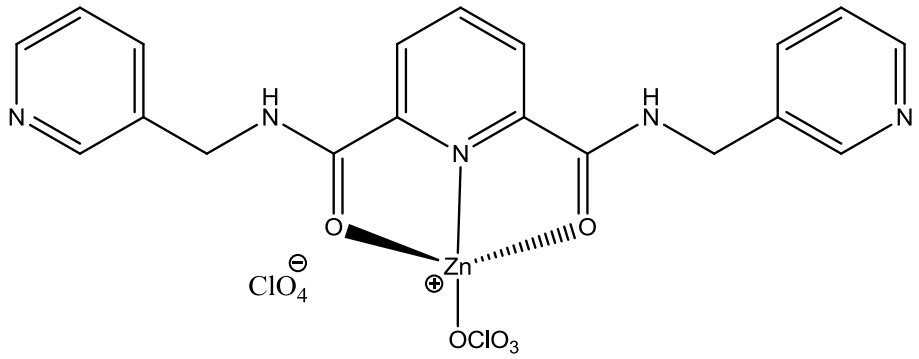

Figure 3.5.7: Possible structure for [Zn(**14**)$(ClO_4)_2$].

3.5.4.3 [Hg(**14**)Cl_2]

The complex of Hg(II) chloride with ligand **14** is formed as a white solid. The ^1H NMR spectrum of compound [Hg(**14**)Cl_2] is shown in Figure 3.5.5 (in purple). The spectrum is very similar to Zn(II) chloride complex. Hence suggesting the bonding of mercury ion could be similar to the one of Zn(II) chloride complex.

The analytical data of the complex [Hg(**14**)Cl_2] in the IR spectrum was also obtained. The carbonyl group is present at 1690 cm^{-1} which is a slight different to the original ligand **14** implying that the oxygen atom in the carbonyl group could be coordinated to the Hg(II) ion. The N-H bend exhibits little to no difference in the complex and the ligand spectra. In addition, the C=N stretch for the pyridine ring is present at 1599 cm^{-1} which was seen the previous one at 1577 cm^{-1} from ligand **14**, indicates that the pyridine nitrogen atom could be binding to Hg(II) ion centre.

Elemental analysis indicated that the complex had the formula [Hg(**14**)Cl_2]. This would suggest that one Hg(II) ion was bonded to ligand and that two chloride ions were also involved to account for neutral charge. The coordination number of the Hg(II) ion is five. The geometry in the Hg(II) ion may possess either a square pyramid or trigonal bipyramid. The possible structure of compound [Hg(**14**)Cl_2] is depicted in Figure 3.5.8.

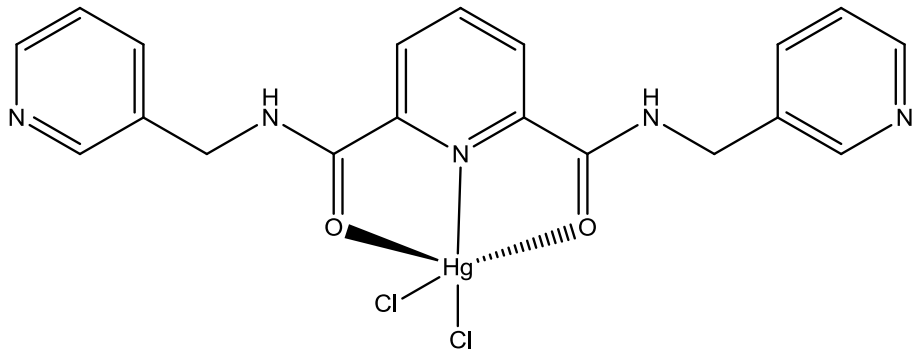

Figure 3.5.8: Possible structure for [Hg(**14**)Cl_2].

3.5.4.4 [Hg(**14**)$(ClO_4)_2 \cdot 2H_2O$]

A white solid was obtained from the reaction of **14** with Hg(II) perchlorate. The ^1H NMR spectrum of compound [Hg(**14**)$(ClO_4)_2 \cdot 2H_2O$] is shown in Figure 3.5.4 (in yellow). The amide protons resonate at 10.00 ppm which were seen at 9.89 ppm indicates that two oxygen atoms from the carbonyl group could be binding to Hg(II) ion centre. Protons Hc and He in the central pyridine ring resonate as a multiplet from 8.19 to 8.27 ppm which is similar to the original ligand **14**. The proton signals of the pyridine rings in each side chains, proton Hd does not change much in comparison to that of free ligand. However, proton Hb, Hf and Hg are observed at 8.55, 8.26 and 7.88 ppm which were seen to have a slight change from ligand **14** at 8.46, 7.73 and 7.36 ppm, respectively.

The IR spectrum of compound [Hg(**14**)$(ClO_4)_2$·$2H_2O$] contains the carbonyl signal of the amide group occurring at 1660 cm^{-1} which has moved from 1674 cm^{-1} in ligand **14** indicating the carbonyl oxygen atoms could be binding to the metal ion centre. In addition, the signal of the C=N stretch for the pyridine rings is observed at 1591 cm^{-1} in comparison to the previous ligand at 1577 cm^{-1} pointing towards that the pyridine nitrogen atom being coordinated to the Hg(II) ion centre. The appearance of the perchlorate group which is observed as a strong broad signal at 1091 cm^{-1} further suggesting that the Hg(II) perchlorate complexation had occurred.

Elemental analysis indicated that the complex had the formula [Hg(**14**)$(ClO_4)_2$·$2H_2O$]. This would suggest that one Hg(II) ion was bonded to ligand and that two perchlorate ions were also involved to account for neutral charge. The coordination number of the Hg(II) ion would be three-coordinate. The possible structure of compound [Hg(**14**)$(ClO_4)_2$·$2H_2O$] is depicted in Figure 3.5.9.

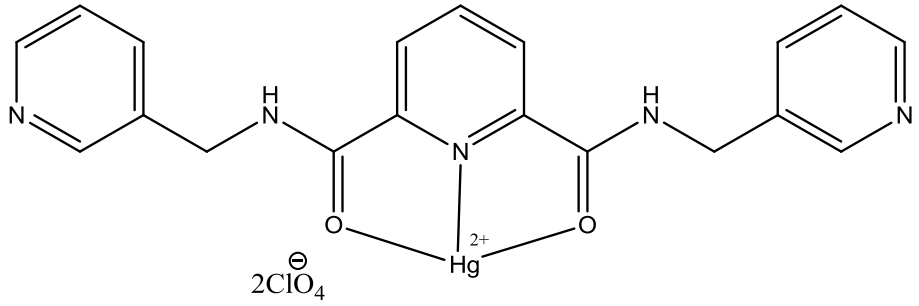

Figure 3.5.9: Possible structures for [Hg(**14**)$(ClO_4)_2$·$2H_2O$].

3.5.4.5 [Ni(**14**)(Cl)·(OH)·2MeOH]

The complex [Ni(**14**)(Cl)·(OH)·2MeOH] is isolated as a blue solid. The IR spectrum of the complex [Ni(**14**)(Cl)·(OH)·2MeOH] is very similar to the one of Zn(II) chloride complex. This would suggest the bonding of the nickel(II) ion is very similar to that of Zn(II) complex.

Elemental analysis suggested that the formula of Ni(II) complex is [Ni(**14**)(Cl)·(OH)·2MeOH]. So this means that one Ni(II) ion was bonded to ligand and that one chloride ion was also involved. The hydroxyl group from deprotonated water was occupied to account for neutral charge. The geometry of Ni(II) complex were obtained from the magnetic moment of complex [Ni(**14**)(Cl)·(OH)·MeOH] which was 1.58 B.M. This value would suggest that the geometry of the Ni(II) chloride complex is either four-coordinate, square planar, or six-coordinate, octahedral. The value obtained

is between 0 BM (indicating diamagnetic Ni^{2+} or square planar geometry) and 2.7 B.M. (indicating paramagnetic Ni^{2+} and octahedral). The possible structures of compound [Ni(**14**)(Cl)·(OH)·2MeOH] are depicted in Figure 3.5.10.

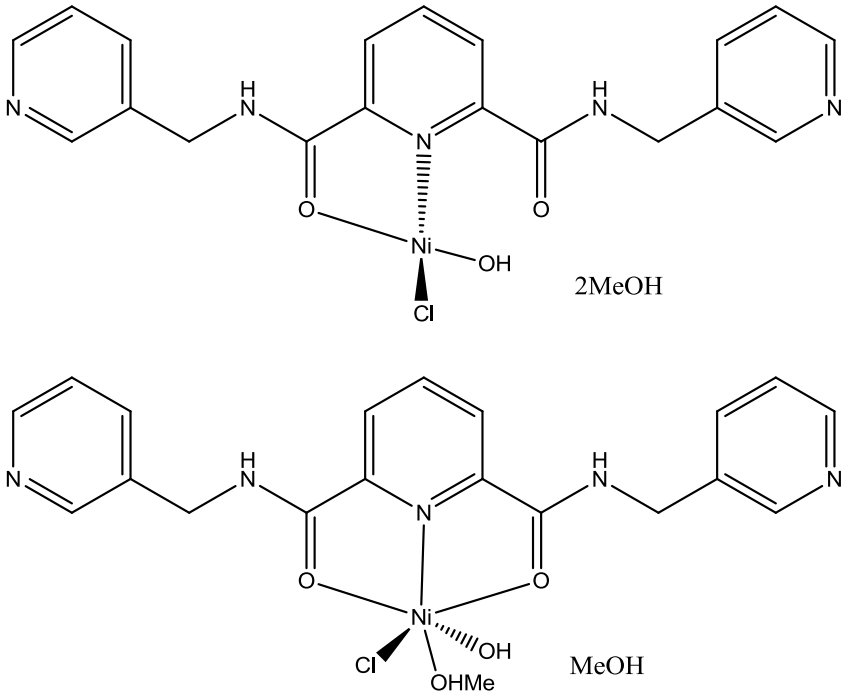

Figure 3.5.10: Possible structures for [Ni(**14**)(Cl)·(OH)·MeOH].

3.5.4.6 [Ni(**14**)(ClO_4)(OH)·$2H_2O$]

The Ni(II) perchlorate complex is formed as a blue solid. In the IR spectrum of compound [Ni(**14**)(ClO_4)(OH)·$2H_2O$], the appearance of a strong broad signal at 3357 cm^{-1} suggests coordinated water molecules could be in the Ni(II) complex. The carbonyl signal of amide group is occurring at 1629 cm^{-1} which is a large shift from the original spectrum at 1674 and 1660 cm^{-1} in ligand **14**. In addition, the C=N stretch from the pyridine ring is observed at 1581 cm^{-1} which is similar to the spectrum of ligand **14**. This would suggest the bonding of Ni(II) ion centre is occurring between the oxygen atoms from the carbonyl group and probable one nitrogen from the central pyridine ring. The observation of the perchlorate group at 1108 cm^{-1} as a strong broad signal confirms that the Ni(II) perchlorate complexation had occurred.

Elemental analysis indicated that the complex had the formula [Ni(**14**)(ClO_4)(OH)·$2H_2O$]. This would imply that one Ni(II) ion was bonded to ligand and that one perchlorate ion was also involved. The hydroxyl group from deprotonated water could be account for neutral charge. The bonding of the Ni(II) ion is through two oxygen atoms from the amide group as well as one hydroxyl group. The obtained

magnetic moment of Ni(II) complex is 2.54 B.M. which has suggests that the geometry of the Ni(II) complex is octahedral sphere. The possible structure of compound [Ni(**14**)(ClO_4)(OH)·$2H_2O$] is depicted in Figure 3.5.11.

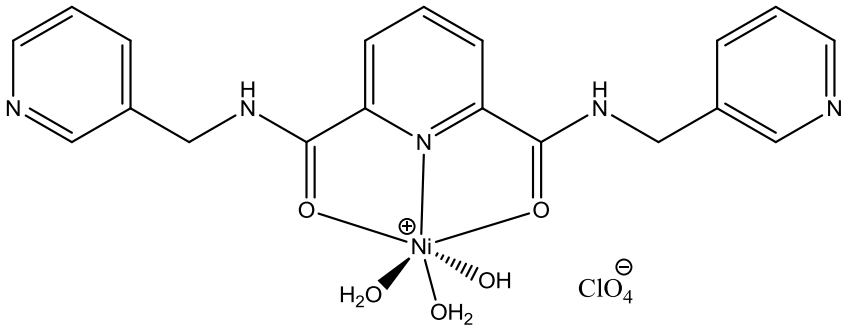

Figure 3.5.11: Possible structure for compound [Ni(**14**)(ClO_4)(OH)·$2H_2O$].

3.5.4.7 [Cu(**14**)Cl_2·H_2O·MeOH]

The complex [Cu(**14**)Cl_2·H_2O·MeOH] is obtained as a blue solid. The observation of Cu(II) chloride complex in both the IR spectrum and the elemental analysis (with the exception of one coordination solvent had been switched to one equivalent of MeOH) is very similar to the data observed for the of Zn(II) chloride complex. Hence, the bonding sites and the geometries of Ni(II) ion should be very similar to that of Zn(II) ion as well. The magnetic moment of the Cu(II) chloride complex is 1.74 B.M. The proposed the structure of [Cu(**14**)Cl_2·H_2O·MeOH] is depicted in Figure 3.5.12.

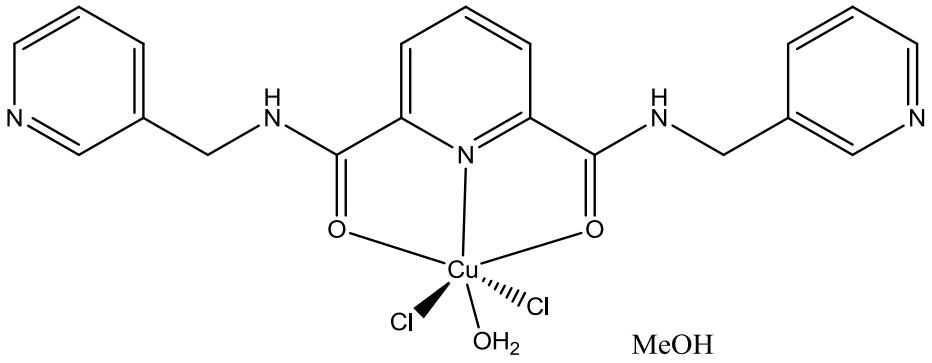

Figure 3.5.12: Possible structure for [Cu(**14**)Cl_2·H_2O·MeOH].

3.5.4.8 [Cu(**14**)(ClO_4)(OH)·$3H_2O$]

The Cu(II) perchlorate complex is isolated as a blue solid. In the IR spectrum of compound [Cu(**14**)(ClO_4)(OH)·$3H_2O$], the appearance of a strong and broad signal at 3550 cm^{-1} suggests that the Cu(II) complex may contain coordinated water molecules. coordinated water could be in the Cu(II) complex. For the other bands, such as the

carbonyl signal, NH stretch are similar to these of the Ni(II) chloride complex. In addition, the C=N stretch occurring at 1611 cm^{-1} which is comparing to the original ligand 1577 cm^{-1} for the pyridine ring suggests that the nitrogen atom from the pyridine ring is coordinated to the Cu(II) ion centre. The Cu(II) perchlorate complexation had occurred due to the observing a strong broad perchlorate signal at 1094 cm^{-1} in the IR spectrum.

Elemental analysis indicated that the Cu(II) complex had the formula [Cu(**14**)(ClO_4)(OH)·$3H_2O$]. This would imply that one Cu(II) ion was bonded to the ligand and that one perchlorate ion was also involved. The hydroxyl group from deprotonated water was occupied to account for the neutral charge. The bonding of Cu(II) ion is *via* the two oxygen atoms from the carbonyl group, one nitrogen atom from the central pyridine ring and additional one hydroxyl group. The magnetic moment of the Cu(II) perchlorate complex is 1.65 B.M. The geometry of Cu(II) ion is octahedral. The possible structure of compound [Cu(**14**)(ClO_4)(OH)·$3H_2O$] is depicted in Figure 3.5.13.

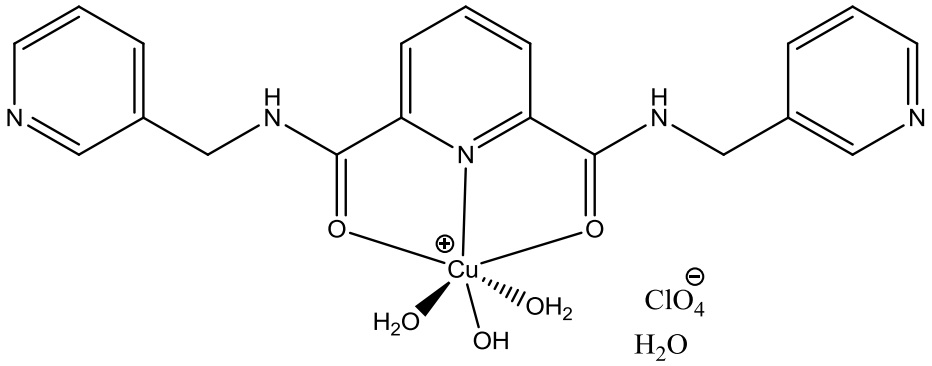

Figure 3.5.13: Possible structure for [Cu(**14**)(ClO_4)(OH)·$3H_2O$].

3.5.4.9 [Cu(**14**)(NO_3)(OH)]

The complex [Cu(**14**)(NO_3)(OH)] is formed as a pale blue solid. In the IR spectrum of compound [Cu(**14**)(NO_3)(OH)], the signal of the carbonyl group which is observed at 1648 cm^{-1} is very similar to the band which was obtained for the Zn(II) chloride complex. In addition, the present signal from the lower pyridine rings of the Cu(II) nitrate complex (1630 cm^{-1}) is slightly higher comparing that of the Zn(II) perchlorate complex. Thus, it suggest that the bonding of Cu(II) ion should be very similar to that of Zn(II) perchlorate complex as well. The observation of the nitrate group is occurring at 1384 cm^{-1} as a strong broad signal indicating the Cu(II) complexation had occurred.

Elemental analysis indicated that the complex had the formula [Cu(**14**)(NO_3)(OH)]. This would imply that one Cu(II) ions was bonded to ligand and that one nitrate ion was also involved. The deprotonated water could be account for neutral charge. The bonding of Cu(II) ion is through two oxygen atoms from the carbonyl group, one nitrogen atom from the central pyridine ring, one nitrate ion and one hydroxyl group. The magnetic moment of the Cu(II) nitrate complex is 1.82 B.M. The geometry of Cu(II) nitrate complex is proposed as an octahedral. The possible structure of compound [Cu(**14**)(NO_3)(OH)] is depicted in Figure 3.5.13.

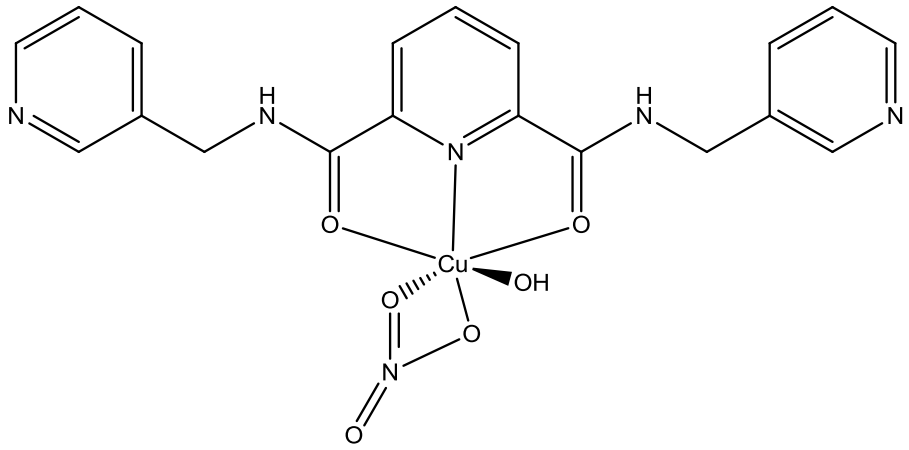

Figure 3.5.13: Possible structure for [Cu(**14**)(NO_3)(OH)].

3.5.4.10 [Cu(**14**)$(OAc)_2 \cdot 4H_2O$]

The complex [Cu(**14**)$(OAc)_2 \cdot 4H_2O$] is isolated as a blue solid. In the IR spectrum of compound [Cu(**14**)$(OAc)_2 \cdot 4H_2O$], the observed signals are similar to those in the Zn(II) chloride complex which suggested that the metal bonding could be similar in these two complexes. In addition, the signal for the acetate group band occurs at around 1590 cm^{-1} as a very strong broad signal implying that the Cu(II) acetate complexation had occurred.

Elemental analysis indicated that the complex had the formula [Cu(**14**)$(OAc)_2 \cdot 4H_2O$]. This would imply that one Cu(II) ion was bonded to the ligand and that two acetate ions were also involved to account for neutral charge. The bonding of Cu(II) ion could be through two oxygen atoms from the carbonyl group, one nitrogen atom from the central pyridine ring and two acetate ions. The magnetic moment of the Cu(II) acetate complex is 1.79 B.M. The geometry of Cu(II) ion possesses an octahedral. The possible structure of compound [Cu(**14**)$(OAc)_2 \cdot 4H_2O$] is depicted in Figure 3.5.14.

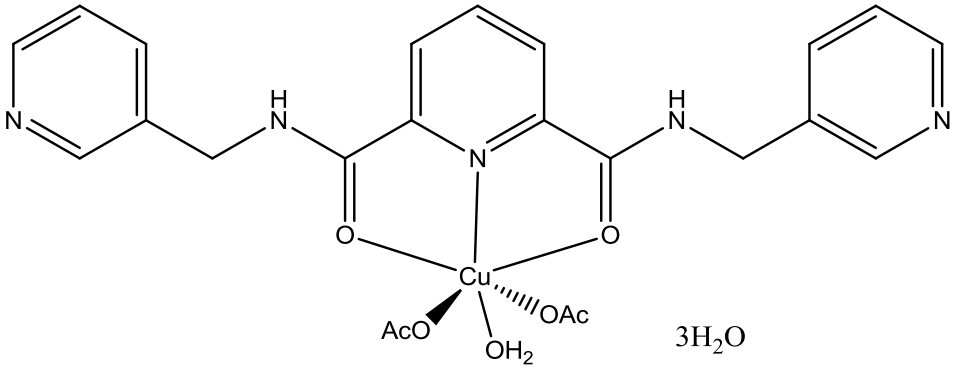

Figure 3.5.14: Possible structure for [Cu(**14**)$(OAc)_2$·$4H_2O$].

3.5.4.11 [Co(**14**)Cl_2·MeOH]

The complex [Co(**14**)Cl_2] is formed as a blue solid. The analytical data in both the IR spectrum and the elemental analysis of Co(II) chloride complex is consistent with the Zn(II) chloride complex. This would suggest that the bonding of the Co(II) ion should be similar to that of the Zn(II) complex. Elemental analysis indicated that the complex had the formula [Co(**14**)Cl_2·MeOH]. This would imply that one Co(II) ion was bonding to the ligand and that two chloride ions were also involved to account for neutral charge. The obtained magnetic moment of Co(II) complex is 3.48 B.M. which is indicative of a high-spin complex either having a square-planar or an octahedral configuration.[146] The bonding of Co(II) ion is analogous to that of Zn(II) chloride complex. The possible structure of compound [Co(**14**)Cl_2·MeOH] is depicted in Figure 3.5.15.

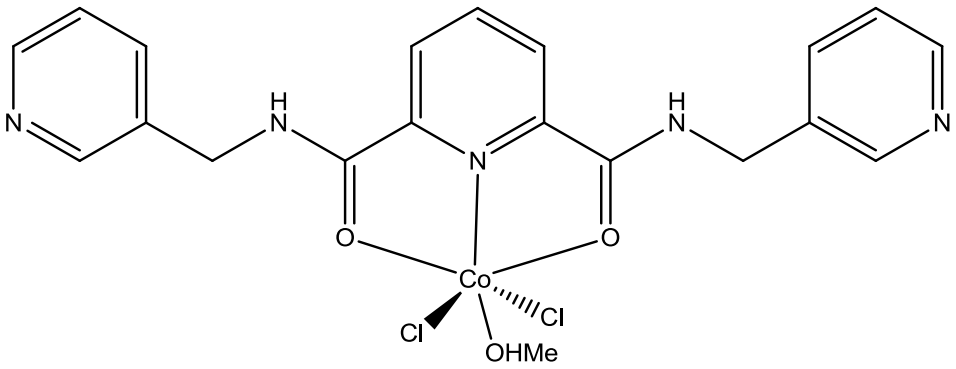

Figure 3.5.15: Possible structure for [Co(**14**)Cl_2·MeOH].

3.5.5 Ligand 15

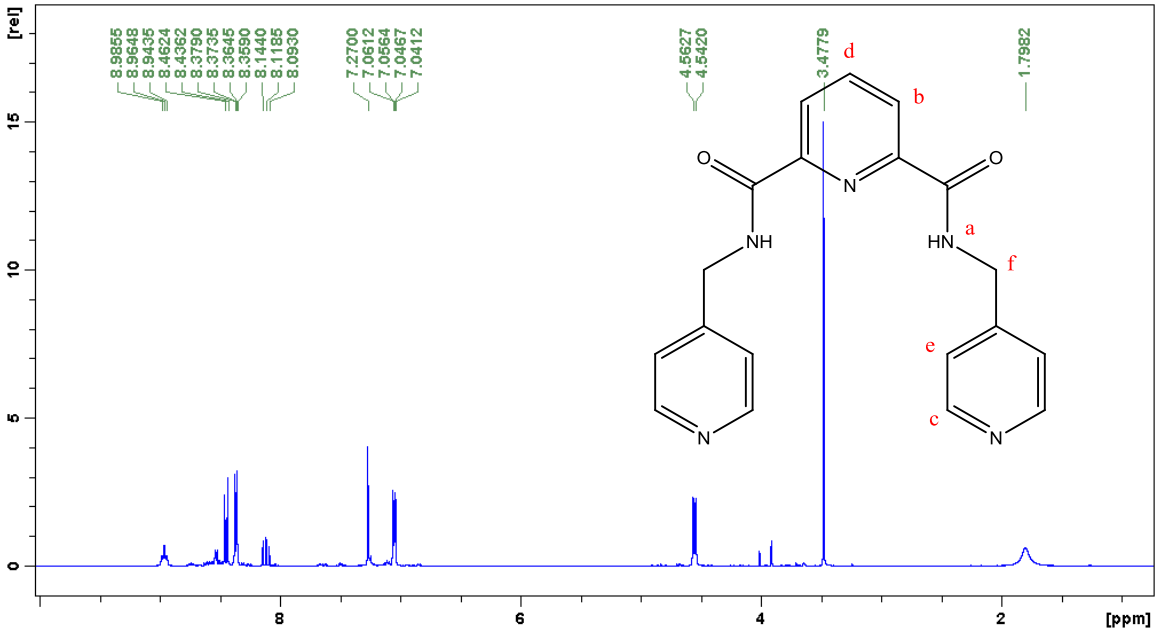

Figure 3.5.16: The ^{1}H NMR spectrum of ligand **15** in $CDCl_3$.

Ligand **15** is obtained as a yellow oil by concentrating from DCM. The ^{1}H NMR spectrum of ligand **15** is shown in Figure 3.5.16. The appearance of the amide proton Ha at 8.86 ppm as a triplet point towards the fact that the amide formation had occurred. The protons Hb and Hd for the central pyridine ring are resonated at 8.46 and 8.12 ppm as a doublet and a triplet, respectively. This is a downfield shift of 0.13 and 0.09 ppm from dimethyl dipicolinate **13**. The proton signals for the lower pyridine ring, Hc and He, are observed at 8.39 and 7.06 ppm and resonated as two doublet of doublets. In addition, the disappearance of the methoxy protons of compound **13** and the appearance of the bridging methylene protons Hf which is occurring as a doublet at 4.57 ppm indicates that the reaction had occurred. In the ^{13}C NMR spectrum of ligand **15**, the signal of amide carbon is observed at 164.0 ppm which suggests that the amide formation had occurred as well. It contains eight carbon peaks to indicate the eight-equivalent carbons now presents in the ligand **15**.

The IR spectrum of ligand **15** was tested under DCM. The signal for ν_{NH} stretch occurs at 3055 cm^{-1} which is slightly lower in comparison to that of ligand **14**. This is due to the lack of hydrogen binding occurring on amide group from DCM solvent. A signal of ν_{C-H} stretch is observed at 2987 cm^{-1}. The carbonyl signal of the amide group appears at 1681 cm^{-1} comparing the ester group at 1740 cm^{-1} suggesting that the amide formation had occurred. The C=N stretch for the pyridine ring is obtained at 1602 cm^{-1}. A signal at

1527 cm^{-1} which is N-H bend indicates that amide formation had occurred. A signal for the C=C stretch from pyridine rings is observed at 1421 cm^{-1}.

3.5.6 Metal complexes of 15

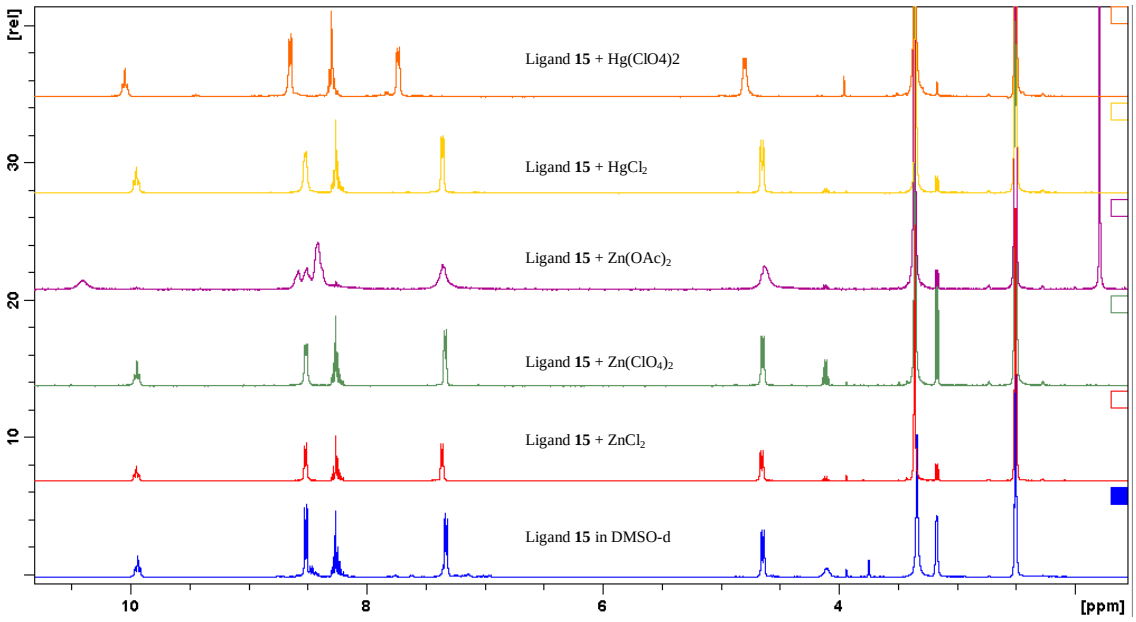

Figure 3.5.17: A comparison of the ^{1}H NMR spectra of ligand **15** and its corresponding ZnX_2 and HgX_2 (X=chloride/perchlorate/acetate) complexes in DMSO-d_6.

Metal complexes reactions of ligand **15** with various metal(II) salts were carried out in MeOH. The reactions were carried out by stirring the ligand and the appropriate metal salts at room temperature for 2 hours in MeOH. The resulting coloured solids were collected by filtration.

3.5.6.1 [Zn(**15**)Cl_2·MeOH·H_2O]

The complex [Zn(**15**)Cl_2·MeOH·H_2O] is isolated as a white solid. The ^{1}H NMR spectrum of the compound [Zn(**15**)Cl_2·MeOH·H_2O] is shown in the Figure 3.5.17 (in red). The amide proton Ha resonating at 9.95 ppm as a triplet is not shifted significantly when compared to the spectrum of ligand **15**. The similarity is also observed for the central pyridine ring protons between the Zn(II) complex and the ligand, Hd and Hb are present as multiplet from 8.20 to 8.30 ppm. The protons of the pyridine rings in each side chains, protons Hc is present at 8.52 ppm in both ligand and Zn(II) complex. However, a slight change had occurred in the signal proton position of He which appears as a doublet at 7.36 ppm and has moved from 7.33 ppm in ligand **15**. These observations indicate that weak bonding could be occurring between the metal ions and

the ligand. Furthermore, the bridging methylene proton Hf is obtained as similar ppm in both Zn(II) complex and its corresponding ligand.

The IR spectrum of compound [Zn(**15**)Cl_2·MeOH·H_2O] contains a signal of ν_{OH} stretch at 3469 cm^{-1} indicating that some coordinated MeOH/H_2O molecules could be present in the Zn(II) complex. The NH stretch is observed at 3068 cm^{-1}, which has moved from the band at 3055 cm^{-1} in ligand **15**. The carbonyl signal of the amide group is occurring at 1675 cm^{-1} as a broad signal in comparison to that of ligand **15** at 1681 cm^{-1}. This suggests that the oxygen atom for the amide group could be coordinated to the Zn(II) ion centre. The appearance of a signal at 1621 cm^{-1} in Zn(II) complex is from pyridine rings which was seen at 1602 cm^{-1} from ligand **15**, implying that the nitrogen atoms at the pyridine rings is binding to the Zn(II) ion centre.

Elemental analysis indicated that the complex had the formula [Zn(**15**)Cl_2·MeOH·H_2O]. This would imply that one Zn(II) ion was bonded to the ligand and that two chloride ions were also involved to account for neutral charge. The geometry of Zn(II) ion possesses octahedral (including one methanol molecule). The possible structure of compound [Zn(**15**)Cl_2·MeOH·H_2O] is depicted in Figure 3.5.18.

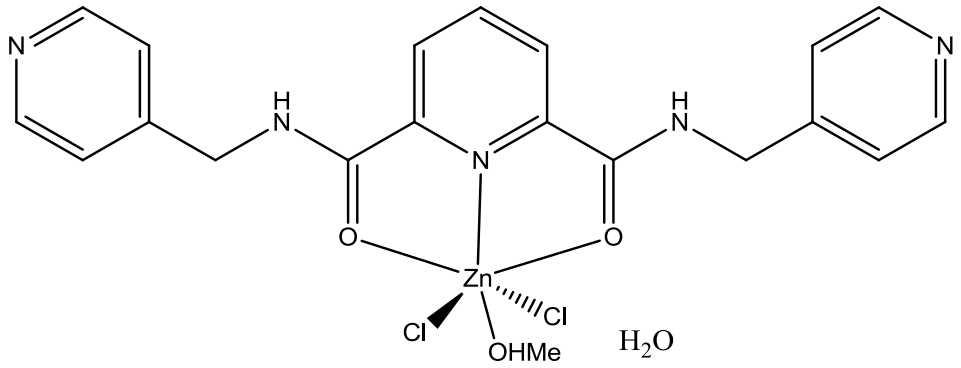

Figure 3.5.18: Possible structure for [Zn(**15**)Cl_2·MeOH·H_2O].

3.5.6.2 [Zn(**15**)$(ClO_4)_2$·H_2O]

The complex [Zn(**15**)$(ClO_4)_2$·H_2O] is isolated as a white solid. The ^{1}H NMR spectrum of compound [Zn(**15**)$(ClO_4)_2$·H_2O] is shown in Figure 3.5.17 (in green). The proton spectrum of Zn(II) perchlorate complex is similar to that of Zn(II) chloride complex suggesting that the bonding of metal ion could be similar in these two complexes .

In the IR spectrum of compound [Zn(**15**)$(ClO_4)_2$·H_2O], a signal for the OH stretch is observed at 3490 cm^{-1} suggesting coordinated water molecule might be in the Zn(II) complex. The carbonyl signal of amide group is observed at 1659 cm^{-1} which has

shifted from the original spectrum at 1681 cm^{-1} in ligand **15** suggesting that the oxygen atom for the carbonyl group is coordinated to the metal ion. The NH bend occurs at 1536 cm^{-1} while the spectrum of ligand **15** has a band at 1527 cm^{-1}. In addition, the C=N stretch for the pyridine ring is observed at 1624 cm^{-1} which was seen the original spectrum at 1602 cm^{-1} in ligand **15** suggesting that the nitrogen atom is binding to the Zn(II) ion centre. The band for the perchlorate group is observed at 1109 cm^{-1} as a strong broad signal pointing towards the Zn(II) perchlorate complexation had occurred.

Elemental analysis indicated the complex had the formula [Zn(**15**)$(ClO_4)_2 \cdot H_2O$]. This would imply that one Zn(II) ion was bonded to the ligand and that two perchlorate were also involved to account for neutral charge. An additional water molecule is also coordinated. The geometry of the Zn(II) ion possesses a tetrahedral, *via* two oxygen atoms for the carbonyl group, one nitrogen atom of the pyridine ring as well as one water molecule. The possible dimeric structure of compound [Zn(**15**)$(ClO_4)_2 \cdot H_2O$] is depicted in Figure 3.5.19.

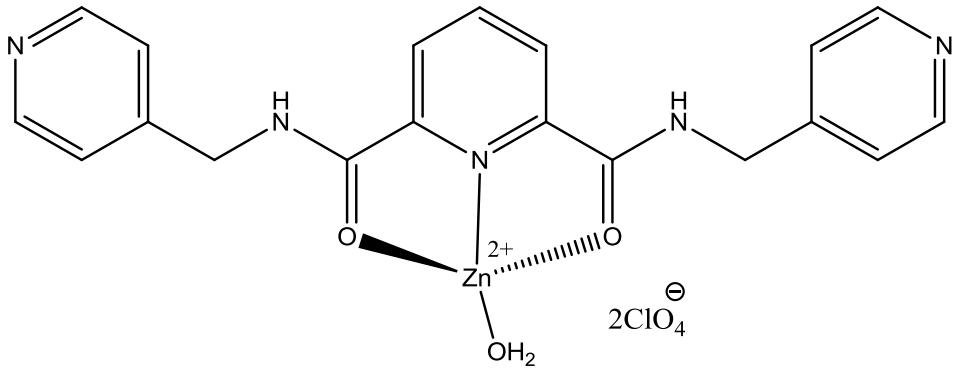

Figure 3.5.19: Possible structure for [Zn(**15**)$(ClO_4)_2 \cdot H_2O$].

3.5.6.3 [Zn_2(**15**)$(OAc)_2(OH)_2 \cdot 2H_2O$]

The complex [Zn_2(**15**)$(OAc)_2(OH)_2 \cdot 2H_2O$] is formed as a white crystalline solid. The ^1H NMR spectrum of compound [Zn_2(**15**)$(OAc)_2(OH)_2 \cdot 2H_2O$] is shown in Figure 3.5.17 (in purple). The amide proton Ha resonates at 10.42 ppm as a broad singlet which was seen to have a shift from the original one at 9.94 ppm from ligand **15** indicating that two oxygen atoms for the amide group are binding to Zn(II) ion centre. The protons in the central pyridine ring, Hd and Hb are present as a broad singlet at 8.41 ppm in contrast to the multiplet which resonates from 8.20 to 8.30 ppm from ligand **15**. Although, the signals of the protons (Hc and He) in each pyridine ring of the side chains are observed very similar to the previous ligand with the exception on closer inspection, both of these

two signals are obtained as broad signals in the Zn(II) complex. This would suggest the nitrogen atoms at the lower pyridine rings are bonding to the metal centre as well.

The IR spectrum of compound $[Zn_2(\mathbf{15})(OAc)_2(OH)_2{\cdot}2H_2O]$, contains a signal for the ν_{OH} stretch at 3432 cm^{-1} indicating coordinated water molecules in the Zn(II) complex. The carbonyl signal for the amide group is observed at 1650 cm^{-1} which has moved from 1681 cm^{-1} in ligand **15** suggesting that the oxygen atoms are coordinated to the Zn(II) ion centre. The appearance of the acetate group occurs at 1674 cm^{-1} suggesting that the Zn(II) acetate complexation had occurred. A band observed at 1621 cm^{-1} in Zn(II) complex which is due to pyridine rings of the side chains, was seen at 1602 cm^{-1} from ligand **15** implying that two nitrogen atoms at the lower pyridine rings are binding to Zn(II) ion centre as well.

Elemental analysis indicated that the complex had the formula $[Zn_2(\mathbf{15})(OAc)_2(OH)_2{\cdot}2H_2O]$. This also suggested that two Zn(II) ions were bonded to the ligand and that two acetate ions were also involved. Two hydroxyl groups from the deprotonated water molecules were involved to account for the neutral charge. One Zn(II) ion possesses an octahedral while the other one is a tetrahedral. The octahedral Zn(II) ion is bonding to two oxygen atoms from the amide group, one nitrogen atom from the central pyridine ring, one acetate ion and one hydroxyl ion as well as one water molecule. The tetrahedral Zn(II) ion is bonding to two nitrogen atoms of the pyridine rings, one acetate ion and one hydroxyl ion. The possible dimeric structure of compound $[Zn_2(\mathbf{15})(OAc)_2(OH)_2{\cdot}2H_2O]$ is depicted in Figure 3.5.20.

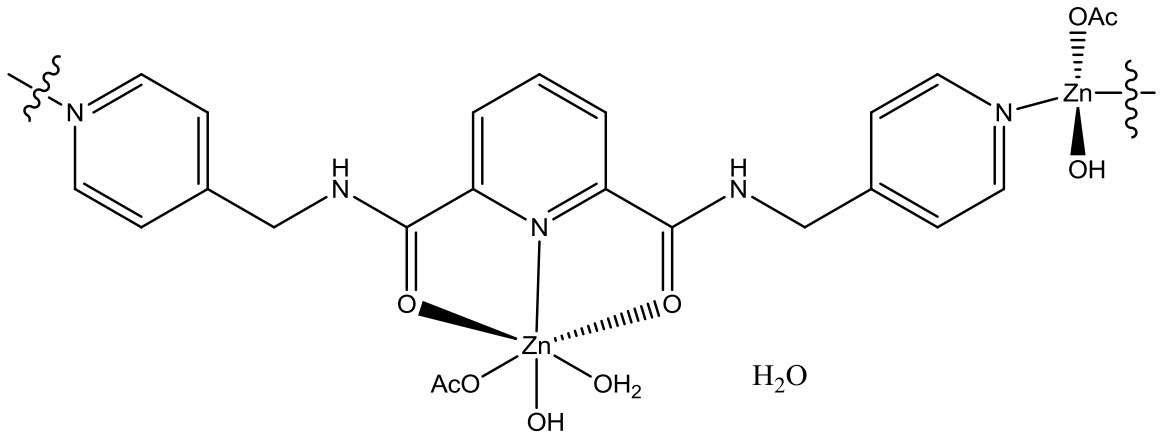

Figure 3.5.20: Possible structure for $[Zn_2(\mathbf{15})(OAc)_2(OH)_2{\cdot}2H_2O]$.

3.5.6.4 [Hg(**15**)Cl_2·H_2O]

The complex of [Hg(**15**)Cl_2·H_2O] is obtained as a white solid. The ^{1}H NMR spectrum of compound [Hg(**15**)Cl_2·H_2O] is shown in the Figure 3.5.17 (in yellow). The spectrum is similar to that of the Zn(II) chloride complex implying a possible similarity in the structure of these two chloride complexes.

The IR spectrum of compound [Hg(**15**)Cl_2·H_2O] contains the OH stretch occurring at 3491 cm^{-1} as a broad band indicating coordinated water molecule in the Hg(II) complex. The signals of both carbonyl group and NH bend are observed very similar to these of ligand **15**, but the carbonyl signal is wider than the original one. This could suggest that the oxygen atom from the amide group is binding to the Hg(II) ion centre. A signal which appears at 1612 cm^{-1} in Hg(II) complex is due to the pyridine rings in each side chains. This has moved from 1602 cm^{-1} suggesting that the two nitrogen atoms at the lower pyridine rings could have a weak bonding to the Hg(II) ion centre.

Elemental analysis indicated that the complex had the formula [Hg(**15**)Cl_2·H_2O]. This would imply that one Hg(II) ion was bonded to the ligand and that two chloride ions were also involved to account for neutral charge. The geometry of the Hg(II) ion is octahedral, with two oxygen atoms from the carbonyl group, one nitrogen atom from the pyridine ring and two chloride ions as well as one water molecule. The possible dimeric structure of compound [Hg(**15**)Cl_2·H_2O] is depicted in Figure 3.5.21.

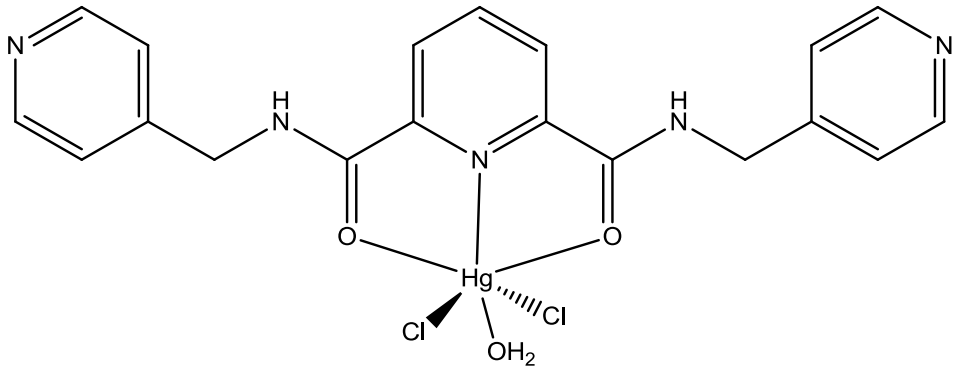

Figure 3.5.21: Possible structure for [Hg(**15**)Cl_2·H_2O].

3.5.6.5 [Hg(**15**)(ClO_4)(OH)]

The complex [Hg(**15**)(ClO_4)(OH)] is isolated as a white solid. The ^{1}H NMR spectrum of compound [Hg(**15**)(ClO_4)(OH)] is shown in the Figure 3.5.17 (in orange). The carbonyl proton Ha is observed at 10.05 ppm, which has shifted from 9.94 ppm in ligand **15**. While the signal protons in the central pyridine ring, protons Hb and Hd, are

obtained to be very similar to the previous signals from ligand **15**. In addition, protons at the lower pyridine rings, Hc is present at 8.65 ppm this has slightly shift from the original spectrum at 8.52 ppm. And He is observed at 7.73 ppm when compared to the ligand spectrum which has shifted from 7.33 ppm. These observations suggest that the bonding of the Hg(II) ion is at the oxygen atom from the carbonyl group and one nitrogen atom from the central pyridine ring.

The IR spectrum of compound [Hg(**15**)(ClO_4)(OH)], the signals such as the carbonyl amide group, the lower pyridine rings and the perchlorate group, are observed very similar to those of Zn(II) perchlorate complex.

Elemental analysis indicated that the complex had the formula [Hg(**15**)(ClO_4)(OH)]. This would suggest that one Hg(II) ion was bonded to the ligand and that one perchlorate ion was also involved. A hydroxyl group from deprotonated water molecule was involved to account for the neutral charge. The coordination number of the Hg(II) ion is four. The possible dimeric structure of compound [Hg(**15**)(ClO_4)(OH)] is depicted in Figure 3.5.22.

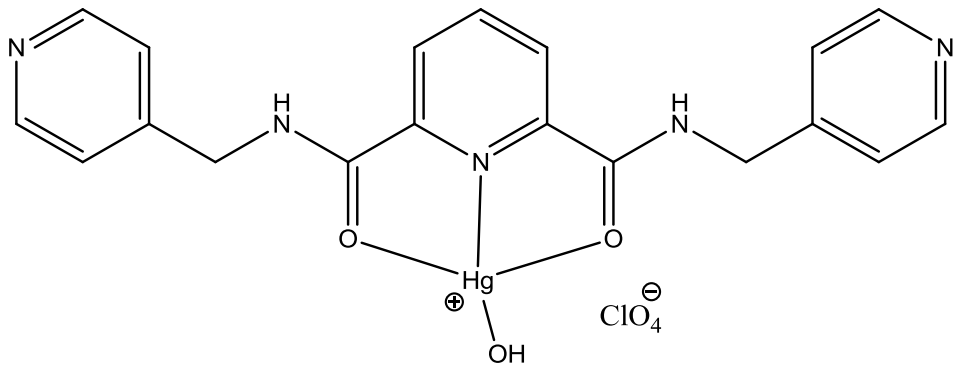

Figure 3.5.22: Possible structure for [Hg(**15**)(ClO_4)(OH)].

3.5.6.6 [Ni(**15**)$Cl_2 \cdot 4H_2O$]

The complex of [Ni(**15**)$Cl_2 \cdot 4H_2O$] was isolated as a brown green solid. In the IR spectrum of compound [Ni(**15**)$Cl_2 \cdot 4H_2O$], the observation of the OH stretch at 3271 cm^{-1} indicates some coordinated water molecules presenting in the Ni(II) complex. The carbonyl signal of the amide group is occurring at 1662 cm^{-1} which has moved from the ligand spectrum at 1681 cm^{-1}. In addition, the observed NH bend is slightly shifted in comparison to the previous ligand. This implies that the oxygen atoms could be bonding to the Ni(II) ion. The C=N stretch for the pyridine ring is obtained to be similar to that

of the Zn(II) chloride complex which would suggest that the bonding of the metal ion in the Ni(II) complex should be similar to that of Zn(II) chloride complex.

Elemental analysis indicated that one Ni(II) ion was bonded to ligand and that two chloride ions were also involved to account for neutral charge. The obtained magnetic moment of Ni(II) complex is 2.86 B.M., this indicates that the Ni(II) possessed an octahedral geometry. The bonding of Ni(II) ion is similar to that of Zn(**15**)Cl_2·MeOH·H_2O]. The possible dimeric structure of compound [Ni(**15**)Cl_2·$4H_2O$] is depicted in Figure 3.5.23.

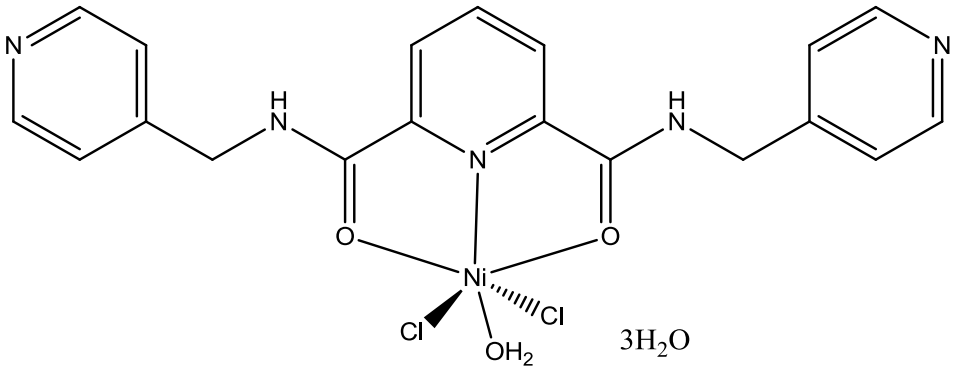

Figure 3.5.23: Possible structure for [Ni(**15**)Cl_2·$4H_2O$].

3.5.6.7 [Ni(**15**)$(ClO_4)_2$]

The complex [Ni(**15**)$(ClO_4)_2$] is isolated as a pale green solid. The analytical data of both the IR spectrum and the elemental analysis of Ni(II) perchlorate complex are very similar to that of the Zn(II) perchlorate complex. This would imply that the bonding of the Ni(II) ion should be very similar to that of Zn(II) perchlorate complex as well.

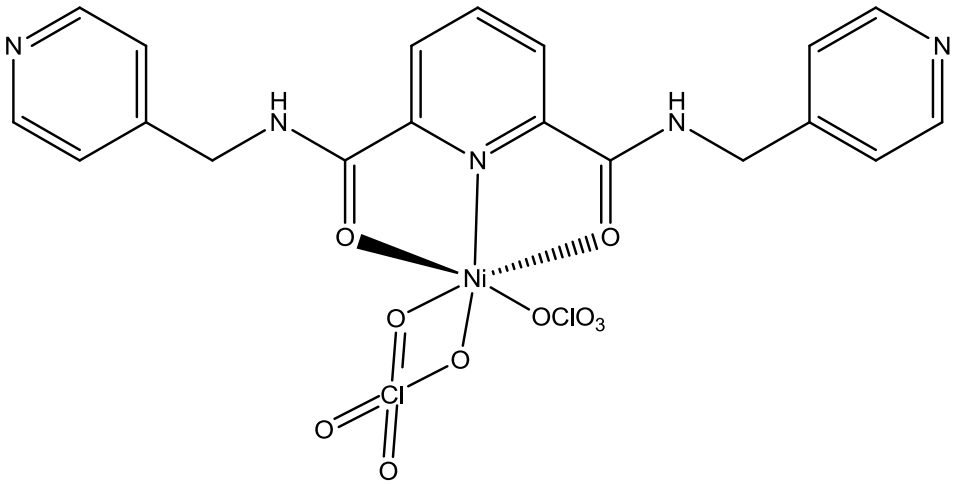

Figure 3.5.24: Possible structure for [Ni(**15**)$(ClO_4)_2$].

Elemental analysis indicated that the complex had the formula [Ni(**15**)(ClO_4)$_2$]. The magnetic moment of Ni(II) complex is obtained at 2.73 B.M. suggesting that Ni(II) complex possesses a octahedral geometry sphere. The possible dimeric structure of compound [Ni(**15**)(ClO_4)$_2$] is depicted in Figure 3.5.24.

3.5.6.8 [Ni(**15**)(NO_3)$_2$·MeOH·2H_2O]

The complex [Ni(**15**)(NO_3)$_2$·MeOH·2H_2O] is formed as a brown green solid. The IR spectrum of the compound [Ni(**15**)(NO_3)$_2$·MeOH·2H_2O] contains a strong broad signal at 3295 cm^{-1} suggesting that coordinated MeOH or water molecules presenting in the Ni(II) complex. The carbonyl signal of the amide group is present at 1648 cm^{-1} which has moved from 1681 cm^{-1} in ligand **15**. This implies that the oxygen atom for the carbonyl group could be coordinated to the Ni(II) ion. The appearance of the C=N stretch for the pyridine ring is observed at 1618 cm^{-1} which was seen in the original spectrum at 1602 cm^{-1} from ligand **15**, this suggests that the bonding of the Ni(II) ion is occurring on the nitrogen atom at the central pyridine rings. Additionally, the presenting strong broad signal at 1384 cm^{-1} which is indicative of nitrate group has pointed out the Ni(II) nitrate complexation had occurred.

Elemental analysis indicated that the complex had the formula [Ni(**15**)(NO_3)$_2$·MeOH·2H_2O]. This would imply that one Ni(II) ion was bonded to the ligand and that two nitrate ions were also involved to account for neutral charge. The geometry of Ni(II) complex is possessing an octahedral sphere which is support by the magnetic moment of the Ni(II) complex obtained as 2.81 B.M. The possible dimeric structure of compound [Ni(**15**)(NO_3)$_2$·MeOH·2H_2O] is depicted in Figure 3.5.25.

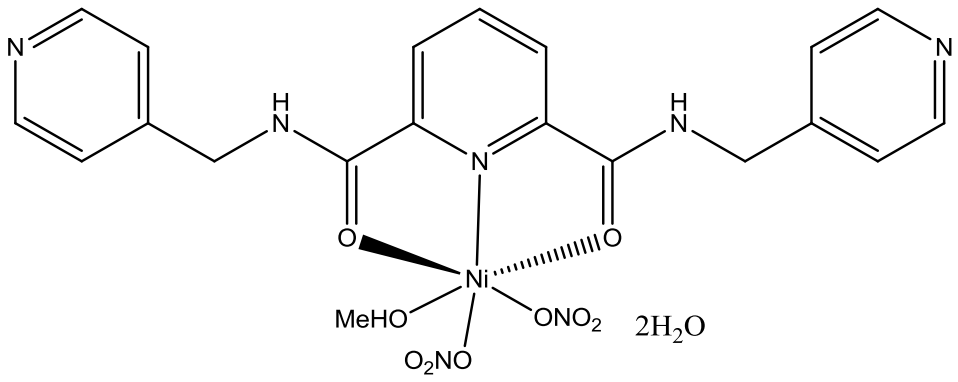

Figure 3.5.25: Possible structure for [Ni(**15**)(NO_3)$_2$·MeOH·2H_2O].

3.5.6.9 [Cu(**15**)$(ClO_4)_2$·H_2O]

The complex [Cu(**15**)$(ClO_4)_2$·H_2O] is isolated as a green solid. The analytical data of both the IR spectrum and the elemental analysis of compound [Cu(**15**)$(ClO_4)_2$·H_2O] obtained is very similar to that of the Zn(II) perchlorate complex, this suggests that the bonding which occurs at the Cu(II) ion centre should be very similar to that of the Zn(II) ion as well. The magnetic moment of the Cu(II) perchlorate complex is 1.87 B.M. Hence, the proposed dimeric structure of complex [Cu(**15**)$(ClO_4)_2$·H_2O] is shown in Figure 3.5.27.

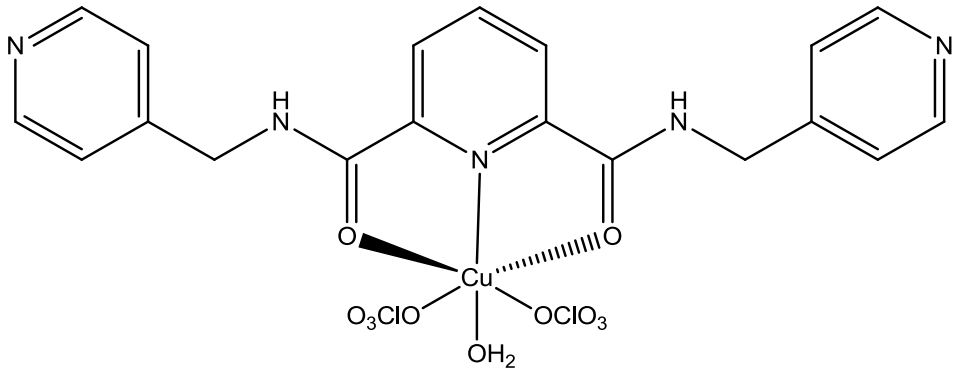

Figure 3.5.27: Possible structure for [Cu(**15**)$(ClO_4)_2$·H_2O].

3.5.6.10 [Cu(**15**)$(NO_3)_2$·2MeOH·H_2O]

The complex [Cu(**15**)$(NO_3)_2$·2MeOH·H_2O] is obtained as a green solid. The analytical data from the IR spectrum of the complex [Cu(**15**)$(NO_3)_2$·2MeOH·H_2O] is very similar to that of [Ni(**15**)$(NO_3)_2$·MeOH·$2H_2O$], with the exception of the carbonyl signal of the amide group. It is observed at 1659 cm^{-1} in the Cu(II) complex which is slightly higher than the spectrum at 1648 cm^{-1} in Ni(II) complex. In addition, the similarity in the rest of the IR spectrum suggests that the bonding of the Cu(II) ion should be similar to that of the Ni(II) ion.

Elemental analysis indicated the complex had the formula [Cu(**15**)$(NO_3)_2$·2MeOH·H_2O]. This also implies that one Cu(II) ion was bonded to the ligand and that two nitrate ions were also involved to account for the neutral charge. The geometry of the Cu(II) ion is similar to that of Ni(II) ion in [Ni(**15**)$(NO_3)_2$·MeOH·$2H_2O$]. The magnetic moment of the Cu(II) nitrate complex is 1.78 B.M. The possible dimeric structure of compound [Cu(**15**)$(NO_3)_2$·2MeOH·H_2O] is depicted in Figure 3.5.28.

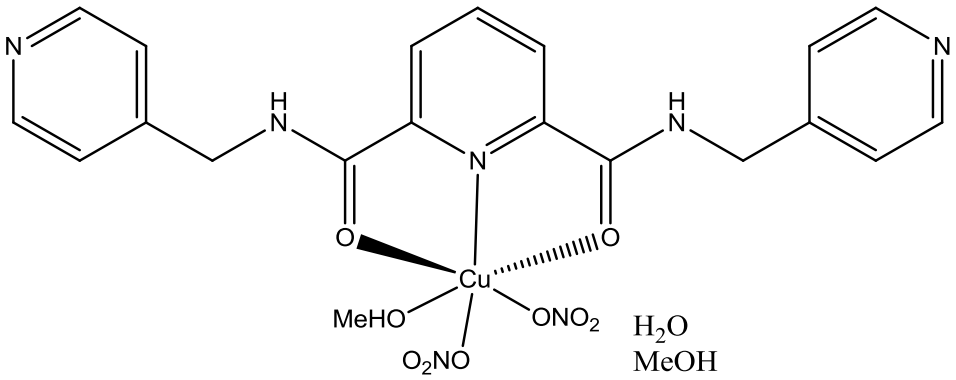

Figure 3.5.28: Possible structure for [Cu(**15**)$(NO_3)_2$·2MeOH·H_2O].

3.5.6.11 [Co(**15**)Cl_2·MeOH·H_2O]

The complex [Co(**15**)Cl_2·MeOH·H_2O] is formed as a green solid. The IR spectrum of compound [Co(**15**)Cl_2·MeOH·H_2O] contains ν_{OH} stretch at 3325 cm^{-1} indicating coordinated MeOH/H_2O molecules present in the Co(II) complex. The signal for the carbonyl group is observed at 1666 cm^{-1} which has moved from 1681 cm^{-1} in ligand **15** suggesting that the oxygen atoms for the carbonyl group could be coordinated to the Co(II) ion. A signal at 1616 cm^{-1} in Co(II) complex which is due to the C=N stretch of the pyridine ring, was seen at 1602 cm^{-1} from ligand **15**. This would suggest that two nitrogen atoms from the central pyridine rings are binding to the Co(II) ion centre.

Elemental analysis indicated that the complex had the formula [Co(**15**)Cl_2·MeOH·H_2O]. This would imply that one Co(II) ion was bonded to the ligand and that two chloride ions were also involved to account for the neutral charge. The obtained magnetic moment of the Co(II) complex at 4.77 B.M. suggested that the high-spin of Co(II) complex and could adopt an octahedral geometry sphere. The bonding of Co(II) ion is similar to that of Ni(II) chloride complex. The possible dimeric structure of compound [Co(**15**)Cl_2·MeOH·H_2O] is depicted in Figure 3.5.29.

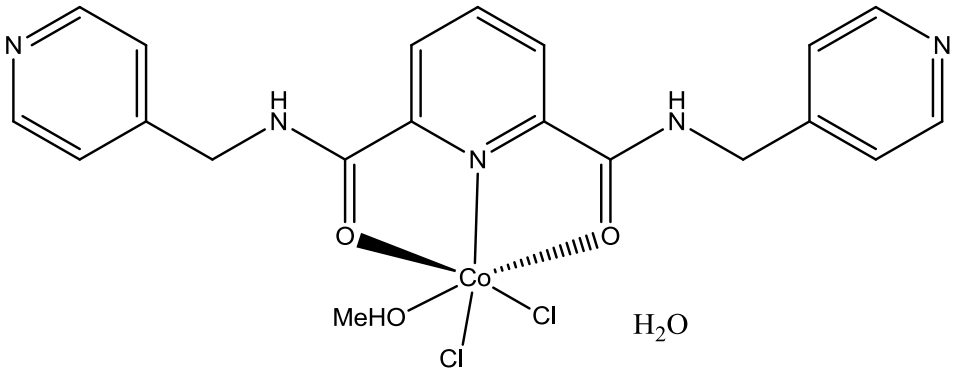

Figure 3.5.29: Possible structure for [Co(**15**)Cl_2·MeOH·H_2O].

3.5.6.12 [Co(**15**)$(ClO_4)_2$·$3H_2O$]

The complex of [Co(**15**)$(ClO_4)_2$·$3H_2O$] is isolated as a yellow solid. The observed analytical data of the complex [Co(**15**)$(ClO_4)_2$·$3H_2O$] in either IR spectrum or the elemental analysis are very similar to that of [Zn(**15**)$(ClO_4)_2$·H_2O]. This would suggest that bonding of Co(II) ion and the structure of the Co(II) complex should be very similar to those of the Zn(II) complex. The magnetic moment of the Co(II) complex is occurring at 3.87 B.M. which suggests that the complex should adopt a square-planar sphere. The possible structure of the compound [Co(**15**)$(ClO_4)_2$·$3H_2O$] is depicted in Figure 3.5.30.

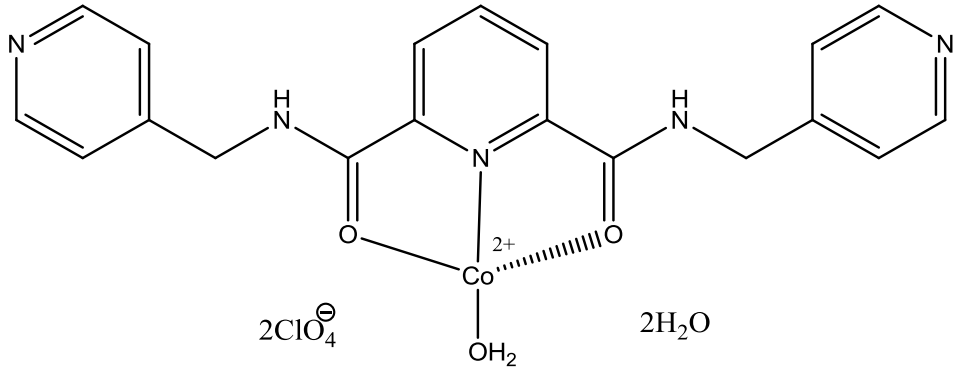

Figure 3.5.30: Possible structure for [Co(**15**)$(ClO_4)_2$·$3H_2O$].

3.5.7 Ligand 16

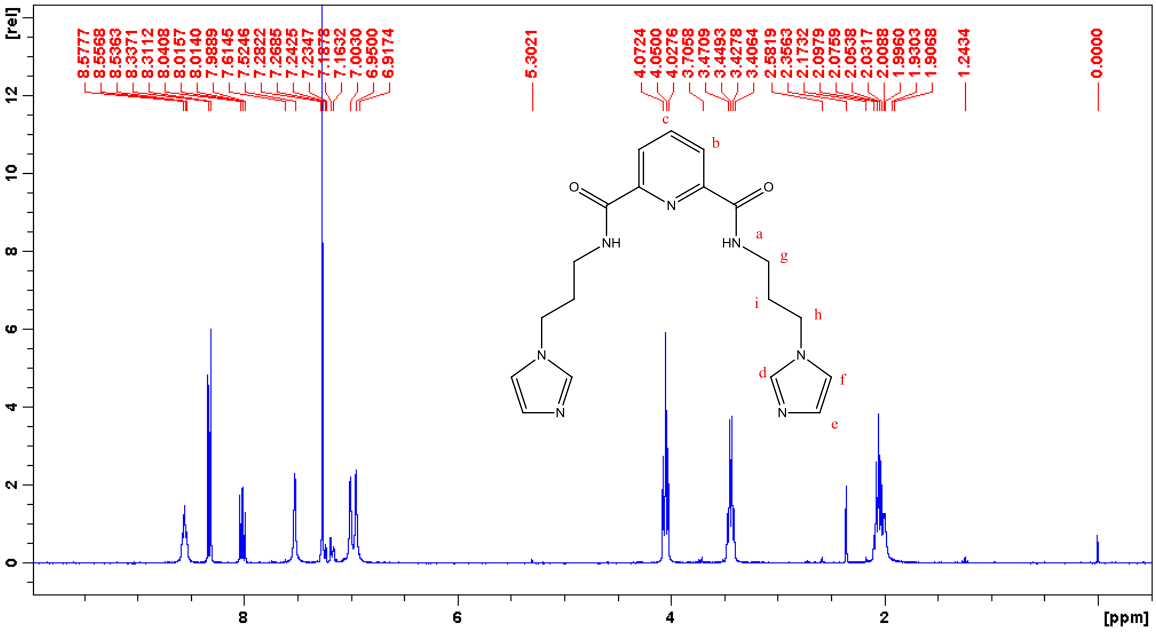

Figure 3.5.31: ^{1}H NMR spectrum of ligand **16** in $CDCl_3$.

The ligand **16** is formed as a yellow oil. The ^{1}H NMR spectrum of ligand **16** is shown in Figure 3.5.31. The appearance of the amide proton Ha which resonates at 8.55 ppm as a triplet and the disappearance of the methoxy protons from compound **13** suggest that the amide formation had occurred. The protons in the central pyridine rings, Hb and Hc, are observed at 8.32 ppm as a doublet and at 8.01 ppm as a triplet, respectively, which are very similar to those two signals of **13**. Three singlets for the protons from the imidazole rings are present at 7.52, 6.95 and 6.91 ppm which are protons Hb, He and Hf, respectively. In addition, the three bridging methylene protons, Hg, Hh and Hi are appeared at 4.05, 3.43 and 2.05 ppm. In the ^{13}C NMR spectrum, the signal of amide group is resonating at 164.2 ppm suggesting that amide formation had occurred. It contains ten carbon peaks to indicate the ten-equivalent carbons now presents in the ligand **16**.

The IR spectrum of ligand **16** is run under DCM solvent. The C-H stretch is present at 2986 cm^{-1}. The carbonyl signal of amide group is observed at 1673 cm^{-1} in comparison to the previous compound **13** at 1740 cm^{-1} suggesting the amide formation had occurred. The N-H bend is observed at 1537 cm^{-1}. It appears a signal at 1508 cm^{-1} which is due to the imidazole rings. And the C=C stretches is observed at 1447 and 1422 cm^{-1} which could be from pyridine rings and imidazole rings, respectively.

The mass spectrum suggests the ligand **16** is pure.

3.5.8 Metal complexes of 16

Metal complexes reactions of ligand **16** with various metal(II) salts were carried out in MeOH. The reactions were carried out by stirring the ligand and the appropriate metal salts at room temperature for 2 hours in MeOH. The resulting coloured solids were collected by filtration.

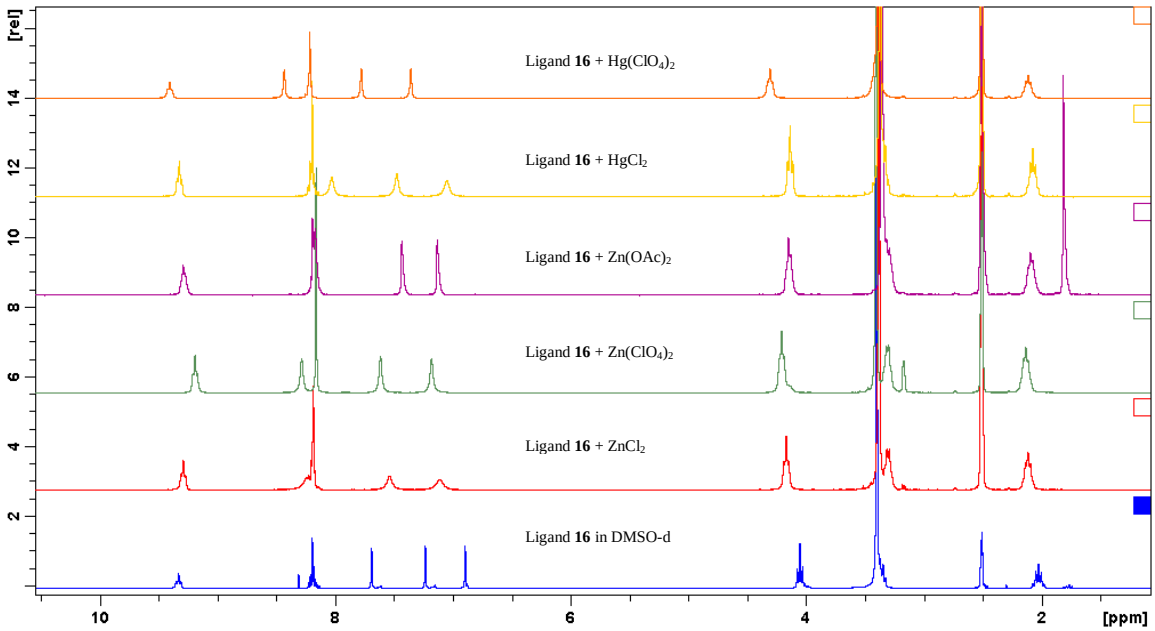

Figure 3.5.32: A comparison of ^{1}H NMR spectra of ligand **16** and its corresponding ZnX_2 and HgX_2 (X = chloride/perchlorate/acetate) complexes in DMSO-d_6.

The exceptions were the Zn(II) acetate complex which formed as white crystals, Ni(II) nitrate which formed as a green solid from slowly evaporated MeOH solvent. In addition, the Cu(II) chloride and nitrate complexes are obtained as blue suspensions. The mixture of each of the Cu(II) complex were reduced under vacuum, the generated blue solids which were collected by filtration and washed with MeOH.

3.5.8.1 [Zn(**16**)Cl_2·$2H_2O$]

The Zn(II) chloride complex of **16** is isolated as a white solid. The ^{1}H NMR spectrum of compound [Zn(**16**)Cl_2·$2H_2O$] is shown in Figure 3.5.32 (in red). The observation of both the proton Ha of amide group and the protons Hb and Hc in the central pyridine rings are observed at 9.29 and 8.19 ppm, respectively, which are very similar to the previous ligand **16** suggesting that the nitrogen atoms from neither amide group nor the central pyridine ring are coordinated to the Zn(II) ion centre. However, several large shifts are obtained between the ligand and complex of the protons in the imidazole rings where the protons Hd, He and Hf, are observed at 8.24, 7.54 and 7.11 ppm in comparison to the original three at 7.69, 7.23 and 6.89 ppm from ligand **16** indicates that the two imine nitrogen atoms from the imidazole rings are binding to Zn(II) ion centre. In addition, the three signals of the bridging methylene protons are also obtained. The proton Hg resonates at 4.16 ppm which was seen to have a slight shift from the original one at 4.05 ppm in ligand **16**. The proton Hd is present at 3.30 ppm which is

very similar to the previous ligand **16**. And the protons Hi is observed at 2.11 ppm in comparison to the original spectrum at 2.02 ppm from ligand **16**.

The IR spectrum of compound [Zn(**16**)Cl_2·$2H_2O$] contains a signal ν_{OH} at 3486 cm^{-1} indicating coordinated water is in the Zn(II) complex. The presence of a broad signal at 1663 cm^{-1} of the carbonyl group was seen to have slightly shifted from the original one at 1673 cm^{-1} from ligand **16**. This suggests that the oxygen atom for the carbonyl group could be coordinated to the Zn(II) ion centre. The C=C stretch for the imidazole rings is present at 1536 cm^{-1} which has moved from 1508 cm^{-1} indicating that two nitrogen atoms from the from imidazole rings could be coordinated to the Zn(II) ion centre. This agrees with the results discussed earlier in the ^{1}H NMR.

Elemental analysis indicated the complex had the formula [Zn(**16**)Cl_2·$2H_2O$]. This would also imply that one Zn(II) ion was bonded to ligand and that two chloride ions were also involved to account for the neutral charge. The complex contains two extra water molecules as well. The geometry of Zn(II) ion is proposed to be an octahedral. The possible structures of compound [Zn(**16**)Cl_2·$2H_2O$] are depicted in Figure 3.5.33.

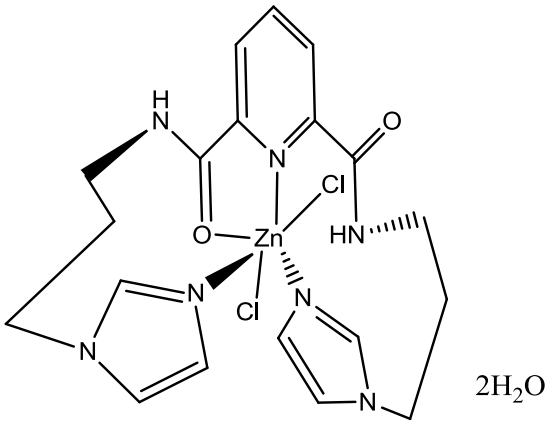

Figure 3.5.33: Possible structure for [Zn(**16**)Cl_2·$2H_2O$].

3.5.8.2 [Zn(**16**)(ClO_4)(OH)·$2H_2O$]

The complex [Zn(**16**)(ClO_4)(OH)·$2H_2O$] is obtained as a white solid. The ^{1}H NMR spectrum of compound [Zn(**16**)(ClO_4)(OH)·$2H_2O$] is shown in Figure 3.5.32 (in green). The amide proton Ha is observed at 9.18 ppm which has moved from the original one at 9.33 ppm in ligand **16**. This suggests that the oxygen atom for the carbonyl group could be coordinated to the Zn(II) ion centre. The protons Hb and Hc in the central pyridine rings are observed to be very similar to that of the ligand. The large chemical shifts occur at the three protons of the imidazole rings, protons Hd, He and Hf, which are

observed at 8.28, 7.61 and 7.18 ppm in comparison to 7.69, 7.23 and 6.89 ppm, respectively, from ligand **16**. This indicates that the two nitrogen atoms from the imidazole rings are binding to the Zn(II) ion centre. The bridging methylene protons are observed to be similar to those of the Zn(II) chloride complex.

The observation of the complex [Zn(**16**)(ClO_4)(OH)·$2H_2O$] in the IR spectrum is very similar to that of Zn(II) chloride complex suggesting that the bonding of the Zn(II) ion should be similar in both two complexes. In addition, the presence of a strong signal of perchlorate group at 1107 cm^{-1} is indicative of the Zn(II) perchlorate complexation had occurred.

Elemental analysis indicated the complex had formula [Zn(**16**)(ClO_4)(OH)·$2H_2O$]. This would imply that one Zn(II) ion was bonded to ligand and that one perchlorate ion was also involved. The hydroxyl group from a deprotonated water molecular was accounted for the neutral charge. The geometry of the Zn(II) ion is an octahedral. The possible structure of compound [Zn(**16**)(ClO_4)(OH)·$2H_2O$] is depicted in Figure 3.5.34.

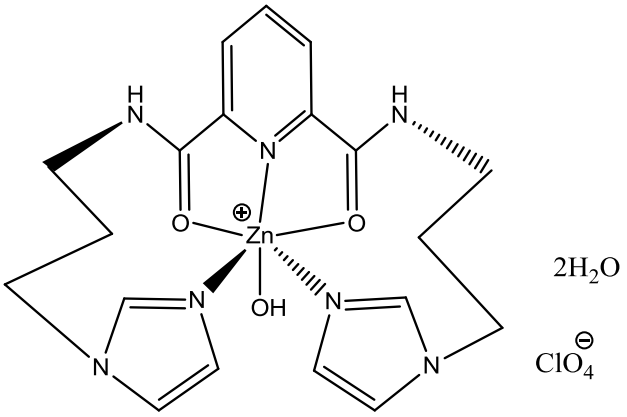

Figure 3.5.34: Possible structure for [Zn(**16**)(ClO_4)(OH)·$2H_2O$].

3.5.8.3 [Zn(**16**)$(OAc)_2$·$2H_2O$]

The complex [Zn(**16**)$(OAc)_2$·$2H_2O$] is isolated as a white crystalline solid. The ^{1}H NMR spectrum of compound [Zn(**16**)$(OAc)_2$·$2H_2O$] is shown in Figure 3.5.32 (in purple). Amide proton Ha is observed at 9.29 ppm which was seen to have a slight shift from the original spectrum at 9.33 ppm in ligand **16**. The signals of protons Hb and Hc in the central pyridine ring in both ligand and complex are obtained to be very similar to each other. However, the three signals of protons Hd, He and Hf from the imidazole rings are observed with large shifts in comparison to the previous ligand **16**. Three are very

similar to what were observed for the Zn(II) chloride complex pointing towards that the bonding of Zn(II) ion should be similar in the chloride and acetate complexes.

The IR spectrum of compound [Zn(**16**)$(OAc)_2 \cdot 2H_2O$] is similar to that of Zn(II) chloride complex indicating that the bonding the Zn(II) acetate complex should be similar to that of the Zn(II) chloride complex as well. The only exception in these two spectra is the appearance of a strong signal at 1612 cm^{-1} which is due to the presence of the acetate group, which indicates that the Zn(II) acetate complexation had occurred.

Elemental analysis indicated that the complex had the formula [Zn(**16**)$(OAc)_2 \cdot 2H_2O$]. The geometry is similar to that of Zn(II) chloride complex. So the proposed structure of compound [Zn(**16**)$(OAc)_2 \cdot 2H_2O$] is depicted in Figure 3.5.35.

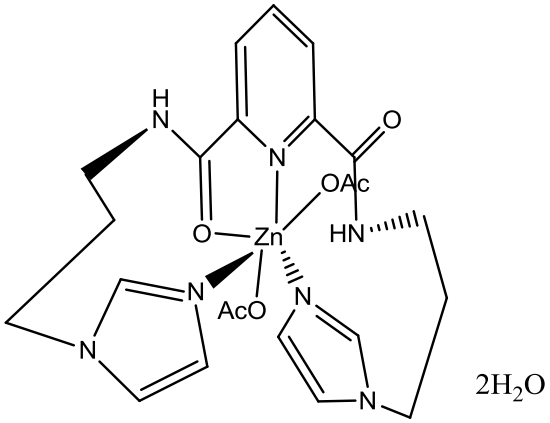

Figure 3.5.35: Possible structure for [Zn(**16**)$(OAc)_2 \cdot 2H_2O$].

3.5.8.4 [Hg(**16**)$Cl_2 \cdot 2H_2O$]

The Hg(II) chloride complex is obtained as a white solid. The ^{1}H NMR spectrum of compound [Hg(**16**)$Cl_2 \cdot 2H_2O$] is shown in Figure 3.5.32 (in red). The ^{1}H NMR spectrum of Hg(II) complex is similar to that of the Zn(II) chloride complex with the exception of the signals of protons Hd and He in the imidazole rings where they resonated at 8.03 and 7.47 ppm in Hg(II) complex in comparison to those of the Zn(II) complex at 8.24 and 7.54 ppm, respectively. However, the similarity of the shifts indicated the bonding of Hg(II) ion should be similar to that of Zn(II) ion.

The observations of either the IR spectrum or the elemental analysis of compound [Hg(**16**)$Cl_2 \cdot 2H_2O$] is similar to that of [Zn(**16**)$Cl_2 \cdot 2H_2O$] as well. So, the proposed structure of complex [Hg(**16**)$Cl_2 \cdot 2H_2O$] is depicted in Figure 3.5.36.

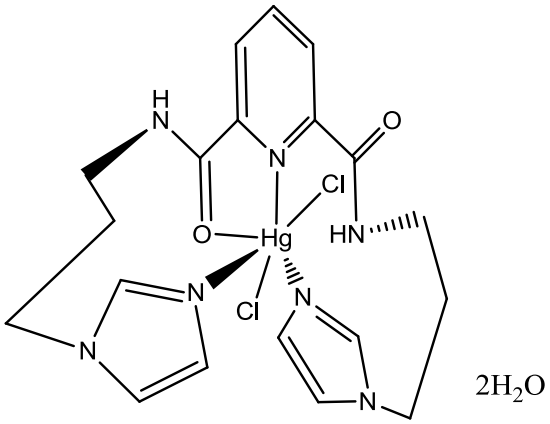

Figure 3.5.36: Possible structure for [Hg(**16**)Cl_2·$2H_2O$]

3.5.8.5 [Hg(**16**)(ClO_4)(OH)·H_2O]

The complex is obtained as a white solid. The observation for the Hg(II) perchlorate complex is very similar to that of Zn(II) perchlorate complex due to the similarity in both ^{1}H NMR spectra and the IR spectra. Hence, this suggests that the bonding of the Hg(II) ion should be similar to that of Zn(II) ion.

Elemental analysis indicated the complex had the formula [Hg(**16**)(ClO_4)(OH)·H_2O]. This would imply that one Hg(II) ion was bonded to the ligand and that one perchlorate ion was also involved. The hydroxyl group from a deprotonated water molecular was accounted for neutral charge. The geometry of Hg(II) ion is similar to that of the Zn(II) perchlorate complex with octahedral geometry. The possible structures for the compound [Hg(**16**)(ClO_4)(OH)·H_2O] is depicted in Figure 3.5.37.

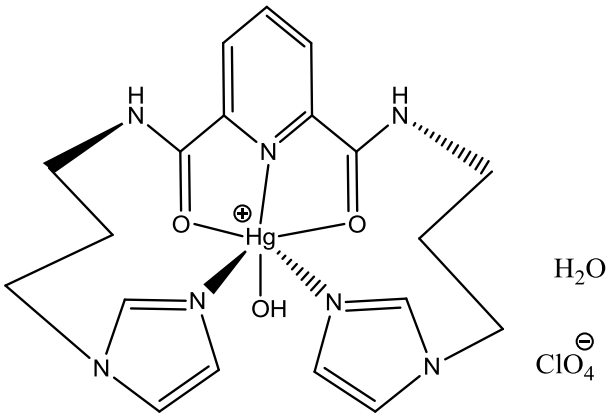

Figure 3.5.37: Possible structure for [Hg(**16**)(ClO_4)(OH)·H_2O].

3.5.8.6 [Ni(**16**)(ClO_4)(OH)·$2H_2O$]

The complex [Ni(**16**)(ClO_4)(OH)·$2H_2O$] is isolated as a green solid. The IR spectrum of compound [Ni(**16**)(ClO_4)(OH)·$2H_2O$] contains a signal ν_{OH} at 3503 cm^{-1} which is due to

some coordinated water molecules in the Ni(II) complex. The carbonyl signal for the amide group is present at 1650 cm^{-1} suggesting the oxygen atoms for the amide group might be coordinating to the Ni(II) ion. The observed signal from the imidazole rings is the analogous to that of Zn(II) perchlorate complex, which suggested the bonding of Ni(II) ion should be consistent with that of the Zn(II) ion. The appearance of a strong broad signal which was due to the perchlorate group is present at 1090 cm^{-1} indicating that the Ni(II) perchlorate complexation had occurred.

Elemental analysis indicated the complex had the formula [Ni(**16**)(ClO_4)(OH)·$2H_2O$]. This would imply that one Ni(II) ion was bonded to the ligand and that one perchlorate ion was also involved as well as one hydroxyl group from a deprotonated water molecular to account for neutral charge. The observation of magnetic moment of the Ni(II) complex at 2.60 B.M. has suggested that the Ni(II) complex adopted an octahedral geometry sphere. The possible structure of compound [Ni(**16**)(ClO_4)(OH)·$2H_2O$] is depicted in Figure 3.5.38.

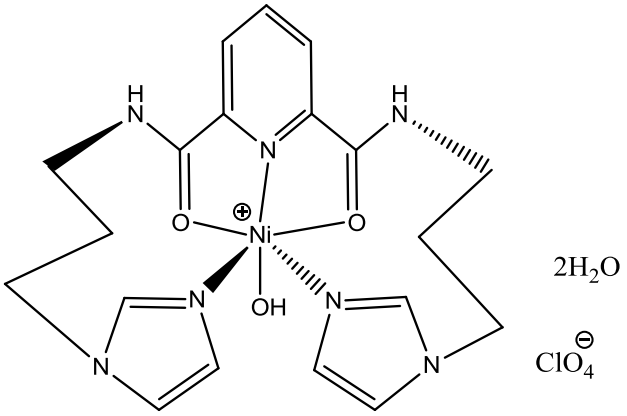

Figure 3.5.38: Possible structure for [Ni(**16**)(ClO_4)(OH)·$2H_2O$].

3.5.8.7 [Ni(**16**)(NO_3)$_2$·MeOH·H_2O]

The complex [Ni(**16**)(NO_3)$_2$·MeOH·H_2O] is obtained as a green solid. In the IR spectrum of compound [Ni(**16**)(NO_3)$_2$·MeOH·H_2O], the appearance of the OH stretch at 3431 cm^{-1} is indicative of coordinated MeOH/H_2O molecules in the complex. The carbonyl signals of amide group are seen at 1656 and 1669 cm^{-1} which has moved from 1673 cm^{-1} in ligand **16**. In addition, the signals of N-H bend are present at 1544 and 1530 cm^{-1}. These two shifts would imply the two carbonyl groups were in different environments. The signal of C=C stretch from the imidazole rings is present at 1530 cm^{-1} which was seen at 1508 cm^{-1} in ligand **16** pointing towards that two nitrogen atoms from the imidazole rings could be coordinated to the Ni(II) ion centre. The observation

of the nitro group which occurs at 1384 cm^{-1} is suggesting the Ni(II) nitrate complexation had occurred.

Elemental analysis indicated the complex had the formula [Ni(**16**)$(NO_3)_2$·MeOH·H_2O]. This would also imply that one Ni(II) ion was bonded to the ligand and that two nitrate ions were also involved to account for the neutral charge. The magnetic moment of Ni(II) nitrate complex is obtained as 3.67 B.M. which indicates that the Ni(II) nitrate complex has a tetrahedral sphere. The possible structure of compound [Ni(**16**)$(NO_3)_2$·MeOH·H_2O] is depicted in Figure 3.5.39.

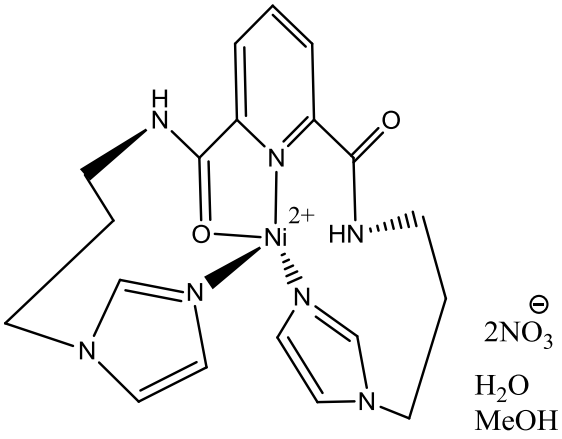

Figure 3.5.39: Possible structure for [Ni(**16**)$(NO_3)_2$·MeOH·H_2O].

3.5.8.8 [Cu(**16**)Cl_2·H_2O·MeOH]

The complex [Cu(**16**)Cl_2·H_2O·MeOH] is formed as a blue solid. The analytical data of complex [Cu(**16**)Cl_2·H_2O·MeOH] for both the IR spectrum and the elemental analysis is very similar to that of [Zn(**16**)Cl_2·$2H_2O$]. This implies that the bonding of the Cu(II) ion is analogous to that of the Zn(II) ion. The one exception for the Cu(II) chloride complex is that the complex has one coordinated water molecule while the Zn(II) complex has two. The magnetic moment of the complex [Cu(**16**)Cl_2·H_2O·MeOH] is 1.77 B.M. The possible structure of complex [Cu(**16**)Cl_2·H_2O·MeOH] is depicted in Figure 3.5.40.

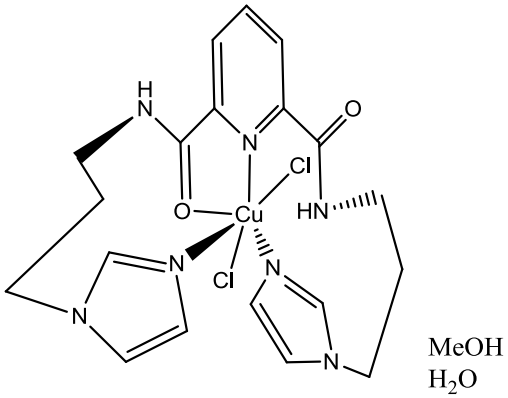

Figure 3.5.40: Possible structure for [Cu(**16**)Cl_2·H_2O·MeOH].

3.5.8.9 [Cu(**16**)$(ClO_4)_2$·H_2O]

The complex [Cu(**16**)$(ClO_4)_2$·H_2O] is isolated as a blue solid. In the IR spectrum of compound [Cu(**16**)$(ClO_4)_2$·H_2O], the observation of OH stretch at 3480 cm^{-1} suggests that the coordinated water molecule is present in the Cu(II) complex. The signal for the amide group is present at 1659 cm^{-1} which has moved from 1673 cm^{-1} in the spectrum of ligand **16**. Therefore, the oxygen atom for the carbonyl group is coordinated to the Cu(II) ion centre. In addition, the classification of the nitrogen atoms from imidazole rings are bonding to the Cu(II) ion centre is the signal from the imidazole rings of the side chains is observed at 1536 cm^{-1} which has moved from 1508 cm^{-1}. The appearance of the perchlorate group at 1099 cm^{-1} as a strong broad signal indicates that the perchlorate complexation had occurred.

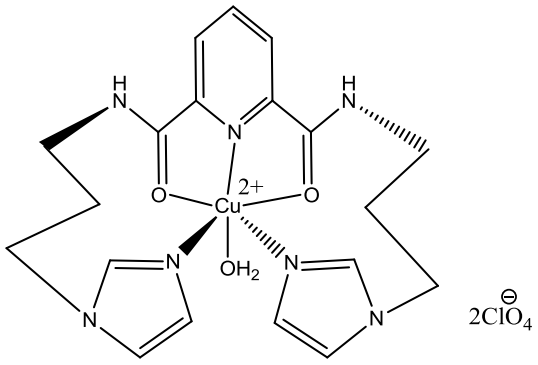

Figure 3.5.41: Possible structure for [Cu(**16**)$(ClO_4)_2$·H_2O].

Elemental analysis indicated the complex had the formula [Cu(**16**)$(ClO_4)_2$·H_2O]. This would also imply that one Cu(II) ion was bonded to the ligand and that two perchlorate ions were also involved to account for the neutral charge. An additional water molecule was occupied in the complex. The magnetic moment of the Cu(II) perchlorate complex

is 1.82 B.M. The geometry of Cu(II) ion is an octahedral. The possible structures of compound [Cu(**16**)(ClO_4)$_2$·H_2O] is depicted in Figure 3.5.41.

3.5.8.10 [Cu(**16**)(NO_3)$_2$·2H_2O]

The complex [Cu(**16**)(NO_3)$_2$·2H_2O] is obtained as a blue solid. The analytical data of either the IR spectrum or the elemental analysis of complex [Cu(**16**)(NO_3)$_2$·2H_2O] obtained are very similar to those of Ni(II) nitrate complex. This implies that the bonding of the Cu(II) ion is analogous to that of the Ni(II) ion as well. The magnetic moment of the Cu(II) nitrate complex is 1.79 B.M. Hence, the proposed structure of complex [Cu(**16**)(NO_3)$_2$·2H_2O] is shown in Figure 3.5.42.

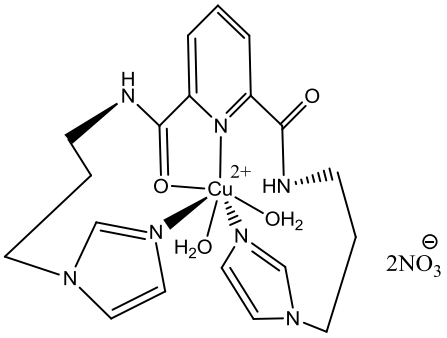

Figure 3.5.42: Possible structure for [Cu(**16**)(NO_3)$_2$·2H_2O].

3.5.8.11 [Co(**16**)Cl_2]

The complex [Co(**16**)Cl_2] is isolated as a blue solid. The signals obtained of the IR spectrum in Co(II) chloride complex is similar to that of Zn(II) chloride complex. The elemental analysis which is also similar would suggest that the bonding of the metal ions in both complexes are analogous. In addition, the magnetic moment of Co(II) chloride complex is obtained as 4.41 B.M. indicating that the geometry of Co(II) complex is an octahedral sphere. Hence, the proposed structure of compound [Co(**16**)Cl_2] is depicted in Figure 3.5.43.

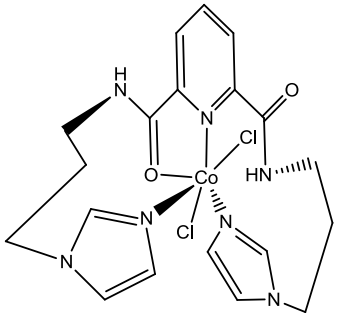

Figure 3.5.43: Possible structure for [Co(**16**)Cl_2].

3.5.8.12 [Co(**16**)(ClO_4)$_2$]

The complex [Co(**16**)(ClO_4)$_2$] is isolated as a light pink solid. In the IR spectrum of compound [Co(**16**)(ClO_4)$_2$], two bands which are observed at 1675 and 1660 cm^{-1} suggests that the two amide groups are in different environments. The signal from the imidazole rings is represented as a strong broad peak at 1539 cm^{-1} which has moved from 1508 cm^{-1} ligand **16** suggesting that the two nitrogen atoms from imidazole rings could be coordinated to the Co(II) ion centre. The appearance of a strong broad signal at 1108 cm^{-1} which is due the perchlorate group provides further evidence for the perchlorate complexation.

Elemental analysis indicated that the complex had the formula [Co(**16**)(ClO_4)$_2$]. This should imply that one Co(II) ion was bonded to ligand and that the two perchlorate were also involved to account for neutral charge. The geometry of Co(II) ion is proposed to be four-coordinate and the magnetic moment of Co(II) complex occurring at 4.19 B.M. is also an indicative of a tetrahedral configuration. The possible structure of compound [Co(**16**)(ClO_4)$_2$] is depicted in Figure 3.5.44.

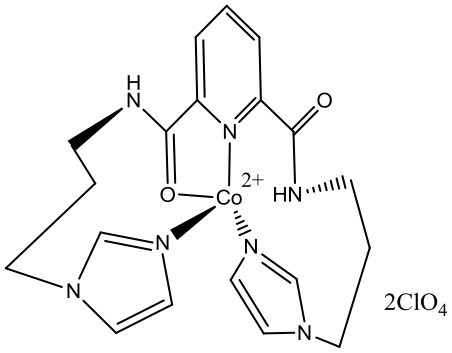

Figure 3.5.44: Possible structure for [Co(**16**)(ClO_4)$_2$].

3.6 Section 4

3.6.1 Preparation of triformylphloroglucinol 17 and ligands 18 - 21

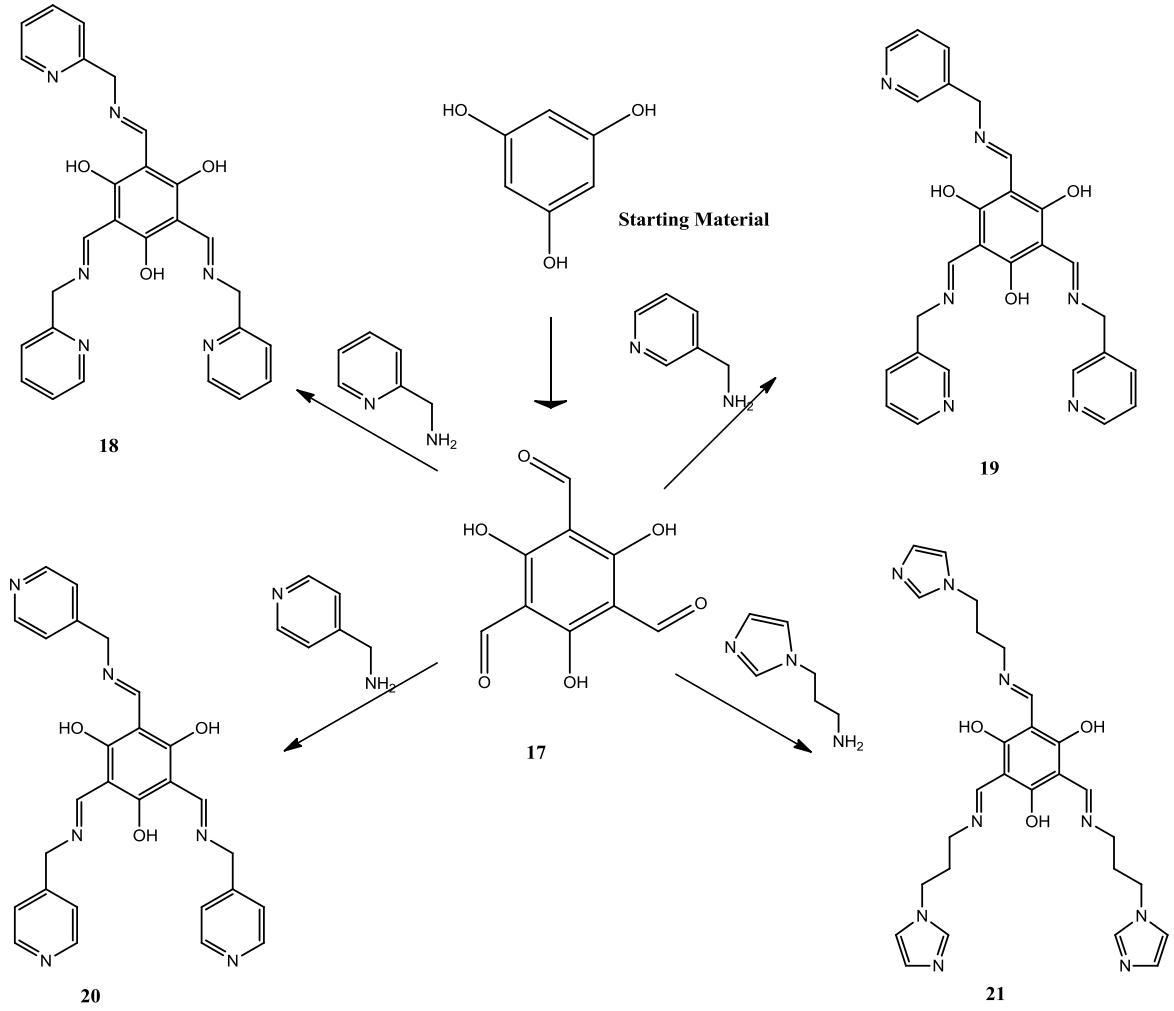

Figure 3.6.1: The formation of triformylphloroglucinol **17** and ligands **18 – 21**.

The formation of compound triformylphloroglucinol **17** in the presence of trifluoroacetic acid and hexamethylenetetramine, as shown in Figure 3.6.1, is reported by Chong and co-workers.[134] This type of reaction is named the Duff formation[147-149] and the mechanism is shown in Figure 3.6.2. The compound **17** can be used for synthesising four new ligands (**18**-**21**) as outlined in Figure 3.6.1. All ligands were synthesised using the same reactions strategy, which was one equivalent of compound **17**, three equivalents of appropriated amine precursors and ten equivalents of anhydrous $MgSO_4$ in DCM with stirring for 12 hours at room temperature. The reason for this

strategy could be seen from **3.2** Schiff base ligand formation and hydrolysis. The starting material phloroglucinol is commercially available.

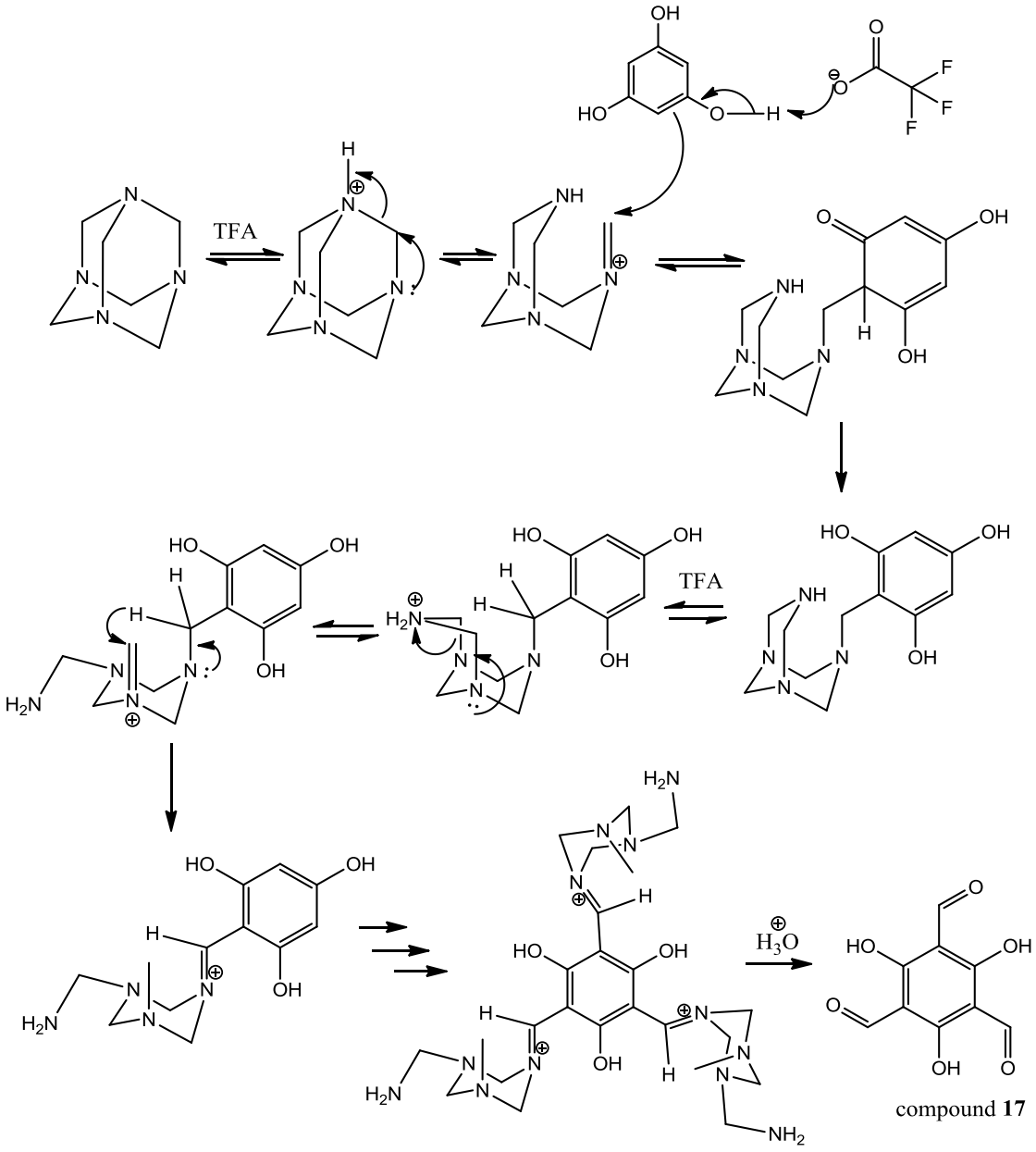

Figure 3.6.2: The mechanism of formation of compound **17**.

3.6.2 Highly stable keto-enamine ligands

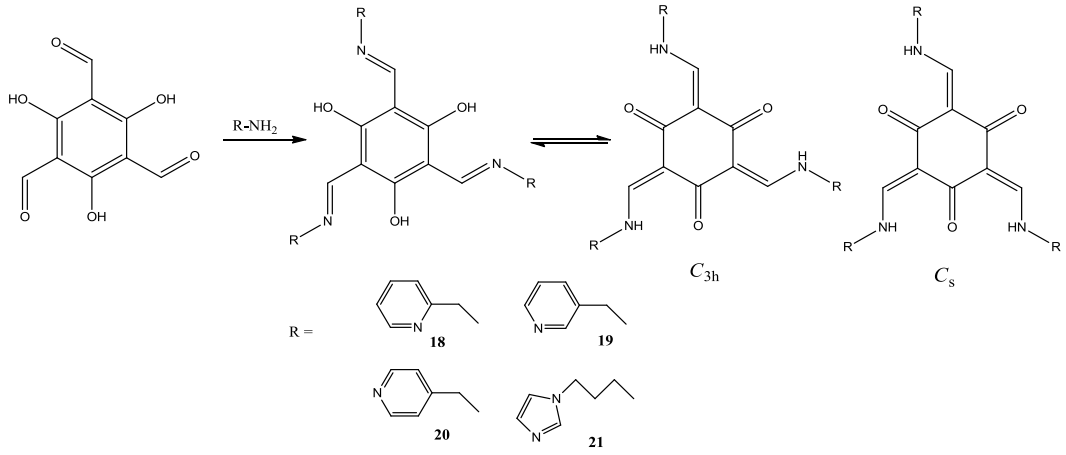

Figure 3.6.3: Highly stable Keto-Enamine ligands.

The three new phloroglucinol-based ligands were prepared by Schiff-base condensation of 2,4,6-triformylphloroglucinol with three equivalents of the appropriate amines. 2,4,6-Triformylphloroglucinol is accessible in one step synthesis through the Duff formation from phloroglucinol. The subsequent reaction with different primary amines in DCM solutions at ambient temperature could generate high yields of ligands. The ^{1}H NMR spectra of all imine-based ligands are surprisingly complicated. Whereas singlets were expected for the imine and phenol protons, the spectra showed multiple peaks between 8.2–8.3 and 11.1–11.6 ppm. The ^{1}H NMR spectra show that exclusively the all keto-enamine form of the four ligands are present in a mixture of two conformational isomers with either C_{3h} or C_s symmetry of the core fragment as shown in Figure 3.6.3. Moreover, this is corroborated by the ^{13}C NMR spectra, as the carbonyl resonances of the central ring are observed in the region between 182 and 188 ppm, which is characteristic of the keto isomer.[150]

3.6.3 Ligand 18

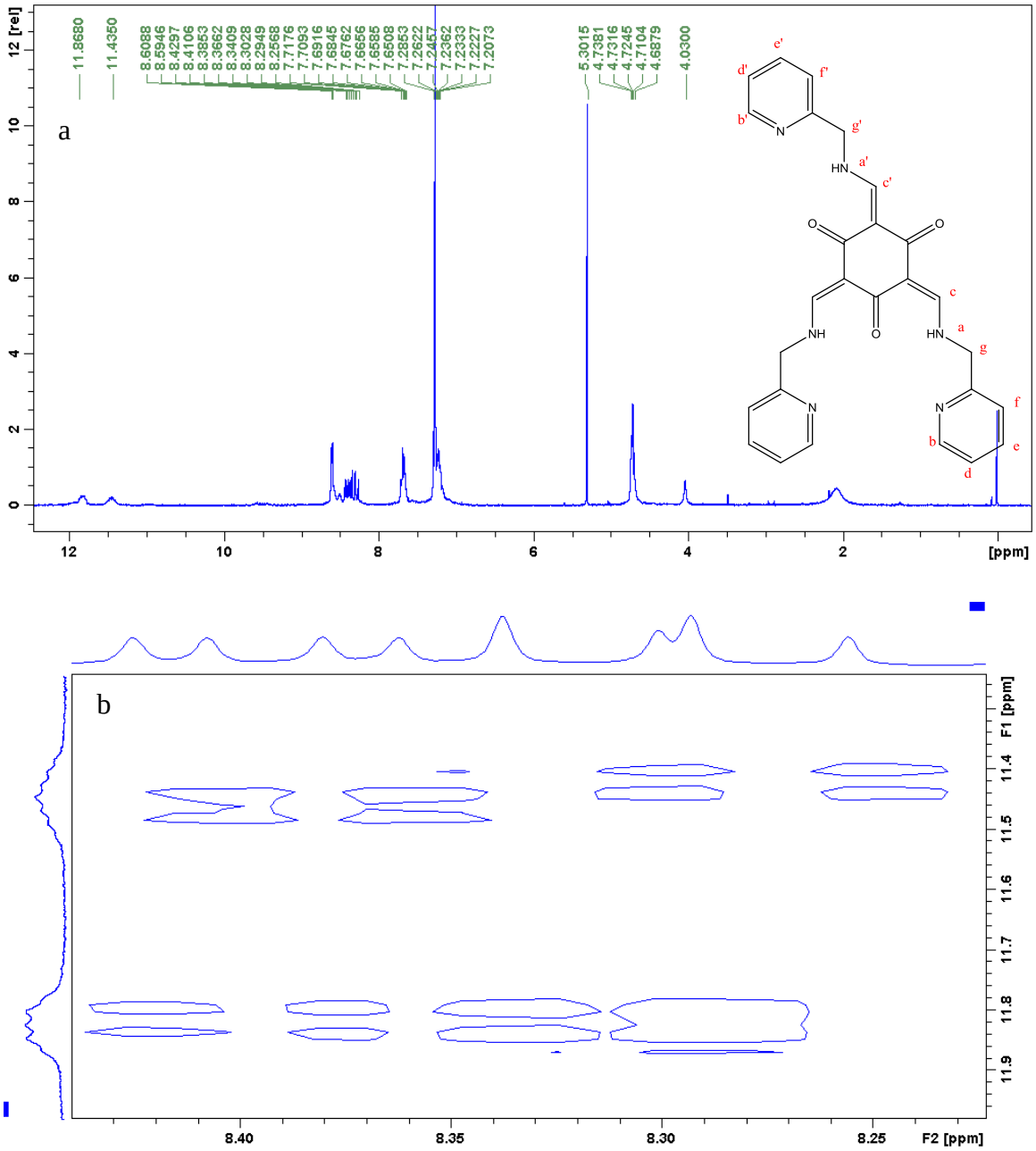

Figure 3.6.4: a) The ^{1}H NMR spectrum of ligand **18** in $CDCl_3$; b) The COSY spectrum of the protons NH and coupling protons CH in ligand **18**.

The ligand **18** is formed as a yellow oil. The ^{1}H NMR spectrum of ligand **18** is shown in Figure 3.6.4. The appearance of the two signals of the NH protons Ha and Ha' at 11.86 and 11.43 ppm and the presenting multiplets from 8.25 to 8.43 ppm for the protons Hc and Hc' are suggested that the ligand **18** is stable in the keto formation. These several multiplets would imply that the ligand **18** would be a mixture of C_{3h} and C_s symmetry structures. In addition, the signals of the pyridine rings protons, both protons Hb and Hb' are observed as a doublet at 8.60 ppm. Protons Hd and Hd' appear as a multiplet from

7.65 to 7.71 ppm. It appears a multiplet from 7.20 to 7.28 ppm which is due four protons signals He, He' and Hf, Hf'. The signals of the bridging methylene protons Hg and Hg', appear as multiplet from 4.69-4.74 ppm.

The ^{13}C NMR spectrum of ligand **18** contains a signal of carbonyl carbon at 185.5 ppm. It appears three signals at 122.8, 121.4 and 121.2 ppm which are assigned to the alkene carbons. From observations, it would suggest that the ligand **18** is stable in keto-formation.

The IR spectrum of ligand **18** is tested under DCM. It contains a weak band of C=O stretch at 1696 cm^{-1} indicates again that the ligand **18** is in the keto-formation. The appearance of a very strong band at 1609 cm^{-1} is due the stretches of the C=C alkene, the C=N of pyridine rings and C=O ketone. The N-H bend is observed at 1552 cm^{-1} as a weak signal. The band C=C stretch representing for the pyridine rings appears at 1422 cm^{-1}.

The mass spectrum suggests the ligand **18** is pure.

3.6.4 Metal complexes of 18

Metal complexes reactions of ligand **18** with various metal(II) salts were carried out in MeOH. The reactions were carried out in MeOH for 2 hours stirring at room temperature. The resulting coloured solids were collected by filtration.

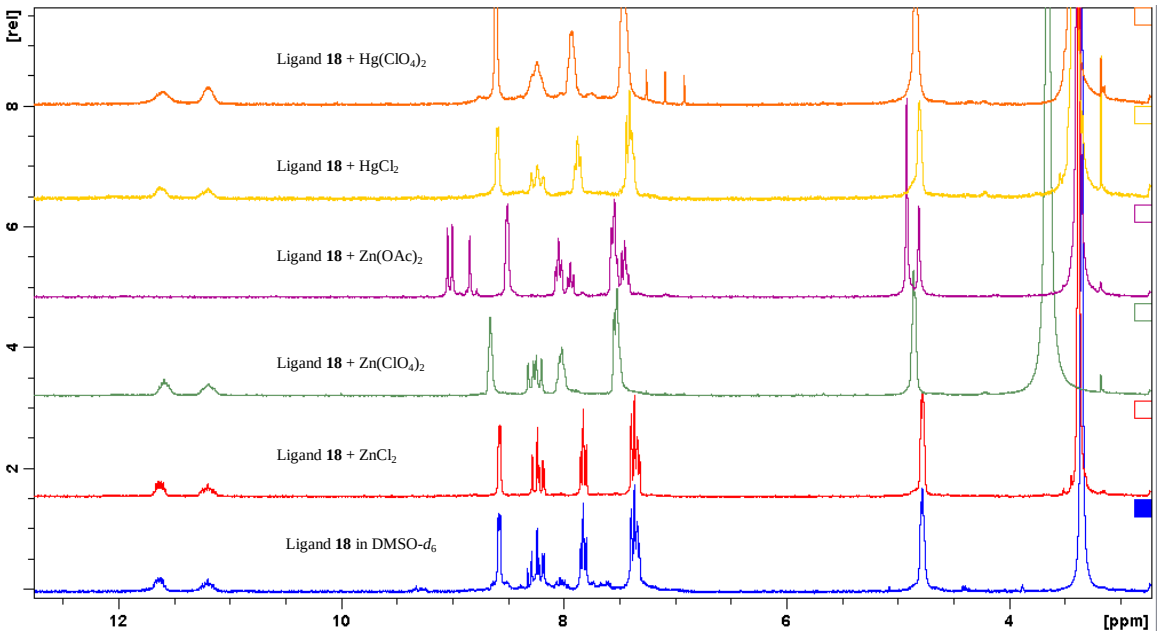

Figure 3.6.5: A comparison of ^{1}H NMR spectra of ligand **18** and its corresponding ZnX_2 (X = Cl, ClO_4, OAc) and HgX_2 (X = Cl, ClO_4) complexes in DMSO-d_6.

Table 3.6.1: A comparison of the analytical data of the IR spectra between the ligand **18** and its corresponding complexes (symbol '/' means no obtained signal; block = obscured by OH stretch; unit = cm^{-1}).

	OH	NH stretch	C=C, C=N	N-H bend	C=C (py)
Ligand **18**			1609	1552	1422
$ZnCl_2$	3451	3224	1607(br)	1547	1440
$Zn(ClO_4)_2$	3434	block	1607 (br)	1546	1433
$Zn(OAc)_2$	3432	/	1607 (br)	/	1443
$HgCl_2$	3431	3240	1610 (br)	1543	1438
$Hg(ClO_4)_2$	3438	block	1606 (br)	1549	1438
$CuCl_2$	3429	block	1599 (br)	1567	1445
$CoCl_2$	3432	block	1615 (br)	1569	1446
$Co(ClO_4)_2$	3427	block	1607 (br)	1569	1446

The comparison of the IR spectra between the ligand **18** and its corresponding complexes is shown in Table 3.6.1. The data of Zn(II) acetate complex in red is due to it has been switched back to the enol-formation complex. There were no changes in the bands of the pyridine rings in the Hg(II) chloride and perchlorate complexes implying that the bonding in these complexes are not through the nitrogen atoms of the pyridine rings. With the other complexes such as Zn(II), Cu(II) and Co(II) complexes, the bonding through the pyridine rings nitrogen atoms. Moreover, in the IR spectra of the various metal complexes of ligand **18**, the bands due to the C=N, C=C or C=O stretching vibrations partly overlap resulting in a broad band centered at about 1600 cm^{-1}. Even the Zn(II) acetate complex which was back to enol-formation, the C=N imine moieties also was occurred at around 1600 cm^{-1}. Therefore these bands at around 1600-1610 cm^{-1} cannot be unambiguously assigned to an individual stretching vibration.[150]

3.6.4.1 $[Zn_2(\mathbf{18})Cl_4 \cdot H_2O]$

The complex $[Zn_2(\mathbf{18})Cl_4 \cdot H_2O]$ is formed as a yellow solid. The ^1H NMR spectrum of compound $[Zn_2(\mathbf{18})Cl_4 \cdot H_2O]$ is shown in Figure 3.6.5 (in red). The spectrum of Zn(II) chloride complex is similar to its corresponding ligand **18** which indicates that a weak bonding could be occurred in this complex.

The IR spectrum of compound $[Zn_2(\mathbf{18})Cl_4{\cdot}H_2O]$ contains a band of ν_{OH} stretch at 3451 cm^{-1} which suggests coordinated water molecule could be present in the Zn(II) complex. A band representing for the NH stretch at 3224 cm^{-1} is indicative of the complex in the keto-formation. A very strong broad signal occurs at 1607 cm^{-1} which are due to the stretches of C=C, C=N and C=O groups which was seen to have a slight change from the original one at 1609 cm^{-1} from ligand **18**. The appearance of the C=C stretch from the pyridine rings at 1440 cm^{-1} indicates that the nitrogen atoms from the pyridine rings are coordinated to the metal ion centre.

Elemental analysis indicated that the complex had the formula $[Zn_2(\mathbf{18})Cl_4{\cdot}H_2O]$. This would also imply that two Zn(II) ions were bonded to the ligand and that four chloride ions were also involved to account for neutral charge. The bonding of the Zn(II) ion is through nitrogen atoms of the either pyridine rings or the secondary amines as well as two chloride ions. Hence, the possible structure for compound $[Zn_2(\mathbf{18})Cl_4{\cdot}H_2O]$ is depicted in Figure 3.6.6.

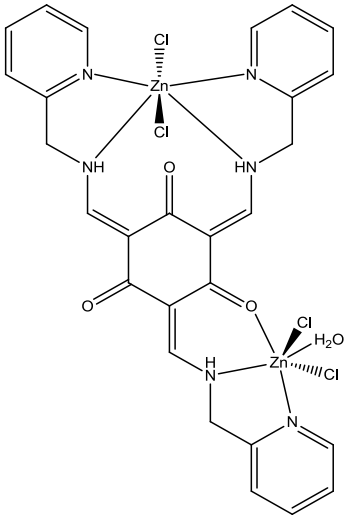

Figure 3.6.6: Possible structure for $[Zn_2(\mathbf{18})Cl_4{\cdot}H_2O]$.

3.6.4.2 $[Zn_3(\mathbf{18})_2(ClO_4)_6{\cdot}2H_2O]$

The complex $[Zn_3(\mathbf{18})_2(ClO_4)_6{\cdot}2H_2O]$ is obtained as a yellow solid. The ^1H NMR spectrum of compound $[Zn_3(\mathbf{18})_2(ClO_4)_6{\cdot}2H_2O]$ is shown in Figure 3.6.5 (in green). The NH protons Ha and Ha' are observed at 11.58 and 11.18 ppm as two broad signals which were seen at 11.57-11.67 ppm and 11.12-11.26 ppm as two multiplets, respectively, form the free ligand. The signals of alkenes protons Hc and Hc' are similar in both the ligand and the complex. Several visible chemical shifts occur at the signals of the pyridine rings protons, Hb and Hb', are observed at 8.65 ppm in comparison to

the original position at 8.57 ppm. Protons Hd and Hd' appear at 8.02 ppm as a broad singlet which have shifted from 7.82 ppm as triple triplets from ligand **18**. Protons He/He' and Hf/Hf' are present together at 7.52 ppm as a broad singlet comparing to the original two signals at 7.31-7.39 ppm as a multiplet in ligand **18**. These observations imply that the nitrogen atoms from the pyridine rings are coordinated to the metal ion centre. The signals of the bridging methylene protons Hg and Hg' are observed at 4.85 ppm which have moved from 4.77 ppm from ligand **18**.

The IR spectrum of the complex $[Zn_3(\mathbf{18})_2(ClO_4)_6{\cdot}2H_2O]$ is similar to that of the Zn(II) chloride complex which points towards the donating atoms of the Zn(II) perchlorate complex should be analogous to those of Zn(II) chloride complex as well. In addition, the appearance of the perchlorate group at 1108 cm^{-1} confirms the Zn(II) perchlorate complexation.

The elemental analysis indicated that the complex had the formula $[Zn_3(\mathbf{18})_2(ClO_4)_6{\cdot}2H_2O]$. This would also imply that three Zn(II) ions were bonded to two ligands and that six perchlorate ions were also involved to account for the neutral charge. The bonding of each Zn(II) ions is through four nitrogen atoms where two from the pyridine rings and the other two from the secondary amines. The possibility of the C=O forming a bond to the Zn(II) ion cannot be ruled out. The possible structure of compound $[Zn_3(\mathbf{18})_2(ClO_4)_6{\cdot}2H_2O]$ is depicted in Figure 3.6.7.

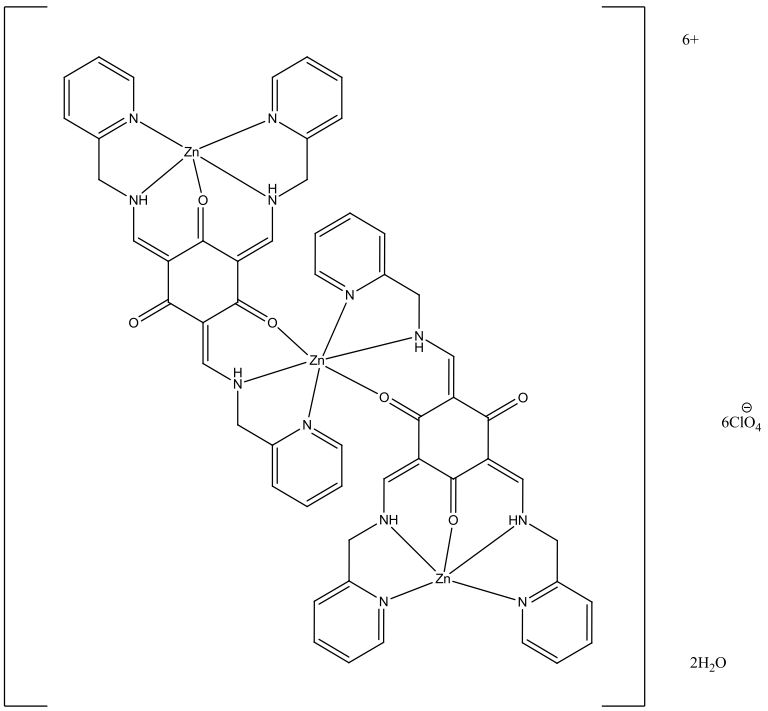

Figure 3.6.7: Possible structure for $[Zn_3(\mathbf{18})_2(ClO_4)_6{\cdot}H_2O]$.

3.6.4.3 [Zn_4(**18**)$(OAc)_5$]

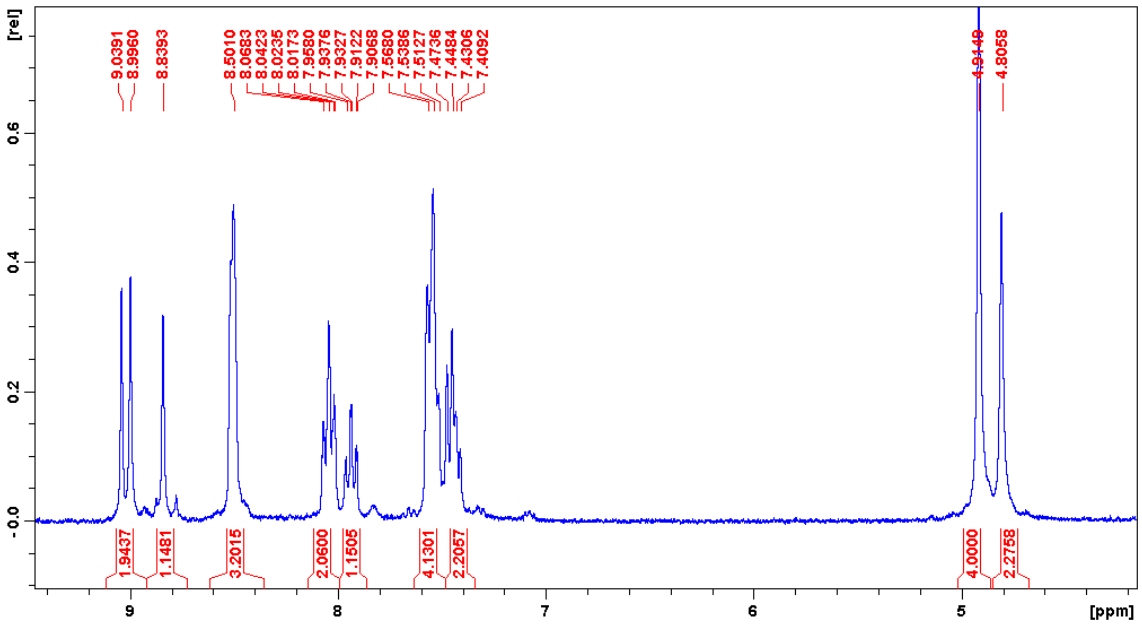

Figure 3.6.8: The ^{1}H NMR spectrum of [Zn_4(**18**)$(OAc)_5$] in DMSO-d_6.

The complex [Zn_4(**18**)$(OAc)_5$] is formed as a yellow solid. The ^{1}H NMR spectrum of compound [Zn_4(**18**)$(OAc)_5$] is shown in both Figure 3.6.5 (in purple) and Figure 3.6.8. The disappearance of the NH protons Ha/Ha' and the alkene protons Hc/Hc' result that the Zn(II) complex has been switched back to the enol-formation complex, and the phenol protons were deprotonated by the Zn(II) ion. In addition, the bridging methane protons are observed as two singlets at 4.91 and 4.80 ppm, respectively, and the ratio of the integrals of these two singlets is 2:1. This suggests that the complex was formed by C_s enol-isomer. The signals protons of the pyridine rings also confirm this results. Three signals appears at 9.04, 8.99 and 8.84 ppm, respectively, indicating three different type of imine protons in Zn(II) complex. While for the signals of pyridine rings protons, protons Hb/Hb' are observed as a broad signal at 8.50 ppm, Hd/Hd' occur at 8.04 and 7.93 ppm, respectively. The signals of protons He/He' and Hf/Hf' resonate at 7.56 and 7.45 ppm as two multiplets.

In the IR spectrum of compound [Zn_4(**18**)$(OAc)_5$] the disappearance of the N-H bend at around 1550 cm^{-1} supports the Zn(II) acetate complex is in enol-isomer formation. The appearance of a band at 1443 cm^{-1} which is due to the C=C stretch pyridine rings indicates that the nitrogen atoms from pyridine rings could be binding to Zn(II) ions centre.

Elemental analysis indicates that the complex had the formula $[Zn_4(\mathbf{18})(OAc)_5]$. This would also imply that four Zn(II) ions were bonded to the ligand and that five acetate group ions were also involved. The ligand itself was deprotonated to account for the neutral charge. The possible structure of compound $[Zn_4(\mathbf{18})(OAc)_5]$ is depicted in Figure 3.6.9.

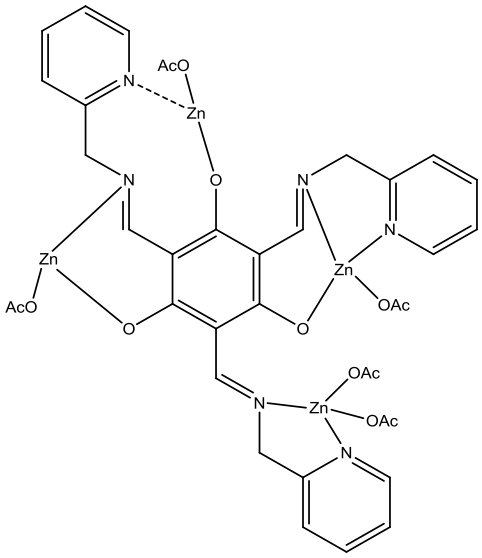

Figure 3.6.9: Possible structure for $[Zn_4(\mathbf{18})(OAc)_5]$.

3.6.4.4 $[Hg_3(\mathbf{18})_2Cl_6]$

The complex $[Hg_3(\mathbf{18})_2Cl_6]$ is formed as a yellow solid. The ^1H NMR spectrum of compound $[Hg_3(\mathbf{18})_2Cl_6]$ is shown in Figure 3.6.5 (in yellow). The spectrum is similar to that of Zn(II) chloride complex.

The IR spectrum of compound $[Hg_3(\mathbf{18})_2Cl_6]$ contains ν_{NH} stretch at 3240 cm^{-1} suggesting the complex is stable in keto-formation and the nitrogen atoms from the secondary amines could be coordinated to the Hg(II) ion centre. It appears a very strong and broad signal at 1610 cm^{-1} which is due to several stretches such as conjugated ketone, alkene and C=N from the pyridine rings. The small difference of the band for the C=C stretch between the free ligand (1422 cm^{-1}) and the complex (1428 cm^{-1}) suggests that the pyridyl nitrogen atoms are not binding to the metal ion centre. So, this broad band at 1610 cm^{-1} would suggest that the bonding of the Hg(II) ion is through two nitrogen atoms from the secondary amines and might be one or two oxygen atoms from the ketone groups.

The elemental analysis indicated that the complex had the formula $[Hg_3(\mathbf{18})_2Cl_6]$. This would also imply that three Hg(II) ions were bonded to two ligands and that six chloride

ions were also involved to account for the neutral charge. The bonding of the each Hg(II) ions is through two nitrogen atoms of the secondary amines and an oxygen atom from the keto group. The possible structure of compound [Hg_3(**18**)$_2Cl_6$] is depicted in Figure 3.6.10.

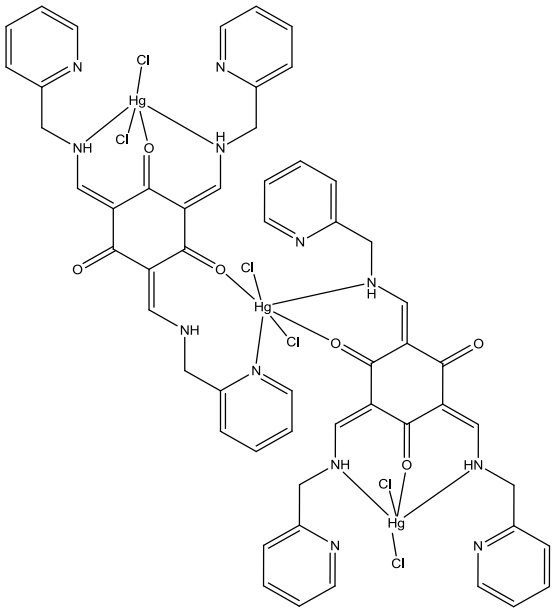

Figure 3.6.10: Possible structure for [Hg_3(**18**)$_2Cl_6$].

3.6.4.5 [Hg_3(**18**)$_2(ClO_4)_6$]

The complex [Hg_3(**18**)$_2(ClO_4)_6$] is isolated as a yellow solid. The ^{1}H NMR spectrum of compound [Hg_3(**18**)$_2(ClO_4)_6$] is shown in Figure 3.6.5 (in orange). The spectra of either the ^{1}H NMR spectrum or the IR spectrum of Hg(II) perchlorate complex are found to be similar to those spectra of Hg(II) chloride complex. The only exception is the appearance of the perchlorate group at 1108 cm^{-1} which confirms the metal complexation. This similarity implies that the bonding of the Hg(II) ion should be similar to that of the perchlorate complex.

The elemental analysis indicated that three Hg(II) ions were bonded to two ligands and that six perchlorate ions were also involved to account for the neutral charge. The possible structure of compound [Hg_3(**18**)$_2(ClO_4)_6$] is depicted in Figure 3.6.11.

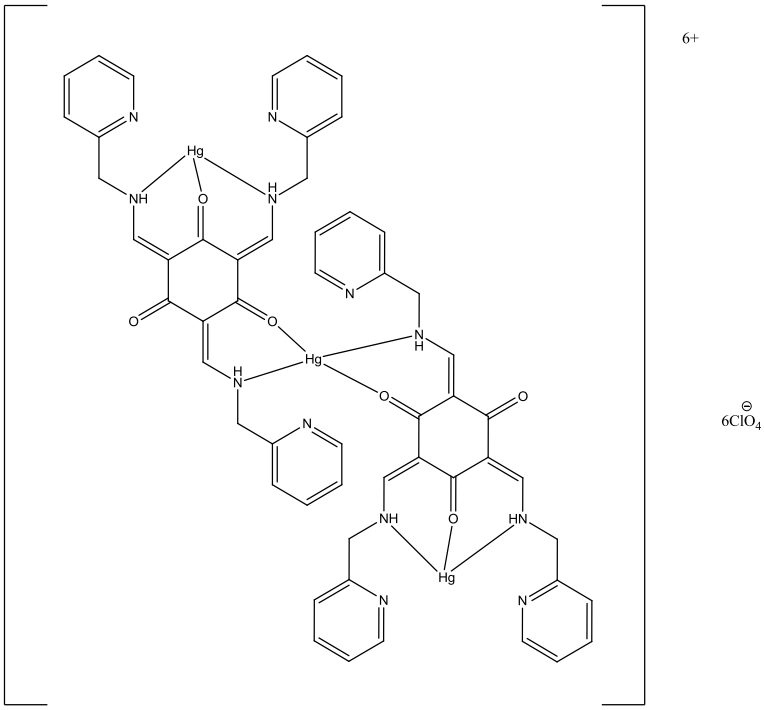

Figure 3.6.11: Possible structure for $[Hg_4(\mathbf{18})_3(ClO_4)_8]$.

3.6.4.6 $[Cu_2(\mathbf{18})Cl_4 \cdot MeOH \cdot 3H_2O]$

The complex $[Cu_2(\mathbf{18})Cl_4 \cdot MeOH \cdot 3H_2O]$ is formed as a green solid. The IR spectrum of compound $[Cu_2(\mathbf{18})Cl_4 \cdot MeOH \cdot 3H_2O]$ contains a band of ν_{OH} stretch at 3431 cm^{-1} indicating some coordinated $MeOH/H_2O$ molecules are present in the Cu(II) complex. The N-H stretch was blocked by OH stretch in the Cu(II) complex. The N-H bend is observed at 1568 cm^{-1} which has moved from 1552 cm^{-1} in ligand **18** indicating that the nitrogen atoms from secondary amines could be binding to Cu(II) ion centre. A strong and broad band at 1599 cm^{-1} is due to several stretches such as (alkene C=C, pyridine C=N) in comparison to the original peaks at 1609 cm^{-1} from ligand **18** indicating that either the oxygen from ketone groups or the nitrogen atoms from the amines might be coordinated to Cu(II) ion centre. The C=C stretch from the pyridine rings appears at 1445 cm^{-1} in comparison to the original band at 1422 which suggests that the two pyridyl nitrogens are binding to the metal ion centre.

The elemental analysis indicated that two Cu(II) ions were bonded to the ligand and that four chloride ions were also involved to account for the neutral charge. The bonding of the Cu(II) ion is *via* four nitrogen atoms where two of the atoms from the pyridine rings and the other two atoms from the amine groups. The magnetic moment of the Cu(II) chloride complex is 1.95 B.M. The possible structure for compound $[Cu_2(\mathbf{18})Cl_4 \cdot MeOH \cdot 3H_2O]$ is depicted in Figure 3.6.12.

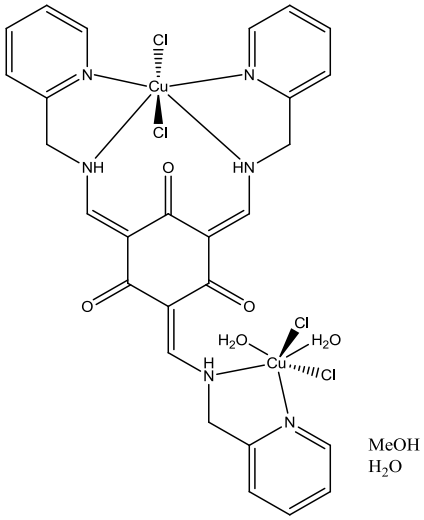

Figure 3.6.12: The proposed structure of complex [Cu_2(**18**)Cl_4·MeOH·3H_2O].

3.6.4.7 [Co_2(**18**)Cl_4·2MeOH]

The complex [Co_2(**18**)Cl_4·2MeOH] is obtained as a dark yellow solid. The IR spectrum of compound [Co_2(**18**)Cl_4·2MeOH] contains a signal of ν_{OH} stretch at 3432 cm^{-1} indicates some coordinated MeOH could be in Co(II) complex. The N-H stretch was blocked by OH stretch. In addition, a very strong broad signal is occurring at 1607 cm^{-1} which is due to the C=C group and the C=N group from the pyridine rings which was seen to have a slight change from the original one at 1609 cm^{-1} from ligand **18**. And the appearance of the band representing for C=C stretch for the pyridine rings at 1499 cm^{-1} points towards the pyridyl nitrogens are coordinated to the metal ion centre. The magnetic moment of the complex is obtained as 2.83 B.M. which suggests that the both high-spin and low-spin Co(II) ions are occurred in this complex. And the geometry of the Co(II) ions could be octahedral.

The elemental analysis indicated that the complex had the formula [Co_2(**18**)Cl_4·2MeOH]. This would also imply that two Co(II) ions were bonded to the ligand and that four chloride ions were also involved to account for the neutral charge. The bonding of the Co(II) complex is similar to that of Co(II) chloride complex. The possible structure for compound [Co_2(**18**)Cl_4·2MeOH] is depicted in Figure 3.6.13.

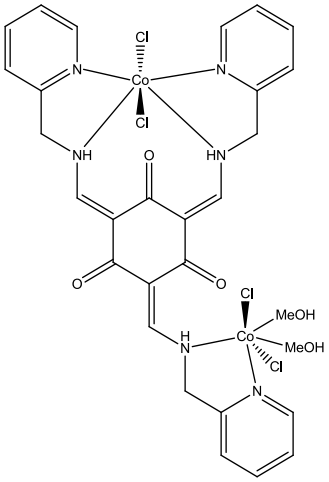

Figure 3.6.13: Possible structure for [Co_2(**18**)Cl_4·2MeOH].

3.6.4.8 [Co(II)Co(III)(**18**)$(OH)_4(ClO_4)$]

The complex [Co(II)Co(III)(**18**)$(OH)_4(ClO_4)$] is formed as a dark yellow solid. The IR spectrum of compound [Co(II)Co(III)(**18**)$(OH)_4(ClO_4)$] is found to be similar to that of Co(II) chloride complex with the only one exception of the appearance of the band for the perchlorate group which are indicative of the metal complexation and the similarity of the bonding in both complexes. The magnetic moment of the complex is 0.67 B.M. This suggests that two different cobalt ions are present which are diamagnetic Co(III) ion and low spin Co(II) ion in the complex.

The elemental analysis indicated that two cobalt ions were bonded to the ligand and that one perchlorate ion and four hydroxyl groups from deprotonated water molecules were also involved to account for the neutral charge. The possible structure for compound [Co(II)Co(III)(**18**)$(OH)_4(ClO_4)$] is depicted in Figure 3.6.14.

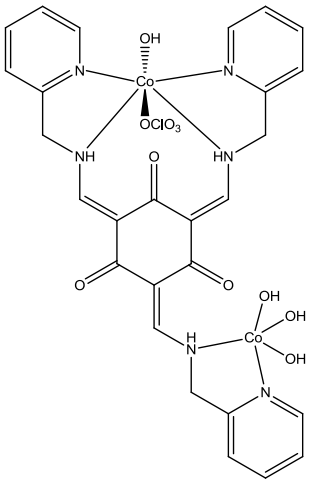

Figure 3.6.14: Possible structure for [Co(II)Co(III)(**18**)$(OH)_4(ClO_4)$].

3.6.5 Ligand 19

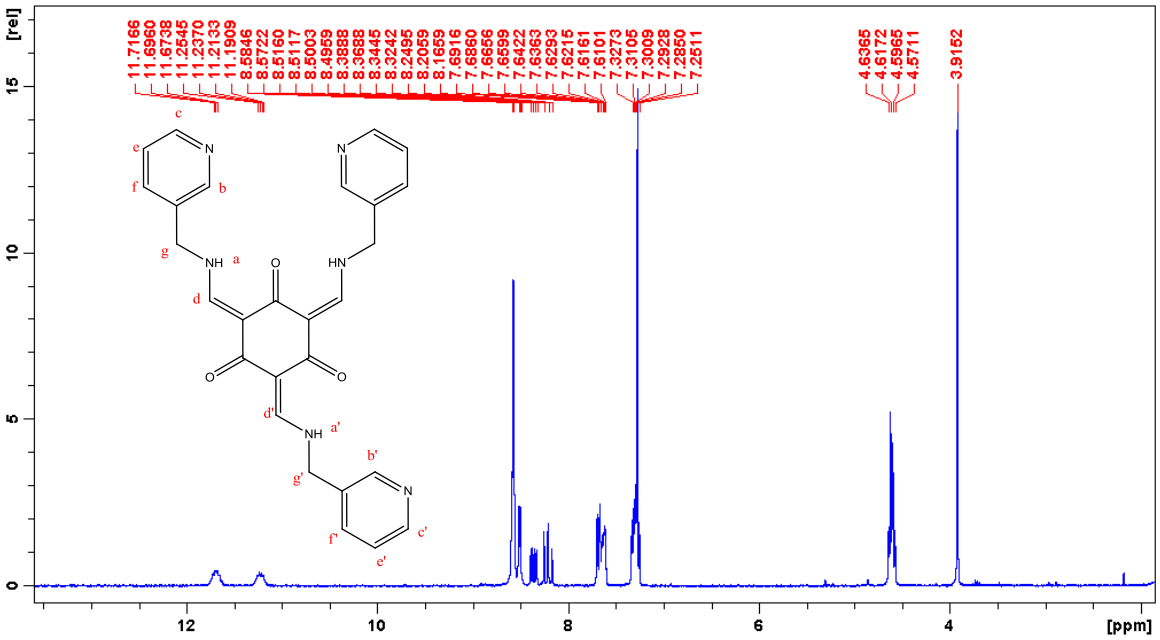

Figure 3.6.15: The ^{1}H NMR spectrum of ligand **19** in $CDCl_3$.

The ligand **19** is formed as a yellow oil. The ^{1}H NMR spectrum of ligand **19** is shown in Figure 3.6.15. The signals of amine protons Ha/Ha' appears as two multiplets at 11.69 and 11.22 ppm, respectively, suggesting the ligand is in keto-formation. And the signals of alkenes protons Hd/Hd' are observed as a quartet and triplet at 8.36 and 8.25 ppm indicating that the ligand **19** are containing both C_{3h} isomer and C_s isomer (Figure 3.6.3). The signals representing for the pyridine rings protons, Hb/Hb', are present at 8.57 ppm as a sharp peak. Proton Hd appears as a doublet at 8.58 ppm which is very close to that of protons Hb/Hb', proton Hd' is observed at 8.50 ppm as a doublet. The signals of protons He/He' appear as a multiplet from 7.25-7.32 ppm and Hf/Hf' resonate as a doublet at 7.68 ppm, respectively.

The ^{13}C NMR spectrum of ligand **19** contains a signal of carbonyl carbon at 185.3 ppm further confirming the keto-formation of ligand **19**.

The IR spectrum of ligand **19** is run under the DCM. The N-H bend is observed at 1553 cm^{-1} as a weak band. A sharp strong band appears at 1607 cm^{-1} which is due to several stretches such as alkene C=C and pyridine C=N and ketone C=O. In addition, the band representing for the C=C stretch of pyridine rings occurs at 1423 cm^{-1}.

3.6.6 Metal complexes of 19

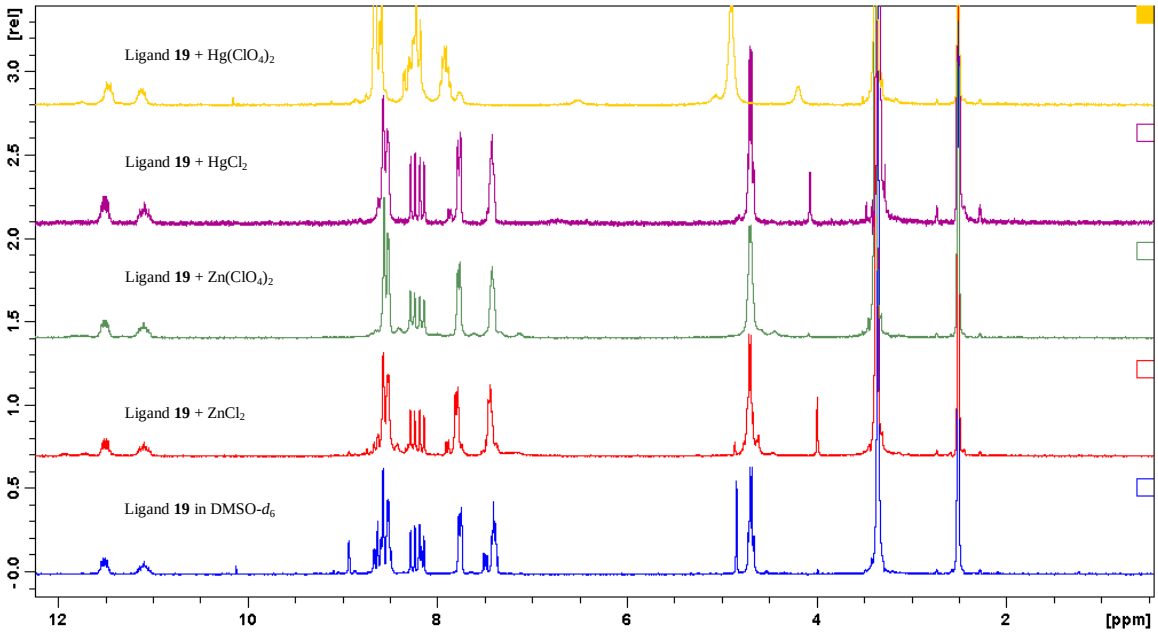

Figure 3.6.16: A comparison of ^{1}H NMR spectra of ligand **19** with its corresponding ZnX_2 and HgX_2 (X = chloride/perchlorate) complexes in DMSO-d_6.

Table 3.6.2: A comparison of the analytical data of the IR spectra between the ligand **19** and its corresponding complexes (symbol '/' means no obtained signal).

	OH	NH stretch	C=C, C=N	NH bend	Pyridine C=C
ligand **19**	/	/	1607	1553	1423
$ZnCl_2$	3435	3240	1606 (br)	1551	1438
$Zn(ClO_4)_2$	3427	3235	1607 (br)	1548	1436
$HgCl_2$	3435	3233	1607 (br)	1546	1434
$Hg(ClO_4)_2$	3460	3234	1607 (br)	1549	1446
$NiCl_2$	3377	3237	1603 (br)	1521 (br)	1432
$Ni(ClO_4)_2$	3405	3238	1604 (br)	1521 (br)	1434
$Ni(OAc)_2$	3387	3232	1593 (br)	1519 (br)	1431
$CuCl_2$	3417	3247	1603 (br)	1539	1435
$Cu(OAc)_2$	3429	3243	1593 (br)	1502 (br)	1428
$Cu(NO_3)_2$	3420	3243	1591 (br)	1505 (br)	1434
$Cu(ClO_4)_2$	3438	3260	1602 (br)	1505 (br)	1436
$CoCl_2$	3406	3227	1603 (br)	1542 (br)	1432
$Co(ClO_4)_2$	3431	3237	1606 (br)	1543 (br)	1434

Metal complex reactions of ligand **19** with various metal(II) salts were carried out in MeOH. The reactions were carried out by stirring the ligand and the appropriate metal salts at room temperature for 2 hours in MeOH. The resulting coloured solids were collected by filtration.

The comparison of the IR spectra of the ligand **19** and its metal complexes is shown in Table 3.6.2. This comparison shows that it is not easy to figure out the specific change between the complexes and the ligand. But it is still indicative of some results. All the complexes are in keto-formation contributed by the fact that the appearance of the NH stretch and bend. The bonding of the metal ion in all metal complexes is through two nitrogen atoms of the pyridine rings due to the bands of C=C stretch of the pyridine rings have a difference about 10-15 cm^{-1} between the complexes and the ligands. The nitrogen atoms of the secondary amines are not coordinated to the metal ion centre in the Zn(II), Hg(II) and Co(II) complexes as well as the Cu(II) chloride complex as no changes occurring at the N-H bend, while in the other Ni(II) and Cu(II) complexes, the nitrogen atoms could be either coordinated to the metal ion centre or forming hydrogen bonds with some solvent molecules. Moreover, in the IR spectra of the various metal complexes of ligand **19**, the bands due to the C=N and C=C stretching vibrations partly overlap resulting in a broad band centered at about 1600 cm^{-1}. Therefore these bands at around 1600-1610 cm^{-1} cannot be unambiguously assigned to an individual stretching vibration.

3.6.6.1 [Zn_2(**19**)Cl_4]

The complex [Zn_2(**19**)Cl_4] is formed as an off-white solid. The ^{1}H NMR spectrum of compound [Zn_2(**19**)Cl_4] is shown in Figure 3.6.16. The spectrum of the Zn(II) complex is similar to the free ligand **19** which indicates that a weak bonding could be occurring between ligand and Zn(II) ion.

The IR spectrum of compound [Zn_2(**19**)Cl_4] contains the NH stretch at 3240 cm^{-1} suggesting the keto-formation. The appearance of a strong band at 1606 cm^{-1} is due to the presence of C=C and C=N stretch in comparison to a sharp signal of the ligand **19** at 1607 cm^{-1} which implies the one of the oxygen atoms from conjugated ketone could be binding to Zn(II) ion centre. The band representing for the C=C stretch of the pyridine rings at 1438 cm^{-1} points to the facts that the nitrogen atoms from the pyridine rings are coordinated to the metal ion centre.

The elemental analysis indicated that the complex had the formula [Zn_2(**19**)Cl_4]. This would suggest that two Zn(II) ions were bonded to the ligand and that four chloride ions were also involved to account for the neutral charge. The geometry of each Zn(II) ions is four-coordinate geometry. The possible structure of compound [Zn_2(**19**)Cl_4] is depicted in Figure 3.6.17.

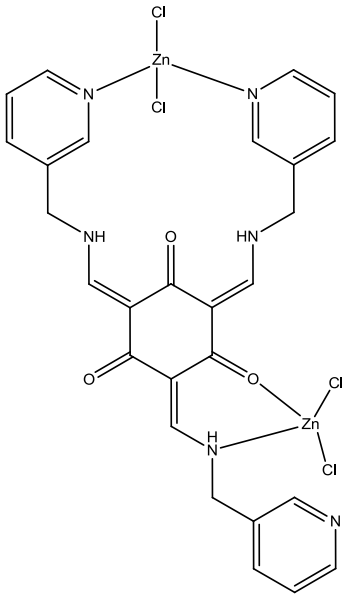

Figure 3.6.17: Possible structure for [Zn_2(**19**)Cl_4].

3.6.6.2 [Zn(**19**)$(ClO_4)_2$]

The complex [Zn(**19**)$(ClO_4)_2$] is formed as an off-white solid. The ^{1}H NMR spectrum of compound [Zn(**19**)$(ClO_4)_2$] is shown in Figure 3.6.16 (in green). The data for the complex [Zn(**19**)$(ClO_4)_2$] in both the ^{1}H NMR spectrum (shown in Figure 3.6.16) and the IR spectrum (shown in Table 3.6.2) are similar to those of the Zn(II) chloride complex with the only one exception of the appearance of perchlorate group as a strong broad band at 1107 cm^{-1} in the Zn(II) perchlorate complex. This would suggest that perchlorate complexation had occurred and the bonding of Zn(II) perchlorate complex should be similar to that of Zn(II) chloride complex.

The elemental analysis indicated that the complex had the formula [Zn(**19**)$(ClO_4)_2$]. This would imply that one Zn(II) ion was bonded to the ligand and that two perchlorate ions were also involved to account for the neutral charge. The bonding of Zn(II) ion is only through three nitrogen atoms of the pyridine rings. The geometry of Zn(II) ion could be either four-coordinate (including one perchlorate ion) or five-coordinate

(including two perchlorate ions). Hence, the possible structure of compound [Zn(**19**)$(ClO_4)_2$] is depicted in Figure 3.6.18.

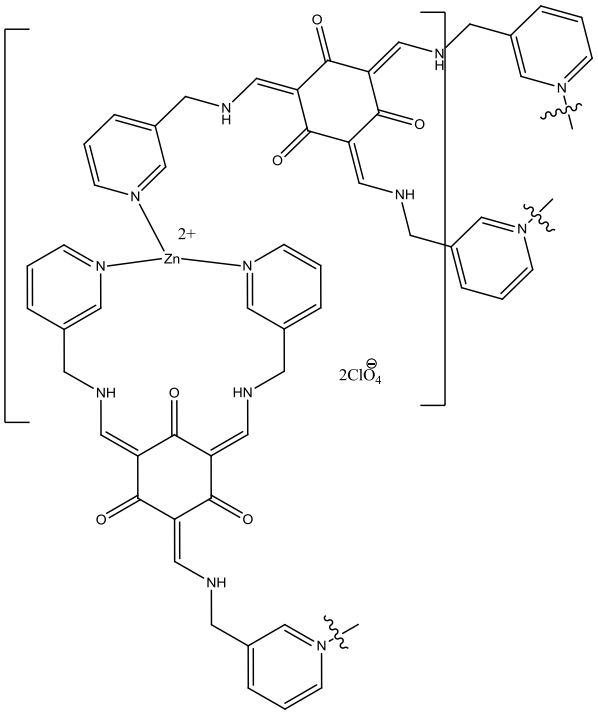

Figure 3.6.18: Possible structure for [Zn(**19**)$(ClO_4)_2$].

3.6.6.3 [Hg(**19**)$Cl_2 \cdot 2H_2O$]

The complex [Hg(**19**)$Cl_2 \cdot 2H_2O$] is formed as an off-white solid. The ^{1}H NMR spectrum of compound [Hg(**19**)$Cl_2 \cdot 2H_2O$] is shown in Figure 3.6.16 (in green). The spectrum of the complex [Hg(**19**)$Cl_2 \cdot 2H_2O$] is similar to its corresponding ligand **19** which is indicative of a weak bonding between the ligand and the Hg(II) ion.

The IR spectrum of compound [Hg(**19**)$Cl_2 \cdot 2H_2O$] contains a band ν_{OH} at 3435 cm^{-1} indicating some coordinated water molecules are present in the Hg(II) complex. The signals of NH stretch and NH bend are found to be very similar to those of Zn(II) perchlorate complex which implied the Hg(II) chloride complex is stable in the keto-formation. In addition, the appearance of a weak signal at 1481 cm^{-1} which is due to the coordinated pyridine rings is suggesting that the bonding of Hg(II) ion is through the nitrogen atoms of the pyridine rings.

The elemental analysis indicated that the complex had the formula [Hg(**19**)$Cl_2 \cdot 2H_2O$]. This would also suggest that one Hg(II) ion was bonded to the ligand and that two chloride ions were also involved to account for neutral charge. The bonding of Hg(II) ion is similar to that of Zn(II) perchlorate complex. The geometry of Hg(II) ion is five-

coordinate. So, the possible structure of compound [Hg(**19**)Cl_2·$2H_2O$] is depicted in Figure 3.6.19.

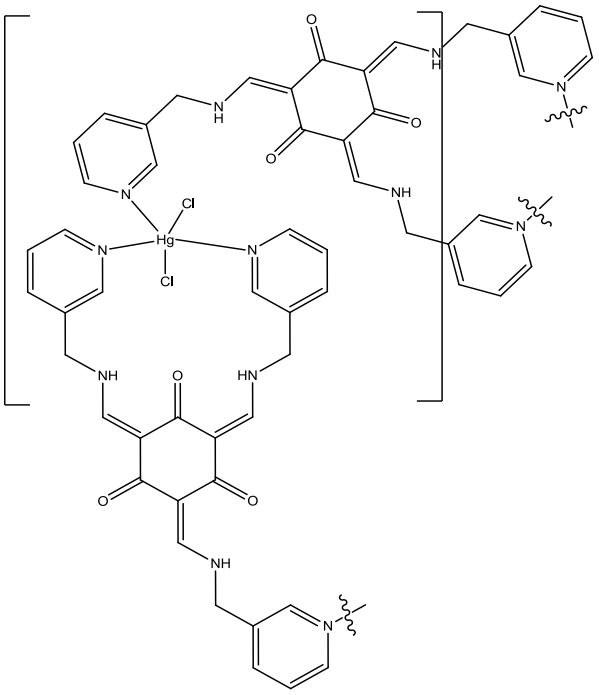

Figure 3.6.19: Possible structure for [Hg(**19**)Cl_2·$2H_2O$].

3.6.6.4 [Hg_2(**19**)$(ClO_4)_4$]

The complex [Hg_2(**19**)$(ClO_4)_4$] is obtained as a yellow solid. The ^{1}H NMR spectrum of compound [Hg_2(**19**)$(ClO_4)_4$] is shown in Figure 3.6.16 (in yellow). The signals of the secondary amines protons, Ha/Ha', resonate as two multiplets at 11.42-11.50 and 11.08-11.16 ppm, respectively, which were seen to shift slightly from the free ligand at 11.46-11.56 and 11.02-11.11 ppm. The appearance signals of alkenes protons Hd/Hd' as a multiplet from 8.18 to 8.31 ppm in Hg(II) complex suggests that the Hg(II) complex is in keto-formation. Several large chemical shifts occur at the signals of pyridine rings protons, Hb/Hb', are present at 8.65 ppm as a broad singlet in comparison to the original positions at 8.57 ppm. The protons Hc/Hc' resonate at 8.59 ppm which were seen as a multiplet from 8.51 to 8.67 ppm in ligand **19**. Protons Hf/Hf' appear as a multiplet which is together with the alkenes protons Hd/Hd' comparing the original signals at 7.76 ppm. Protons He/He' resonate as a multiplet from 7.86 to 7.96 ppm in Hg(II) complex which were seen as a multiplet from 7.36 to 7.43 ppm in ligand **19**. These shifts of the protons from the pyridine rings would suggest the pyridine nitrogen atoms are coordinated to the metal ion centre. In addition, the signal of bridging

methylene protons Hg/Hg' are observed at 4.90 ppm as a broad peak which have moved from the free ligand at 4.69 ppm.

In the IR spectrum of compound [Hg_2(**19**)(ClO_4)$_4$], the NH stretch is observed at 3234 cm^{-1} confirming the Hg(II) complex is in keto-formation which agrees with the results discussed earlier in the ^{1}H NMR spectrum. A strong broad band at 1606 cm^{-1} is due to the presence of C=C, C=O and C=N stretches in comparison to a sharp signal of the ligand **19** at 1607 cm^{-1} which indicates that one of the oxygen atoms from conjugated ketone could be binding to the Hg(II) ion centre. While the other bands (shown in Table 3.6.2) in the Hg(II) perchlorate complex are found to be very similar to those of the Hg(II) chloride complex implying that the bonding of these two complexes should be similar. The appearance of perchlorate group band at 1107 cm^{-1} as a strong broad peak is indicative of the Hg(II) perchlorate complexation.

Elemental analysis indicated that the complex had the formula [Hg_2(**19**)(ClO_4)$_2$]. This would also imply that two Hg(II) ions were bonded to the ligand and that four perchlorate ions were also involved to account for the neutral charge. The geometry of each Hg(II) ions is two-coordinate. The possible structure of compound [Hg_2(**19**)(ClO_4)$_4$] is depicted in Figure 3.6.20.

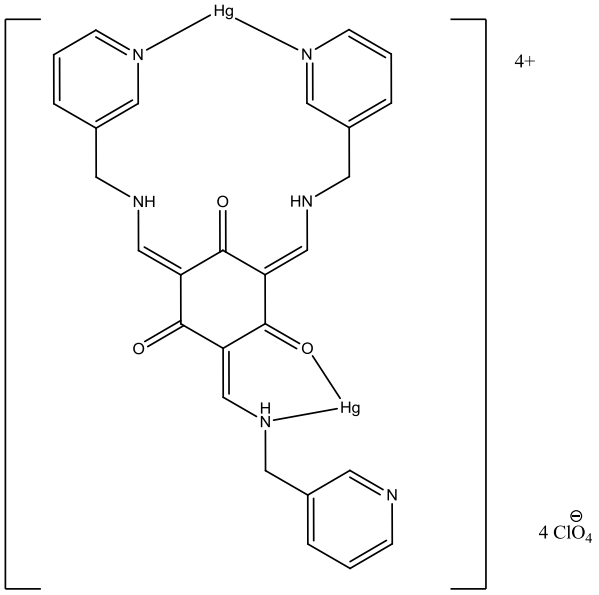

Figure 3.6.20: Possible structure for [Hg_2(**19**)(ClO_4)$_4$].

3.6.6.5 [Ni_2(**19**)Cl_4·MeOH·2H_2O]

The complex [Ni_2(**19**)Cl_4·MeOH·2H_2O] is obtained as a pale red solid. The IR spectrum of compound [Ni_2(**19**)Cl_4·MeOH·2H_2O] contains a band ν_{OH} at 3377cm^{-1} indicating

some coordinated water or methanol molecules are present in the Ni(II) complex. The signals of NH stretch occurs at 3237 cm^{-1} which is indicative of the keto-formation. The band representing for the C=C stretch of the pyridine rings at 1432 cm^{-1} which was seen at 1423 cm^{-1} in free ligand implying that that the nitrogen atoms of the pyridine rings could be coordinated to the metal ion centre. Although the appearance of several stretches of ketone C=O, alkene C=C, and pyridine rings C=N is found to be very similar at around 1605 cm^{-1} in either the complex and the ligand, the more broad band observed in the complex might also suggest that the nitrogen atoms and the oxygen atoms are binding to the metal ion centre. The NH bend is occurring at 1521 cm^{-1} as a broad peak which would suggest the nitrogen atoms of the amine groups are involved some hydrogen bonding with some water molecules. The magnetic moment of the complex $[Ni_2(\mathbf{19})Cl_4 \cdot MeOH \cdot 2H_2O]$ is obtained at 3.92 B.M. which could suggest the geometry of the Ni(II) ions are tetrahedral.

Elemental analysis indicated that the complex had the formula $[Ni_2(\mathbf{19})Cl_4 \cdot MeOH \cdot 2H_2O]$. This would imply that two Ni(II) ions were bonded to the ligand and that four chloride ions were also involved to account for the neutral charge. The bonding of the Ni(II) chloride complex is similar to that of the Zn(II) complexes. Hence, the possible structure of compound $[Ni_2(\mathbf{19})Cl_4 \cdot MeOH \cdot 2H_2O]$ is depicted in Figure 3.6.21.

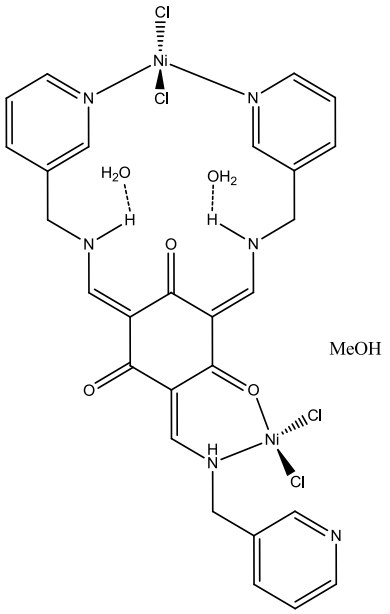

Figure 3.6.21: Possible structure for $[Ni_2(\mathbf{19})Cl_4 \cdot MeOH \cdot 2H_2O]$.

3.6.6.6 [Ni(**19**)$(ClO_4)_2$·$4H_2O$]

The complex [Ni(**19**)$(ClO_4)_2$·$4H_2O$] is formed as a brown-red solid. The IR spectrum of compound [Ni(**19**)$(ClO_4)_2$·$4H_2O$] is similar to that of Ni(II) chloride complex which would suggest the bonding the these two Ni(II) complexes should be similar. The broad signal of the NH bend is occurring at 1521 cm^{-1} which would suggest the nitrogen atoms of the amine groups are involved the hydrogen bonding with water molecules. In addition, the magnetic moment of the complex [Ni(**19**)$(ClO_4)_2$·$4H_2O$] is 4.29 B.M. implying that the Ni(II) perchlorate complex adopts a tetrahedral geometry.

Elemental analysis indicated that the complex had the formula [Ni(**19**)$(ClO_4)_2$·$4H_2O$]. This would also indicate that one Ni(II) ion was bonded to the ligand and that two perchlorate ions were also involved to account for neutral charge. The bonding of the Ni(II) ion is through three nitrogen atoms of the pyridine rings and one water molecule. The possible structure of compound [Ni(**19**)$(ClO_4)_2$·$4H_2O$] is depicted in Figure 3.6.22.

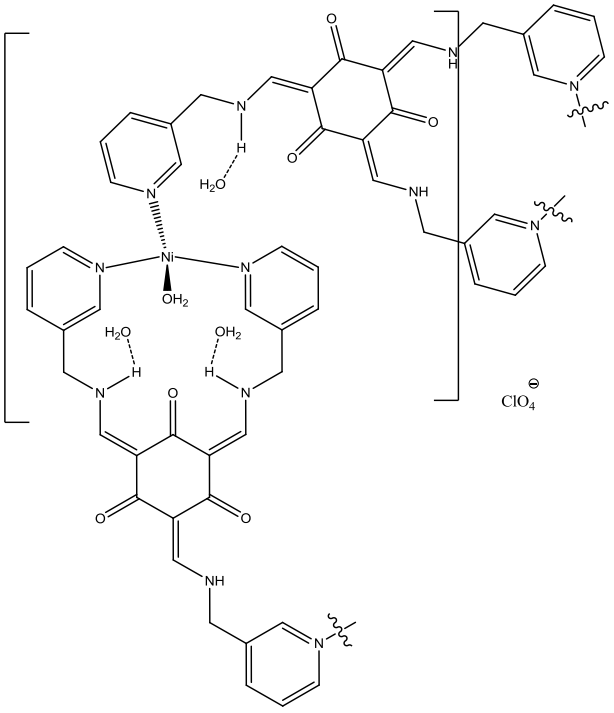

Figure 3.6.22: Possible structure for [Ni(**19**)$(ClO_4)_2$·$4H_2O$].

3.6.6.7 [Ni_3(**19**)$(OH)_3(OAc)_3$·$3H_2O$]

The complex [Ni_3(**19**)$(OH)_3(OAc)_3$·$3H_2O$] is formed as a light-red solid. The IR spectrum of the complex [Ni_3(**19**)$(OH)_3(OAc)_3$·$3H_2O$] contains a band of OH stretch at 3405 cm^{-1} which suggests some coordinated water molecules are present in the Ni(II) acetate complex. The observation of the NH stretch at 3232 cm^{-1} is indicative of the

keto-formation. A slight change occurred at the band around 1600 cm^{-1} (shown in Table 3.6.2). The appearance of a strong broad peak at 1593 cm^{-1} in comparison to the original band at 1607 cm^{-1} as a very sharp signal in ligand **19** suggests that the nitrogen atoms in either the amine groups and the pyridine rings (due the observed NH bend in Table 3.6.2) could be coordinated to the metal ion centre, and the structure of the Ni(II) acetate complex could be slightly different to the other complexes of ligand **19**. While the other bands such as the C=C stretch of the pyridine rings are found to be very similar to that of Ni(II) chloride complex suggesting the nitrogen atoms of the pyridine rings are coordinated to the metal ion centre. The magnetic moment of the complex $[Ni_3(\mathbf{19})(OH)_3(OAc)_3{\cdot}3H_2O]$ is 3.27 B.M. which suggests that the Ni(II) ion adopts a tetrahedral geometry.

The elemental analysis indicated the complex had the formula $[Ni_3(\mathbf{19})(OH)_3(OAc)_3{\cdot}3H_2O]$. This would also imply that three Ni(II) ions were bonded to one ligand and that three acetate ions were also involved. Three hydroxyl groups from the deprotonated water molecules are account for the neutral charge. The bonding of each Ni(II) ions is through two nitrogen atoms from one amine group and one pyridine ring and one oxygen atom of the keto group, as well as one acetate ion and one hydroxyl group. Hence, the possible structure of the complex $[Ni_3(\mathbf{19})(OH)_3(OAc)_3{\cdot}3H_2O]$ is depicted in Figure 3.6.23.

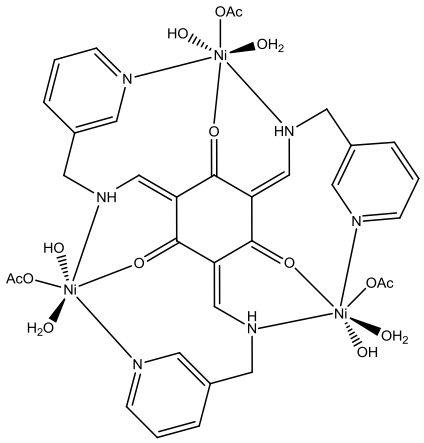

Figure 3.6.23: Possible structure of the complex $[Ni_3(\mathbf{19})(OH)_3(OAc)_3{\cdot}3H_2O]$.

3.6.6.8 $[Cu_2(\mathbf{19})Cl_4{\cdot}2H_2O]$

The complex $[Cu_2(\mathbf{19})Cl_4{\cdot}2H_2O]$ is obtained as a brown-green solid. The data of the complex $[Cu_2(\mathbf{19})Cl_4{\cdot}2H_2O]$ in the IR spectrum and the elemental analysis are found to be very similar to that of Zn(II) chloride complex (shown in Table 3.6.2) which would

suggest the bonding of the Cu(II) ion should be very similar to the Zn(II) ion as well. The magnetic moment of the Cu(II) chloride complex is 2.38 B.M. Hence, the proposed structure of the complex is depicted in Figure 3.6.24.

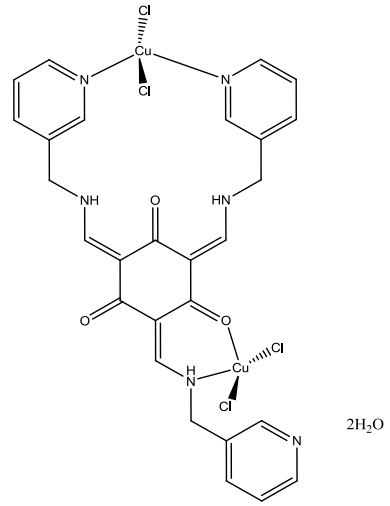

Figure 3.6.24: Possible structure for [Cu_2(**19**)Cl_4·$2H_2O$].

3.6.6.9 [Cu_3(**19**)$(OH)_3(OAc)_3$·$3H_2O$]

The complex [Cu_3(**19**)$(OH)_3(OAc)_3$·$3H_2O$] is formed as a dark green solid. The bonding of the complex [Cu_3(**19**)$(OH)_3(OAc)_3$·$3H_2O$] is very similar to that of Ni(II) acetate complex is due to the obtained data in both the IR spectrum and the elemental analysis of the Ni(II) acetate complex are similar to those of Cu(II) acetate complex. The only one small difference is occurring at the signal of the NH bend which is obtained at 1502 cm^{-1} as a broad signal in comparison to 1519 cm^{-1} in Ni(II) acetate complex. The magnetic moment of the Cu(II) acetate complex is 2.82 B.M., this would imply that the complex is in trigonal-bipyriamidal geometry. Hence, the proposed structure of the complex [Cu_3(**19**)$(OH)_3(OAc)_3$·$3H_2O$] is shown in Figure 3.6.25.

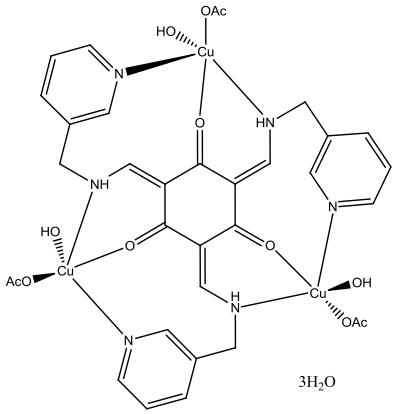

Figure 3.6.25: The proposed structure of the complex [Cu_3(**19**)$(OH)_3(OAc)_3$·$3H_2O$].

3.6.6.10 $[Cu_3(\mathbf{19})(OH)_3(NO_3)_3]$

The complex $[Cu_3(\mathbf{19})(OH)_3(NO_3)_3]$ is formed as a brown-green solid. The main bands (shown in Table 3.6.2) of the Cu(II) nitrate complex are similar to those of Cu(II) acetate complex as well as the elemental analysis. In addition, the appearance the band representing for the nitrate group at 1384 cm^{-1} as a strong signal is indicative of the nitrate complexation. The bonding of the Cu(II) ion is through two nitrogen atoms from pyridine rings and amine groups, one oxygen atom of ketone group and as well as one hydroxyl group and nitrate ion. The magnetic moment of the Cu(II) nitrate complex is 2.87 B.M. The geometry of the Cu(II) ion is five-coordinate trigonal-bipyriamidal geometry. So, the possible structure of the complex $[Cu_3(\mathbf{19})(OH)_3(NO_3)_3]$ is depicted in Figure 3.6.26.

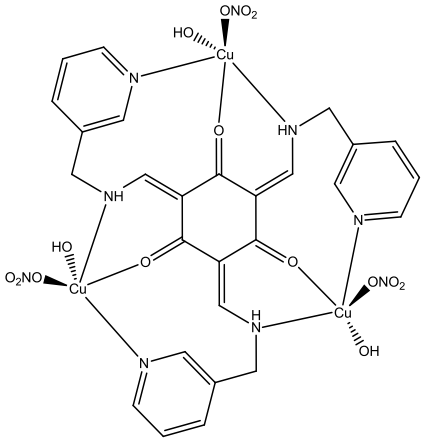

Figure 3.6.26: Possible structure of the complex $[Cu_3(\mathbf{19})(OH)_3(NO_3)_3]$.

3.6.6.11 $[Co_3(\mathbf{19})_2Cl_6{\cdot}2MeOH{\cdot}2H_2O]$

The complex $[Co_3(\mathbf{19})_2Cl_6{\cdot}2MeOH{\cdot}2H_2O]$ is formed as a dark-green solid. The IR spectrum of compound $[Co_3(\mathbf{19})_2Cl_6{\cdot}2MeOH{\cdot}2H_2O]$ is found to be similar to that of Zn(II) chloride complex which implies the similar bonding between these two complexes. The magnetic moment of the complex $[Co_3(\mathbf{19})_2Cl_6{\cdot}2MeOH{\cdot}2H_2O]$ is 5.45 B.M. indicating the octahedral geometry is occurring in the Co(II) complex.

Elemental analysis indicated that the complex had the formula $[Co_3(\mathbf{19})_2Cl_6{\cdot}2MeOH{\cdot}2H_2O]$. This would also suggest that three Co(II) ions were bonded to two ligands and that six chloride ions were also involved to account for the neutral charge. The two methanol and two water molecules are regarded as coordination solvents in the Co(II) complex. Hence, the possible structure of compound $[Co_3(\mathbf{19})_2Cl_6{\cdot}2MeOH{\cdot}2H_2O]$ is depicted in Figure 3.6.27.

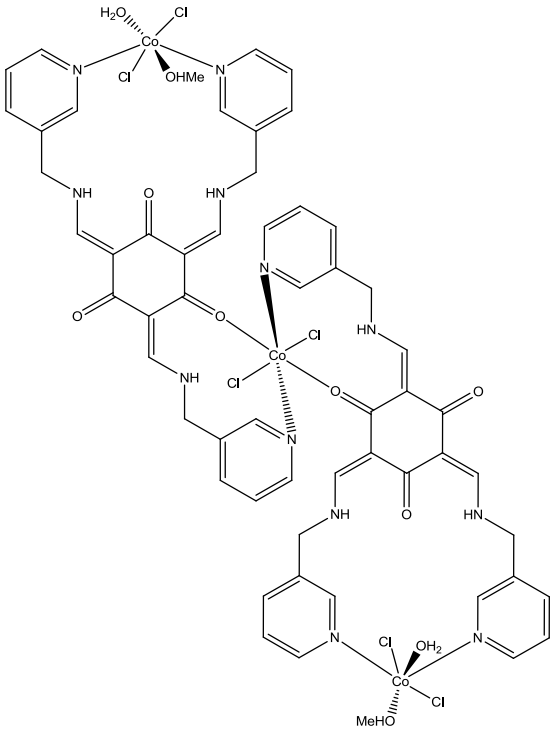

Figure 3.6.27: Possible structure for [Co_3(**19**)$_2Cl_6$·2MeOH].

3.6.6.12 [Co(**19**)(ClO_4)$_2$]

The complex [Co(**19**)(ClO_4)$_2$] is formed as a pale solid. The bonding of the Co(II) perchlorate complex is very similar to that of Zn(II) perchlorate complex as the similar data of the IR spectra and the elemental analysis in both complexes. However, the obtained two signals of the perchlorate group at 1121 and 1108 cm^{-1}, respectively, suggests that the two perchlorate group could be in different environments in comparison to only one signal of perchlorate group in Zn(II) complex. The magnetic moment of the complex [Co(**19**)(ClO_4)$_2$] is occurring at 4.25 B.M. implying a tetrahedral geometry in the complex.

Elemental analysis indicated that the complex had the formula [Co(**19**)(ClO_4)$_2$]. This would also suggest that one Co(II) ion was bonded to the ligand and that two perchlorate ions were also involved to account for neutral charge. The bonding of the Co(II) ion is through three nitrogen atoms of the pyridine rings and one perchlorate ion. The possible structure of compound [Co(**19**)(ClO_4)$_2$] is depicted in Figure 3.6.28.

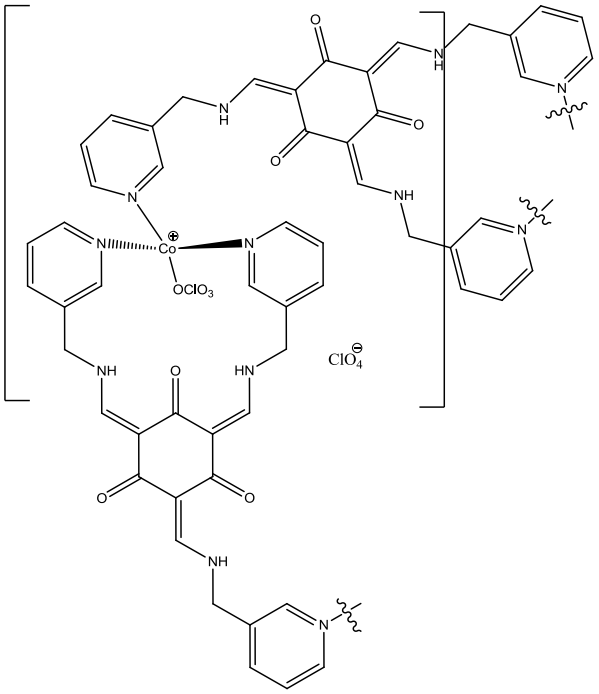

Figure 3.6.28: Possible structure for [Co(**19**)$(ClO_4)_2$].

3.6.7 Ligand 20

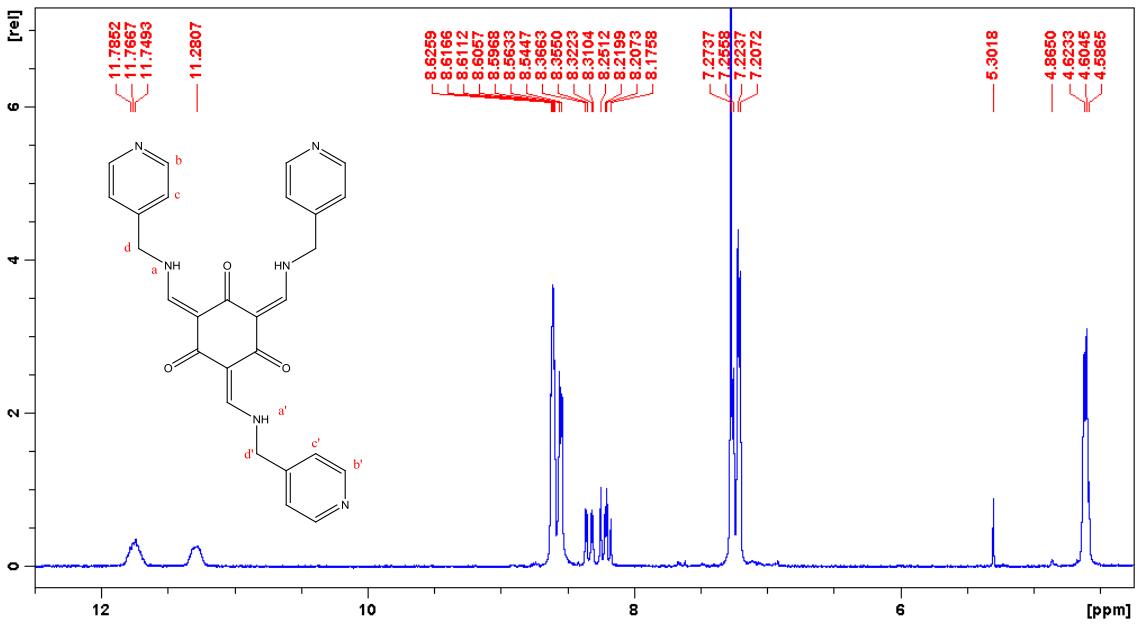

Figure 3.6.29: The ^{1}H NMR spectrum of ligand **20** in $CDCl_3$.

The ligand **20** is formed as a yellow oil. The ^{1}H NMR spectrum of ligand **20** is shown in Figure 3.6.29. Either the two signals of amine protons Ha/Ha' which are observed at two broad singlets at 11.76 and 11.28 ppm or the alkenes protons resonating as a multiplet from 8.17 to 8.36 ppm imply that the ligand **20** is in the stable keto-formation. In addition, the signals of the pyridine rings protons, Hb/Hb', are observed as a

multiplet from 8.54 to 8.62 ppm, and the protons Hd/Hd', appear at a multiplet from 7.20 to 7.27 ppm in Figure 3.6.29. The bridging methylene protons He/He' are present as a multiplet from 4.58 to 4.62 ppm.

The ^{13}C NMR spectrum of ligand **20** appears three signals of carbonyl carbon at 188.3, 185.4 and 182.5 ppm suggesting the ligand **20** is in both C_{3h} and C_3 isomers (shown in Figure 3.6.3). And the signals of alkenes carbon are observed at 122.7 and 121.8 ppm, respectively, could further confirm this result.

The IR spectrum of ligand **20** is run under DCM. A strong sharp band occurring at 1610 cm^{-1} is due to the presence of C=C, C=O and C=N stretches. The N-H bend is observed at 1553 cm^{-1} as a medium signal. The band representing for the C=C stretch from the pyridine ring is present at 1456 cm^{-1}.

The mass spectrum suggests that the ligand **20** is pure.

3.6.8 Metal complexes of 20

Metal complexes reactions of ligand **20** with various metal(II) salts were carried out in MeOH. The reactions were carried out by stirring the ligand and the appropriate metal salts at room temperature for 2 hours in MeOH. The resulting coloured solids were collected by filtration.

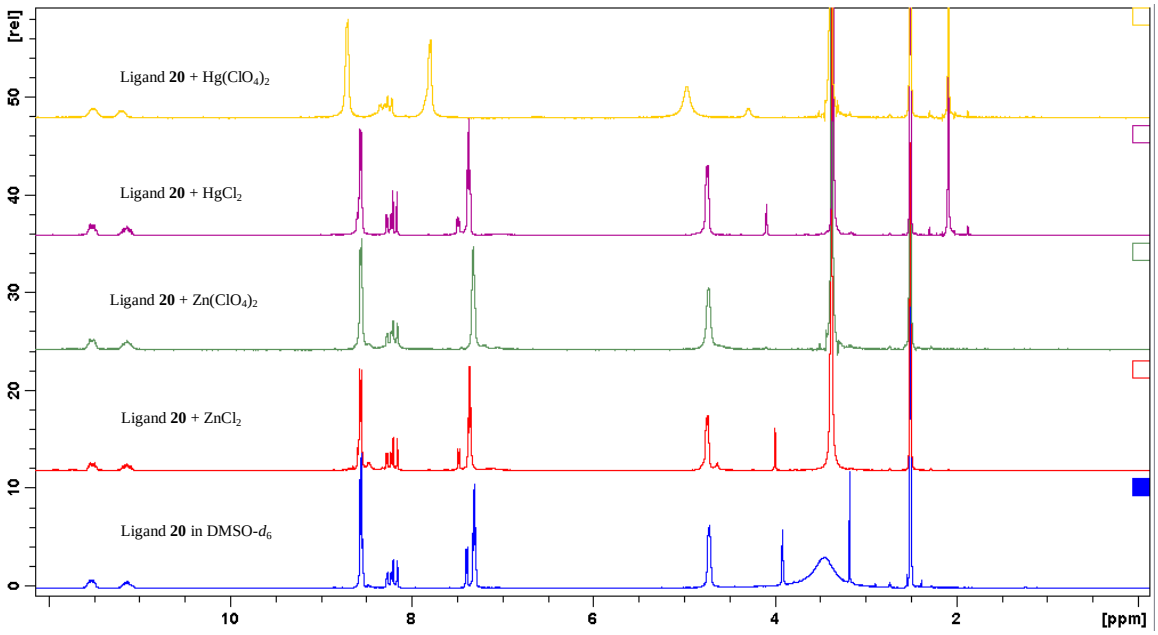

Figure 3.6.30: A comparison of ^1H NMR spectra of ligand **20** with its corresponding ZnX_2 and HgX_2 (X = chloride, perchlorate) complexes in DMSO-d_6.

Table 3.6.3: A comparison of the analytical data of the IR spectra between the ligand **20** and its corresponding complexes.

	OH	NH stretch	C=C, C=N	N-H bend	Pyridine
ligand **20**			1610	1553	1421
$ZnCl_2$	3447	3250	1607 (br)	1549	1431
$Zn(ClO_4)_2$	3423	3240	1606 (br)	1546	1431
$HgCl_2$	3444	3257	1604 (br)	1532	1426
$Hg(ClO_4)_2$	3454	block	1605 (br)	1546	1427
$NiCl_2$	3387	3233	1603 (br)	1520	1426
$Ni(ClO_4)_2$	3407	3240	1604 (br)	1521	1426
$Ni(OAc)_2$	3414	block	1599 (br)	1520	1424
$CuCl_2$	3433	block	1603 (br)	1535	1428
$Cu(ClO_4)_2$	3436	3256	1603 (br)	1503	1429
$Cu(OAc)_2$	3430	block	1587 (br)	1505	1427
$Cu(NO_3)_2$	3432	3240	1589 (br)	1504	1427
$CoCl_2$	3384	3227	1606 (br)	1540	1426
$Co(ClO_4)_2$	3428	3253	1606 (br)	1544	1426

The comparison data of the IR spectra between the ligand **20** and its metal complexes is shown in Table 3.6.3. Some results will be indicative according to this table. All the complexes are in keto-formation due to the presence bands of the NH stretch and bend. The bonding of these complexes are normally through the nitrogen atoms of the secondary amines due to the difference of the signals of NH bends between the ligand and the complexes excluding the Zn(II) complexes, Hg(II) perchlorate complex and the Co(II) complexes. While the bonding of these exceptions complexes are through the nitrogen atoms of the pyridine rings as a slight change of the NH bends between the ligand and these complexes. Moreover, in the IR spectra of the various metal complexes of ligand **20**, the bands due to the C=N, C=O and C=C stretching vibrations partly overlap resulting in a broad band centered at about 1600 cm^{-1}. Therefore these bands at around 1590-1610 cm^{-1} cannot be unambiguously assigned to an individual stretching vibration.

3.6.8.1 [Zn_2(**20**)Cl_4]

The complex is [Zn_2(**20**)Cl_4] formed as an off-white solid. The ^{1}H NMR spectrum of compound [Zn_2(**20**)Cl_4] is shown in Figure 3.6.30 (in red) which is similar to that of ligand **20** suggesting a weak bonding is occurring in this complex.

In the IR spectrum of compound [Zn_2(**20**)Cl_4], the N-H stretch and N-H bend are present at 3250 and 1549 cm^{-1}, respectively, which confirms the complex is in keto-formation. As the NH bend presented at 1553 cm^{-1} in ligand **20** without significant change, it implies that the three nitrogen atoms of the secondary amines are not coordinated to the metal ion centre. However, the appearance of a broad band at 1607 cm^{-1} could point towards one oxygen atom from ketone group is coordinated to the metal ion centre. In addition, a band representing for the C=C stretch from the pyridine ring at 1431 cm^{-1} which shifted from 1421 cm^{-1} in free ligand suggest that the nitrogen atoms from pyridine rings are coordinated to Zn(II) ion centre.

The elemental analysis indicated that the complex had the formula [Zn_2(**20**)Cl_4]. This would also imply that two Zn(II) ions were bonded to the ligand and that four chloride ions were also involved to account for neutral charge. The possible structure of compound [Zn_2(**20**)Cl_4] could be depicted in Figure 3.6.31.

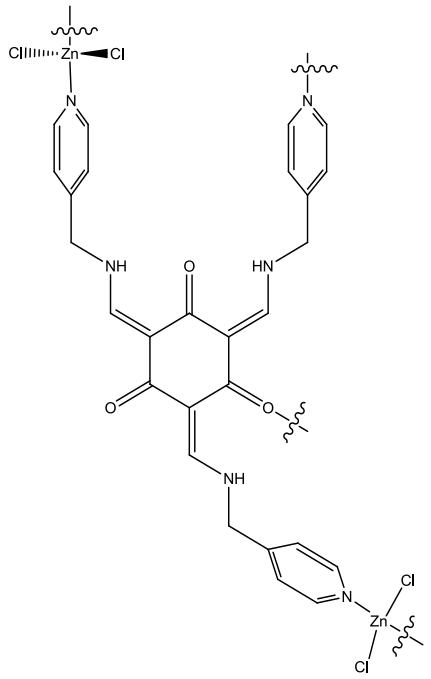

Figure 3.6.31: Possible structure for [Zn_2(**20**)Cl_4].

3.6.8.2 [Zn(**20**)(ClO_4)$_2$]

The complex [Zn(**20**)(ClO_4)$_2$] is obtained as an off-white solid. The ^{1}H NMR spectrum of compound [Zn(**20**)(ClO_4)$_2$] is shown in Figure 3.6.30 (in green) which is very similar to that of the ligand implying a weak bonding could be occurred between the metal ion and the ligand.

The IR spectrum of the complex [Zn(**20**)(ClO_4)$_2$] is found to be very similar to that of Zn(II) chloride complex (shown in Table 3.6.3) which suggests that the bonding of these two complexes should be analogous. The only one exception of the Zn(II) perchlorate complex is the appearance of the perchlorate group at 1121 cm^{-1} which is indicative of the perchlorate complexation.

The elemental analysis indicated the complex had the formula [Zn(**20**)(ClO_4)$_2$]. This would also imply that one Zn(II) ion was bonded to the ligand and that two perchlorate ions were also involved to account for the neutral charge. The bonding of the Zn(II) ion is through three nitrogen atoms of the pyridine rings and one perchlorate ion. The possible structure of compound [Zn(**20**)(ClO_4)$_2$] is depicted in Figure 3.6.32.

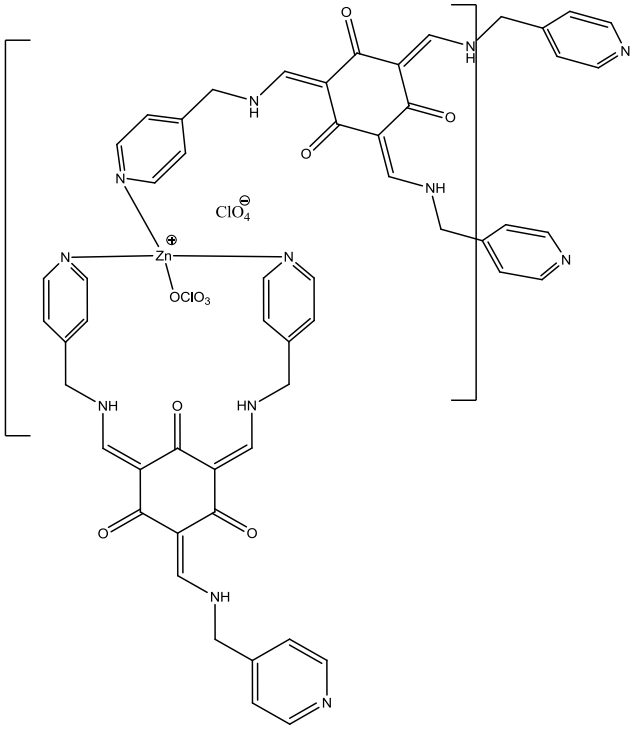

Figure 3.6.32: Possible structure for [Zn(**20**)(ClO_4)$_2$].

3.6.8.3 [Hg_5(**20**)$_2Cl_{10}\cdot 2H_2O$]

The complex [Hg_5(**20**)$_2Cl_{10}\cdot 2H_2O$] is isolated as an off-white solid. The ^{1}H NMR spectrum of compound [Hg_5(**20**)$_2Cl_{10}\cdot 2H_2O$] is shown in Figure 3.6.30 (in purple).

The IR spectrum of compound [Hg_5(**20**)$_2Cl_{10}\cdot 2H_2O$] contains a signal ν_{OH} at 3444 cm^{-1} suggesting some coordinated water molecules are present in the Hg(II) complex. The NH stretch and NH bend were present at 3257 cm^{-1} and 1532 cm^{-1}, respectively, in comparison to the original NH bend at 1553 cm^{-1} implying the bonding of the Hg(II) ion is through the nitrogen atoms from the secondary amines. The appearance of a broad band at 1604 cm^{-1} could suggest that one or two oxygen atoms from the ketone group are coordinated to the metal ion centre. In addition, there is no significant change of the C=C stretch from pyridine rings in between the ligand and the complex which implies that the pyridyl nitrogens are not binding to the metal ion centre.

Elemental analysis indicated that the complex had the formula [Hg_5(**20**)$_2Cl_{10}\cdot 2H_2O$]. This would imply that five Hg(II) ions were bonded to two ligands and that ten chloride ions were also involved to account for the neutral charge. The possible structure of compound [Hg_5(**20**)$_2Cl_{10}\cdot 2H_2O$] is depicted in Figure 3.6.33.

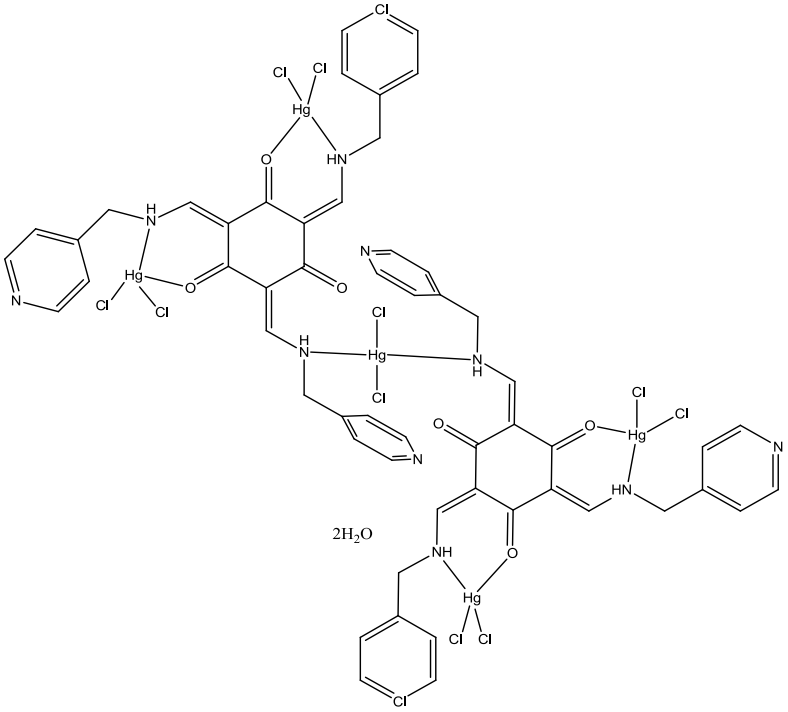

Figure 3.6.33: Possible structure for [Hg_5(**20**)$_2Cl_{10}\cdot 2H_2O$].

3.6.8.4 $[Hg_2(\mathbf{20})(ClO_4)_4]$

The complex $[Hg_2(\mathbf{20})(ClO_4)_4]$ is obtained as an off-white solid. The ^1H NMR spectrum of compound $[Hg_2(\mathbf{20})(ClO_4)_4]$ is shown in Figure 3.6.30 (in yellow). The signals of secondary amine protons, Ha/Ha', and the alkene protons, Hc/Hc', are found to be similar to those in ligand **20**. However, the signals of pyridine rings protons, Hb/Hb', are observed as a broad singlet at 8.71 ppm in comparison to the original positions as a multiplet from 8.53 to 8.57 ppm in ligand **20**. The protons Hd/Hd' are present at 7.80 ppm as a broad signal in Hg(II) complex which were seen as a multiplet from 7.30 to 7.40 ppm in the free ligand. These two shifts imply that the nitrogen atoms from pyridine rings could be binding to Hg(II) ion centre. The signals of the bridging methylene protons He/He', resonate at 4.97 ppm in Zn(II) complex which have moved from 4.71 ppm.

The IR spectrum of compound $[Hg_2(\mathbf{20})(ClO_4)_4]$ is similar to that of Zn(II) chloride complex which confirms that the bonding of Hg(II) ion is through the nitrogen atoms of the pyridine rings not *via* the nitrogen atoms of the secondary amines. This similarity could suggest the bonding of these two complexes should be analogous. The appearance of the perchlorate group at 1109 cm^{-1} as a strong broad signal is indicative of the perchlorate complexation.

Elemental analysis indicated that the complex had the formula $[Hg_2(\mathbf{20})(ClO_4)_4]$. This would imply that two Hg(II) ions were bonded to the ligand and that four perchlorate ions were also involved to account for the neutral charge. The possible structure of compound $[Hg_2(\mathbf{20})(ClO_4)_4]$ is depicted in Figure 3.6.34.

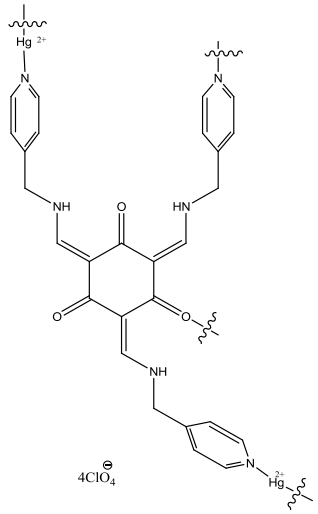

Figure 3.6.34: Possible structure for $[Hg_2(\mathbf{20})(ClO_4)_4]$.

3.6.8.5 [Ni_2(**20**)Cl_4]

The complex [Ni_2(**20**)Cl_4] is isolated as a pale-pink solid. In the IR spectrum of compound [Ni_2(**20**)Cl_4], the NH stretch and NH bend are observed at 3233 cm^{-1} and 1520 cm^{-1}, respectively, confirming the keto-formation. The original NH bend was seen at 1553 cm^{-1} from ligand **20**. It suggests that the nitrogen atoms of the amine groups are coordinated to the metal ion centre. There is no significant change of the C=C stretch in pyridine rings between the complex and the ligand. The appearance of a more broad signal at 1603 cm^{-1} would point towards that one or two oxygen atoms from the ketone group could be coordinated to the metal ion centre. In addition, the magnetic moment of the complex [Ni_2(**20**)Cl_4] is obtained at 3.50 B.M. which suggests that the Ni(II) ions adopt tetrahedral geometries.

Elemental analysis indicated that the complex had the formula [Ni_2(**20**)Cl_4]. This suggested that two Ni(II) ions were bonded to the ligand and that four chloride ions were also involved to account for the neutral charge. The possible structure of compound [Ni_2(**20**)Cl_4] is depicted in Figure 3.6.35.

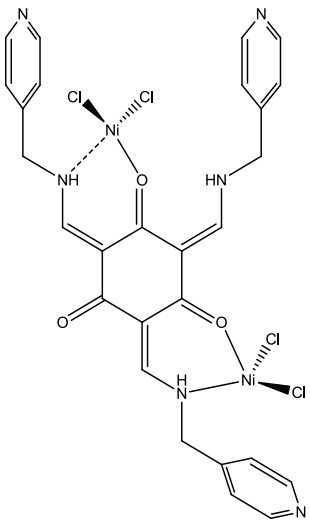

Figure 3.6.35: Possible structure for [Ni_2(**20**)Cl_4].

3.6.8.6 [Ni(**20**)$(ClO_4)_2$·MeOH·H_2O]

The complex [Ni(**20**)$(ClO_4)_2$·MeOH·H_2O] is obtained as a pale-pink solid. The IR spectrum of compound [Ni(**20**)$(ClO_4)_2$·MeOH·H_2O] is similar to that of Ni(II) chloride complex which suggests that the bonding in these two complexes should be analogues. The appearance of a strong broad band at 1109 cm^{-1} which is due to the perchlorate group, is indicative of the perchlorate complexation. The magnetic moment of the

complex [Ni(**20**)$(ClO_4)_2$·MeOH·H_2O] is obtained as 2.87 B.M. indicating an octahedral geometry could be occurred in complex [Ni(**20**)$(ClO_4)_2$·MeOH·H_2O].

Elemental analysis indicated that the complex had the formula [Ni(**20**)$(ClO_4)_2$·MeOH·H_2O]. This would also imply that one Ni(II) ion was bonded to ligand and that two perchlorate ions were also involved to account for neutral charge. The possible structure of compound [Ni(**20**)$(ClO_4)_2$·MeOH·H_2O] could be depicted in Figure 3.6.36.

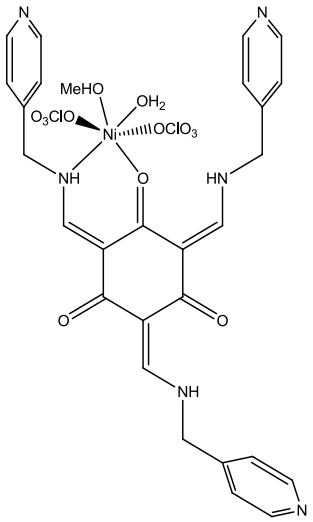

Figure 3.6.36: Possible structure for [Ni(**20**)$(ClO_4)_2$·MeOH·H_2O].

3.6.8.7 [Ni_3(**20**)$(OH)_4(OAc)_2$·H_2O]

The complex [Ni_3(**20**)$(OH)_4(OAc)_2$·H_2O] is formed as a pale-pink solid. The IR spectrum of the complex [Ni_3(**20**)$(OH)_4(OAc)_2$·H_2O] contains OH signal at 3430 cm^{-1} suggesting water molecule is present in the Ni(II) acetate complex. The band representing for the NH stretch was block by the broad OH peak, but the appearance of the NH bend at 1520 cm^{-1} suggests that the complex is in keto-formation. With a comparison to the original NH bend at 1553 cm^{-1}, it implies that the nitrogen atoms from the amine groups are coordinated to the metal ion centre. The presence of a strong broad signal at 1599 cm^{-1} is due to the stretches of the C=C, C=N and C=O which has moved from 1610 cm^{-1}. This could imply that the oxygen atoms of the ketone groups may be binding to the metal ion centre. The magnetic moment of the complex [Ni_3(**20**)$(OH)_4(OAc)_2$·H_2O] is obtained at 4.32 B.M. indicating the complex is in tetrahedral geometry. So, the possible structure of the complex [Ni_3(**20**)$(OH)_4(OAc)_2$·H_2O] is depicted in Figure 3.6.37.

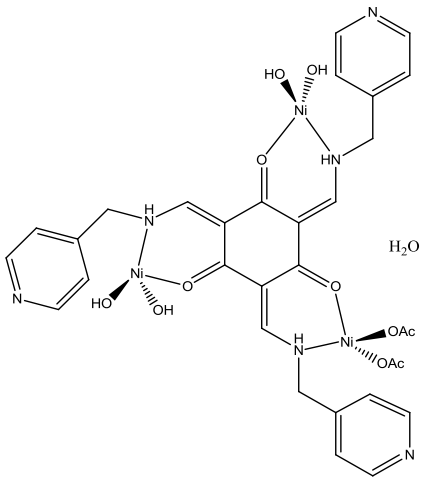

Figure 3.6.37: Possible structure of the complex [Ni_3(**20**)$(OH)_4(OAc)_2 \cdot H_2O$].

3.6.8.8 [Cu_5(**20**)$_2Cl_{10} \cdot 4H_2O$]

The complex [Cu_5(**20**)$_2Cl_{10} \cdot 4H_2O$] is formed as a brown solid. The analytical data of the complex [Cu_5(**20**)$_2Cl_{10} \cdot 4H_2O$] in either the IR spectrum or the elemental analysis are found to be very similar to that of Hg(II) chloride complex implying the bonding of these two complexes should be analogues. The magnetic moment of the Cu(II) chloride complex is 2.06 B.M. The proposed structure of the complex [Cu_5(**20**)$_2Cl_{10} \cdot 4H_2O$] is depicted in Figure 3.6.38.

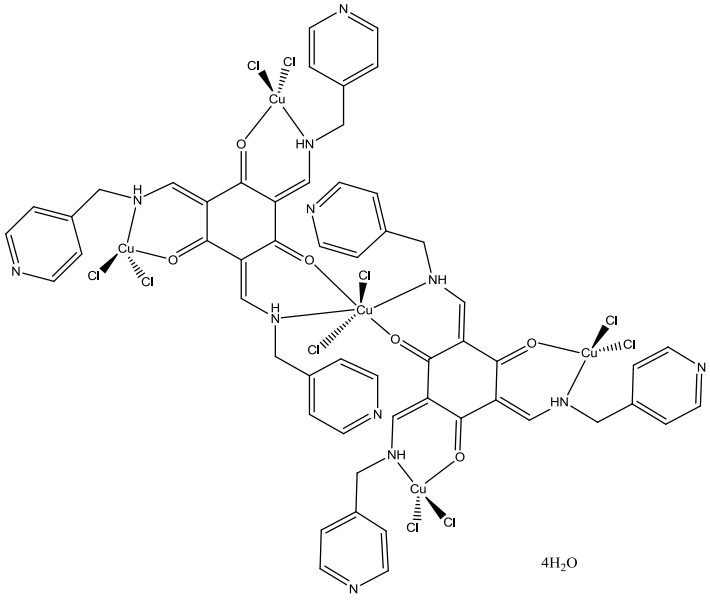

Figure 3.6.38: Possible structure for [Cu_5(**20**)$_2Cl_{10} \cdot 4H_2O$].

3.6.8.9 [Cu_2(**20**)$(ClO_4)_3 \cdot (OH)$]

The complex of [Cu_2(**20**)$(ClO_4)_3 \cdot (OH)$] is formed as a brown solid. The IR spectrum of compound [Cu_2(**20**)$(ClO_4)_3 \cdot (OH)$] is found to be similar to that of the Ni(II) perchlorate

complex with the only one exception of the signal of NH bend which was occurred at 1503 cm^{-1} in the Cu(II) perchlorate complex in comparison to the band at 1521 cm^{-1} from the Ni(II) perchlorate complex. But this similarity still suggested the bonding of the metal ion in both complexes should be analogues.

The elemental analysis indicated that the complex had the formula [Cu_2(**20**)$(ClO_4)_3$·(OH)]. This would also suggest that two Cu(II) ions were bonded to the ligand and that three perchlorate ions and one hydroxyl group from deprotonated water molecule were also involved to account for neutral charge. The magnetic moment of the Cu(II) perchlorate complex is 2.11 B.M. The possible structure of compound [Cu_2(**20**)$(ClO_4)_3$·(OH)] is depicted in Figure 3.6.39.

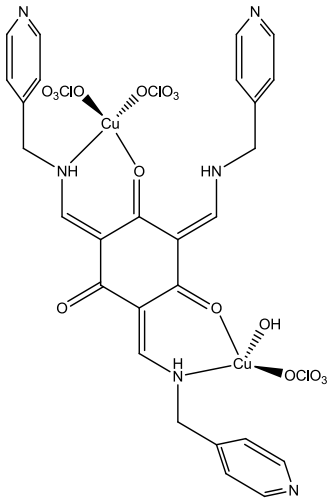

Figure 3.6.39: Possible structure for [Cu_2(**20**)$(ClO_4)_3$·(OH)].

3.6.8.10 [Cu_3(**20**)$(NO_3)_3(OH)_3$·$2H_2O$]

The complex [Cu_3(**20**)$(NO_3)_3(OH)_3$·$2H_2O$] is obtained as a dark green solid. The data of the complex [Cu_3(**20**)$(NO_3)_3(OH)_3$·$2H_2O$] in both the IR spectrum and the elemental analysis are similar to those of the Ni(II) acetate complex with the only one small exception of the NH bend signal which occurred at 1504 cm^{-1} in nitrate complex in comparison to the one at 1520 cm^{-1} in acetate complex. The appearance of the band representing for the nitrate group is indicative of the nitrate complexation. However, this similarity is still suggesting the bonding of the complex [Cu_3(**20**)$(NO_3)_3(OH)_3$·$2H_2O$] should be similar to that of Ni(II) acetate complex as well. The magnetic moment of the Cu(II) nitrate complex is 2.94 B.M. The geometry of the Cu(II) nitrate complex is square-pyramidal. The proposed structure of the complex [Cu_3(**20**)$(NO_3)_3(OH)_3$·$2H_2O$] is depicted in Figure 3.6.40.

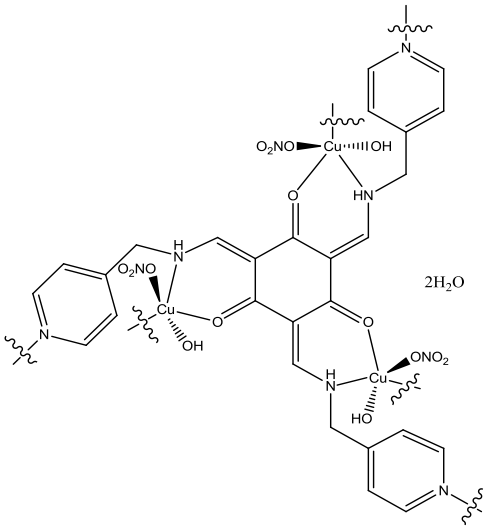

Figure 3.6.40: Proposed structure of the complex [Cu_3(**20**)$(NO_3)_3(OH)_3 \cdot 2H_2O$].

3.6.8.11 [Co_2(**20**)$Cl_4 \cdot 2MeOH \cdot 2H_2O$]

The complex [Co_2(**20**)$Cl_4 \cdot 2MeOH \cdot 2H_2O$] is isolated as a green solid. The difference of the IR spectrum between the complex [Co_2(**20**)$Cl_4 \cdot 2MeOH \cdot 2H_2O$] and the ligand **20** is that the presence of a more broad signal at 1606 cm^{-1} and the signal of NH bend occurring at 1540 cm^{-1} in the Co(II) chloride complex. These two observations would imply that the bonding of each Co(II) ions is through the nitrogen atoms of the amine groups and might be involved one or two oxygen atoms from the ketone groups as well. In addition, the magnetic moment of the complex [Co_2(**20**)$Cl_4 \cdot 2MeOH \cdot 2H_2O$] is 5.70 B.M. which suggests that the complex is in octahedral geometry sphere.

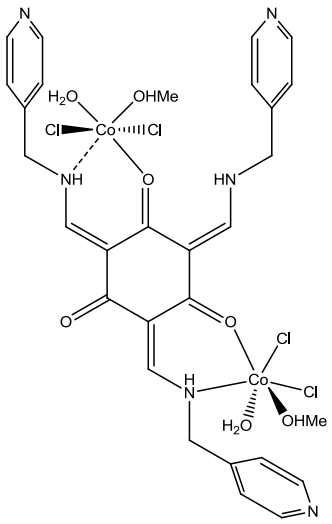

Figure 3.6.41: Possible structure for [Co_2(**20**)$Cl_4 \cdot 2MeOH \cdot 2H_2O$].

Elemental analysis indicated that the complex had the formula [Co_2(**20**)Cl_4·2MeOH·2H_2O]. This would also suggest that two Co(II) ions were bonded to the ligand and that four chloride ions were also involved to account for the neutral charge. Two methanol molecules and two water molecules could be also involved as coordination solvents. The possible structure of compound [Co_2(**20**)Cl_4·2MeOH·2H_2O] is depicted in Figure 3.6.41.

3.6.8.12 [Co(**20**)(ClO_4)$_2$·MeOH·H_2O]

The complex [Co(**20**)(ClO_4)$_2$·MeOH·H_2O] is formed as a dark-green solid. The IR spectrum of compound [Co(**20**)(ClO_4)$_2$·MeOH·H_2O] contains a band ν_{OH} at 3428 cm^{-1} which suggests that coordinated MeOH/H_2O molecules are present in the Co(II) complex. The NH stretch and NH bend observed at 3253 cm^{-1} and 1544 cm^{-1} are indicative of the keto-formation. The original NH bend presented at 1553 cm^{-1}, and no significant change occurring at the C=C band for the pyridine rings between the ligand and the complex (shown in Table 3.6.3). It would suggest that the bonding of the Co(II) ion is through the nitrogen atoms of the amine groups. The appearance of a broad band at 1606 cm^{-1} indicates that one or two oxygen atoms from the ketone groups could be coordinated to the metal ion centre as well. The magnetic moment of the complex [Co(**20**)(ClO_4)$_2$·MeOH·H_2O] is obtained at 4.05 B.M. which is indicative of a tetrahedral geometry in the Co(II) complex.

Elemental analysis indicated that the complex had the formula [Co(**20**)(ClO_4)$_2$·MeOH·H_2O]. This would also suggest that one Co(II) ion was bonded to the ligand and that two perchlorate ions were also involved to account for neutral charge. The possible structure of compound [Co(**20**)(ClO_4)$_2$·MeOH·H_2O] could be depicted in Figure 3.6.42.

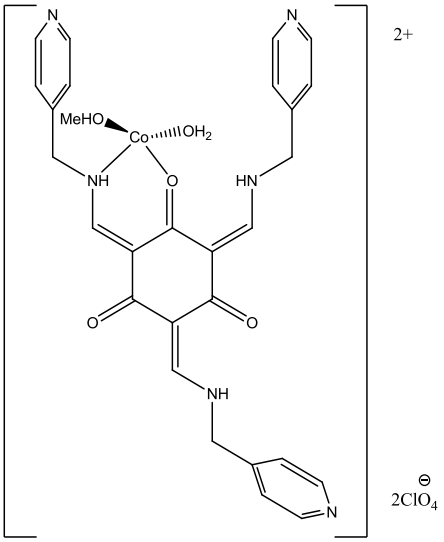

Figure 3.6.42: Possible structure for [Co(**20**)$(ClO_4)_2$·MeOH·H_2O].

3.6.9 Ligand 21

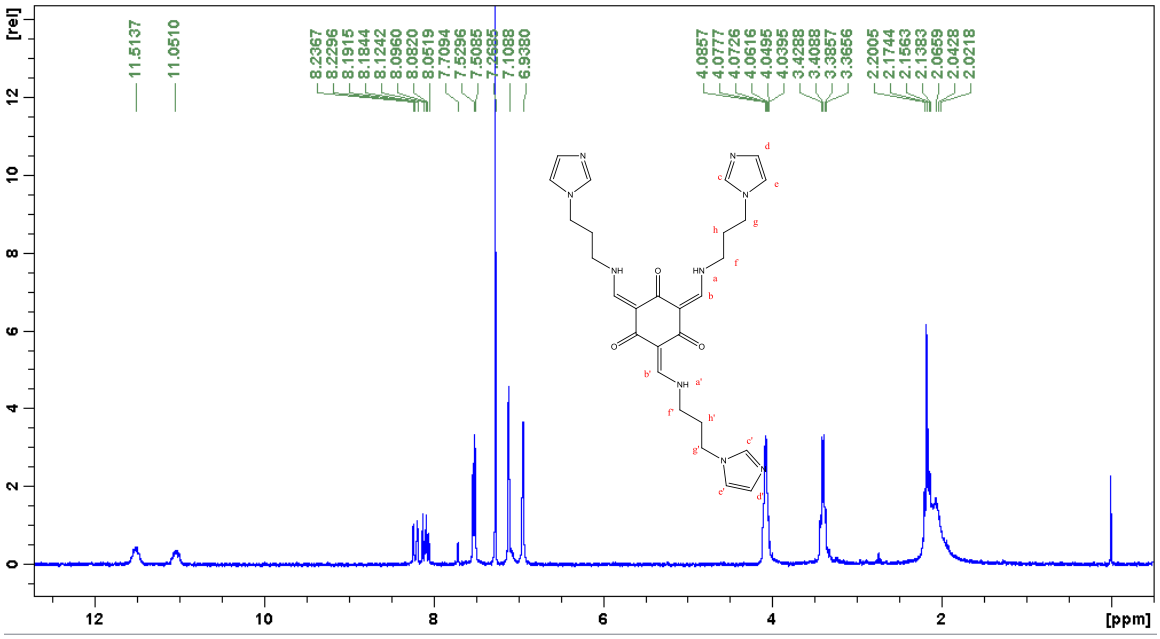

Figure 3.6.43: The ^{1}H NMR spectrum of ligand **21** in $CDCl_3$.

The ligand **21** is isolated as a yellow oil. The ^{1}H NMR spectrum of ligand **21** is shown in Figure 3.6.43. The appearance signals of the secondary amine protons Ha/Ha' occurring as two broad singlets at 11.51 and 11.05 ppm and alkenes protons Hb/Hb' resonating from 8.08 to 8.23 ppm as a multiplet suggest that the ligand **21** is in the keto-formation. The multiplet of protons Hb/Hb' also indicates the occurrence of the both C_s and C_{3h} isomers (shown in Figure 3.6.3) in ligand **21**. The signals for the imidazole rings protons, Hc/Hc', Hd/Hd' and He/He', resonate at 7.52, 7.10 and 6.93 ppm, respectively, as three singlets. The three bridging methylene protons Hf/Hf', Hg/Hg'

and Hh/Hh', are observed as three multiplets at 4.04–4.08 ppm, 3.36–3.42 ppm and 2.02–2.20 ppm, respectively.

In the ^{13}C NMR of ligand **21**, it appears a carbonyl carbon at 185.2 ppm and the alkene carbon at 118.6 ppm which confirm the keto-formation.

The IR spectrum of ligand **21** is tested under the DCM solvent. It contains a signal ν_{NH} bend is at 1551 cm^{-1} as a weak signal. The appearance sharp strong signal at 1610 cm^{-1} which is due to be C=C, C=O and C=N stretches. For the imidazole rings, it appears a signal at 1422 cm^{-1}.

The mass spectrum suggests that the ligand **21** is pure.

3.6.10 Metal complexes of 21

Metal complexes reactions of ligand **21** with various metal(II) salts were carried out in MeOH. The reactions were carried out by stirring the ligand and the appropriate metal salts at room temperature 2 hours in MeOH. The resulting coloured solids were collected by filtration.

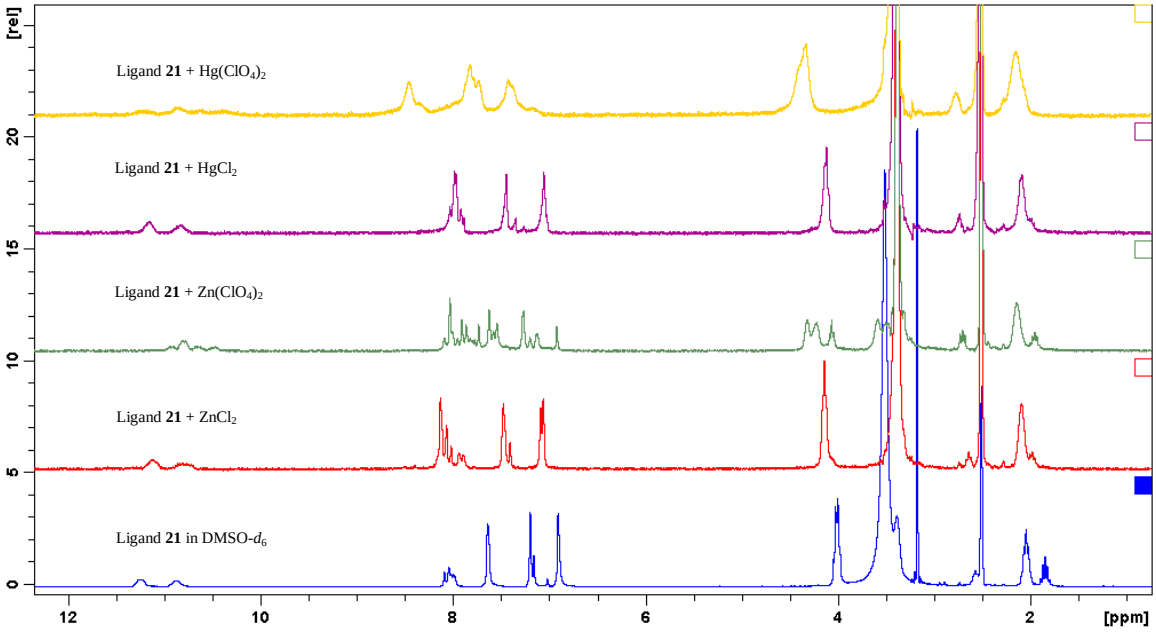

Figure 3.6.44: A comparison of ^{1}H NMR spectra of ligand **21** and its corresponding ZnX_2 and HgX_2 (X = chloride/perchlorate) complexes in DMSO-d_6.

Table 3.6.4: A comparison of the analytical data of the IR spectra between the ligand **21** and its corresponding complexes (cm^{-1}).

	OH	NH stretch	C=O, C=N, C=C	NH bend	Imidazole
ligand **21**			1610	1551	1422
$ZnCl_2$	3469	3246	1614 (br)	1535	1453
$Zn(ClO_4)_2$	3428	block	1614 (br)	1539	1453
$HgCl_2$	3442	3243	1611 (br)	1540	1451
$Hg(ClO_4)_2$	3527	block	1614 (br)	1529	1453
$Ni(ClO_4)_2$	3426	block	1611 (br)	1524	1454
$CuCl_2$	3434	3245	1610 (br)	1520	1452
$CoCl_2$	3392	block	1610 (br)	1521	1451
$Co(ClO_4)_2$	3420	block	1611 (br)	1526	1453

The comparison data of the IR spectra between the ligand **20** and its metal complexes is shown in Table 3.6.4. Although some of the NH stretch signals were blocked by the OH stretch, the appearance of NH bend in all complexes confirms the complexes are in keto-formations. The nitrogen atoms from either the secondary amine groups or the imidazole rings are coordinated to the metal ion centre due to the difference of the signals between the ligand and the metal complexes observed in the appropriate spectra. Moreover, in the IR spectra of the various metal complexes of ligand **21**, the bands due to the C=N, C=O and C=C stretching vibrations partly overlap resulting in a broad band centered at about 1610 cm^{-1}. Therefore these bands at around 1590-1610 cm^{-1} cannot be unambiguously assigned to an individual stretching vibration.

3.6.10.1 $[Zn_5(\mathbf{21})_2Cl_{10}\cdot 2H_2O]$

The complex $[Zn_5(\mathbf{21})_2Cl_{10}\cdot 2H_2O]$ is obtained as an off-white solid. The ^1H NMR spectrum of compound $[Zn_5(\mathbf{21})_2Cl_{10}\cdot 2H_2O]$ is shown in Figure 3.6.44 (in red). The signals representing for the secondary amine protons, Ha/Ha', resonate at 11.13 and 10.81 ppm as two broad singlets, respectively, in comparison the original peaks at 11.51 and 11.05 ppm in ligand **21** indicating the nitrogen atoms from amine groups could be binding to Zn(II) ion centre. The signals for the alkenes protons Hb/Hb' are observed as a multiplet from 7.89 to 8.06 ppm which are similar to those in the free ligand. Several large shifts occurred at the signals for the imidazole protons, Hc/Hc' resonate at 8.14

ppm which were seen to shift from 7.64 ppm in ligand **21**. The protons Hd/Hd' and protons He/He' occur at 7.48 and 7.08 ppm, respectively, which were seen at 7.20 and 6.91 ppm from ligand **21**. These shifts imply that the nitrogen atoms from imidazole rings are coordinated to Zn(II) ion centre.

The IR spectrum of compound $[Zn_5(\mathbf{21})_2Cl_{10}\cdot 2H_2O]$ contains a band ν_{OH} at 3469 cm^{-1} which suggests that coordinated water molecules are present in the Zn(II) complex. The signals for the NH stretch and NH bend are observed at 3122 cm^{-1} and 1535 cm^{-1} suggesting the complex is in keto-formation and the nitrogen atoms from the amine groups are coordinated to the metal ion centre. The C=C stretch for the imidazole rings occurs at 1543 cm^{-1} in comparison to the original band at 1422 cm^{-1} which implies that the nitrogen atoms from the imidazole rings are binding to the metal ion centre.

Elemental analysis indicated that the complex had the formula $[Zn_5(\mathbf{21})_2Cl_{10}\cdot 2H_2O]$. This would also imply that five Zn(II) ions were bonded to the ligand and that ten chloride ions were also involved to account for the neutral charge. The possible structure of compound $[Zn_5(\mathbf{21})_2Cl_{10}\cdot 2H_2O]$ is depicted in Figure 3.6.45.

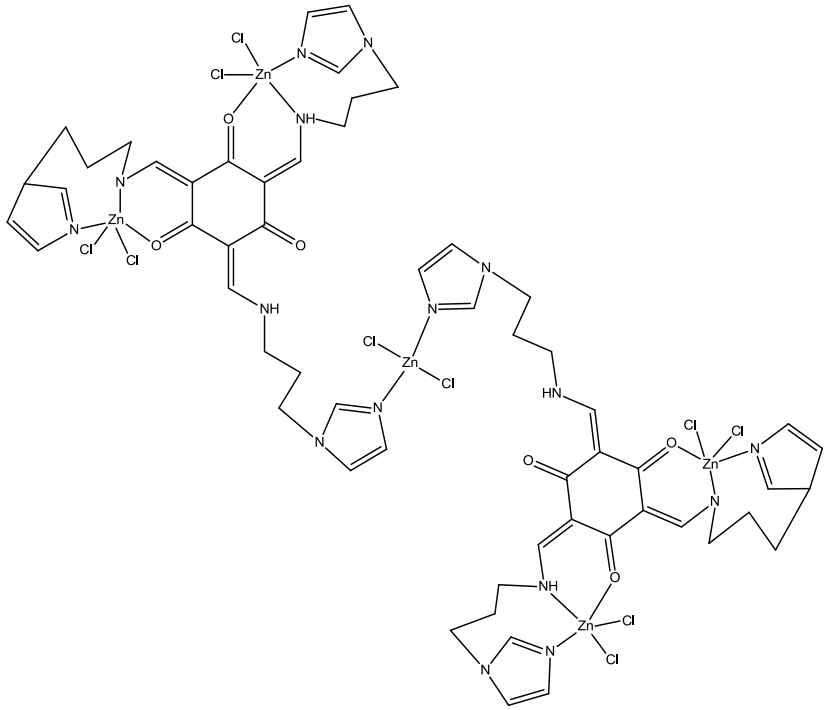

Figure 3.6.45: Possible structure for $[Zn_5(\mathbf{21})_2Cl_{10}\cdot 2H_2O]$.

3.6.10.2 $[Zn(\mathbf{21})(ClO_4)_2\cdot 4H_2O]$

The complex $[Zn(\mathbf{21})(ClO_4)_2\cdot 4H_2O]$ is isolated as an off-white solid. The ^1H NMR spectrum of compound $[Zn(\mathbf{21})(ClO_4)_2\cdot 4H_2O]$ is shown in Figure 3.6.45 (in green). The

reason why it presents lots of peaks in the spectrum could be only one or two imidazole rings bonded to the Zn(II) ions centre.

The IR spectrum of compound [Zn(**21**)$(ClO_4)_2 \cdot 4H_2O$] is found to be similar to that of Zn(II) chloride complex (shown in Table 3.6.4). The appearance of the perchlorate group at 1109 cm^{-1} is indicative of the perchlorate complexation.

Elemental analysis indicated that the complex had the formula [Zn(**21**)$(ClO_4)_2 \cdot 4H_2O$]. This would also imply that one Zn(II) ion was bonded to the ligand and that two perchlorate ions were also involved to account for the neutral charge. The possible structure of compound [Zn(**21**)$(ClO_4)_2 \cdot 4H_2O$] is depicted in Figure 3.6.46. The imidazole nitrogen atoms are probably involved in intermolecular interactions (not shown) to other Zn or perchlorate ions

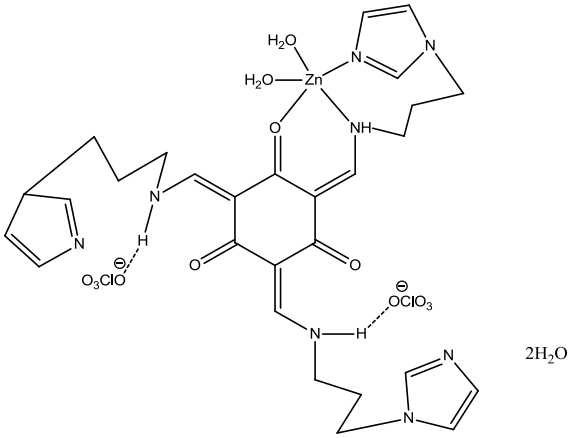

Figure 3.6.46: Possible structure for [Zn(**21**)$(ClO_4)_2 \cdot 4H_2O$].

3.6.10.3 [Hg_3(**21**)Cl_6]

The complex [Hg_3(**21**)Cl_6] is obtained as an off-white solid. The analytical data of the complex [Hg_3(**21**)Cl_6] in either the ^{1}H NMR spectrum or the IR spectrum are similar to those of the Zn(II) chloride complex which suggest the bonding of the Hg(II) ion should be similar to that of Zn(II) ion.

Elemental analysis indicated that the complex had the formula [Hg_3(**21**)Cl_6]. This would also suggest that three Hg(II) ions were bonded to ligand and that six chloride ions were also involved to account for neutral charge. The possible structure of compound [Hg_3(**21**)Cl_6] is depicted in Figure 3.6.47.

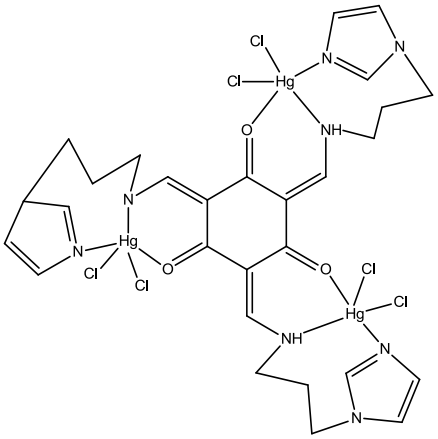

Figure 3.6.47: Possible structure for $[Hg_3(\mathbf{21})Cl_6]$.

3.6.10.4 $[Hg_2(\mathbf{21})(ClO_4)_4{\cdot}2H_2O]$

The complex $[Hg_2(\mathbf{21})(ClO_4)_4{\cdot}2H_2O]$ is obtained as an off-white solid. The ^1H NMR spectrum of compound $[Hg_2(\mathbf{21})(ClO_4)_4{\cdot}2H_2O]$ is shown in Figure 3.6.44 (in yellow). The signals for the secondary amine protons, Ha/Ha', resonate at 11.85 ppm as a broad singlet comparing the original one at 11.51 and 11.05 ppm, respectively, in ligand **21** indicating the nitrogen from amine could be binding to Hg(II) ion centre. The signals for the alkenes protons, Hb/Hb', occur as a broad singlet at 8.45 ppm which was seen to shift from 7.88 to 8.05 ppm in ligand **21** as a multiplet. Several large shifts were also occurring at the signals protons of the imidazole rings, protons Hc/Hc' and Hd/Hd' present at 7.83 ppm as a broad signal which have moved from 7.64 ppm of protons Hc/Hc' and 7.45 ppm of protons Hd/Hd', respectively, in free ligand. Protons He/He' are observed at 7.05 ppm in comparison to the original peaks at 6.91 ppm in ligand **21**, which implies that the nitrogen from imidazole rings could be binding to Hg(II) ion centre. The broadness of the signals suggests a polymeric structure.

The observed IR spectrum of the complex $[Hg_2(\mathbf{21})(ClO_4)_4{\cdot}2H_2O]$ is found to be similar to that of the Zn(II) perchlorate complex with the only one exception of the NH bend which was obtained at 1529 cm^{-1} in the Hg(II) perchlorate complex in comparison to the peak at 1539 cm^{-1} from the Zn(II) perchlorate.

Elemental analysis indicated that the complex had the formula $[Hg_2(\mathbf{21})(ClO_4)_4{\cdot}2H_2O]$. This would imply that two Hg(II) ions were bonded to the ligand and that four perchlorate ions were also involved to account for the neutral charge. The possible structure of compound $[Hg_2(\mathbf{21})(ClO_4)_4{\cdot}2H_2O]$ is depicted in Figure 3.6.48.

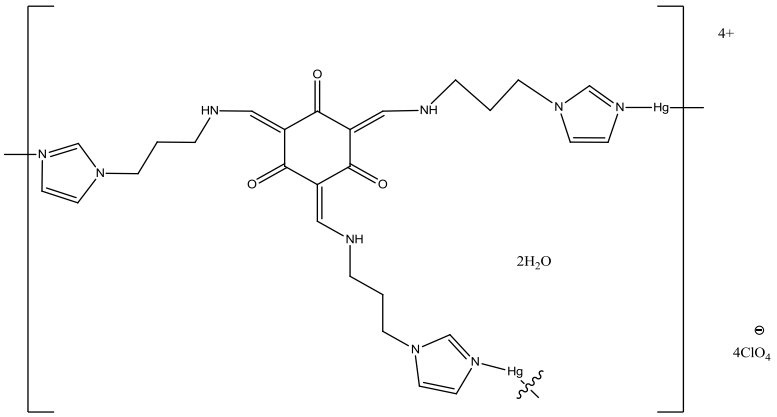

Figure 3.6.48: Possible structure for $[Hg_2(\mathbf{21})(ClO_4)_4 \cdot 2H_2O]$.

3.6.10.5 $[Ni(\mathbf{21})(ClO_4)_2 \cdot MeOH \cdot 2H_2O]$

The complex $[Ni(\mathbf{21})(ClO_4)_2 \cdot MeOH \cdot 2H_2O]$ is obtained as a pale-pink solid. The data of the complex $[Ni(\mathbf{21})(ClO_4)_2 \cdot MeOH \cdot 2H_2O]$ in both the IR spectrum and the elemental analysis are similar to that of Zn(II) perchlorate complex which would suggest the bonding of Ni(II) ion should be similar to that of Zn(II) ion. The magnetic moment of the complex $[Ni(\mathbf{21})(ClO_4)_2 \cdot MeOH \cdot 2H_2O]$ is 3.07 B.M. which suggests that the Ni(II) perchlorate complex adopts a tetrahedral geometry. The possible structure of the complex $[Ni(\mathbf{21})(ClO_4)_2 \cdot MeOH \cdot 2H_2O]$ is depicted in Figure 3.6.49.

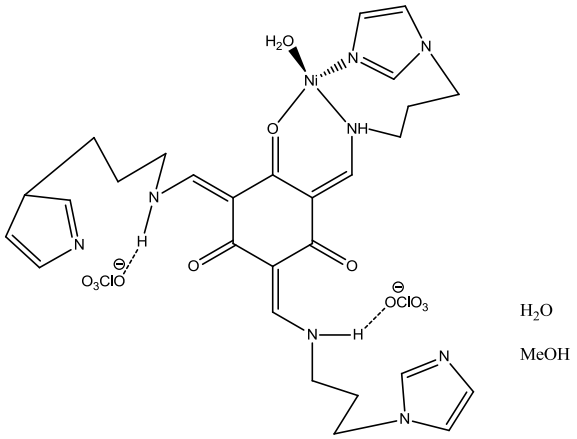

Figure 3.6.49: Possible structure for $[Ni(\mathbf{21})(ClO_4)_2 \cdot MeOH \cdot 2H_2O]$.

3.6.10.6 $[Cu_3(\mathbf{21})Cl_6]$

The complex $[Cu_3(\mathbf{21})Cl_6]$ is isolated as a dark-green solid. The analytical data in either the IR spectrum or the elemental analysis of the complex $[Cu_3(\mathbf{21})Cl_6]$ are found to be similar to that of the Hg(II) complex. The only one exception is occurred at the signal of the NH bend which was appeared at 1520 cm^{-1} in Cu(II) complex in comparison to the one at 1540 cm^{-1} in Hg(II) complex. However, this similarity still suggests that the

bonding of the Cu(II) ion should be similar to that of Hg(II). The magnetic moment of the Cu(II) chloride complex is 2.86 B.M. This would suggest an square pyramidal geometry. The proposed structure of the complex [Cu_3(**21**)Cl_6] is depicted in Figure 3.6.50.

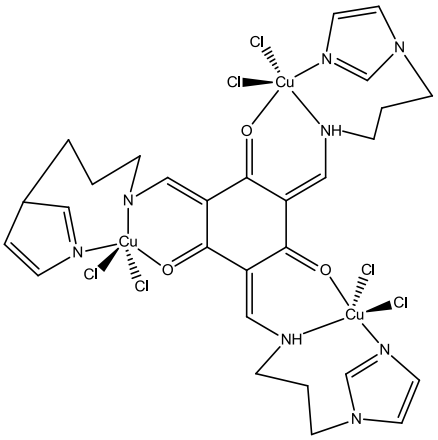

Figure 3.6.50: Possible structure for [Cu_3(**21**)Cl_6].

3.6.10.7 [Co_3(**21**)Cl_6·H_2O]

The complex [Co_3(**21**)Cl_6·H_2O] is obtained as a brown solid. Again, the bonding of the complex [Co_3(**21**)Cl_6·H_2O] is similar to that of Cu(II) chloride complex due to the similar data in IR spectra and the elemental analysis. The magnetic moment of the complex [Co_3(**21**)Cl_6·H_2O] is obtained at 5.35 B.M. which suggests the complex adopts a tetrahedral geometry. The proposed structure of the complex [Co_3(**21**)Cl_6·H_2O] is depicted in Figure 3.6.51.

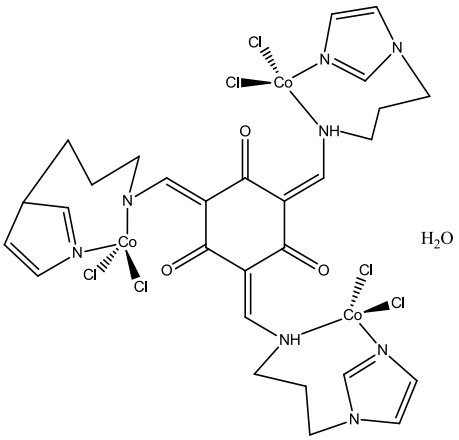

Figure 3.6.51: Possible structure for [Co_3(**21**)Cl_6·H_2O].

3.7 Section 5

3.7.1 Preparation

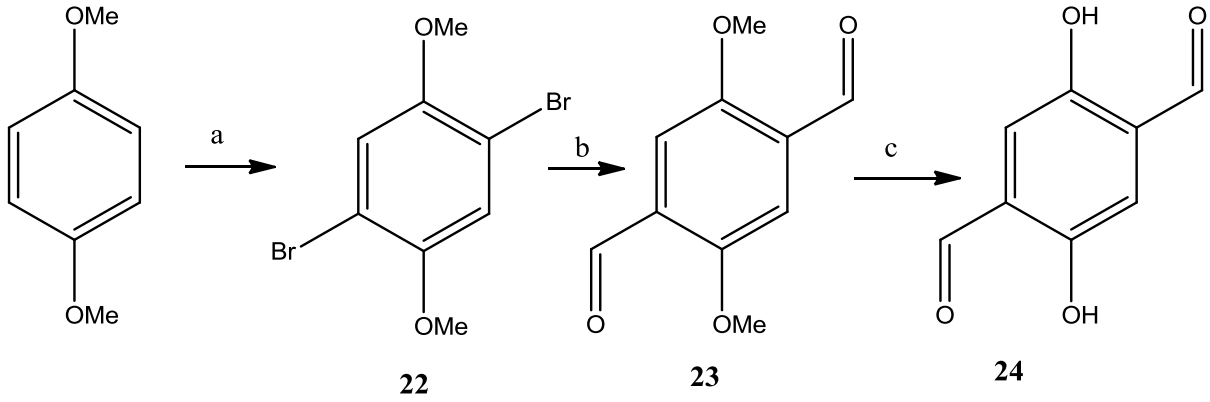

Conditaoins: (a) CH_3COOH, Br_2; (b) (i) 2.5M *n*-Butyllithium, THF, N_2, -78 C; (ii) DMF, 3M HCl; (c) HBr, CH_3COOH

Figure 3.5.1: The synthetic route of compound **24**.

The synthetic route of compound **24** is shown in Figure 3.5.1. The starting material 1,4-dimethoxybenzene was commercially available. The compound 1,4-dibromo-2,5-dimethoxybenzene **22** was synthesized by using acetic acid and bromine with the temperature below 40 ℃ which was reported by Andreas and co-workers.[135] The white crystalline solid of **22** was crystallized from the solution after 2 hours. 2.5M *n*-butyllithium was used in dry THF at -78 ℃ to form 4-dimethyloxy-2,5-difromylbenzene **23**, as reported by Nikolai and co-workers.[136] The **23** is isolated as a yellow solid without further purification. Acidification of **23** with hydrobromic acid (48%) and acetic acid under reflux gives compound 1,4-dihydroxy-2,5-diformylbenzene **24** as a dark yellow crystals with 61 % yield.[137] The mechanism of the formation **23** from the starting material 1,4-dimethoxybenzene is shown in Figure 3.5.2.

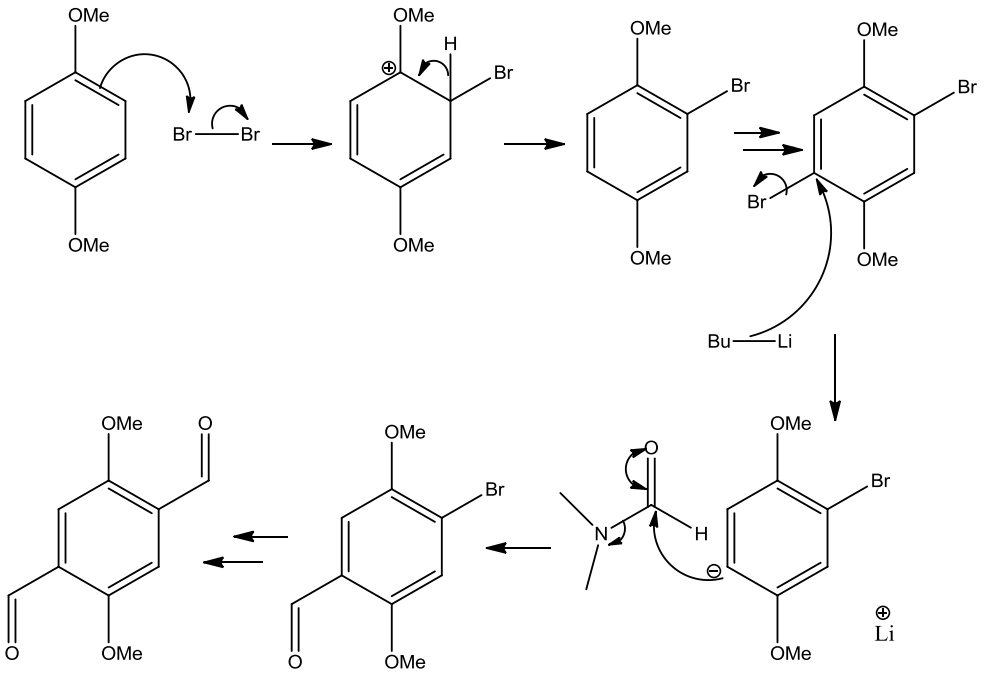

Figure 3.5.2: The mechanism of the formation of **24** from 1,4-dimethoxybenzene.

3.7.2 Ligand synthesis

Compound **24** can be used to synthesize two new ligands (**25** – **26**) as obtained in Figure 3.5.3. Two ligands were synthesized using the same reaction strategy, which was one equivalent of 1,4-dihydroxy-2,5-diformylbenzene **24**, two equivalents of appropriate amine with stirring at room temperature in MeOH for 2 hours. Corresponding ligands **25** and **26** would be precipitated as crystalline yellow solids with about 50 % yield.

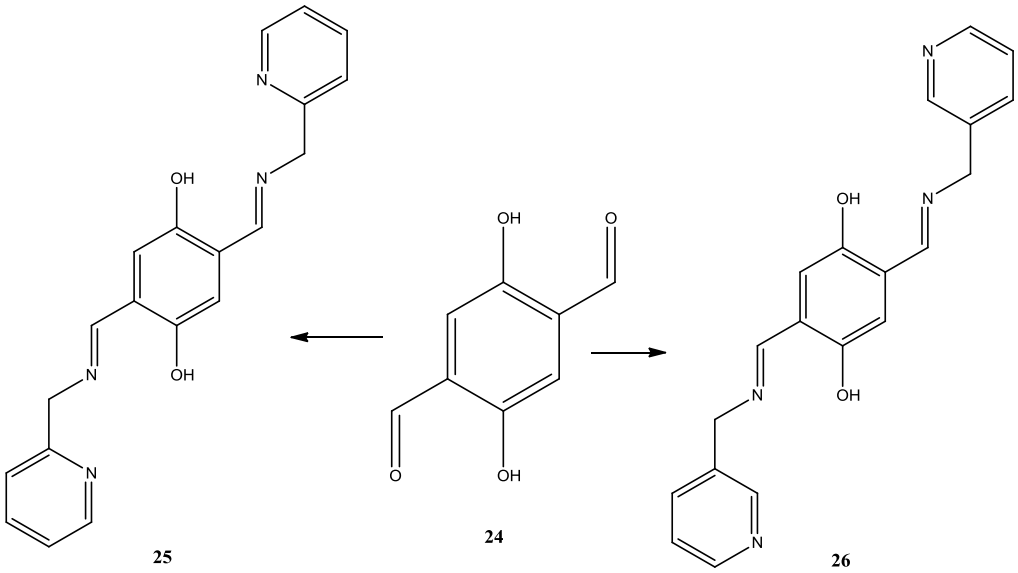

Figure 3.5.3: The Synthetic routes of ligands **25** and **26**.

3.7.3 Ligand 25

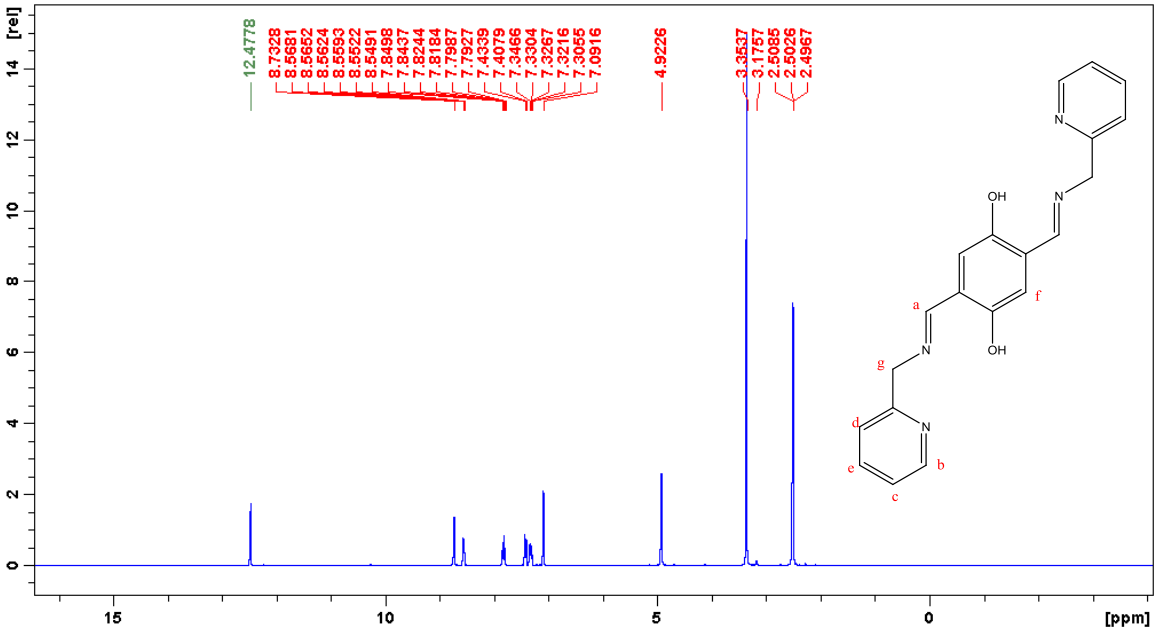

Figure 3.5.4: The ^{1}H NMR spectrum of ligand **25** in DMSO-d_6.

The ligand **25** is formed as a yellow crystalline solid. The ^{1}H NMR spectrum of ligand **25** is shown in Figure 3.5.4. The signal of phenol proton resonates at 12.47 ppm as a sharp singlet. The disappearance of the aldehyde proton at around 10 ppm in di-carbonyl **24** and the appearance of the imine proton Ha at 8.73 ppm indicate that imine formation had occurred. The signals of the pyridine ring protons, Hb is observed as a doublet at 8.55 ppm, Hc and Hd resonate at 7.82 and 7.42 ppm as a double triplets and a doublet, respectively; proton He presents as a multiplet from 7.30 to 7.34 ppm. The signals of the aromatic proton Hf and bridging methylene protons Hg resonate at 7.09 and 4.92 ppm as two singlets.

In the ^{13}C NMR spectrum of ligand **25**, the imine carbon resonates at 166.5 ppm which suggests that imine formation had occurred. The spectrum contains ten carbon peaks which are match with ligand **25**.

The IR spectrum of ligand **25** contains a band ν_{OH} at 3437 cm^{-1} indicating phenol OH stretch in comparison to the band at 3280 cm^{-1} of **24** indicates that stronger hydrogen bond is formed between the imine and the phenol rather formed between the aldehyde and the phenol. The imine C=N stretch appears 1642 cm^{-1} which has moved from the C=O stretch at 1669 cm^{-1} from compound **24**, further confirming the imine formation. The bands of the C=N stretch from the pyridine rings and the aromatic C=C stretch are

observed at 1590 cm^{-1} and 1472 cm^{-1}, respectively. The elemental analysis suggested the ligand **25** is pure.

3.7.4 Metal complexes of 25

Metal complexation reactions of ligand **25** with Zn(II) and Hg(II) salts were carried out in MeOH. The reactions were carried out by heated to reflux for 12 hours in MeOH. The resulting dark dark-coloured solids were collected by filtration.

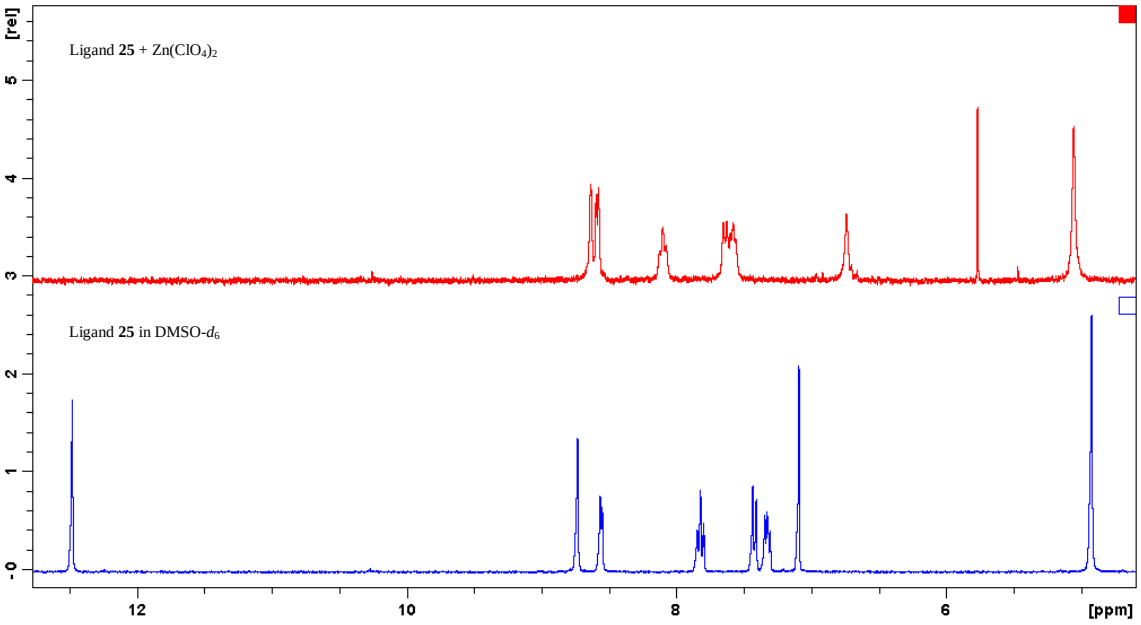

Figure 3.5.5: A comparison of ^{1}H NMR spectra of ligand **25** with its corresponding Zn(II) perchlorate complex in DMSO-d_6.

All the metal complexes of ligand **25** are dark coloured solids, the Zn(II) acetate complex is appears as a dark purple solid which gives a very broad ^{1}H NMR spectrum. The ^{1}H NMR spectra of the metal(II) chloride complexes (such as Zn(II) chloride or Hg(II) chloride) are occurring as broad signals. The reason for this could be metal(II) chloride complexes were formed as polymeric complexes, these compounds will not be discussed further. The ^{1}H NMR spectrum of the Zn(II) perchlorate complex is shown in Figure 3.5.5.

3.7.4.1 [Zn_2(**25**)$(ClO_4)_2$·MeOH]

The complex [Zn_2(**25**)$(ClO_4)_2$·MeOH] is obtained as a dark-yellow solid. The ^{1}H NMR spectrum of compound [Zn_2(**25**)$(ClO_4)_2$·MeOH] is shown in Figure 3.5.5 (in red). The phenol group was deprotonated by the Zn(II) ion due to no peak occurring more than 10 ppm. The signal of imine proton Ha presenting at 8.63 ppm which has moved from 8.73

ppm in ligand **25**, has suggested the nitrogen atoms from the imine group are coordinated to Zn(II) ion centre. While the signals protons of the pyridine rings, protons Hb is observed at 8.57 ppm which is similar to the previous one in ligand, but the proton Hc appears at 8.10 ppm in Zn(II) complex which was seen at 7.82 ppm; and for the protons Hd and He are presented as a multiplet from 7.55 to 7.65 ppm in Zn(II) complex in comparison to the original proton Hd at 7.42 ppm as doublet and proton He as a multiplet from 7.30 to 7.34 ppm, respectively, in ligand **25** implying that the two nitrogen atoms from pyridine rings are binding to Zn(II) ion centre as well. And aromatic signal proton Hf appears at 6.74 ppm in Zn(II) complex which was seen to have a slight change from 7.09 ppm in ligand **25**.

In the IR spectrum of the complex [Zn_2(**25**)$(ClO_4)_2$·MeOH], a MeOH molecule could be present in the Zn(II) complex due to the presence of the OH stretch at 3433 cm^{-1}. The imine C=N stretch is occurring at 1636 cm^{-1} which has moved from 1642 cm^{-1} suggesting that nitrogen atoms from the imine groups are coordinated to Zn(II) ions centre. In addition, the presence of the C=N stretch for the pyridine rings is obtained at 1609 cm^{-1} in comparison to the original one at 1590 cm^{-1} in ligand **25** pointing out that nitrogen atoms from pyridine rings are binding to Zn(II) ion centre as well. The reason for the Zn(II) perchlorate complexation had occurred is the observed perchlorate signal at 1109 cm^{-1}.

The elemental analysis indicated the complex had the formula [Zn_2(**25**)$(ClO_4)_2$·MeOH]. This would also imply that that two Zn(II) ions were bonded to ligand and that two perchlorate ions were also involved. The ligand itself was deprotonated to account for neutral charge. The possible structure for [Zn_2(**25**)$(ClO_4)_2$·MeOH] is depicted in Figure 3.5.6.

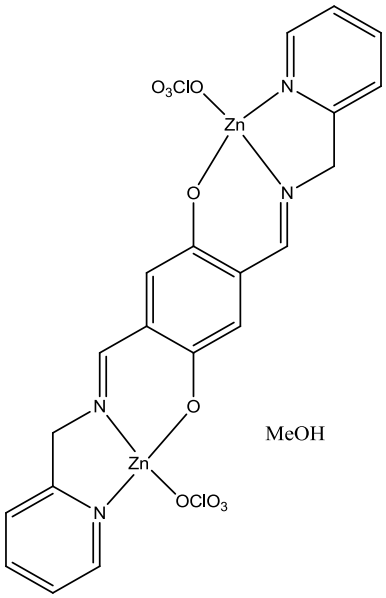

Figure 3.5.6: Possible structure for $[Zn_2(\mathbf{25})(ClO_4)_2 \cdot MeOH]$.

3.7.4.2 $[Zn_2(\mathbf{25})(OAc)_2 \cdot 2H_2O]$

The complex $[Zn_2(\mathbf{25})(OAc)_2 \cdot 2H_2O]$ is isolated as a dark-purple solid. The unusual dark colour of the metal complex suggested the presence of a radical species. This was confirmed by the proton NMR spectrum which gave very broad signals.

The IR spectrum of $[Zn_2(\mathbf{25})(OAc)_2 \cdot 2H_2O]$ contains a signal ν_{OH} at 3431 cm^{-1} indicated coordinated water molecules could be in Zn(II) complex. It appears a broad signal at 1625 cm^{-1} which is due to the presence of the imine C=N stretch and acetate group suggesting the Zn(II) acetate complexation had occurred. The original imine stretch resonated at 1642 cm^{-1} suggesting that imine nitrogen atoms are coordinated to Zn(II) ions centre. The C=N stretch for the pyridine rings appears at 1575 cm^{-1} which was seen to have a slight shift from 1590 cm^{-1} in ligand **25** indicating that nitrogen atoms from pyridine rings could be binding to Zn(II) ion centre as well.

The elemental analysis indicated that the complex had the formula $[Zn_2(\mathbf{25})(OAc)_2 \cdot 2H_2O]$. This would also imply that two Zn(II) ions were bonded to ligand and that two acetate ions were also involved to account for neutral charge. The ligand itself was deprotonated to account for neutral charge. The possible structure of compound $[Zn_2(\mathbf{25})(OAc)_2 \cdot 2H_2O]$ is depicted in Figure 3.5.7.

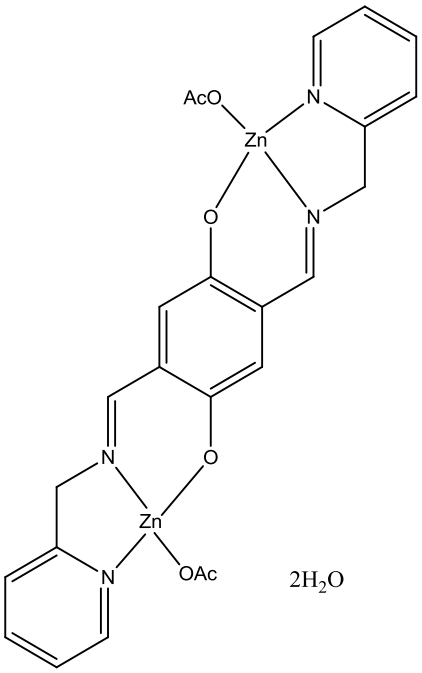

Figure 3.5.7: Possible structure for [Zn_2(**25**)$(OAc)_2$·$2H_2O$].

3.7.5 Ligand 26

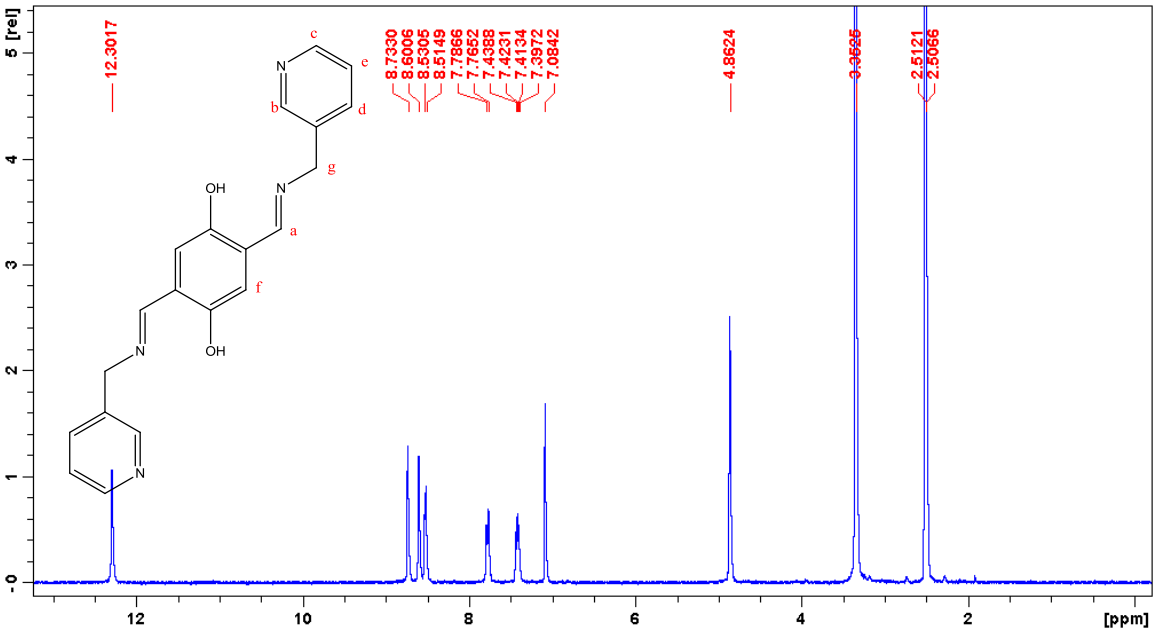

Figure 3.5.8: The ^{1}H NMR spectrum of ligand **26** in DMSO-d_6.

The ligand **26** is isolated as a dark-yellow crystalline solid. The ^{1}H NMR spectrum of ligand **26** is shown in Figure 3.5.8. The signal of phenol proton resonates at 12.30 ppm in comparison to the one of 1,4-dihydroxy-2,5-diformylbenzene **24** at 10.62 ppm again indicating stronger hydrogen bond is formed between the imine and the phenol rather formed between the aldehyde and the phenol. There is no signal of the aldehyde proton

appearing from 9 to 11 ppm, and the imine proton Ha occurs at 8.73 ppm as a singlet indicating that the imine formation had occurred. The aromatic protons is observed at 7.08 ppm comparing the original one at 7.20 ppm of **24**. While the signals of the pyridine rings protons, protons Hb, Hc and Hd are present at 8.60, 8.52 and 7.77 ppm as singlet, doublet and doublet, respectively.

The ^{13}C NMR spectrum of ligand **26** contains the signal of imine carbon at 166.1 ppm implying imine formation had occurred. And it contains ten carbon peaks which are match with ligand **26**.

The IR spectrum of ligand **26** contains a signal ν_{OH} at 3436 cm^{-1} suggesting the phenol OH stretch. It appears a signal at 1637 cm^{-1} which is due to the imine C=N stretch which has moved from the C=O stretch at 1669 cm^{-1} from compound **24**. The signals of the pyridine rings and aromatic are present at 1576 cm^{-1} and 1479 cm^{-1}.

3.7.6 Metal complexes of 26

Metal complexes reactions of ligand **26** with various metal(II) salts were carried out in MeOH. The reactions were carried out by heated to reflux for 12 hours in MeOH. The resulting dark coloured solids were collected by filtration.

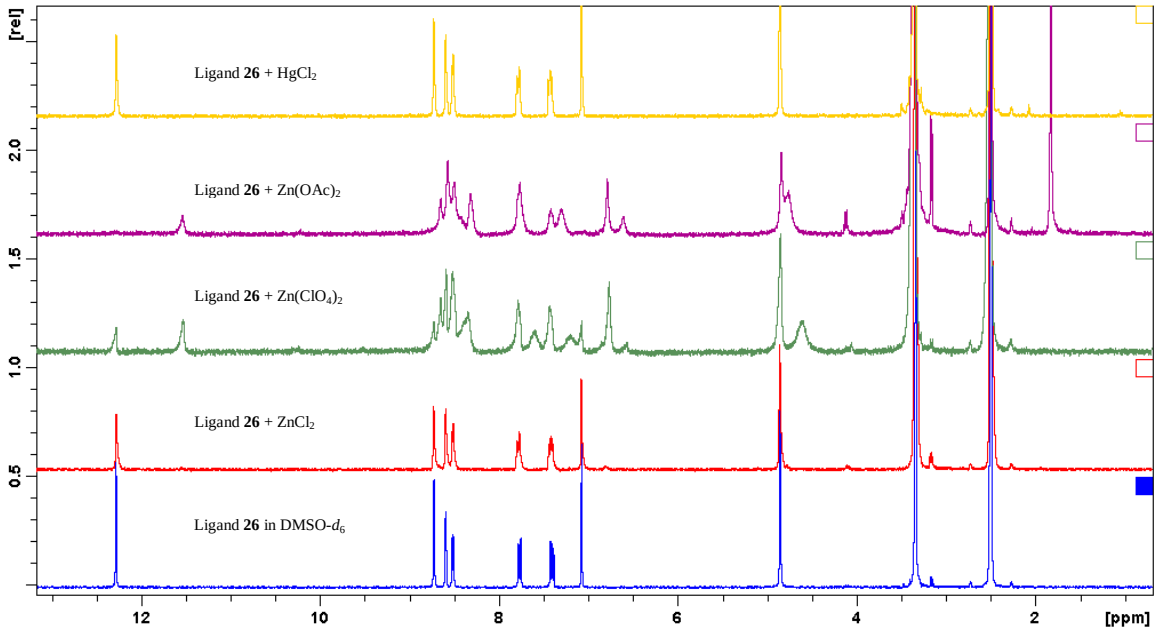

Figure 3.5.9: A comparison of ^{1}H NMR spectra of ligand **26** and its corresponding ZnX_2 and HgX_2 (X = chloride, perchlorate and acetate) complexes in DMSO-d_6.

The comparison ^{1}H NMR spectra of the ligand **26** and its corresponding complexes is shown in Figure 3.5.9. The spectra of both Zn(II) and Hg(II) chloride complexes are

similar to the one of ligand **26** implying a weak bonding could be occurred between the metal ion and the ligand. But the Zn(II) acetate and perchlorate complexes, which are shown as green and purple spectra, respectively, in Figure 3.5.9, show many broad signals suggesting the both type of metal(II) complexes were formed to be polymeric complexes.

3.7.6.1 [Zn(**26**)Cl_2]

The complex [Zn(**26**)Cl_2] is obtained as a brown-orange solid. The ^{1}H NMR spectrum of compound [Zn(**26**)Cl_2] is similar to that of ligand.

The IR spectrum of compound [Zn(**26**)Cl_2] contains a signal $\nu_{C=N}$ at 1637 cm^{-1} which was seen to have a slight shift from 1630 cm^{-1} in ligand **26** suggesting that the imine nitrogen atoms may be binding to the metal ion centre. There appears a signal at 1611 cm^{-1} which probable is due to the C=N stretch for the pyridine rings in comparison to the original one at 1576 cm^{-1} implying that nitrogen atoms from pyridine rings are bonding to Zn(II) ion centre as well.

Elemental analysis indicated that the complex had the formula [Zn(**26**)Cl_2]. This would also suggest that one Zn(II) ion was bonded to ligand and that two chloride ions were also involved to account for neutral charge. The bonding of Zn(II) ion is through two nitrogen atoms from the pyridine rings, as well as two chloride ions. The geometry of Zn(II) ion is four-coordinate sphere. The possible structure of compound [Zn(**26**)Cl_2] is depicted in Figure 3.5.10.

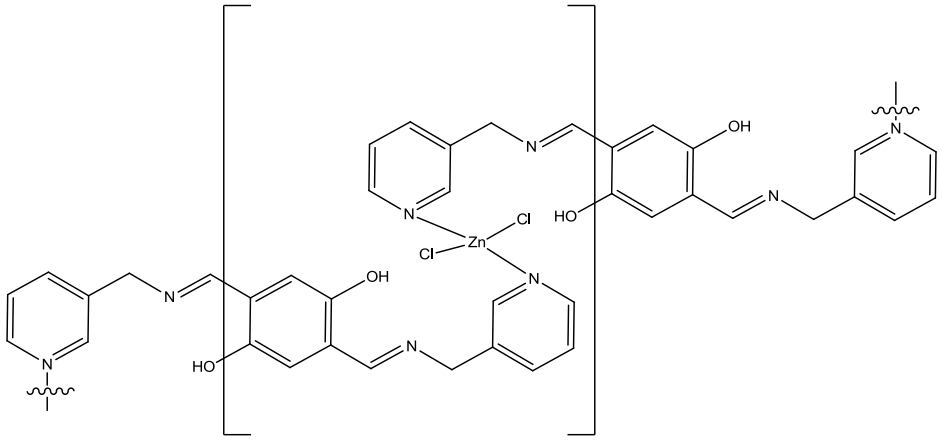

Figure 3.5.10: Possible structure for [Zn(**26**)Cl_2].

3.7.6.2 [Zn(**26**)(ClO_4)·(OH)·2MeOH]

The ^{1}H NMR spectrum of compound [Zn(**26**)(ClO_4)·(OH)·2MeOH] is shown as green spectrum in Figure 3.5.9. From the comparison with the blue spectrum of the ligand, it is clear that some peaks in the Zn(II) complex are same with its corresponding ligand **26** while some are not. The phenol proton for the Zn(II) complex is appeared two signals which are resonating at 12.30 and 11.55 ppm, respectively. The signal at 12.30 ppm is similar to that of the ligand while the signal at 11.55 ppm is presumed that only one oxygen atom from the phenol group is coordinated to the Zn(II) ion.

The IR spectrum of compound [Zn(**26**)(ClO_4)·(OH)·2MeOH] contains a signal ν_{OH} at 3435 cm^{-1} indicated the phenol OH stretch and coordinated MeOH molecules could be present in the Zn(II) complex. The imine C=N stretch is observed at 1613 cm^{-1} as a broad signal which was seen to have a shift from 1630 cm^{-1} in ligand **26**, indicates that nitrogen atoms from the imine group could be coordinated to Zn(II) ion centre. The C=N stretch for the pyridine rings is obscured of imine stretch but there is no peak around 1576 cm^{-1} which is the original signal of co-ordinated pyridine in ligand **26**, suggests that nitrogen from pyridine rings are bonding to Zn(II) ion centre. The aromatic stretch is observed at 1471 cm^{-1} which was similar with the original one at 1479 cm^{-1} in ligand **26**. It appears a strong broad signal at 1108 cm^{-1} which is expected to be perchlorate group, indicates that Zn(II) perchlorate complexation had occurred.

The elemental analysis indicated that one Zn(II) ion was bonded to ligand and that one perchlorate ion was also involved to account for neutral charge. One water molecule was deprotonated to account for neutral charge. The possible structure of compound [Zn(**26**)(ClO_4)·(OH)·2MeOH] could be depicted in Figure 3.5.11.

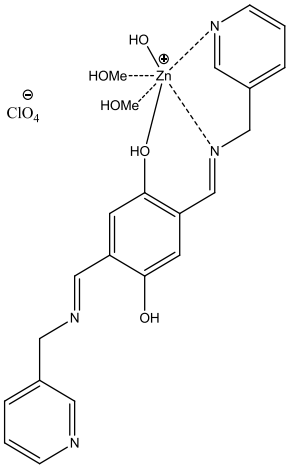

Figure 3.5.11: Possible structure for [Zn(**26**)(ClO_4)·(OH)·2MeOH].

3.7.6.3 [Zn_2(**26**)$(OAc)_2 \cdot 4H_2O$]

The ^{1}H NMR spectrum of the compound [Zn_2(**26**)$(OAc)_2 \cdot 4H_2O$] is shown as the purple spectrum in Figure 3.5.9. There appears a broad signal at 11.56 ppm which is due to the phenol protons, but the integrals suggested very low number on phenol protons, indicating phenol protons could be deprotonated by the Zn(II) ion. And there are also many broad peaks in the spectrum, suggesting that complexation could have occurred. These broad signals also suggests the polymeric complexation. For the signals of imine protons Ha, pyridine protons Hb and Hc, are observed as a multiplet together from 8.32 to 8.66 ppm, comparing the original protons at 8.73 ppm (Ha), 8.60 ppm (Hb) and 8.52 ppm (Hc), respectively. This suggests that the nitrogen atoms from both the imine groups and the pyridine rings could be binding to Zn(II) ion centre. While the other signals of pyridine protons Hd and He are observed to be similar to the original positions in ligand **26**. But the aromatic protons Hf resonates at 6.79 and 6.93 ppm as two singlets in Zn(II) complex.

The IR spectrum of compound [Zn_2(**26**)$(OAc)_2 \cdot 4H_2O$] contains a broad signal ν_{OH} at 3385 cm^{-1} indicating that some coordinated water molecules could be present in the Zn(II) complex. The imine C=N stretch is observed at 1621 cm^{-1} which was seen to have a shift from 1637 cm^{-1} in ligand **26**, suggesting nitrogen atoms from the imine group could be binding to the Zn(II) ion centre. The signal C=N stretch for the pyridine ring occurs 1609 cm^{-1} in comparison to the original signal at 1576 cm^{-1} in ligand **26**. This indicates that nitrogen atoms from the pyridine rings are coordinated to Zn(II) ion centre as well. The presence of several signals in the range of 1600-1300 cm-1 makes it difficult to assign the binding mode of the acetate group.

The elemental analysis indicated that two Zn(II) ions were bonded to ligand and that two acetate ions were also involved. The ligand itself was deprotonated to account for neutral charge. The possible structure of compound [Zn_2(**26**)$(OAc)_2 \cdot 4H_2O$] is depicted in Figure 3.5.12.

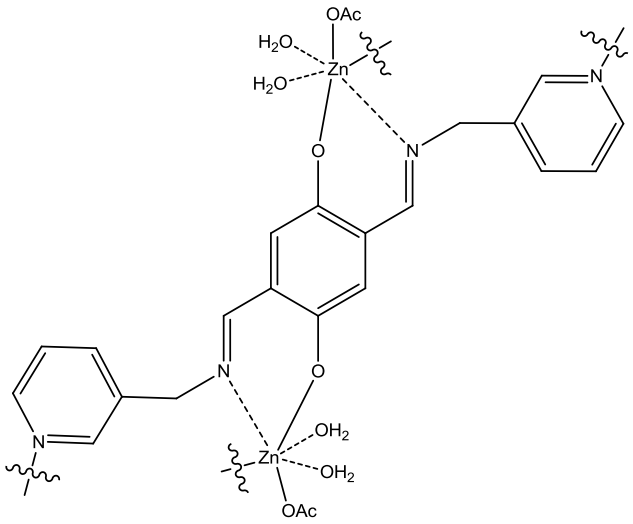

Figure 3.5.12: Possible structure for $[Zn_2(\mathbf{26})(OAc)_2{\cdot}4H_2O]$.

3.7.6.4 $[Hg(\mathbf{26})Cl_2{\cdot}MeOH]$

The complex $[Hg(\mathbf{26})Cl_2{\cdot}MeOH]$ is formed as a yellow solid. The analytical data of the complex $[Hg(\mathbf{26})Cl_2{\cdot}MeOH]$ in either the ^1H NMR spectrum or the IR spectrum or the elemental analysis are found to be very similar to that of Zn(II) chloride complex which would imply that the bonding of the Hg(II) ion should be similar to that of Zn(II) ion as well. Hence, the proposed structure of the complex $[Hg(\mathbf{26})Cl_2{\cdot}MeOH]$ is depicted in Figure 3.5.13.

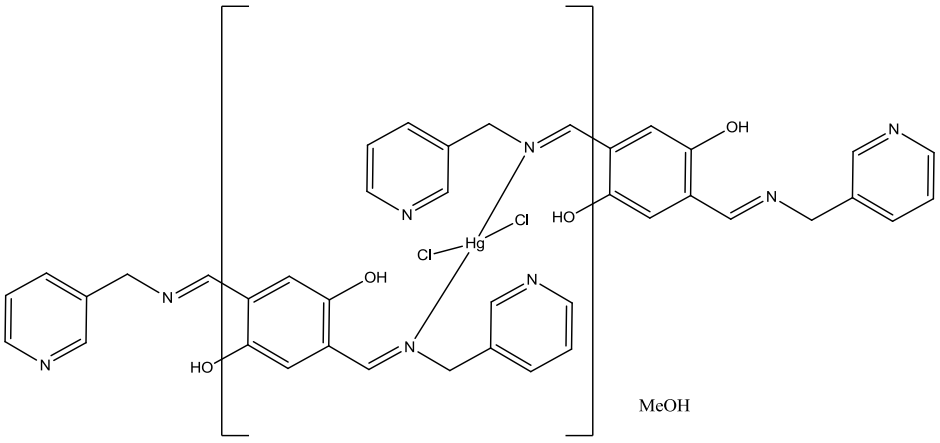

Figure 3.5.13: Possible structure for $[Hg(\mathbf{26})Cl_2{\cdot}MeOH]$.

3.8 Section 6

3.8.1 Preparation

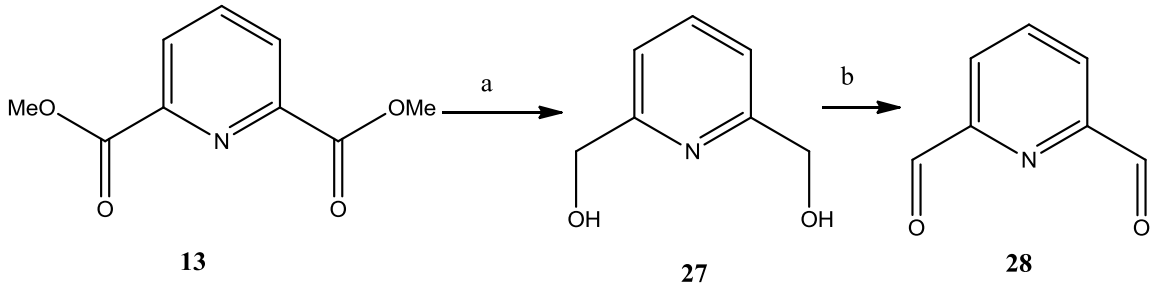

Condition: (a) (i) $NaBH_4$, THF; (ii) 2M HCl (b) SeO_2, 1,4-dioxane

Figure 3.6.1: The synthetic route of compound **28**.

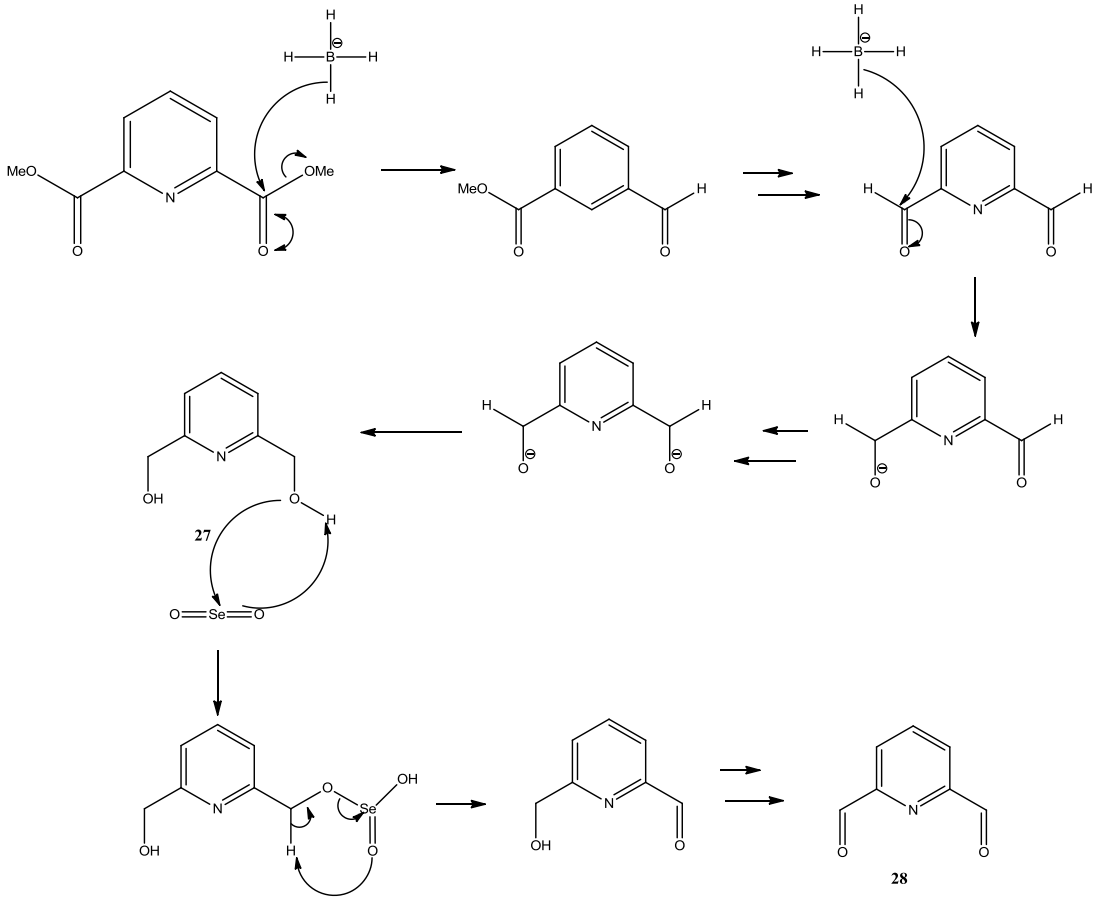

Figure 3.6.2: The mechanism of synthesising compound **27** and **28**.

The compound dimethyl pyridine-2,6-dicarboxylate **13** was obtained in **Section 3**. The synthesis of the di-carbonyl compound **28**, 2,6-diformyl-pyridine, is shown in Figure 3.6.1. Reduction of compound **13** by using sodium borohydride in THF has been

reported by Xiao-Ming and co-workers.[138] The generated 2,6-bis-(hydroxymethyl)-pyridine **27** as a white solid which was then oxidizing by with SeO_2 in 1,4-dioxane to leave pyridine-2,6-dicarboxaldehyde **28** as a white solid with 82 % yield.[139] The mechanism of this synthesis route has been shown in Figure 3.6.2.

3.8.2 Ligand synthesis

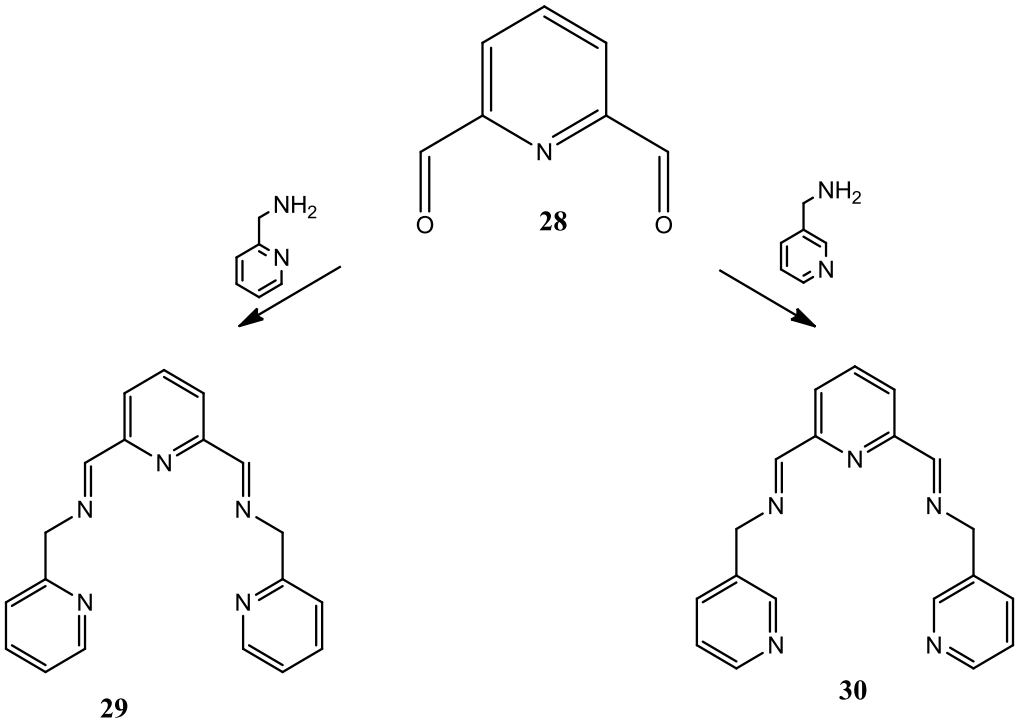

Figure 3.6.3: Synthesis of ligands **29** – **30**.

Compound **28** can be used to synthesize two new ligands (**29** – **30**) as shown in Figure 3.6.3. Both ligands were synthesized using the same reaction strategy, which was one equivalent of compound **28**, two equivalents of appropriate amine, and ten equivalents of anhydrous $MgSO_4$ in $CHCl_3$ with reflux for 12 hours. The reason for this can be seen from Schiff base ligand formation and hydrolysis.

3.8.3 Ligand 29

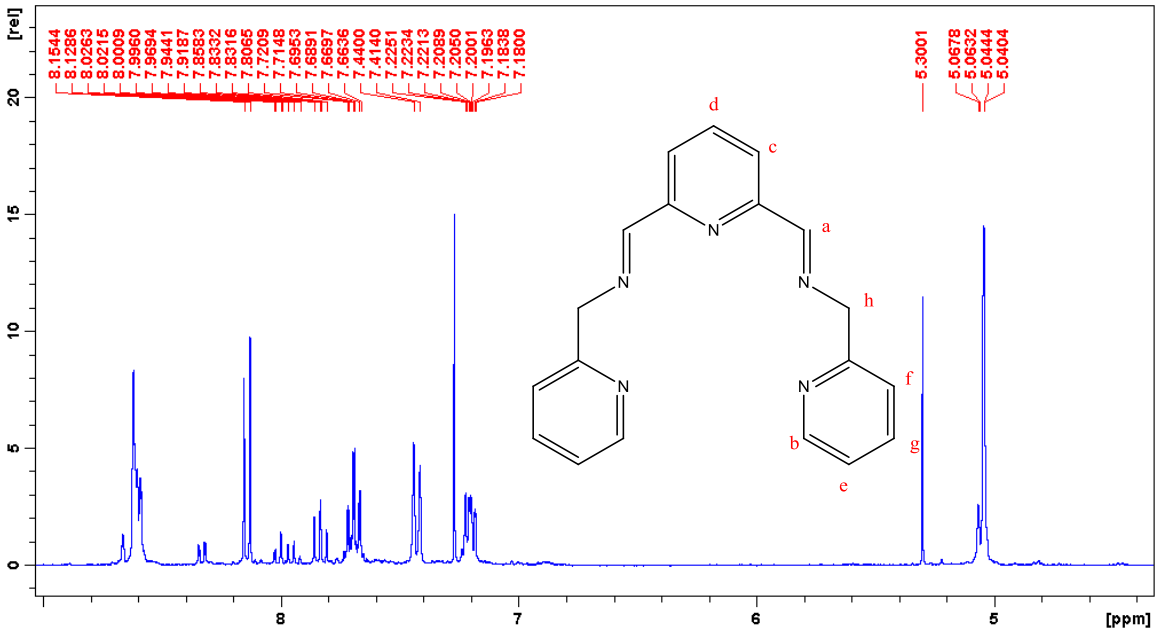

Figure 3.6.4: The ^{1}H NMR spectrum of ligand **29** in $CDCl_3$.

The ligand **29** is isolated as a yellow oil. The ^{1}H NMR spectrum of ligand **29** is shown in Figure 3.6.4. The signals of imine protons Ha is observed at 8.62 ppm, and the disappearance of the carbonyl proton at around 10 ppm are suggesting the imine formation had occurred. The signals protons Hc and Hd from the central pyridine rings are observed as a doublet and a triplet at 8.14 and 7.83 ppm in comparison to the original two at 8.19 and 8.10 ppm from 2,6-diformylpyridine **28**. While the signals for the lower pyridine rings, proton Hb resonates from 8.58 to 8.61 ppm as multiplet, and protons He appears as a double triplet at 7.69 ppm. Proton Hf is present as a doublet at 7.42 ppm and proton Hg is observed from 7.18 to 7.22 ppm as a multiplet. The signal of bridging methylene proton Hh is occurring at 5.04 ppm.

The ^{13}C NMR spectrum of ligand **29**, it appears a imine carbon signal at 163.9 ppm which confirms the imine formation had occurred.

The IR spectrum of ligand **29** contains a signal of imine C=N stretch at 1652 cm^{-1} in comparison to the carbonyl signal at 1710 cm^{-1} confirming that imine formation had occurred again. It appears two C=N stretches at 1594 and 1573 cm^{-1} which are expected to be from different pyridine, respectively.

3.8.4 Ligand 30

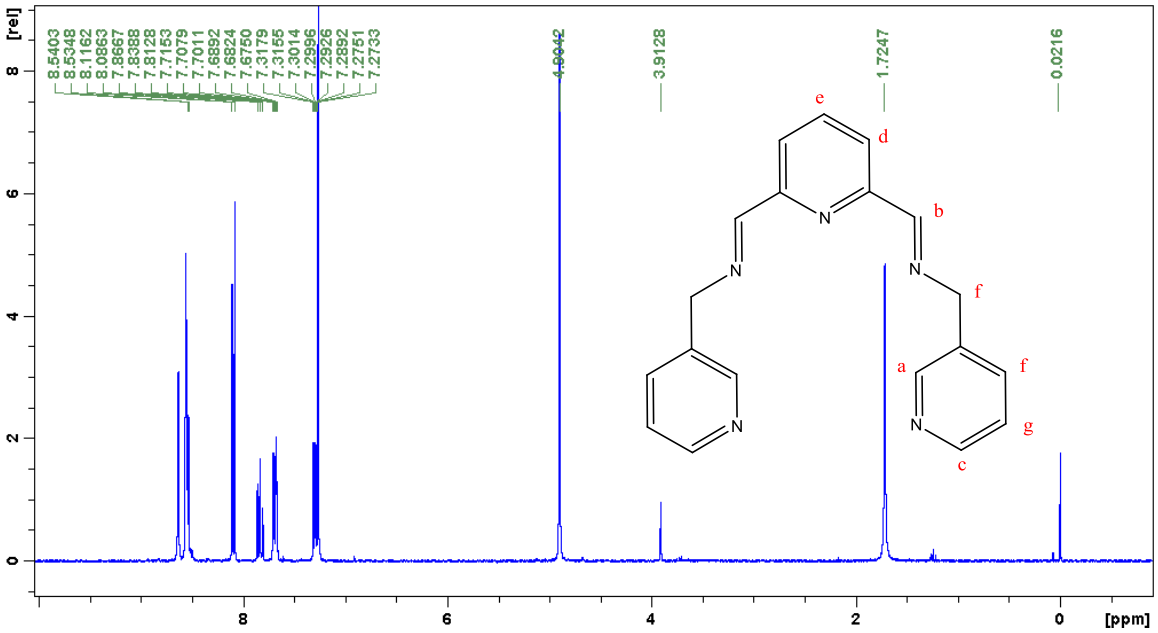

Figure 3.6.5: The ^{1}H NMR spectrum of ligand **30** in $CDCl_3$.

The ligand **30** is formed as a yellow oil. The ^{1}H NMR spectrum of ligand **30** is shown in Figure 3.6.5. The signals of central pyridine rings, protons Hd and He are observed as a doublet and a triplet at 8.10 and 7.83 ppm, respectively, which have moved from 8.19 and 8.10 ppm in compound **28**. The appearance of the imine proton Ha at 8.64 ppm and the disappearance of the aldehyde proton at around 10 ppm are indicating the imine formation had occurred. The signals at the lower pyridine rings, proton Ha is observed as a multiplet at 8.64 ppm; Hc appears as a multiplet from 8.53 to 8.55 ppm; Hf resonates from 7.67 to 7.71 ppm as a multiplet and Hg presents as a multiplet from 7.27 to 7.31 ppm as well. The bridging methylene proton Hh is occurring at 4.90 ppm as a singlet.

In the ^{13}C NMR spectrum of ligand **30**, there appears a signal for the imine carbon at 163.1 ppm confirming the imine formation had occurred. The spectrum also contains ten carbon peaks which are match with ligand **30**.

The IR spectrum of ligand **30** contains a signal of imine C=N stretch at 1648 cm^{-1} which has moved from 1710 cm^{-1} in di-carbonyl compound **28** suggesting that imine formation had occurred again. The signal C=N stretch for the pyridine ring occurs at 1591 cm^{-1}.

Due to the time constraints, no metal complexation reaction were carried out with either ligand.

4 Conclusion

Conclusion

The goal of the work carried out in this thesis was to prepare an array of novel ligands based on either a Schiff-base (imine) or amide design. This thesis can be divided into 6 sections, depending on the aldehyde used in the imine reaction. In addition, five of the sections discuss imine metal complexes while the remaining section discusses di-amide complexes. The formation of different Schiff-base ligands by using anhydrous magnesium sulphate in chloroform or dichloromethane had been proved to be the best way in this thesis. All of the ligands (except the two ligands **29** and **30** in section **6**) were subjected to complexation studies resulting in the formation of novel coordination complexes. Different divalent d-block metal(II) salts, cobalt(II), nickel(II), copper(II), zinc(II) and Hg(II) with counterions being acetate, chloride and perchlorate, were employed in these complexation reactions.

Using 5-(1,1-dimethylethyl)-2-hydroxy-1,3-benzenedicarboxaldehyde **2**, four new Schiff-base ligands were prepared in good yield in section 1 of chapter 3. The ligand **4** based on 3-aminomethyl pyridine was isolated as a yellow solid while the other three ligands (**3**, **5** and **6**) were observed as yellow oils. The ligands, once formed, were stable for an extended period. Complexation reactions were carried out using the above metal salts by stirring with the ligands in methanol at room temperature. No hydrolysis of the Schiff-base complexes occurred in this chapter. The NMR spectra of the metal complexes of ligands **3** and **6** were more simple than the complexes of ligand **4** and **5**, whose proton spectra (shown in Figure 3.3.10 and Figure 3.3.21) were more complicated. The phenol protons in all complexes based on ligands **3**, **4**, **5** and **6** were deprotonated by the metal ions with the exception of the Hg(II) complexes of ligand **6**.

The di-carbonyl compound 5,5'-methylene-bis-salicylaldehyde **7** was employed in order to synthesis the four new ligands **8 – 11** in section 2 of chapter 3. Again, the ligand **9** based on the 3-aminomethylpyridine was isolated as a yellow solid. The other ligands **8**, **10** and **11** were obtained as yellow oils. The metal complexation reactions can be separated by two synthetic routes. The first route was stirring the ligands and the appropriate metal salts which was similar to the metal complexation in section 1. The second route was to react directly from the di-carbonyl compound **7** with appropriate amines and the metal salts in a one-pot reaction. Both methods gave the same results. All the phenol groups were deprotonated by the metal ions in the complexes of ligand **8**. For the rest of the complexes, according to the observations in the proton NMR spectrum and the IR spectrum, the phenol groups in some complexes were deprotonated while some were not. The '$Zn(SCN)_2$' and '$Ni(SCN)_2$' metal complexation reactions

with ligand **8** were carried out initially with Zn(II) or Ni(II) acetate salts resulting in a clear solution. The appropriate thiocyanate complexes were formed on the addition of sodium thiocyanate to the solution which resulted in coloured solids, which precipitated from solution.

The three novel acyclic di-amide ligands **14 – 16** also had been explored in chapter 3, section 3. In comparison to the formation of Schiff base ligands, a different reaction strategy was involved to synthesis the amide ligands. The excess of appropriate primary amines precursors and the higher boiling point of the toluene solvent were used in the formation of the amide ligands. Ligand **14** was isolated as a crystalline white solid while the other two ligands were observed as yellow oils. The metal complexation reactions were carried out by stirring the ligands and the appropriate metal salts at room temperature for 2 hours. No amide protons were deprotonated by the metal ions in any case. The proton spectra of all Zn(II) and Hg(II) metal complexes formed in the presence of either ligands **14** or **15** are found to be similar to the spectra of corresponding ligands. Large protons shifts occurred, however, between the ligand **16** and its Zn(II) and Hg(II) complexes.

The [1+3] acyclic Schiff-base complexes were synthesised by using the compound triformylphloroglucinol **17** in section 4. Only 10-15 % yield was achieved for the formation of **17**. The formation of ligands **18 – 21** and the corresponding metal complexations were prepared in reaction strategies similar to those of section 1. However, the observations of the ligands in either the proton spectra or the IR spectra confirmed that the ligands were stable in the keto-form, rather than enol-form. In addition, both the C_{3h} and C_s isomers were present in all ligands. The complexes from all ligands were in the keto-form with the exception of the Zn(II) acetate complex in the presence of the ligand **18**. This acetate complex was switched back to the enol-formation and the phenol groups were deprotonated by the metal ion. It was difficult to assign the specific bonding sites in this chapter due to the presence of several donating atoms in each ligand.

Only the formation of Zn(II) and Hg(II) complexes was undertaken in section 5 which involved the compound 1,4-dihydroxy-2,5-diformylbenzene **24**. Two new Schiff-base ligands **25** and **26** were formed as yellow crystalline solids which crystallized directly from the solution. The dark coloured Zn(II) and Hg(II) complexes were precipitated by stirring the ligand and the appropriate metal salts in methanol. It was found that the

chloride complexes of ligand **25** gave broad signals in the proton spectra while the perchlorate complexes are much more clear. The Zn(II) acetate complex of ligand **25** was obtained as a dark purple solid which could indicate the formation of a radical complex. The observed spectra of the Zn(II) and Hg(II) chloride complexes of ligand **26** are found to be similar to that of ligand. However, broad signals appeared in the acetate and the perchlorate complexes of ligand **26**.

In the last section, the reduction of dimethyl pyridine-2,6-dicarboxylate **13** by using sodium borohydride in THF yielded the di-hydroxyl-pyridine derivative **27**. This was then oxidised using selenium dioxide to form pyridine-2,6-dicarboxaldehyde **28**. Two novel acyclic Schiff base ligands **29** and **30** were synthesized by stirring the di-aldehyde **28** and the appropriate amines in chloroform under reflux. Due to the time constraints, no metal complexation reactions were carried out with either ligands.

The future work can be summarised as follows: i) the completion of sections 4 and 5, using various metal ion salts; ii) deprotonating of all these phenol groups with a weak base, such as triethylamine, in the metal complexation reactions in order to get better interaction between the metal ions and the ligands; and iii) further investigation of the ligands based on triformylphloroglucinol **17** in section 4 in order to get a better understanding of the keto-enol tautomerism and also to get interaction with different metal ions with the same ligand in these systems.

5 Bibliography

References

1. R. Hernández-Molina and A. Mederos, *Comprehensive Coordination Chemistry II 2003*, Elsevier Ltd, 2003, 411
2. P. Anand, V.M. Patil, V.K. Sharma, R.L. Khosa and N. Masand, *International Journal of Drug Design and Discovery*, 2012, **3**, 851
3. K.C. Gupta, A. Kumar Sutar and C.-C. Lin, *Coord. Chem. Rev.*, 2009, **253**, 1926.
4. K.C. Gupta and A.K. Sutar, *Coord. Chem. Rev.*, 2008, **252**, 1420.
5. A. Zoubi and Wail, *J. Coord. Chem.*, 2013, **66**, 2264.
6. H. Schiff, *Justus Liebig's Annalen der Chemie*, 1864, **131**, 118.
7. P. Pfeiffer, E. Breith, E. Lübbe and T. Tsumaki, *Justus Liebig's Annalen der Chemie*, 1933, **503**, 84
8. R. Atkins, G. Brewer, E. Kokot, G.M. Mockler and E. Sinn, *Inorg. Chem.*, 1985, **24**, 127
9. K.N. Campbell, A.H. Sommers and B.K. Campbell, *J. Am. Chem. Soc.*, 1944, **66**, 82
10. J. Hine and C.Y. Yeh, *J. Am. Chem. Soc.*, 1967, **89**, 2669.
11. I.A. Savich, A.K. Pikaev, I.A. Lebedav and V.I. Spitsyn., *Vestnik. Moskov. Univ*, 1956, **11**, 225.
12. H. Tazoki and K. Miyano., *J. Am. Chem. Soc.*, 1959, 9769.
13. C.M. Brewster, *J. Am. Chem. Soc.*, 1924, **46**, 2463.
14. J.M. Sayer, B. Pinsky, A. Schonbrunn and W. Washtien, *J. Am. Chem. Soc.*, 1974, **96**, 7998.
15. P. Wothers, N. Greeves, S. Warren and J. Clayden, *Organic Chemistry*, Oxford University Press, Oxford, 1st edn., 2001, 348.
16. B.S. Furniss, A.J. Hannaford, P.W.G. Smith and A.R. Tatchell, *Vogels text book of practical org. chem.*, 2006, **5**, 782.
17. N.P. Kushwah, M.K. Pal, A.P. Wadawale and V.K. Jain, *J. Organomet. Chem.*, 2009, **694**, 2375.
18. J.-C. Andrez, *Tet. Lett.*, 2009, **50**, 4225.
19. Y. Zhang, L. Xiang, Q. Wang, X.-F. Duan and G. Zi, *Inorg. Chim. Acta*, 2008, **361**, 1246.
20. G.J.P. Britovsek, V.C. Gibson, B.S. Kimberley, P.J. Maddox, S.J. Mctavish, G.A. Solan, A.J.P. White and D.J. Williamsa, *Chem. Commun.*, 1998, 849
21. R. Jackson, J. Ruddlesden, D.J. Thompson and R. Whelan, *J.Organomet. Chem.*, 1977, **125**, 57

22. F.a.R. Kaul, G.T. Puchta, H. Schneider, F. Bielert, D. Mihalios and W.A. Herrmann, *Organometallics*, 2002, **21**, 74
23. I. Kim, B.H. Han, C.-S. Ha, J.-K. Kim and H. Suh, *J. Am. Chem. Soc.*, 2003, **36**, 6989.
24. S.D. Ittel and L.K. Johnson, *Chem. Rev.*, 2000, **100**, 1169.
25. G.J.P. Britovsek, V.C. Gibson and D.F. Wass, *Angew. Chem. Int. Ed.*, 1999, **38**, 428
26. K. Kervinen, H. Korpi, M. Leskel ä and T. Repo, *J. Mol. Catal. A: Chem.*, 2003, **203**, 9.
27. A. Soroceanu, M. Cazacu, S. Shova, C. Turta, J. Kožíšek, M. Gall, M. Breza, P. Rapta, T.C.O. Mac Leod, A.J.L. Pombeiro, J. Telser, A.A. Dobrov and V.B. Arion, *Eur. J. Inorg. Chem.*, 2013, **2013**, 1458.
28. M. Rong, J. Wang, Y. Shen and J. Han, *Catal. Commun.*, 2012, **20**, 51.
29. P. Oliveira, A. Machado, A.M. Ramos, I. Fonseca, F.M.B. Fernandes, A.M.B.D. Rego and J. Vital, *Microporous Mesoporous Mater.*, 2009, **120**, 432.
30. J. Hu, K. Li, W. Li, F. Ma and Y. Guo, *Appl. Catal., A,*, 2009, **364**, 211.
31. W. Adam, F.G. Gelalcha, C.R. Saha-Moller and V.R. Stegmann, *J. Org. Chem.*, 2000, **65**, 1915
32. E.D.P. Carreiro and A.J. Burke, *J. Mol. Catal. A: Chem.,*, 2006, **249**, 123.
33. G. Grivani, S. Tangestaninejad and A. Halili, *Inorg. Chem. Commun.*, 2007, **10**, 914.
34. Y.R.D. Minguel, *J. Chem. Soc., Perkin Trans.*, 2000, **1**, 4213.
35. D. Rechavi and M. Lemaire, *Chem. Rev.*, 2002, **102**, 3467.
36. D.E.D. Vos, M. Dams, B.F. Sels and P.A. Jacobs, *Chem. Rev.*, 2002, **102**, 3615.
37. A.H. Lu and F. Schuth, *Adv. Mater.*, 2006, **18**, 1793.
38. Y. Jung, S. Kim, S.J. Park and J.M. Kim, *Colloids Surf., A*, 2008, **313**, 292.
39. A.R. Massah, R.J. Kalbasi and S. Kaviyani, *RSC Advances*, 2013, **3**, 12816.
40. W. Zhang, J.L. Loebach, S.R. Wilson and E.N. Jacobsen, *J. Am. Chem. Soc*, 1990, **112**, 2801
41. E.N. Jacobsen, W. Zhang, A.R. Muci and L.D. James R. Ecker *J. Am. Chem. Soc*, 1991, **113**, 7063
42. K. Srinivasan, P. Michaud and J.K. Kochi, *J. Am. Chem. Soc.*, 1986, **108**, 2309
43. R. Irie, K. Noda, Y. Ito, N. Matsumoto and T. Katsuki, *Tetrahedron Lett.*, 1990, **31**, 7345
44. E.M. Mcgarrigle and D.G. Gilheany, *Chem. Rev.*, 2005, **105**, 1563

45. R. Irie, K. Noda, Y. Ito and T. Katsuki, *Tetrahedron Lett.*, 1991, **32**, 1055

46. R. Irie, Y. Ito and T. Katsuki, *Synlett*, 1991, **4**, 265

47. R. Irie, K. Noda, Y. Ito, N. Matsumoto and T. Katsuki, *Tetrahedron: Asymmetry*, 1991, **2**, 481

48. K.C. Nicolaou, S.A. Snyder, T. Montagnon and G. Vassilikogiannakis, *Angew. Chem. Int. Ed.*, 2002, **41**, 1668

49. C.J. Magesh, S.V. Makesh and P.T. Perumal, *Bioorg. Med. Chem. Lett.*, 2004, **14**, 2035.

50. C.E. Housectrof and A.G. Sharpe, *Inorganic Chemistry 2nd Edition*, Pearson Education Limited, England, 2nd edn., 2005, 639.

51. F.A. Cotton and G. Wilkinson, *Advanced Inorganic Chemistry*, John Wiley & Sons, New York, 5th edn., 1988.

52. R. Ocampo and W.R.D. Jr, *Tetrahedron*, 2004, **60**, 9325.

53. H.E. Simmons and R.D. Smith, *J. Am. Chem. Soc*, 1958, **50**, 5323.

54. A.H. M. Nakamura and E. Nakamura, *J. Am. Chem. Soc*, 2003, **125**, 2341.

55. X.-X. Sun, C.-M. Qi, S.-L. Ma, H.-B. Huang, W.-X. Zhu and Y.-C. Liu, *Inorg. Chem. Commun.*, 2006, **9**, 911.

56. M.H. Chisholm, J.C. Gallucci and H. Zhen, *Inorg. Chem.*, 2001, **40**, 5051

57. J. Yang, J.W. Yuan, R.H. Zha and Q.F. Zeng, *Acta Crystallogr., Sect. E: Struct. Rep. Online*, 2009, **65**, m1090.

58. A.P. Deshmukh, V.G. Akerkar and M.M. Salunkhe, *J. Mol. Catal. A: Chem.*, 2000, **153**, 75

59. J.S. Kumaran, S. Priya, J. Muthukumaran, N. Jayachandramani and S. Mahalakshmi, *Journal of Chemical and Pharmaceutical Research*, 2013, **5**, 56

60. R.B. King, *Encyclopedia of Inorganic Chemistry*, John Wiley & Sons, Inc., 2nd edn., 2005.

61. C.E. Housecroft and A.G. Sharpe, *Inorganic Chemistry (2nd Ed)*, 2005, 694.

62. X. Wang, L. Andrews, S. Riedel and M. Kaupp, *Angew Chem Int Ed Engl*, 2007, **46**, 8371.

63. A.D. Khalaji, K. Fejfarova and M. Dusek, *Russ. J. Coord. Chem.*, 2012, **39**, 68.

64. A.D. Khalaji, G. Grivan, M. Rezaei, K. Fejfarova and M. Dusek, *Russ. J. Coord. Chem.*, 2012, **39**, 104.

65. A.D. Khalaji, G. Grivani, M. Seyyedi, K. Fejfarova and M. Dusek, *Polyhedron*, 2013, **49**, 19.

66. S. Chattopadhyay, K. Bhar, S. Das, S. Satapathi, H.-K. Fun, P. Mitra and B.K. Ghosh, *Polyhedron*, 2010, **29**, 1667.

67. T.S. Basu Baul, S. Kundu, S. Mitra, H. Hopfl, E.R. Tiekink and A. Linden, *Dalton Trans.*, 2013, **42**, 1905.

68. A. Kumar, M. Agarwal, A.K. Singh and R.J. Butcher, *Inorg. Chim. Acta*, 2009, **362**, 3208.

69. W. Kaim and B. Schwederski, *Bioinorganic Chemistry: Inorganic Elements in the Chemistry of Life*, John Wiley & Sons, Inc., 1997.

70. A. Earnshaw and N. Greenwood, *Chemistry of the Elements (2nd ed.) Butterworth–Heinemann.*, 1997.

71. C.E. Housecroft and A.G. Sharpe, *Inorganic Chemistry (3rd ed.). Prentice Hall.*, 2008.

72. G.C. Congress, *Green Car Congress*, 2008.

73. A.G. Sharpe, *Inorganic Chemistry*, Pearson Education Limited, England, 2nd edn., 2005, 563.

74. P.J. Mccarthy, R.J. Hovey, K. Ueno and A.E. Martell, *J. Am. Chem. Soc*, 1955, **77**, 5820.

75. M. Franks, A. Gadzhieva, L. Ghandhi, D. Murrell, A.J. Blake, E.S. Davies, W. Lewis, F. Moro, J. Mcmaster and M. Schroder, *Inorg. Chem.*, 2013, **52**, 660.

76. S. Anbu, M. Kandaswamy and B. Varghese, *Dalton Trans.*, 2010, **39**, 3823.

77. M. Jian-Ying, *Synthesis and Reactivity in Inorganic, Metal-Organic, and Nano-Metal Chemistry*, 2013, **43**, 1361

78. P. Mukherjee, M.G.B. Drew and A. Ghosh, *Eur. J. Inorg. Chem.*, 2008, **2008**, 3372.

79. V.C. Gibson and E.L. Marshall, *Comprehensive Coordination Chemistry II*, 2003, **9**, 1

80. K. Anuradha and R. Rajavel, *international Journal of Pharmacy and Technology*, 2011, **3**, 3175

81. R. Katwal, H. Kaur and B.K. Kapur, *Sci. Revs. Chem. Commun*, 2013, **1**, 1

82. O.I.A. El-Salam, A.M. Shalaby, A.A. El-Sawy, S. Elshihaby and M. Abdulla, *Open Journal of Synthesis Theory and Applications*, 2013, **02**, 56.

83. A. Ourari, D. Aggoun and L. Ouahab, *Inorg. Chem. Commun.*, 2013, **33**, 118.

84. A.P. Mishra, N. Sharma and R.K. Jain, *Open Journal of Synthesis Theory and Applications*, 2013, **02**, 56.

References

85. A.F. Holleman, N. Wiberg and E. Wiberg, *Lehrbuch der Anorganischen Chemie*, , German Edition, Germay, 102nd edn., 2007, vol. "Cobalt", 1146
86. A.G. Sharpe, *Inorganic Chemistry (2nd Ed)*, Pearson Education Limited, England, 2nd edn., 2005, 665.
87. A.G. Blackman, *Cobalt: Inorganic & Coordination Chemistry*, 2006.
88. D. Chen, A.E. Martell and Y. Sun, *Inorg. Chem.*, 1989, **28**, 2647
89. Roman Boca, H. Elias, Wolfgang Haase, Martina Hu ¨Ber and E. Robert Klement, *Inorg. Chim. Acta*, 1998, **278**, 127
90. C. Rajnák, J. Titiš, R. Boča, J. Moncol' and Z. Padělková, *Monatsh Chem*, 2011, **142**, 789.
91. P. Pfeiffer, E. Breith, E. Lübbe and T. Tsumaki, *Justus Liebigs Annalen der Chemie*, 1933, **503**, 84
92. M. Salavati-Niasari, E. Esmaeili, H. Seyghalkar and M. Bazarganipour, *Inorg. Chim. Acta*, 2011, **375**, 11.
93. F. Saliu, B. Putomatti and B. Rindone, *Tetrahedron Lett.*, 2012, **53**, 3590.
94. P.A. Vigato and S. Tamburini, *Coord. Chem. Rev.*, 2004, **248**, 1717.
95. V. Alexander, *Chem. Rev.*, 1995, **95**, 273.
96. S.R. Collinson and D.E. Fenton, *Coord. Chem. Rev.*, 1996, **148**, 19.
97. A. Martell, J. Penitka and D. Kong, *Coord. Chem. Rev.*, 2001, **216 - 217**, 55.
98. P.D. Beer, D.K. Smith and K.D. Karlin (Ed.), *Progress in Inorganic Chemistry*, John Wiley & Sons, New York, USA, 1997, vol. 46, 1.
99. H. Okawa, H. Furutachi and D.E. Fenton, *Coord. Chem. Rev.*, 1998, **174**, 51
100. P. Guerreiro, S. Tamburini and V.A. Vigato, *Coord. Chem. Rev.*, 1995, **139**, 17
101. J. Nelson, V. Mckee and G. Morgan, *Prog. Inorg. Chem.*, 1998, **47**, 167
102. D.A. House and N.F. Curtis, *Chem. Ind.*, 1961, **42**, 1708
103. P. Gurumoorthy, J. Ravichandran, N. Karthikeyan, P. Palani and A.K. Rahiman, *Bull. Korean Chem. Soc.*, 2012, **33**, 2279.
104. Z.H. Chohan, M. Arif, M.A. Akhtar and C.T. Supuran, *Bioinorg. Chem. Appl.*, 2006.
105. Z.H. Chohan, A. Scozzafova and C.T.J. Supuran, *J. Enzyme Inhib. Med. Chem.*, 2003, **18**, 259
106. K. Matsufuji, H. Shiraishi, Y. Miyasato, T. Shiga, M. Ohba, T. Yokoyama and H. Okawa, *Bull. Chem. Soc. Jpn.*, 2005, **78**, 851.
107. B.-H. Ye, X.-Y. Li, I.D. Williams and X.-M. Chen, *Inorg. Chem.*, 2002, **41**.
108. R. Rl, T. Wb and L. Sj, *New J. Chem.*, 1991, **15**, 417

109. G.S. Papaefstathiou, I.G. Georgiev, T. Friscic and L.R. Macgillivray, *Chem. Commun. (Cambridge, U. K.)*, 2005, 3974.

110. G.S. Papaefstathiou, Z. Zhong, L. Geng and L.R. Macgillivray, *J. Am. Chem. Soc.*, 2004, **126**, 9158

111. O. Belda and C. Moberg, *Coord. Chem. Rev.*, 2005, **249**, 727.

112. H.R. Khavasi, K. Sasan, M. Pirouzmand and S.N. Ebrahimi, *Inorg. Chem.*, 2009, **48**, 5593.

113. A.K. Singh, W. Jacob, A.K. Boudalis, J.-P. Tuchagues and R. Mukherjee, *Eur. J. Inorg. Chem.*, 2008, **2008**, 2820.

114. W. Jacob and R. Mukherjee, *Inorg. Chim. Acta*, 2006, **359**, 4565.

115. A. Rajput and R. Mukherjee, *Coord. Chem. Rev.*, 2013, **257**, 350.

116. C.R. Bondy and S.J. Loeb, *Coord. Chem. Rev.*, 2003, **240**, 77.

117. P. Wothers, N. Greeves, S. Warren and J. Clayden, *Organic Chemistry*, Oxford University Press, England, 1sd edn., 2001, 288.

118. B.S. Jursic and Z. Zdravkovski, *Synthetic Communications: An International Journal for Rapid Communication of Synthetic Organic Chemistry*, 1993, **23**, 2761.

119. E. Valeur and M. Bradley, *Chem Soc Rev*, 2009, **38**, 606.

120. J.C. Sheehan and G.P. Hess, *J. Am. Chem. Soc.*, 1955, **77**, 1067.

121. Z.J. Kamiński, B. Kolesińska, J. Kolesińska, G. Sabatino, M. Chelli, P. Rovero, M. Błaszczyk, M.L. Główka and A.M. Papini, *J. Am. Chem. Soc.*, 2005, **127**, 16912.

122. M. Kunishima, C. Kawachi, J. Monta, K. Terao, F. Iwasaki and S. Tani, *Tetrahedron*, 1999, **55**, 13159.

123. A.D. Bond, B.S. Creaven, D.F. Donlon, T.L. Gernon, J. Mcginley and H. Toftlund, *Eur. J. Inorg. Chem.*, 2007, **2007**, 749.

124. E. Fischer and E. Fourneau, *Ber. Dtsch. Chem. Ges.*, 1901, **34**, 2688

125. L. Stoicescu, C. Duhayon, L. Vendier, A. Tesouro-Vallina, J.P. Costes and J.P. Tuchagues, *Eur. J. Inorg. Chem.*, 2009, **2009**, 5483.

126. A. Mishra, N.K. Kaushik, A.K. Verma and R. Gupta, *European journal of medicinal chemistry*, 2008, **43**, 2189.

127. N.W. Alcock, G. Clarkson, P.B. Glover, G.A. Lawrance, P. Moore and M. Napitupulu, *Dalton Trans.*, 2005, 518.

128. F.A. Chavez, M.M. Olmstead and P.K. Mascharak, *Inorg. Chim. Acta*, 1998, **269**, 269

References

129. K. No and K.M. Kwon, *Synthesis*, 1996, **11**, 1293
130. W. Huang, S. Gou, D. Hu and Q. Meng, *Synth. Commun.*, 2000, **30**, 1555.
131. C.S. Marvel and N. Tarkoy, *J Am Chem Soc*, 1959, **79**, 6000
132. H. Dai and H. Xu, *Chin. J. Chem.*, 2012, **30**, 267
133. E.J.T. Chrystal, L. Couper and D.J. Robins, *Tetrahedron*, 1995, **51**, 10241
134. J.H. Chong, M. Sauer, B.O. Patrick and M.J. Maclachlan, *Org. Lett.*, 2003, **5**, 3823.
135. A. Palmgren, A. Thorarensen and J.-E. Bäckvall, *J. Org. Chem.*, 1998, **63**, 3764.
136. N. Kuhnert, G.M. Rossignolo and A. Lopez-Periago, *Organic & Biomolecular Chemistry*, 2003, **1**, 1157.
137. J.-I. Kadokawa, Y. Tanaka, Y. Yamashita and K. Yamamoto, *Eur. Polym. J.*, 2012, **48**, 549.
138. X.M. Shi, R.R. Tang, G.L. Gu and K.L. Huang, *Spectrochimica acta. Part A, Molecular and biomolecular spectroscopy*, 2009, **72**, 198.
139. A.M. Costero, M.J. Baños, M.J. Aurell, L.E. Ochando and A. Doménech, *Tetrahedron*, 2005, **61**, 10309.
140. Y. Fu, Z. Xing, C. Zhu, H. Yang, W. He, C. Zhu and Y. Cheng, *Tetrahedron Lett.*, 2012, **53**, 804.
141. Y.-P. Chan, L. Fan, Q. You, W.-H. Chan, A.W.M. Lee and S. Shuang, *Tetrahedron*, 2013, **69**, 5874.
142. R.P. Bell, K.N. Bascombe and J.C. Mccoubrey, *J. Am. Chem. Soc.*, 1956, **1956**, 1286
143. Baekellte, *The New York Times*, 1909.
144. J. Clayden, N. Greeves, S. Warren and P. Wothers, *Organic Chemistry*, *Oxford, New York*, 2001 1455.
145. H. Dai and H. Xu, *Chin. J. Chem.*, 2012, **30**, 267.
146. D.R.L.a.S. A, *Elements of magnetochemistry*, Affiliated East West Press Pvt. Limited, New Delhi:Elsevier, 1992.
147. J.C.B. Duff, E. J, *J. Am. Chem. Soc.*, 1932, 1987.
148. J.C.B. Duff, E. J., *J. Am. Chem. Soc.*, 1934, 1305.
149. J.C.B. Duff, E. J, *J. Am. Chem. Soc.*, 1941, 547.
150. D. Plaul and W. Plass, *Inorg. Chim. Acta*, 2011, **374**, 341.